CCC2011
Proceedings

Central European Congress on Concrete Engineering

Main organizer
fib Hungary

22-23 September 2011
Hotel Flamingó Balatonfüred
Balatonfüred, Hungary

BALATONFÜRED 2011

The 7th Central European Congress on Concrete Engineering

FOUNDING MEMBERS

Innovative Materials and Technologies for Concrete Structures

Proceedings

www.fib.bme.hu

INNOVATIVE MATERIALS AND TECHNOLOGIES FOR CONCRETE STRUCTURES

INNOVATIVE MATERIALS AND TECHNOLOGIES FOR CONCRETE STRUCTURES

Proceedings of the ***fib*** Congress

Balatonfüred, Hungary
22 to 23 September 2011

Edited by

György L. Balázs
Professor
Department of Construction Materials and Engineering Geology
Budapest University of Technology and Economics
Budapest, Hungary
President of the Hungarian Group of *fib*

and

Éva Lublóy
Assistant Professor
Department of Construction Materials and Engineering Geology
Budapest University of Technology and Economics
Budapest, Hungary

This Volume was edited by György L. Balázs and Éva Lublóy

Both the abstracts and the papers were reviewed by the members of the Scientific Committee.

ISBN 978-963-313-036-0

PREFACE

A new tradition started in 2005 that is called *CENTRAL EUROPEAN CONGRESS ON CONCRETE ENIGNEERING*. This is a series of yearly congresses to provide a forum for engineers of our neighbouring countries to meet and exchange experiences regularly. Engineers from all fields are addressed working in design, execution, prefabrication, material production, research or quality control.

In our Congresses new achievements are presented to a specific field of concrete engineering: The *1st* CCC Congress in Graz (Austria) 2005 was devoted to *Fibre Reinforced Concrete* in Practice; the *2nd* Congress in Hradec Kralove (Czech Republic) 2006 had the main topic *Concrete Structures for Traffic Network*. The *3rd* Congress in Visegrád (Hungary) 2007 focused on *Innovative Materials and Technologies for Concrete* Structures.; the *4th* CCC Congress in Opatija (Croatia) in 2008 concentrated on *Concrete Engineering in Urban Development*; the *5th* Congress in Baden (Austria) was devoted *to Innovative Concrete Technology in Practice*; the *6th* Congress in Mariánské Lazně (Czech Republic) in 2010 had the main topic *Concrete Structures for Challenging Time*.

The 7thCentral European Congress on Concrete Engineering will take place in Balatonfüred, Hungary. The Congress focuses on *Innovative materials and technologies for concrete structures*. Concrete is an ever developing construction material. There is a continuous development on material properties, constructability, economy as well as aesthetics. The Congress in Balatonfüred intends to overview properties of new types of concretes (including all constituent materials) and reinforcements as well as their possible applications which already exist or can exist in the future.

Therefore, we selected the following 5 topics:

Topic 1: Tailored properties of concrete
Topic 2: Advanced reinforcing and prestressing materials and technologies
Topic 3: Advanced production and construction technologies.
Topic 4: Advanced conctere structures
Topic 5: Modelling , design and testing

The Congress in Balatonfüred will be organized in a beautiful ambient provided by the Lake Balaton.

The host organisation of the Congress is the Hungarian Group of ***fib***. Co-organizers of the Congress are the Hungarian Concrete Association and the Association of Hungarian Concrete Elements Manufacturers.

We have a pleasure to invite representatives of clients, designers, contractors, academics and students to take part at this regional event, which will give excellent social and technical conditions for exchange of experience in the field of concrete engineering. We are happy to meet you in Balatonfüred.

György L. Balázs — Éva Lublóy

7th European Congress on Concrete Engineering
22-23 September 2011 Balatonfüred, Hungary

Scientific Committee

BALÁZS, György L., Chairman (Hungary)
BERGMEISTER, Konrad (Austria)
BÓDI, István (Hungary)
BOROSNYÓI, Adorján (Hungary)
CSÍKI, Béla (Hungary)
FARKAS, György (Hungary)
GLATZL, Johann (Austria)
HELA, Rudolf (Czech Republic)
KALNỲ, Milan (Czech Republic)
KOLLEGGER Johann (Ausrtia)
KOPECSKÓ, Katalin (Hungary)
KORIS, Kálmán (Hungary)
KREMNITZER, Peter (Austria)
NEHME, G. Salem (Hungary)
PIČULIN, Srečko (Croatia)
RADIĆ, Jure (Croatia)
SAVOR, Zlatko (Croatia)
SIMON, Tamás (Hungary)
TKALČIĆ, Damir (Croatia)
VÍTEK, Jan L. (Czech Republic)

Organizing Committee

BARTA, János, Chairman (Hungary)
ARANY, Piroska (Hungary)
BELUZSÁR, Levente (Hungary)
CZOBOLY, Olivér (Hungary)
DANCS, László (Hugary)
FOGARASI, Gyula (Hungary)
KARSAINÉ, Katalin (Hungary)
KOLOZSI, Gyula (Hungary)
KOVÁCS, Tamás (Hungary)
LUBLÓY, Éva (Hungary)
MÁRKUS, Kristóf (Hungary)
PAUSER, Michael (Austria)
PLUZSIK, Tamás (Hungary)
SÁNTA, Ildikó (Hungary)
SRŮMA, Vlastimil (Czech Republic)
SZARKÁNDI, János (Hungary)
TEITER, Zoltán (Hungary)
VASS, Viktória (Hungary)

Sponsoring Organizations

Holcim
Hídépítő Co.
Form+Test Hungary Ltd.
Mapei
Sika Hungary Ltd.
Červenka Consulting Ltd.
Lafarge Cement Hungary
Beton-Star Ltd.
ÉMI-TÜV Süd Ltd.
Duna – Dráva Cement Ltd.
Via Pontis Co.
Lábatlani Vasbetonipari Co.
Főtaxi

7th European Congress on Concrete Engineering
22-23 September 2011 Balatonfüred, HUNGARY

CONTENT

TOPIC 5
MODELLING, DESIGN AND TESTING

SELECTED PAPERS

DESIGN OF THE M43 TISZA RIVER BRIDGE

Mátyássy László[1], Nagy András[1], Dezső Berkó[2]
[1] Pont-TERV Zrt., Thán Károly utca 3. 1119, Budapest, Hungary
[2] Hídépítő Co., Karikás Frigyes u. 20. 1138, Budapest, Hungary

SUMMARY

Motorway M43 connects Szeged with Makó in the southern part of Hungary. Móra Ferenc bridge crosses there the Tisza river. The main goal of the design tender was an esthetic shape and innovative technology. The Fig.1 shows the computer visualization of the new structure bridge for the tender.

Fig. 1 Computer visualization of the bridge

1. INTRODUCTION

The Fig. 2 shows the main data of the bridge. The total length of the Tisza bridge is 661.20 m, there are 2 approach bridges and a river bridge. Spans of the river-bridge are: 95.00+180.00+95.00 m. The superstructure consists of a 29.94 m wide box cross section beam with three cells. (Fig. 3) The bridge is an extradosed superstructure. Corrugated steel web was applied between the top and bottom prestressed concrete slabs. Those two solution have several advantageous features in comparison with ordinary box beam bridges: the beam height as well as the self-weight were successfully reduced resulting in a slender superstructure. The pylon height is 20 m. The VSL stay cables are driven through the pylon with saddles. The river-bridge is made by the in-situ balance cantilever method.

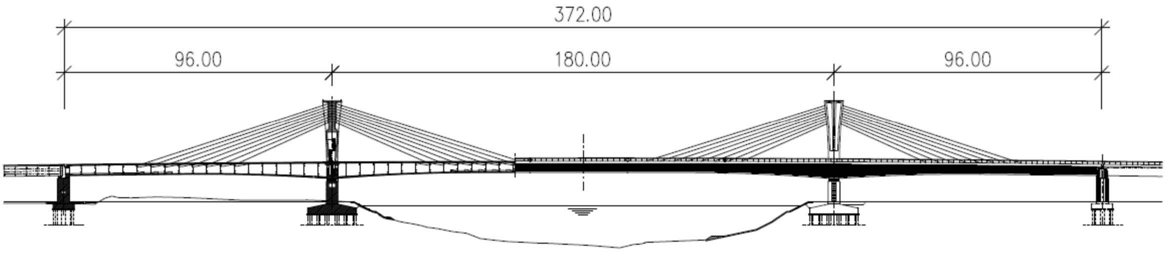

Fig. 2 General view

2. DESIGN OF THE SUPERSTRUTURE

2.1 Statical calculation

For the global statical calculation of the superstructure, beam elements were applied. It was a big challenge to find a good modeling method for the corrugated steel web part in the statical system. The corrugated steel web has anisotropic behavior. The Austrian bridge software company TDV helped us to develop a new special elements to connect the top and bottom slab. We tested this element by using several FEM verifying model in order to get a correct deformation for the main girder.

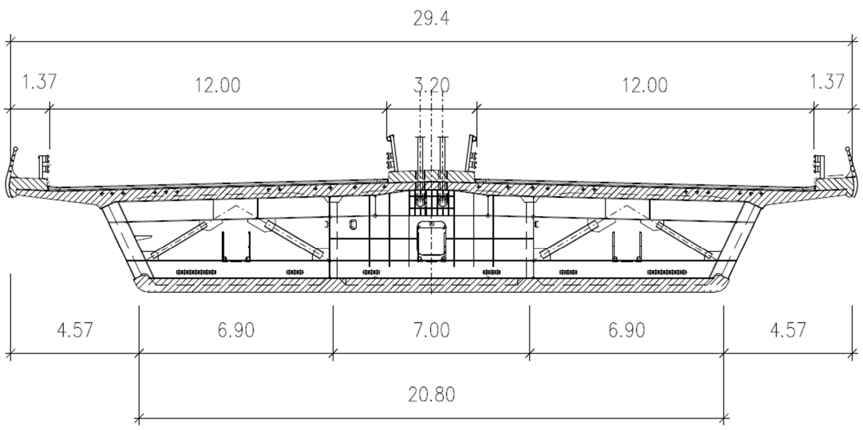

Fig. 3 Cross section

2.2 Cross section

The main girder is a three cell box girder with four corrugated steel webs. Every 5 m long segment has a steel cross girder. There are DSI inner stressing cables in the top slab. For the bottom slab VT external stressing cable are applied. These cables are driven trough the steel cross girders. The corrugated steel web withstands the shear force without receiving significant normal force from the axial tensioning. Due to this effect, the tension force stays in the slab and therefore the stressing is more effective. Shear bolts connect the top and bottom slab via the steel structure.

2.3 Stay Cable

The pylon height is 20 m. Eight pairs of VSL stay cables are placed in a special saddle structure in the upper part of the pylon. The stay cables connect to the main girder in the middle of the cross section. Detailing of the anchorage was a very complicated engineer problem. The steel part of the anchorage can be seen in Fig. 4. The steel cross girder together with the top slab are capable of handling the large cable forces.

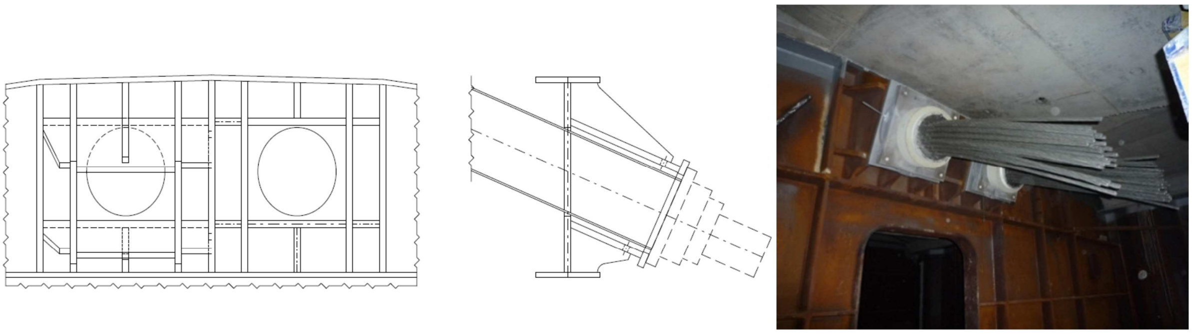

Fig. 4 Stay Cable anchorage

3. FATIGUE AND WIND TUNNEL TEST

The Hungarian Technical University made a fatigue test of the corrugated steel web, because there is no any guidance in the Hungarian Standard for such a structure.
Wind tunnel tests were also made in order to determine the aerodynamic performance of the cross section and to get data for the computer simulation of the whole bridge.

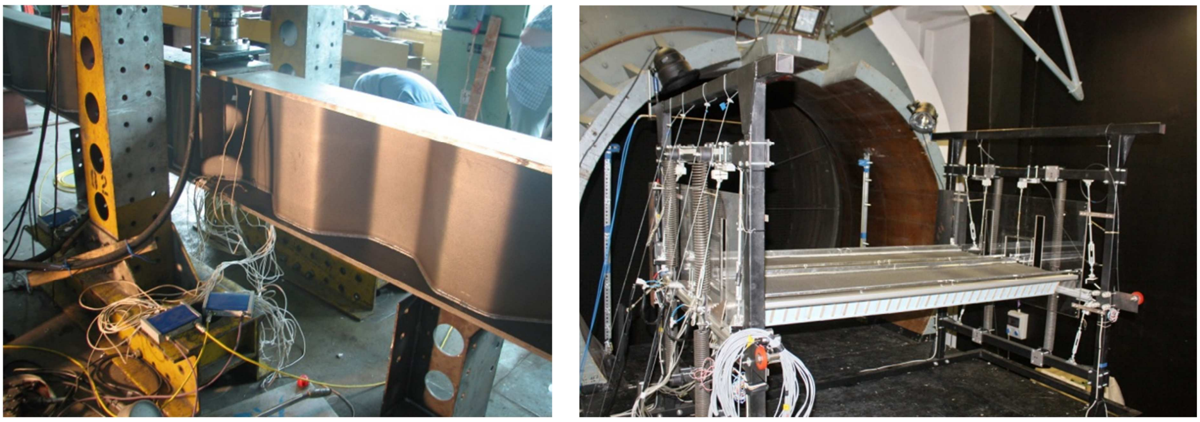

Fig. 5 Fatigue and wind tunnel test

4. CONSTRUCTION

During the construction the most important thing was to measure the shape of the growing cantilever. After concreting a segment the whole bridge shape was measured and compared with the calculated camber line of the superstructure.

The bridge was built by using a balanced cantilever method. The DOKA traveler assembled 5 m long segments. First steps was the assembly of the steel frame on the shore. Fig. 6. Every single steel frame was lifted into the traveler by cranes. By positioning the traveler, the difference between the measured and designed camber lines can be compensated according to the geodesy. There are 75 segments in the superstructure.


Fig. 6 Assembled steel frame

The two cantilever were built in same time. There were two closing segment in the shore side and the final closing was over the river. Other construction description can be read in the next paper written by the constructor.



Fig. 7 Traveler in work and the VSL saddle before concreting

Fig. 8 The completed bridge

5. CONCLUSIONS

This paper dealt with an extradosed bridge combined with corrugated steel webs, which is the first such structure in Europe. This solution enable the bridge to get a very slender and aesthetic appearance. During the construction good cooperation was achieved between the designer and the contractors. As to the calculation and detailing of the structure, it was a challenging engineering work.

MAJOR DEVELOPMENT IN ENVIRONMENTAL PROTECTION OF CENTRAL-EUROPE, THE BUDAPEST CENTRAL WASTEWATER TREATMENT PLANT

András Sármay[1], *Dr. Béla Csíki*[2]
[1] *Hidrokomplex Engineering Ltd.Budapest, III. Bécsi út 122-124, Hungary*
[2] *DCB Engineering Ltd. Budapest, IX. Mester u. 9., Hungary*

SUMMARY

As is well-known by the Hungarian public and mainly by the engineering professionals the Budapest Central Wastewater Treatment Plant, the largest environmental development in the area, has been put in its regular operation, recently. The project has been completed as a result of cooperation of a few typical civil engineering specialities, such as; hydraulic-, wastewater treatment- and structural engineering, civil- and structural construction.

The paper gives a general view of the project, presents the main objectives, the special conditions of the realization, the characteristic data of the water treatment technology and also those of the technological buildings. To the construction of the latter ones about 180.000 m^3 of reinforced concrete was to be used. The structural specialities of the largest complex technological buildings are also outlined in the paper.

1. INTRODUCTION

The Budapest Central Wastewater Treatment Plant (BCWWTP) completed in 2010 was realized as the most important part of a gigantic environmental development in Hungary called Living Danube Project (Élő Duna Projekt).

The daily amount of wastewater originating from the 790.000 households of Budapest is almost 600.000 m^3. Before the realization of the project the two existing wastewater treatment plants of the Hungarian capital has been able to receive and - by appropriate removal of biologic nutriments - suitably treat only about the half of the whole quantity. Namely 200.000 m^3 per day is treated at the Northern-Pest Wastewater Treatment Plant and an other 80.000 m^3 per day is treated at the Southern-Pest Wastewater Treatment Plant.

In addition to establishing the Central Wastewater Treatment Plant the Living Danube Project included also several other developments, such as: the flood control dam protecting of the plant, the construction of the accessing road, development of three pumping stations (in Ferencváros, in Albertfalva and in Kelenföld), the Main Collector Canal of Buda at the riverside of Danube and, moreover, the pressure pipes from the pumping stations crossing the Danube under the riverbed and leading to the new treatment plant. The proper handling of the wastewater-sludge, the end product of the treatment has also been taken care of.

The total investment cost of the Living Danube Project has been about 428.7 million Euros. This sum has been financed according to the following: 65% by the Cohesion Fund of the European Union, 20% by the Hungarian State and 15% by the Municipality of Budapest.

The new Budapest Central Wastewater Treatment Plant is able to treat an equivalent wastewater quantity of 1,6 million inhabitants by its dry period hydraulic capacity of 300.000 m^3. By the development the biological wastewater treatment capacity of Budapest has become almost 100 %. In rainy weather the plant has the ability to biologically treat a 500.000 m^3 per day, and to mechanically pre-treat a 950.000 m^3 per day of peak time water flow, respectively.

The selection of the main contractor happened to be by way of a public procurement procedure. The construction contract - including also the whole design task - with the winner Csepel 2005 FH Consortium was signed at the end of 2005.

The Consortium consisted of four companies. Two French companies, the Degremont SUEZ and the OTV France were responsible for the technological mounting and its commission. Two Hungarian companies, the Hídépítő Inc. and the Colas Alterra Inc. were responsible for the civil design and execution of buildings, structures and objects. As a subcontractor the Hidrokomplex Ltd. was the general designer of the plant. The leader of the Hungarian participants was the **Hídépítő Inc.**

The most difficult tasks facing the contractors can be summarized as follows:
Due to the development location keeping the strictest noise and odour emission values were defined to the contractors. Moreover, securing green surfaces up to 70% of the 24 hectares building site was also prescribed. The fulfilment of these demands required, on the one hand, the complete covering of the structures at the plant. On the other hand, in order to occupy as little area as possible the technologists have put different elements of the technology over each other. This way the technological buildings became multi-storied to allow the reduction of the occupied terrain.

2. ABOUT THE TREATMENT TECHNOLOGIES

The wastewater forwarded by the two pumping stations is received at the plant on an initial geodetic height, high enough to allow the water to flow through the total treatment process by gravity, even in case of ruling water level of the Danube.

Wastewater cleaning
The mechanical pre-treatment at the plant begins by 6+2 fine screens followed by 7+1 3D Sedipack structures. Each of these letter structures includes an aerated sand-trap and a lamellar pre-settling device. Following the mechanical pre-treatment the water flows into one of the 18 biologic-treatment water lines consisting of an anaerobe labyrinth and a sectional aerated carousel basin. This – at each line - is followed by a final sedimentation basin securing longitudinal streaming through, with space also to provide disinfections, eventually. The separated pre-settling devices and the biologic water lines can be operated simultaneously ensuring a relatively great enough flexibility for the plant. At the end of the process an underground pipe leads the treated water to the river bed.

Sludge handling
The primary sludge divided at the pre-settling devices is first thickened in gravitational condensers. Then, the condensed sludge mixed with the excess sludge settled by the post-settling devices, pasteurised at a temperature of 70°C before rendering rotten in the three thermofill digester towers. The digested sludge is forwarded into an intermediate storage basin for thickening it gravitationally. After the thickening the sludge dewatered by

centrifuges. The remaining sludge of about 23 to 27 % water containment is transported away from the plant.

Usage of biogas
The biogas created during the process of digesting is collected in 2 gasholder tanks and burned in gas-motors (3 pieces of 1,5 MW each) and in boilers. This way, on the one hand, the electric power demand of the plant can be partially (up to 30%) ensured. On the other hand, the entire thermal energy necessary for heating the buildings, for sludge pasteurising and digesting can also be supplied by the usage of biogas.

3. BUILDINGS AND STRUCTURES

The buildings and structures serving the technology may be divided into four characteristic groups (Fig. 1):

1. Large structures (technological buildings of the water lines)
    a. Mechanical pre-treatment building (screens, sand-traps, primary settling basins)
    b. Biological treatment building (basins with activated sludge and final sedimentation devices)
2. Circular structures
    a. Gravitational thickeners
    b. Digester towers
    c. Storage tank of digested sludge
    d. Foundations of gas-holder tanks
3. Other technological buildings
    a. Odour machine-house
    b. Sludge dewatering building
    c. Gas-motor- and boiler machine-house
    d. Electrical building (power receiver and control building)
4. Non-technological buildings
    a. Central office and laboratory building
    b. Workshop, storeroom
    c. Reception house

From structural engineering viewpoint the, so called, “large structures”, the technological buildings are the most interesting because of their complexity and measures. A few of their characteristic data and design aspects are summarized in the next chapters.

Fig. 1: Bird's eye view of the large structures during construction

3.1 Mechanical pre-treatment building

The main (middle) level of the multi-storey building contains the following water-technological basin-blocks: fine screens, sand-trap basins, primary settling basins and a system of channels securing the appropriate water flow (Fig. 2). Below this whole level, at the basement of the building there are storage and handling spaces and the air-blower rooms of the whole plant. The third level (at the top of the basin-blocks), mainly, secures spaces and walkways for handling and serving the devices and checking the operation.

The layout measures of the large and rather complex building are about 60,0x110.0 m. The total height of the building containing the above three main levels is about 15.0 m, from which 10 m height is below the ground-surface. The complexity of the building well can be seen in an axonometric view. The characteristic water pressure in the water holding units is about 6.0 m. (The water holding capacity of each of the eight primary settling basins in the building is 2.000 m^3, for example.)

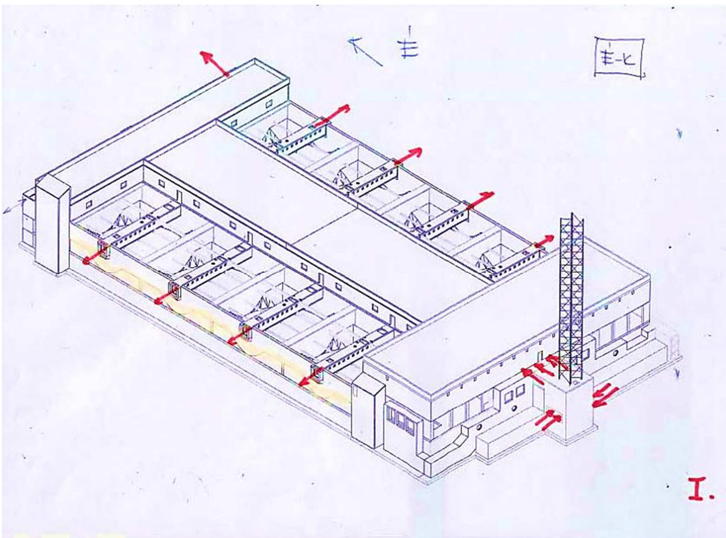

Fig. 2: Axonometric view of the mechanical pre-treatment building

Structurally the building and its dilatation units are reinforced concrete "box-structures" with stiff wall to wall, floor to wall and column to floor connections.

The whole building stands in one common foundation plate. Then, the basement level and the middle level is separated by a cross-directed expansion joint-surface into two dilatation units. The third (upper) level, which is above the ground surface, is divided by two additional expansion joint-surfaces into four structurally independent parts.

The amount of structural concrete and reinforcing steel used for the elements of the building is summarized in Tab. 1:

Tab. 1: Summary of concrete and steel amounts

	Concr. (m^3)	Steel (t)	Ratio C/S (kg/m^3)
Foundation plate	4250	578	136
Southern block	8090	1095	135
Northern block	2900	375	128
Summary	15240	2048	133

The value of the ratio of built in steel per concrete m^3 is a little bit higher, then it was expected. The reasons for this are, on the one hand, the substantial occurring of restrained shrinkage due to the complexity of the building and, on the other hand, the "close to square shape" of the elements of the technological units (Fig. 3). (One can hardly find an element in the whole structure with only one load bearing direction.)

Fig. 3: View of the mechanical pre-treatment building during construction

3.2 Biological treatment building

Significant parts of the plant are the two huge biological blocks (150x170 m each) on the two sides of the pre-treatment block (Fig. 4). Each block has 9 independent treatment lines, which contains:

- Pre-anoxic zone,
- Anaerobic labyrinth,
- Aeration tank (61x18 m; water depth: 8.3 m),
- Degazing zone,
- Final sedimentation tank (above the anaerobic and the chlorination labyrinth),
- Chlorination labyrinth,
- Recirculated and excess sludge removal system,
- Scum collecting and removal system.

The water is distributed by an inlet channel, and after the treatment process is collected by the treated water channel. Two main service corridors provide a comfortable operation. The whole block is covered, and equipped by a sophisticated aeration system. Exhaust air is handled in the separate biological and chemical odour control building.

As the final sedimentation tank is situated above the anaerobic and the chlorination labyrinth the built-in surface of the plant could be reduced considerably. On the other hand even the foundation became more practical as the base plate of the whole block could have the same level. Interesting detail is, that the intermediate slab between the labyrinth and the final sedimentation tank may get under pressure not only from the topside, but from the bottom side, as well, when the upper tank is empty. An extreme care has been taken to avoid shrinkage problem because of the restraining effect of the walls underneath.

Because of the huge dimensions (150x170 m) of the blocks, each block has been split into six structurally independent pieces by three expansion joints. The transversal joint is between the aeration tanks and the final sedimentation tanks, and in the longitudinal direction two expansion joints split the structure into three parts, consisting 3-3-3 treatment lines.

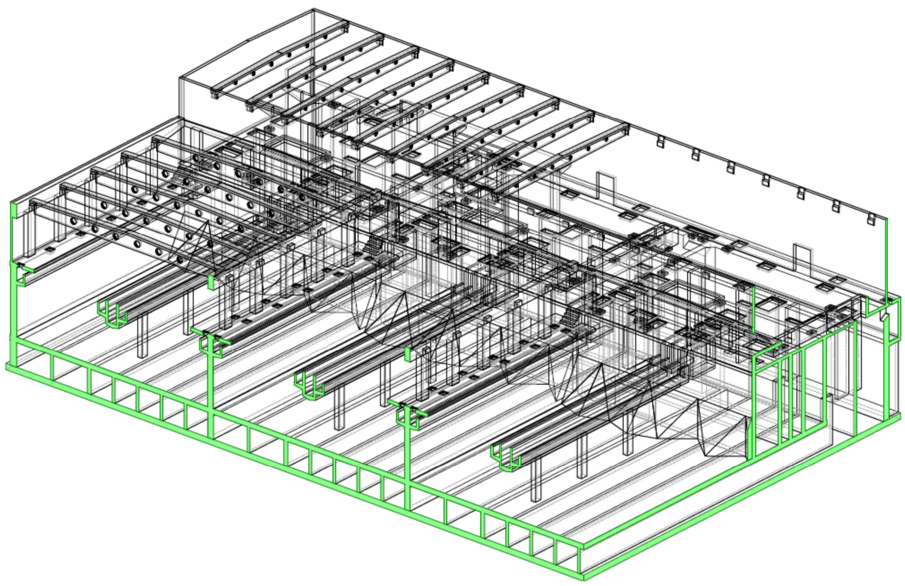

Fig. 4: Axonometric detail of the biological treatment building

As the construction time was extremely short, the building companies decided to prefabricate the whole cover of the building. It was a real challenge to design and build the wall-roof connection especially in the case of the aeration tank, because the 13 m high wall retaining 8.3 m deep water has no intermediate support (Fig. 5). For the emplacement of the elements of the prefabricated roof Hídépítő Inc. developed a special crane, running on the top of the walls. It was the only possibility because any normal crane wasn't able to this emplacement due to the large dimension.

The base plates, slabs and especially the long walls have been poured by smaller pieces to avoid the problem due to the restrained shrinkage. In the case of the walls usually the first poured elements was "L" and "T" forms, or 10.6 m long strait peaces. The length of the closing elements was 3-4 m.

Fig. 5: The walls during construction

In the two blocks ~100.000 m^3 structural concrete has been poured, the reinforcement ratio was 120 kg/m^3.

4. A FEW CONSTRUCTION DETAILS AND DATA

Following the contract signature the tasks of the Consortium were the preparation of the design-drawings to apply for building permissions, the preparation of the executing drawings and the construction of the plant.

During the design phase the archaeological survey of the building site and the required ground works were being done.

The archaeologists found on the near 50.000 m^2 area of the large structures - surveyed at the same time - more than 6.000 findings from the Ludanice culture of the Middle Copper Age (4th thousand B. C.), from the culture of Nagyrév (2nd thousand B. C.), from the Celtic migration period in the Iron Age (5th century B. C.) up to the findings of the Arpadian Age (11th to 12th century A. C.).

Simultaneously with the archaeological works, as the first step of the execution, a long diaphragm wall in the ground – surrounding the large technological buildings under the ground surface - made of clay and bentonite was being built. This watertight wall confines the working pit required to reach the foundation level deeper then the high water level of the near Danube river. On the one hand, during the construction the wall made possible the proper lowering of the ground water to secure the building process. On the other hand, during operation the wall can localise the contaminations arising accidentally at the large technological buildings. The material of the diaphragm wall was Solidur 274RV selected appropriately to the aggressive soil contaminated with heavy metals. The diaphragm wall along its lower 1.5 m length is bound into the "kiscelli" clay-layer occurring in the site at about 10-15 m depth. Thus, a closed "basin" made of clay-wall has been formed. The diaphragm wall of 60 cm thickness surrounds the large technological buildings in a length of about 2.5 km (Fig. 6).

Fig. 6: Sectional detail of the diaphragm wall

Having received the legally valid permission of water-rules, the execution of the buildings and structures started in January 2007 and were completed in December 2008.

For preparing and finishing the construction works an approximate amount of 400.000 cubic m of ground were necessary to move, twice in particular, once at phase of digging out the places for the structures and later on for refilling and landscaping. The remaining quantity was used to form the final "wavy" ground surface.

During the construction of the buildings and the complex civil engineering structures about 180.000 m^3 of structural concrete and 22.000 tons of reinforcing steel were built in (Lengyel, Sármay and Csíki, 2010). The necessary quantity of concrete was provided by 2 mixing plants settled on the building site. The applied concrete mixture was developed specially to the large structures of the plant in cooperation with the Department of Building Materials and Engineering Geology of the Technical University of Budapest. The concrete had to fulfil the following requirements:

C30/37-XV2(H)-XD2-XA2-32-F4

- Strength (at age of 56 days on a cube of 15 cm) 40 N/mm^2
- Impermeability (at age of 56 days in case of XV2(H) environmental class) 40 mm
- Keeping the principle of „White tub"

- Max. w/c = 0.5
- Min. cement content 320 kg/m^3
- Consistency measured by outstretch after 1.5 hours min. 450 ± 30 mm (at casting, according to the experiences, the best consistency 500 to 550 mm)
- Non-perishability for 2 hours of the green concrete

Winter and summer mixtures were worked out for the execution. In the summer period in order to reach a low value of the heat generation CEM III/B 32.5 N-S cement was used. In wintertime for reaching a larger initial strength CEM II/A-V 32.5 R-S cement was used in the mixture (Kovács, Lengyel, Martin, Orbán and Tóth, 2008).

The implementation works of the technologic-mechanical installations started in October 2007, very closely after the structural works had begun. Until the 1st August 2009, the starting time of the trial operation all the execution works - excepting the horticultural development – had been completed. Thus the trial operation could be started in the scheduled time (Lengyel, 2009), and finished in the middle of 2010. Since the technical handling over in summer 2010 the new, odourless, durable and aesthetic wastewater plant has been regularly operating (Fig. 7).

Fig. 7: The completed large structures

5. CONCLUSIONS

Recently, the construction of the Central Wastewater Plant of Budapest has been the largest environmental innovation in Hungary and, moreover, in the Central European Area, as well (Fig. 8). A short review of the main goals of the project, of the applied wastewater treatment technology and of the erection circumstances of the technological buildings and objects have been presented in the paper. Experiences of the more then one year regular operation of the plant confirm the successful contribution of the project to reach almost 100%-level of biological treatment of wastewater arising in Budapest.

Fig. 8: View of the whole plant after completion

6. ACKNOWLEDGEMENTS

The authors gratefully thank Hídépítő Inc., the leader of the Hungarian participants of the international Consortium responsible for the project realization, for the help and support during the time of preparing to the Congress.

7. REFERENCES

Kovács, J., Lengyel, G., Martin, B., Orbán, Z. and Tóth, L. (2008), "The concretes of the wastewater treatment plant at Csepel using sulphate-resistant cements CEM III/B 32,5 N-S and CEM II/A-V 32,5 R-S", *Beton*, Vol. 16. No. 1., January 2008, pp. 8-11.

Lengyel, G. (2009), „In the course of trial operation… war and peace", *Hídépítők*, Vol. 38. No. 2009/5-6. pp. 4-5.

Lengyel, G., Sármay, A. and Csíki, B. (2010), "Major environmental innovation in Central-Europe, the Budapest Central Wastewater Plant", *Concrete Structures*, Vol. 11. No. 1., 2010, pp. 32-37.

RECENT STRUCTURAL ENGINEERING ACHIEVEMENTS IN CROATIA

Jure Radić[1,2]
[1] *University of Zagreb – Faculty of Civil Engineering*
Croatia, 10000 Zagreb, Kačićeva 26
[2] *Institute IGH*
Croatia, 10000 Zagreb, J. Rakuše 1

SUMMARY

This paper highlights several projects at the design or construction level or completed in last three years in Croatia. The desicribed structural engineering projects are related with sustainable development of the capital city Zagreb, Adriatic coast as well as other part of the land through furher improvement of the Croatian motorway network. Structures described within this paper still largely resort to concrete as the predominant construction material, although there are some examples of various combinations of concrete and steel providing for efficient and exceptional structures.

1. INTRODUCTION

Croatia has long-standing tradition of concrete construction celebrating an entire century of structural concrete. This paper highlights several projects at the design or construction level or recently completed in Croatia. Many of the structures constructed in course of these projects are made of concrete, as it allows for utilization of local materials and is thus cheaper.

Fast growing city and economic development of Zagreb brought about an increase in design and construction of bridges and buildings: planned two new bridges across Sava River and new pasanger terminal at Zagreb Airport are curently at design level, while several ofice-residental building has been built recently.

The 21st World Handball Championship took place in January 2009 in Croatia and six large sport halls were constructed to host the event.

Recent development of the Croatian motorway network is related to the upgrading of existing routes to full motorway profile, while activities relating to construction and maintenance of motorways are limited by present-time financing possibilities which are, due to global financial crisis and recession, less favourable when compared to previous periods.

In a country of over 1,000 islands, of which 66 are inhabited, providing fixed road connection to the mainland is of major importance. Therefore, many bridges have been built so far, and two undergoing projects will be present in this paper.

2. NEW PROJECTS FOR SUSTAINABLE DEVELOPMENT OF ZAGREB CITY AND ITS REGION

Zagreb is the capital and the largest city of the Republic of Croatia. The transport connections, concentration of industry, scientific and research institutions and industrial tradition underlie its leading economic position in Croatia. Fast growing city and economic development brought about an increase in design and construction of bridges and buildings, many of them in concrete.

2.1. New bridges across Sava River in Zagreb

Solving the problem of the inadequate capacity of the Sava River crossing in Zagreb, the City Council of Zagreb and the Croatian Society of Structural Engineers organized public competitions for the preliminary bridge designs for the two new bridges located near the lakes, Jarun and Bundek, popular recreational and sports areas. The new bridges should be city landmarks providing six traffic lanes, and light rail crossing. These bridges has been designed as part of the solution for sustainable development of the Sava River banks area in Zagreb, as the most dominant natural and urban city motif. So far, the littoral area of the Sava River was used only as a protection from floods. In order to integrate the river into the urban area, the regulation of the river flow is also planned to enable bringing new life to riverbanks and the river boat service.

The Jarun Bridge is designed as a cable-stayed bridge and is inserted in the urban structure at the outside perimeter of the city. For this city bridge asymmetrical layout was chosen with one inclined pylon as a dominant structure element. The main span is 150 m with the overall bridge length of 625 m. Respecting the vertical urbanism and cultural heritage, pylon height of 88 m does not surpass the tallest building in the Zagreb City, the historical Cathedral.

The main characteristic and uniqueness of the Bundek Bridge is its urban design which is manifested through its vertical organization and attitude toward the content of public space and urban environment. The bridge structure is carrying the communication longitudinally on two levels. The bridge has four (4) spans: $2 \cdot 93 + 2 \cdot 124 = 434$ m, and total length of 462 m. The new structure forming principals, based on intersected arches forming frames, are already applied in the new passenger terminal design for Zagreb Airport, but it can be also transformed for other future landmark buildings, e.g. central metro station, as a modern style of the 21st century Croatian capital.


Fig. 1 Jarun bridge (left) and Bundek Bridge (right) – computer rendering.

2.2. New passenger terminal at Zagreb Airport

Zagreb Airport, located only 10km from the centre of Zagreb, is the Croatian main international airport Zagreb Airport and handles over two million passengers and 12 000 tonnes of cargo annually, and it is also an important military base for fighter jets. With growing passenger numbers the old terminal facilities cannot handle the additional volume and are in desperate need of upgrading. The new terminal will have around 65,600m² of floor space – nearly five times greater than the size of the current terminal. The new terminal has been designed as a result of an international architectural and urban planning competition in 2008, which was finally won by a consortium of between Institute IGH, Neidhardt arhitekti and Kincl chosen from 17 other proposals. The design includes a retail area that will have banks, shops, cafes and restaurants, a luxury hotel with a direct underground link to the terminal and a railway station. The main building of new terminal is reinforced concrete structure wile roof structure is made of steel. An international, public tender for the selection of a strategic partner to build and operate the new passenger terminal was published in October 2010.


Fig. 2 Winning design of the new passenger terminal at Zagreb Airport

2.3. New public and office-residential buildings in Zagreb

In the city centre two new business and residental complexes will improve quality of life in Zagreb. Office residential building currently under construction, Ban Centar is located at the most prestigious location in the historic center of Zagreb, next to the Cathedral. The building consists of 5 underground storeys and 8 storeys above the ground level. The entire covered area amounts to 33 222 m^2. The structure is reinforced concrete frame with span of 8.00 m. Recently built office residential building, Cvjetni Centar, located close to main Zagreb's square, occupies 42000 m^2 in plan area. Out of this, the underground part accounts for 20000 m^2 in 6 storeys, 8 more storeys are built above the ground level. The structure is mostly made of reinforced-concrete, and also of steel and concrete combination. The quality of life in the other parts of the city has been also increased by construction of the new building complexes, such as Bundek Centre, consisting of business and residential complexes as well as sports and recreational facilities and hotels; and Arena Centre, commercial and amusement centre close to the sporting hall.




Fig. 3 New office-residential centres in Zagreb: Ban, Cvjetni, Bundek and Arena

3. SPORTING HALLS FOR THE WORLD CHAMPIONSHIP IN CROATIA

The 21st World Handball Championship took place in January 2009 in Croatia and six large sport halls were constructed in Zagreb, Split, Osijek, Varaždin, Poreč and Zadar. Building according to public private partnership model was used in most cases and the entire investment was distinguished by very short terms. The all six structers are made of concrete or combine members of reinforced concrete and steel. The largest hall is Zagreb Arena, with seating capacity of 15200.

Fig. 4 Sporting halls in Zagreb, Split, Osijek, Varaždin, Poreč and Zadar

4. RECENT DEVELOPMENT OF CROATIAN MOTORWAY NETWORK

The road network in Croatia is by far the most important element of the land transport. Over the last decades Croatia made large investments in order to complete the 1500 km long motorway network, which shall integrate the most distant parts of the country. As on 1 January 2011, the total length of the motorway network in the Republic of Croatia amounted to 1,240.7 km. Over last four years more efforts was put into the upgrading of existing routes to full motorway profile (Tab.1), including construction or competition of complex engineering structures. Left-side tubes of the Mala Kapela (5.78 km) and Sveti Rok (5.68 km) tunnels were opened to traffic in May 2009. Widening of the south-side pavement of the Rijeka city beltway to the full motorway profile was completed at the end of 2009, including construction of the new Rječina Bridge. Upgrading of the Istrian Y route to the full motorway profile is currently in progress. 10 km long section of motorway A1: Zagreb-Split-Dubrovnik between Ravča and Vrgorac, including four viaducts, five overpasses and one tunnel, was completed at the end of June 2011. At the beginning of July 2011 construction of new cable-stayed bridge across Drava River as the most comprehensive project of the motorway A5 between Beli Manastir and Osijek was announced.

Tab. 1 Motorway network in service 2008 – 2010

Year	New motorways [km]	Upgrading to the full motorway profile [km]	Total network [km]
2008	41.50	36.90	1198.70
2009	42.00	20.32	1240.70
2010	0.00	28.00	1240.70
2011 (planned)	11.50	67.00	1252.20
Total	95.00	155.22	1252.20

According to the Strategy of Sustainable Development of the Republic of Croatia a high level of Croatian motorway network development has so far been achieved. In the current four-year period (2009 - 2012), all activities relating to construction and maintenance of motorways are limited by present-time financing possibilities which are, due to global financial crisis and recession, less favourable when compared to previous four-year periods.


Fig. 5 Twin Rječina Bridges (left) and the bridge across Drava River near Osijek (right)

5. UNDERGOING PROJECTS FOR SUSTAINABLE DEVELOPMENT OF ADRIATIC COAST AND ISLANDS

Croatia is a country with more than a thousand islands. Connection with the mainland is of the greatest importance for the development of the Adriatic coast and islands. Therefore, many bridges have been built so far, and two undergoing projects will be present in this paper.

2.1. Pelješac Bridge

The bridge across the sea strait between Croatian mainland and the Pelješac peninsula is a major new investment in the region. The southern part of Croatia, including the city of Dubrovnik, is currently separated from the rest of Croatia by a small coastal stretch belonging to the state of Bosnia and Herzegovina. The idea of fixed road link to connect the whole of Croatia, without having to cross state borders twice has been investigated for more than a decade. The new bridge crossing the sea strait between the Croatian mainland and the Pelješac peninsula shall fulfil this purpose and also further the development of the Pelješac peninsula and adjacent islands. The total bridge length is 2.4 km, and it consists of 17 spans. The central bridge is a cable-stayed bridge with a main span of 568 m – the second longest cable-stayed span in Europe . The bridge superstructure is made of steel. The pylon below the road level is made of concrete, while the upper part is to be constructed in steel. The pylons are founded on open caissons with depth of 90 m below the sea level. Concrete piers are founded on tubular steel driven piles with the concrete pile cap at the sea level. There is a specific requirement on the construction of the bridge issued by the Croatian Ministry of environmental protection, physical planning and construction regarding the protection of Mali Ston bay shellfish culture. The construction of the bridge is currently in progress, although the speed of construction is limited by present-time financing possibilities.


Fig. 6 Pelješac Bridge: computer rendering (left) and construction site (right)

2.2. Mainland – Čiovo Island Bridge

The new Mainland – Čiovo Bridge in Trogir is planned to relieve traffic congestion on the existing movable bridge, which is close to the historic town centre. Historic centre of Trogir is under UNESCO protection, thus the terms of competition were very restrictive. The bridge was to be designed as almost invisible, with the alignment as low as possible and no structural members above the roadway. One span of the bridge was to be movable to allow the passage of sailing boats. The bridge is designed as continuous steel beam-type bridge, while columns are made of reinforced concrete. The bridge is 535 m long, consisting of 14 spans. The largest span is 43.3 m long and includes a bascule bridge. Designers chose the bridge which is simple, with as few structural members as possible, has a slender superstructure, with structural members of continuous contours which at the same time reflect the force flow.


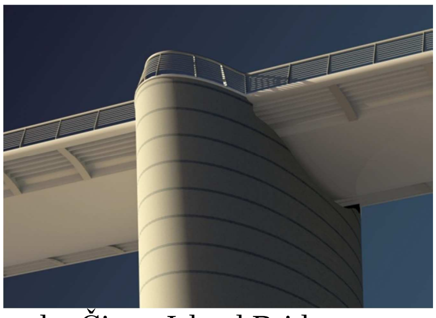

Fig. 7 Computer rendering of the Mainland – Čiovo Island Bridge

6. CONCLUSION

Sustainable development requires a holistic approach to secure environmental protection, economic development and high quality of life. This paper highlights several undergoing projects at the design or construction level or recently completed in Croatia. Investments in infrastructure, buildings and other engineering structures need to be carefully balanced with the requirements to protect natural and man-made environment, in the sense of both environmental or aesthetic degradation.

Structures described within this paper still largely resort to concrete as the predominant construction material, although there are many examples of various combinations of concrete and steel providing for efficient and exceptional structures. We do not consider this as a shortcoming, but an added value to concrete structures which enabled bridging of larger distances and rising to greater heights.

6. REFERENCES

HUKA-the Croatian Association of Toll Motorways Concessionaires (2011) „National Report 2010", Zagreb

Radić, J., Kušter, M., Kincl, B. (2010) „Structural – Architectural Approach to Bridge Design"˝, Proceedings of 34th International Symposium on Bridge and Structural Engineering „Large Structures and Infrastructures for Environmentally Constrained and Urbanised Areas" , Venice, Italy, pp. 422-429.

Radić, J., Šavor, Z., Hrelja, G., (2008) „Preliminary design of Mainland – Čiovo Bridge in Trogir", Proceedings of Int. Conf. & EurekaBuild Event Networks for sustainable environment and high quality of life, SECON, Zagreb, pp. 265-272.

Radić, J., Šavor, Z., Hrelja, G., Mujkanović, N., Vlašić, A., Franetović, M., (2008) „Design of Pelješac Bridge", Proceedings of Int. Conf. & EurekaBuild Event Networks for sustainable environment and high quality of life, SECON, Zagreb, pp. 31-38.

Šavor, Z., Gukov, I., Bleiziffer, J. & Hrelja, G., (2007): "Twin bridges across Rječina river canyon", Proceedings fib Symposium Dubrovnik 2007 "Concrete Structures – Stimulators of Development, SECON, Zagreb, pp. 83-92.

CONSTRUCTION OF THE TROJA BRIDGE IN PRAGUE

Jan L. Vítek[1], Ladislav Šašek[2],Petr Nehasil[2], Robert Brož[1], Alexandr Tvrz[1]
[1] *Metrostav a.s.*
Koželužská 2246, 180 00 Praha 8, CZ
[2] *Mott MacDonald Praha, s.r.o.*
Národní 15, 110 00 Praha 1, CZ

SUMMARY

The new Troja Bridge in Prague, which is now under construction, has a main span of 200,4 m long. The steel network arch with the bridge deck made of prestressed concrete represents an advanced bridge structure. The construction combines several technologies, including incremental launching and assembly of the arch from the bridge deck supported on temporary piers in the river.

1. INTRODUCTION

The new Troja Bridge is a part of the road system which is built within the Blanka Tunnel Complex. It carries 4 lanes of road, 2 tram tracks, which connect the city centre to the northern parts of the city, and also two wide pedestrian lanes used also by cyclists. The bridge crosses the Vltava River. The bridge has two spans; the main span crossing the river is 200.4 m long and the side span on the Troja riverside, which is 40.4 m long. The bridge is about 35 m wide. There are no supports located in the river.

In 2006, the architectural competition was organized by the client (City of Prague) and the winning project submitted by J. Petrak and L. Šašek (Mott MacDonald Prague) and by R. Koucky and L. Kabrt (R. Koucky arch. office, Prague) is under construction. The bridge should be open to traffic in June 2013.

2. DESCRIPTION OF THE BRIDGE

The main span and the side span are almost independent structures; there is an expansion joint over the pier no.2 between them. The basic theme of the elegance of the bridge lies in the ratio of the rise and span of the arch of 1/10. The slender network arch structure of the main span is a tied arch (rise of the arch is only 20 m) with inclined hangers (Fig.1 and 2). The arch is made of steel – the central part is formed by a multiple box section (Fig.3), which is then divided into two legs on each side approaching the bridge deck at the ends of the span. The tie of the arch is located above the bridge deck and has a composite steel concrete cross-section. The longitudinal tensile force is carried mainly by 6 prestressing cables located inside the tie section. Each cable is composed of 37 strands 0.6” (15.7 mm). The bridge deck is completely made of prestressed concrete. The deck has transverse precast prestressed beams (C70/85) (Fig.4), which are suspended on the composite tie and which support a thin prestressed concrete slab (C50/60). The concrete deck carries the tram tracks and the road lanes, the pedestrian lanes are located on steel cantilevers.

The side span is completely made of cast in situ concrete (C50/60). The two longitudinal beams form the main load carrying element. The transversal beams have the same shape as those in the main span. The slab on the top is also very similar to that in the main span. The complete structure is prestressed longitudinally and transversely.

Fig. 1 Visualization of the complete bridge

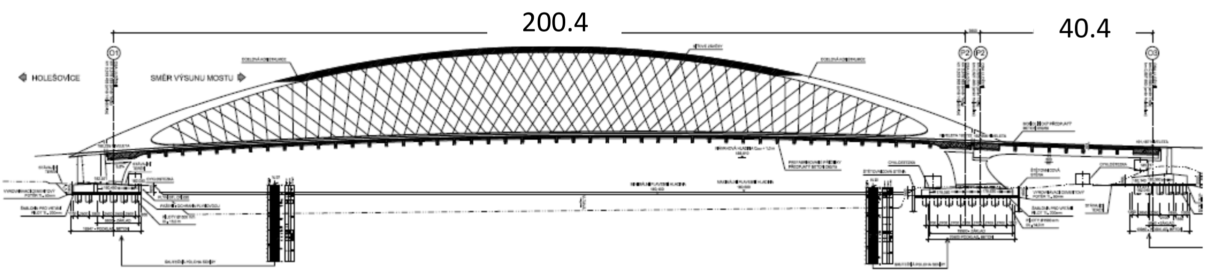

Fig. 2 Longitudinal section

3. CONSTRUCTION OF THE BRIDGE

The construction process of the main span was an object of many discussions. Initially the design assumed the process when first the arch with the tie and hangers would be built and then the bridge deck would be subsequently assembled and cast above the river. Due to the slenderness of the arch and very soft steel structure, the contractor saw many risks in such construction process. Also the economical evaluation was not favourable. Considering many alternatives, finally it was decided to build the deck first and then to assemble a steel arch using the deck as a fixed platform. A limited space on both sides of the river resulted in the following construction process.

The steel tie and the precast beams are assembled on the Holesovice riverside at the production yard. Since the bridge has no stiff longitudinal element, a temporary steel truss is used in order to work as a couple of stiff longitudinal beams. Top chord of the truss is definitive – the tie of the arch. The bottom chord and the diagonals are temporary and they will be removed after completion of the bridge. The 5 temporary piers were built in the river. The temporary truss with the precast transversal beams is assembled in the production yard

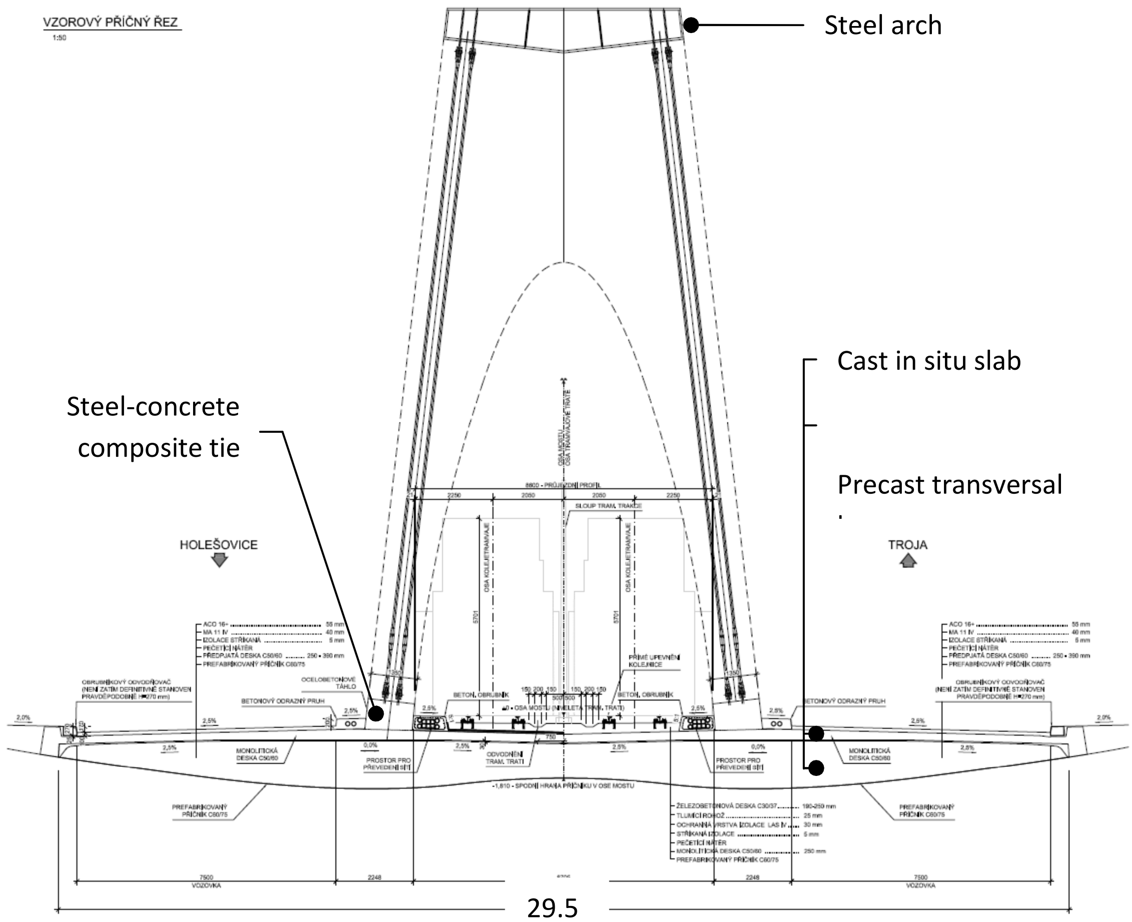

Fig. 3 Cross-section of the main span (without steel cantilevers)

Fig. 4 Precast transversal beams stored on the site prior to assembly

and then incrementally launched across the river in steps 16 m long using the temporary supports (Fig. 5). A short launching nose was used in front of the temporary steel truss. The hydraulic system with 8 cylinders with the capacity of 60 t each was used for moving the structures forwards. The stroke of cylinders was 250 mm. The structure was suspended on 8 steel bars. A special independent braking device was used when the steel bars where moved to the next position between individual launching stages. The structure was launched initially upwards to the slope of almost 7%, finally downwards due to the geometry of the bridge. The maximum capacity of 8 cylinders was used only for a short time. In the most of the launching process only 4 cylinders were able to push the structure. Very simple sliding bearings, where the bottom steel flange of the temporary truss moved directly on the teflon plates, were designed. No stainless steel sheets and inserted teflon plates were necessary. The friction coefficient varied between 2 and 4%.

After launching, the end elements (footings) of the arch will be connected to the tie and the end transversal beams will be cast in situ. The ends of the steel arch will be embedded into the end transversal beams. Their steel structure is extremely complex. The anchorage of 6 prestressing cables (each composed of 37 strands) represents a large force which has to be transferred to the steel arch. A number of stiffeners in the steel structure of the arch footing would be too high. Therefore the footing will be filled with high strength self-compacting concrete (C80/95). The self-compacting concrete will be pumped into the steel structure in several layers approximately 2 m thick. The concrete will distribute the forces from the anchorage into the entire steel section. The welded studs and steel reinforcement are used for connection of steel and concrete.

A complete deck slab will be subsequently cast from the ends to the centre of the main span in the sections again 16 m long. The formwork will be transported on ships, lifted and finally anchored to the transversal precast beams. The transversal prestressing will be activated immediately when the appropriate strength of concrete is achieved. When the slab is completed, approximately 1/3 of the longitudinal prestressing force will be activated. The slab supported on the temporary truss and on the 5 temporary supports in the river will form a platform with sufficient load carrying capacity for the assembly of the arch.

The steel parts of the arch will be delivered to the bridge deck and welded together into 3 parts of the arch. The temporary towers will be built on the deck. The three parts will be then lifted to the position and welded together in order to complete the arch (Fig.6). All the manipulations with steel elements on the arch will be carried out using hydraulic systems without any heavy crane. The hangers then may be installed and slightly prestressed to the stress level about 10% of their strength in order to avoid their excessive deflection. Very small deformations of the arch are expected in this stage which allows for a relatively precise specification of forces in hangers. All these activities will be executed in stable temperature conditions, preferably during the night. An extensive monitoring system will be used for detailed check of forces in individual hangers.

Then it will be possible to activate the second level of the prestressing in the longitudinal direction, interrupt the bottom chord of the temporary truss and release the supports in the river. The bridge will deform and all the hangers become activated simultaneously. After that it will be possible to remove the temporary truss, finalize the prestressing (level 3) in the longitudinal direction and complete the works on the bridge (pavements, lighting, tram rails, etc.).

The side span will be cast in situ on the fixed scaffolding and then prestressed. The side span will be cast in three stages after the completion of the launching process and will be used for delivery of steel parts of the arch to the main span.

Fig. 5 Incremental launching of the steel truss and precast transversal beams

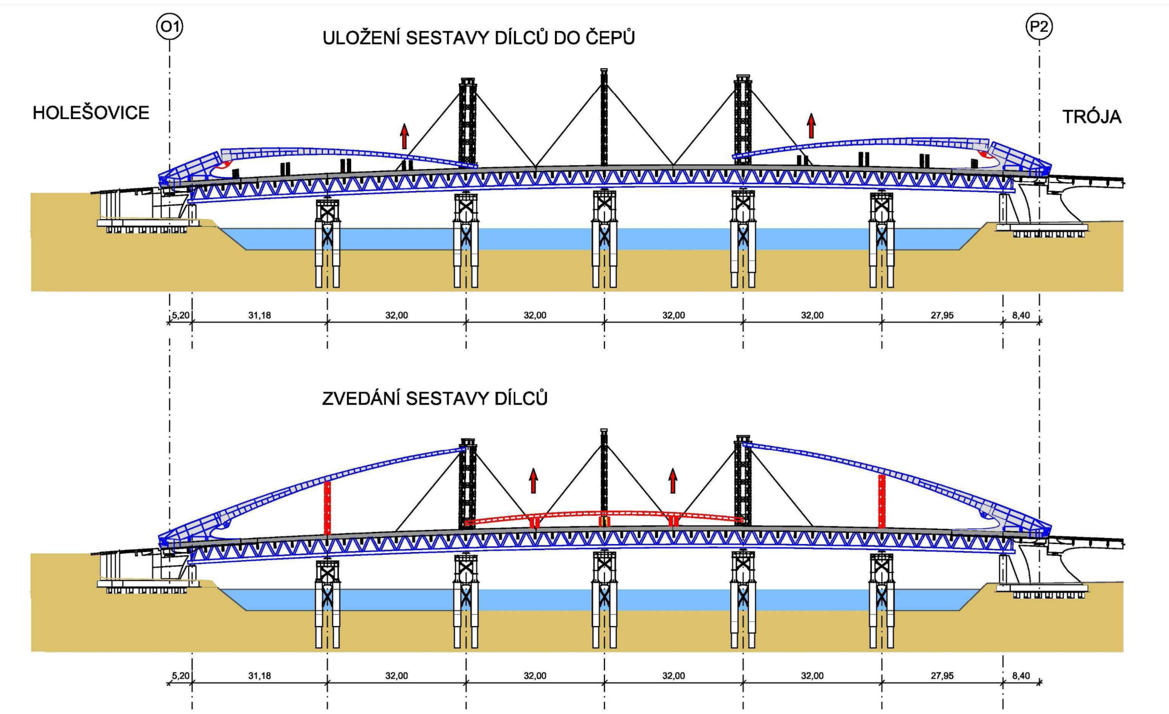

Fig. 6 Assembly of the arch

4. CONCLUSIONS

The structure of the new Troja bridge is rather complex. On the other hand the bridge is elegant and fits well into the environment of the recreation area of the city, which will be further developed and in some years it becomes a central area. The city representatives decided to build this bridge because the arrangement and shaping of the bridge, with a span of 200.4 m, form an internationally unique structure. Taking into account the tradition of architectural development of the historical city of Prague it is certainly the right decision.

Now (June 2011) the launching process has been completed. The steel elements of the arch are produced in two factories – in Metrostav and in MCE. The short construction time requires excellent organisation of all activities on the site and in factories. The structural performance is monitored using many strain and temperature gauges installed on the main parts of the structure. Additionally the detailed surveying provides information on deformations and movements of the structure. Execution of complex details is verified on models or trial structures in the scale 1:1. The executing team believes that it is able to finalize this sophisticated project on time and in adequate quality.

5. MAIN PARTICIPANTS OF THE CONSTRUCTION

Client:	City of Prague
Client represented by:	IDS – Engineering of transport structures.
General consulting office:	Mott MacDonald Prague, R.Koucky, arch. office
Consulting office – steel structure:	Excon, j.s.c.
Supervision and construction process analysis:	Novak and Partner, Ltd.
Contractor:	Metrostav j.s.c.
Steel production:	Metrostav j.s.c., MCE Czech branch in Slany
Concrete production:	TBG Metrostav, Ltd.
Other partners:	VSL-CZ, Ltd., SMP CZ, j.s.c., SM7, Ltd. MTEK, Ltd., CCE, Ltd. PONTEX, Ltd.

6. ACKNOWLEDGEMENT

Some results of the research carried out under the support of the Ministry of education, youth and sports of the Czech Republic (Research centre CIDEAS – Project no.1M0579) were used during the construction. This support is gratefully acknowledged.

MONITORING OF LONGITUDINAL DEFLECTIONS OF RAILWAY BRIDGES

Markus Vill[1], *Michael Reiterer*[2]
[1] *Austrian Federal Railways (ÖBB-Infrastruktur AG)*
Praterstern 3, 1020 Vienna
[2] *RED Bernard GmbH, Research & Development*
Nordbahnstrasse 36/2.7, 1020 Vienna

SUMMARY

The presented paper considers two railway bridges where the longitudinal deflections of the bridges due to temperature loading have been monitored over a period of one year. The background for the one year monitoring was to identify the real seasonal variation of longitudinal deflections and to compare the measured values with results of the calculation according to Eurocode. The monitoring results show, that the measured longitudinal deflections of the bridges are much smaller than the calculated values and that big differences of the bridge deck temperature and the air temperature are present on-site. The results are an important basis for the further development of the Eurocodes and the design of bearings and dilatations.

1. INTRODUCTION

In the design process of bridges the temperature loading has to be chosen according to Eurocode 1. The bearings and dilatations of bridges have to be designed for the calculated temperature range. The Eurocode demands to apply a very large temperature range and in addition safety factors have to be taken into account. The result is that bearings of bridges become very large dimensions and hence expensive.

The objective of the performed measurements was to identify the real seasonal variation of longitudinal deflection of railway bridges. Therefore, a monitoring system was installed at two different construction types of railway bridges where the longitudinal deflections and the structural temperatures of the bridges have been monitored over a period of one year. The first bridge is the new bridge over the Salzach river in Salzburg, Austria. It is a 3 span steel-concrete composite bridge with a box girder cross section of steel and a concrete slab with a total length of 157.26 m. The second bridge is the FW26 Bridge at Koralmbahn in sytria in the southern part of austria. It is a conventional 5 span concrete T-Beam Bridge with a total length of 77 m.

2. MONITORING OF SALZACHBRIDGE

The Salzachbridge in the city of Salzburg consist of three single-track steel-concrete composite structures. The bridges have three spans and span lengths of 50.63 m, 56 m and 50.63m, i.e the total bridge length is 157.26 m. The cross section of the Salzachbridge is a steel-box girder with a concrete composite plate, see Fig. 1. The box girder has a rounded edge on the bottom side of the cross section. The three bridges are not connected to each other in longitudinal direction, i.e there is an expansion joint between the bridge structures of rail 1 and 2. The two piers of the Salzachbridges are placed in the river Salzach. The fixed bearings of the bridges are located at the abutment. All other bearings at the piers and at the abutment Freilassing are free moveable in longitudinal direction.

Fig. 1 Picture of all 3 structures of the Salzachbridge, bridge 1 to be monitored in the front

Fig. 2 shows the front view and cross section of the Salzachbridges. The installed displacement sensors W1, W2 and W3 are located at the abutment and bridge pier Freilassing, respectively. The temperature sensors T1 – T5 are installed in the centre of the midspan. The sensors T1 – T4 are installed at the surface of the steel girder and they measure the steel temperature. The sensor T5 measures the air temperature inside the box girder. In order to get information of the seasonal air temperature a temperature sensor T6 was placed outside of the girder close to the bridge.

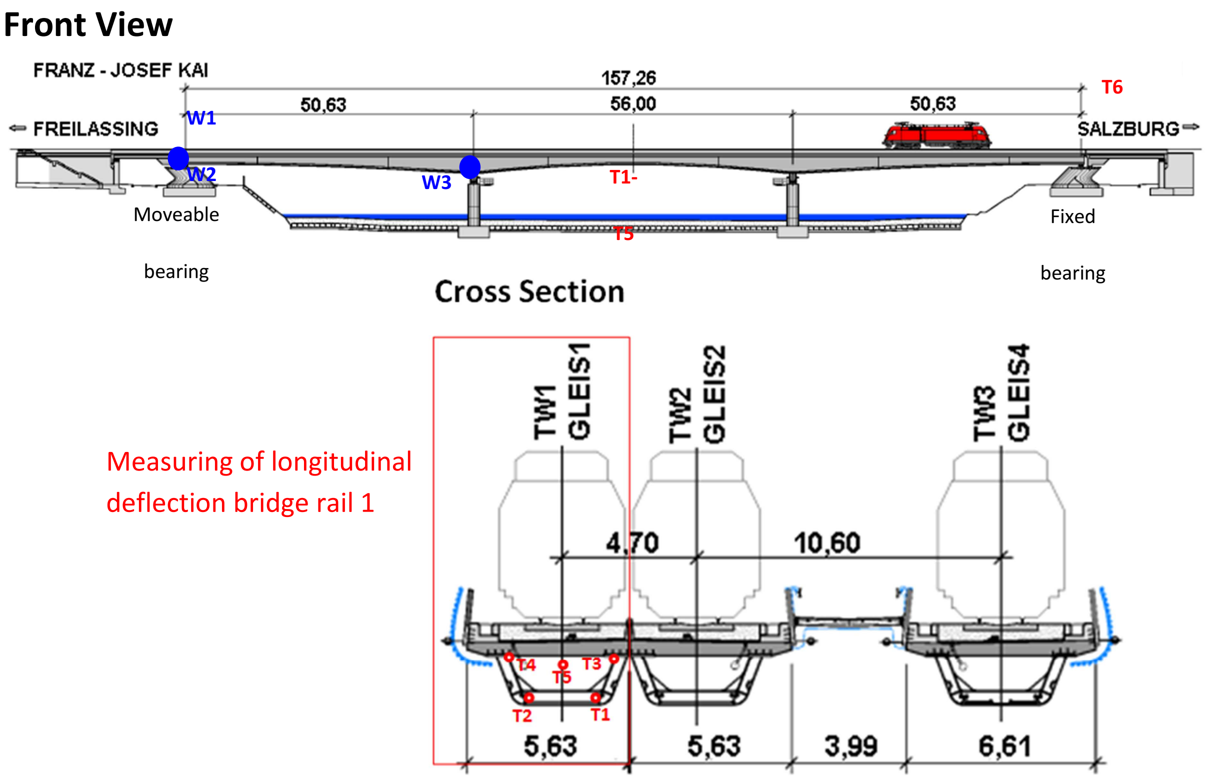

Fig. 2 Front view and cross section of Salzachbridge with installed sensors

The Fig. 3 shows the seasonal variation of longidutinal deflection and of steel and air temperature inside the box girder of the Salzachbridge.

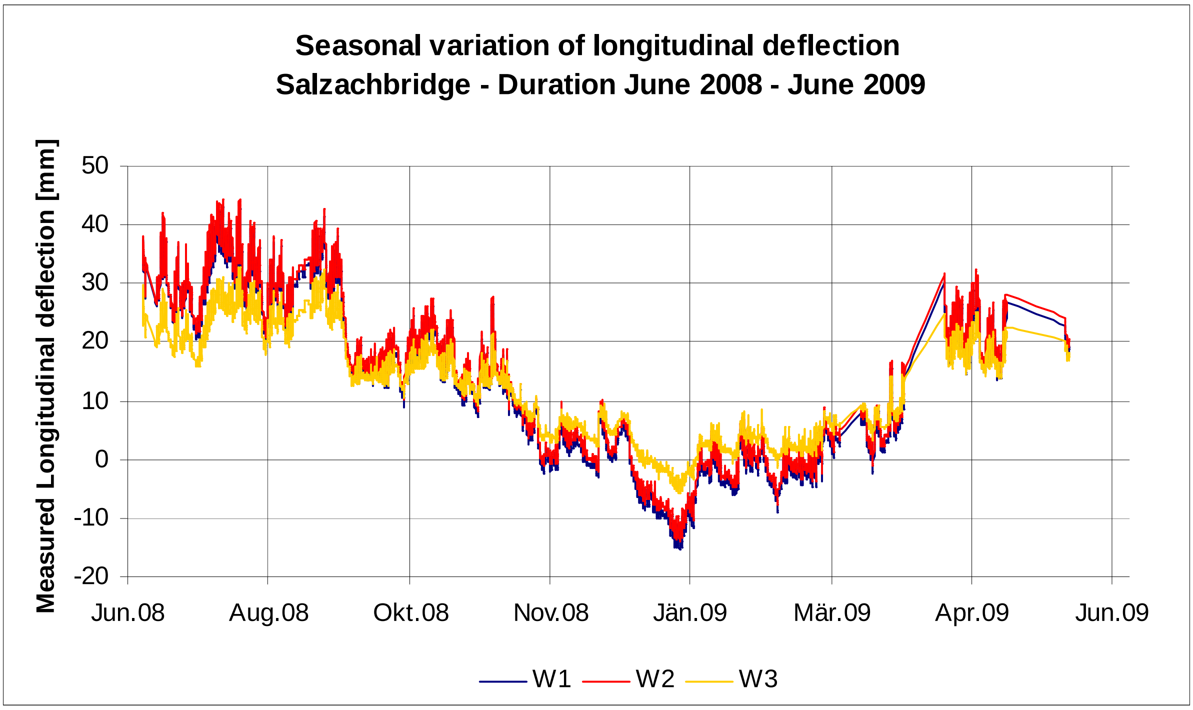

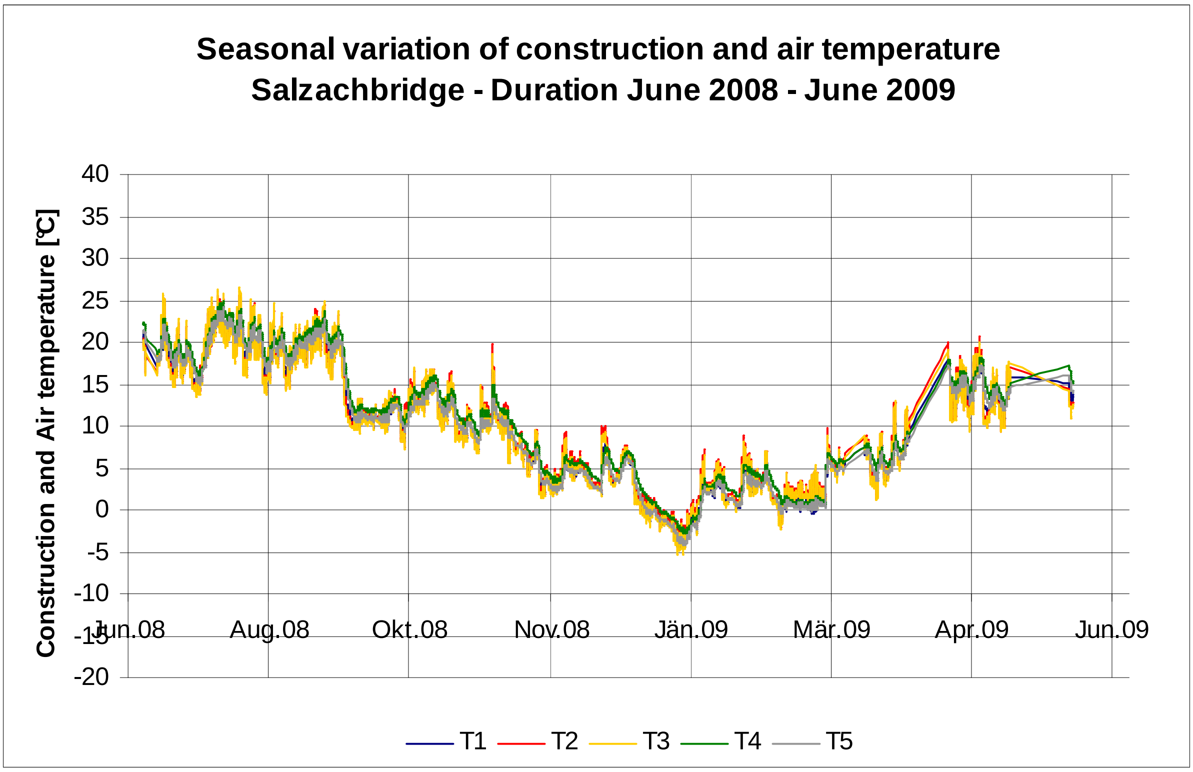

Fig. 3 Seasonal variation of longidutinal deflection and of steel and air temperature inside the box girder of the Salzachbridge

The result of the measurements show that seasonal longidutinal deflection of the bridge is from +43 mm to –12 mm which is a total deflection of 55 mm. The maximal temperature variation is from +25 to -5 °C which is a total seasonal temperature variation of 30°C.

In the design process of the Salzachbridge a maximal seasonal temperature variation of 84°C was chosen according to Eurocode EN 1991-1-5 and a safety factor of 1.5 was taken into account. Hence, the calculated total longitudinal deflection was $\Delta w_{,calc}$ = 84°C*1.5*1.0e-5*157260 mm = 198.15mm. The comparison of real measured and calculated deflections show that the calculated values are nearly 4 times higher.

Fig. 4 shows the seasonal variation of air temperature outside of the box girder with a maximum and minimum of 32 °C and -15 °C. The comparison with the temperature of the bridge structure show that the bridge responds very slowly to changes of the air temperature. A temperature difference of -7 °C and +9 °C was measured.

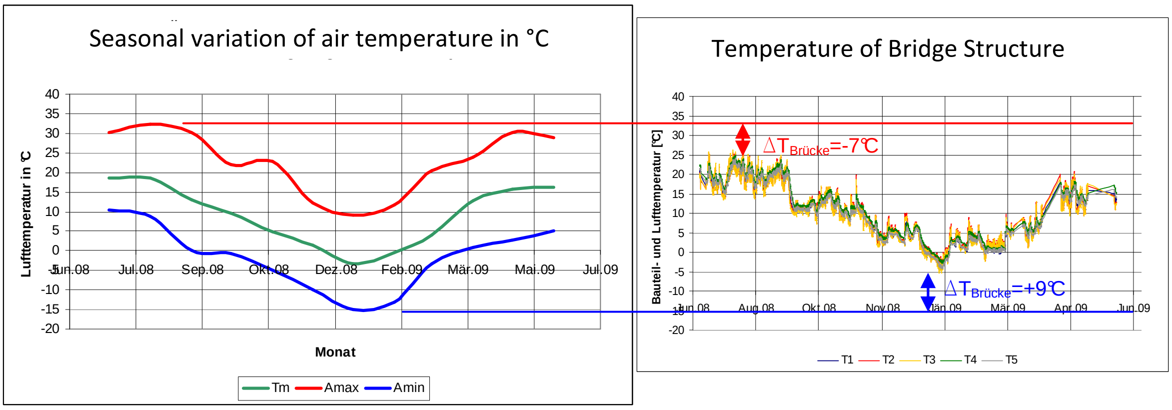

Fig. 4 Seasonal variation of air temperature close to the bridge and temperature of bridge structure

3. MONITORING OF FW26 BRIDGE AT KORALMBAHN

The railway bridge FW26 at Koralmbahn in sytria in the southern part of austria is a conventional 5 span concrete T-Beam Bridge with a total length of 74 m, see Fig. 5. It is a railway bridge with spans of 11.6m + 3x16.0m + 14.4m and two separate superstructures for each rail.

Fig. 5 Picture of FW26 bridge at Koralmbahn in Carinthia, Austria

Fig. 6 and Fig. 7 show the ground view and cross section of the FW26 bridge at Koralmbahn. The installed displacement sensors W1 and W2 are installed at the abutment Klagenfurt. The sensors BT1 – BT4 and BT6 are installed into the concrete structure also at the abutment Klagenfurt. The temperature sensor LT5 measures the air temperature.

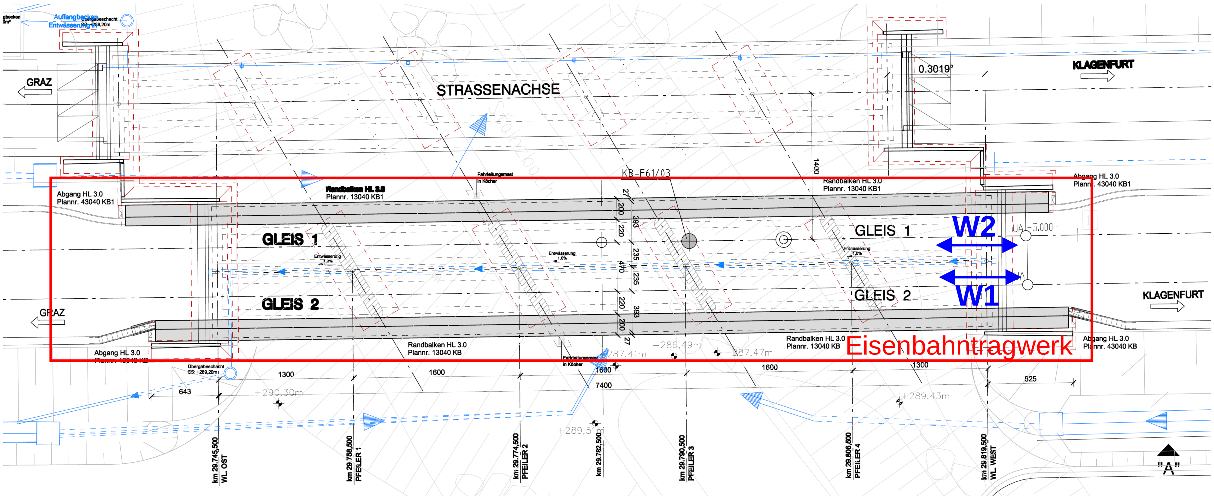

Fig. 6 Ground view of FW26 bridge at Koralmbahn with location of installed sensors

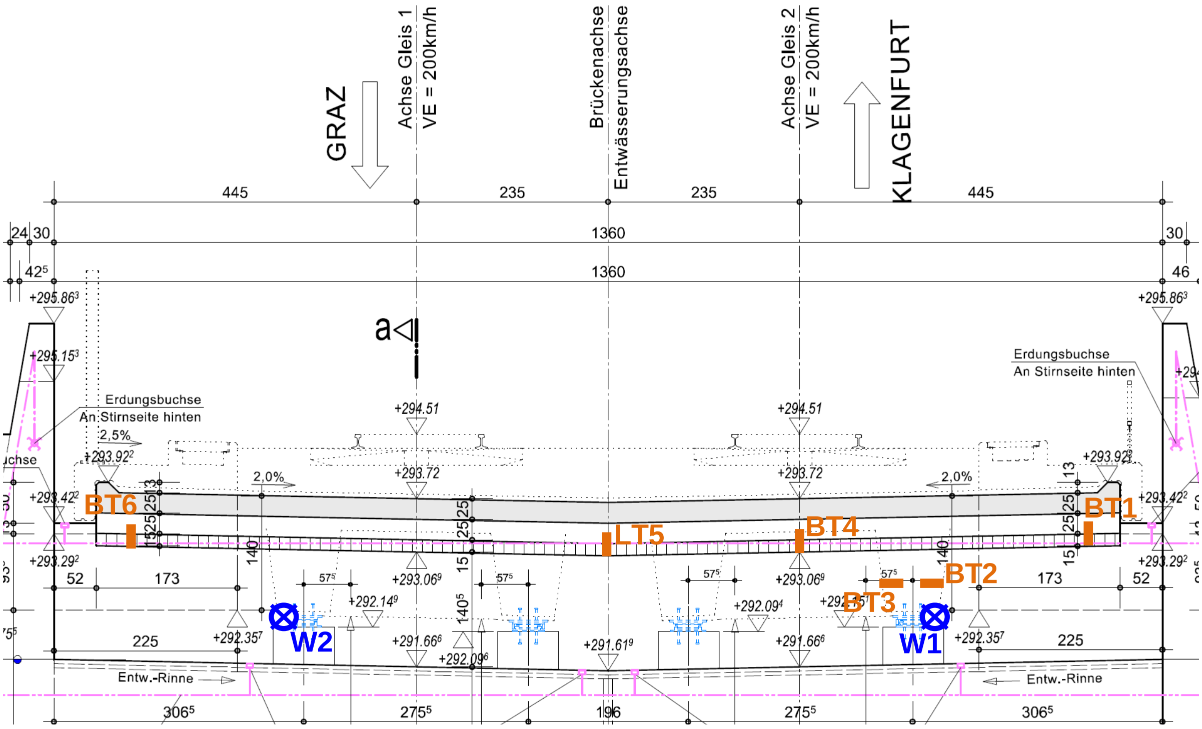

Fig. 7 Cross section of FW26 bridge at Koralmbahn with location of installed sensors

Fig. 8 shows the seasonal variation of longidutinal deflection and of concrete and air temperature of the FW26 bridge. The result of measurements show that seasonal longidutinal deflection of the bridge until now varies from -12 mm to +16 mm which is a total deflection of 28 mm. The maximal concrete temperature variation is from -7 to -25 °C, which is a total seasonal temperature variation of 32 °C until now.

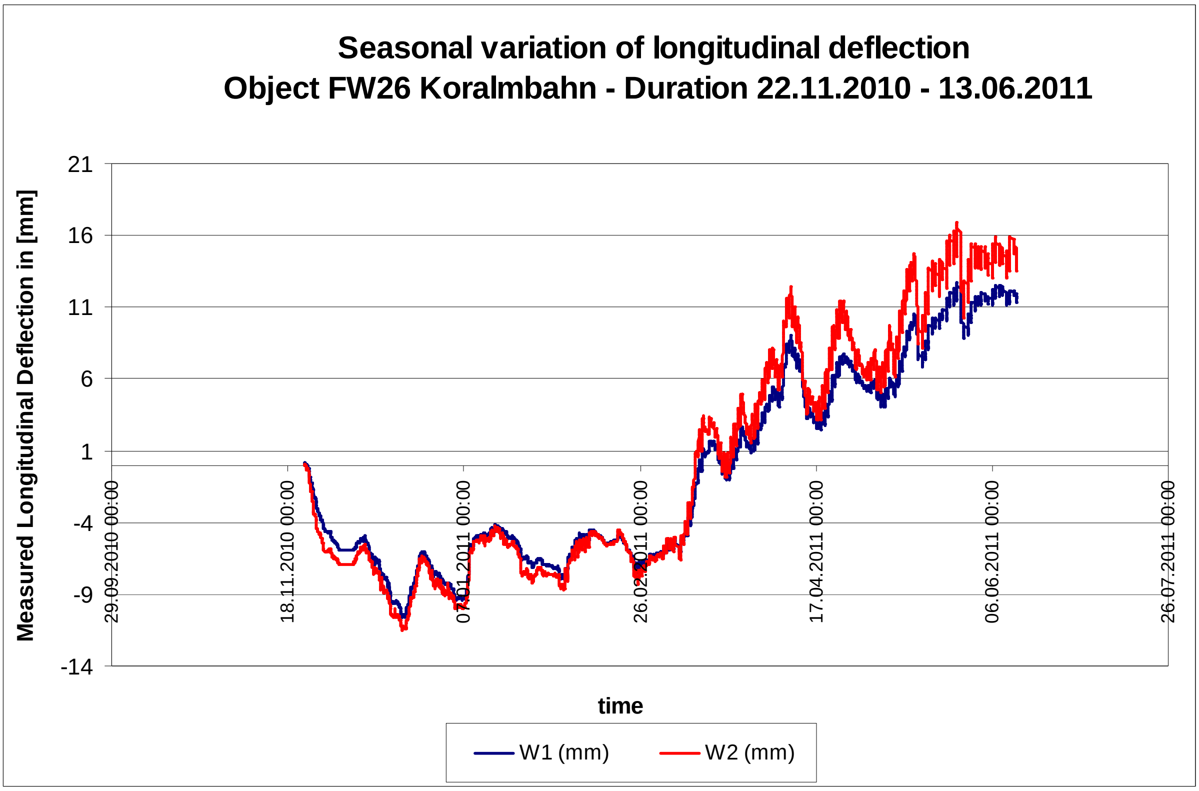

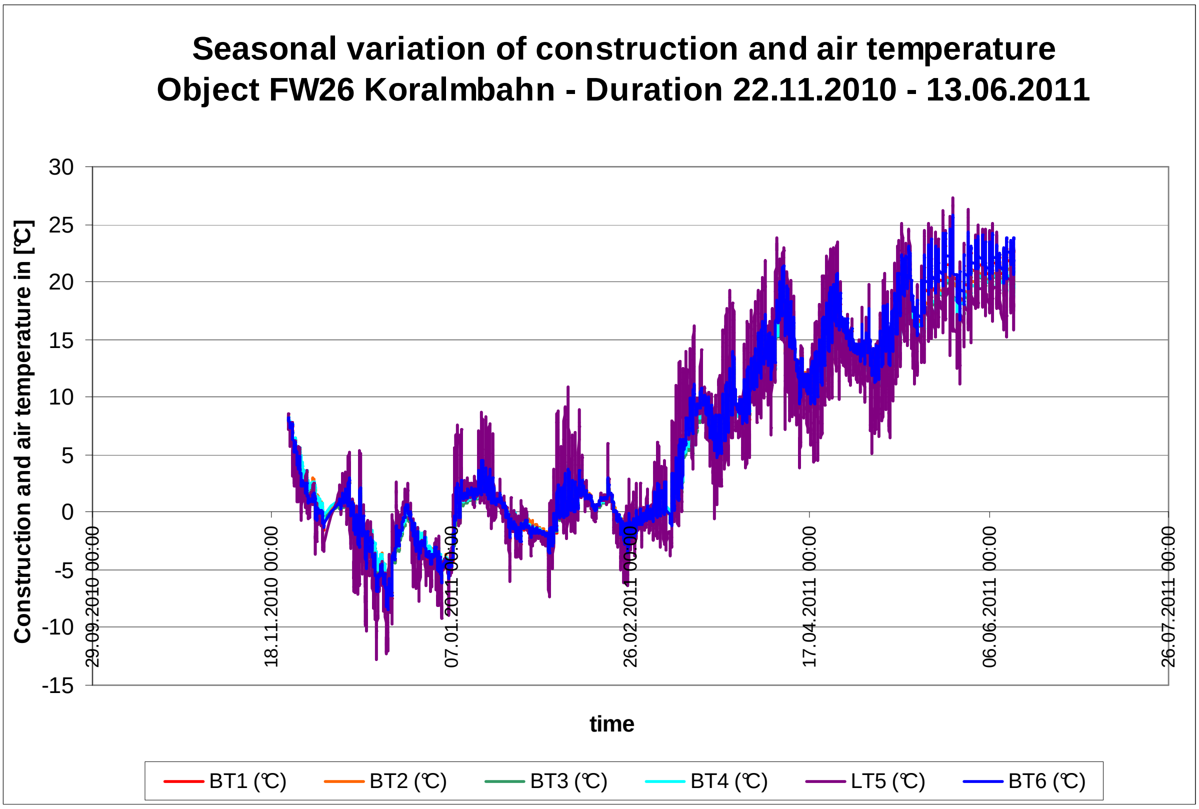

Fig. 8 Seasonal variation of longidutinal deflection and of concrete and air temperature of FW25 bridge at Koralmbahn

In the design process of the FW26 bridge a maximal seasonal temperature variation of 75 °C was chosen according to the previous Austrian Standard ÖNorm B4703 and no safety factor was taken into account. Hence, the calculated total longitudinal deflection was $\Delta w,_{calc}$ = 75 °C*1.0*1.2e-5*74000 mm = 66.6 mm. The comparison of real measured and calculated deflections show that the calculated values till now are nearly 3 times higher.
Fig. 8 shows also that the difference of air temperature to bridge temperature is up to 8 °C (+11 °C air temperature and +3 °C bridge temperature).

4. CONCLUSIONS

In order to identify the real longitudinal deflection of railway bridges altogether two bridges were attached with a permanent monitoring system and the deflection and temperatures were measured over a period of 1 year. The results of the measurements show that the measured longitudinal deflections of the railway bridges is much lower than the theoretical calculated values according to Eurocode and/or ÖNorm. The results show also that there is a big temperature difference between actual air temperature and bridge temperature, i.e. the bridges are reacting very slowly to changes of air temperature.
It can be summarized that the regulations according to Eurocode concerning the temperature loading is very conservative and follows a high safety comparing to the measured bridge temperature. Especially the safety factor which needs to be taken into account according to Eurocode is very high. Thus, huge bearing elements and expansion joints are resulting of the calculation which are expensive and complex for maintenance.

The measurements results are now an important basis for the further development and improvement of the Eurocodes and the design of bearings and dilatations.

5. ACKNOWLEDGEMENTS

The authors are grateful to financial support of the project by the Austrian Federal Railways (ÖBB Infrastruktur AG).

6. REFERENCES

EN 1991-1-5: 2003 Eurocode 1: Actions on structures: General Actions: Part 1.5: Thermal Actions
ÖNorm B4703: 01. März 1995. Eisenbahnbrücken aus Beton und Stahlbeton - Berechnung und konstruktive Durchbildung

TOPIC 1
TAILORED PROPERTIES OF CONCRETE

POTENCIALS IN USE OF X-RAY COMPUTER TOMOGRAPH (CT) TO STUDY CONCRETE PROPERTIES

Éva Lublóy[1], Támás Földes[2], György L. Balázs[1]
[1] *Department of Construction Materials and Engineering Geology*
Budapest University of Technology and Economics
1111 Budapest Műegyetemrakpart 1-3
[2] *Diagnostic Institute of University of Kaposvár*
7400 Kaposvár Guba Sándor u. 40

SUMMARY

The pore structure of cement-based materials is of primary importance for understanding and modelling the transport phenomena that influences the durability. Several methods have been developed to observe and quantify aggregate size and distribution, crack size and distribution as well as pore structure of concrete. In this study we would like demonstrate the potentials of Computer Tomography (CT) to study the three dimensional (3D) microstructure of concrete.

1. INTRODUCTION

As a new, non-destructive analysis method, the Computer Tomography (CT) technique originally was used for medical analysis. During the time of data processing the quality of the picture depends on many factors. The displayed image is calculated from electrical signals by the imager, so it is not a real picture like a traditional photograph or a radiogram. The theoretical foundation was made by Hounsfield and Cormack in '70s .

X ray is weakening as it goes through different materials and textures. The degree of absorption is smaller or higher in materials of different densities therefore it depends on the attributes of the measured materials. The capability of X ray absorption can be characterized by the coefficient of X ray absorption. If the transfer of energy is constant, the absorption of X ray depends only on the material through which it goes. This degraded radiation reaching the detectors generates electrical signals dependent on the intensity of radiation .

As the system of tube detector turns around the analysed object during the time of data collection hundreds or thousands of measurements are made by the CT while the incoming data is organized into a matrix. At the end of the process the imager calculates each element of the matrix and assigns a scale to the points of the matrix whose points are actually the coefficients of X ray absorption. This scale is the so called Hounsfield scale, its unit is the Houndsfield unit. (Nobel Prize was awarded jointly to Alan M. Cormack and Sir Godfrey N. Hounsfield for the development of computer assisted tomography in 1979.) Assigning the different values of the matrix to the appropriate values of the Hounsfield scale the image can be displayed. We can visualize the image using predefined colour tables or our own colour ones .

The Hounsfied scale is a calibrated one where the value of air is -1024 HU, and the value of water is 0 HU .

The experiments were made with Simens Sensation CT with multislice technique. The resolution of a matrix depends on several factors. Using the best resolution of our CT the smallest size of a cell of a slice can be 0.1 mm x 0.1 mm x 0.8 mm in reality. The duration of time of the measurement can be set within the range of 0.1 to 1 second for one slice .

2. CT FOR NATURAL ROCK

Several techniques and evaluations were developed in Diagnostic Institute of Kaposvár University for petrophysical, lithological and structural characterisation of different rocks based on CT measurement. With the help of CT measurements rock samples can be measured in their original state without any destruction. The CT measurement also makes it possible to study dynamic systems which can vary in time and to determine the various parameters of these systems *(Bogner et al 2003, Földes et al 2004, 2011).*

The Hounsfield values of the different minerals were determined and it was found that there was a strong – but not perfect linear relationship between the Hounsfield unit of the minerals and their densities. Taking the above mentioned fact into consideration the image, derived from the data matrix of the CT measurement, can be handled as a density map of the specified slice of the rock sample. After displaying this density map, the main features of the sample, such as granularity, joint, fractures, sedimentological features, changes in lithology, can be clearly seen. Displaying the images of the slices one after the other the inner characteristics of the rock samples (core samples) come to light. The Hounsfield values of the cells are influenced by two factors. The first factor is the Hounsfield value of the mineral grains of the specified cell, while the other factor is the Hounsfield value of the pore space filled with liquid and/or gas (air) .

If a rock sample is properly prepared, drained, vacuumed out, then saturated with liquid, its effective porosity can be determined by the CT measurement since the effective pore space of the cells (which can be filled up with liquid or gas) can be specified that is the effective porosity of each cell can be quantified. With the help of the CT not only the final stage of the saturation but also the behavior and state of the saturation of each cell can be investigated at regular time intervals. Since the saturation of the cells can be measured in time the complexity of the interior structure of the cells can become known. The saturation of the rock samples with liquid may result in flushing out of the dry material content such as drilling mud, left over in the samples. This process can be also investigated by means of CT measurements. If the value of the effective porosity of a cell has become known (calculated) then the Hounsfield value of the mineral grain or grains of the cell can be also calculated. On the basis of the above fact the mineral composition can be determined in a case of a coarse grained rock in which the grain size exceeds the resolution, and can be estimated in a case of a fine grained sample in which the grain size is smaller than the applied resolution.

Further investigations can be made using different liquids, acids or gels. With the help of the repetition of measurements at the same position a conclusion can be drawn on the mineral composition and the petrophysical properties of the rock samples and on the interaction between the various acids or other types of liquid and the rock samples.

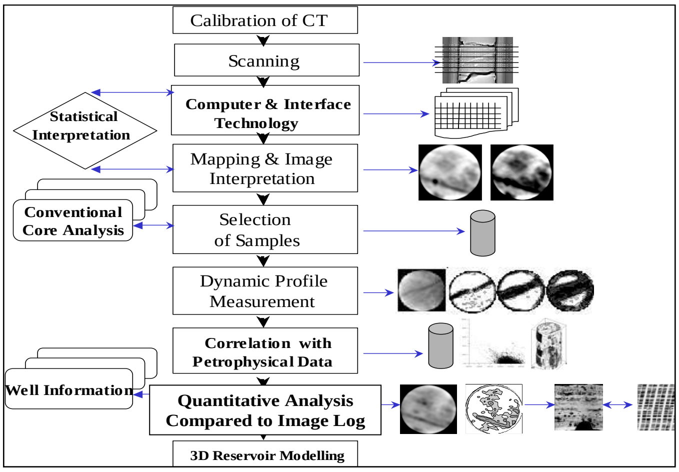

Fig. 1 Integrated processing based on CT measurement interpretation *(Földes, 2004)*.

3. CT FOR CONCRETE

Computer Tomography (CT) seems to able to demonstrate density differences in concrete sections. Further analysis of several subsequent sections may lead to 3D visualisation. In order to carry out CT measurements concrete specimens need special preparation (1) preparated concrete sections are measured (2) concrete specimens are vacuum cleaned (3) concrete specimens are by water (4) saturated concrete sample are scanned (5) effective pore structure is analysed (6) pore structure can be used to study e.g. freeze-thaw and fire resistance.

Test variables were *for concrete specimens*: silica fume content (0, 3, 9 m_c%) and maximum temperature (-20, 20, 50, 150, 300, 500 and 1000°C).

Concrete compositions:
Mix1: cement 400 kg/m^3, water 140 kg/m^3, aggregate 1888 kg/m^3, plastificator 6 kg/m^3;
Mix2: cement 400 kg/m^3, silica fume 12 kg/m^3, water 140 kg/m^3, aggregate 1871 kg/m^3, plastificator 7.2 kg/m^3;
Mix3: cement 400 kg/m^3, silica fume 36 kg/m^3, water 140 kg/m^3, aggregate 1840 kg/m^3, plastificator 8 kg/m^3

Studied characteristics were: porosity, effective porosity surface cracking, spalling, reduction of compressive strength. The porosity and the effective porosity were measured in the laboratory with experiments and by computer tomography. Test result are demonstrated in Tab. 1.

Tab. 2 Measured porosity values

	Total porosity [%]	Total porosity measured by CT [%]	Effective porosity [%]	Effective porosity measured by CT [%]
Mix1	9.23	7.373	8.00	8.41
Mix2	11.67	9.07	9.49	6.89
Mix3	9.62	7.30	8.29	8.92
Mix4	10.38	6.72 (unsaturated)	8.59	4.90 (unsaturated)

Our observations:

- The ratio of effective and total porosity (1.15) of Mix1 was the smallest. Mix1 was the unfavourable in case of fire (the specimens spalled) and freeze-thaw resistances.

- The ratio of effective and total porosity of Mix 2 was the biggest (1.23). Mix 2 was the favourable in case freeze-thaw resistances.
- The best fire resistance was observed by Mix 3, that could be explain with the high strength of this composition.
- The porosity and effective porosity values have influences on the fire and freeze-thaw resistances. Informations on distribution of pores is also necessary (Fig.2).

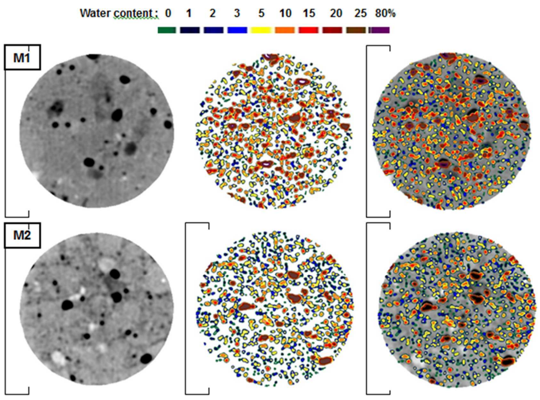

Fig. 2 Saturations map of concrete segments

4. CONCLUSIONS

The pore structure of cement-based materials is of primary importance for understanding and modelling the transport phenomena that influence the durability.

Computer Tomography (CT) seems to able to demonstrate density differences in concrete sections.

Preliminary tests were carried out on four different concrete mixes in order to determine porosity and effective porosity. These measurements may help to judge the durability of concrete.

5. ACKNOWLEDGEMENTS

The authors are grateful to the Diagnostic Institute of University of Kaposvár for the use of their CT equipment.

6. REFERENCES

Bogner, P., Földes, T., Závoda, F., Repa I., (2003) „Application of CT and MR in the carbon hydrogen research“, Radiology 2003. pp. 231-237

Földes, T., Kiss, B., Árgyelán, G., Bogner, P., Repa, I., Hips, K. (2004.) ”Application of medical computer tomograph measurements in 3D reservoir characterization” Acta Geologica Hungarica, Vol.47/1, pp. 63-73

Elliott, J. C., Dover, S. D. (1982), „X-ray microtomography”. Journal of Microscopy-Oxford Vol.: 126 (May) pp. 211-213.

EN 206-1: 2002 Concrete-Part1: Specification, performance, production and conforming, European Standard

Földes, T. (2011), „Integrated processing based on CT measurement” News in Geometry 2011 vol1, pp. 23-41.

INNOVATION IN AGGREGATES FOR CONCRETE; MANUFACTURED SAND, LIGHTWEIGHT AGGREGATE, ALKALI-SILICA REACTION

Tor Arne Martius-Hammer[1], Bård Pedersen[2], Rolands Cepuritis[3], Markus Bernhardt[3], Hilde Tellesbø[4], Jan Lindgård[1]

[1] *SINTEF Building and Infrastructure, COIN, N-7465 Trondheim*
[2] *The Public Norwegian Road Administration, Postboks 8142 Dep, 0033 Oslo*
[3] *The Norwegian Institute of Science and Technology (NTNU), Dep. of structural Engineering, N-7491 Trondheim*
[4] *Weber Saint Gobain, Postboks 216 Alnabru, 0614 Oslo*

SUMMARY
The wish to avoid waste material from a quarry for manufactured sand production, has created a challenge because of the negative influence of the fines on workability. The present work suggests methods to modify the fines to meet the challenge. Extensive progress has been made in order to develop a consensus method for performance based testing of ASR, allowing utilization of many local potentially alkali-silica reactive aggregates, enhanced flexibility for the concrete producer with respect to material selection and optimization of the concrete mix design. The idea to further develop the expanded clay LWA to get a strong but thin outer shell and a light but strong internal structure has been explored, and the present work show that a considerbale strength improvemnt can be reached without compromising the density.

1. INTRODUCTION

Continious stricter environmental requirements is one driving force for innovation in concrete construction with all its elements. This is also true for the aggregates. As natural aggregate resources near urban areas terminate, the availability diminishes and the transport distances increase. Also, the search more tailor made concretes enforce research on the aggregates. In line with this, COIN - the COncrete INnovation Centre in Norway (www.coinweb.no) focuses on three areas within aggregate research: 1. High Quality Manufactured Sand for Concrete. The objective to develop manufactured sand to give concrete properties equal to or better than concrete with natural sand. 2. Development of superlightweight high strength aggregates, LWA. The idea is to further develop the expanded clay LWA to get a strong but thin outer shell and a light but strong internal structure. 3. Performance based testing of alkali-aggregate reactivity of aggregates, AAR. The objective is to develop a reliable and performance based test method for assessment of the alkali reactivity of aggregates, knowing that the existing methods may be too conservative and thus may erroneously exclude aggregate sources.

2. HIGH QUALITY MANUFACTURED SAND FOR CONCRETE

As described in a State-of-the-art (*Wigum et al, 2009*), there is an increasing miss balance between the need for aggregates in the society and the available geological sources traditionally used for concrete. Some of the glaciofluvial deposits in Norway best suited for concrete purposes have an expected lifetime of less than 10 years. Transportation distances from the good resources to the urban areas increases and consequently also the environmental impact. The need to develop technology for 100 % use of manufactured aggregate in concrete is then obvious, and is the main objective of the Manufactured Sand project in COIN.

Naturally weathered sand differs from most fine crushed aggregates (manufactured sand) by grading, particle shape and surface texture. The differences are more expressed if the crushed fine aggregate is a by-product (also known as "waste sand" or leftover rocks from quarrying) of coarse aggregate production and no special processing techniques are utilized to improve the characteristics. Typically crushed fine aggregate would incorporate a lot more fines, different particle size distribution (than natural sand) and be more angular with rougher surface. Due to these differences concrete with crushed aggregate often displays higher water demand and lower workability that the corresponding concrete with glaciofluvial aggregate (*Ahn, 2000, Quiroga, 2003, Westerholm, 2006, Kim et. al., 2008*).

Two different approaches can be used to enable the transfer from natural to crushed aggregate possible. 1) The first is trying to copy "mother nature" by putting extreme effort into shaping of aggregates and design of grading curves. This may be expensive and would also make it very difficult to achieve mass balance of the quarries. 2) The other way, which in most cases is more realistic, is to learn how to use materials with different properties. This would mean finding an approach on how to effectively improve the aggregate properties to make them "good enough" for different applications. The key to such an approach is more innovative concrete mix design and increased knowledge on the interactions of fine aggregates with other concrete constituents (such as superplasticizers, cements etc.).

The properties of the manufactured sand can be changed in many ways. Thus the main task for the first phase of the COIN-project has been to study the effect of different parameters and to distinguish which ones are the most relevant to be investigated in more detail. The issue of using manufactured sand has been divided into four main keystones based on the main differences between natural and crushed fine aggregates: 1) the shape of the particles below 4 mm; 2) particle size distribution; 3a) the question of very high filler (< 125 µm) content – how much should be removed; 3b) particle size distribution of filler (< 125 µm) – using new technologies such as air classification it's even possible to modify the filler itself for example by removing basically only particles below a certain size; 4) to what extent and in what way should the concrete mix design be changed.

Rather extensive studies on aggregates from 3 selected quarries have been carried out and are still in progress within the project. The most significant results so far (*Cepuritis, 2011*) indicate that the filler part and particle size distribution of the fine aggregates are the parameters that have the most crucial effects on the fresh concrete rheology. The effect of those has been found to be best expressed by packing measurements that confirms some recognized previous research results (*Ferraris and de Larrard, 1998*). Though some other phenomena related to specific surface has also been observed we presently still do not understand fully why packing measured on packed fine particles relates to the properties of the same particles when dispersed in a lubricating phase together with coarse particles. This must be further investigated. Based on the present knowledge we may conclude that most of the efforts for the future research should be focused on the filler phase of the manufactured fine aggregate and how the fillers interact with the other concrete constituents.

3. DEVELOPMENT OF HIGH PERFORMANCE LIGHTWEIGHT AGGREGATES

Expanded clay is a common used material for artificial lightweight aggregates (LWA) for concrete. For this purpose the material should combine a low density and low water absorption with a high strength. Expanded clay is produced by adding oil as an expansion agent to clay and firing in a rotary kiln. The rotation of the kiln gives the product a spherical shape and the development of gaseous carbon oxides - generated by the reduction reaction of iron-(III)-oxide through carbon (motor oil) - leads to the expansion and the porous structure of the aggregate.

By increasing the strength of LWA without compromising the density, new application fields could be opened up. The strength and density of the lightweight aggregate depends generally on the composition of the clay, the amount and type of additives used during the production process, the heating rate, the cooling rate, the pore structure, the total porosity, the surface structure and the final composition after burning. One approach to increase the strength of the brittle LWA matrix is to reinforce it with small stainless- or carbon-steel fibres. For this purpose the fibres are mixed into the clay before firing. Challenges for this approach are the shape and thermal resistivity of the fibres. The reinforcement has to withstand the high temperatures during the burning process while not hindering the expansion of the clay. Since the matrix of the LWA consists of a high amount of glass phase (usually around 85 %) the expanded clay aggregates could be toughened through thermal pre-tensioning like a flat glass. The idea is to create a tension in the outer shell of the pellet by quenching it. This tension counteracts an applied mechanical stress and toughens therefore the material. Quenching could on the other hand lead to irregular stresses inside the pellet due to the inhomogeneous and porous structure and weaken the material. In this case slow annealing of the product after the burning process could lead to an increased strength. Furthermore, the cooling rate will influence the ratio between mineral phases and glass phase. With a slower cooling rate or by keeping the sample at certain temperatures crystal growth could be promoted and a higher strength level could be reached.

Besides fibre reinforcement and different heat treatments the usage of additives is another possibility of influencing the strength of the aggregate. SiO_2 in the form of reactive silica fume influences the viscosity of the matrix within the expansion process. A higher viscosity leads to a more equal distribution and size of bubbles which are formed during the expansion process. The pore structure of the end product - which results from the formed bubbles - will influence the strength of the aggregate. Traditional LWA has uneven pore structure of ordinary expanded clay which could be improved by the usage of additives. Many small pores seem to show better mechanical properties than few big pores. A high Si content in the glass phase leads, due to its network forming properties, to a higher viscosity and could therefore influence the strength properties of the end product in a positive way. Work is in progress along these lines.

4. PERFORMANCE BASED TESTING OF ALKALI-SILICA REACTIVITY OF AGGREGATES

National regulations for preventing alkali-silica reactions (ASR) in concrete structures are based on various principles that have to take into account a range of material properties and local experience. Some countries have also incorporated the option of performance testing in their provisions. Such options are meant to partly replace technically and commercially restrictive prescriptive requirements by performance-oriented requirements (e.g. *EN 206-1*). Several national ASR performance tests have been used worldwide for more than 15 years, but none of the methods have proven to be reliable for use with all aggregate types and all binders. Some of the methods also lack documentation on the link to the field behaviour during the concrete service life. As basis to agree on a general international ASR performance based testing concept, one of the objectives of RILEM TC 219-ACS 'Alkali-silica reactions in Concrete Structures' (2007-2012) is to develop and validate one or more ASR performance tests for assessment of the alkali reactivity of various aggregate/ binder combinations. The innovation potential for such performance tests is high, since general ASR regulations are rather restrictive. It will e.g. allow utilization of many local potentially alkali-silica reactive aggregates, enhance the flexibility for the concrete producer with respect to material selection and optimization of the concrete mix design.

Developing a reliable performance test requires both theoretical considerations and practical verification. A comprehensive research program is being performed in a PhD study within COIN, where one aim is to give input to the RILEM task group. As a base for the work within RILEM TC 219-ACS and the PhD study, a literature survey on influencing parameters when moving from aggregate testing to performance testing has recently been finalized (*Lindgård et al, 2011*). The main objective of the review was to identify parameters and limitations for accelerating ASR under elevated moisture and temperature conditions. In the PhD study, an extensive laboratory program is being performed focusing on the impact of the curing and storage conditions (that vary a lot from test method to test method) on the internal humidity in the test specimens, the extent of alkali leaching and the measured ASR expansions.

The most important preliminary conclusion from the laboratory testing is that the ASR expansion is very sensitive to the extent of alkali leaching, that may vary significantly even for small modifications of the test setup. Based on these preliminary findings, two of the three RILEM concrete prism tests have been withdrawn. An extensive follow-up program has recently been actuated within COIN, comprising eight aggregate types and four commercial binders, as well as two field exposure sites, one at SINTEF in Trondheim and one at LNEC in Lisbona. One aim is to verify if some of the present test variants might work as a commercial performance test method. Another aim is to document the laboratory field correlation with various aggregate/binder combinations.

5. REFERENCES

Ahn N. (2000), "An experimental study on the guidelines for using higher contents of aggregate micro fines in Portland cement concrete", Ph.D, The University of Texas.

Cepuritis R. (2011), "Effects of Concrete Aggregate Crushing on Rheological Properties of Concrete and Matrix", Master Thesis, Norwegian University of Science and Technology.

Ferraris C. F. and de Larrard F. (1998), "Testing and Modelling of Fresh Concrete Rheology. NIST (National Institute of Standards and Technology) Report 6094", Washington: NIST.

Kim et.al. (2008), "Rheological and mechanical properties of mortars prepared with natural and manufactured sands", Cement and Concrete Research, 38, pp. 1142-1147.

Quiroga P. N. (2003), "The effect of the aggregate characteristics on the performance of Portland cement concrete", Ph.D, The University of Texas.

Westerholm M. et. al. (2006), "Influence of fine aggregate characteristic on the rheological properties of mortars", Cement & Concrete Composites, 30, pp. 274-282.

Wigum, B.J., Danielsen, S.W., (Editors), Hotvedt, O. & Pedersen, B., (2009): Production and Utilisation of Manufactured Sand. COINProject report 12 – 2009. 62 pp.

EN 206-1 Concrete – Part 1: Specification, performance, production and conformity, 2001.

Lindgård, J., Ö. Andiç-Çakır, I. Borchers, M. Broekmans, E. Brouard, I. Fernandes, C. Giebson, B. Pedersen, C. Pierre, T.F. Rønning, M.D.A. Thomas, B.J. Wigum, RILEM TC219-ACS-P: Literature survey on performance testing, COIN project report 27, ISBN: 978-82-536-1209-6, in, 2011, pp. 164.

RECOVERY BEHAVIOUR OF HYBRID FIBRE REINFORCED HIGH STRENGTH CONCRETE AFTER HIGH TEMPERATURE EXPOSITION

Takashi HORIGUCHI
Hokkaido University, Faculty of Engineering, Sapporo, Japan

SUMMARY

Recently the addition of polypropylene fibres into high-strength concrete (PFRHSC) was reported to be very effective against the explosive spalling. However, it is hopeless to maintain the residual strength and the fracture toughness when the fibres melt. Steel fibre reinforcement can help to maintain the residual strength and fracture toughness after heated. In this point of view, author has proposed the hybrid fibre reinforcement with the combination of polypropylene and steel fibres, HFRHSC is proposed for improving the strength as well as the fracture characteristics after heating. In this paper, the recovery behavior of the strength as well as the others physical properties of HFRHSC is investigated.

1. INTRODUCTION

High-strength concrete shows particular characteristic behaviour at elevated temperatures, such as explosive spalling, that is rarely observed in normal-strength concrete. This behaviour has been attributed to the very dense concrete matrix usually associated with high-strength concrete (*Ali et.al., 1996, Phan, 1996, Khoury et.al, 1999)*. Recently the addition of polypropylene fibres into high-strength concrete was reported to be very effective against the explosive spalling (*Takano et.al., 2000, Horiguchi*, *2002*). As heating increases, the fibres in the cement matrix start to melt at about 160 ˚C and increase the total pore area. This melting effect mitigates the explosive spalling as it provides pore space in which moisture vapour can accumulate at lower vapour pressures. However, it is hopeless to maintain the residual strength and the fracture toughness when the fibres melt. Steel fibre reinforcement can help to maintain the residual strength and fracture toughness after heated.

In this point of view, authors have proposed the hybrid fibre reinforcement systems with the combination of polypropylene and steel fibres for improving the residual strength as well as the residual fracture characteristics after heating (*Suhaendi, 2006, Horiguchi*, *2008*). This paper investigates the residual properties as well as recovery possibility of heated hybrid fibre reinforced high-strength concrete.

2. EXPERIMENTAL PROCEDURE

2.1 Materials

The cement was a normal Portland cement, and river gravel (Sand stone) (5 - 20 mm of particle size) was used as the coarse aggregate and river sand was used as the fine aggregates. A maleic acid based super-plasticizer (SP), air entraining agent (AE), and bubble cutter agent (BC) were used. For bubble cutter agent, this chemical admixture was used only in the concrete mix containing fibres since this particular mix had the tendency to form more additional air bubble. Steel and polypropylene fibres were added into concrete mix in this study. The steel fibres came in bundles where each bundle consisted of 10 to 12 single steel fibres bound by special glue that would dissolve in water. As for polypropylene fibres, they came in fine fibrillated bundles that would disperse into monofilament fibres inside the concrete mix.

2.2 Mix Design of Concrete

There were eleven series of concrete mix as shown in Table 1 to be tested in this experimental study. These are plain concrete, four series of polypropylene fibre reinforced concrete (PFRC), two series of steel fibre reinforced concrete (SFRC), and four series of hybrid fibre reinforced concrete (HFRC). In this mix proportions, all series had the same value of these factors: water to cement ratio (W/C) of 0.3, sand to aggregate ratio (s/a) of 60 %, and unit water content of 170 kg/m3. The main factor differentiated each series of concrete mix was the fibres. The valuable included fibre material (polypropylene fibre, steel fibre, and combination of the two fibres), fibre volume fraction (Vf), fibre length (lf), and Vf composition. The Vf composition in hybrid fibre reinforced concrete was selected intentionally so that correlation between single type fibre reinforced concrete and hybrid fibre reinforced concrete could be maintained.

Tab. 1 Mix design of plain and fibre reinforced high-strength concrete

Series	Code	w/c	s/a (%)	Fiber volume (%)		SP[1] (% x c)	AE[2] (A)	BC[3] (T)
				pp	steel			
Plain	Plain	0.3	60	~	~	1.3	7	~
PFRC 6 - 0.25	P6-0.25			0.25	~	1.3	3	1
PFRC 6 - 0.5	P6-0.5			0.5	~	1.3	3	1
PFRC 30 - 0.25	P30-0.25			0.25	~	1.7	3	2
PFRC 30 - 0.5	P30-0.5			0.5	~	1.9	3	2
SFRC 30 - 0.25	S30-0.25			~	0.25	1.3	3	1
SFRC 30 - 0.5	S30-0.5			~	0.5	1.3	3	1
P_6-0.25 S_{30}-0.25	H1			0.25	0.25	1.35	3	2
P_6-0.25 S_{30}-0.5	H2			0.25	0.5	1.3	1	4
P_6-0.5 S_{30}-0.25	H3			0.5	0.25	1.4	1	4
P_6-0.5 S_{30}-0.5	H4			0.5	0.5	1.5	1	4

[1] Superplasticizer= Paric FP300U

[2] Air entraining agent= Flowric AE200, 1A= 0.004% x cement (by weight)

[3] Bubble cutter agent, 1T= 0.0002% x cement (by weight)

2.3 Experimental test procedures

For fresh concrete, the performed tests included slump and air content tests. Some features of the hardened concrete like density, voids, and ultrasonic pulse velocity (UPV test according to ASTM C 597-83) were also conducted. The main tests in this study consisted of compressive strength (ASTM C 39-86 and ASTM C 469-87a), splitting tensile strength (ASTM C 496-90), and permeability test (modified DIN1048). Specimens were heated using computer-controlled electric furnace. The heating rate was set at 10°C per minute with peak temperature maintained at 200°C and 400°C for 2 hours.

3. TEST RESULTS AND DISCUSSION

3.1 Recovery properties of heated concrete

Fig.1 to Fig.4 show the properties of heated concrete after being cured under ambient temperature (dry curing) and under water (saturated curing), respectively.

The compressive strength, tensile strength and Young's modulus do not seem to recover clearly in the case of heated concrete specimens being cured under ambient temperature. Meanwhile, for heated concrete specimens that had been cured under saturated curing, the recovery in UPV, compressive strength, tensile strength and Young's modulus can be observed as shown in Fig. 1 to Fig. 3. This might indicate that re-hydration of heated concrete had taken place for the heated specimens cured under saturated condition. The recovery rate under saturated curing showed a rapid increase in the first 2 months and slows down after that.

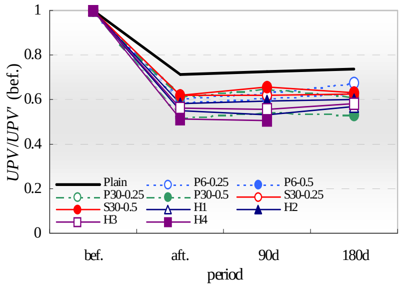

(a) Under dry curing

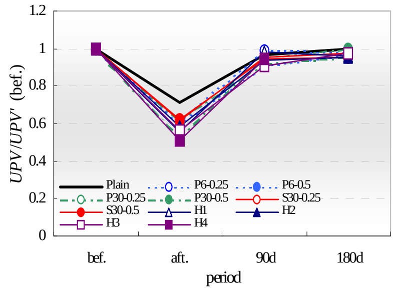

(b) Under saturated curing

Fig. 1 Relative UPV value before and after heat exposure under dry curing

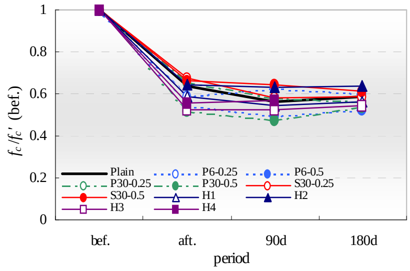

(a) Under dry curing

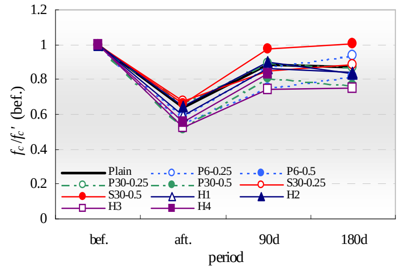

(b) Under saturated curing

Fig. 2 Relative compressive strength before and after heat exposure

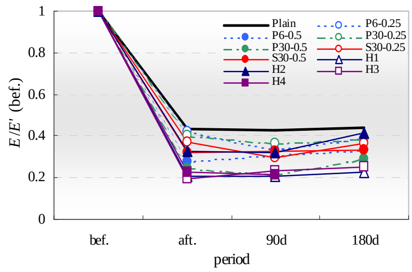

(a) Under dry curing

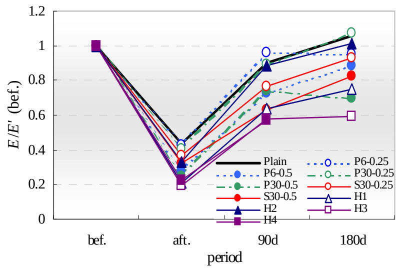

(b) Under saturated curing

Fig. 3 Relative Young's modulus before and after heat exposure

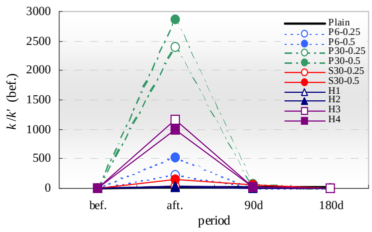

(a) Under dry curing

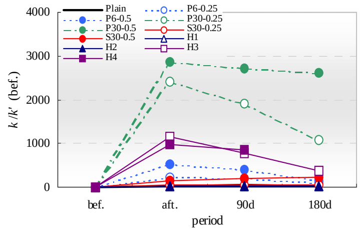

(b) Under saturated curing

Fig. 4 Relative permeability coefficient before and after heat exposure

4. CONCLUSIONS

From the experimental test results, the following conclusions were made:
Average reduction of 30%, 20%, and 15% was observed in modulus of elasticity, splitting tensile strength, and compressive strength, respectively, for specimens heated up to 200°C. For specimens heated up to 400°C, average reduction in modulus of elasticity of 70% was observed while both compressive strength and splitting tensile strength showed an average reduction of 40%.

As polypropylene fibers melted at its fusion point of 160-170°C, polypropylene fiber reinforced concrete (PFRC) showed more reduction in its residual properties compared to steel fiber reinforced concrete (SFRC). More inclusion of polypropylene fibers will tend to reduce most of PFRC and HFRC residual properties, especially its residual permeability performance. On the other hand, more inclusion of steel fibers may improve the splitting tensile strength of SFRC and HFRC.

In residual permeability performance, more inclusion of steel fibers was found to be quite effective in the series also consisting 0.25% of polypropylene fibers in the HFRC, at both 200°C and 400°C. For PFRC, fiber length significantly affected the residual water permeability coefficient. The longer the fiber, the higher the residual water permeability coefficient

Properties recovery was observed significantly on heated concrete specimens cured under saturated condition compared to the ones cured under ambient temperature.
The recovery rate showed a rapid increase in the first two months on heated concrete being cured under saturated condition and slowed down after that

5. REFERENCES

Ali, F.A., Connolly, R. and Sullivan, P.J.E.(1996) , "Spalling of High Strength Concrete at Elevated Temperatures," Journal of Applied Fire Science, Vol.6, No.1, pp.3-14,

Horiguchi, T., Takano, T., N. Saeki, T. D. Lin(2002), "Effect of Fiber Reinforcement on Residual properties of high strength concrete under elevated temperature," American Concrete Institute, ACI SP-209, 53-64,

Horiguchi, T., Watanabe, K. and Suhaendi, S. L.(2008) : Study on fracture toughness of hybrid fiber reinforced high strength concrete at high temperature environment, Proceedings of 11th International Conference on Durability of Building Materials and Components, 11dbmc, pp.117-124, 2008

Khoury, G.A. and Algar, S.(1999), "Mechanical behaviour of HPC and UHPC concrete at high temperatures in compression and tension, "ACI International conference on State-of-the-Art in High Performance Concrete, Chicago

Phan, L.T.(1996), "Fire Performance of High-Strength Concrete: A Report of the State-of-the-Art," NISTIR 5934, NIST

Suhaendi, S. L. and Horiguchi, T.(2006): Effect of short fibres on residual permeability and mechanical properties of hybrid fibre reinforced high strength concrete after heat exposition, Cement and Concrete Research, Vol.36, Issue 9, pp.1672-1678,

Takano, T., Shimura, K., Horiguchi, T. and Saeki, N.(2000), "Fire Resistance of High-strength Mortars with Several Types of Fibers and Polymers," 3rd Joint Symposium on the Structural Materials between Korea & Japan, pp.65-72

TAILORING THE INNATE PROPERTIES OF PORTLAND CEMENT: THE APPLICATION OF CARBON NANOTUBES

Péter Ludvig[1,2], José Marcio Calixto[1],Luiz Orlando Ladeira[2]

[1] *Department of Structural Engineering, Federal University of Minas Gerais, Av. Antônio Carlos, 6627, Pampulha, Belo Horizonte-MG, CEP 31.270-901, Brazil*

[2] *Nanomaterials Laboratory, Department of Physics, Federal University of Minas Gerais, Av. Antônio Carlos, 6627, Pampulha, Belo Horizonte-MG, CEP 31.270-901, Brazil*

SUMMARY

Carbon nanotubes are a promising material to solve the low tensile strength and ductility of Portland cement based materials. Carbon nanotubes (CNTs) and nanofibers (CNFs) synthesized directly on cement clinker particles can also reduce production costs and help dispersion. Mortar specimens prepared with such nanostructured material were tested to determine tensile and compressive strength. The effects of different functionalizing agents were compared. Test results showed some enhancement of mechanical characteristics of Portland cement matrices made with CNT/CNF.

1. INTRODUCTION

Concrete made with Portland cement is the largest consumed construction material worldwide. Among the reasons for this fact are the availability of the raw materials and the excellent compressive behavior. On the other hand, tensile characteristics of cementitious materials are poor due to their low tensile strength and brittle behavior. In reinforced concrete, steel reinforcement bars are used to resist the tensile stresses. The distribution of cracks is more uniform and their width is reduced when small diameter steel rebars are used.

Recent investigations showed that the poor tensile behavior of cement based materials is partly due to macroscopic defects (pores) and partly to the innate properties of calcium silicate hydrate (C-S-H), the main constituent of hardened cement paste.

Carbon nanotubes (CNTs) are among the highest tensile strength materials known, up to 100 times higher than that of steel, yet only one hundredth of its density. Their tubular structure is composed of one or several graphene sheets rolled up in specific directions. The high tensile strength is due to the bond between carbon atoms that compose the CNTs which is the strongest link that exists. At the same time, the failure strain of CNTs can be as high as 15-20%. The typical dimensions of CNTs are between 2 and 50 nm in diameter and up to hundreds of microns in length, thus aspect ratios as high as 1:1,000,000 can be found.

These properties of CNTs make them a promising candidate to be incorporated in cementitious matrices in order to achieve a novel material with tailored characteristics: increased tensile strength and ductility. The length of CNTs is comparable to smaller cement grains and their diameter to C-S-H crystals. This size would allow a nano-scale distribution of tensile stresses with lower stress peaks, more crack bridging and smaller crack width at this nano-level. Several worldwide investigations have been conducted producing and testing cementitious composites with CNT addition. Their results show some increase in tensile and compressive strength, as well as in the modulus of elasticity (Li *et al.*, 2005; Musso *et al.*, 2009; Konsta-Gdoutos *et al.*, 2010; Melo *et al.*, 2011). In all these studies employed physical mix of high quality CNT in cement matrices. CNTs with different types of functionalization were used in a content between 0.025 % to 0.75 % with respect to the cement weight.

The aim of this work is to present the results of Portland cement mortars made with *in situ* synthesized nanostructured clinker. The research group based at the Nanomaterials Laboratory at the Federal University of Minas Gerais (UFMG) developed a process to synthesize CNTs and carbon nanofibers (CNFs) directly on cement clinker particles which can reduce production costs and make processing and dispersion easier (Ladeira *et al.*, 2008). Since as-produced CNTs are highly hydrophobic, special surface treatment (functionalization) is necessary to allow the incorporation in water based composites like Portland cement mortar. The effects of different concrete admixtures as well as hydrogen peroxide as functionalizing agents on the mechanical behavior of mortars are compared.

2. METHODOLOGY

CNTs and CNFs were grown directly on cement clinker in a process described by Ludvig *et al.* (2011). Products were characterized by scanning electron microscopy (SEM). Mortar specimens of 40 x 40 x 160 mm^3 in size were cast using slag Portland cement, sand in equal amounts of four fractions (0.15 mm, 0.30 mm, 0.60 mm and 1.2 mm), water, plasticizer/superplasticizer and nanostrucutred clinker. Water to cement ratio was 0.4. Based on the results of Melo *et al.* (2011), the amount of CNTs and CNFs was 0.3 % with respect to cement weight. For untreated CNTs/CNFs the plasticizer served as a non-covalent functionalizing agent. Three different types of plasticizers/superplasticizers were employed: a combination of sulfonated polinaphtalene and policarboxylate (PP), lignosulfonate (LS) and sulfonated melamine (ME) based concrete admixtures. The mortar compositions are given in Tab. 1. Flexural tensile and compressive strength of the mortar beams were determined. These tests were performed at the age of 28 days.

Tab. 1 Mortar mix proportion

Composition (kg/m^3)	**CNT/CNF content (kg/m^3)**	**W/C [b]**	**Plasticizer content (kg/m^3)**
530 : 1590[a]	1.59	0.4	7.95

[a] – cement : fine aggregates

[b] – water/cement ratio

In an attempt to achieve better functionalization of the CNTs/CNFs, and thus a better link between nanotubes and the cement matrix, a hydrogen peroxide treatment was carried out on the synthesis products prior to casting. Some 80 ml of H_2O_2 was applied to 50 g of CNT-clinker composite. The preparation was dried at 105 °C immediately after the reaction stopped. The composition of mortars made with peroxide functionalized CNTs/CNFs was the same as the others, including lignosulfonate plasticizer.

3. RESULTS AND DISCUSSION

3.1 Synthesis

Typical synthesized products are shown on Fig. 1. The products had heterogeneous dimensions and morphology when compared to high quality CNTs. The products were well-distributed on the surface of clinker particles.

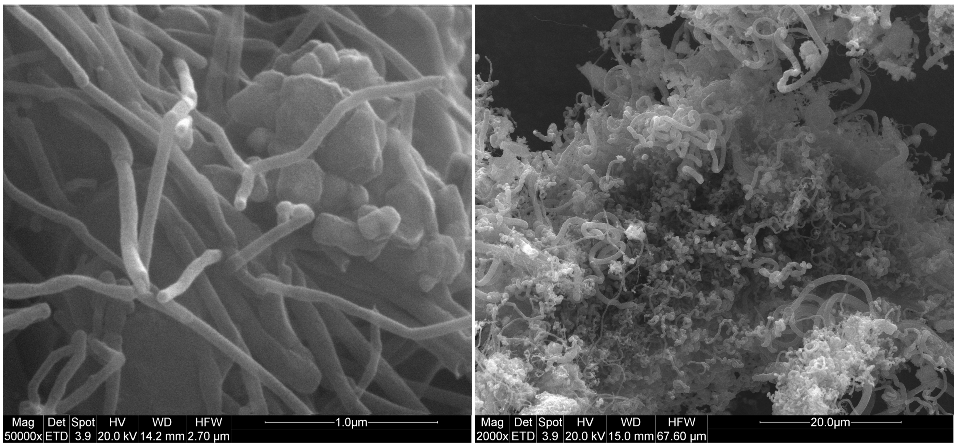

Fig. 1 SEM images of CNTs and CNFs grown on clinker under different magnifications

3.2 Mechanical behaviour

Tensile and compressive strength results of the test specimens are presented in Fig. 2. Compressive strength of mortars with CNTs showed more enhancement than flexural tensile strength. The mortar prepared with lignosulfonate plasticizer presented the best results, both in flexure and in compression, with 14 % gain in tensile and a 90 % gain in compressive strength. The addition of H_2O_2 treated CNTs to the mortar resulted in higher compressive and flexural tensile strengths with 33 % and 13 % gain at 28 days respectively.

Legends: PP – sulfonated polinaphtalene and policarboxylate surfactants;
LS – lignosulfonate plasticizer;
ME – sulfonated melamine plasticizer;
PO – hydrogen peroxide treated CNTs/CNFs with lignosulfonate plasticizer

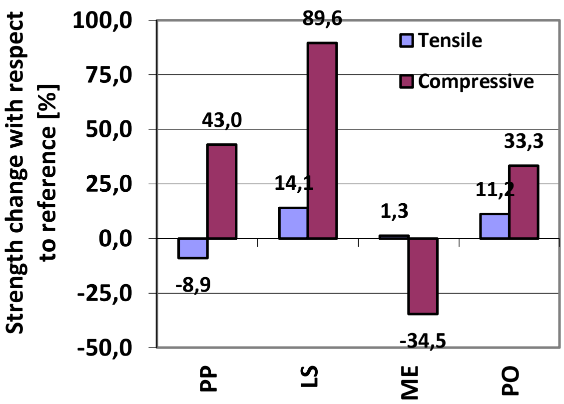

Fig. 2 Compressive and tensile strength results of mortar specimens at the age of 28 days.

Gain in compressive strength was in all cases higher than in flexural strength. The addition of CNTs and CNFs to the mortars had a micro filling and hydration catalyst effect rather than a crack-bridging effect. This can be explained by the poor dispersion and adherence of the CNTs/CNFs in the cement matrix. At the same time, the high surface area CNTs and CNFs – if an adequate surface treatment is applied – may act as nucleating sites for cement hydration product formation, as it was observed by Makar and Chan (2009), resulting in a more complete hydration and thus in higher compressive strength.

4. CONCLUSIONS

CNTs and CNFs were synthesized in a CVD process on Portland cement clinker. The resulting products had a fibrous structure with high level of defects. The reinforcing effect of these nanostructured materials was evaluated on cement mortar specimens.CNT/CNF addition to the mortars affected the degree and speed of hydration of cement. Some improvements in both compressive and flexural strength were observed. Flexural strength enhancement remained lower than compressive strength, suggesting a micro filling and/or hydration catalizator effect rather than crack-bridging and fiber reinforcement.

5. ACKNOWLEDGEMENTS

The authors would like to express their gratitude to Intercement SA for providing materials and financial support and to INCT – Nanomateriais de Carbono for the funds provided for this research project. The authors would like to acknowledge the Center of Microscopy at the Federal University of Minas Gerais (http://www.microscopia.ufmg.br) for providing the equipment and technical support for experiments involving electron microscopy. Péter Ludvig was funded by a Fapemig Grant.

6. REFERENCES

Konsta-Gdoutos, M. S.; Metaxa, Z. S. and Shah, S. P. (2010) “Multi-scale mechanical and fracture characteristics and early-age strain capacity of high performance carbon nanotube/cement nanocomposites”, Cement & concrete composites, Vol. 32, 2010, pp. 110-115.

Ladeira, L. O.; Silva, E. E.; De Oliveira, S.; Lacerda, R. G.; Ferlauto, A. S.; Ávila E. and Lourençon, E. (2008) “Processo de síntese contínua e em larga escala de nanotubos de carbono sobre o clínquer de cimento e produtos nanoestruturados”, Brazilian Patent, INPI 014080002727 (30.04.2008).

Li, G.Y.; Wang, P.M. and Zhao, X. (2005), „Mechanical behavior and microstructure of cement composites incorporating surface-treated multi-walled carbon nanotubes”, Carbon, Vol. 43, 2005, pp. 1239-1245.

Ludvig, P.; Calixto, J. M.; Ladeira, L. O. and Gaspar, I. C. P. (2011), “Using Converter Dust to Produce Low Cost Cementitious Composites by *in situ* Carbon Nanotube and Nanofiber Synthesis”, Materials, Vol. 4, 2011, pp. 575-584.

Makar, J.M. and Chan, G.W. (2009) “Growth of cement hydration products on single-walled carbon nanotubes”, J. Amer. Ceram. Soc. Vol. 92, 2009, pp. 1303-1310.

Melo, V. S.; Calixto, J. M.; Ladeira, L. O. and Silva, A. P. (2011), “Macro- and Micro-Characterization of Mortars Produced with Carbon Nanotubes”, ACI Materials Journal, Vol. 108, No. 3, May-June 2011, pp. 327-332.

Musso, S.; Tulliani, J.-M.; Ferro, G. and Tagliaferro, A. (2009), “Influence of carbon nanotubes on the mechanical behavior of cement composites”, Composites science and technology, Vol. 69, 2009, pp. 1985-1990.

NON DESTRUCTIVE TESTING OF LIFETIME CONCRETE

Luboš Pazdera[1], Libor Topolář[1], Vlastimil Bílek[2], Jaroslav Smutný[1], Marta Kořenská[1]

[1] *Department of Physics and Department of Railway Structures and Construction*
Brno University of Technology, Faculty of Civil Engineering
602 00 Brno, Veveri 331/95, Czech Republic

[2] *ZPSV a.s.*
Ostroh, Czech Republic

SUMMARY

Concrete is a composite construction material frequently used in civil engineering. We know that concrete is as a man – when concrete is made it is as a baby, then it ages and its properties change in accordance to its baby life. That means it is better to monitor and change its properties when it is young as soon as possible. However, using the methods immediately after concrete birth (making the mixture) is difficult *(Pomeroy, 1991)*. The main aim of the article is to show the application of Acoustic Emission Method, Impact Echo Method, Non-Linear Ultrasonic Method, Ultrasonic Method and temperature measuring during concrete lifetime, particularly during the first days after the mixture has been made.

1. INTRODUCTION

Concrete is one of the most popular building materials *(Aitcin 2005)*. Its lifetime properties determinate the whole construction lifetime period. Concrete setting and hardening processes are the most critical phases during construction work, influencing the properties of concrete structure. For this reason applying non destructive testing in the early age of concrete lifetime can be useful *(Mikulic, Sekulic, Stirmer, Bjegovic 2005)*. Some Non-Destructive Testing Methods were applied for describing concrete properties in the early age.

Acoustic emission is elastic radiation generated by the rapid release of energy from sources within the material. These elastic waves are detected and converted to voltage signals by small piezoelectric sensors mounted to convenient surface of the material. The results is that acoustic emission can be used to monitor a structure for active damage even when ambient noise levels are extremely high. Sources of acoustic emission include fracture and plastic deformation, phase transformation and other processes. Acoustic emission is sensitive enough to detect newly formed crack surfaces down to a few hundred square micrometers and less.
Non-linear acoustic spectroscopy methods can be split into resonant and non-resonant. One or more (harmonic) signals are broadcast into a sample structure. Sensors fixed on the sample surface detect structure responses. Harmonics and non-harmonic frequencies imply structure quality *(Finlayson, Friesel, Carlos, Cole and Lenain 2000).*

Impedance spectroscopy, which belongs to the methods of non-destructive testing of concrete, monitors spectrum changes during cement hydration. Differences are observed in the spectra of tangents delta and capacity, respectively. The resistance for samples and its quality is described by the dominant type of loss in material.

2. EXPERIMENTAL SETUP

Two different concretes mixture were prepared. The first mix was "classical" concrete and the second mix was concrete with a mixture of fly ash and grounded recycled concrete. Specimen 100 x 100 x 400 mm were made from "classical" mix (marked S1) and with fly ash and grounded recycled concrete, respectively (marked S2).

Fig. 1 Experimental set up of concrete samples (S1 and S2) with sensors for acoustic emission and impedance spectroscopy before unmolding

Acoustic emission signals were taken by measuring equipment DAKEL XEDO *(Mazal; Liskutin, 2007)*. Four acoustic emission sensors (two and two) were placed on the samples for each system. Acoustic emission events were measured "continuously" during a fortnight. A sinusoidal generator and two recorded sensors were applied. Impedance spectroscopy used RLCG bridge for measuring loss-factor and ohmmeter for monitorin temperature and switch for controlling a lot of measured channels. Each sample contained two plates and two cylinder bars for measuring electrical impedance *(Pazdera, Topolar, Bilek, Smutny, Korenska 2010)*.

Acoustic emission and impedance spectroscopy (electrical properties) were measured simultaneously on two and two different types of concrete samples for a long time (Fig. 1).

3. RESULTS

The mechanical properties (compressive strength and bulk density) of individual mixtures are in Tab. 1.

Tab. 1 Mechanical properties

	Specimen S1		Specimen S2	
Time	24 h	28 days	24 h	28 days
Compressive strength [MPa]	25	67.5	14.7	58.6
Bulk density [$kg\cdot m^{-3}$]	2300	2326	2277	2291

In the diagram (Fig. 2) is shown the dependence cumulative counts (Nc) on time (t). The specimen (marked S1 - solid blue line) has got significantly higher the acoustic emission count event than specimen (marked S2 - dashed red line) during at the measurement period (7 days). It can be assumed that the greater numbers of acoustic emission events are caused by higher numbers of microcracks in the concrete specimen.

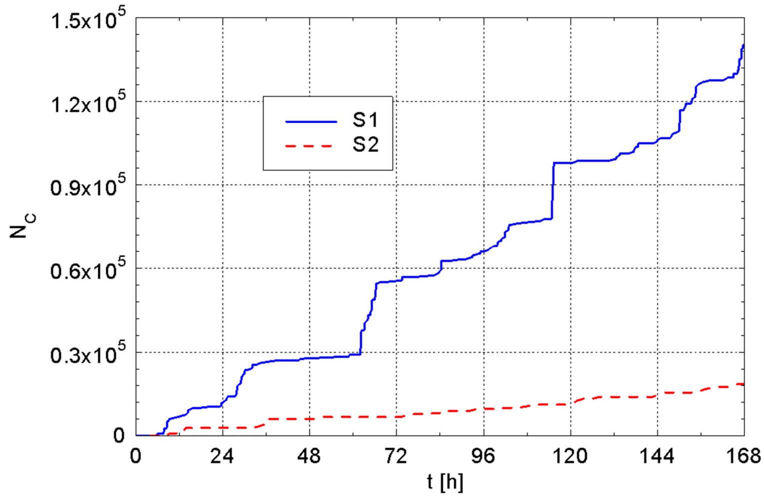

Fig. 2 Dependences of acoustic emission activity (N_C) on time (t)

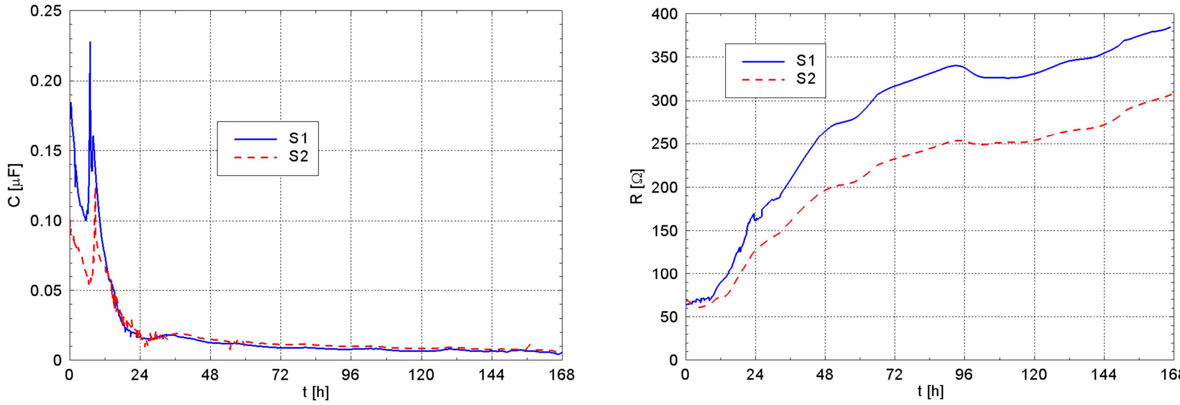

Fig. 3 Time history of capacity and resistance at 1 kHz

The capacity and resistance dependence on time at frequency 1 kHz of both types of samples is shown in graphs in Fig. 3 – capacity on the left and resistance on the right. The maximum capacity (specimen S1) is reached at 7 hours after mixing and maximum capacity (specimen S2) is reached at 8.5 hours after mixing. The capacity slightly increased after unmolding, but continued to decline.

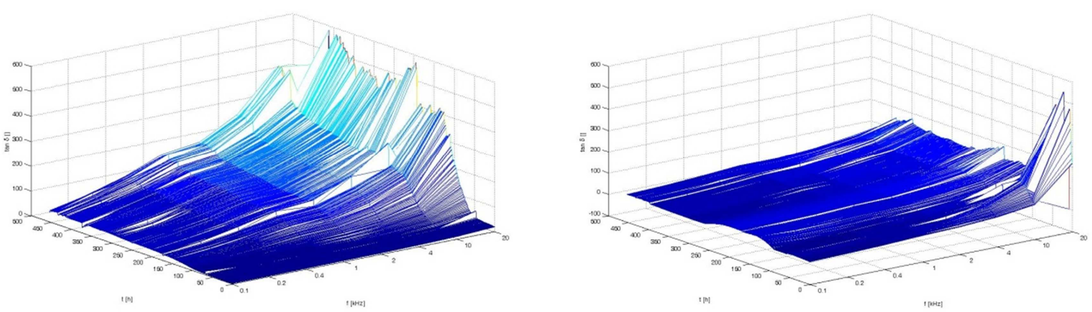

Fig. 4 Dependence loss factor on time and frequency (S1 – left, S2 – right)

The capacities decrease and resistances increase – these changes show that structural changes continue in the course of time.

Values of loss factor are higher at specimen mixed from classical mixture as shown in Fig. 1 and their shape dependents on monitoring frequency. Note, that time increases from down to upward.

4. CONCLUSIONS

Applying the methods described in the paper can help to determine the behaviour and the properties of concrete mixture mainly during the early age or during the whole lifetime without its destruction. Nevertheless, their application immediately after mixing the concrete is not easy.

Acoustic emission appears as a powerful tool for determining the rise of microcracks in the hardening concrete. It can be assumed that the greater numbers of acoustic emission events are caused by higher numbers of microcracks in the concrete specimen. The application of acoustic emission method during the hardening of the concrete structure can help to obtain better properties of the concrete structures.

Impedance spectroscopy can monitor electrical property changes during the whole concrete lifetime. Its disadvantage is mainly the inclusion of electrodes in the structure. Concrete properties are changed mainly during the first day of concrete structure setting as shown in Figs. 3 to 5. Although major changes take place immediately after mixing, important changes continue to happen for a long time.

5. ACKNOWLEDGEMENTS

This research has been supported by the project of GACR No. GAP104/10/1430 and by the part of the research project MSM 0021630519.

6. REFERENCES

Aitcin P.C.(2005): Vysokohodnotny beton (High-Performance Concrete), EBS, Prague,

Finlayson R. D., Friesel M., Carlos M., Cole P. and Lenain J. C. (2000), Health monitoring of aerospace structures with acoustic emission and acousto-ultrasonics, 15th World Conference on NDT, Rome

Mazal P.; Liskutin, P. (2007): Mechanicke zkousky materialu s vyuzitim NDT postupu (Mechanical tests of material with utilize NDT progress), NDT Welding Bulletin.. 17(1). p. 21 - 26. ISSN 1213-3825.

Mikulic D., Sekulic D., Stirmer M., Bjegovic D. (2005): Application of Ultrasonic Methods for Early Age Concrete Characterisation, The 8th International Conference of the Slovenian Society for Non-Destructive Testing, “Application of Contemporary Non-Destructive Testing in Engineering”, Portoroz, Slovenia

Pazdera L, Topolar L, Bilek V, Smutny J, Korenska M (2010): Is It Possible to Applied Acoustic Emission Method during Concrete, The 29th European Conference on Acoustic Emission (EWGAE), Wien, Austria

Pomeroy, C. (1991), Properties of fresh concrete. Materials and Structures, Vol. 24, No. 2, pp. 159. ISSN: 1359-5997

WORKING CHARACTERISTICS OF CEMENT COMPOSITES WITH CRUSHED PLASTIC AGGREGATE

Martin Križma, Oľga Koronthályová, Peter Matiašovský
Institute of Construction and Architecture SAS
845 03 Bratislava, Dúbravská cesta 9, Slovakia

SUMMARY

At present, due to continual progress in information technology, permanently new and increasing demands are put on information and computation systems. On the other hand the rational disposal of the physically worn and inadequate components of the computer and information technique (IT) becomes concern of the whole society. The study deals with one of possible ways of the disposal of plastic waste from IT components.

1. INTRODUCTION

The rational disposal of the physically worn, inadequate components of the computer and information technique – plastics in this case – becomes concern of the whole society. Furthermore, there is a permanent tendency to limit the extraction of the natural, chiefly filling building materials and thus to save the natural environment. The rational application of the cement composites using "PC crushed material" as partial additive into conventionally employed concrete mixtures may solve the above mentioned problems to a great extent. Since the year 2004 we have been occupied by the investigation of the cement composites CPA containing plastic crushed material PA (plastic aggregates). Introductory research has been initiated by the requirements of the Slovak Environmental Agency *(Bágeľ et al, 2004)*. The research has been focused mainly on the mechanical and physical properties of the composites CPA of PC and TV screens. The short-term and long-term tests were carried out as well as tests of bond between composites and the reinforcing bars. In the year 2006, the programme was extended on the tests of the composites CPA based on the print circuits.

2. EXPERIMENTAL PROGRAMME

2.1 Experimental part - mechanical properties

In years 2004 till 2007 seven types of the composite CPA mixtures were designed, which contained plastics of the PC and TV screens (mixtures labelled A to G) and four mixtures with plastics of the printed circuits (labelled H(i), i = 1 – 4), *(Križma and Nürnbergerová, 2007)*. The mixtures labelled A to E, and H1, H2, and H4 may be applied as thermo-insulating or sound proofing material. The mixtures labelled F, G, H3, which are described in this paper, are comparable with the corresponding mixtures for the undemanding structures**.** The working characteristics of the mentioned mixtures are given in Tab. 1, together with the working characteristics of the reference concrete **–** RC, which contains only standard river aggregates.

All mixtures given in Tab. 1 are of the type SCC (self consolidating concrete). Therefore the primary tests were performed for the verification of bond between predominant material PCA and reinforcement. The following tests for the determination of the working characteristics of the composite material were performed *(Križma and Nürnbergerová, 2010)*:

Tab. 1 Average values for the bulk density ρ_c, cube strength f_{cc}, prism strength f_{cp}, Young's modulus of elasticity E_c, flexural strength $f_{ct,f}$, tensile strength f_{ct} .

Designation of mixtures	ρ_c (kg.m^{-3})	f_{cc} (MPa)	f_{cp} (MPa)	E_c (GPa)	$f_{ct,f}$ (MPa)	$f_{ct,}$ (MPa)
F	1689	22.18	20.09	11.65	3.50	2.28
G	1792	29.19	24.10	12.32	3.44	2.24
H3	1863	15.90	11.90	12.83	3.89	2.53
RC	2430	48.67	47.50	41.07	6.43	4.18

- bond strength between composite and reinforcement,
- the effect of the time factor on the deformations of the composites in compression,
- the effect of the time factor on the deformations under free/restricted shrinkage.

As a super plasticiser (Stachement NN) has been applied, the commonly used compressive strength may not be decisive for the classification of the concrete. Corresponding tests were performed in compliance with (STN 73 1328, 1993).

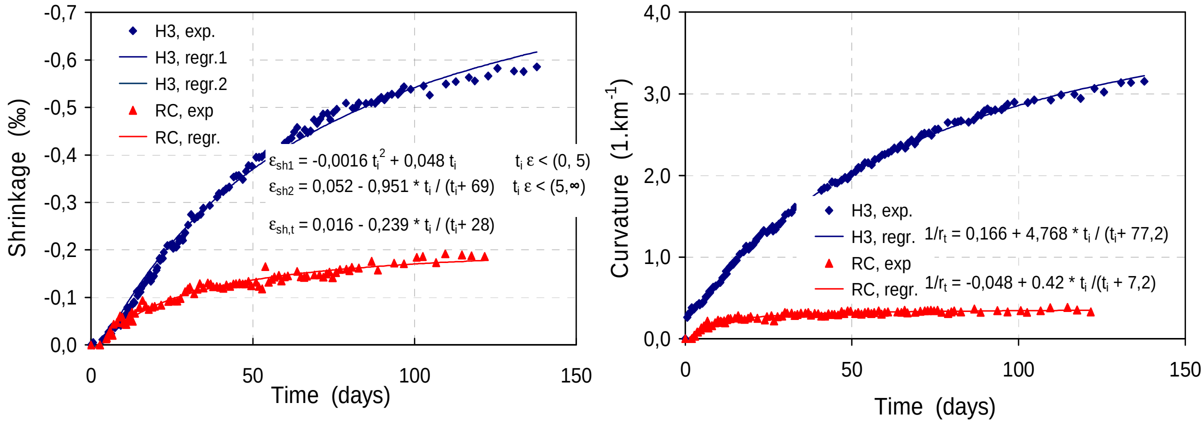

Fig. 1 Shrinkage of the composites CPA; a) comparison of the results of free shrinkage for the mixtures H3/reference mixture RC, b) comparison of the shrinkage induced curvatures of the mixtures H3/reference mixture RC

On the basis of the above mentioned results six floor slabs were designed. The slabs designated PC – Printed Circuit – 1, 2 were made of the mixture H3. The slabs designated PC – Cases – 1, 2 were made of the mixture F. The slabs PC – sandwich – 1, 2 were manufactured as two-ply slabs. The reinforced lower part with the height of h = 100 mm was made of the mixture F, the upper part with the height of h = 50 mm was made of the concrete RC. The working characteristics of all types of the composites are given in Tab. 1. The geometrical characteristics of the floor slabs are as follows: length l = 4.0 m, theoretical span l_t = 3.6 m, width b = 0.75 m, depth h = 0.15 m. The reinforcing characteristics for the former two types of slabs – symmetric longitudinal reinforcement 5 ø10 (f_{sy} = 410 MPa), transversal reinforcement ø6 by 0.3 m, the anchorage of the longitudinal reinforcement behind the theoretical support was executed by two transversal bars ø6. For the slabs PC – sandwich there was proposed the bottom reinforcement 5ø10, the transversal reinforcement ø6 by 0.3 m. The design was performed in compliance with (STN 73 1201, 1993) with the increased cover a_c = 35 mm. It is the case of the SCC composites processed by punching.

The real uniformly distributed load was simulated by the two concentrated forces F, which acted in the thirds of the theoretical span. The floor slabs were loaded by the short-term step-by-step increasing load under stress rate controlled procedure. The tests were terminated when the loading force has reached the value of $F = 2F_s$ (service load), or when the capacity of the loading hydraulic jack has been reached. The test set up is shown in Fig. 2a.

The loading force F vs. midspan deflection a relationships are plotted in Fig. 2b for all tested slabs.

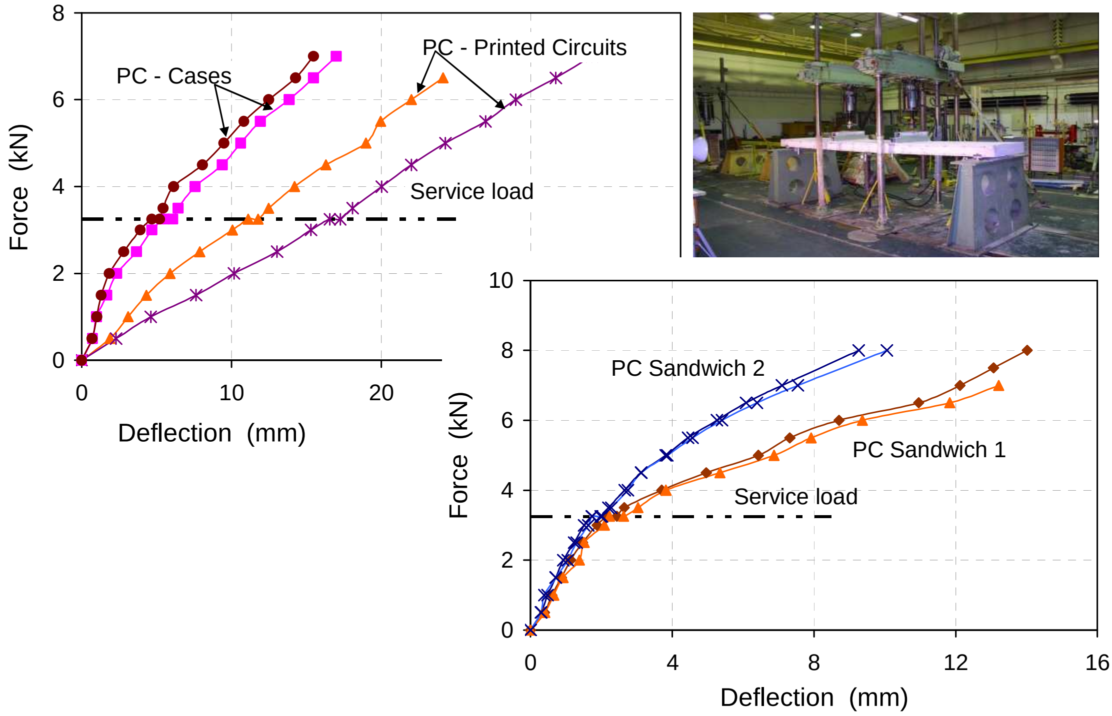

Fig. 2 Tests of the floor slabs a) test set up, b) loading force F vs. midspan deflection a

Based on afore mentioned results two sandwich slabs were chosen for the long-term tests, partial results have been published in *(Križma and Nürnbergerová, 2010)*.

2.2 Experimental part - parameters of heat transport and accumulation

Generally, the specific heat capacity as well as the bulk density of composites can be estimated by using the additivity rules (AR), where the resultant value is calculated as the weighted mean of the particular components. The resultant thermal conductivity of the composites with plastic aggregate (PA) can be estimated by the relation for the composite with the non-ideal serial configuration of components *(Matiašovský and Koronthályová, 2008)*:

$$\frac{1}{\lambda_c} = \frac{(1-1.1\cdot\pi)^{n1}}{\lambda_1} + \frac{(1.1\cdot\pi)^{n2}}{\lambda_2} \qquad (1)$$

where λ_1 and λ_2 are the thermal conductivities of high and low conductivity components, $n1$=1, $n2$=2.2 are coefficients. Transport and accumulation parameters of 4 types of PA composites were determined by the regular regime method. It was also shown that the thermal conductivity of PA itself corresponds to the value of the prevailing PA component – polyethylene (PE); $\lambda_{PE} \approx 0.3$ W/(m·K) *(Bágeľ et al, 2004)*. In Tab. 2, the estimated and measured parameters of heat transport and accumulation are compared for 4 types of PA composites.

Tab. 2 Comparison of measured *(Bágeľ et al, 2004)* and estimated thermo-physical parameters of plastic aggregate composites

Designation of mixtures	ρ_c measured (kg.m^{-3})	ρ_c (AR) (kg.m^{-3})	c_c measured (J.kg^{-1}.K^{-1})	c_c (AR) (J.kg^{-1}.K^{-1})	λ_c measured (W.m^{-1}.K^{-1})	λ_c (Eq.1) (W.m^{-1}.K^{-1})
A	1111	1059	1561	1640	0.255	0.30
B	1109	1079	1682	1689	0.320	0.31
C	1510	1421	1424	1177	0.504	0.66
D	1631	1596	1235	1181	0.853	0.86

From the results it follows that the thermo-physical parameters of composites are dependent on the composite total porosity and the portions of the plastic and the river aggregate. An improvement of the thermo-insulation ability of the composites can be obtained by the lowering the portion of the river aggregate or the cement, however, at the expense of the worse mechanical parameters.

3. CONCLUSIONS

The cement composite with the content of the plastic crushed material has specific mechanical properties in comparison with the reference standard concrete. The performance in bond – the composite/reinforcement is concerned as well as shrinkage and creep in compression. The achieved results were applied as input values for the design of the undemanding ceiling structures. The results of the short-term tests point out the suitability to design floor slabs of the sandwich type with the upper layer of the standard concrete. The long-term tests have confirmed these assumptions. The effects of the environment on the tested elements will be dealt separately. The heat transfer of the aggregates markedly affects the resulting heat conductivity of the composite in case of the composite with the lower values of the total porosity (< 50%). It is also the case of the cement composites with the plastic crushed material, where its use decreased the value of the heat conductivity to the level of the light concretes.

4. ACKNOWLEDGEMENTS

This paper was supported by the grant project GP 2/0088/09 of the Grant Agency VEGA of the Ministry of Education and Slovak Academy of Sciences.

5. REFERENCES

Bágel, Ľ., Križma, M. and Matiašovský, P. (2004), "Analysis of the applicability of the plastic crushed material at the production of the cement composites", Customer – SAŽP Banská Bystrica, Expert's report, ICASA SAS Bratislava, October 2004.

Križma, M. and Nürnbergerová, T. (2007), "Utilisation of Cement Composites with Plastic Crushed Material in Building Production", In: Proceedings of 5th Conference „Special Concretes", SEKURKON Prague, Czech Republic, October 2007, pp.148-155.

Matiašovský, P. and Koronthályová, O., (2008), "Analysis and modelling of effective thermal conductivity of dry porous building materials". In: Proceedings of the eigth Symposium in the Nordic Countries, vol. 1, pp. 285-291. Copenhagen, Denmark; 2008.

Križma, M. and Nürnbergerová, T. (2010), "Effect of the Time Factor on the Deformations of the Cement Composites with the Content of the PlasticCrushed Materials", In: Proceedings of 7th Conference „Special Concretes", SEKURKON Prague, Czech Republic, October 2010, pp.124-131.

USE OF ADMIXTURES TO ACCELERATE THE SETTING AND HARDENING OF HIGH SLAG CEMENT BASED CONCRETE

Julie Piérard[1], Valérie Pollet[1], Gunther Mosselmans[2], Christian Pierre[2]
[1] *Belgian Building Research Institute (BBRI), Concrete Technology Laboratory Limelette, Belgium*
[2] *Belgian Research Center for the Cement Industry (CRIC-OCCN) Brussels, Belgium*

SUMMARY

One of the problems most often mentioned when using cements incorporating high percentages of ground granulated blast-furnace slag (GGBFS) is the lower hydration rate of the concrete, this in comparison with ordinary Portland cement. Therefore in this study, chemical admixtures and mineral additions have been used to reduce the setting time and improve the initial strength development of cements containing 70% to 85% of GGBFS. Preliminary results seem to indicate that calcium nitrate and sodium nitrate based accelerators are the most effective. Encouraging results were also obtained with mortar mixes incorporating very fine metakaolin particles.

1. INTRODUCTION

Cements containing high percentages of ground granulated blast-furnace slag (GGBFS), classified as CEM III/B or CEM III/C, are usually recommended for use in concrete exposed to aggressive environments (chloride, sulphate and acid attack) and to minimise the risk of alkali-silica reaction in case suspicious aggregates have to be used *(Bijen, 1996)*. Another advantage of these cements is the possibility to produce light-colored concrete for esthetic purposes. Moreover, the environmental effects of GGBFS cements are substantially lower than those of ordinary Portland cement (OPC) since the partial replacement of clinker with slag (a by-product of the iron industry) leads to a reduction in carbon dioxide emissions and raw material demand.

Apart from all these benefits, GGBFS cements are characterised by a considerably lower hydration rate compared to OPC *(Neville, 1999)*. This makes the concrete more sensitive to drying, especially at early age. In this study, chemical admixtures and mineral additions have been used to reduce the setting time and improve the initial strength development of cements containing 70% to 85% of GGBFS. The influence on the mortar fluidity and the 28-day compressive strength was also investigated.

2. MATERIALS AND EXPERIMENTAL PROCEDURE

Two GGBFS cements produced in Belgium were investigated in this paper: CEM III/B 42.5 N LH HSR LA (69% slag) and CEM III/C 32.5 N HSR LA (85% slag). An OPC type CEM I 42.5 R HES was also used as a reference. The Blaine finenesses of these cements are respectively 490, 455 and 320 m²/kg.

Tests were carried out on mortars prepared according to NBN EN 196-1:2005 and consisting of one part of cement and 3 parts of normalized sand, by mass. The water to binder ratio was 0.50 and no superplasticizer was added. As mentioned previously, some adjustments were made in order to enhance the early age performances of the mortars: (1) a commercially available accelerator among those listed in Tab.1 was added to the mix or (2) the cement was partially substituted by a pozzolanic addition. In both cases, the total amount of mixing water was kept constant. In addition to silica fumes, one of the tested mineral products is a metakaolin (MK) which is an amorphous aluminosilicate ($Al_2O_3.2SiO_2$) obtained by calcination of kaolin clay, followed by fine grinding. Its mean particle size is about 1 or 2 µm.

Tab. 1 Accelerating admixtures (accelerators) used in this study

Product ref.	Chemical composition (main constituent)		Dry extract (EN 480-8) [%]
ACC 1	Calcium formate	$Ca(HCOO)_2$	100
ACC 2	Calcium nitrate (+ others)	$Ca(NO_3)_2$	58
ACC 3	Sodium nitrate	$NaNO_3$	43
ACC 4	Sodium thiocyanate	NaSCN	13
ACC 5	Calcium chloride	$CaCl_2$	61
ACC 6	Calcium nitrate (only)	$Ca(NO_3)_2$	58

The fluidity, the setting time and the compressive strength of all the mixes were determined at 20°c, respectively according to nbn en 1015-3:1999 (by flow table), nbn en 480-2:2006 and nbn en 196-1:2005.

3. RESULTS AND DISCUSSION

The flow values of the reference mortars made of OPC and the two GGBFS cements (without admixtures or additions) are all in the range of 200±10 mm. Tab. 2 compares the strength development of these mortars. As expected, the initial hydration of the GGBFS cements is very slow. The average 28-day compressive strength ($f_{cm,28}$) seems to be related to the cement strength class.

Tab. 2 Compressive strength of the reference mortars after 1, 2 and 28 days hardening

		CEM I 42.5	CEM III/B 42.5	CEM III/C 32.5
$f_{cm,1}$	[N/mm²]	15	4	1
$f_{cm,2}$	[N/mm²]	25	12	10
$f_{cm,28}$	[N/mm²]	57	53	44
$f_{cm,2} / f_{cm,28}$	[-]	0.44	0.23	0.23

The graphs presented below show the influence of the accelerator type on the setting time (Fig.1) and the early age strength (Fig.2) of the mortar made with CEM III/B 42.5. The dosage (dry extract) was 0.8 wt.% of cement. If we exclude the chloride accelerator (ACC5), which is now forbidden for use in reinforced and prestressed concrete (see EN 206-1:2000), the calcium nitrate (ACC2 and ACC6) and sodium nitrate (ACC3) based products seem to be the most effective to reduce the initial setting time and improve the strength development. An increase in the dosage (dry extract) from 0.8 to 1.1 wt.% even gave better results in some cases.

Additional tests conducted on mortars made with CEM III/C 32.5, which is particularly rich in slag, confirmed the effectiveness of ACC2 and ACC3 to enhance the initial hydration rate.

Compared to the reference mortar, we observed a reduction in the initial setting time of up to 120 minutes (Fig. 3) and an increase in the compressive strength of up to 150% after 24 hours and 75% after 48 hours hardening (Fig.4). No negative effect was observed on the 28-day compressive strength.

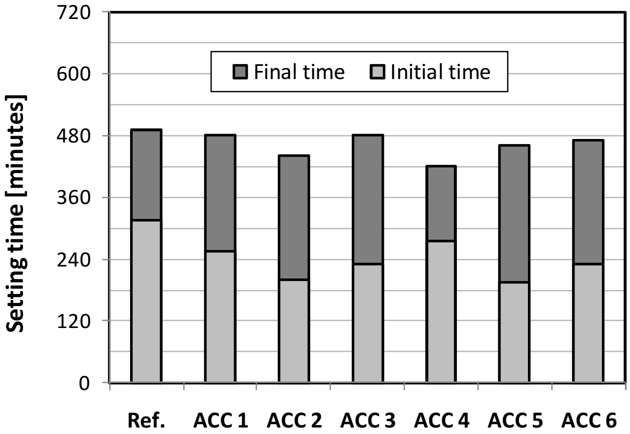

Fig. 1 Effect of the accelerators on the setting times of mortars made with CEM III/B 42.5

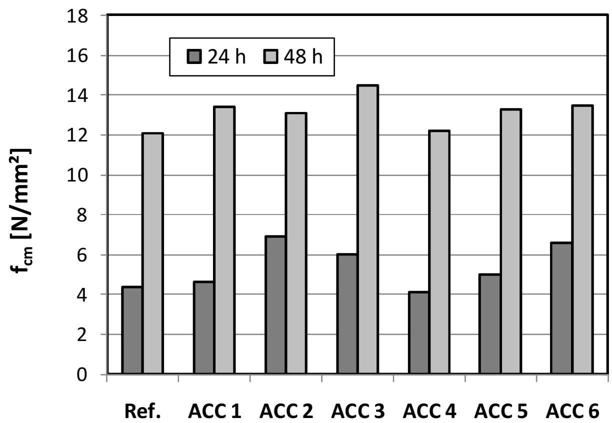

Fig. 2 Effect of the accelerators on the early age strength of mortars made with CEM III/B 42.5

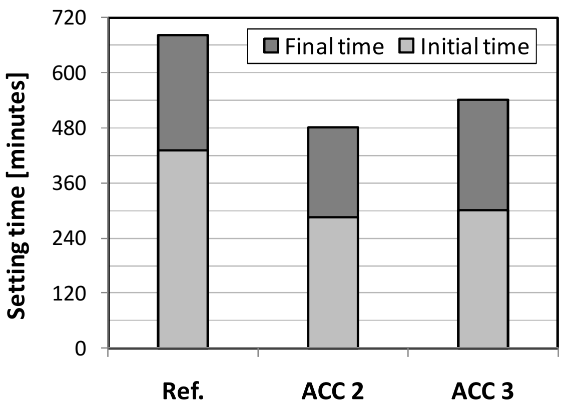

Fig. 3 Effect of the accelerators on the setting mortars made with CEM III/C 32.5

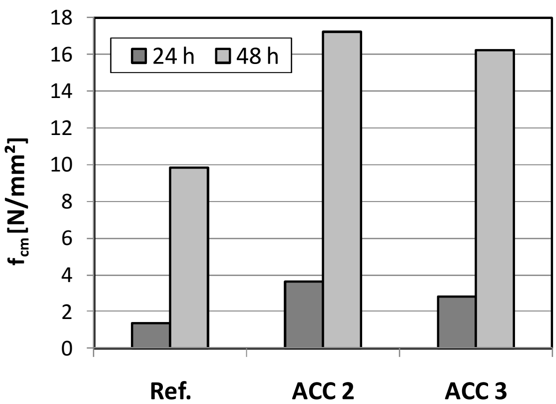

Fig. 4 Effect of the accelerators on the early age strength of mortars made with CEM III/C 32.

This study also showed that the use of some mineral additions as partial cement replacement can accelerate the hardening of GGBFS cements. Especially, the influence of a very fine MK (see section 2) was investigated within this study in combination with a CEM III/C 32.5 (see Fig. 5). The early age compressive strength tends to increase with increased cement replacement level from 2.5 to 7.5 wt.%. Compared to the reference mortar, a gain of up to 70% is obtained on the 2-day compressive strength (from 10 to 17 N/mm²). This improvement could be explained by a combination of a physical (*filler effect*) and a chemical (*pozzolanic activity*) effect. Some negative effects were however observed such as:

- a loss in fluidity (up to 15% for replacement level of 7.5 wt.%) probably due to the high fineness and the lamellar shape of the MK particles ;
- a loss in the 28-day compressive strength (up to 20%) probably related to the fact that MK consumes calcium hydroxide that is then no more available for the later hydration of GGBFS. This last assumption needs to be verified by X-ray and/or microscopic examination of hardened mortar samples.

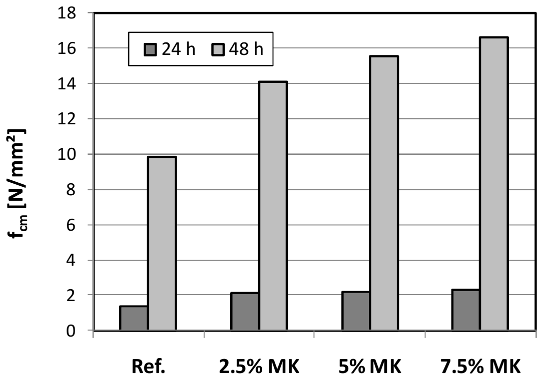

Fig. 5 Effect of MK on the early age strength of mortars made with CEM III/C 32.5 (cement replacement in wt.%)

4. CONCLUSIONS

In this study, chemical admixtures and mineral additions have been used to enhance the hydration rate of high GGBFS cements. Preliminary results seem to indicate that calcium nitrate and sodium nitrate based accelerators are the most effective to reduce the setting time and increase the early age strength of these cements. Encouraging results were also obtained with mortar mixes incorporating very fine metakaolin particles.

From a practical point of view, methods for accelerating the hardening of high slag cement based concrete could lead to a reduction of the minimum moist curing period to be applied on-site, as specified in the new standard EN 13670:2009 – related to the execution of concrete structures.

5. ACKNOWLEDGEMENTS

The results presented in this paper are part of the research project *BeSlag*. The authors would therefore like to gratefully acknowledge the Public Service of Wallonia (SPW – DGO6) for the financial support. The scientific contribution of Julien Deramaix, student at the University College ECAM (Brussels), was also appreciated.

6. REFERENCES

Bijen, J. (1996), "Blast Furnace Slag Cement for Durable Marine Structures", Association of The Netherlands Cement Industry.
Neville, A.M. (1999), "Properties of concrete", Fourth Edition, Longman.

FORMWORK FOR BRIDGE CONSTRUCTION

Hermann Stift[1], Sergej A. Ksengenko[2], Alfred Preuer[1], András Sütő[3]
[1]Doka GmbH, Amstetten, Austria
[2]NPO "Mostovik", Omsk, Russia,
[3]Magyar Doka Kft., Budapest, Hungary

SUMMARY

A summit meeting of the Asia-Pacific Economic Cooperation (APEC) will be held in Vladivostok in 2012. A 4-lane motorway bridge, 3.100 metres in length, is being erected as a future link to the mainland. With a pylon height of 320 m and a free span of 1104 m this project breaks two world records at the same time. The Doka self-climbing formwork systems are being used so that the pylon will be finished on time. To ensure high-quality concrete placement even at extremely low temperatures Doka covered all seven platform levels with a robust scaffold tarpaulin and constructed a roof consisting of seven sliding segments.
Under the use of the Doka Cantilever Forming Traveller with integrated formwork a 459 m long bridge, as part of the highway R1, is under construction by Hídépítő Zrt. The superstructure is a 3-box girder with inclined webs, span length 85 m, width 26 m, 4+2 lanes, construction time of superstructure 5 month, 6 travellers are in operation.

1. DOKA FORMWORK SYSTEMS FOR BRIDGE CONSTRUCTION

More and more complex bridge structures are typical of the architecture of our times. All over the world. Doka technicians work closely with the clients and bridge designers to put together the most suitable solutions, exactly tailored to each individual situation and to the requirements of the structure. Doka offers formwork systems for:

Fundations, Abutments, Piers and pylons, Pierheads, Falswork constructions, Launching-girders, Cantilevering constructions, Incremental launching, Composite constructions, Arched constructions, Cantilevered parapets.

2. SELF CLIMBING SYSTEMS

2.1 Introduction

Automatic climbing formwork is an efficient solution for every type of high structure. No crane is required for lifting climbing scaffold and formwork, the system is permanent connected to the building. Overview about Doka climbing systems Fig. 1.

With its modular design concept, the crane-independent automatic climbing formwork provides a flexible solution. The platform sizes can be freely selected and accommodated to the geometry (inclination infinitely variable ± 15°) of each structure. The casting height of the casting sections is freely selectable from 2.70 m up to 5.50 m. The system makes possible a weather-independent construction workflow and maximum crew safety. Safety and speed are further ensured by the wide working platforms, railed-in on all sides, and the integrated ladder or stairtower system.

In every case are safe working conditions like on the ground guaranteed. The hydromechanical drive provides an optimum control and operational safety.

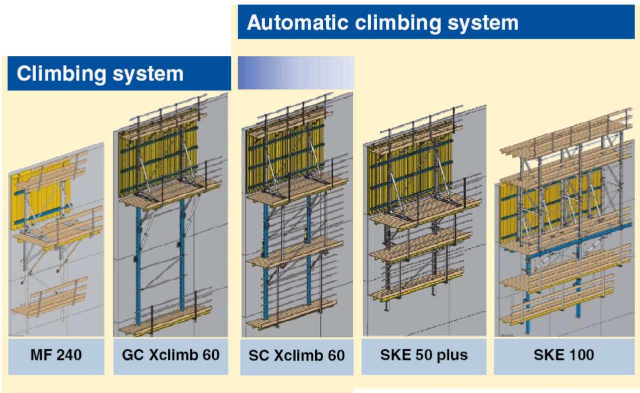

Fig. 1 Overview climbing systems

Fig. 2 Remote control

The hydraulic system allows synchronised repositioning of the entire climbing gang. Up to 25 automatic climbers can be lifted together with one hydraulic unit. A radio remote-control system is an effective way to drive the hydraulic cylinders, Fig. 2.
Due to the high load bearing capacity of the automatic climbing system, payloads can remain on the scaffold while climbing – saving crane capacity.

2.2 Pylon Vladivostok

Data Pylon:

- Location: Vladivostok, Russia
- A – shape pylon
- Height: 320.9 m
- Client: NPO Mostovik
- 71 casting steps
- Casting height: 4.50 m
- Width at base: 12.83m
- Width at top: 7.27 m
- Inclination in front of bend: 5.1°
- Inclination after bend: 2.1°

Solution Doka:

- Outside: SKE 100
- Inside: SKE 50
- Special roof construction

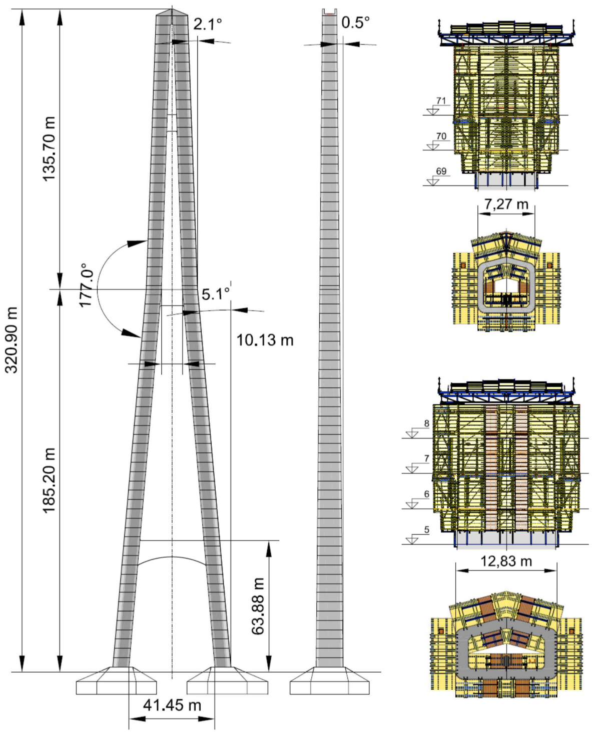

Fig. 3 Pylon

On the Vladivostok project, however, it is not just the geometry of the structure that challenges formwork planning to the utmost. The extremes of the geographic location with frequent stormy weather and bitter cold in the winter months are a major influencing factor on this build. Extremely strict specifications for achieving optimum-strength concrete necessitated yet another formwork-engineering innovation. To ensure high-quality concrete placement even at extremely low temperatures, Doka enclosed all seven platform levels inside a robust scaffolding tarpaulin and built a roof consisting of seven sections. The workplace is fully enclosed inside this structure and can be heated in winter. When ambient temperatures rise and when reinforcing bars have to be manoeuvred into position, the individual sections of the roof slide one above the other on rollers, Fig. 6. The high adaptability of SKE to different geometries and angles of inclination is another advantage on this project, because the cross-section of each tower leg tapers from 12.83 m to a mere 7.27 metres in section 71, Fig. 3. Wall thickness too diminishes gradually from 2.0 metres to 0.75 metre. Adaptation in each concreting section is rapid and straightforward, thanks to telescopic platforms and reducible beam-formwork assemblies.

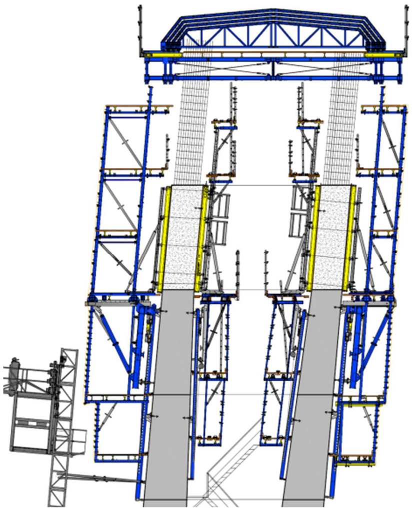
Fig. 4 Regular section


Fig. 5 Super view


Fig. 6 Roof construction

3. CANTILEVER FORMING TRAVELLER

3.1 Introduction

Cantilever forming travellers are the movable skeleton structures carried integrated formwork units used to cast the two cantilever arms of the bridge's superstructure. These skeleton structures cantilever away from the pier, taking the fresh-concrete load of the casting sections that are between 3 and 5 metres in length and weigh up to approximately 250 metric tons, and transfer this load back to the section cast beforehand and capable of carrying this load. When the concrete has set and the two concreting sections have been prestressed, a hydraulic drive advances the CFT along rails to the next section, where it is again anchored, Fig. 6

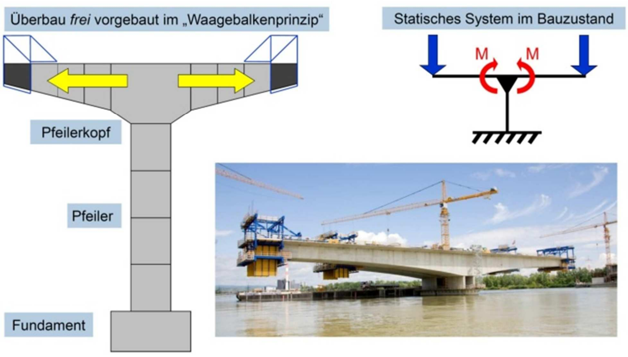

Fig. 6 Principle of free balanced cantilever construction methode

Innovations of the Doka Cantilever Forming traveller see (*Preuer, Broichgans, 2009*)

3.2 Speedway bridge Nitra, Slovakia

Under the use of the Doka Cantilever Forming Traveller with integrated formwork, a 360 m long bridge, as part of the highway R1, is under construction by Hídépítő Zrt. The superstructure is a 3-box girder with inclined webs, span length 85 m, width 26 m, 4+2 lanes, construction time of superstructure 5 month, 6 travellers are in operation. Maximum concrete load per casting segment is 310 t, in total 59 casting steps, Fig. 7

Fig. 7 Panorama-View Free balanced cantilever bridge construction, Nitra Slovakia

Cross section of the 3-box girder, inclined webs with top blisters, requires complex formwork design integrated into the traveller, Fig. 8, 9, 10.



Fig. 8 left, Cross section of bridge, assembly of traveller at pierhead
Fig. 9 middle, View to Top slab, ready for casting
Fig. 10 right, Postion of travellers last casting step, before closure poor

4. REFERENCES

Preuer, A. and Broichgans, M. (2009), "Innovative Cantilever Forming Traveller (Doka CFT) for Bridge Building", 5th Central European Congress on Concrete Engineering, Baden, September 2009, pp. 229-233

EXPERIMENTAL STUDIES OF STEEL REINFORCED POLYMER CONCRETE

Orsolya Ilona NÉMETH[1], *György FARKAS*[1]
[1] Department of Structural Engineering, Budapest University of Technology and Economics Hungary, 1111 Budapest, Műegyetem rkp. 3-9.

SUMMARY

Polymer concrete (PC) is used more and more often in the building industry. As its use in load-bearing structures requires precise knowledge of material properties, tests were carried out on polymer concrete of specified composition to determine its principal parameters.

The present study determined the binding of reinforcement steel, and compared it with cement concrete. To determine resistance against damage from de-icing salt, cement concrete and polymer concrete test pieces were tested under identical corrosion conditions.

1. INTRODUCTION

Polymer concrete is the material system which comprises a polymer binder, a solid aggregate and possibly modifying and auxiliary agents; it may be formed in the fresh state and sets to stone-like hardness in conditions of normal application.
Tab. 1 shows the results of our previous experiments.

Tab. 1 Strength determined by previous experiments

Flexural strength	28.49 N/mm²
Tensile strength	17.67 N/mm²
Compressive strength	98.70 N/mm²

The reinforcement of structures and the establishment of a connection between structures have two pivotal points, namely the binding strength between rebar steel and polymer concrete together with the minimum anchorage length and the corrosion resistance of polymer concrete, which influences significantly the thickness of the concrete cover.

2. MATERIAL COMPOSITION

The following tests were carried out to determine the properties for the present recipe (Tab. 2). The construction material made by the recipe will here be referred to as “UP polymer concrete”, meaning polymer concrete whose binder is unsaturated polyester.

3. TEST OF BINDING STRENGTH BETWEEN REBAR STEEL AND POLYMER CONCRETE

The binding strength of rebar steel set into UP polymer concrete was determined by a pull-out test (Fig. 1).

The series of experiments involved 60x60x250 mm edge-length UP polymer concrete test pieces with S500 rebar steel rods of diameters Φ_1=8 mm and Φ_2=12 mm embedded in them.

Test pieces were prepared with embedded lengths between 50 and 250 mm, in 50 mm steps (Fig. 2). Five test pieces were made with each embedded length, so that there was a total of 2x5x5 = 50 test pieces.

Tab. 2 The components of polymer concrete

Binder	POLIMAL 144-01 unsaturated polyester	16 w%
Aggregate	2-4 mm particle-size dried bulk graded quartz gravel	38 w%
	0-2 mm particle-size quartz sand	38 w%
Other components	Trigonox 44 B catalyst	3 w%
	CO-1 Cobalt initiator	
	Calcium-Carbonate	5 w%

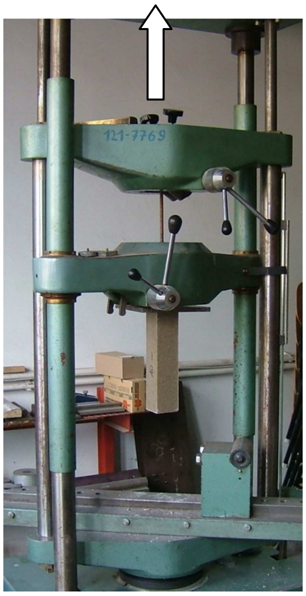

Fig. 1 Arrangement of testing for binding strength

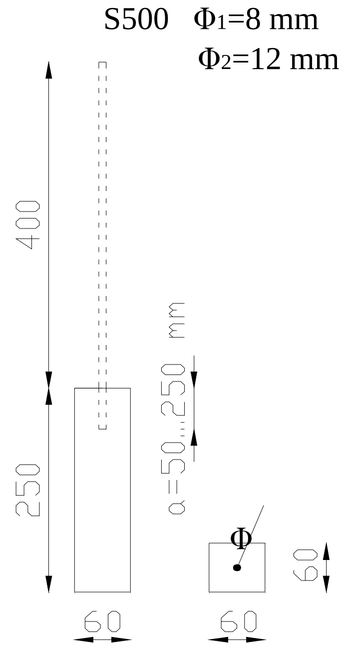

Fig. 2 Design of test pieces for pull-out test (all in mm)

Failure in most test pieces was caused by breaking of the rebar (Fig. 3). As the embedding length was reduced, failure came to be caused by the pulling-out of the rebar.

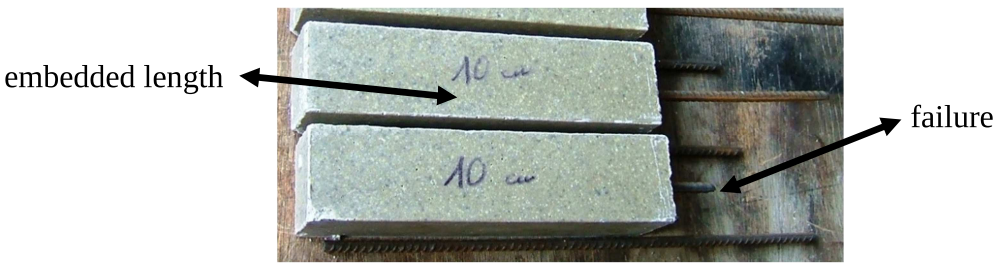

Fig. 3 Failure mode after pull-out test

The binding strength and required anchorage length may be calculated from the force causing the pull-out of rebars. The results for test pieces which failed by rebar pull-out are shown in Tab. 3.

Tab. 3 Results of pull-out test

SD: Standard deviation (N/mm²), CV: Coefficient of variation (%)

Diameter (mm)	**Depth greater (mm)**	**Failure force (kN)**	**Binding strength (N/mm²)**	Average of binding strength (N/mm²)	**SD (N/mm²) CV (%)**	**Anchorage length (mm)**	**Average of grip length (mm)**	**SD (N/mm²) CV (%)**
8	50	37.70	30.00			29.00		
8	50	36.10	28.73			30.28		
8	50	34.30	27.30	28.68	1.08 (3.8)	31.87	30.39	1.15 (3.8)
8	50	36.90	29.36			29.63		
8	50	35.10	27.93			31.15		
12	50	42.30	22.44			58.15		
12	50	43.00	22.81			57.21		
12	50	43.30	22.97	21.19	2.28 (10.7)	56.81	59.26	6.76 (11.4)
12	50	46.20	24.51			53.24		
12	50	34.70	18.41			70.89		

These values show that the minimum recommended anchorage length for UP polymer concrete is 5Φ, much shorter and more economical than the 30Φ - 40Φ values usually used for normally cemented concrete.

4. UP POLYMER CONCRETE CORROSION RESISTANCE TEST

The purpose of this test was to compare the behaviour of steel-reinforced cement concrete and UP polymer concrete test pieces exposed to an aggressive environment.
Nine test pieces of each material were prepared for the experiment in two different geometric forms. Prism-shaped test pieces were made with cross-sections of 20x20mm and 40x40 mm, all of them 160 mm long. A 10 mm diameter steel rebar was placed in the geometric centre of each test piece, parallel with the long side (Fig. 4).

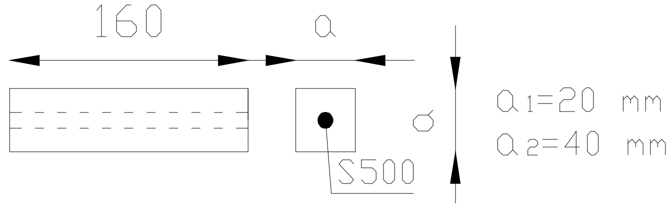

Fig. 4 Design of test pieces for corrosion resistance (all in mm)

Three of each kind of test piece were kept as controls, and the others were placed in a 1:5 ws/ww salt solution. In the first half of the 6-month test, the test pieces were laid horizontally and completely covered by the solution. In the second three months, to enhance the aggressive effect, the prisms were placed standing, with only half of them in the solution, and turned round every two weeks, so that each end was alternately in the solution and in the air.

After six months (Fig. 5), only a tiny amount of corrosion was visible at the ends of the rebars in the UP polymer concrete test pieces. Damage to the cement-concrete pieces had progressed much further (Fig. 6). Those of both material discoloured slightly compared with the controls.

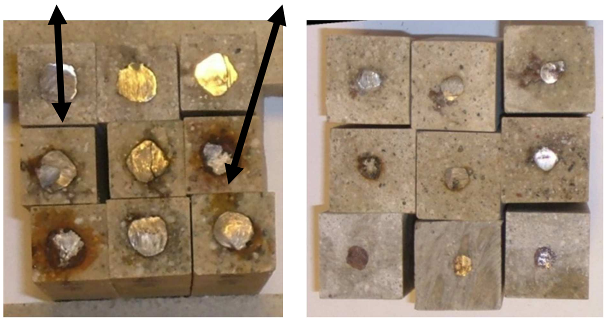

a. 20x20 mm b. 40x40 mm

Fig. 5 UP polymer concrete at the end of corrosion resistance test

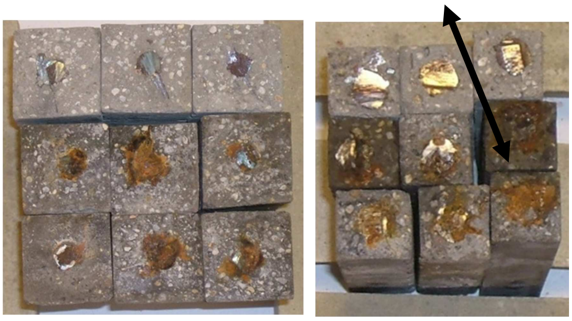

a. 20x20 mm b. 40x40 mm

Fig. 6 Cement concrete at the end of corrosion resistance test

To determine the actual corrosion, the test pieces were sheared paralelly, with the rebar steel. The extent of deterioration was also consistent on the exposed rebars.
The rebars in the UP polymer concrete pieces retained their original condition (metallic shine), the only corrosion being visible at the ends of the steel rods (blackening). By contrast, there was incipient corrosion across the whole surface of the rebar rods in the cement concrete pieces: the surface was matt overall, with rust in some places.

6. CONCLUSIONS

The observations and measurements made during the experiments yield the following conclusions. There is excellent binding between UP polymer concrete and rebar steel. The direct consequence of good steel binding is reduction of the minimum anchorage length. The recommended grip length is about one eighth of that for cement concrete. This is both economical and advantageous for rebar arrangements, enabling simpler and less crowded nodes to be designed.
UP polymer concrete has a high degree of corrosion resistance. The corrosion experiment simulated the effects of winter salting, and caused no substantial damage to the test piece. The steel rebar only corroded at the point where it directly contacted the salt solution. The corrosion experiment bears out the hypothesis that polymer concrete inhibits the permeation of corrosive agents, and so is very well suited to environmental protection applications.
The qualities found in these experiments support the applicability of polymer concrete in load-bearing structures and for connection. Our future research will be extended in this direction.

7. ACKNOWLEDGEMENTS

This work is connected to the scientific program of the " Development of quality-oriented and harmonized R+D+I strategy and functional model at BME" project. This project is supported by the New Széchenyi Plan (Project ID: TÁMOP-4.2.1/B-09/1/KMR-2010-0002).

8. REFERENCES

Farkas, Gy., Nemeth, O.I, “Experimental study of polymer concrete’s mechanical properties” Proccieding of 15th International Conference on Civil Engineering and Architecture, pp.117-123., 2011

INVESTIGATION OF CEM V ECO-CEMENTS BY USING ELECTRONIC SPECKLE PATTERN INTERFEROMETRY (ESPI)

Klaus Voit[1], Konrad Bergmeister[1], Ivan Janotka[2], Markus Klambauer[1]

[1] *Department of Civil Engineering and Natural Hazards, Institute of Structural Engineering University of Natural Resources and Life Science Vienna 1190 Wien, Peter-Jordan-Straße 82*

[2] *Building Testing and Research Institute 82104 Bratislava, Studená 3*

SUMMARY

Due to EU regulations for decreasing the emission of CO_2, new cement kinds are gaining in importance. Therefore a research project between Austria and Slovakia, funded by the EU (Project ENVIZEO), was initiated in 2010. The main ambition of this project is to develop new CEM V eco-types of cements and certificate them for common usage.

The aim of this paper is now to give an overview of the status of the project research and forecast of the usage of the Electronic Speckle Pattern Interferometry (ESPI) to characterize and compare the physical properties of the new CEM V mixtures to standard CEM I cements/concrete. The investigations with ESPI started early in June 2011.

1. INTRODUCTION

CEM V is a Portland clinker saving cement kind that allows the reduction of clinker to a proportion of 40-64% for CEM V/A and 20-38% for CEM V/B respectively by the input of slag sands, puzzolanas and fly ash (according to *EN 197-1, 2000*).

Therefore four new CEM V kinds were created, two Austrian kinds based on slag and fly ash, and two Slovak kinds, one based on slag and fly ash, the other on slag and natural pozzolana. The pozzolana consists of zeolite of clinoptilolite type that is gained from a nearby Slovak deposit. Intensive material testing for the Slovak and Austrian CEM V/A and CEM V/B was performed by the Slovak partner TSUS to determine the technical characteristics. With the help of the processed survey results the application potential for practical use of the new CEM V/A and CEM V/B cement kinds should be justified.

2. CEMENT PROPERTIES

Austrian (AT) CEM V/(A, B) cement kinds are characterized by normal consistencies and mortar workabilities equal and better than those of the reference CEM I 32,5 R (SK). Lower normal consistencies and mortar workabilities are typical for Slovak CEM V/(A, B) products. The use of superplasticizer (polycarboxylate-based, 27 % of dry solids coming from Slovakia) is necessary to improving normal cement consistencies and mortar workabilities. All cements are adjustable on constant workabilities of the mortars around 160 mm. The 90-day compressive strengths of CEM V/A - SK mortars 63,3 MPa and 68,2 MPa of CEM V/A - AT relative to 59,0 MPa of the reference CEM I mortar give clear evidence on the same and higher achieved strength parameters. The 90-day compressive strengths of CEM V/B - SK and AT mortars 46,8 MPa (SK) and 51,4 MPa (AT) relative to 59,0 MPa of the reference CEM I mortar show still sufficiently high strength parameters.

Chemical composition of the CEM V/A and CEM V/B cements (AT and SK) is very similar; typical feature is markedly reduced (by 17 to 25 %) CaO content in the composite cements opposite to CEM I having 60,82 % CaO content. Reduced CaO contents in composite cements indicate improved resistance to chemical attack compared to CEM I cement kind. The pH values of cement extracts between 12.41 and 12.55 (CEM I, both CEM V/A and CEM/V cement kinds - AT and SK) suppose the sufficient embedded steel passivation.

3. ESPI - METHODOLOGY

ESPI is optical measurement equipment that allows contact-free extensive recording of displacement and deformation respectively. It enables 3D measurement of local displacement distribution within a certain strain field with an accuracy of up to 0.1 μm *(Eberhardsteiner, 2002; Buksnowitz et al., 2010)*. For data recording the full-field 3D-ESPI measurement system Q 300 by Dantec-Ettmeyer AG in Ulm, Germany, is implemented. After collecting the raw speckle data (speckle patterns) and calculating the displacement data by the ESPI system, the data is transformed into in-plane strain maps using the post processing software ISTRA *(Dantec-Ettmeyer, 2001)*. For this purpose in-plane displacements were differentiated numerically to calculate strain maps of the different strain components.

The ESPI analyses are performed during compression tests of the various CEM V concrete specimens at different load levels. Strain maps of the different concrete specimens are calculated at certain load steps to visualize strain distribution. For this reason cubic concrete specimens with a lateral length of 150 mm were produced for testing with the ESPI device. The basic composition of the concrete is: 370 kg cement, 176 l water (w/c ≈ 0,47), 1825 kg of aggregate with a maximum grain size of 16 mm. In case of the Slovak cement kinds additionally a superplasticizer was applied.

For each specimen one side of the cube was measured during increase of load that was superimposed in increments of approximately 40 kN. At every step, in-plane deformation in longitudinal and tangential direction as well as out-of-plane deformation is measured in the observed field of view. The observed field of view is a square with a side length of ca. 130 mm. The outer margins of the concrete cube surface (ca. 10 mm each side) is not examined because of the irregular edges of the concrete specimens.

4. PRESENT RESULTS WITH ESPI

For a first analysis several load steps were integrated and the raw speckle pattern, displacement distribution (including vector maps) and strain maps were calculated for the added load step. Finally the load was increased until failure to receive the maximum strength of the sample.

Exemplarily the following figures show the preliminary ESPI analysis of sample CEM V/A1 AT (CEM V/A from Austria) and CEM-V/A3 SK (CEM V/A from Slovakia). For illustration the vector plot derived from the displacement in x- and y-direction is overlaid with the displacement plots. The strain maps were calculated by differentiation of the displacement once horizontally for x-direction, and once vertically for y-direction.

Sample CEM V/A1 AT (shown is load step: 630,5 – 758,9 kN, max. strength: 1152,8 kN) shows the development of a crack in the central part of the specimen. Sample CEM-V/A3 SK (shown is load step: 654,8 – 768,8 kN, max. strength: 1226,1 kN) is not yet broken, but shows a linear high strain area, where a crack will be developing during further load.

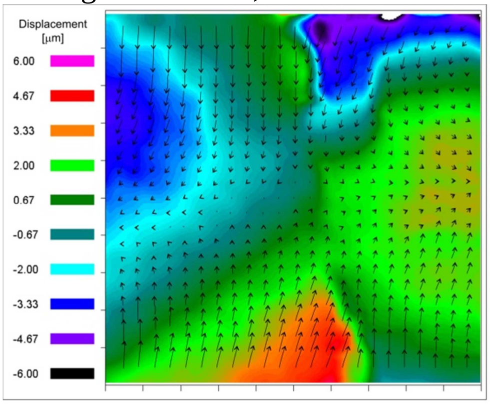

Fig.1 Displacement of CEM V/A1 AT in x

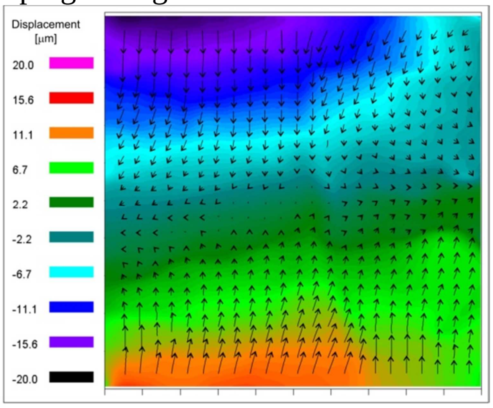

Fig.2 Displacement of CEM V/A1 AT in y

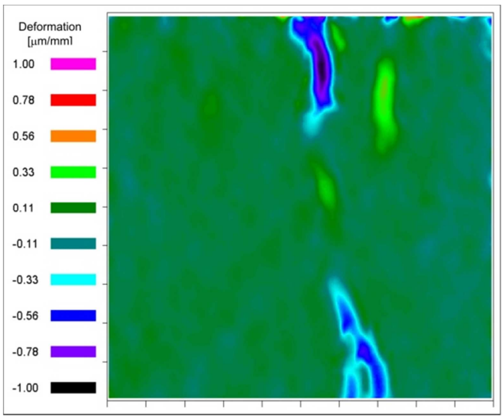

Fig.3 Strain distribution of CEM V/A1 AT in x

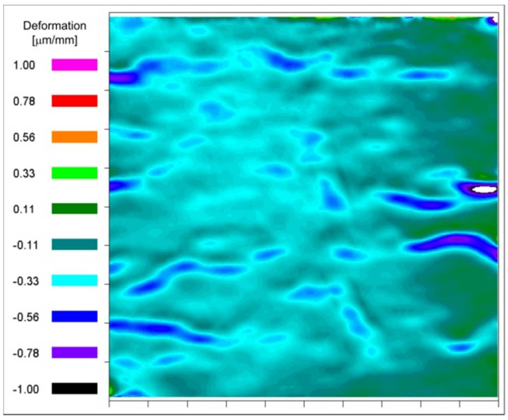

Fig.4:Strain distribution of CEM V/A1 AT in y

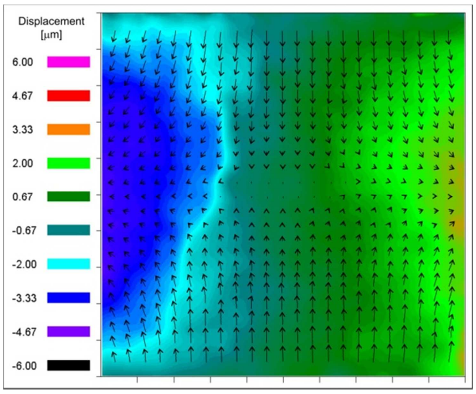

Fig.5 Displacement of CEM V/A3 SK in x

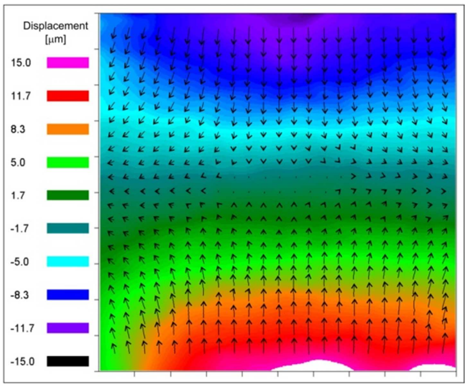

Fig.6:Displacement of CEM V/A3 SK in y

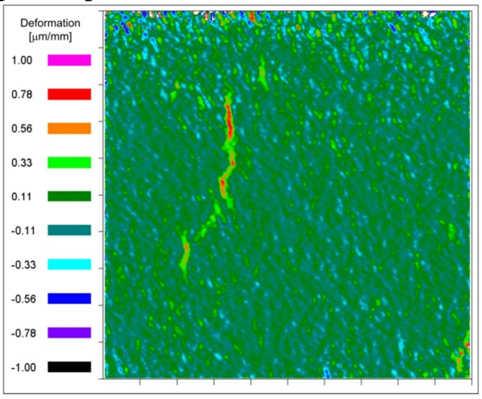

Fig.7 Strain distribution of CEM V/A3 SK in x

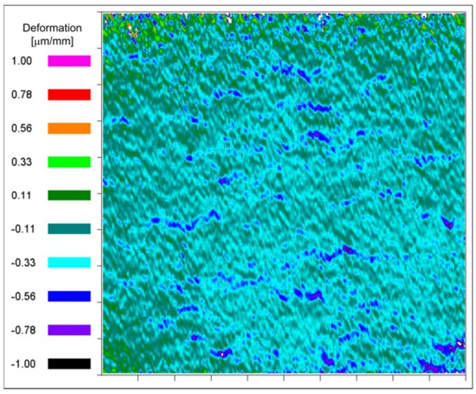

Fig.8 Strain distribution of CEM V/A3 SK in y

5. FORECAST

The concretes are adjusted on the same workabilities and therefore are comparable from the viewpoint of obtained results. The adjustment of concrete mixture composition is based on: 1.) the same cement content – 370 kg/m^3; 2.) the same content of the same aggregates: 710 kg/m^3 of 0/4mm; 420 kg/m^3 of 4/8 mm and 695 kg/m^3 of 8/16 mm (river aggregate from Vysoká pri Morave); 3.) almost the same w/c ratios 0,475 – 0,476 – 0,464 (around 0,47) and 4.) the use of superplasticizer Berament 05-10 (producer BetonRacio, Trnava, SK) necessary for Slovak CEM V/(A,B) cement kinds to maintaining the constant workabilities of the concrete (slumps) between 40 and 50 mm.

The 28-day cube strengths between 42,0 - 47,0 MPa for CEM V/A (AT, SK) concretes and 30,0 - 38,0 MPa for CEM V/B (AT, SK) concretes are comparable with those of the reference CEM I 32,5 concrete (43,0 to 45,0 MPa). Cube strengths of CEM V/(A,B) - SK concretes are enhanced by the superplasticizer use. Suction capacity values are below 6 weight %. The tests performed on cements, mortars and ongoing tests on concrete specimens indicate the suitability of CEM V/(A, B) cement kinds from Austria and Slovakia for the use in construction concrete.

As already shown, ESPI speckle interferometry is a powerful instrument to observe crack development in concrete *(Unterweger et al., 2008)*. By using the ESPI technique it is possible to identify the velocity of crack development and to estimate the ductile-brittle behaviour and the tensile capacity respectively. Thus this method should allow to identify the differences in physical properties of the various CEM V types of cement and concrete and to compare them to standard CEM I. The first experiments show that the ESPI test arrangement is working. The displacement distributions of several samples were recorded at different load steps and strain maps were calculated. The analysis of the existing data and further measurements are in progress.

6. ACKNOWLEDGEMENT

The authors are grateful for the financial support of EU structural funds *Creating the future*: *N00086 „Utilization of ecocements of CEM V (A, B) kind according to EN 197-1 in construction concrete"* in the program of the over border collaboration Slovak Republic - Austrian Republic 2007 – 2013.

7. REFERENCES

Buksnowitz C., Hackspiel C., Hofstetter K., Müller U., Gindl W., Teischinger A., Konnerth J. (2010): Knots in trees: strain distribution in a naturally optimised structure. Wood Sci Technol. 2010; 44(3): 389-398. Springer, Berlin, Heidelberg, New York.

Dantec-Ettemeyer (2001): ISTRA for windows, vers. 3.3.12. Dantec Ettemeyer GmbH, Ulm.

EN 197-1 (2000): Zement – Teil 1: Zusammensetzung, Anforderungen und Konformitäts-kriterien von Normalzement. Europäische Norm.

Eberhardsteiner J. (2002): Mechanisches Verhalten von Fichtenholz – Experimentelle Bestimmung der biaxialen Festigkeitseigenschaften. Springer Wien, New York.

Unterweger A., Spyridis P., Mihala R., Bergmeister K. (2008): Randnahe Vierfachbefestigungen unter Querlast - Experimentelle und numerische Untersuchung. Beton- und Stahlbetonbau 103; Heft 11: 741-747. Ernst&Sohn, Berlin.

SUPERDISPERSED WASTES OF THE FERROMAGNETIC ALLOYS IN THE HIGH-STRENGTH CONCRETE TECHNOLOGY

Irakli Giorgadze[1], Malkhaz Turdzeladze[1], George Tatarashvili[1]
[1] *Faculty of Civil Engineering*
Georgian Technical University
0175 Tbilisi, Georgia, Kostava str.77

SUMMARY

The use of the chemical and active mineral additions in the concrete and reinforced concrete production allows to improve the cement stone structure that conditions the improvement of concrete technical-operational properties. The research of the new additions and their use in combination with known additions allows the more full realization of possibilities of the adhesion substances, solution of cement economy, utilization of the residues and environment defense problems. From standpoint of the utilization of the wastes, the big significance is given to the use of the metallurgy wastes, particularly, of superdispersed ones in the technology of the heavy concrete and reinforced concrete.

1. INTRODUCTION

The use of other plasticizers in combination with superdispersed wastes of the ferromagnetic alloys is one of effective ways of the solution of the engineering-economical problems of the building industry. From this standpoint the wastes of Zestafoni ferromagnetic manufactory in Georgia - the dust of the silicomanganese (SiMn) - are most remarkable. These wastes we have used for production of high strength, rational and durable reinforced concrete.

In result of the experimental research there is established that, when in the heavy concrete the superdispersed wastes of Zestafoni manufactory of ferromagnetic alloy is added, in the system -“cement-aggregate-water”- the maximum approaching of the solid grains is achieved by way of increasing of their number. In such environment, the pozzolanic reaction between the calcium hydroxide, created in result of cement hydrolyze and hydration , and amorphous silicon, existing in composition of superdispersed wastes, actively runs, in result of which the high strength, durable and high density concrete is obtained.

There is known that in result of above mentioned reaction the high-strength , small-crystal calcium hydro-silicates type of CSH (B) are created that conditions the additional increasing of the density of the concrete structure.

There is established as well that the dynamics of increasing of the strength of the concrete, containing the small-dispersed wastes of Zestafoni manufactory of ferromagnetic alloy as addition, conventionally can be represented as a unity of two processes – Mechanical and Chemical.

2. BASIC PART

It should be noted that Zestafoni ferroalloys plant currently produces only silicomanganese. Silicomanganese – SiMn – is a silicious alloy that represents finely dispersed, powdered (dustlike) mixture and that is catched by bag-type filters of air-treatment facilities. In case of plant's operation at full load the quantity of waste in the filters reaches 80000-100000 ton per year. Chemical compositions of finely dispersed waste of ferroalloys melted in the near-abroad countries and their basic properties are represented in the Tab. 1 and Tab. 2. It should be noted that chemical inhomogeneity is characteristic for SiMn dust of Zestafoni ferroalloy plant, that is caused by chemical composition of raw materials and different grades of melted SiMn.

Tab. 1 Chemical Composition

Microfiller's origin	microsaturator's name	Chemical Composition %							
		SiO_2	Fe_2O_3	AAl_2O_3	CaO	MgO	K_2O+ Na_2O	MnO	SO_3
Novokuznetst	Ferro-silico	89.7	2.0	1.7	2.5	1.76	O1.89	_	0.3
Chelyabinsk	Ferro-silico	89.2	2.84	1.68	2.1	1.75	1.43	_	0.5
Yermak	Ferro-silico	70.1	3.43	2.03	11.4	0.9	0.9	_	0.4
Aktyubinsk	Ferrosilicochrome	66.1	2.2	1.3	0.44	14.65	1.8	_	4.2
Zestafoni 1	Silicomanganese	25.2	2.64	4.27	18.6	4.0	2.1	35.8	4.2
Zestafoni 2	Silicomanganese	35.4	2.3	3.86	4.58	4.2	2.4	39.1	3.4
Tbilisi	Fly Ash	58.8	5.5	31.4	0.2	1.0	2.2	_	0.1

Tab. 2 Some physical and technical characteristics of ultradisperse waste of ferroalloy production

Plant	Novokuznetst	Chelyabinsk	Yermak	Aktyubinsk	Zestafoni 1	Zestafoni 2
Ultradispersed leavings	Ferro-silico	Ferro-silico	Ferro-silico	Ferro-silico-chrome	Silico-manganese	Silico-manganese
% of SiO_2	89.7	89.2	70.1	66.1	25.2	35.4
hydravlic activity	98	94	58	40	14.2	25
water requirement	40	33	137	43	26	33
general density of bulk, kg/m^3	260	228	130	266	621	800
specific surface area, g/cm	20 000 – 25 000	20 000 – 22 000	25 000 50 000	20 000 – 22 000	8 000 – 10 000	12 000 – 14 000

3. EXPERIMENTAL RESEARCH OF HIGH STRENGTH CONCRETE

Experimental part of the work has been carried out in the Georgian Technical University's laboratory, while other part has been done in the Kiriak Zavriev Institute of Structural Mechanics and Earthquake Engineering.

Portlandcement produced by "HeidelbergCement" CEM II 32.5 A-S has been used during tests.

Finely disperced waste (SiO_2 content – 35.4%) of Zestafoni ferroalloy plant have been used as ultradisperse additions, while ,,Glenium 27'' as plasticizing agent.

Content of $1m^3$ of B40 grade concrete, with demonstration of its component materials' fractions is given in Tab. 3.

Tab. 3 The composition of concrete mixture

Cement kg/m^3	Gravel kg/m^3		Sand kg/m^3		Water l/m^3	Plasticizer „Glenium 27'' %	SiMn, kg/m^3	water/ cement
	5-10 mm	10-20 mm	0-2 mm	2-5 mm				
420	251.7	671.2	167.8	587.3	145	1.3	70	0.345

The samples were made – cubes 15x15x15cm, to establish the concrete strength on compression were tested in age t_0=3; 7; 14 and 28 days. The results of experiments are given in Tab. 4.

Tab. 4 Concrete compression strengths

№ №	B40 Concrete Compression Strength, Mpa			
	3 Days	7 Days	14 Days	28 Days
1	25.6	40.5	44.3	51.8
2	26.1	38.8	45.5	52.5
3	27.6	38.1	46.5	54.3
4	26.5	37.9	45.6	50.2
5	25.9	37.1	46.1	55.5
6	27.1	36.5	44.3	51.9
7	26.0	39.7	45.8	51.4
8	28.1	38.2	43.5	50.3
9	25.6	39.3	45.6	50.8
10	26.3	40.1	47.5	52.7
11	25.8	38.6	48.0	53.8
12	25.0	39.8	44.8	50.8
$R_{Ave.}$	26.3	38.7	45.6	52.3

It should be noted that 25 km length road pavement has been arranged by above mentioned concrete in the one of the regions of Western Georgia, namely in Guria. Application of mentioned type of concretes is also foreseen at other facilities of Georgia (in the construction of roads, bridges, tunnels and in hydrotechnical construction).

4. CONCLUSIONS

Experiments have shown, that Silicomanganese from Zestafoni ferroalloys plant, with 35% of SiO_2 is good for the production of High Strength Concrete.

5. REFERENCES

Batrakov V., Kaprielov S., Sheinfeld A., (1992) "Influence of Different Types of Silica Fume Having Varying Silica Content on the Microstructure and Properties of Concrete". Fourth Int Conf. On Fly Ash, Silica Fume, Slag and Natural Pozzolans in Concrete, Istanbul, Turkey, May 1992, Proceedings, pp.943-964

Kaprielov S., Sheinfeld A., Krivoborodov Yu. (1992) "Influence of Cement Paste Structure with Silica Fume and Superplasticizer on the Properties of Concrete". Concrete and Reinforced Concrete No.7, 1992, pp.4-7 (in Russian)

EN 206-1: 2002 Concrete-Part1: Specification, performance, prodution and conforming, European Standard

LIGHTWEIGHT AGGREGATE CONCRETE PAVEMENT ON MARGIT BRIDGE IN BUDAPEST

Zsuzsanna Józsa[1], Rita Nemes[1], Olivér Fenyvesi[1]
[1] Department of Construction Materials and Engineering Geology
Budapest University of Technology and Economics
1111 Budapest Műegyetem rakpart 3.

SUMMARY
The reconstruction of Margit Bridge in Budapest is a significant project in the life of the city. The bridge is a protected national monument and has to serve the increasing traffic and public transport too. Several new solutions are used during the design and the building processes too. In this paper some material properties of the temporary pavement of the Bridge are evaluated and discussed, which was built with an innovative technology in Hungary.

1. INTRODUCTION

The Margit Bridge in Budapest is a roadway above arch bridge with six spans and has a side bridge to the Margit Island. The middle of the bridge is curved (at 30° angle), here the pillar is wider because of the connection of the side bridge. The bridge has key importance in the traffic of Budapest; its last reconstruction was more than 30 years before 2009. The reinforced concrete structure of the bridge was rebuilt after the Second World War, but at 2009 was in completely deteriorated condition and needed replacement. Due to the requirements changes in the traffic it was also necessary to widen the pavement of the bridge.

During the reconstruction it had to be maintained on the bridge of the tram traffic and of the wheeled vehicles (building traffic, vehicles marked with distinctive, public transport, etc.) too. Due to this the bridge was divided along the longitudinal axis of the construction and the reconstruction was built in two sections. In the first building period tram rails were moved to the south-side from the middle of the bridge (Fig. 1).

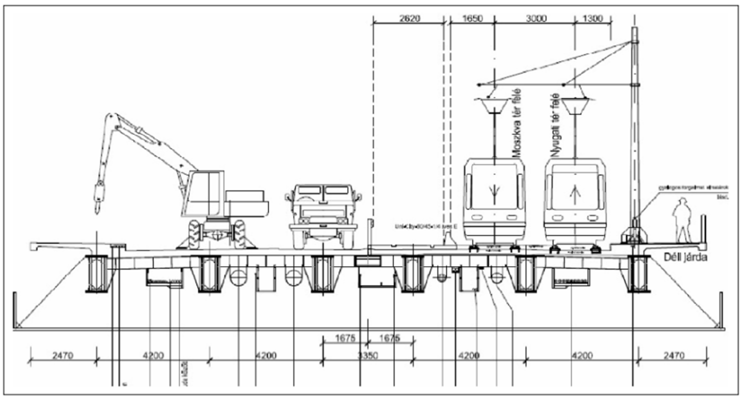

Fig. 1 Cross-section of the bridge during first period of reconstruction *(Benedek et al. 2010)*

After milling of the asphalt layer the temporary tram rails were put to the existing reinforced concrete slab. To ensure the wheeled vehicles traffic on the bridge, the gap between the rails had to be filled up to the top of the rails. Because of the bad conditions of the structure no additional load could have been put on the existing bridge. The milled asphalt layer was 12 cm thick, the new temporary layer should be 20 cm thick because of the height of the rails and the rails had also loaded the structure. In the first idea the pavement would be wood. For this the installation would be difficult and cca. 450 m^3 wood were needed, maintenance and environmental problems encountered too. This pavement would be very noisy and in winter weather also dangerous. So the contractor MH-2009 Consortium (Közgép Machine and Metal Structure Manufacturing Company Limited., A-Híd Építő Zrt.(Hídépítő Co.), Strabag MML Ltd.) commissioned the Department of Construction Materials and Engineering Geology of the Budapest University of Technology and Economics to give alternative structures and materials instead of the wooden pavement. It was obvious to investigate the opportunity of using lightweight aggregate concrete (LWAC) pavement. According to the statical design, body density of the applied lightweight aggregate concrete had to be under 1500-1600 kg/m^3 (Fig. 2).

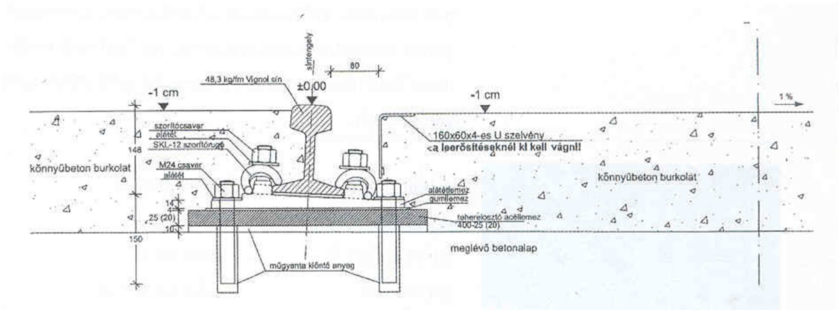

Fig. 2 The temporary LWAC pavement and a tram rail in it *(Nemes et al. 2010)*

In Hungary earlier there was no example for using LWAC on bridges, but in worldwide there are several examples for this, mostly in case of the structures not of pavements *(fib, 2000)*. Based on earlier experiments we suggested to build LWAC pavement on the bridge, which was finally allowed. The pavement had to work cca. one year long. The strength requirement was low: LC 20/22 compressive strength grade was enough. This should not be increased because of the durability requirements as the pavement was temporary. (e.g. 25 cycles of frost resistance was enough instead of the common tested 150 cycles.) There was very short time for the design procedure, so the optimal concrete mixture could not be tested and defined correctly, so the requirements were defined based on earlier test results and technical literature data *(Faust, 2003)*.

2. DURABILITY

There are limited data are available about the durability of LWACs in aggressive environment. LWAC due to its closed cement-stone structure is as waterproof as normal concretes at the same water-cement ratio and hydration level.

The *frost resistance* of LWAC is good, if the aggregate itself is frost resistant. Resistance against de-icing salt frost of concretes made with aggregate with high porosity is better as others made with quartz aggregate. (e. g. in Canada instead of air entrainer admixture fine crushed clay brick aggregate was used *(Erdélyi, 1997)*.)

The *water content and absorption capacity* of concrete especially influence durability of the structure, because most of the corrosive materials (e. g. chloride, sulphates) penetrate in the material with water. Beside this other corrosion processes need water (e. g. steel corrosion). The porosity of LWAC is higher than of normal concrete, so the water content of LWAC can be higher by air dry conditions, which could be important in the point of view of durability.

LWACs are rarely applied for construct abrasion-resistant surfaces, because most of the aggregates have bad abrasion resistance, so there are only few research results in this field. So we have made a test to compare the abrasion resistance of a normal concrete and LWAC made with expanded clay aggregate with the same cement mortar matrix. The volume reduction of abrasion showed, that the normal concrete corresponded to the highest XK4(H) grade, and the LWAC to the XK3(H) grade. Altogether lightweight particles did not bleeded from the surface during the abrasion test due to the better bond between lightweight aggregate and cement stone.

3. LWAC MIX DESIGN FOR THE TEMPORARY PAVEMENT ON MARGIT BRIDGE

Based on our research results and the references the following described LWAC was suggested: cca. 1600 kg/m^3 body density, minimum LC20/22 compressive strength grade, expanded clay aggregate (with min. 4 N/mm^2 crush resistance). This mixture by adequate quality controll can be correspondent to abrasion, forst and deiceing frost resistance in the designed one year lifetime. The mix design was made by Holcim Zrt. With the leadership of Béla Migály tests were made for determine definitive mix parameters.

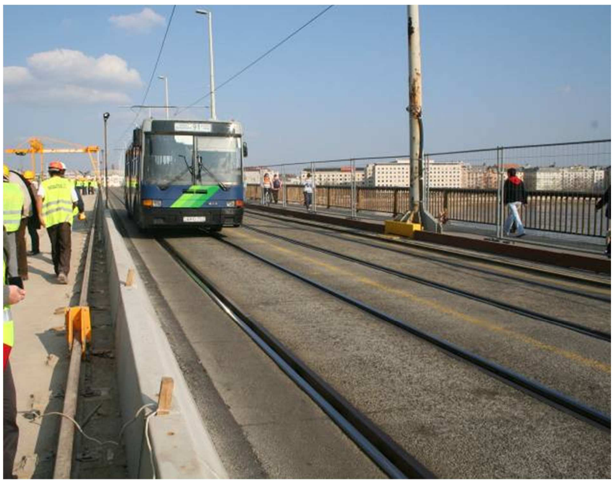

Fig. 3 LWAC pavement

Sign of concrete:
LC20/22-XC1-XF4-8-F2

Mix:

CEM I 42.5 R	360 kg/m^3
Water	180 kg/m^3
Water-cement ratio:	0.5
0-4 mm sand	420 kg/m^3
Liapor HD 4-8 (5N):	600 kg/m^3
Averak FM 66T:	0.5 %
Ravenit V7:	0.5 %
Ravenit LP Mischöl:	0.2 %

To reduce body density and increase frost resistance of LWAC 8-10 V% air content was taken in the concrete.

Before the mix design procedure the following properties of expanded clay aggregate were determined (EN 13055-1:2002):

- Water content: 10 m%;
- Dry bulk density: 730 kg/m^3;
- Water absorption capacity: 18 m%;
- Particle density: 1210 kg/m^3.

After testing six test mixtures, changing the cement content, the lightweight aggregate content and admixture dosages the target properties were reached.

4. TESTS AFTER UNBUILDING

The temporary LWAC pavement was unbuilded in July 2010. This did not mean the end of our investigations. During unbuild of the pavement (after it worked one year long) we took specimens from the LWAC and later took several tests on them. The same tests were taken on specimens were made at the building of the pavement and stored in laboratory conditions. So we could determine the affect of the environmental conditions on LWAC properties. In the

laboratory long term tests were also taken, which could not be made before building of the pavement. New results can be applied later in LWAC constructions.
The *frost resistance* was tested on prism (non-standardized 70 x 70 x 250 mm) specimens for 50, 100 and 150 cycles, with the same reference specimens. The requirement was 25 cycles. Each tested specimen case the compressive strength was reduced by 15%. However the specimens were not standardized it can be seen that this is almost the limit of the compliance. It was interesting that the compressive strength did not reduce between 50 and 150 cycles.

The *Young's modulus* was also tested on 70 x 70 x 250 mm prism specimens on 100 mm length, with loading the specimen up to the 1/3-th of the compressive strength in 3 cycles. The average of measured values of the Young' modulus was 14 070 N/mm^2. This corresponds with the calculated value of the standard ModelCode 1990 based on the compressive strength and the body density of LWAC:

$$E_C = 2.15 \times 10^4 \times \left(\frac{f_{cm}}{10}\right)^{\frac{1}{3}}$$

The reducing coefficient for LWAC:

$$\left(\frac{\rho}{2200}\right)^2 = \left(\frac{1450}{2200}\right)^2 = 0.435$$

Calculating with LC20/22 the result is: 13 500 N/mm^2.

Shrinkage was measured also on 70x70x250 mm prism specimens from 1 to 421 days age on the surface of the concrete on 200 mm basic length. 6 specimens were tested. After 421 days the average shrinkage was 0.8 ‰, which is unexpectedly good value in case of LWAC. At 1 week age 0.1 ‰ and at 3 months age 0.7 ‰ average shrinkage was detected (Fig. 4).

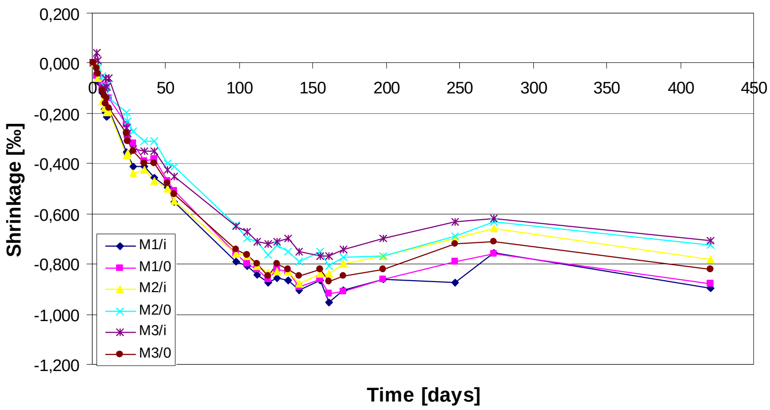

Fig. 4 Shrinkage of LWAC specimens

5. REFERENCES

Benedek B., Józsa Zs., Nemes R., Migály B. (2010) „Ideiglenes pályaburkolat a Margit hídon könnyűbetonból", in Hungarian (LWAC temporary pavement on Margit Bridge) in Beton vol. 2010/7-8. pp. 3-8.

EN 13055-1:2002 "Lightweight aggregates – Part 1: Lightweight aggregates for concrete and mortar" Brussels 2002

Erdélyi, A. (1997) „Fagyállóak-e a légpórusképző szer nélküli nagyszilárdságú betonok", in Hungarian (Are frost resistant the HSCs made without air entraining admixtures?) in Beton vol. 1997/12 pp. 10-11

Faust (2003) „Leichtbeton im Konstruktiven Ingenieurbau", Ernst&Sohn

fib (2000) „Lightweight Aggregate Concrete", CEB-FIP guidence documents bulletin 8.

Nemes R., Józsa Zs., Benedek B., Migály B. (2010) „Miért is készült könnyűbetonból az ideiglenes pályaburkolat a Margit hídon?", in Hungarian (Why the temporary pavement of Margit Bridge was built with LWAC?) in Építési Megoldások vol. 2010/4 pp. 20-25.

STRUCTURAL BEHAVIOR OF ULTRA-HIGH PERFORMANCE CONCRETE (UHPC) ELEMENTS (PRISMS) SUBJUCTED TO BENDING-FRACTURE ENERGY

Victor Văgîi[1], *Cornelia Măgureanu*[1], *Ciprian Ţibea*[1]
[1] *Civil Engineering Faculty*
Tehnical University of Cluj-Napoca
Str. Gh. Bariţiu No. 25,400027 Cluj-Napoca, Romania

SUMMARY

The Ultra-High Performance Concrete (UHPC) is a new type of concrete, used more and more in slender prefabricated structures. There are many worldwide researches regarding this type of concrete that have revealed very good mechanical and durability properties (such as compressive strengths larger than 150 MPa, durability, etc). UHPC matrix is brittle and, consequently, different types of steel fibers are added in order to increase its ductility.

This paper presents the experimental research towards bending behavior and fracture energy of UHPC elements. The UHPC compositions were designed using different parameters such as fibers type and fibers volume. Two types of steel fibers were used: short straight fibers and long hooked-end fibers. The fibers were added as hybrid (50% short+50%long fibers) or as single type (100 % long fibers).

1. INTRODUCTION

In scientific literature can be found many parameters that can describe the ductility of ultra-high performance concrete reinforced with fibers, or building materials in general.

The most important parameters to describe the ductile character of a material are: fracture energy and characteristic length (the minimum anchorage length of a fiber in the concrete matrix).The purpose of this project is studying the fracture energy depending on three parameters: the volumic percent of fibers (1.5% to 2.55%), type of fiber used (only the long and hybrid ones), but also the dimensions variation of the samples (prisms with 100x100x400 mm and 150x150x600 mm).

The fracture energy $\left(G_f\right)$ is defined as the amount of energy needed to completely separate a sample (ex: a prism submitted to bending). The characteristic value of this can be determined computing the area beneath the effort diagram and the deflection measured at mid-span. As the value of the fracture energy increases, the more ductile the material is (it has a large deforming capacity even after reaching the maximum bearing capacity and the fracture occurs slowly).

The most frequently, fracture energy is determined on prism samples submitted to bending in 4 points. Between the two applied forces, the moment has a constant value and the shear force is zero.

These two have a slot in the middle with a minimum height of $0.1 \cdot a$ (a-the dimension of the cross-section) to induce the starting point of the fissure (due to weakening of the section).

Both RILEM (*RILEM –Technical Recomandation for the testing and use of construction materials*) and Japanese standards (*JCI-S-001-2003*) specify the fact that they can be used to determine both forced-crack mouth opening displacement curve (F-CMOD) and forced-load point displacement curve (F-LPD) from the mid-span.

2. EXPERIMENTAL PROGRAMME

To achieve ultra-high strength concrete were used steel fibers having the following characteristics: long fibers with Lf_1/d_1=6/0.175 and short fibers with Lf_2/d_2=6/0.175 (where Lf_1; Lf_2 - fiber length and d_1; d_2 - fiber diameter) (*Şoşa I. 2011*)

The fracture energy was determined on prism samples with following dimensions: 100 x 100 x 400 mm and 150 x 150 x 450 mm. The volumetric percentages of the elements were 1.5% respectively 2.55%. The elements were realized with hybrid fibers (50% long fibers and 50% short fibers), and also only with long fibers for each volumetric percent separately. There were executed minimum 6 elements separately for each type of prism, reinforcing percent and type of fibers. In Fig. 1 is presented the testing mode of the elements:

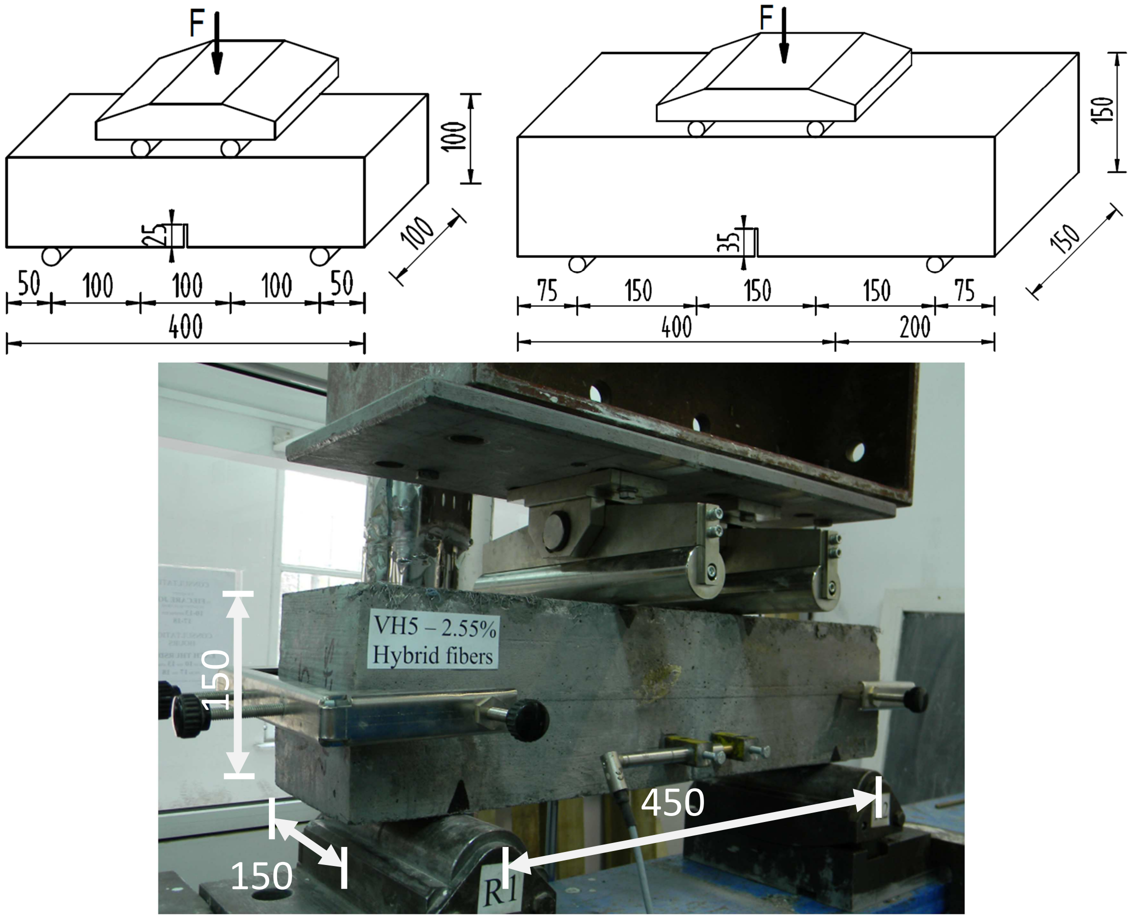

Fig. 1 The characteristics of a section and the test mode

3. RESULT AND DISCUSSIONS

The fracture energy was calculated by determining the characteristic curve between the load and deflection related to the RILEM methodology, on prism samples (100x100x400 mm and 150x150x450 mm) submitted to bending in 4 points. The experiment was performed with a digital hydraulic press with both deforming velocity and constant loading. During the determination there were measured both the deflection at the mid-span and the opening of the fissure after reaching the ultimate deformation of the concrete matrix. Loading velocity has the value of 250 μm/min. In Fig. 2 and Fig. 3, there is presented the relation load-deflection, in the case of studied elements.

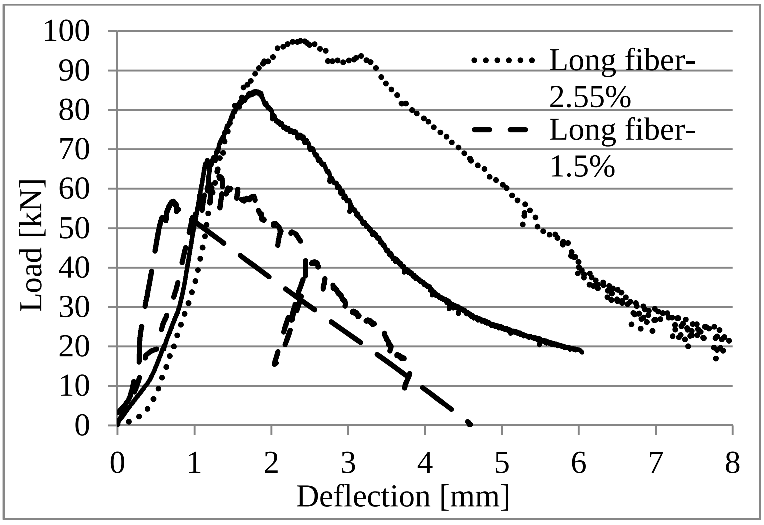

Fig. 2 Characteristic curves load-deflection for prisms with 150x150x450mm dimensions

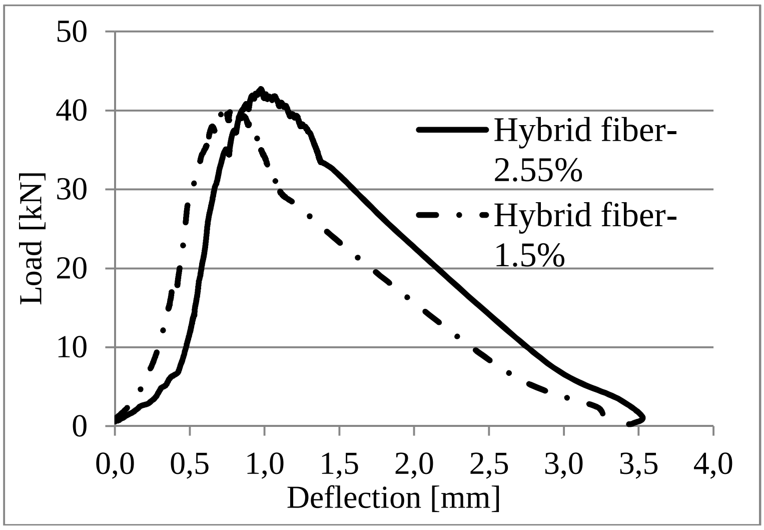

Fig. 3 Characteristic curves load-deflection for prisms with 100x100x400mm dimensions

The tensile strength in bending and the ductility of the realized elements, are influenced by volumetric percentage of fibers and by the type of used fibers. Both experimental values and geometrical characteristics are presented in Tab. 1.

The sample dimensions's influence over the fracture energy (G_f) is the following:

- For prisms of 150x150x450mm with volumetric percent of 2.55% fibers, G_f increases with 29% besides the case of the 100x100x400mm prisms.
- In the other cases (for volumetric percentages of 1.5%; 2.55% - hybrid fibers,but also for volumetric percent of 1.5% long fibers) G_f decreases indirect proportionaly with the increase of the sections, as shown in Tab 1.

Tab. 1 Fracture energy G_f

Concrete type	Specimen dimensions [mm]	Ligament dimensions [mm]	Volumetric percentage [%]	Type of fibers	**G_f** [N/m]	**$f_{cm,cub}$** [MPa]
UHPFRC	100x100x400	100x75	2.55	hybrids	8923	189
	100x100x400	100x75	1.5	hybrids	7535	178
	100x100x400	100x75	2.55	long	19930	184
	100x100x400	100x75	1.5	long	7345	172
	150x150x450	150x115	2.55	hybrids	5210	189
	150x150x450	150x115	1.5	hybrids	3840	178
	150x150x450	150x115	2.55	long	25776	184
	150x150x450	150x115	1.5	long	3435	172

4. CONCLUSIONS

- Higher strengths lead to a significant reduction in elements' deadweight thus lowering their transportation costs while also achieving greater spans.
- Increased ductility and greater energy absorption recommend their use in Seismic Areas.
- The reduction of concrete volume for structural elements to only 1/3÷1/2 of their conventional volume.
- Due to the ductile behavior of UHPC with steel fiber reinforcement, no shear reinforcement is needed.

5. ACKNOWLEDGEMENTS

This paper was supported by the project "Doctoral studies in engineering sciences for developing the knowledge based society-SIDOC" contract no. POSDRU/88/1.5/S/60078, project co-funded from European Social Fund through Sectorial Operational Program Human Resources 2007-2013. Also, the authors would like to express their gratitude to CNCSIS for financing the research program within the PCE-PN II-IDEI Program, code 1053/2007.

6. REFERENCES

RILEM (1993) „Technical recomandations for the testing and use of construction materials", pp. 99-110

Japan Concrete Institute Standard (2007), Method of test for bending moment–curvature curve of fiber-reinforced cementitious composites, JCI-S-003-2007, Japan.

Şoşa I. (2011), „Proprietăţile fizico-mecanice ala betoanelor de ultra-înaltă performanţă".Ph Thesis.

UTILIZING CONCRETE SAWING SLUDGE AS EFFECTIVE MICRO FILLER

Genadij Shakhmenko [1], Janis Justs [1], Girts Bumanis[1], Patricija Kara[1]
[1] Department of Building Materials and Units
Riga Technical University
Kalku 1, Riga, Latvia, LV-1658, e-mail: gs@apollo.lv

SUMMARY

Concrete sawing waste is sludge (SL) containing small concrete particles and water. The idea of presented work is application of the sawing sludge in concrete production as micro filler. Micro particle size distribution of sludge was determined and compared with traditional micro filler. Experimental work included preparation of traditional and self-compacting concrete containing sawing waste. Test results indicate good workability characteristics of the concrete mixes containing sawing sludge. In the case of self-compacting concrete containing high dosage of sludge, reduction of mechanical properties was recorded. Experimental results indicate that it is possible to find the optimum dosage of sludge, which ensures the required performance characteristics of concrete.

1. INTRODUCTION

Extrusion technology in modern pre-cast concrete plant provides sawing of concrete elements with diamond tool in water environment. Concrete sawing sludge (SL) is stored in special tanks for further utilization. The average amount of produced waste is about 0.5-1% of the total amount of concrete. Sludge utilization is a problem in operation of a pre-cast concrete plant. The main idea of the presented work is application of the sawing sludge in concrete production as micro filler.

The information about utilization of the sawing sludge is not sufficient. With the increasing volumes of concrete production it is turning into a serious environmental issue. The information, which is generally available, is about the waste water and water sludge containing residual cement from concrete mixing plants and agitator trucks *(Chatveera et al, 2006).* The authors *(Sato et al, 1999)* declare that sludge water with 3% of solid content ratio can be used up as mixing water if the constant amount of ready-mixed concrete is produced every day.

2. SLUDGE CHARACTERISTICS

Concrete sawing sludge (SL) being investigated is material taken from real pre-cast concrete plant. Used waste material contains 70% of water and 30% of dry small concrete particles. The size of more than 95% of particles being less than 0.063 mm. Bulk density of sludge paste 1240 kg/m^3 and dry particle density 2650 kg/m^3.
Particle grading analysis was determined by laser diffraction method, test was performed in water environment. The results indicated the presence of fine particles with a wide size range from 1 up to 20 μm, the average particle diameter being 6-8 μm.

Significant differences of gralunometric composition among samples which were delivered at different times were not observed (Fig. 1). Grading curves determined for traditional micro-materials: dolomite powder, silica fume (microsilica) and normal Portland cement type I are shown for comparison on Figure 1. According to the data of grading analysis, the particle size distribution of sludge is similar to cement. Particles of dolomite powder are more coarse 10-100 μm) but silica fume is the finest material with smaller particle diameter up to 1 μm. Granulometric composition results are necessary in order to design the concrete composition. It makes possible to provide an optimum particle packing.

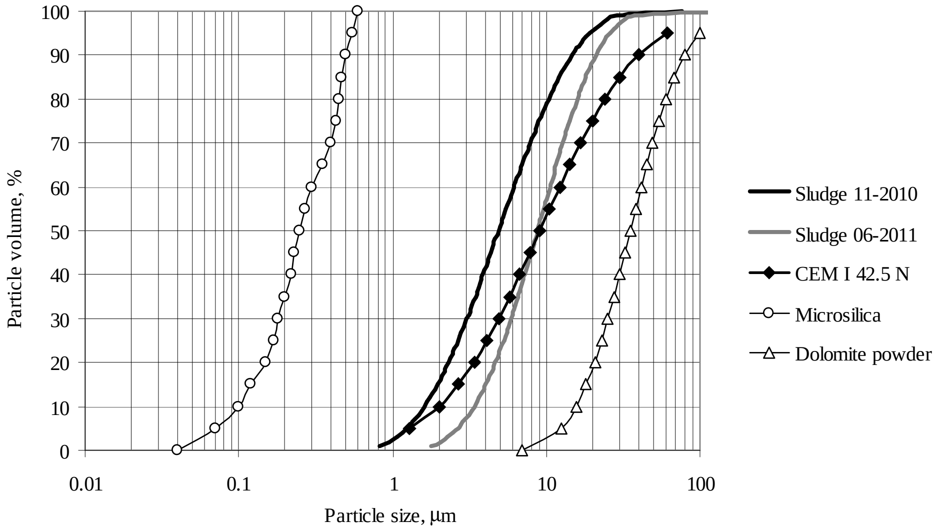

Fig. 1 Comparing of grading size distribution

3. METHODS AND MATERIALS

Experimental part included preparation of ordinary concrete mixes (OC) and self-compacting concrete (SCC) containing saw sludge as micro filler. Sawing waste was added to the concrete mixes in the initial paste form. It allowed avoiding additional drying and grinding of the material.

Local commercially available materials were used as fine and coarse aggregates. Dolomite powder (D), silica fume (SF) and concrete sawing sludge (SL) were used as micro fillers. Standard portlandcement CEM I 42.5 was used as binding agent. Concrete components were mixed in the laboratory drum mixer for 4 minutes, testing samples – 100 × 100 × 100 mm cubes were produced. Standard curing conditions (temperature 20±2°C, RH > 95±5%) were provided during the process of hardening. Sample compressive strength testing was performed according to LVS EN 12390-3:2002 standard, rate of loading was 0.7 MPa/sec.

Consistency of ordinar concrete mix was tested using standard cone slump test, but self-compacting concrete consistency was tested by means of cone flow and V-funnel methods.

4. CONCRETE MIX COMPOSITIONS AND TEST RESULTS

The first part of experimental work consists of making reference concrete mix and replacing part of sand by sawing sludge. Mix design and compressive strength results are summarized in Tab. 1. It was observed, that concrete mixes containing sawing sludge have more plastic and homogeneus consistency comparing to reference mix. Experimental results indicate that optimum dosage of sawing sludge 1.5 % (36 kg/m^3), maximum compressive strength result was achieved in this case.

Tab. 1 Concrete mix compositions and compressive strength

Percent of sludge:	**0**	**1.5**	**2.5**	**5.0**
Portlandcement CEM I 42.5 N	350	350	350	350
Gravel 10/20 mm	520	520	520	520
Gravel 2/10 mm	520	520	520	520
Sand 0/4 mm	730	719	712	694
Sludge		36	61	122
Water (added + sludge water)	215	215	220	225
Water / cement ratio	0.61	0.61	0.63	0.64
Concrete mix:				
Cone slump, mm	190	190	160	155
Charecteristics of concrete mix:	Little segregation	Quite homo-geneous	Plastic and homogeneous	Plastic and homogeneous
Compressive strength, MPa:				
2 Day	20.8	21.0	19.9	20.0
7 Day	29.5	31.4	29.4	29.0
28 Day	**37.3**	**41.5**	**36.0**	**36.7**

The second part of experimental work consists of making self-compacting concrete mix (SCC). Two types of SCC mixes were elaborated: with cement content 360 and 445 kg/m^3. Mix compositions and compressive strength results are summarized in Tab. 2.

Tab. 2 SCC mix compositions and compressive strength

Mix composition:	**SF-1**	**D**	**SL-1**	**SF-2**	**50/50**	**SL-2**
Portland cement I CEM 42.5 N	360			445		
Gravel 2/16mm	900			820		
Sand 0/2mm	830			790		
Silica fume	60			90	45	
Dolomite powder		60				
Saw sludge, moisture content 70%			*200*		*150*	*300*
Saw sludge, recalculated to dry			60		45	90
Super plasticizer	7.0	7.0	7.0	10	10	11
Water, incl. sludge water	193	187	204	190	201	233
Water / Cement ratio	0.54	0.52	0.57	0.43	0.45	0.52
Properties of fresh concrete:						
Cone flow, mm	510	595	510	510	510	490
Time 500 mm, sec	3.7	3.2	3.4	5.6	5.9	2.5
V-funnel time, sec	5.6	18.5	6.9	8.7	9.1	5.9
Compressive strength, MPa						
2 Day	30.6	30.0	29.0	40.5	37.1	36.3
7 Day	52.6	52.9	43.9	64.3	56.9	51.5
28 Day	**71.4**	**65.5**	**53.9**	**92.3**	**86.9**	**68.3**

Water dosage in concrete mixtures was selected in order to provide the required SCC concrete flowability. The results of the experiment showed that concrete mixes with concrete saw sludge require more water to achieve mix consistency. The most prospective results were demonstrated by the 50/50 mix based on the composite micro filler containing 50% of silica fume and 50% of saw sludge fine particles. At the age of 28 days, the compressive strength of that mix (86.9 MPa) was just 8% lower in comparison to the mix with silica fume (92.3 MPa) and 27% higher in comparison to the mix SL-2 with saw sludge (68.3 MPa). Such satisfactory results can be attributed to improved micro particle packing properties resulting from optimal micro filler combination.

5. CONCLUSIONS

Test results indicate good workability characteristics of the concrete mixes containing sawing sludge as micro-filler. Adding concrete sawing sludge to ordinary concrete (OC) improves homogeneity of the mix and prevents segregation. Sludge amount above 50 kg/m^3 requires more water, as a result decrease in compressive strength takes place. Experimental results indicate that it is possible to find the optimum dosage of sludge, which ensures the required performance characteristics of concrete.

Experiments with self-compacting concrete (SCC) mixtures confirms possibility to obtain good self leveling properties using only sawing sludge as a micro filler (200-300 kg/m^3). Unfortunently decrease in compressive strength takes place as high dosage of sludge requires more water and higher water/cement ratio.
Composite micro-filler (microsilica + sludge) was proposed as a compromise solution. The mix with the combined micro filler 50/50 content (50% silica fume and 50% of the sludge particles) looks prospective. It shows satisfactory results of compressive strength by utilizing a relatively small quantity of silica fume (it is the most expensive part of concrete mix).
The results of research help to select the most effective way to utilize concrete sawing waste, taking into account economical and ecological aspects.

6. ACKNOWLEDGEMENTS

The financial support of the ERAF project Nr. 2010/0286/2DP/2.1.1.1.0/10/APIA/VIAA/033 „High efficiency nanoconcretes" and RTU ZP-2010/03 project "Recycling of concrete cutting waste as micro filler" is acknowledged.
The authors would like to express appreciation to SIA Betonelements for the provided material – concrete saw sludge – which was used in experimental work.

7. REFERENCES

Chatveera, B., Lertwattanaruk, P., Makul, N. (2006) „Effect of sludge water from ready-mixed concrete plant on properties and durability of concrete", Cement and Concrete Composites, 28, 2006, pp. 441–450.

Sato, Y., Kiyohara, C., Chia-Ming, L. (1999) „Studies on the effective use of concrete sludge - sludge water and pulverized dry sludge", Exploiting wastes in concrete: seminar 5, p. 37-46.

EN 12390-3:2002. Testing hardened concrete - Part 3: Compressive strength of test specimens. LVS. Riga, 2002. 16 p.

Draft prEN 12350-8. Testing fresh concrete – Part 8: Self-compacting concrete – Slump-flow test. Brussels, 2007. 8 p.

MAKING DRYING SHRINKAGE CRACK-FREE STRUCTURES REALITY IN EUROPE BY USING SHRINKAGE-COMPENSATING CONCRETE

Noémi Nagy[1], István Zsigovics [1]
[1]Department of Building Materials and Engineering Geology,
Budapest University of Technology and Economics
Műegyetem rakpart 3., H-1111, Budapest, Hungary

SUMMARY

Present paper introduces the advanced drying shrinkage solution for reinforced concrete structures: Shrinkage-Compensating Concrete. The concept of full shrinkage compensation by means of restrained expansion of concrete will be explained. Shrinkage-Compensating Concrete mixtures made with commercially available expansive additives in Europe will be evaluated regarding their expansive properties, fresh and hardened concrete performance.

1. INTRODUCTION

Shrinkage-Compensating Concrete is customized to eliminate the destructive effects from drying shrinkage on reinforced concrete structures: it provides full shrinkage compensation by achieving the controlled expansion of the material. If designed and built properly it results in concrete structures with zero net volume change and zero stress induced by restrained length change (from drying shrinkage) *(ACI Committee 223).* The objective of present study is to adapt Shrinkage-Compensating Concrete to the European conditions and to educate the engineer community about the beneficial effects of shrinkage compensation by the mechanism of restrained expansion of concrete.

1.1 Research motivation

Volume change from shrinkage is one of the most detrimental properties of concrete, which affects the load-bearing capacity, durability, serviceability and causes unsightly cracks. Shrinkage comes about due to the moisture loss from concrete. The mixing water in concrete is only partially consumed by the chemical reactions of cement hydration. Depending on the cement type, above 0,2÷0,3 water to cement ratio, there is residual free water in the hardened concrete upon hydration. In general the w/c ratio is around 0,5 for normal concrete. Thus concrete structures subjected to drying conditions will shrink due to the departure of free water from the concrete body *(Mindess, S., Young, J., F., Darwin D.)(Mehta, P., Monteiro, P.).* Volume change due to shrinkage is of considerable importance because in practice these movements are usually partly or completely restrained (by reinforcement, subgrade friction, adjacent structure, etc.) therefore inducing stress. Concrete cracks upon shrinkage due to the tensile stress introduced by restraints opposing to the shortening from shrinkage. It is difficult to make concrete which does not shrink and crack. All concrete shrinks. It is only a question of magnitude. The question is how to reduce the shrinkage and shrinkage cracks in concrete structures. As shrinkage is an inherent property of concrete it demands greater understanding of the various properties of concrete, which influence its shrinkage characteristics. It is only when the mechanism of all kinds of shrinkage and the factors affecting the shrinkage are understood, an engineer will be in a better position to control and limit the shrinkage in the body of concrete. As one cannot avoid shrinkage the principle in current engineering practice is to employ various gimmicks (e.g. contraction joints) to accommodate the stresses from restrained drying shrinkage in order to preserve structural soundness. Unlike *Shrinkage-Compensating Concrete*: it *eliminates the tensile stress from restrained drying shrinkage without the need for any discontinuities (=crack, joint) in the concrete structure*. Shrinkage-Compensating concrete has not been utilized to its full potentialities in Europe yet thus to launch that process became the governing motive of the study.

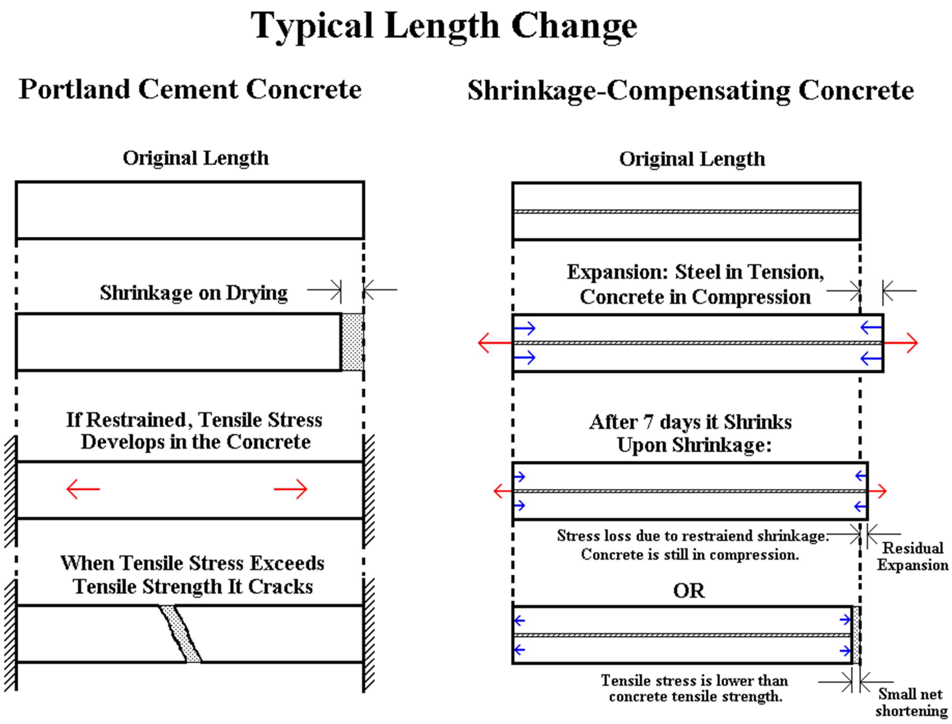

Fig.1 Length change of Portland Cement and Shrinkage-Compensating Concrete

1.2 Concept

The idea of shrinkage compensation by utilizing the induced prestress coming from the restrained expansion of expansive concrete was initiated in the U.S. The purpose of Shrinkage-Compensating Concrete is the full compensation of drying shrinkage in concrete by achieving the controlled expansion (right degree, interval and rate) of the material that is under restraint. Shrinkage-Compensating Concrete expands in the first few days upon pouring, and a form of prestress is obtained by restraining this expansion with steel reinforcement. Since concrete is bonded to steel, expansion stretches the steel reinforcement thereby it is put in tension and concrete –as a reaction– into compression. When moist curing is over Shrinkage-Compensating Concrete shrinks just as Portland cement concrete does. However the tension introduced by subsequent restrained drying shrinkage will be offset by the pre-compression in concrete so there is no harmful tensile stress from shrinkage length change in the structure *(ACI Committee 223)*. Fig. 1 is the graphical representation of length change compared to portland cement concrete. By means of the above described phenomenon we are able to construct reinforced concrete structures with no shrinkage cracks without the need for further provisions to accommodate the harmful stresses from restrained drying shrinkage.

2. EXPERIMENTAL PROGRAM

2.1 Material properties

In the scope of present study one typical concrete mixture has been looked at with various types and ratios of expansive additive to create Shrinkage-Compensating Concrete. As for the concrete mixture itself, it was made with natural river sand and gravel, maximum aggregate diameter was 32 mm; CEM I 42,5 N type Portland cement was used as binder; to achieve Shrinkage-Compensating Concrete different ratios of Portland cement was replaced by expansive additive. The expansive additive is a hydraulic cement with expansive properties so when determining the water to cement ratio the whole amount of binder entails the joint quantity of cement and expansive additive. The amount of binder was kept constant, 330 kg/m^3, for each mixture with w/c=0,53. Polycarboxylate based superplasticizer was used to increase workability - 1% by weight of binder - and also kept constant in order to reveal the effect of the different types of expansive additive on workability. Tab.1 contains the mineral compositions of each expansive additive.

Tab. 1 Expansive additive mineral compositions

Mineral	EXP#1 (%)	EXP#2 (%)	EXP#3 (%)
$C_4A_3\overline{S}$	30	58	29
C_2S	-	20	-
$C\overline{S}$	40	7	50
C_3S	5	-	-
C_4AF	2	-	2
CA	-	-	8,5
$C_{12}A_7$	-	-	0,5
C_2AS	-	-	8
free CaO	20	-	-
other	3	15	2
∑	100	100	100

Tab. 2. Concrete mixture composition

constituents		specific density	composition
binder	cement	3,15	330 kg/m^3
	expansive additive	2,8	
water		1	175 l/m^3
sand 0/4		2,64	680,4 kg/m^3 (36%)
gravel 4/8		2,64	264,6 kg/m^3 (14%)
gravel 8/16		2,64	472,5 kg/m^3 (25%)
gravel 16/32		2,64	472,5 kg/m^3 (25%)
MC Powerflow 2743 superplasticizer		1,1	1% by weight of binder
unit weight			2398,4 kg/m^3
w/c			0,53

Concrete expansion, in the case of Shrinkage-Compensating Concrete, comes about due to the hydration of Alumina-Sulfate-Calcium Oxide ternary system *(Klein, A. 1966)*:

$$C_4A_3\overline{S} + 6C + 8C\overline{S} + 96H \rightarrow 3C_6A\overline{S}_3H_{32}$$

The reaction product is Ettringite (6CaO●Al_2O_3●$3SO_3$●$32H_2O$). The underlying reason of expansion is that Ettringite occupies more space than those constituents it evolved from. The expansion takes place during the first few days under wet curing. It is completely controlled, meaning the desired degree of expansion on the right rate occurs during the right period of time. Upon the removal of curing concrete starts drying. Tab. 2 presents the concrete mixture composition that was kept constant except for the cement÷expansive additive ratio. Three types of –in Europe commercially available- expansive additives have been used. EXP#1 and EXP#3 are expansive systems, containing all the minerals needed for the above mentioned reaction. EXP#2 is a high Calcium-Sulfoaluminate content material, for the expansive reaction it requires the further addition of Sulfates (in the form of Calcium Sulfate). From the concrete mixtures that have been looked at five is presented in the paper with the binder compositions shown in Tab. 3.

Tab. 3 Binder composition for each of the tested concrete mixtures

	Binder				
	Portland cement	EXP#1	EXP#2	EXP#3	Calcium Sulfate
Mixture designation					
EXP#1	90%	10%	-	-	-
EXP#2-1	90%	-	66%	-	33%
EXP#2-2	90%	-	5%	-	5%
EXP#2-3	90%	-	43%	-	57%
EXP#3-1	85%	-	-	15%	-
EXP#3-2	80%	-	-	20%	-

2.2 Sample fabrication and test methods

Since to adapt Shrinkage-Compensating concrete to European application was the main aim of the research the most important fresh and hardened concrete properties have been investigated: compressive strength gain – measured on 15 by 15 by 15 cm cubes according to EN 12390-3:2009 *(EN 12390-3:2009)* at the age of 3,7 and 28 days; expansion – measured on 7,5 by 7,5 by 25 cm bars according to ASTM C878 *(ASTM C878/C 878M-03)* for 28 days and even after; workability – measured by drop table flow test according to EN 12350-5:2009 *(EN 12350-5:2009)* 10, 30 and 60 minutes upon adding water to the system. The strength gain and expansion potential are very closely connected to each other. Some of the aspects: if not sufficient strength you lose the expansion, without the bonds the solid particles reorganize themselves without the increase of the whole volume of concrete (1); if the early strength is very high it reduces the expansion (2); if it expands beyond 7 days the excessive expansion causes microcracks and reduces the compressive strength (3). These are the most important aspects by reason I chose (and everybody who is involved in Shrinkage-Compensating Concrete) to monitor these properties. All further concrete properties are basically the same as for Portland cement concrete since only a minor portion of cement is substituted with the expansive additive. The addition of expansive additive influences the fresh concrete characteristics so it has been checked to ensure sufficient workability for concrete placement. To determine the expansive potential of a certain mixture restrained length change concrete bars are used having two end plates of concrete connected by a threaded rod according to ASTM C878 *(ASTM C878/C 878M-03)* (Fig. 2).

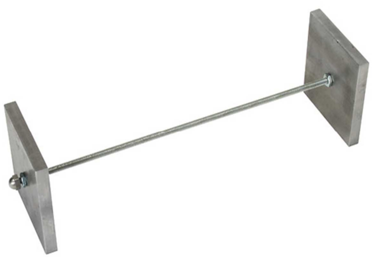

Fig. 2 Restraining cage for determining restrained expansion

3. RESULTS AND DISCUSSION

Expansion is the most relevant property of Shrinkage-Compensating Concrete. The expansion takes place in the first 7 days upon casting. All expansion that takes place beyond 7 days is detrimental regarding the compressive strength and durability of concrete *(ASTM C845 – 04)*. Furthermore we will not achieve the full potential of expansion without wet curing, as the creation of Ettringite requires water in vast quantities. The concrete expansion bars were wet cured –as determined in ASTM C878– for 7 days. With 10-20% substitution of Portland cement by various expansive additives we get 7 days expansion between 0,023 and 0,046% (Fig. 3). The goal is to obtain an expansion strain that equals to or slightly greater than the anticipated drying shrinkage strain of the reinforced concrete structure. Thus EXP#1, EXP#2-2 are proper Shrinkage-Compensating Concrete mixtures in terms of expansive potential.

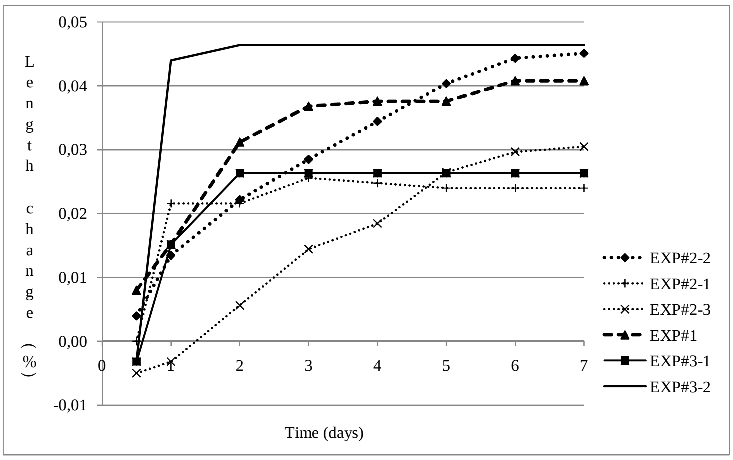

Fig. 3 7 days expansion for different expansive additives

Upon the removal of curing water Shrinkage-Compensating Concrete shrinks the same amount on the same rate as conventional Portland cement concrete and eventually the net volume change from drying shrinkage becomes 0. Fig. 4 presents the 28 days volume change (EXP#3 mixtures are not presented since those are younger than 28 days yet).

It shows that after 7 days all concrete mixtures shrink, so excessive expansion does not occur in any of the cases. The type and quantity of expansive additive of this order of magnitude (10%) does not affect the drying shrinkage characteristics. As it can be seen for mixtures EXP#2-1 and EXP#2-3 the net volume change is already close to 0 at the age of 28 days. However in 28 days only part of the drying shrinkage appears so they are very likely to go into contraction at later ages. To achieve full shrinkage compensation, concrete never goes to contraction. The net volume change is either 0 or little above. In turn the curves of EXP#1 and EXP#2-2 mixtures are very promising and based on literature and practice that kind of expansion will preserve the structure in slight expansion or about 0 net volume change from drying shrinkage.

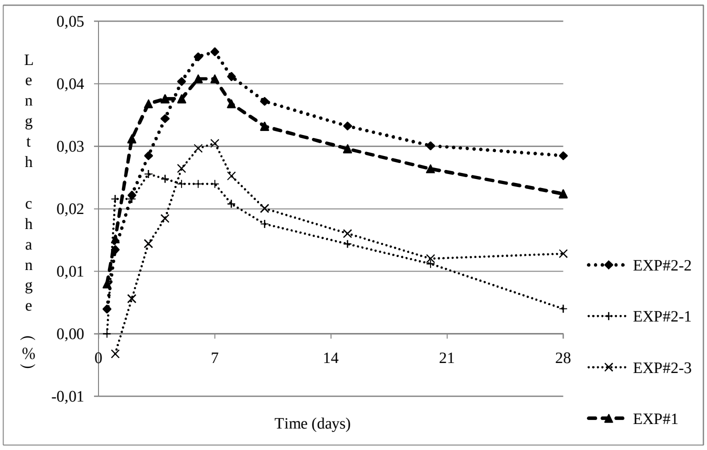

Fig 4 28 days volume change for different expansive additives

The performance of Shrinkage-Compensating Concrete is best monitored by tracking both the volume change and compressive strength. Fig. 5 presents the 3 to 28 days compressive strength values for the above 4 mixture. The compressive strength gain and final values are practically the same for each mixture. In each cases we get C25/30 concrete. With pure Portland cement (330kg/m^3, w/c=0,53) we would get the same strength class.

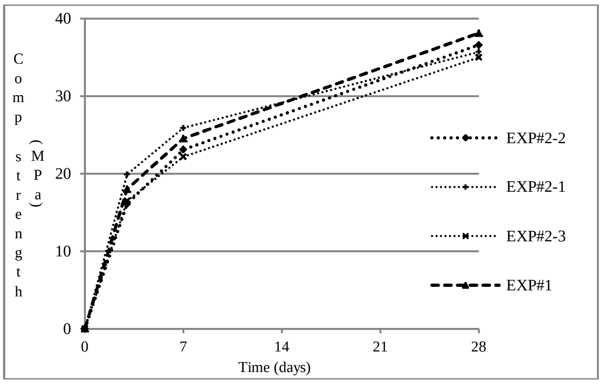

Fig. 5 Compressive strength

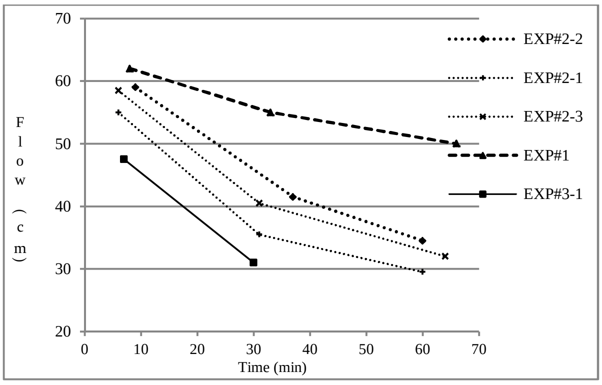

Fig. 6 Fresh concrete performance by drop table flow test

For the proper quality of concrete in the structure good concrete workability is inevitable. The desired workability varies from project to project. As the present mixture composition was not made for a specific job the desired workability is determined as 52±2 cm drop table flow diameter that should be kept for at least an hour. Only EXP#1 mixture satisfies this (Fig. 6), the rest of the mixtures are not even close to meet this requirement. However it was not the point to make all mixtures comply with the prescribed workability characteristics but to present the effect of expansive additives of different types. By changing the type and amount of superplasticizer or by employing different admixtures the workability can be adjusted to the current needs. This is the subject of further research.

4. CONCLUSION

Current design and practice considerations assume that concrete will crack to relieve the restrained strains from drying shrinkage *(Mehta, P., Monteiro, P.)*. With Shrinkage-Compensating Concrete finally a new era of shrinkage solutions dawned on us. Shrinkage-Compensating Concrete is available in Europe. It is adapted to the local materials and its performance meets the requirements set by US research and experience. There are 3 companies commercializing the expansive additive in Europe that it has to be mixed with. For each expansive additives: 1.) adequate expansion and 2.) satisfactory compressive strength increase throughout the first 28 days was proved. Virtually, Shrinkage-Compensating Concrete is recommended for any type of structure where the provisions that have to be done due to drying shrinkage are too expensive, time-consuming, need excessive maintenance during the life-span or simply a high quality structure without drying shrinkage joints and cracks is needed.

6. REFERENCES

ACI Committee 223, Standard Practice for the Use of Shrinkage-Compensating Concrete
Adams, D., L. (1997) Ettringite, the positive side
ASTM C845 – 04, Standard Specification for Expansive Hydraulic Cement
ASTM C878/C 878M-03, Standard Test Method for Restrained Expansion of Shrinkage-Compensating Concrete
EN 12350-5:2009, Testing Fresh Concrete, Part 5: Flow table test
EN 12390-3:2009: Testing Hardened Concrete: Compressive strength of test specimens
Klein, A. (1966) United States Patent 3,251,701, Exp. and Shrinkage Compensated Cements
Mehta, P., Monteiro, P., Concrete: Microstructure, Properties and Materials
Mindess, S., Young, J., F., Darwin D., Concrete

A FORMULA TO PREDICT THE MAXIMUM DIRECT SHEAR LOAD OF SFRC

Tim Soetens[1], Stijn Matthys[1]
[1] *Magnel Laboratory for Concrete Research, Department of Structural Engineering Faculty of Engineering and Architecture, Ghent University, Ghent, Belgium*

SUMMARY

New design approaches to predict the ultimate load capacity of SFRC beams subjected to shear are based on fracture mechanics. These recently developed design models are able to predict the ultimate shear loads more accurate than the semi empirical formulas who were developed in the past. However, when the fracture mechanics based approach is applied, a widely accepted test method to characterise the mode II fracture process of SFRC is of great importance. As a first step to gain more insight in this fracture process, a new formula is proposed to calculate the maximum shear load of SFRC subjected to direct shear by means of a modified JSCE SF-6 test setup.

1. INTRODUCTION

In the past, mainly Z-type push-off specimens were used to characterize the behaviour of SFRC in direct shear. Regarding the complex stress fields showing up around the shear plane during these tests, several researchers *(Mirsayah, 2002)*, *(Majdzadeh, 2006)* and (Appa Rao, 2009) adopted a standard test setup developed by the Japanese Standards for Civil Engineering (JSCE SF-6, 1990) which can be defined as a push-through test rather than a push-off test. The main goal of these experiments is to investigate the influence of fibres to the direct shear behaviour of SFRC. Based on the results obtained by the authors and similar tests conducted by *(Majdzadeh, 2006)* and *(Appa Rao, 2009)*, a general applicable formula is proposed to predict the maximum shear load of SFRC subjected to a push-through test.

2. EXPERIMENTAL TEST SETUP

A total of four different concrete mixes (with a volume fraction of fibres equal to 0%, 0.25%, 0.50% and 0.75%) were adopted. The cement content of the concrete mix was equal to 390 kg/m³ and the w/c ratio was kept constant at 0.48. All SFRC mixes contained low-carbon Dramix® RC 80/60 BN end-hooked steel fibres, which are 60 mm long and have a diameter of 0.75 mm.

Each mixture was used to cast six 150 x 150 x 500 mm³ prisms for the determination of the direct shear strength as well as three cubes with side length 150 mm and three cylinders of 150 mm diameter and 300 mm height to determine the compressive strength and modulus of elasticity. After 24 h of casting, all specimens were demoulded and notches of 4 mm width and 10 mm deep were cut in the two vertical faces of the direct shear prisms (i.e. modification with respect to the original JSCE SF-6 specimens). Until the age of 28 day, when all specimens were tested, the push-through specimens were stored at 20 °C and 95 % of relative humidity.

The push-through shear test was conducted by means of a modified JSCE SF-6 standard test method, which is shown in Fig. 1. The test is conducted in two stages. In the first stage, to avoid undesired effects of bending, both ends are fixed vertically and the specimen is loaded until first visible appearance of the two imposed shear cracks. In the next stage of the test, crack dilation should occur, so the vertical restraints were removed to eliminate the development of internal forces due to friction. During removal of the vertical restraints, the applied force was kept constant. The vertical displacement of the middle part, denoted as the slip, was monitored by means of an Linear Variable Displacement Transducer (LVDT). All performed tests were displacement-controlled (0.01 mm/s) to investigate the post-peak direct shear behaviour of SFRC. The tests are stopped when reaching a slip of at least 15 mm.

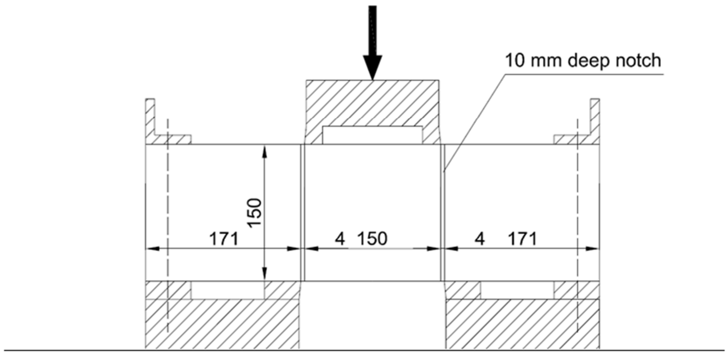

Fig. 1 Used specimen and test setup for a modified JSCE SF-6 push-trough test.

3. RESULTS

As expected, all tested specimens failed along the predefined shear planes which are induced by the vertical notches. For approximately one third of the specimens, a small vertical bending crack appears due to small geometrical imperfections inherent to the test configuration. These fine crack openings (ca. 0.02 mm) close while load is increasing and the prism is failing in shear.

The mean curve (mean of six specimens) of the measured load-slip response is shown in Fig. 2 per volume fraction of fibres. Hereby, the shear load is the load that acts on one shear plane (i.e. the measured applied load divided by two). It is clear that this load can significantly be increased by adding fibres to the concrete matrix: the ratio of maximum shear load between SFRC with 0.75% of fibres and the 0% reference mix is about 2.5. The ascending branch of the load-slip curves is quasi linear. When no fibres are added, a brittle failure has been observed. While in case of the SFRC prisms, the post-peak branch of the load-slip curves indicates a more ductile behaviour when failing in shear. After the peak, the direct shear load decreases exponentially and the residual load at higher slip values seems to converge to the same ultimate load for all different types of SFRC. The same tendency was found by *(Majdzadeh, 2006).*

The mean value of the maximum shear stress as a function of the volume fraction of fibres is shown in Fig. 3. Hereby, the shear stresses are calculated by dividing the average shear load by the cross-section of a single shear plane. Also the lowest and highest maximum shear stress of each series is set out to give an idea of the scatter of the test results. Fig. 3 shows, for the tested range, a linear relationship between the mean value of the maximum shear stress and the volume fraction of fibres. This is quite similar to the conclusions of others researchers (Majdzadeh, 2006 & Appa Rao, 2009).

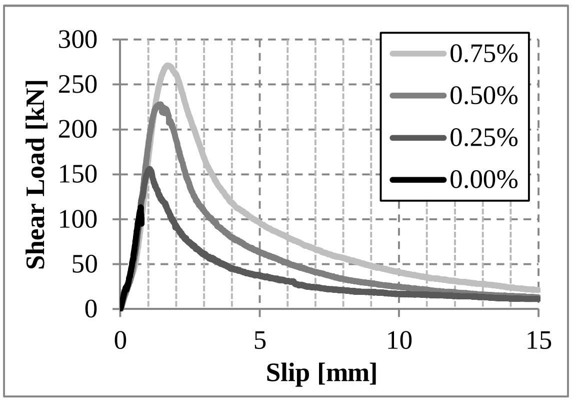

Fig. 2 Load-slip curves for each volume fraction of fibres from 0% to 0.75%.

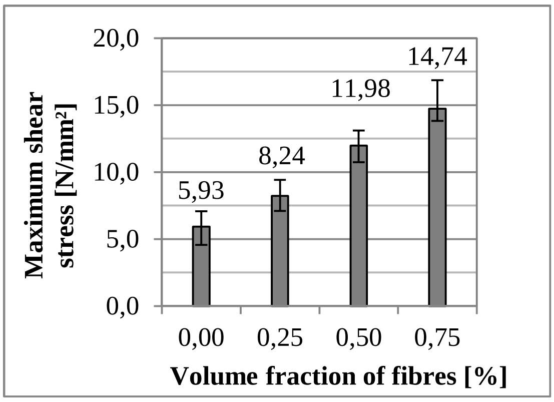

Fig. 3 Maximum shear load vs. V_f.

4. PROPOSED FORMULA

During testing, the observed crack width at maximum shear load are relatively small in comparison to the slip. This might indicate that all fibres are first subjected to a very local shear force before being pulled out (which is necessary for the ductile post-peak behaviour). Therefore the increase in shear stress was found to be in relationship with the amount of fibres crossing the shear plane, the concrete compressive strength, the dowel force that a fibre can reach before it breaks and the fibre volume fraction.

For the experimental test results of (Majdzadeh, 2006 & Appa Rao, 2009) and the current research project, a relationship between the increase of shear stress $\Delta\tau_{max}$ and the fibre volume fraction V_f was found, taking into account the aforementioned influencing parameters (Eq. 1).

$$\Delta\tau_{\max} = f_{cm}^{2.5}\sqrt{\frac{N_f F_d}{A_{sh}}}\frac{V_f}{8.2\left(1+198.9V_f\right)} \qquad \text{(Eq. 1)}$$

With

V_f	volume fraction of fibres	[%]
N_f	the amount of fibres crossing the shear crack	[-]
F_d	ultimate dowel force of a single fibre	[N]
A_{sh}	shear crack surface	[mm²]
f_{cm}	mean concrete compressive strength	[N/mm²]

This equation can be formulated as follows (Fig. 4):

$$\Delta k = \frac{V_f}{8.2\left(1+198.9V_f\right)}\ \text{, with}\ \Delta k = \frac{\tau_{\max}}{f_{cm}^{2.5}\sqrt{\frac{N_f F_d}{A_{sh}}}} \qquad \text{(Eq. 2)}$$

The amount of fibres crossing the shear plane was calculated by means of the Buffon theory for short needles *(Dörrie, 1965)*. The dowel force depends on fibre diameter and tensile strength of fibres.

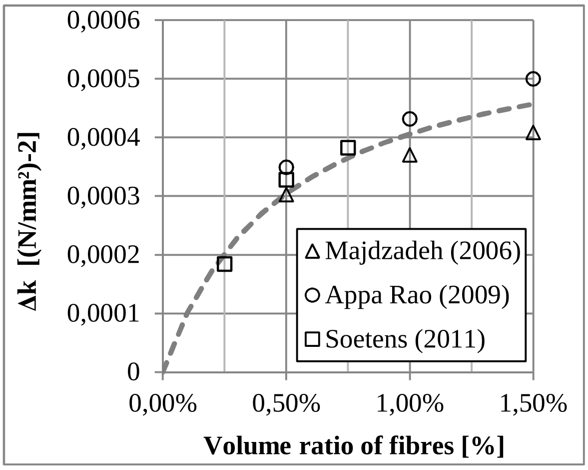

Fig. 4 Δk vs. V_f (Eq. 2).

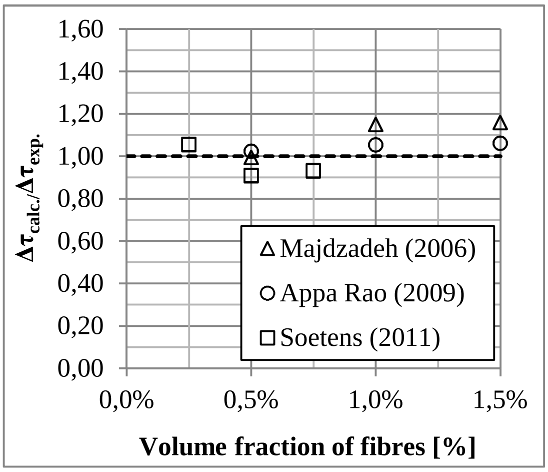

Fig. 5 $\Delta\tau_{calc.}/\Delta\tau_{exp.}$ vs. V_f

With Eq. 1, it is possible to calculate the predicted increase in shear stress due to the presence of fibres. The ratio between the calculated and the measured shear stress increase is shown in Fig 5. This figure shows that the proposed formula is able to predict the beneficial effect of fibres bridging a shear crack. For higher volume fractions an overestimation of shear stress increment occurs while for lower values the prediction is more accurate.

5. CONCLUSIONS

The proposed formula is able to predict the incremental shear load for SFRC prisms subjected to direct shear, taking into account influencing parameters such as volume ratio of fibres, concrete compressive strength and fibre type. However, the proposed relationship is based on a few experimental results, so it is necessary to verify the formula on a wider range of experimental data to improve its accuracy.

For testing of SFRC in direct shear, specific test methodologies are applicable. Hereby, the use of a standardized test configuration is desired, given the inherent sensitivity of direct shear testing to size effects.

6. REFERENCES

Appa Rao, G. and Sreenivasa Roa, A. (2009), „Thoughness indices of steel fiber reinforced concrete under mode II loading", Materials and Structures, nr. 42, pp.1173-1184

Dörrie, H., (1965), „Buffon's needle problem. In 100 Great Problems of Elementary Mathematics: Their History and Solutions", New York, Dover.

JSCE-SF6 (1990), „Method of Test for Shear Strength of Steel Fiber Reinforced Concrete (SFRC)", Japan Society of Civil Engineers, Tokyo, pp.67-69

Majdzadeh, F., Mohamad, F. and Banthia, N. (2006), „Shear Strength of Reinforced Concrete Beams with a Fiber Concrete Matrix", Canadian Journal of Civil Engineering, nr. 33, pp.726-734.

Mirsayah, A. A., Banthia, N. (2002), „Shear strength of steel fiber-reinforced concrete. ACI Material Journal, 66(5), pp. 473-479.

STRUCTURAL BEHAVIOUR OF SINGLY REINFORCED BEAM WITH AER-TECH NOVEL MATERIAL

F.G. Dan-Jumbo, M. Saidani and S. George
Faculty of Engineering and Computing, Department of Built Environment, Coventry University, Priory Street, Coventry CV1 5FB, United Kingdom
E-mail: fubarajumbo@yahoo.co.uk , m.saidani@coventry.ac.uk and samgeorge@orange.net

SUMMARY

The Aer-Tech material is a cement sand bond admixture that comes in various density, with more than 10% by volume of foam in its base mix. It is cooperatively developed by Aer-Tech group as an innovative technological breakthrough offering up to 28MPa compressive strength and a reasonable tensile strength with true ductile behaviour. This paper synthesises the method for complete structural characterisation of tensile properties of Aer-Tech material.
Keywords: Investigating, material, structural, lightweight, Aer-Tech material.

1.INTRODUCTION

Aer-Tech has evolved out of concrete but where stone aggregates were replaced with air cells. The Aer-Tech machine equipment uses a patented screw, mixing system and atomised liquid dosing system which produces a regular, consistent homogeneous mix. The atomiser injects air cells as small as 20 micron into the mix replacing the stone aggregate and the mixing screw mixes sand, cement and water with consistency and even distribution, creating a geodesic structure (see Fig.1). The consistent structure created provides the strengths achieved without using any stone aggregates. This remarkable consistent distribution of air cells creates a geodesic structure, which in effect makes the material unique.
Similar studies have shown that base mixes of uniform distribution of air-cells in a plastic mortar give a higher strength (Nambiar and Ramamurthy, 2006). It is also said that bigger pores in a base mix influence the strength. This is correct as the pore system in cement-base material is conventionally, classified as gel-pores, capillary pores, macro- pores due to deliberately entrained air. However, the gel pores do not influence the strength of Aer-Tech material through it porosity. But the capillary pores and other large pores are responsible for reduction in strength and elasticity (Neville and Brooks, 2004).

2. EXPERIMENTAL PROGRAMME

Tab. 1 Experimental strain

Load	**Demec1**	**Demec2**	**Demec3**	**Demec4**	**Demec5**
0	0.00908	0.00916	0.009317	0.00943	0.008814
3	0.009084	0.009148	0.00968	0.009793	0.009184

The constituent material used to produce Aer-tech material were comprised of: Pro-chem cement conforming to BS8110, pulverized river sand finer than 300µ (specific gravity 2.5), and foam produced by aerating a foaming agent (Aer-Tech Sol) (dilution ratio 1:5 by weight) using an indigenously Aer-tech machine calibrated to a density of 1810kg/m^3.

3. RESULTS AND ANALYSIS

Three reinforced beam were tested for each Aer-Tech mix of 4.78:1, 4.44:1 and 5., Ultimately, all beams showed typical structural behaviour in flexure. Also, during the test of the three beams no horizontal cracks were observed at the level of the reinforcement, which confirms non occurrence of bond failure. Fig. 1 shows that experimental deflection is lower than the theoretical deflection. The illustration of load against deflection graph confirms that in both experimental and theoretical results, the relationship between load and deflection is linear.

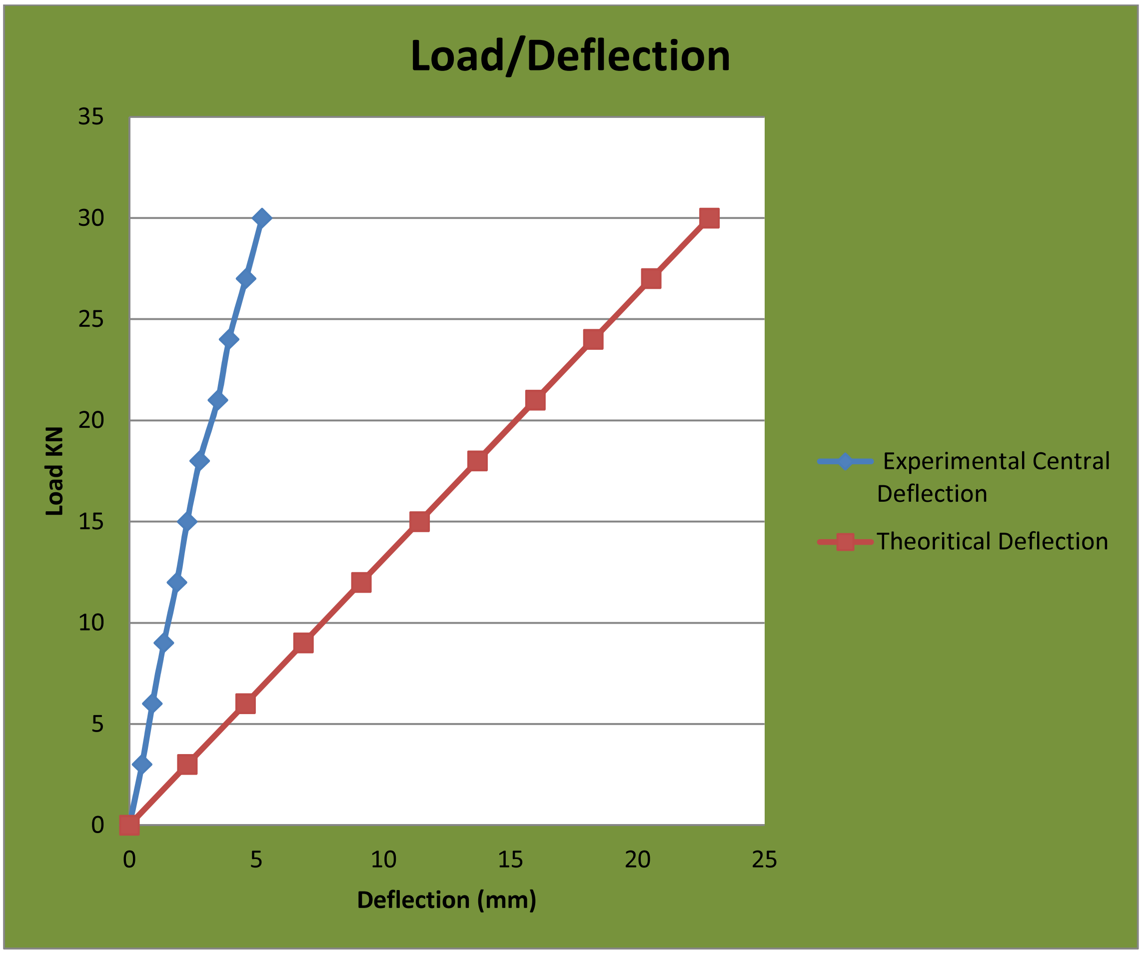

Fig. 1 Experimental and theoretical deflection values for reinforced beam mix one

Ultimately, the ductility of reinforced Aer-Tech beam is primarily important in justifying structural capability of the material. Since, from structural standard it is paramount for a ductile structural material to undergo large deflection at near maximum load carrying capacity, by providing ample warnings to an impending failure.

Aer-Tech reinforced beams had two different modes of failure,. respectively. Obviously, the beam failed in total bending. Thus the ultimate experimental failure load of Aer-Tech material is 38.7 KN, whilst the theoretical calculated ultimate load is 35 KN.

4. CONCLUSIONS

The experimental investigation of reinforced Aer-Tech beam has shown that Aer-Tech structural behaviour is comparable to other lightweight concrete.Apparently, structural assessment of Aer-Tech material has shown that the Aer-Tech beam suffered tension at the bottom and compressive forces at the top, which resulted in the diagonal tension cracks being produced mid span at the bottom of the beam.

5. ACKNOWLEDGEMENT

This study forms part of a research programme supported by Aer-Tech development Ltd

6. REFERENCES

British Standards BS8110 (2000). Testing Hardened Concrete: Part 14.

Nambiar, E. K. K. and Ramamurthy, K. (2006). "Air-void characterization of foam concrete". *Elsevier*, 37 221-230

Narayanan, N. and Ramamurthy, K. (2000). "Structure and properties of aerated concrete: a review". *Elsevier Science Ltd*.

Neville, A.M. and J.J. Brooks, J.J. (2004). *"Concrete Technology"*, Pearson Education Pvt. Ltd., Singapore.

BEHAVIOR OF ULTRA HIGH PERFORMANCE FIBER REINFORCED CONCRETE ELEMENTS SUBJECTED TO SHEAR ACTION

Ţibea Ciprian[1], Cornelia Măgureanu[1], Victor Văgîi
[1] Faculty of Civil Engineering
Technical University of Cluj Napoca
Str. G. Baritiu nr. 25, 400027 Cluj-Napoca, Romania

SUMMARY

Ultra High Performance Fiber Reinforced Concrete is a new material with unique properties like compressive strength, ductile behavior, good behavior in aggressive environment, etc.
The addition of steel fibers to the mix is known to increase its shear strength and, if sufficient fibers are added, a brittle shear failure can be suppressed in favor of a more ductile behavior. The use of steel fibers is particularly attractive for Ultra High Strength Concrete which exhibits relatively brittle behavior without fibers; also the addition of fibers may reduce reinforcement congestion by eliminating conventional stirrups.

This paper presents experimental results of Ultra High Performance Fiber Reinforced Concrete specimens subjected to shear action, casted with different percentage by volume of fibers (1.5%, 2.0% and 2.5%) consisting of hybrid fibers (50% long fibers and 50% short fibers).

1. INTRODUCTION

UHPC is a type of concrete with enhanced properties compared to Normal Strength Concrete due to composition and curing treatment applied. Those parameters increase the ductility and also make UHPC a water resistant material which has almost zero porosity. A major discovery in concrete technology is Reactive Powder Concrete which has compressive strength up to 200 MPa or even more.

Adding steel fibers to the mix further improves the qualities of this unique material. Based on the very good bond between fibers and concrete, the material has enhanced properties in tension and flexure. Fibers can also be used as a replacement for standard shear reinforcement. Even if failure in tension is caused by the failure of the concrete matrix, it is not a brittle failure because the load and deformations are taken up by the steel fibers. The shape of the steel fibers has a direct influence on the deformation and failure behavior of the concrete. Results show that this new material has a better ductile behavior than standard concrete making it therefore suitable for structures with high performance requirements. The further addition of superplasticizers do not impair on any of the characteristics of this material (including workability).

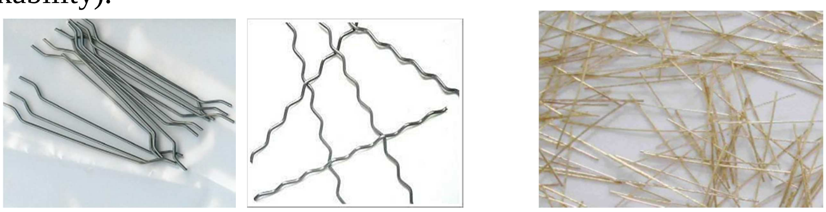

Fig. 1 a) Long fibers; b) Micro fibers.

2. EXPERIMENTAL PROGRAM

Push-off specimens were casted with an Ultra High Performance Fibre Reinforced Concrete mix that has a disperse hybrid steel fibre reinforcement made of 50% long fibres and 50% micro fibres with an mean compressive strength after heat treatment of about 180 MPa . The geometrical characteristics for fibres are: long fibre Lf1/d1=25/0,4 and micro fibre Lf2/d2=6/0,175 (Lf-fibre length; d-fibre diameter). Each specimen was casted with various steel fibre percentage by volume (1,5%, 2,0% and 2,55%) and has the geometrical dimensions as presented in Fig.2.

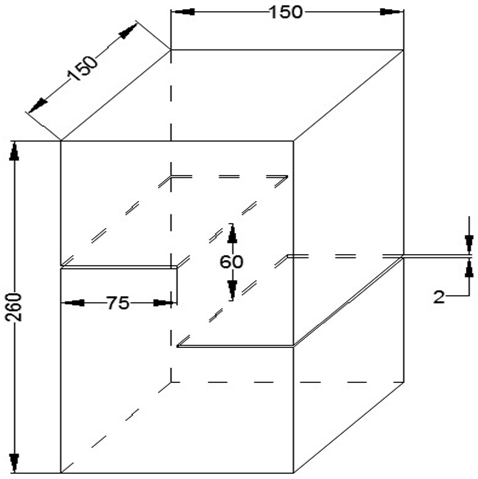

Fig. 2 Geometrical characteristics of push-off specimen.

3. TESTING PROCEDURE

The test was performed on a digital loading machine type Advantest 9 with displacement and force control. Two displacement transducers with a precision of 10^{-4}mm positioned as show in Fig. 3. were used (for recording the vertical and the horizontal displacement, respectively).

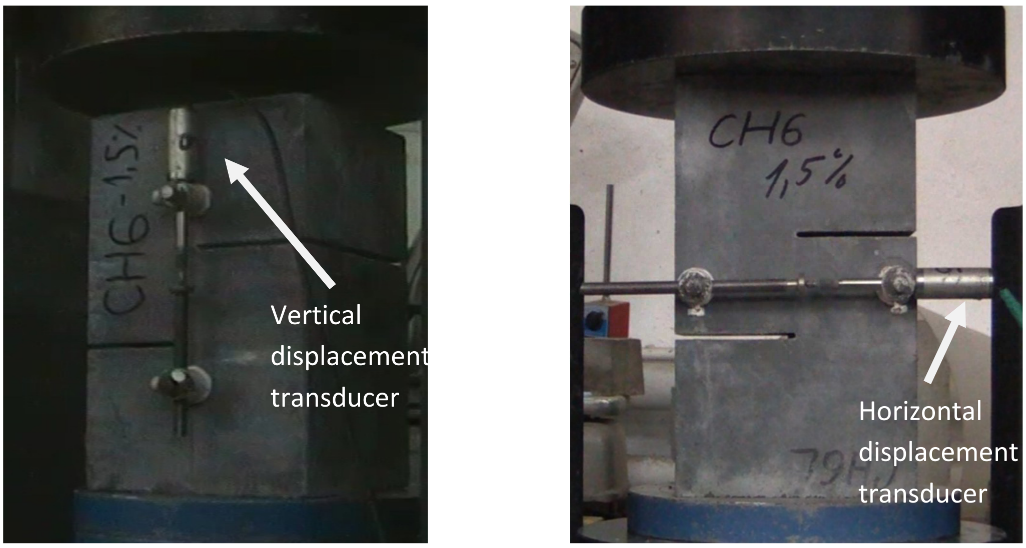

Fig. 3 Test setup of push-off specimen

4. RESULTS OBTAINED

The load-deformation relation experimentally obtained is shown in Fig. 4. Shear failure maximum force related to fibre reinforcement percentage by volume is presented in Fig. 5. The deformation for the peak value of shear force related to fibre reinforcement percentage by volume is presented in Fig. 6.

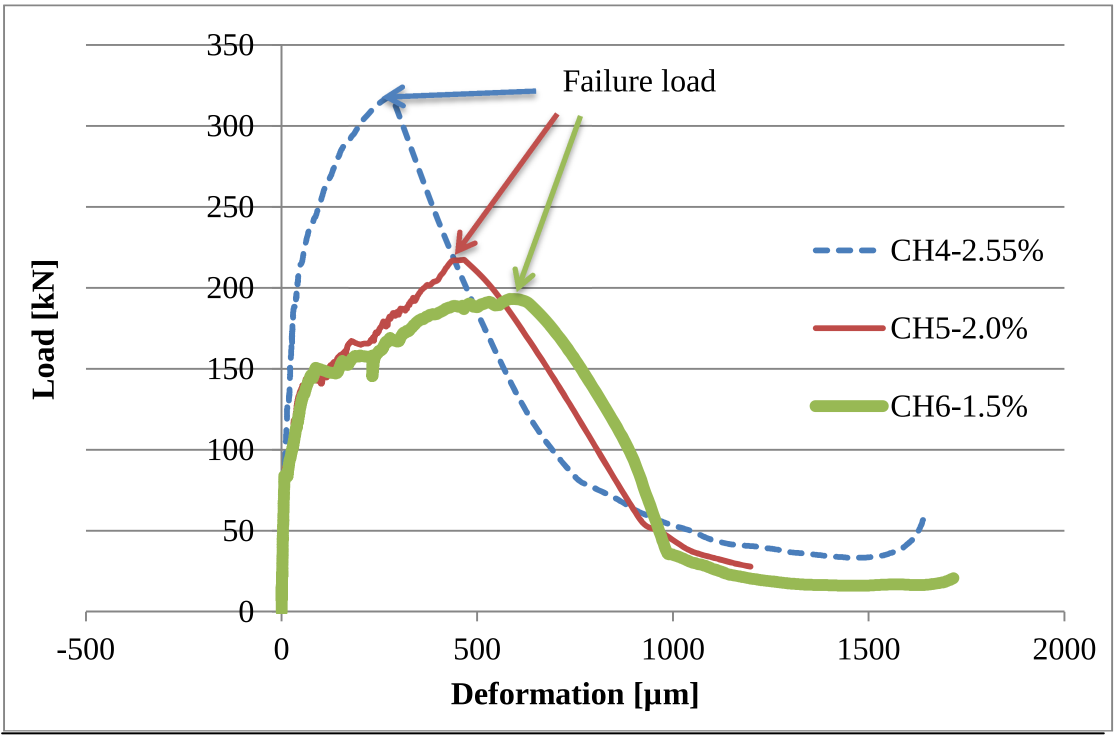

Fig. 4 Load – Deformation graphic for the 3 push-off specimens with different fibre reinforcement percentage by volume

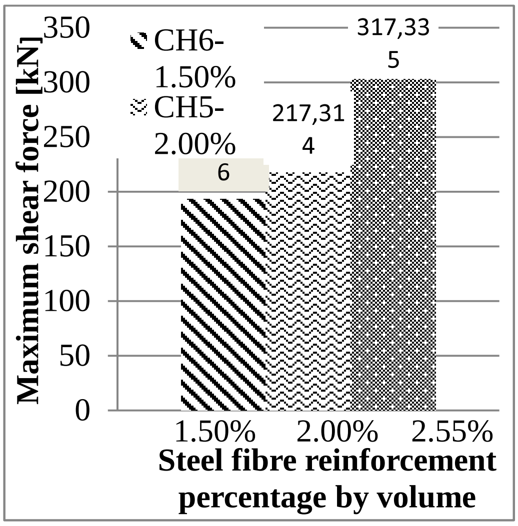

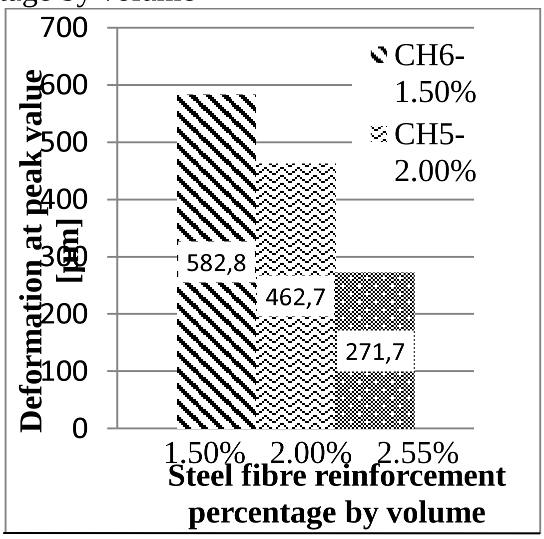

Fig. 5 Shear failure maximum force related to fibre reinforcement percentage by volume

Fig. 6 Horizontal deformation for the peak value of shear force related to fibre

Tab. 1 shows the values of the maximum shear force and different ratios between the push-off specimens like maximum shear force ratios, horizontal deformation for the peak value ratios.

Tab. 1 The values of the maximum shear force and different ratios

ρ_v	symbol	P_U [kN]	$P_U/P_u^{1.5\%}$	$P_U/P_u^{2.0\%}$	W_l [µm]	$W_l/W_l^{1.5\%}$	$W_l/W_l^{2.0\%}$
1.50%	CH6	193.226	1.00	0.89	582.8	1.00	1.26
2.00%	CH5	217.314	1.13	1.00	462.7	0.79	1.00
2.55%	CH4	317.335	1.64	1.46	271.7	0.47	0.59

ρ_v - fibre reinforcement percentage by volume; P_u-maximum shear force value; $P_u^{1.5\%}$- maximum shear force value for CH6; $P_u^{2.0\%}$maximum shear force value for CH5; W_l- deformation for the peak value of shear force; $W_l^{1.5\%}$- deformation for the peak value of shear force for CH6; $W_l^{2.0\%}$- deformation for the peak value of shear force for CH5;

5. CONCLUSIONS

The toughening effect shown in Fig. 4 is a result of the dowel action of steel fibres crossing the shear crack. Fig. 5 shows that the peak load increases with the increase of steel fibre percentage by volume (CH4 has an ultimate shear force with 64% higher than CH6 while CH5 has an ultimate shear force with 13% higher than CH6). In Fig. 6 we can observe a decrease of deformation at peak shear force caused by the increase of steel fibre percentage by volume, CH4 having a decrease in deformation at the peak load.

6. ACKNOWLEDGEMENTS

This paper is possible due to project "Doctoral studies in engineering sciences for developing the knowledge based society-SIDOC” contract no. POSDRU/88/1.5/S/60078, project co-funded from European Social Fund through Sectorial Operational Program Human Resources 2007-2013. Also, the authors would like to express their gratitude to CNCSIS for financing the research program within the PCE-PN II-IDEI Program, code 1053/2007.

7. REFERENCES

American Concrete Institute (2008), Specification ACI 318-08

Brian Barragan, Ravindra Gettu, Luis Agullo and Raul Zerbino, „Shear Failure of Steel Fiber-Reinforced Concrete Based on Push-Off Tests”

CEB-FIP(2008),”Constiitutive modelling of high strenght/high performance concrete”,Task Group 8.2, International Federation for Structural Concrete, ISSN 1562-3610

EUROCODE 2 (2004): Design of concrete structures – Part 1.1:”General rules and rules for buildings”,European Committe for Standardisation

Mariano Valle, “Behavior of Fiber Reinforced High-Strenght Concrete Under Direct Shear”

Sosa Pavel, „Proprietatile fizico-mecanice ale betoanelor de ultra inalta performanta”

INFLUENCE OF INCINERATION REGIMES ON POZZOLANIC PROPERTIES OF WHEATSTRAW ASH FOR HPC/SCC

Syed Ali Rizwan[1], Arsalan Rao[2], and Thomas. A. Bier[3]

1. Professor of Civil Engineering, HoD Structural Enginering Department, NUST Institute of Civil Engineering (NICE), National University of Sciences & Technology (NUST), Islamabad, Pakistan.Member ACI committees 237, 234 &232. Email: syedalirizwan@hotmail.com.Corresponding Author.
2. Post Graduate student, NUST Institute of Civil Engineering (NICE), National University of Sciences & Technology, Islamabad (NUST), Islamabad, Pakistan. Email: rao_nust@yahoo.com Author.
3. Professor and Chair of Construction Materials Technology, Institute of Ceramics, Glass and Construction Materials (IKGB), Technical University Freiberg Germany. E mail: thomas.bier@ikgb.tu-freiberg.de.

SUMMARY

This study is a continuation of a research programme aimed at findings suitable locally available secondary raw materials in High Performance Concrete (HPC) and Self Compacting cementitios Systems (SCPS). Wheat straw is an important agricultural product in Pakistan as well as in the entire world. This paper looks in to the role of various controlled and uncontrolled Incineration regimes on properties of wheat straw ash produced which in turn affects the properties of fresh and hardened cementitious systems. The microstructure, chemical, morphological and mechanical properties of resultant ash were studied using Scanning Electron Microscope (SEM), X-Ray Diffraction (XRD) and X-Ray Florescence (XRF) procedures. It was observed that burning temperature, hold time, burning environment and burning volume all affect the properties of resultant ash and therefore one has to optimise these parameters to get the wheat straw ash (WSA) with excellent properties required for use in high performance self-compacting cemenetitious systems.

1. INTRODUCTION

HPC and SCC both require high powder amounts and essentially containing cement and mineral admixture replacing a part of cement. If mineral admixtures are pozzolanic in nature, then it becomes more advantageous from performance view point. According to ACI 116R, “pozzolan is a siliceous or aluminous and siliceous material, which in itself possesses little or no cementitious value but will in finely divided form and in presence of moisture, chemically react with calcium hydroxide produced during cement hydration at ordinary temperatures to form compounds possessing cementitious properties” *(ASTM C 125 – 00, 2004)*. The pozzolonic property greatly depends on the content of amorphous silica present in addition to particle size and specific surface area of pozzolan *(Rizwan,2006).*

There are both natural and man made artificial pozzolans which are used in cement based systems.The natural pozzolans include volcanic ash or pumicite, opaline cherts and shales, tuffs, and some diatomaceous earths.The artificial pozzolans consist of calcined clay (Metakaolin) and some industrial by products such as fly ash, ground granulated blast furnace slag, wheat straw ash, rice husk ash and silica fume etc *(Mirza; Riaz,; Naseer; Rehman; Khan, and Ali,2009) (Mehta, 2006).*

In developing countries fly ash and silica fume is not available so research is being carried out on pozzolans obtained from basic agricultural products. Wheat straw is composed of both organic and inorganic matter. The major inorganic matter is silica *(Biricik, Akoz, Berktay, Tulgar, 1999)*. Wheat plant takes up silicon component from soil and fertlizers and deposits it in its straw and as an outer covering of the grain and similar situation exists with rice husk. When burnt, organic matter is decomposed and the silica rich inorganic residue is left behind *(Ajay Goyal et al.,)*. Wheat straw in Pakistan has average ash content of 8.0% and average silica content of 74%, when burnt under controlled conditions.
Chemical composition of wheat straw ash (WSA) depends upon a number of factors; type of soil for growing wheat plants, the type of fertilizers used, environment, burning temperature, burning volume and duration of burning *(Biricik,. Akoz, Berktay, Tulgar, 1999)*. Two main issues associated with wheat straw ash are its unburnt carbon and and amorphous silica content which play important role in the hydration kinetics of cement based systems using such pozzolans. The presence of unburnt carbon, greatly increases water demand and reduces silica content of the ash *(Biricik et al., 2000)*. The unburnt carbon (LOI, loss on ignition) is identifiable by dark color of wheat straw ash. Ideal wheat straw ash should have very little LOI.

According to H. Biricik et al *(Biricik, Akoz, Berktay, Tulgar, 1999)*, the ash content and SiO_2 content of wheat straw also depends upon environmental conditions, burning temperature, burning volume and duration of burning. Wheat straw burned at 575±25^{o}C for 5 hrs and then air cooled produces an ash content of 8.6% and has SiO_2 content of (73-74)%. According to Visvesvaraya *(Visvesvaraya 1986)*, the ash content produced is 8–11% and SiO_2 content is 88–91%. The difference in SiO_2 content depends upon soil and environmental conditions exiting during develpinment of wheat crop.

In this research, various incineration regimes of wheat straw were investigated and the comparison was made on the basis of their chemical composition, ash content and their crystalline or amorphous nature.

2. METHODS EMPLOYED FOR INCINERATION OF WHEAT STRAW ASH

Three methods have been employed.

2.1 First Incineration Regime

This comprised of uncontrolled gradual burning of wheat straw sample in electric furnace, weighing 75gm, using a gas burner (outside electric furnace) in a steel tray (6”x12” in size) for about fifteen minutes. During preburning wheat straw was continuously stirrered to have uniform distribution of heat and to avoid the accumulation of smoke. After pre burning the wheat straw sample was inducted in to specially designed and manufactured electrical furnance having a smoke vent and maintained at a temperature of 600 ^{o}C for controlled burning for a duration of 75 minutes. Then the specimen was cooled in air to 20^{o}C to achieve maximum pozzolonic properties. This incineration regimeis shown graphically in Fig. 1.

2.2 Second Incineration Regime

No uncontrolled burning was carried out using a gas burner and a 75 gm sample was directly inducted in to the specially designed and locally manufactured electric furnance already at a temperature of 600 ^oC and then furnace door was closed. After 2-3 minutes the wheat straw sample caught fire due to extensive high temperature inside the furnace and the initial burning process got completed just in five or six minutes because of fire. During fire the temperature did not remain constant and risen to 750 ^oC during these five minutes, as recorded by the temperature measuring device. After the ceasure of fire, specimen was retained in furnance for about 75 minutes and then was cooled rapidly in air to 20^oC to achieve maximum pozzolonic properties. This incineration regimeis shown graphically in Fig. 2.

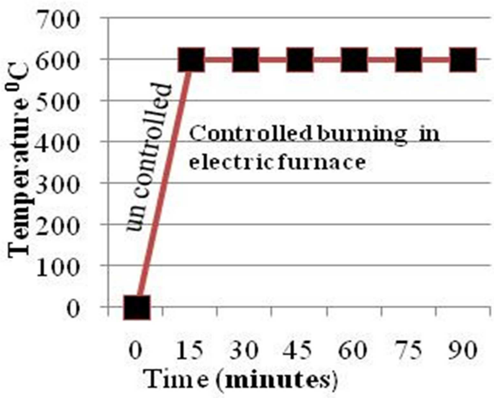

Fig 1. Burning of wheat straw in two stages as per first incineration regime.

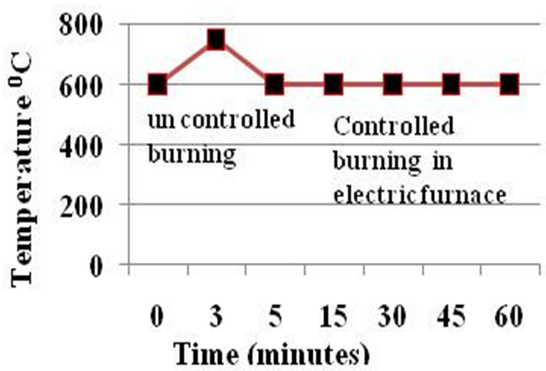

Fig 2. Burning of wheat straw as per second incineration regime.

2.3 Third Incineration Regime

No controlled burning was initially carried out. Wheat straw weighing 300 gm was put in a steel container which was open to the atmosphere and burnt using a gas burner. During initial fifteen minutes, the entire smoke got emitted like the uncontrolled burning stage of the first incineration regime but the sample still kept on burning for about 75 minutes. During burning wheat straw was continuously stirrered to have almost uniform temperature and to enable unburnt carbon get oxidized.

3. RESULTS AND DISCUSSIONS

3.1 Physical Properties of Wheat Straw Ash

Tab. 1. gives the physical properties of WSA produced by the incineration regimes used.

Tab. 1. Physical properties of Wheat straw Ash

Ash produced	1st Regime	2nd Regime	3rd Regime
Colour	white	grey	dark blackish grey
Specific Gravity	2.3	2.34	2.45
Ash Content (%)	8	8.6	10
Avg. Particle Size (μm)	12.22	12.42	12.77
Blain Fineness(cm^2/gm)	3200	3125	2800

According to Tab. 1, ash produced by first two controlled incineration regimes was pozzolanic in nature as per ASTM standards and had lower specific gravity values and higher surface areas, which facilitates pozzolanic reaction, when used in High Performace Concrete

(HPC) and Self Compacting Concrete(SCC) systems as locally available secondary raw materials.

3.2 Chemical Analysis by X-Ray Florscence (XRF)

Tab. 2 Chemical Analysis of Wheat straw Ash

	Ist Regime	*2nd Regime*	*3rd Regime*
Constituents	***% by wt***	***% by wt***	***% by wt***
SiO_2	73.95	71.21	60.39
TiO_2	1.92	0.93	0.93
Al_2O_3	0.91	0.52	2.49
Fe_2O_3	1.15	0.99	2.51
MgO	1.83	1.92	2.75
CaO	5.21	5.25	7.45
K_2O	11.51	11.86	13.92
(SiO_2 + Al_2O_3+Fe_2O_3)	76.25	72.15	65.21

According to Tab. 2 ash produced by using first two controlled incineration regimes contains higher amount of silica and therefore it may have less unburnt carbon *(Biricik, Akoz, Berktay, Tulgar, 1999).* According to Tab. 2 ash produced by first two contrlled incineration regimes meet ASTM C618 requirement for being a pozzolan, that is (SiO_2 + Al_2O_3+Fe_2O_3) must be greater than 70%.

3.3 Particle Characterization By Scanning Electron Microscope (SEM)

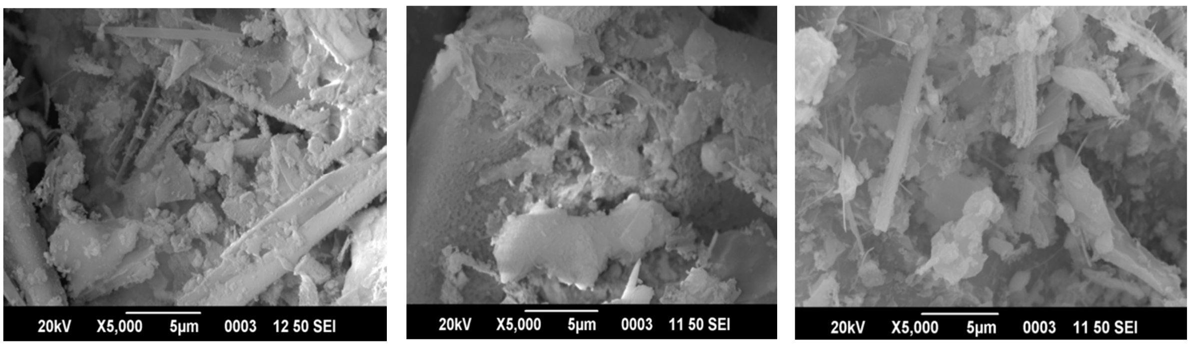

(a) First Regime WSA (b) Second Regime WSA (c) Third Regime WSA
Fig. 3 SEM images of wheat straw ash produced by various incineration regimes

The mean particle sizes of all three WSA was almost similar, however, their surface areas were different with the first two regimes giving more surface areas. It may be possible that first two regimes introduced some degree of internal porosity in the particles which resulted in higher surface areas. Also as per literature *(Rizwan, 2006) (Rizwan, and Bier, 2009),* this may be one of the reason of higher surafce areas. From SEM images of WSA samples, it is clear that ash particles produced by all the three incineration regimes are long, flaky and irregular shaped with rough and abrasive texture. Also these ash particles contain small surface pits which may show their high water demand when used as cement based material in concrete.

3.4 X-Ray Diffraction (XRD)

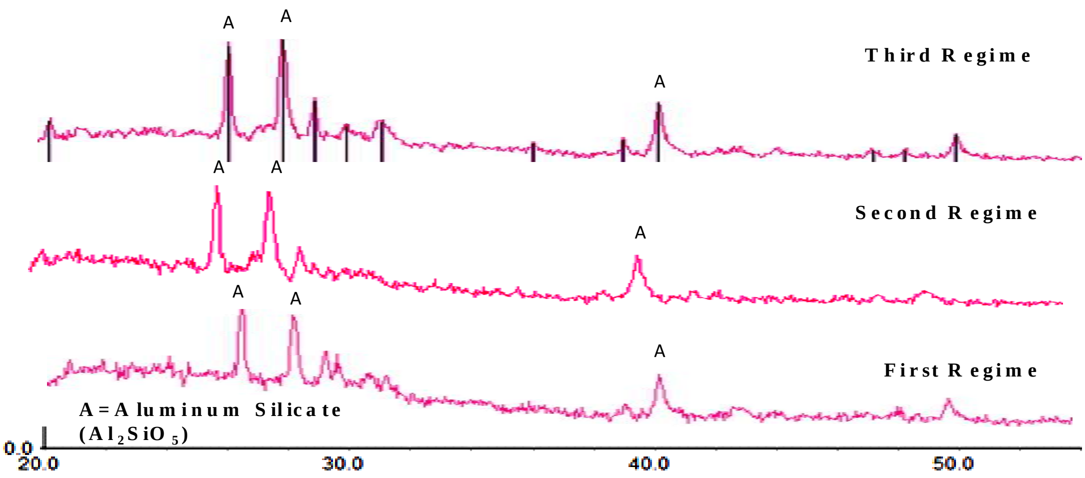

Fig. 4. XRD analysis of wheat straw ash produced by various incineration regimes

XRD technique is used to determine whether wheat straw ash produced is crystalline or amorphous in nature [Rizwan, S. A. and Bier, T. A.]. According to XRD data shown in Fig. 4 wheat straw ash produced under various incineration regimes contained some crystalline minerals (aluminate silicate phase peaks) and amorphous phases. The amorphous phases seem to dominate though the crystal planes shift to slightly lower angles (see the shift of angle towards left) coupled with slightly narrowerer and higher peaks showing increase in degree of crystalanity in wheat straw ash produced by first two controlled incineration regimes. Due to higher oxidation available in the third regime, the peaks shift towards right and height of peaks increases showing it to be more crystalline than other two.

4. CONCLUDING REMARKS

Specific gravity of WSA is lowest in the first regime and it increases towards third regime. The ash became heavier indicating a possible reduction in internal porosity coupled with reduced specific areas.The first and second controlled incineration regimes yeild good quality pozzolanic ash meeting ASTMC618 standard, while the third uncontrolled incineration yeilds an ash, that may not be 100% pozzolan.The avialability of oxygen in the thee regimes was different and seems to be principally responsible for the change in cystalanity degree.The WSA produced in the first two incineration regimes seems to be usable in HPC/SCC as a pozzolanic secondary raw material from view points of strength and durability for a given mix.The mixture rheology can be adjusted using superplasticizer.

5. ACKNOWLEDGEMENTS

The authors are grateful to the NUST Institute of Civil Engineering (NICE) and Military College of Engineering (MCE) for allowing some spare time for the completion of this work.

6. REFERENCES

Ajay Goyal et al., “synergic effect of wheat straw ash and rice husk ash on the strength properties of mortar” Journal of Applied Sciences.

ASTM C 125 – 00, (2004) "Standard Terminology Relating to concrete and concrete aggregate", Annual Book for ASTM Standards, American Society of Testing and Materials, Vol. 04.02, pp.150-155.

Biricik H., F. Akoz, I. Berktay, A. Tulgar, (1999) "Study of pozzolanic properties of wheat straw ash", Cement and Concete Research 29 637– 643.

Biricik H. et al., "Resistance to magnesium sulfate and sodium sulfate attack of mortars containing wheat straw ash", Cement and Concrete Research 30 (2000) 1189-1197.

James J., M. Subba Rao, (1986) Silica from Rice Husk through Thermal Decomposition, Thermochimica Acta 97, Elsevier Science, Amsterdam, pp. 329–336.

Massazza F., (1998): Pozzolana and pozzolanic cements, in: P.C. Hewlett (Ed.), Lea's Chemistry of Cement and Concrete, 4th edn., Arnold Publishers, London, pp. 471-631.

Mehta, P.K. (2006). "Concrete structure, properties and material." *The McGraw-Hill Companies*, *Inc.*, *USA*, *New York*, 232, 299, 307-310, and 638.

Mehta. P. K, (1987) "Natural Pozzolans, Supplementary Cementing Materials for Concrete", Canadian Government Publishing Center, Supply and Services, CANMET-SP-86-8E, Ottawa.

Mirza, J.; Riaz, M.; Naseer, A.; Rehman, F.; Khan, A. N. and Ali, Q. (2009); "Pakistani Bentonite in Mortars and Concrete as Low Cost Construction Material", Applied Clay Science, 42, pp. 220 – 226.

Rizwan, S. A. (2006); "High – Performance Mortars and Concretes using Secondary Raw Materials", PhD thesis, Technical University, Freiberg, Germany, ISBN 978-3-639-17878-4, pp. 1-132

Rizwan, S.A and Bier, T.A, (2009) "Self Compacting Mortars Using Various Secondary Raw Materials", ACI Materials Journal, Vol 1.

Rizwan, S. A. and Bier, T. A.; "Application of XRD, Calorimetry and Thermal Analysis Techniques in the Study of Hydration Kinetics of Cement Based Systems", Paper submitted to Construction and Building Materials Journal.

Visvesvaraya H. C., (1986): Recycling of Agricultural Wastes with Special Emphasis on Rice Husk Ash, Use of Vegetable Plants and Fibres as Building Materials Joint Symposium RILEM/CIB/NCCL, Baghdad, pp. 1–22.

MECHANICAL PROPERTIES AND DURABILITY OF CONCRETES CONTAINING NATURAL ZEOLITE

A. A. Ramezanianpour[1] , R. Mousavi[2] , M .Kalhori [2], M.Nikravan[2]
[1] *Concrete Technology & Durability Research Center, Amirkabir University of Technology, Tehran, Iran*
[2] *Departments of Civil and Environmental Engineering, Amirkabir University of Technology, Tehran, Iran*
Amirkabir university, Hafez avenue, Tehran , Iran .

SUMMARY

One ton of CO_2 is emitted per one ton of cement production. Hence, sustainable development goals, necessary for optimal use of material and environmental pollution leads us to use Pozzolanic materials as cement replacement material to reduce CO_2 emission. Zeolite is a natural pozzolanic material and found in nature abundantly especially in Iran. In this work, the mechanical and durability properties of concretes containing a natural zeolite is investigated. The percentages of zeolite that replace Portland cement in this research are 0%, 10%, and 15% by mass. The water/binder ratios are 0.35, 0.4, 0.45 and 0.5. Experimental tests are compressive and tensile strengths, electrical resistivity and chloride diffusion at different ages.

Generally, results showed that zeolite decreases chloride permeability and increases compressive and tensile strengths and electrical resistivity. Therefore concretes containing various contents of zeolite showed improved durability and mechanicall properties.

1. INTRODUCTIN

Concrete is one of the most widely used man-made construction material, owing to its good durability and low cost.

Cement is the most produced and used binding material in the world with its 1.6 billion tons of annual production *(Worrell, Martin, Price 2000).* The world cement industry is responsible for 7% of the total CO2 emission *(Mehta PK. 2002)*. Thus, the cement industry has a crucial role in the global warming.

The use of pozzolanic materials as partial replacement for Portland cement in concrete has been increasing, not only for energy-saving and CO2 emission and economical benefits without causing any degradation to cement properties, but also improving concrete strength and durability *(Cahit Bilim. 2011) (Cenk Karakurt ,Ilker Bekir Topcu. 2011) (Uzal, Turanlı, Yücel, Göncüoğlu, Çulfaz. 2010) (Bu¨ lent Yılmaza, Ali Uc-arb, Bahri O¨ teyakab, Veli Uza. 2007).*

Zeolite has been widely used as a cement replacement material to increase the mechanical properties of concrete for many years. Natural zeolite particles contain large quantities of reactive SiO_2 and Al_2O_3 *(Breek 1974)*. Zeolite substitution can improve the strength of concrete, due to high pozzolanic activity. Also chemical, physical, environmental and economic properties of these particles make zeolite attractive for the construction materials technology *(Feng, Yang, Zu 1988) (Fragoulis, Chaniotakis, Stamatakis 1997) (Naidenov 1991) (Perraki, Orfanoudaki 2004).*

Natural zeolite has low cost and is accessible pozzolanic material in Iran. Additionally, it has positive effect on enhancing mechanical and durability properties of concrete.

Therefore, In this experimental study the effects of natural zeolite on mechanical and durability properties are investigated.

2. MATERIALS

(a) Cement: type 1-425Ordinary Portland cement (OPC).
(b) Zeolite︰clinoptilolite type from north of Semnan, Iran.
The chemical compositions and physical properties of the ordinary Portland cement and zeolite used in the experiments are summarized in Tables 1 and 2.
(c) Coarse aggregate: maximum size 19 mm the Karaj River region
(d) Fine aggregate: sand in grading zone between A and C in accordance with IRAN standard.
(e)Superplasticizer: polycarboxilate based with gravity of 1.2. For the purpose of producing high strength and sufficient workability concrete .

Tab. 1 . Physical properties in clinoptilolite

material	Specific gravity (g/cm^3)	Specific surface area (cm^2/g)	Remained on sieve (%)	
			45 µm	90 µm
clinoptilolite	1.19	10000	0	0
cement	3.15	3060	20	4.2

Tab. 2 .Chemical compositions of ordinary Portland cement and zeolite

Oxide composition	Sio_2	Al_2o_3	Fe_2o_3	Tio_2	Cao	Mgo	Na_2o	K_2o	S	LOI
cement	23.73	4.83	3.11	0.265	54.98	3.92	0.24	0.68	6.188	1.44
zeolite	67.44	10.90	0.84	0.19	1.24	0.33	3.71	4.39	0.47	11.05

3. MIXTURE PROPORTION

Zeolite was in turn used to replace 0%, 10%, 15% by weight of cement. The Coarse aggregate content was 40 % and fine aggregate 60 % of all aggregate while the 19 mm sized coarse aggregates were maximum, respectively. Superplasticizer was added to attain a slump of about 70-100 mm. The water to total cementations materials ratio W/(C + P) was 0.35, 0.4, 0.45, and 0.5 for this study.

4. SPECIMEN PREPARATION, CURING AND TESTING

(1) Mixing procedure : The dry aggregates of concrete were mixed first followed by the addition of 1/3 water. Then mixture of cement and zeolite added by addition of another 1/3 of water. Superplasticizer was added at the last stage of mixing with the rest of water. The total mixing time was about 5 min.

(2) Casting and curing of specimens : Concrete specimens were demoded 24 h after casting, and then placed immediately in a water curing tank. The temperature of water was maintained at 25±2 °C.

(a) Compressive strength: At 7, 28, and 90 days of age, three 100-mm cube specimens of each concrete mixture were tested for compressive strength.
(b) Tensile strength: At 28, and 90 days of age, four 150x300 mm cylinder specimens of each concrete mixture were tested for tensile strength.
(c) Electrical resistivity: Electrical resistivity testing was conducted on two 100 x 200 mm cylinders prepared for every concrete mixture at 28 and 90 days after casting of concretes.
The specimens were submerged in water until the testing age. The 4 point electrical resistivity measurement device (wenner array probe) is used to measure the electrical resistivity of concrete for analyzing the corrosion potential and offers an indication of its permeability.
(d) Chloride Penetration: The Rapid Chloride Permeability Test was conducted in accordance with ASTM C-1202 for each mixture. Two specimens of 100 mm in diameter and 50 mm in thickness which had been conditioned were subjected to a 60-V potential for 6 hours. The total charge passed through the concrete specimens was determined and used to evaluate the chloride permeability of each concrete mixture. The ages of specimens for the tests were 28 and 90 days.

5. RESULTS

5.1. Compressive strength

Fig. 1 shows the effect of zeolite on compressive strength of concrete. It is clear that regardless of replacement level, zeolite decreased concrete strength at 7 days. This reduction is about 6% for 10 % replacement and around 9 % for 15 % replacement. Compressive strength increased at 28 days due to the pozzolanic reaction . it is apparent that the optimum replacement level was about 10 %. Although it didn't show considerable difference at 15% replacement. Replacement of cement by zeolite at different levels increased the 28-day compressive strength of concrete of about 8-10 %. Except in w/c =0.35 the compressive strength of concrete of the control mixture was higher than that of zeolite mixtures at 90 days. This can be attributed to the experimental error.

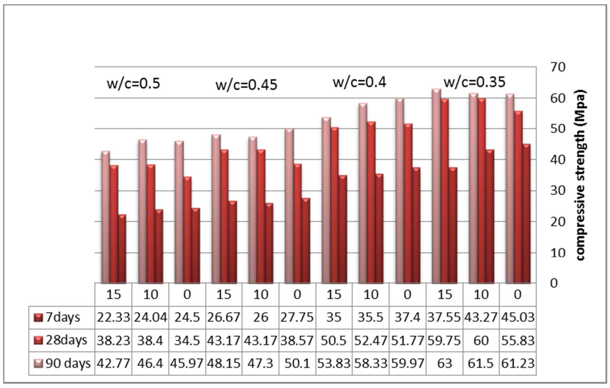

Fig. 1 Compressive strength of control and zeolite concretes at different ages with various w/c ratios.

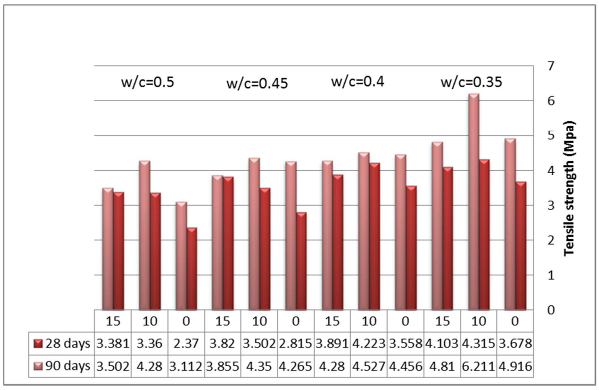

Fig. 2 Tensile strength of control and zeolite concretes at different ages with various w/c ratios.

5.2. Tensile strength

Results of the tensile strength of the natural zeolite compared with the control mixture are shown in Fig. 2. As seen in Fig. 2, replacement of zeolite improves the tensile strength at all ages. Optimum replacement level of zeolite at 90 days was about 10 %.

5.3. Electrical resistivity

As shown in Fig. 3 electrical resistivity of specimens considerably increases versus time. It is clear that mixtures containing zeolite have higher resistivity than control mixtures at various w/c ratios.The resistivity of concrete increases by increasing zeolite content up to 15 %. According to the report of CEB committee it can be seen that the corrosion rate of reinforcing steel is low when the resistivity of concrete exceeds 20 kΩcm . All the zeolite mixtures have resistivity higher than 20 kΩcm.

5.4. Chloride permeability

As presented in Fig. 4 zeolite decreases charge passing from specimens considerably and increases resistivity of concrete against chloride ion permeability at various ages. This is observed mostly in mixtures containing high w/c ratios. As an example 15 % zeolite replacement decreases the chloride permeability ion of mixtures (w/c=0.5) of about 59.4 % at 28 days and 70.3 % at 90 days.

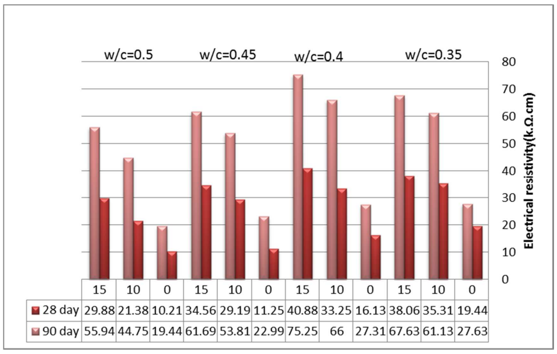

Fig. 3 electrical resistivity of control and zeolite concretes at different ages with various w/c ratios.

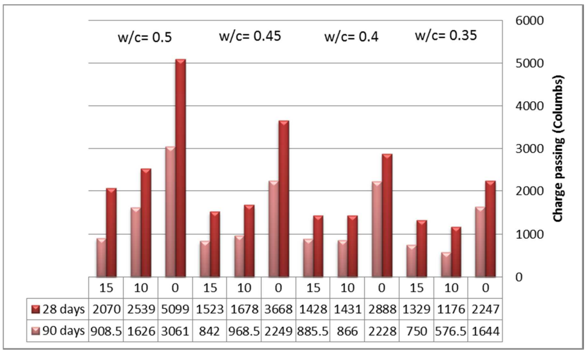

Fig. 4 result of RCPT test of control and zeolite concretes at different ages with various w/c ratios

6. CONCLUSIONS

- Natural zeolite concrete mixtures displayed higher compressive and tensile strengths than the control mixture at 28 days. Natural zeolite was not more effective in increasing the compressive strength at 90 days.
- The substitution of cement with 15% natural zeolite reduced chloride penetration of concrete mixtures according to the RCPT test and increased its electrical resistivity.
- Due to the reduction in chloride diffusion and increase in electrical resistance, concretes containing natural zeolite are expected to perform better in corrosive environments.

7. REFERENCES

Breek D.W., (1974).Zeolite Molecular Sieves: Structure, Chemistry and Use.

Bu¨ lent Yılmaza, Ali Uc-arb, Bahri O¨ teyakab, Veli Uza. (2007). Properties of zeolitic tuff (clinoptilolite) blended portland cement.

Cahit Bilim. (2011).Properties of cement mortars containing clinoptilolite as a supplementary cementitious material.

Cenk Karakurt ,Ilker Bekir Topcu. (2011).Effect of blended cements produced with natural zeolite and industrial by-products on alkali-silica reaction and sulfate resistance of concrete.

Feng NQ, Yang HM, Zu LH. (1988).The strength effect of mineral admixture on cement concrete.

Fragoulis D, Chaniotakis E, Stamatakis MG. (1997).Zeolitic tuffs of Kimolos Island, Aegean Sea, Greece and their industrial potential.

Mehta PK. (2002).Greening of the concrete industry for sustainable development.

Naidenov V. (1991).Rapid hardening cement-gypsum composites for shotcreting on the base of Bulgarian raw materials: Part I.Introduction, materials, design of the compositions, strength and deformability.

Perraki Th, Orfanoudaki A. (2004).Mineralogical study of zeolites from Pentalofos area, Thrace, Greece. Applied Clay Science.

Uzal B., L. Turanlı, H. Yücel, M.C. Göncüoğlu, A. Çulfaz. (2010). Pozzolanic activity of clinoptilolite: A comparative study with silica fume, fly ash and a non-zeolitic natural pozzolan.

Worrell E, Martin N, Price L. (2000) .Potentials for energy efficiency improvement in the US cement industry.

STUDY OF PROPERTIES OF HIGH PERFORMANCE CONCRETE WITH A FOCUS ON HIGH STRENGTH AND SELF COMPACTING CONCRETE

Klára Křížová[1], Rudolf Hela[2], David Procházka[3]
[1,2,3] Department of Buildings Materials and Components
Brno University of Technology, Faculty of Civil Engineering
602 00 Brno Veveří 95

SUMMARY

The paper presents results of tests of physico-mechanical properties of High Performance Concrete HPC, in particular, High Strength Concrete HSC and Self Compacting Concrete SCC. Both types of concrete were designed with respect to their character, which is also grasped in their names. Mix-design of SCC included ground lime stone to increase proportion of fine parts smaller than 0.25 mm. Silica fumes were added into HSC. Both types of concrete were tested on compressive strength, static and dynamic elasticity modulus including development of the values in time. The aim of the paper is introduction into basic parameters of these types of concrete and consideration of current methods of evaluation of elasticity modulus based on compressive strength.

1. INTRODUCTION

Current development of concrete technology brings new knowledge and modern views of concrete. New types of concrete gradually emerge and find their applications, like High Performance Concrete (HPC). Such concrete show outstanding properties and frequently surpass currently used concrete. Both Self Compacting Concrete (SCC) and High Strength Concrete (HSC) rank among HPC. Concrete in this group shows one or more properties or characteristics of high performance compared to common, traditional concrete. Considerable difference of such concrete is apparent as early as in their composition, which bases required high performance properties. The basic principle lies in enhancing classic model of concrete design: aggregate, water, cement. Mix-design contains other components like mineral additions in the function of fine parts and partly replacing cement and plasticizer or superplasticizers of new generation. Industrial production of cement, which heavily loads environment, contributes to ecological efforts as mineral additions are mostly secondary waste materials.

Research activities focus on modern types of concrete, which is proved in many research projects both home and abroad. However, it is necessary to admit that wider application in construction practice is limited by economical factors and certain worries and doubts concerning use of new, modern concrete in traditional construction practice. Current cost saving trends show necessity of extending our knowledge and developing research focused on optimization of composition of concrete. High performance concrete complies with such conception very well since good design can bring considerable cost saving, let alone higher end use properties. Design of type and proportion of individual components is very important factor with influence on final characteristics of hardened concrete, hence concrete structures. It was found, that e.g. mineral additions have unambiguously positive effect on most of properties of both fresh and hardened concrete. However, designing of structures made from such concrete also brings new problems, which will have to be solved. Strength behavior of HPC needs solution as well as relation between dynamic and static elasticity modules characterizing deformational properties of concrete. Practice and experience show that empirical relationship between elasticity modules and compressive strength used for common concrete cannot be fully applied for high performance concrete. Construction practice also shows differences compared to standardized procedures and relationships determined for common concrete and therefore these need to be updated for modern types of concrete to define their characteristic properties as exactly as possible.

High Strength Concrete in constructions is designed for reasons of higher bearing capacity in pressed areas of cross sections or because of denser and stronger microstructure and higher durability of structures. Strengths of HSC are between 55 and 180 MPa *(Fiala. C.)* according to European Standard EN 206 for strength classes C 50/60, LC 55/60 to LC 80/88 for high strength concrete with light weight aggregate *(Reinhardt, H.W, 2000).* High strength concrete differs from concrete with normal strength by strong and dense cement matrix and enhanced bond between matrix and aggregate. Therefore, this concrete shows higher increase of strength and lower tensile deformation under stress. Strength of matrix is higher because of low water cement ratio and pozzolanic additions, which fill up voids and make microstructure denser. Since water cement ratio is low, cement in high strength concrete does not hydrate completely unlike cement in concrete with normal strength. This includes all processes dependent on hydration – volumetric changes, strength development and development of hydration heath (Alonso, M.T.).

Self Compacting Concrete is a modern type of concrete, which requires no vibrating during placing. It is capable of flowing only by means of its own weight and gravity and completely fill up formwork even with dense reinforcement. Hardened concrete is dense, homogeneous and shows properties and durability comparable to traditional vibrated concrete. Fresh mix of self compacting concrete shows high movability and capability of flowing without action of external dynamic force, high resistance to segregation and sedimentation of coarse components. Concrete mix can be placed very quickly since it flows through dense reinforcement easily and thus all construction can be speeded up. Fluidity and resistance to segregation of SCC ensures high degree of homogeneity, minimal volume of pores and uniform strength, which shows in high quality of surface and high durability of whole structure. Self compacting concrete is often manufactured with low water cement ratio, which brings fast development of strength, possibility of early removing of formwork and thus faster rotation of construction parts and formwork. Elimination of vibration decreases level of noise at the construction site, improves working conditions both on construction sites and in prefabrication plants. Improved construction procedures combined with positive influence on health and safety make self compacting concrete attractive for prefabrication as well se civil construction *(Krizova, K. 2007).*

2. EXPERIMENTAL WORK

Mixes were designed with respect to character of individual types of concrete. In SCC, mined aggregate was used for its positive effect on this specific property of self compacting concrete. To reach higher strengths of HSC, mineral addition – micro silica was used. Consistency of fresh mixes was determined. SCC reached 560 – 630 mm of slump, i.e. category SF1. Consistency of HSC was determined as S1 with respect to character of the concrete and low water cement ratio.

Concrete compositions:
HSC concrete
Mix1: cement 467 kg/m^3, water 146 kg/m^3, aggregate 1723 kg/m^3 (fraction 0/4 796, 4/8 335 and 8/16 592), silica fume 46,7 kg/m^3 plasticizer 8,3 kg/m^3;
Mix2: cement 435 kg/m^3, lime-stone 43,5 kg/m^3, water 136 kg/m^3, aggregate 1735 kg/m^3 (fraction 0/4 693, 4/8 182 and 8/16 860), plasticizer 7,2 kg/m^3;
Mix3: cement 436 kg/m^3, lime-stone 43,6 kg/m^3, water 144 kg/m^3, aggregate 1739 kg/m^3 (fraction 0/4 1063, 4/8 336 and 8/16 340), plasticizer 7,3 kg/m^3

SCC concrete
Mix1: cement 400 kg/m^3, water 180 kg/m^3, aggregate 1590 kg/m^3 (fraction 0/4 880, 4/8 210 and 8/16 500), plasticizer 5,2 kg/m^3;
Mix2: cement 380 kg/m^3, lime-stone 130 kg/m^3, water 184 kg/m^3, aggregate 1590 kg/m^3 (fraction 0/4 880, 4/8 210 and 8/16 500), plasticizer 3,4 kg/m^3;
Mix3: cement 395 kg/m^3, lime-stone 140 kg/m^3, water 181 kg/m^3, aggregate 1580 kg/m^3 (fraction 0/4 880, 4/8 220 and 8/16 480), plasticizer 3,6 kg/m^3

Following characteristics were studied: compressive strength, static elasticity modulus, dynamic elasticity modulus. All mentioned characteristics were tested at the age of 7 - 90 days or 7 – 28 days. Compressive strength was tested on testing specimens with dimensions 150 x 150 x 150 mm, elasticity modules on testing specimens with dimensions 100 x 100 x 400mm. Test result are given in Tab. 1.

Tab. 1 Measured values of compressive strength and elasticity modules

	Compressive strength [MPa]/days			Static elasticity modulus [MPa]/days			Dynamic elasticity modulus [MPa]/days			Specific elasticity modulus* [MPa]/days
	7	28	90	7	28	90	7	28	90	28
HSC										
Mix1	78.8	92.8	-	37000	38500	-	51000	54000	-	41000
Mix2	69.3	68.5	-	32000	33500	-	52000	55000	-	37000
Mix3	70.2	75.8	-	33500	36500	-	48000	52500	-	38000
SCC										
Mix1	28.4	40.9	37.8	27500	28000	31500	36000	38500	38000	32000
Mix2	28.5	36.6	39.0	23500	26500	28000	32000	33500	34000	31000
Mix3	28.3	34.1	33.5	25000	26000	24500	32000	33500	32500	31000

*EN 1992-1-1 Euro Code 2: Designing of concrete structures – Part 1-1: General rules and rules for civil engineering. Defines dependency of elasticity modulus on compressive strength of concrete. There is empirical relationship between strength class and elasticity modulus.

3. CONCLUSIONS

The aim of the paper was introducing into new trends of concrete technology and their place in current construction practice, in particular, characteristics of modern types of concrete, their difference from traditional concrete and inadequateness of current values of empirical relationships between static elasticity modulus and compressive strength. Compressive strength, static and dynamic elasticity modulus of each type of concrete were determined.
Mix design of SCC containing only cement reached the highest values. However, there was no considerable difference from the values of other SCC. The only marked difference

observed was the value of dynamic elasticity modulus of SCC containing only cement: the value at the age of 28 days was by 5000 MPa higher. Comparison of values static elasticity modules measured and those recommended in regulations was surprising. Neither of the mix designs reached required values. The values are lower by ca 4000 MPa. The trend of development of elasticity modules is rising, only in one case decrease was observed, which cannot be unambiguously proved because of small amount of testing specimens. Among HSC, mix design with micro silica reached the highest values of compressive strength and elasticity modules (both static and dynamic). The other two mix designs with addition of lime stone reached comparable values of strength at the age of 7 days, while the values of strength and static elasticity modulus of mix designs 3 with higher content of sand increased at the age of 28 days. Dynamic elasticity modules grew by ca 3000 MPa between 7 and 28 days. Comparison of specific values of elasticity modulus and measured values showed the same trend as SCC: neither of the mix designs reached the values derived from strength classes of concrete according to EN 1992-1-1.

Test results may imply that theoretical trends of different elasticity behavior of new types of concrete can manifest in practice. Formulation of wider range of mix designs of modern concrete and observation of their characteristics would be recommendable. Then, current empirical relationships could be re-evaluated and new computation models formulated with respect to mentioned factors, in particular design of composition of concrete and different quality and character of individual input materials.

4. ACKNOWLEDGEMENTS

This paper was supported by the project MPO FR – TI1/387 „Development of High Strength Carrying Composite Construction for Civil Engineering on Base Epoxide Compposite Profile Interlocked with Strength Concrete“ and project FAST-S-11-44 "Efficiency of High Volume of Fine Admixtures in Current Concrete Mix Design in the Czech Republic (CR)".

5. REFERENCES

Fiala, C. High performance concretes. Technical University in Prague, Department of Building Structures.

Reinhardt, H.W (2000). Structural behaviour of high performance concrete. Otto-Graf-Journal Vol. 11, 2000.

Alonso, M.T. High strength concrete. Düsseldorf.

Křížová, K (2007). Study of possibilities of the further development og high performance concrete. Thesis VUT Brno, 2007, pp 19-20.

The European Guidelines for Self-Compacting Concrete. Specification, Production and Use, May 2005.

CSN ISO 6784 Determination of static modulus of elasticity in compression.

CSN 73 1371 Method of ultrasonic pulse testing of concrete.

EN 1992-1-1 EuroCode 2: Designing of Concrete Structures – Part 1-1: General Regulations for Civil Engineering.

EN 206-1 Concrete - Part 1: Specification, properties, manufacture and Compliance.

MECHANICAL AND THERMO-INSULATION CHARACTERISTICS OF BIO-COMPOSITES

Oľga Koronthályová[1] Martin Križma[1] Anatolij Guzun[2]
[1] Institute of Construction and Architecture SAS
845 03 Bratislava, Dúbravská cesta 9, Slovakia
[2)] RPIC Malacky
901 01 Malacky, Bernolákova 1, Slovakia

SUMMARY

Ten different composites on basis of the biomass have been tested, whereas the wood chips, reed, straw and sawdust were used as fillers. The research has been focused on bio-composites manufactured without heavy technical and technological equipment. Experimental results show that the mechanical properties as well as the thermo-insulation ability are dependent on the composite dry density and its equilibrium moisture content. The coupled effect of these parameters can be expressed by the parameter 'actual density at equilibrium moisture content'. The wood chips composite with cement binder has got the best mechanical properties while the foam-lightened composite with straw filler achieves the lowest thermal conductivity.

1. INTRODUCTION

In the recent 30 years a lot of research has been done in the field of using wood chips and non-wood vegetable materials in bio-composite manufacture. The research has been focused mainly on the compatibility between the wood (or non-wood vegetable materials) and cement, the ways of the compatibility improvement and the mechanical properties of bio-composites (*Wei and Tomita 2001, Bederina et al 2009*). Due to the high variability of wood and lignocelluloses a generalization is often difficult. Therefore definition of manufacturing methods and measurement of properties should be made again if raw materials come from a different plant species.

Theoretic-experimental investigation focused on lingo-cellulosic bio-composites has been carried out at the Institute of Construction and Architecture SAS in Bratislava since the year 2007. From the very beginning a complex approach, dealing with the mechanical as well as the thermo-insulation properties of the composites has been applied in the investigation. The paper is focused on the effect of the bulk density and moisture content on mechanical and thermo-insulation properties of the composites.

2. EXPERIMENTAL PART

The description of the tested composites is in Tab. 1. After manufacturing the specimens were conditioned in the laboratory room with 23±3°C and relative humidity 51±4% for ca 6 weeks in order to mature. The actual bulk density was determined from the weight and dimensions of the specimens. The mechanical tests (verification of static modulus of elasticity in compression and verification of flexural tensile strength – four – point loading) were done on prism specimens with dimensions of 150x150x600 mm, using the servo-hydraulic machine

SCHENCK (STN ISO 6784 or STN EN 12390-5). The thermal conductivity was measured by guarded hot plate method (STN EN 12664) on the samples with dimensions of 0.5x0.5x0.08 m. After tests, the samples were oven dried at 105±1°C and the equilibrium moisture content as well as the dry bulk density was calculated (Tab. 1, Tab. 2) (*Krizma et al, 2008*).

3. RESULTS AND DISCUSSION

The mechanical parameters and thermal conductivity of tested composites are presented in Tab. 2. The obtained mechanical properties as well as the thermo-insulation ability are dependent on the dry density and the equilibrium moisture content. The coupled effect of the parameters can be expressed by the parameter 'actual density at equilibrium moisture content'. The mechanical parameter/actual bulk density relations involve also the effect of the used filler whereas a positive effect of the fibrous filler (reed, straw) is noticed. For composites with the same type of filler (wood chips), the relationship between the actual bulk density and mechanical parameter is linear (Fig. 1). In case of thermal conductivity the linear dependence on the actual bulk density is obtained independently of the filler used (Fig. 2). The wood chips composite with cement binder (A2) has got the best mechanical properties that are comparable with the AAC ones. On the other hand its thermal conductivity is higher than the AAC one. In case of A1, B1, B2, C, D and F composites, the better thermo-insulation ability is obtained at expense of the lower mechanical parameters. In case of foam-

Tab. 1 Designation, description of mixtures and dry density (ρ_0) of tested composites

Designation of composite	Description of mixtures	ρ_0 (kg.m^{-3})
A1	wood chips, cement PC, $CaCl_2$, sodium-silica glass, water	640
A2	as A1; by 1.2 higher amount of cement	800
B1	wood chips, MgO, $MgCl_2$, water	540
B2	wood chips, MgO, $MgSO_4$, water	530
C	mineralised reed, MgO, $MgCl_2$, water	510
D	mineralised straw, MgO, $MgCl_2$, water	590
E	mineralized sawdust, MgO, $MgCl_2$, water	680
F1	wood chips, MgO, $MgCl_2$, water, foam	380
F2	wood chips, MgO, $MgCl_2$, water, foam	350
FD	mineralised straw, MgO, $MgCl_2$, water, foam	140

Tab. 2 Density at equilibrium moisture content (ρ_{um}), equilibrium moisture content (u_m), prism strength (f_{cp}), static modul of elasticity (E_c), flexural strength ($f_{ct,f}$) and thermal conductivity (λ) of tested composites. Mean values of three measurements.

Designation of composite	ρ_{um} (kg.m^{-3})	u_m (kg.kg^{-1})	f_{cp} (MPa)	E_c (MPa)	$f_{ct,f}$ (MPa)	λ (W.m^{-1}.K^{-1})
A1	740	0.15	1.655	0.903	0.705	0.19
A2	910	0.13	2.345	1.240	1.279	0.25
B1	640	0.19	1.107	0.621	0.927	0.20
B2	650	0.22	1.322	0.634	0.802	0.20
C	580	0.12	2.172	2.393	2.223	0.16
D	660	0.13	1.257	1.548	1.092	0.18
E	790	0.18	0.753	0.478	0.296	0.26
F1	450	0.18	0.722	0.500	0.722	0.13
F2	410	0.18	-	-	-	0.11
FD	160	0.20	-	-	-	0.07

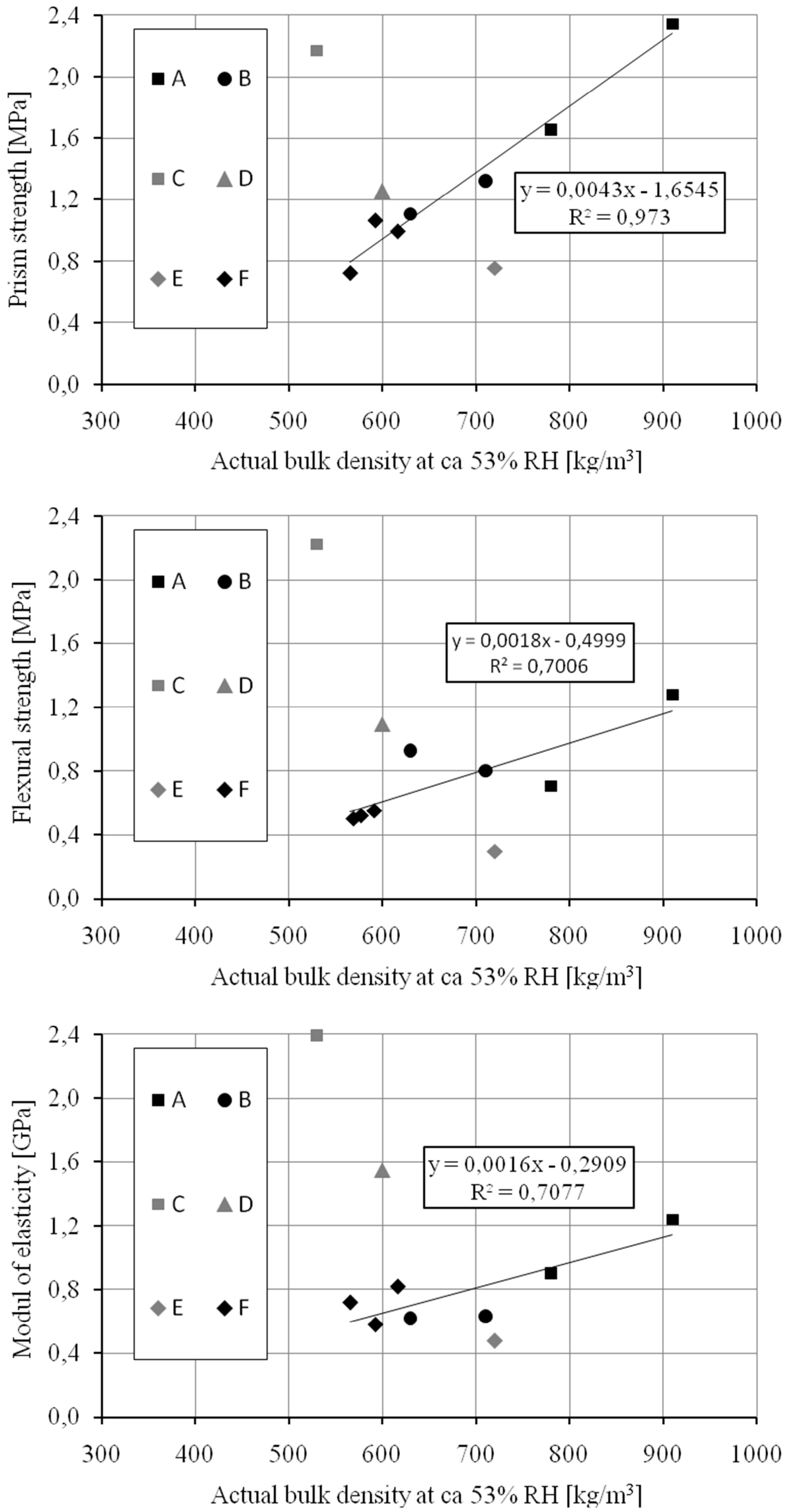

Fig. 1 Prism strength, flexural strength and modul of elasticity versus actual bulk density for composites of A, B, C, D, E and F. Linear interpolations of mechanical parameter/actual bulk density relation are done for composites with wood chips filler

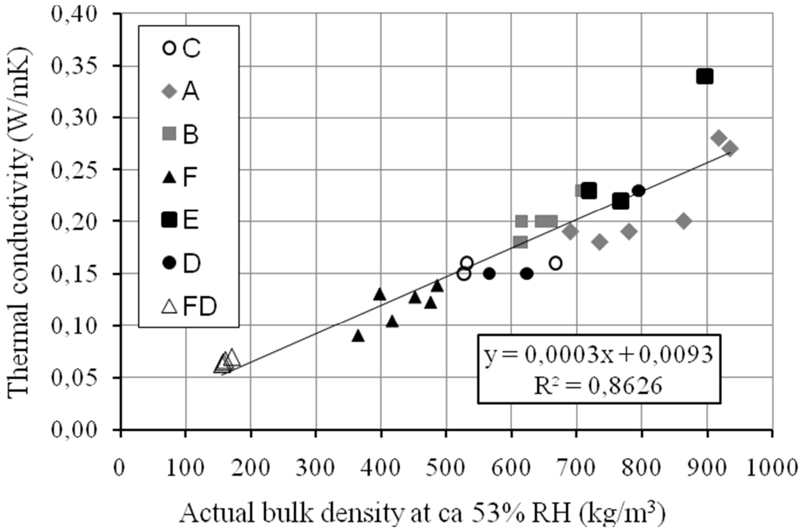

Fig. 2 Thermal conductivity versus actual bulk density for composites of A, B, C, D, E, F and FD type

lightened mixtures (F1, F2 and FD) a significant improvement of thermal conductivity is reached that enables their application as thermo-insulating filling of the load-bearing global framework.

4. CONCLUSIONS

The mechanical properties as well as the thermo-insulation ability of the tested composites have been dependent on the dry density and the equilibrium moisture content. The coupled effect of the parameters could be expressed by using the parameter 'actual density at equilibrium moisture content'.

The thermo-insulation properties of the foam-lightened wood chips/straw composites satisfy their application as the thermal insulation material for external walls of residential buildings.

5. ACKNOWLEDGEMENTS

This work was supported by the Slovak Research and Development Agency under the contract No. APVV-0031-10 and by the Scientific Grant Agency VEGA under the contract No. 2/0159/10.

6. REFERENCES

Bederina M., Laidoudi B., Goullieux A., Khenfer M.M., Bali A., Quéneudec M., (2009). „Effect of the treatment of wood shavings on the physico-mechanical characteristics of wood sand concretes", *Construction and Building Materials*, Vol. 23, p. 1311-1315.

Križma M., Nürnbergerová T., Koronthályová O., Guzun A., Kočiš I. (2003) „Working characteristic of building materials on the basis of the biomass", In *70 Years of FCE STU Proceedings of the International Scientific Conference.* Ed. A. Grmanova, M. Minarik, ISBN 978-80-227-2979-6, STU, Bratislava 2008

Wei Y. M., Tomita B. (2001) „Effects of five additive materials on mechanical and dimensional properties of wood cement-bonded boards", *Journal of Wood Science*, Vol. 47, p. 437-444.

SELF-COMPACTING CONCRETE WITH RECYCLED CONCRETE AGGREGATE AND HIGH FINENESS SLAG

R. Sri Ravindrarajah [1&2], James David Saltmer [1], Pek Qia Quan [1] and Chng Xian Ming [1]
[1] Nanyang Technological University, Nanyang Avenue, Singapore
[2] University of Technology, Sydney, Australia

SUMMARY

An environmentally friendly concrete uses minimum cement, maximum supplementary cementitious materials (SCM) and recycled concrete aggregate. Ground granulated blast furnace slag (ggbfs) is an effective binder material for concrete due to its cementitious and pozzolanic reactivity. However, due to the low fineness its usage is limited in high strength concrete. This paper reports the results of a study into the use of high f ineness ggbfs in high strength self-compacting concrete with either natural or recycled concrete aggregates. The slag content was about 10% or 30% of the binder content. The results showed that the fine ggbfs performed superior to cement in SCC mixes. The use of recycled concrete aggregate had produced manageable reductions in strengths and stiffness, and increased the chloride permeability of SCC.

1. INTRODUCTION

I ncrease in the complexity of construction, intricate reinforcement details of modern day concrete structures and lack of skilled construction workers resulted in the development of self-compacting concrete (SCC). The fresh SCC has several advantages over conventional concrete, namely: (a) ability to ow under its own weight; (b) high resistance to segregation; and (c) improved filling capacity. The properties of SCC ar e found to be sensitive to the superplasticiser dosage and fine materials content (*Sri Ravindrar ajah et. al., 2003, Kheder and Al Jadiri,2010*) proposed a mix design method for SCC based on compressive strength requirements using cement and inert limestone powder. I n this research the ef fectiveness of high f ineness ggbfs on SCC mixes with natural or recycled concrete aggregates is studied.

Tab. 1: Properties of coarse aggregate

Property	Natural coarse aggregate	Recycled concrete coarse aggregate
Specific gravity	2.55	2.20(mean)
Water absorption (%)	1.23	6.33 (mean)
Ten percent fines (kN)	204	122
Impact strength (% fines)	19.7	24.9

2. EXPERIMENTAL DETAILS

2.1 Materials and Mix Compositions

Ordinary Portland cement and ultra-high fine ground granulated blast furnace slag (fineness of 870m^2/kg) were used in combination as binder materials in the concrete mixes. Fine aggregate was natural siliceous sand with the fineness modulus of 2.90. Coarse aggregate was either natural (granite) aggregate or recycled concrete aggregate, obtained from the demolished sewage concrete plant. The coarse aggregate grading was such that 75%, and 25%

passing through 12.5mm and 9.5mm standard sieves. Table 1 summarises the properties of natural and recycled concrete coarse aggregates. The recycled concrete aggregate is notably weaker than the natural aggregate due to the porous attached mortar (Sri Ravindrarajah and Tam (1985), as reflected from the differences in the water absorption capacity. The water absorption for recycled aggregate was 6.33% compared to 1.23% for the natural aggregate.

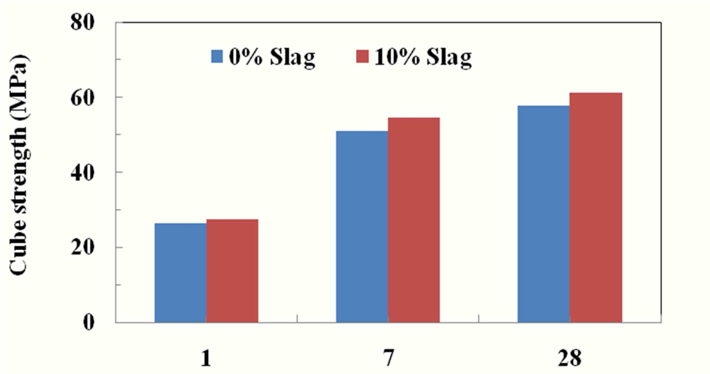

Fig. 1 Effect cement replacemet with fine slag on mortar strength

The reactivity of fine slag was assessed using mortar strength tests at the ages of 1, 7 and 28 days. Mortar mixes with and without slag had the sand to binder ratio of 2.75 and the water to binder ratio of 0.43, by weight. Fig. 1 shows the development of mortar strength with age for both control mortar (100% cement) and mortar with cement and slag (90% cement plus 10% slag). The results show that the strength activity index for slag at the 10% cement replacement level is 1.05, 1.07 and 1.08 at 1, 7 and 28 days, respectively.

Tab.2 Mix compositions (in kg/m) of self-compacting concrete

Materials	Grade 35		Grade 75	
	NAC 35	RAC 35	NAC 75	RAC 75
Cement	0	60	534	534
Fine slag	170	170	70	70
Fine aggregate	978	1020	977	1020
Coarse aggregate (ssd)	742	673	742	673
Water	173	173	155	155
Superplasticiser (% of binder)	1,33	1.63	2.60	2.60
Water/Binder Ratio	0.48	0.48	0.29	0.29
Slag content (%)	32.1	32.1	9.9	9.9

Compositions for Grades 35 and 75 SCC mixes were obtained using the mix design procedure reported by Kheder and Al Jadiri (2010) . Superplasticiser, containing polycarboxylate ether polymers, was used. Table 2 summarizes the mix compositions of all four mixes. Concrete mixes with recycled concrete coarse aggregate required more sand for both concrere grades. The slag content of Grades 35 and 75 concrete mixes were 32.1% and 9.9%, respectively.

2.2 Mixing and Testing of Concrete

A pan-type of concrete mixer was used for mixing the concrete. The coarse aggregate were batched at saturated surface dry moisture condition. The superplasticiser dosage was adjusted/for each mix to achieve the slump flow above 600mm. The slump flow recorded for the SCC mixes were varied between 625mm and 675mm. For each mix, 12Nos. of 100mm cubes; 3Nos. of 100mm diameter by 200mm high cylinders; 1No. of 150mm diameter by 300mm high cylinder; and 2Nos. of 100mm by 100mm by 500m prisms were cast in steel mould for testing the hardened concrete. No compaction was applied while casting the specimens. The specimens were demoulded after 24 hours and cured in water at the room temperature of 28 C, until testing. Using 100mm diameter by 50mm thick concrete slices, chloride migration coeff icient for concrete was determined using the Rapid Migration Test (NT BUILD 492).

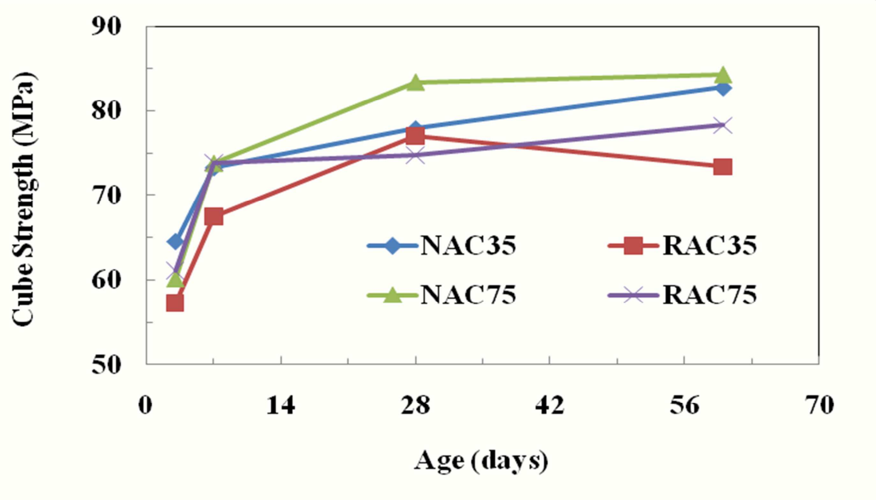

Fig. 2 Effect of recycled concrete coarse aggregate on strength development for SCC

Tab. 3 Hardened properties of self compacting concrete

Property	NAC35	NAC75	RAC35	RAC 75
28d Cube strength (MPa)	74.7	83.4	77.0	74.8
28d Tensile strength (MPa)	5.01	5.33	4.55	4.98
60d Elastic Modulus (GPa)	31.3	33.3	29.3	28.4
28d UPV (km/s)	4.73	4.73	4.56	4.51
60d Migration Coefficient (10 - 12 m 2 /s)	-	3.78	-	5.02

3. RESULTS AND DISCUSSION

Fig. 2 shows the development of compressive strength for SCC mixes with either natural or recycled concrete aggregates. Table 2 shows that the cement and binder contents f or NAC35 mix were 174kg/m 3 and 74kg/m 3 less than those for the NAC75 mix. In addition, NAC35 mix had the water to binder ratio of 0.48 compared to 0.29 f or NAC75 mix. The results showed that there is no significant difference in the compressive strength between these two mixes at all ages. *Nakumara et. al. (1992)* produced that high strength concrete with high water to cement ratio with the use of ultra fine slag. This is due to the combined effect of pore filling and high reactivity of slag due to its fineness as shown by *Isaia (2003). Dinakar (2010)* reported comparable performance of ultra fine slag with silica fume.

Table 3 summarizes the hardened concrete properties for SCC mixes at either 28 or 60 days. The results show that the SCC with recycled concrete aggregate had reduced the compressive strength, tensile strength, modulus of elasticity and increased the chloride permeability coeff icient when compared with SCC mix with natural aggregate. For Grade 35 concrete, the 60-day compressive strength dropped from 82.3MPa to 73.4MPa, a reduction of 10.8%. However, for Grade 75 concrete, the compressive strength had dropped from 84.3MPa to 78.3MPa, a reduction of 7.1%. at the same age. At the age of 28 days, the tensile strength was reduced by 9.2% and 6.6% and the modulus of elasticity was dropped by 6.4% and 14.7%, for Grade 35 and 75 concretes, respectively. The reactivity of ultra fine slag may have contributed to the strengthening of aggregate-cement paste bond.

The chloride migration coefficient at 60 days was 3.78 x 10 -12 m 2 /s and 5.02 x 10 -12 m 2 /s for NAC75 and RAC75, respectively. Although the SCC with recycled concrete aggregate increased the chloride migration potential, the resistance against chloride ingress is much lower to the limit for migration coefficient is 8 x 10 -12 m 2 /s for low chloride ingress concrete. As expected, the presence of weak porous attached mortar in the recycled concrete aggregates is responsible for the increase in porosity (indicated by UPV in Table 3) and chloride permeability of concrete.

5. CONCLUSIONS

The use of finely ground granulated blast furnace slag is shown to be a highly effective cement replacement material in producing high strength self -compacting concrete with reduced cement content. Such concrete is found to be less sensitive to the variation in the water to binder ratio. The use of recycled concrete aggregate as a full replacement to natural coarse aggregate reduced strengths and modulus of elasticity and increased the chloride permeability potential of SCC. However, such changes can be accommodated and should not be considered as undesirable in producing SCC with reduced environmental impact.

6. ACKNOWLEDGEMENTS

The authors wish to thanks EnGro Corporation Limited and BASF South East Asia Pte Ltd for their kind contribution of the concrete making materials used in this investigation.

7. REFERENCES

Dinakar, P. (2010), “Effect of ultra fine slag on the fresh and hardened properties of ultra high strength concrete”, Proceedings of the Asian Conf erence on Ecstasy in Concrete 2010,
Chennai, India, Dec. 2010, pp. 527-532.

Kheder, G. F. and Al Jadiri , R. S. (2010), “New method for proportioning self-consolidating concrete on compressive strength requirement”, ACI Materials Journal Vol. 107, No. 5, Sept. - Oct. 2010, pp. 490-497.

Isaia, G. C., Gastaldini, A. L. G., and Moraes, R. (2003), “Physical and pozzolanic action of mineral additions on the mechanical strength of high performance concrete”, Cement Concrete Composites, Vol. 25, No. 1, pp. 69-76.

Nakamura, N., Saki, M., and Swamy, R.N. (1992), “Effect of slag fineness on the development on concrete strength and microstructure”, Proceedings of the 4th International Conference on Fly Ash, Silica Fume, Slag, & Natural Pozzolans in Concrete, Turkey, pp. 1343-1366.

Sri Ravindrarajah, R. and Tam, C. T. (1985), “Properties of concrete made with crushed concrete as coarse aggregate”, Magazine of Concrete Research, Vol. 37, pp. 29-38.

Sri Ravindrarajah, R., Farrokhzadi, F. and Lahoud, A. (2003) Properties of flowing concrete and self -compacting concrete with high-performance superplasticiser, Proceedings of the 3rd International RILEM Symposium , Reykjavik, Iceland.

Sri Ravindrarajah, R. (2010), "Concrete for sustainable construction", Proceedings of the Asian Conference on Ecstasy in Concrete 2010, Chennai, India, Dec. 2010, pp. 135-153.

EXPERIMENTAL STUDIES ON STRENGTH AND COST OF RPC

Renyuan Du[1]*, Qingwei Huang*[1]*, Baochun Chen*[1]
[1] *College of Civil Engineering of Fuzhou University*
350108 Fuzhou Fujian China

SUMMARY

Reactive powder concrete (RPC) is a new concrete material with super-high compressive strength, high toughness, good durability and stability. But prices of the raw materials of RPC are much higher than those of normal concrete, and have an influence on its application to some extent. It is shown that the steel fiber is the most expensive raw material in RPC. Therefore experimental studies on influence of steel fiber ratio by volume to RPC mechanical properties including axial compressive strength, tensile strength, and flexural strength were carried out in this paper. The relationship between cost-performance ratio and content of steel fiber was also analyzed for applications and future studies.

1. INTRODUCTION

RPC had studied much since 1993, and had been applied to some bridges*(Adeline et al 1998, Cavill et al 2003, Bum et al 2005, Zimmermann et al 2008,)*, but not yet popular. Main reasons are as follows: (1) high price, the price of RPC was between RMB 4000 to 8000 per cubic meter*(Huang 2008, Zhou et al 2000)*, much higher than normal concrete. Furthermore, steel fiber is main cost of RPC. (2) Lack of basic research. Many studies focused on compressive strength of RPC, but there is a lack of research on tensile, flexural and shear strength*(Richard et al 2003, Wu et al 2003, He et al 2000)*. (3) Lack of relevant criteria. Studies in different countries are limited just to internal criteria, there is still short of unified standard *(Guo 2008)*. Axial compressive, splitting tensile and flexural strength of RPC were tested, as reported in this paper, and cost-performance ratio of RPC was also analyzed for engineering applications.

2. EXPERIMENTAL PROGRAMME

The compressive strength of 7 sets of specimens with side lengths of 150 mm × 150 mm × 300 mm, and the tensile strength of 7 sets of cubic specimens with side length of 150mm, and the flexural strength of 7 sets of specimens with side lengths of 150 mm × 150 mm × 550 mm were carefully measured.

RPC mix: Cement: Silica fume: Sand: super-plasticizer: water is 1: 0.3: 1.17: 0.025: 0.234. Taking the content of steel fiber as parameter, the contents are 0, 0.5%, 1%, 1.5%, 2%, 2.5% and 3% by volume respectively. Steam curing system was adopted, and contained modeling (24h), standard curing (24h) and steam curing (8h, 180℃). Specimens were tested after three days.

3. RESULTS OF ANALYSIS

Fig. 1 shows the axial compressive strength versus the content of steel fiber. The compressive strength of RPC without steel fiber reaches up to 95MPa, for RPC increased homogeneity through the elimination of coarse aggregates; and steam curing for RPC furthers activity of silica fume. When the content of steel fiber is 0.5%, the strength of the RPC is 28MPa higher than that of RPC without steel fiber. While the content is in the range of 0.5% to 2%, the strength increases slowly; when the content of steel fiber is 2%, the strength of the RPC is 21MPa higher than that of RPC with 0.5% fiber content. The results indicate that steel fiber can improve RPC compressive strength, but affects the strength less when the content is above 0.5%.

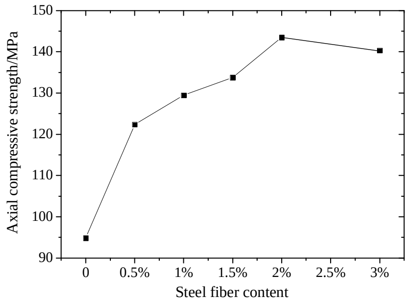

Fig. 1 The axial compressive strength of RPC versus steel fiber content

The tensile strength versus content of steel fiber is presented in Fig. 2. The growth of each phase is almost same, and about 3 MPa. RPC without steel fiber failed as soon as cracking began; but RPC mixing with steel fiber failed due to steel fiber pulled out. The fiber effectively controls the development of the cracks, and can sustain loads after RPC cracking. The results indicate that steel fiber has great influence on RPC splitting tensile strength, and the strength will higher with the inclusion of more steel fiber.

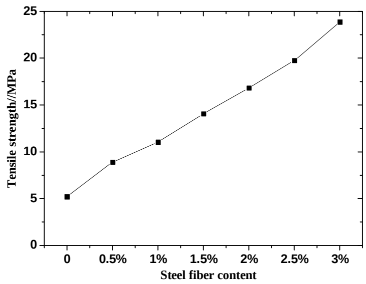

Fig. 2 The tensile strength of RPC versus steel fiber content

The flexural strength of RPC depends much on steel fiber, because matrix of RPC has a poor crack resistance; the tensile strength of RPC was improved by tension of steel fiber and the bond between steel fiber and matrix. Fig. 3 shows the flexural strength versus content of steel fiber. The results manifest that the flexural strength grows as steel fiber content increases, and the highest strength reaches up to 15.06MPa.

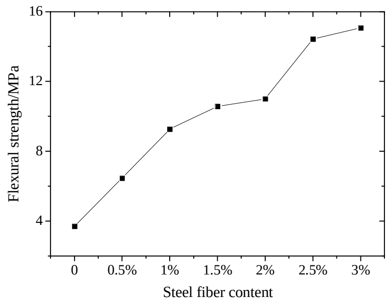

Fig. 3 The flexural strength of RPC versus steel fiber content

4. COST-PERFORMANCE RATIO ANALYSIS

The strength (S) of RPC is taken as a parameter due to RPC characterized by super-high strength, and the price (P) of RPC is taken as the other parameter. The relationship of R (the cost-performance ratio), S and P is presented in Eq. (1).

$$R = S / P \tag{1}$$

In paragraph 3, it is shown that growth trends of compressive, tensile and flexural strength are different with increasing content of steel fiber. Therefore, the synthetical strength (S) is introduced as a parameter.

$$S = (\sum_{i=1}^{n} K_i S_i) / n \tag{2}$$

In the equation (2):

K_i —a parameter for strength; the value should be taken according to the practical application. In this paper, compressive, tensile and flexural strength are assumed to be equally important, K_1, K_2 and K_3 are the parameters of the compressive, tensile and flexural strength respectively. The value of K_1 is 1, the value of K_2 and K_3 are 10.

S_i —a particular strength of RPC; S_1 S_2 and S_3 correspond to compressive, tensile and flexural strength respectively.

P—the price of one cubic meter of RPC

Many factors have effect on RPC price, such as raw materials price, preparation and curing costs, equipment costs, transport costs, labor wages and so on. As this is an initial study, raw materials price (details in Table 1) is taken as the only factor.

Tab. 1 The prices of raw materials in RPC

Raw materials	Cement	Silica fume	Sand	Super-plasticizer	Steel fiber
Price (Yuan/kg)	0.4	2.8	0.03	11.2	30

Costs for one cubic meter of RPC are calculated and presented in Table 2. When steel fiber content is 0.5%, the price of RPC is the lowest, and is RMB 2500 per cubic meter. The price grows with the increase of steel fiber. In addition, failure mode of RPC without steel fiber is likely explosive. It is not proper for application, and not listed in the table.

For engineering applications, it is demanded that not only requirements of mechanical properties are fulfilled, but also that materials with the highest cost-performance ratio are chosen.

Tab. 2 The cost-performance ratio of RPC versus steel fiber content

Steel fiber content (%)	0.5	1	1.5	2	2.5	3
Price of one cubic meter RPC (Yuan)	2500	3663	4827	5990	7177	8340
Axial compressive strength (MPa)	122.4	129.5	133.8	143.5	141.9	140.3
Splitting tensile strength (MPa)	9.68	7.99	11.32	18.12	20.44	23.64
Flexural strength (MPa)	6.5	9.3	10.6	11.0	14.4	15.1
Synthetical strength (MPa)	94.7	100.8	117.7	144.9	163.4	175.9
Cost-performance ratio	0.038	0.028	0.024	0.024	0.023	0.021

5. CONCLUSIONS

The incorporation of steel fiber significantly improved the strength of RPC. The axial compressive increases firstly but then decreases with the increase of steel fiber content, the changing point of steel fiber content is 2%. The splitting tensile strength and the flexural strength mainly increase with increasing of steel fiber content.

RPC cost-performance ratio is inversely proportional to the content of steel fiber. According to the analysis, the cost-performance ratio is the highest, when the steel fibers are introduced into RPC at the ratio of 0.5% by volume.

6. REFERENCES

Adeline, R., Lachemi, M., Blais, P.,(1998),,Design and behavior of the Sherbrooke footbridge. Proceeding of the international symposium on high-performance and reactive powder concretes, Sherbrooke, August 1998

Cavill, B., Chirgwin, G.,(2003),,The world’s first RPC road bridge at Shepherds Gully Creek, NSW. 21st Biennial conference of CIA, Brisbane, July 2003.

Bum, H. S., Joo, B. Y.,(2005),,Sim-Yu Pedestrian Arch Bridge, Seoul, Korea. Structural Engineering International: Journal of the International Association for Bridge and Structural Engineering, 15(1): 32—34, 2005.

Zimmermann, W.,(2008),,UHPC-First applications with ultra high performance concrete in Austria. 4th CCC Symposium in Opatija, Croatia, Oct 2008.

Huang, Z. B.,(2008),,The mix proportion design of permeability resistance and cracking resistance reactive powder concrete based on artificial neural network. Master's Thesis, Fujian: Fuzhou University, 2008. (in Chinese)

Zhou, Y. Q., Du, Y. F.,(2000),,The first precast prestressed structure of RPC in the world-the Sherbrooke footbridge[J]. Foreign bridges, 2000(3): 18-23. (in Chinese)

Richard, P., Cheyrezy, M.,(1995),,Composition of Reactive Powder Concretes. Cement and Concrete Research, 25(7): 1501-1511, 1995

Wu, Y. H., He, Y. B., Y. H.,(2003),,Yang: Investigation on RPC200 mechanical performance. Journal of Fuzhou University, 31(5), 598-602, 2003. (in Chinese)

He, F., Huang, Z. Y.,(2000),,Research on preparation of 200～300MPa RPC. China concrete and cement products, (4), 3-7, 2000. (in Chinese)

Guo, M.,(2008),,RPC Research on RPC Arch and its Mechanical Behaviors. Master's Thesis， Beijing: Beijing Jiaotong University， 2008. (in Chinese)

LOCALLY AVAILABLE SECONDARY RAW MATERIALS FOR SELF COMPACTING CEMENTITIOUS SYSTEMS

Syed Ali Rizwan[1], Arsalan Rao[2], and Thomas. A. Bier[3]

1. Professor of Civil Engineering, HoD Structural Enginering Department, NUST Institute of Civil Engineering (NICE), National University of Sciences & Technology (NUST), Islamabad, Pakistan.Member ACI committees 237, 234 &232. Email: syedalirizwan@hotmail.com.Corresponding Author.
2. PostGraduate student, NUST Institute of Civil Engineering (NICE), National University of Sciences & Technology, Islamabad (NUST),Islamabad, Pakistan. Email: rao_nust@yahoo.comAuthor.
3. Professor and Chair of Construction Materials Technology, Institute of Ceramics, Glass and Construction Materials (IKGB), Technical University Freiberg Germany. Email: thomas.bier@ikgb.tu-freiberg.de.

SUMMARY

This study is a continuation of a research programme aimed at finding suitable locally available secondary raw materials for making High Performance Concrete (HPC) and Self Compacting cementitios Systems(SCPS) in Pakistan. Secondary raw materials are used in all modern concrete systems due to advantages offered. This study evaluates the feasibility of using Bentonite (BN), a naturally occurring pozzolan and Wheat Straw (Toori) Ash, an artificial pozzolanic material, in self compacting paste systems with ultimate aim to produce self compacting concrete with desired properties. The parameters studied include secondary raw material's particle characterization, flow behavior and strength development of self compacting paste systems.

1. INTRODUCTION

Self Compacting Concrete (SCC), a kind of high performance concrete (HPC) possesses excellent deformation (low yeild stress)and adequate segregation resistance(adequate viscosity). A paste type of SCCwas firstdeveloped in university of Tokyo Japan *(Su, Husand Chai, 2001) (Okumura, Ouchi, 2003)* and now many developed countries are exploring the potential of this technology in their construction projects.

The European Guidelines for Self Compacting Concrete *(European Guidelines for Self Compacting Concrete 2005)* give some basic information and lately ACI committee 237 is developing the specifications. The paste phase of self compacting cementitious system acts as a vehical for the transport of aggregate phase and also plays the most important role in service life performance of the structures. This phase mainly consists of cement, secondary raw materials, chemical admixtures and water. The study was made on the use of locally available SRMs including "As Obtained" Bentonite as well as "Calcined" Bentonite at 150^{o}C for 8 hrs and Toori ash(wheat straw ash) for which specially designed burning regimes were found and the details are available in another paper by the authors *(Rizwan, Arsalan, and Bier 2011).*

2. EXPERIMENTAL PROGRAMME

2.1 Materials

The material used in this investigation consisted of Pakistani Fouji Brand Grade 53 OPC cement. SRM's consisted of "As Obtained" and "Calcined" Bentonite as well as Toori (wheat straw) ash. Melflux powder, a third generation poly-carboxylate ester based superplasticizer has been used for producing target flow of 30±1 cmmeasured by Hagerman's mini slump cone of 6x7x10 cm^3dimentions. 4x4x16 cm^3 prisms were cast at temperature of 20^oC and relative humidity greater than 90%. The samples were covered with plastic sheet for the first 24 hours and were later water cured till the age of testing in SSD conditions as per DIN EN 196 standard. The partical size and BET surface areas of powders were measured. Tab. 1 gives physical and chemical properties of powders used.

Tab. 1 Physical and Chemical Properties of Powders Used

Parameters	**Cement Grade 53**	**Bentonite (Calcined)**	**Bentonite (As Obtained)**	**Toori ash**
Particle size (µm)	22	4.75	4.32	12.5
Surface Area(cm^2/gm)	1650	4800	2535	3200
Specific gravity	3.10	2.82	2.79	2.3
Chemical Analysis				
SiO_2	17.15	53.96	41.69	73.95
TiO_2	0.32	0.93	1.92	1.92
Al_2O_3	5.60	20.27	10.67	0.91
Fe_2O_3	3.21	8.92	31.34	1.15
MgO	1.44	4.02	0.88	1.83
CaO	64.09	7.05	9.09	5.21
K_2O	1.19	3.93	4.05	11.51

2.2 Mixing Regime

The mixing was done using Hobart Mixer of 5L capacity. The constituents including cement, secondary raw material and powder superplasticizer were first manually mixed in closed plastic container in dry state. These were then fed into the bowl of mixer containing requisite mixing water. A slow mixing (145 rpm) was carried out for 30 seconds and then interior of bowl was cleaned. Thereafter, again slow mixing was done for 30 seconds and finally, the formulation received 120 seconds of fast mixing (285 rpm) *(Rizwan, 2006)*. The total mixing time was thus 3 minutes (180 seconds) as per EN-D/N 197.

2.3 Specimen Designation

A typical formulation used in the experimental program may be written as; C + 10 TA, where the first letter donates cement, followed by a numeral which indicates mass of secondary raw material in percent mass of cement and the next letters denote secondary raw material type i-e "TA" for Toori Ash and "BN" for Bentonite.

3. RESULTS AND DISCUSSIONS

3.1 Water Demand, Superplasticizer Demand and Setting Times

Fig. 1 shows the water demand, superplasticizer demand and setting times of self compacting paste formulations using the SRMs. Results of "As Obtained" Bentonite have been taken from MS thesis at NUST *(Niazi, 2010)* for comparison.

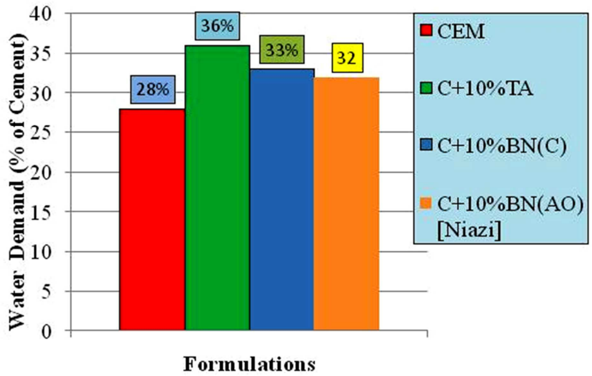

Fig. 1(a) Water Demand

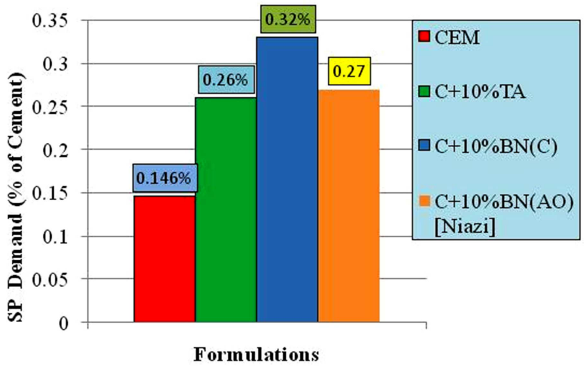

Fig. 1(b) Superplasticizer Demand

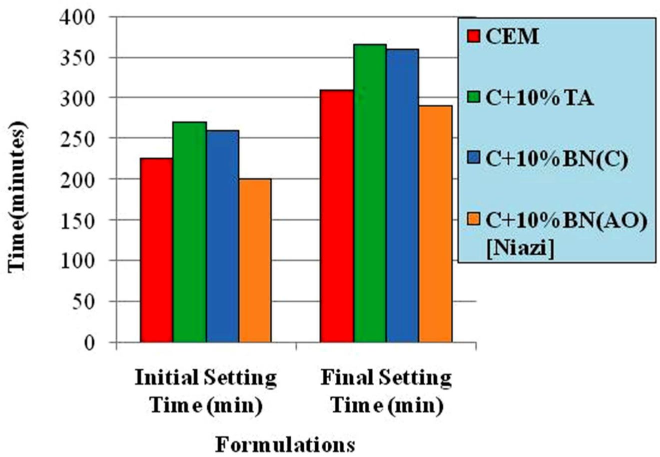

Fig. 1(c) Setting Times

Fig. 1 Water Demand, Superplasticizer Demand and Setting Times of SCP Formulations

Particle shape, size and morphology of secondary raw materials are quite important parameters for understanding their role in terms of water and superplasticizer demands, flow, strength, shrinkage and microstructure of self compacting paste systems. The details can be seen in the literature *(Arsalan, 2011).*

Toori (wheat straw) ash and "Calcined" Bentonite had much smaller average particle sizes and much greater specific surface areas as compared to local Faugi brand Pakistani Ordinary Portland Cement (OPC) as mentioned in Tab. 1. Large surface area of Bentonite and Toori ash particles might indicate the presence of small internal pores. SCP formulations containing

Bentoniteand Toori ash in replacement mode have high water demand and superplasticizer demand due to their small particle size and large surface area.

Retardation in setting time of self compacting formulation is also recorded with Toori Ash and Bentonitereplacementas shown in Fig. 1 (c). The increase in the setting time of SCP formulations containing Toori Ash and “Calcined” Bentonite in replacement is due to dilution.

3.2 Flow of SCP Formulations

Fig. 2 shows the Hagerman’s mini slump cone time for a spread of 25 cm. T 25 time was noted for a target flow of 30±1cm achieved by a superplasticizer Melflex 2651 powder. Fig. 3 shows the V Funneltime of formulations to have an idea regarding the viscosity of different paste formulations. The funnel consisted of a rectangular cross section with top dimension as 270 x 30 mm and bottom opening as 30 x 30 mm. The total height of funnel was 315 mm with a 75 mm long straight bottom square or rectangular section with a gate at bottom.

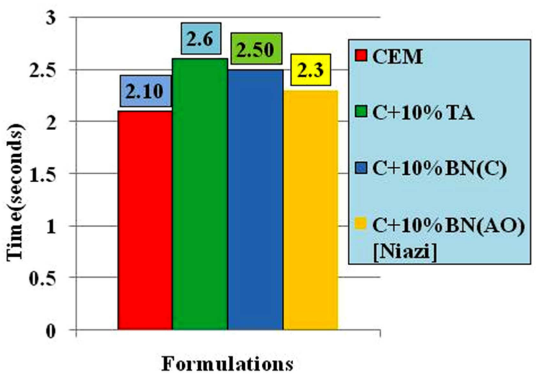

Fig. 2 Variation of T25 cm time of SCP Formulations

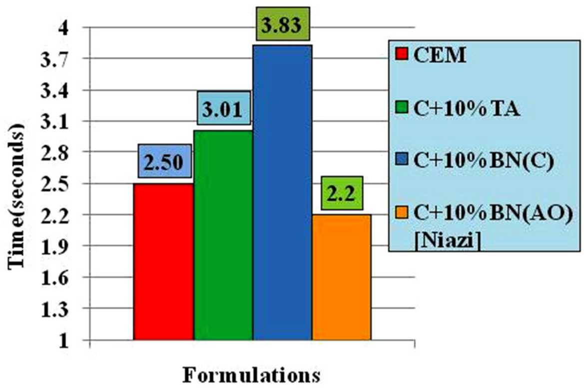

Fig. 3 Variation of V Funnel time of SCP Formulations

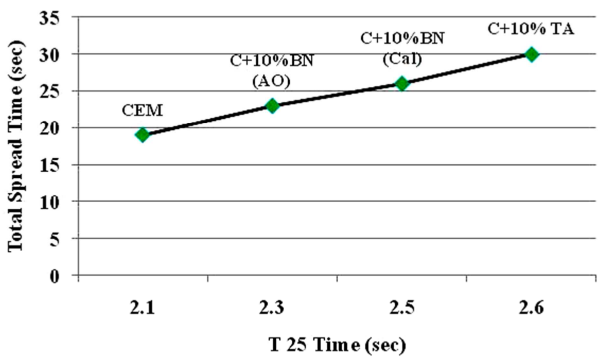

Fig. 4 Variation between T25 Time and time for total spread of 30±1 cm

SCP formulations containing “Calcined” Bentonite and Toori Ash in replacement mode had high yield stress and high viscousity as indicated by increase in T25 cm time and V Funnel time (Fig. 2 and Fig. 3). The increased viscousity and yield stress might be due to the absorption of water in the porous structure of Toori Ash and “Calcined” Bentonite particles and thus less effective water was available in the system to help the flow.

Fig. 4 shows the variation between T25 time and time for total spreadof 30±1 cm. As total spread time is a function of yield stress and T25 time is a function of viscosity and rate of deformation therefore we may conclude that viscosity is also a function of yield stress. Also there is a very little variation in the slope of the graph.

3.3 Strength of SCP formulations

Results for compressive strength of SCP system for various formulations are shown by bar charts in Fig. 5.

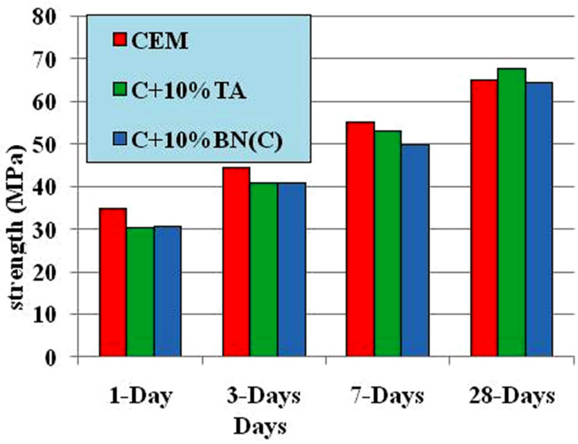

Fig. 5 CompressiveStrength of SCP with Various Secondary Raw Materials

Strength of self compacting paste system is defined and governed by combination of maximum pore size, degree of pozzolanic activity and degree of packing *(Rizwan and Bier, 2009).* Higher the pore size, lower pozzolanic activity and loose packing all results in the reduction of strength.

At the age of 1, 3 and 7 days self compacting paste formulations containing “Calcined” Bentonite and Toori Ash, in replacement mode, gave lesser value of compressive strength as as compared to control mix but at the age of 28 days, SCP formulations with Bentonite achieved strength almost equal to that of control mix and SCP with Toori Ash gave four percent high compressive strength (Fig. 5).

4. CONCLUSIONS

Toori (wheat straw) ash and Bentonite seems to be quite suitable local SRMs for use in modern concrete systems in Pakistan**.**

The SRM’s shape, size and morphology (particle characterization) is very important for modern cement based systems, as it affects almost all the resulting properties of self compacting paste systems.

Toori (wheat straw) Ash and Calcined Bentonite based self compacting paste formulations SCP give maximum strength activity index (Fig 4) even higher than the control mix.Seeing the trends, even higher strength beyond 28 days are expected.

5. ACKNOWLEDGEMENTS

The authors are grateful to the NUST Institute of Civil Engineering (NICE) and Military College of Engineering (MCE) Pakistan for providing facilities for the completion of this work. Thanks are due to Laboratory staff at IKGB, TU Freiberg, Germany for providing help.

6. REFERENCES

Arsalan, R. (2011). “A study of self compacting cementitious systems using Calcined Bentonite and Toori (wheat straw) ash.” MSc. Thesis, NIT (NUST) Islamabad.

Biricik H. et al., (2000)“Resistance to magnesium sulfate and sodium sulfate attack of mortars containing Wheat Straw Ash”, *Cement and Concrete Research* 30 1189-1197.

Birick H., (1995): Pozzolanic Properties of Wheat Straw Ash and Effects on Durability of Mortar, The Institute for Graduate Studies in Science and Technology of Yildiz Technical University, PhD Thesis

European Guidelines for Self Compacting Concrete, (2005), EFNARC, http://www.efnarc.org/publications.html, accessed on 15 February 2010, pp.1-163.

Niazi, B. (2010). “A study of self compacting cementitious systems using bagasse ash and Bentonite.” MSc. Thesis, NIT (NUST) Islamabad.

Okumura. H, Ouchi. M,(2003): “Self Compacting Concrete”, *Journal of Advanced Concrete Technology* Vol. 01, No. 05, 5-15.

Rizwan, S.A., Arsalan, R.,and Bier, T. A. (2011); “Influence of Incineration Regimes on Pozzolanic properties of Toori (wheat straw) ash”, paper submitted in7rd European Congress on Concrete Engineering, Balatonfüred, Hungary

Rizwan, S. A. (2006); “High – Performance Mortars and Concretes using Secondary Raw Materials”, PhD thesis, Technical University, Freiberg, Germany, ISBN 978-3-639-17878-4, pp. 1-132

Rizwan, S.A. and Bier, T. A. (2009); “Self Consolidating Mortars Using Various Secondary Raw Materials”, *ACI Materials Journal*, V. 106, No. 1, , pp. 1-8

Rizwan, S.A. and Bier, T. A. (2005): “Role of Mineral Admixtures in High Performance Cementitious Systems”, 2nd All Russian International Conference on, ‘Concrete and Reinforced Concrete-Development Trends’, Vol. 3, Concrete Technology, 5-9, Moscow, Russia. pp. 727-732.

Su, N.; Hus, K. C. and Chai, H. W. (2001); “A Simple Mix Design Method for Self Compacting Concrete”, *Cement and Concrete Research*, 31, pp. 1799 – 1807.

PERFORMANCE OF REACTIVE POWDER CONCRETE PRODUCED USING FINE QUARTZ SAND

Shamsad Ahmad [1], Mohammed Maslehuddin [2], Abul Kalam Azad [1]
[1] *Civil Engineering Department, King Fahd University of Petroleum & Minerals, Dhahran-31261, Saudi Arabia*
[2] *Center for Engineering Research, Research Institute, King Fahd University of Petroleum & Minerals, Dhahran-31261, Saudi Arabia*

SUMMARY

Reactive Powder Concrete (RPC) is an ultra-high performance concrete having excellent mechanical properties and high resistance against water and chloride penetration. RPC consists of very low water-to-binder ratio, very high superplasticizer dosage, fine quartz sand, crushed quartz, silica fume, and small-size steel fibers for improving toughness. In RPC, fine quartz sand replaces coarse aggregate and crushed quartz replaces fine aggregate. This enables in producing high performance concrete mixtures even in the absence of good quality coarse aggregates. This paper presents the experimental program and preliminary test results of an ongoing research project on assessing the mechanical properties and durability of RPC trial mixtures produced using local dune sand characterized as fine quartz sand with particle size ranging from 75 to 600 μm.

1. INTRODUCTION

Reactive powder concrete (RPC) with compressive strength of more than 150 MPa and other superior material properties is a new generation cementitious material that originated through intensive research work mostly conducted in France and Canada since 1994 (*Ma and Schneider, 2002*). Different applications of RPC include: heavily reinforced precast elements for bridge decks; in situ applications for the rehabilitation of deteriorated concrete bridges and industrial floors (*Buitelaar, 2004*). With or without additional "passive" reinforcement it is used for precast elements and other applications like offshore bucked foundations. In addition, coarse grained RPC with artificial or natural high strength aggregates were developed for heavily loaded columns and for extremely high-rise buildings (*Schmidt et al., 2003*).

The basic principle on which RPC is based is to achieve a cement matrix as dense as possible (by reducing micro cracks and capillary pores in the cement matrix) and a dense transition zone between matrix and aggregate. Following measures are suggested to produce RPC:

- Enhancing the homogeneity by elimination of coarse aggregate. It is suggested that the maximum aggregate size in RPC should be less than 600 μm. Fine quartz sand (150 to 600 μm) replaces coarse aggregate and quartz powder (smaller than 10 μm) is used as micro-filler replacing fine aggregate (*Richard and Cheyrezy, 1995; Ma and Schneider, 2002*).
- Improving the properties of cement matrix by the addition of supplementary cementing materials, such as silica fume. The amount of the silica fume (micro-silica with size ranging from 0.1 to 1.0 μm) may go up to 30% of the mass of cement (*Richard and Cheyrezy, 1995*). The silica fume content in RPC is normally in the range of 25-30% of the cementitious material. An ordinary Portland cement (Type I) with low C_3A content is used. Cement and silica fume together is termed as 'binder' in RPC.

- Improving the properties of cement matrix by reducing water to binder ratio (0.15 to 0.24).
- Using a high dosage of superplasticizer to achieve the desirable fluidity.
- Using short high carbon steel or polymer fibers at various volume fractions to improve its tensile and flexural strength, toughness, decrease cracking, and alter the mode of failure by increasing post cracking ductility (*Shah and Weiss, 1998*).
- Enhancing the microstructure by post-set heat-treatment.

(Tam et al. 2010) in their study on optimal conditions for producing RPC have found that RPC with a water-to-binder ratio of 0.2, superplasticizer dosage of 2.5%, 150 – 600 μm quartz sand cured at 27 °C in water conditions provides the best results in terms of mechanical and composite properties. They found that the heat treatment of RPC can result in a significant increase in compressive strength.

Though sufficient information is available on the development of RPC in the other parts of the world, there is a lack of data on the RPC prepared utilizing the local fine aggregate, which is characterized as very fine with a low fineness modulus. Also, very limited information is available on the durability of RPC, particularly under the local aggressive environmental conditions. Considering this, a research work is in progress where an attempt is being made to evaluate the performance of various possible mixtures of RPC produced using local dune sand characterized as fine quartz sand with particle size ranging from 75 to 600 μm. The experimental program and preliminary test results are presented in this paper

2. EXPERIMENTAL PROGRAM

The ongoing research work is being carried out in the following steps:

1. Collection of information on locally available ingredients and procurement of ingredients from different local sources to examine their suitability for the production of RPC.

2. Characterization of the ingredients to assess their chemical composition and physical properties.

3. Selection of the optimum grading of the local fine quartz sand. As described in the next section, the natural grading of the local dune sand (96.2%, 61.4%, 21.9%, and 1.0% passing through 600 μm, 300 μm, 150 μm, and 75 μm sieves, respectively) has been found to be the optimum grading.

4. Design of a total number of 27 trial mixtures of RPC using absolute volume method considering three values of each of the mixture variables (water-to-binder ratio, cement content, silica fume content), as follows:
   Water-to-binder ratio: 0.15, 0.175, 0.20
   Cement content (Kg/m^3): 1000, 1100, 1200
   Silica fume content: 15%, 20%, 25% by mass of cement
   For all trial mixtures, natural grading of sand and a fiber content of 150 kg/m^3 will be used. Glenium 51 will be used as superplasticizer. Dosage of the superplasticizer for each mixture will be selected for acheiving a flow value of 200±20 mm.

5. Preparation of plain and reinforced concrete specimens for all trial mixtures of RPC.

6. Testing specimens to evaluate: compressive strength, tensile strength (both split cylinder and modulus of rupture), modulus of elasticity, fracture toughness, shrinkage, chloride permeability, sulphate resistance, and reinforcement corrosion resistance. The sulphate-resistance would be evaluated by placing RPC specimens in a sodium sulphate plus magnesium sulphate solution. For this purpose, the specimens would be exposed to 2.1% SO_3 (50% sodium sulphate plus 50% magnesium sulphate) solution. The sulphate resistance would be evaluated by measuring the reduction in compressive strength after 9, 12, and 24 months of exposure to the sulphate solution. Control specimens immersed in water will also be tested at same ages. The corrosion resistance will be evaluated by immersing the specimens in 5% sodium chloride solution. Reinforcement corrosion would be evaluated by measuring corrosion potentials and corrosion current density every 30 days. Specimens will also be subjected to impressed current corrosion to determine the time to cracking.

7. Based on the analysis of the experimental data generated through this study, recommendations regarding the design and preparation of the preferred mixtures of RPC will be made as the major outcome of this research work.

3. PRELIMINARY TEST RESULTS

In order to select an optimum grading of the sand, six trial mixtures of RPC were considered with different sand grading, as mentioned in Tab. 1. For each mixture, a water-to-binder ratio of 0.2 (by mass), a cement content of 1000 kg/m^3, a silica fume content of 150 kg/m^3, a water content of 230 kg/m^3, and a sand content of 977 kg/m^3 were used. Glenium 51was used as superplasticizer (SP). Suitable dosages of SP (% by mass of the binder), as given in Tab. 1, were used for the different trial mixture for maintaining a flow of around 20 cm. All samples were water cured at normal room temperature.

Tab. 1 Preliminary test results

Trial Mix	Sand grading	SP %	Flow (cm)	Compressive strength (MPa)		
				7-day	14-day	28-day
1	Natural grading (taken as supplied)	1.5	20.0	92	109	126
2	Passing 600 μm sieve and retained on 150 μm sieve	1.7	18.0	81	102	117
3	All passing 600 μm sieve	1.8	16.0	87	91	113
4	All passing 300 μm sieve	2.0	21.5	88	96	109
5	All passing 150 μm sieve	2.1	17.5	78	85	101
6	Mixed (one-third of each passing through 600, 300, and 150 μm sieve)	1.9	19.5	57	63	64

It can be observed from Tab. 1 that the natural grading of the sand is most suitable because it has resulted in a maximum strength at a minimum dosage of the superplasticizer. However, the strength is still less than the minimum strength of 150 MPa for a RPC. This is because of lower silica fume content and a higher water-to-binder ratio selected for the preliminary trial mixtures. Based on these feedbacks, it has been decided to use the natural grading of sand in another 27 trial mixtures considering three cement contents (two values more than 1000 kg/m^3), three silica fume contents (two values more than 150 kg/m^3), and three values of water-to-binder ratio (two values less than 0.2) for achieving desired strength and other properties of the RPC.

4. CONCLUSIONS

The preliminary test results show that the natural grading of the local dune sand is most suitable for producing RPC. However, even the best mixture produced under preliminary trials failed to provide a minimum compressive strength of 150 MPa needed for RPC. The information obtained through the preliminary part of the research has been utilized to carry out a suitable experiment design for achieving the desirable properties of the RPC mixtures.

5. ACKNOWLEDGEMENTS

The authors gratefully acknowledge the financial support received from King Fahd University of Petroleum & Minerals (KFUPM), Saudi Arabia for carrying out this project under the CRG funding (Project No. RG1005-1 and RG1005-2). The support of the Department of Civil Engineering and the Center for Engineering Research at the Research Institute of KFUPM are also acknowledged.

6. REFERENCES

Ma, J. and Schneider, H., (2002), "Properties of Ultra-high-performance Concrete", LACER, No.7, pp. 25-32.

Buitelaar, P., (2004), "Heavy Reinforced Ultra Reactive Powder Concrete", *Proceedings of the International Symposium on Ultra Reactive Powder Concrete,* Kassel University Press, Kassel, Germany.

Schmidt, M., Fehling, E., Teichmann, T., Bunje, K., and Bornemann, R., (2003), "Ultra Reactive Powder Concrete: Perspective for the precast concrete industry", *Beton und Fertigteil-Technik*, 3, pp. 16-29.

Richard, P. and Cheyrezy, M., (1995), "Composition of Reactive Powder Concretes" *Cement and Concrete Research*, 25(7), pp. 1501-1511.

Shah, S.P. and Weiss, W.J., (1998), "Ultra High Strength Concrete; looking toward the future", *ACI special proceedings from the Paul Zia symposium*, Atlanta.

Tam, C.M., Tam, V.W.Y., and Ng, K.M., (2010), "Optimal Conditions for Producing Reactive Powder Concrete". *Magazine of Concrete Research*, 62(10), October, pp. 701-716.

CALCINED MARL AS ALTERNATIVE POZZOLAN

Tone Østnor[1], Harald Justnes[1], Tor Arne Martius-Hammer[1] and Tobias Danner[2]
[1] *SINTEF Building and Infrastructure, Concrete Inovation Centre (COIN)*
7465 Trondheim, Norway
[2] *Norwegian University of Science and Technology*
Department of Materials Science and Engineering
7491 Trondheim, Norway

SUMMARY

Marl with 10-20% $CaCO_3$ was calcined over a range of temperatures from 600 to 1000°C, and the optimum calcination temperature with respect to reactivity as pozzolan seemed to be 800°C.

The compressive strength of mortars was tested at equal water-to-cementitious material ratio when Ordinary Portland Cement (OPC) was replaced with calcined marl. Mortar with 20, 35 and 50% marl calcined at 800°C achieved 62, 64 and 55 MPa (equal to reference without cement replacement) compressive strength, respectively, after 28 days curing at 20 ºC. The 1 day strength for mortar with 50% calcined marl replacing cement was sufficient for removing formwork in practical concreting (close to 10 MPa).

1. INTRODUCTION

Marl is considered ”bad” clay for production of burnt clay products (e.g. bricks and light weight aggregate) since it is clay contaminated with substantial amounts of calcium carbonate that will form CaO after burning that can lead to “pop outs” in reaction with water during service. Calcined marl is shown to be an effective pozzolan and for this reason marl can be a large resource that is not exploited to make blended cements or as a mortar/concrete additive.

Calcined marl can be considered “industrial pozzolan” within the European cement standard (EN 197-1), and it may be feasible to make a pozzolanic cement with up to 55% clinker replacement (CEM IV/B) considering the 28 day strength and sufficient early strength documented in this paper.

2. MATERIALS AND METHODS

2.1 Materials

- The cement used was Standard cement (CEM I according to EN 197-1) from the Norwegian cement producer NORCEM (part of Heidelberg Group), Brevik, Norway.
- The calcium hydroxide used was *pro analysi* (laboratory grade) from Merck, Germany.
- The marl (or rather calcareous clay) calcination was done at IBU-Tec in Germany, in a small rotary kiln (7m in length) to simulate technical and industrial conditions.
  Grinding of the calcined materials to d_{50} = 3 µm was performed at UVR-FIA GmbH in Freiberg.

2.2 Mortar mix designs

The consistency of fresh mortar was determined using a flow table. The aim was to obtain a w/b ratio of 0.5 in all mortars by varying the amount of super-plasticizer. 0.1 – 0.8 % (of binder weight) of super-plasticizer was added in the mortar mixes. The flow of all mortars was within ± 5 % of the reference. The mortar mixes were cast in 3 pc. 40x40x160 mm moulds and stored in a cabinet with 23 ± 2°C and 90% RH for 24 hours. After 24 hours the prisms were removed form the moulds and stored in saturated lime water for 28 days. After 28 days storage the compressive strength and the flexural strength was determined according to NS-EN 196-1.

2.3 Paste for pozzolanicity test

In order to simplify the system, clinker was excluded in the mixes for thermal analysis. In stead an excess of laboratory grade calcium hydroxide, $Ca(OH)_2$, and alkaline mixing water (i.e. pH 13.2 and KOH/NaOH = 2:1) was used to simulate the conditions in a hydrating cement paste. The ratio between calcined marl and calcium hydroxide (CH) was 2/1.

The samples were analyzed by thermogravimetric analysis and simultaneous differential thermal analyses (TGA/SDTA) with a Mettler Toledo TGA/SDTA 851. About 150 mg of the frozen sample was weighed into aluminum oxide crucibles. Prior to the thermal analysis the samples were submitted to a drying step in order to avoid interference by the non-reacted free or adsorbed water. During the drying step the sample was kept at 20°C and dried in the instrument by the purge gas, N_2, at a flow of 50 ml/min. After drying the sample was heated from 30°C to 1100°C with a heating rate of 10°C/min.

3. RESULTS

3.1 Compressive and flexural strength

The compressive and flexural strength of mortars with 20% replacement of OPC with marl calcined at different temperatures are plotted in Fig. 1. The sample marked 650/800 gave the best results. This calcined marl was then chosen for 35 and 50% replacement as well, and the compressive and flexural strengths of these mortars after 28 days curing are plotted in Fig. 2. The early strengths for mortar where 50% cement is replaced with marl calcined at 800°C are presented in Fig. 3.

3.2 Pozzolanicity

The pozzolanic effect was documented by lime consumption after the calcined marl was mixed with lime and simulated concrete pore water of pH 13.2. From Table 1 it can be seen that marl/lime blend cured for 28 days at 20 °C and 38 °C consumed 62 and 61 % of the added calcium hydroxide, respectively. For marl/lime blend cured for 6 months the consumption of calcium hydroxide was 73 % and 72 %. Typical lime consumption for silica fume is 78 % under otherwise equal conditions (Justnes, 1992). The hydration products of the pozzolanic reaction are likely to be similar to those of siliceous fly ash (CSH, CAH and CASH), after all fly ash is formed from clay contaminations in coal burnt in thermal power plants. The calcium aluminate hydrates can then combine with any present calcium carbonate to calcium carboaluminate hydrates as documented for fly ash *(Weerdt K. De and H. Justnes 2008), (Weerdt De 2009) (Weerdt De, , Justnes, Kjellsen and Sellevold, 2010) (Weerdt De, , Kjellsen, Sellevold and Justnes, 2011)* and thereby increase the overall amount of hydrates and subsequently strength.

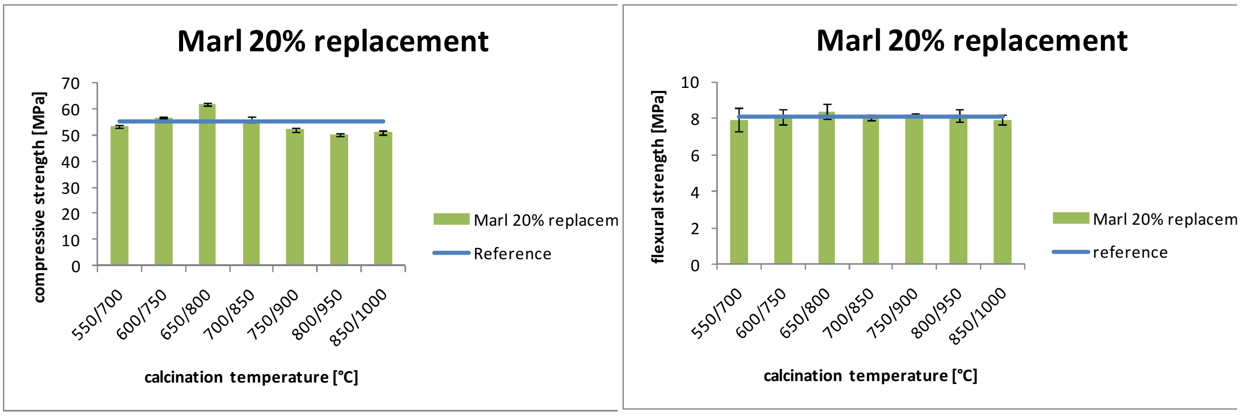

Fig. 1. Compressive and flexural strength of mortars with 20 % replacement of cement by calcined marl as a function of calcination temperature for the marl.

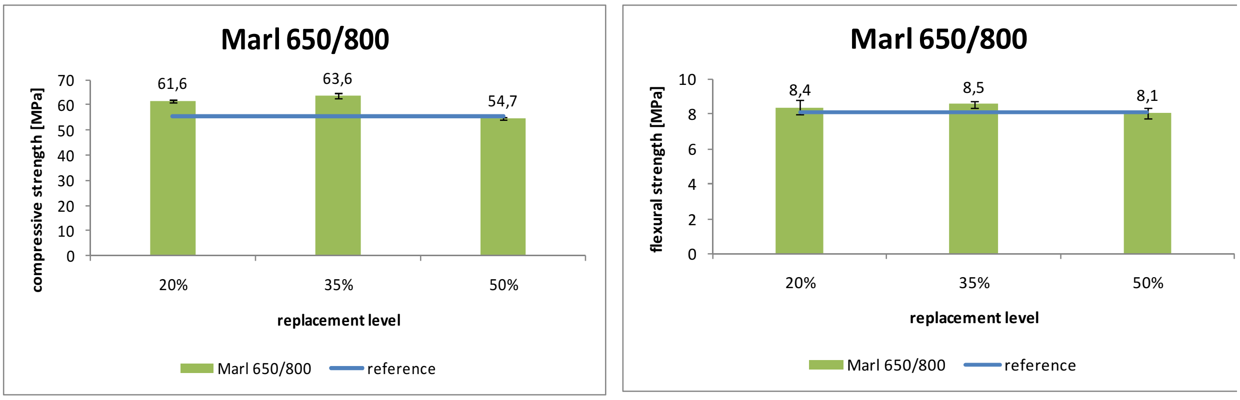

Fig. 2. Compressive and flexural strength of mortars with 20, 35 and 50 % replacement of cement by marl calcined at 800°C. Reference is mortar based on 100% Portland cement with strength level according to the blue line.

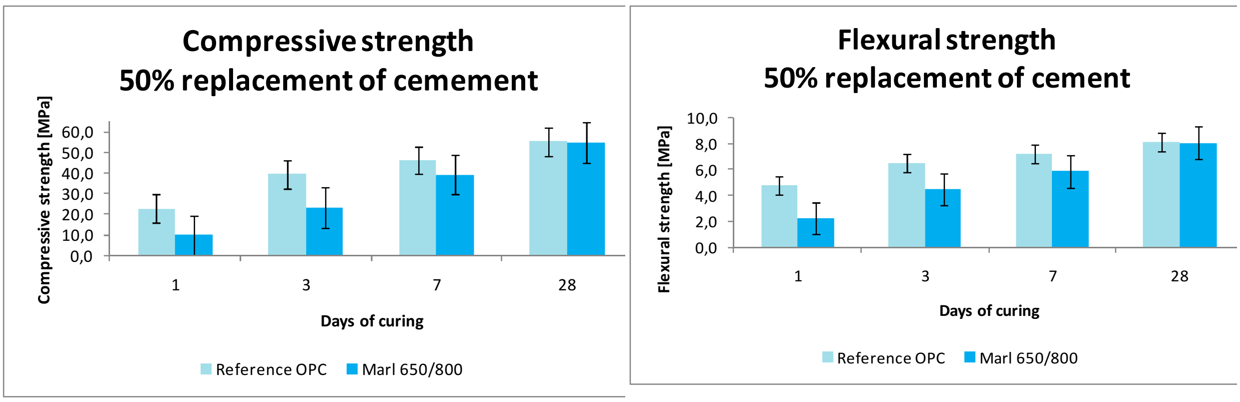

Fig. 3. Compressive and flexural strength of mortars with 50 % replacement of cement by marl calcined at 800°C cured for 1, 3, 7 and 28 days. Reference is mortar without cement replacement.

Tab. 1. Calcium hydroxide (CH) consumption in the marl paste

Curing	**20 °C moist**	**38 °C moist**
CH at 0 days	31.7	31.7
CH at 28 days	11.9	12.3
Consumed CH [%] 0-28days	62.4	61.2
CH at 6 month	8.6	9.0
Consumed CH [%] 0-6 mouth	72.8	71.6

4. CONCLUSIONS

It has been demonstrated that carefully calcined marl, or calcareous clay, can be transformed to a very effective pozzolan that can replace cement as binder in mortar.
Up to 50% calcined marl can replace Portland cement and still the 28 days strength can be maintained.
From an environmental perspective it is clear that replacing Portland cement with 50% calcined marl can have a large impact on reduced CO_2 emissions, which is a challenge for the cement industry as a whole.

5. ACKNOWLEDGEMENTS

The paper is based on the work performed in COIN - Concrete Innovation Centre (www.coinweb.no) - which is a Centre for Research based Innovation, initiated by the Research Council of Norway (RCN) in 2006. COIN has an annual budget of NOK 25 mill, and is financed by RCN (approx. 40 %), industrial partners (approx 45 % of which ¼ is cash) and by SINTEF and NTNU (in all approx 15 %). The Centre is directed by SINTEF, with NTNU as a research partners and with the present industrial partners: Aker Solutions, Norcem, Norwegian Public Roads Administration, Rescon Mapei, Skanska, Spenncon, Unicon, Veidekke and Weber Saint Gobain.

6. REFERENCES

Justnes, H. (1992); "Hydraulic binders based on condensed silica fume and slaked lime", The 9th International Congress on the Chemistry of Cement, New Delhi, India, Vol. III, pp. 284-290.

Weerdt K. De and H. Justnes (2008): ”Microstructure of Binder from the Pozzolanic Reaction between Lime and Siliceous Fly Ash, and the Effect of Limestone Addition”, Proceedings of 1st Int. Conf. on Microstructure Related Durability of Cementitious Composites, Nanjing, China, pp. 107-116, RILEM Proceeding PRO 61.

Weerdt K. De (2009): “Synergic Reactions in Triple Blended Cements”, Proceedings of the 11th NCB International Seminar on Cement and Building Materials, New Delhi, India, pp. 257-261.

Weerdt De, K., Justnes, H., Kjellsen, K.O. and Sellevold, E. (2010): ”Fly Ash-Limestone Ternary Composite Cements: Synergy Effect at 28 days”, Nordic Concrete Research, Publication No. 42, 2/2010, pp. 51-70 (ISBN: 978-82-8208-023-1).

Weerdt De, K., Kjellsen, K.O., Sellevold, E.J. and Justnes, H. (2011): ”Synergy between Fly Ash and Limestone Powder in Ternary Cements”, Cement and Concrete Composites Vol. 33, Issue 1, pp. 30-38.

EXPERIMENTAL STUDY OF SOME HIGH-STRENGTH CONCRETE ISOLATED STRUTS

A. Arabzadeh [1], R. Aghayari [2]

1. *Assistant Professor of Structural Engineering Dept., Tarbiat Modarres University, Tehran, IRAN, Tel: 021-82883323, Email: arabzade.a@gmail.com*
2. *Assistant Professor of Civil Engineering Dept, Razi University, Kermanshah, IRAN, Tel: 0831-4283264, Email: r.aghayari@gmail.com*

SUMMARY

Strut-and-Tie Model (STM) can be used to model the flow of compression within a concrete strut. Concrete struts are formed in various shapes such as prismatic or bottle-shaped. Eighteen reinforced concrete isolated struts with compressive strength of 65 MPa were tested to failure under point loading in the plane of specimens. The tested specimens were reinforced by various reinforcement layouts. Observations were made on transverse displacement, primary cracking and ultimate failure load and distribution of strain on the face of tested panels.

1. INTRODUCTION

Strut-and-tie method (STM) is one of the most simple and applicable methods that can be used to reduce complex states of stresses within concrete structures to a collection of simple stress paths. Struts as important element of strut-and-tie model carry compressive forces and their forming shapes varies depend on the force path. The most basic type of struts is prismatic with uniform cross-section over its length. The compressive stress block in the pure-bending region of deep beams can be an example of prismatic strut *(Michael Brown, Cameron Sankovich, Oguzhan Bayrak, and James Jisra 2006)*. When the flow of compressive stress is not confined to a portion of structural element, a bottle-shape strut forms that the force is applied to a small zone and disperses as they flow through the member. Its bulging stress paths cause the significant transverse strain perpendicular to strut axis. The formed transverse strain is compressive in near of both neck of bottle-shape strut and tensile further away *(Michael, Brown and Oguzhan Bayrak 2006).* Consequently, those strains cause longitudinal cracks and initiate an early failure. It is therefore necessary to reinforce the stress field in transverse direction or to consider the transverse tension to predict the ultimate strength of strut. Some studies have been published to investigate the behavior of RC bottle-shape struts and establish their ultimate strength and the minimum requirement transverse reinforcement on the basis of mechanic-based models *(Michael Brown, Cameron Sankovich, Oguzhan Bayrak, and James Jisra 2006), (Michael Brown and Oguzhan Bayrak 2006).*

2. EXPERIMENTAL PROGRAM

2.1. Specimen details

Test specimens consisted of eighteen concrete plain panels that measured 400×400×60 mm and were loaded using steel bearing plates that were 120×60×12 mm defining the nodal zone. The concrete was prepared by Type II Portland Cement and river fine aggregate. Maximum aggregate size was 9.5 mm (3/8 inch) and the slump was approximately 90 mm. The concrete strength was defined 65 MPa based on the average value of three standard cylinders (300×150 mm). The primary variables were the amount and placement of the reinforcing bars. The specimens were classified in the following series based on the various patterns of used transverse reinforcement. Each of the specimens is described in detail of Fig. 1; the tested panels were employed supplemental confinement at the nodal zones. This confinement consisted of short pieces of reinforcing 6D (6 mm-dia.) bars welded to a steel plate and surrounded by ties bent from 6D (6 mm-dia.) bars.

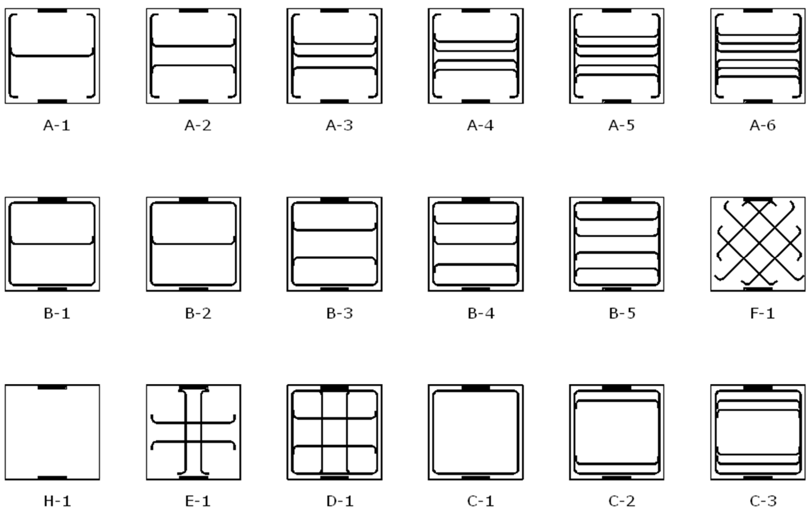

Fig. 1 The typical schema of specimens

2.2. Test setup and loading

The test setup was similar to split-cylinder testing by a monotonic load with an increasing rate applied at top face of specimen trough bearing steel plate. The basic setup of test is shown in Fig. 2, To report and record the magnitude of applied load, a load cell placed between the hydraulic jack and the strong girder of reaction frame.

3. EVALUATION OF TEST RESULTS

3.1. General behavior

All specimens presented a same behavior. As in initial steps of loading a vertical crack was formed approximately at the mid-height of the specimens. By increasing the applied load, this crack propagated toward the top and bottom loaded edges. As the crack reached near to top or bottom loading surface, it changed direction and curved toward out of loaded zone (Fig. 3). However the ultimate failure occurred due to extreme splitting of concrete at mid-height of tested strut. In The over-reinforced specimens, ultimate failure was initiated by crushing of the concrete near, but not adjacent to the loading points (Fig. 3). Table 1 presents the cracking and ultimate failure load obtained from tests. To calculate the efficiency factor υ on the basis of experimental data, the applied load at failure of the specimens was divided by the bearing area of that particular specimen times the compressive strength.

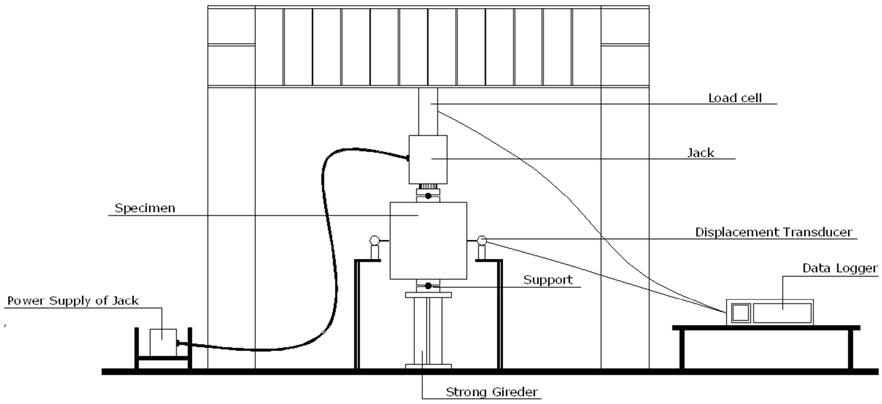

Fig.2 Testing setup

Fig.3 general behavior of tested specimens

3.2. Effect of transverse reinforcement

In each group, there is a considerable variation in the experimental strength, as the amount of transverse reinforcement increased, the ultimate capacity of specimens increases and the failure mode changed from a tensile failure of concrete away from the crushing of concrete at or near the loaded edges. The marked increase in percentage of transverse reinforcement was not associated with significant increase in ultimate strength of over-reinforced specimens than under-specimens. It means that, by satisfying the requirement reinforcement the bottle-shaped strut can be able to maintain equilibrium and additional transverse reinforcement only controls the width of cracks and cannot prevent tensile failure. The ultimate capacity of specimens contained reinforcement lumped at the middle region of strut was measured greater than other specimens with same amount of transverse reinforcement. Because of high transverse tensile straining at the center of struts, it is logical that, the concentration of reinforcement at this region can resist the occurred tensile stresses and be more effective compared with specimens despite the presence of reinforcement that was distributed by uniform spacing. In addition, lumping of transverse reinforcement near to the loading surfaces decreases the efficiency of transverse reinforcement, as the experimental capacity of specimens in series C was less in comparison with those in series A and B that were reinforced with same percentage of reinforcement. It is concluded that from experimental observations, once the initial crack appears, the concrete stiffness reduces significantly. By increasing the applied load, the system of STM was changed and the vertical crack propagates toward loading surfaces of strut. At least before ultimate failure of strut a series of secondary-ties appears with slight level of stress due to redistribution of middle tensile stresses.

Tab. 1 experimental results

Specimen ID	Ultimate Load **(kN)** V_u	Cracking Load **(kN)** V_{cr}	$\upsilon * = \frac{\text{Ultimate Load}}{f'_c \times \text{Bearing Area}}$	$\frac{V_u}{V_{cr}}$
A-1	258	205	0.55	0.79
A-2	371	271	0.79	0.73
A-3	432	307	0.92	0.71
A-4	465	330	0.99	0.71
A-5	479	325	1.02	0.69
A-6	481	325	1.04	0.66
B-1	221	172	0.47	0.78
B-2	343	257	0.73	0.75
B-3	418	288	0.89	0.69
B-4	461	323	0.98	0.70
B-5	465	293	0.99	0.65
C-1	268	155	0.57	0.58
C-2	343	170	0.73	0.49
C-3	423	260	0.90	0.61
D-1	401	230	0.87	0.57
E-1	381	243	0.81	0.64
F-1	353	215	0.75	0.61
H-1	184	137	0.39	0.74

4. CONCLUSION

a) The ultimate capacity of concrete strut depends on the amount of transverse reinforcement, but if the minimum requirement reinforcement is satisfied the additional reinforcement only can improve the purposes of serviceability.
b) Because of high transverse tensile straining at the center of struts, the concentration of reinforcement at this region can be more effective compared with specimens despite the presence of reinforcement that was distributed by uniform spacing.

6. REFERENCES

Michael D. Brown, Cameron L. Sankovich, Oguzhan Bayrak, and James O. Jisra (2006), Behavior and efficiency of bottle-shaped struts, ACI STRUCTURAL JOURNAL, Vol.103, No.3. pp. 348-355.

Michael D. Brown and Oguzhan Bayrak (2006), Minimum Transverse Reinforcement for Bottle-Shaped Struts, ACI STRUCTURAL JOURNAL, Vol.103, No.6. pp. 813-821.

SOME PERSPECTIVES OF APPLICATION OF ALKALI ACTIVATED CONCRETE IN PRODUCTION OF PRECAST ELEMENTS

Vlastimil Bílek
ZPSV a.s.
Krizikova 68
687 24 Uhersky Ostroh
Czech Republic

SUMMARY

Meeting the requirements of the lowering of CO_2 emissions is nearly impossible without the development of new building materials which can replace Ordinary Portland Cement based concrete – (OPCC). As OPCC shows many excellent properties and is also customer-friendly, only a limited range of applications seems reasonable for Alkali Activated Concrete (AAC). Some of these applications are discussed in this paper. It focuses on the utilisation of precast elements from AAC in applications where some of its advantageous properties might be important. The properties of AAC and OPCC are compared.

1. INTRODUCTION

Alkali-Activated Materials and geopolymers are rather intensively studied materials. The reason of the interest in these materials is especially the lowering of CO_2 emissions during their production. It is a well-known fact that during the production of 1 ton of ordinary portland cement nearly 1 ton of CO_2 is emitted (decomposition of limestone, burning, grounding,...).

A number of practical applications of AAC can be found in the Ukraine, see for example (*Rostovskaya et al. 2007)*, in Australia, see (*van Deventer 2010)*, in China, see (*Pan 2010)* and some other countries. But some problems do still persist, following from the relatively complicated composition of AAC. In the case of OPCC practically only water to binder ratio affects the properties of concrete. However, in the case of AAC not only water to binder ratio affect these, but also the amount of activator (Σ) and the ratio between alkalis´ content and anionic group; in this case (Na_2O + K_2O) / SiO_2 ratio. All these characteristics affect the properties of fresh and hardened concrete.

Some results for AAC produced from Czech ground granulated blast furnace slag are summarised in *Bilek et al. (2010).* A suitable course of setting and hardening was found for mixtures with Na_2O + K_2O) / SiO_2 ratio ≈ 50/50 – 70/30. For these ratios also the maximum compressive strengths were recorded. Early strenghts cause some problems – they are usually low. They can be increased by an enhancement of the dry content of activator (Σ > 9 %), see (*Szklorzova, Bilek 2008).* Other problems are caused by efflorescence. It can be eliminated by the use of potassium ions instead of sodium, (*Szklorzova, Bilek 2008).* The workability of mixtures is also enhanced in this way.

A wide range of applications can be found for mineral admixtures; some of them enhance workability – for example fly-ash or limestone, while others enhance early strengths – for example powder from recycled concrete (concrete filler).

As a result of the above mentioned results it is possible to design self compacting alkali activated concrete (SCAAC) with water to binder ration 0.45 – 0.52, with compressive strength cca 60 MPa, a good frost resistance and resistance to some aggressive solutions. In addition, the application of admixtures reduces the cost of materials of SCAAC. From the view-point of the production of concrete elements it is interesting to compare SCAAC with SCC on the basis of OPC. SCCs also contain a big portion of mineral admixtures which reduce the negative impact of OPC on ecology. On the other hand, mineral admixtures can lower some mechanical properties – especially early strengths or frost resistance.

2. MATERIALS

GBFS which was used had been produced in blast furnaces in the Czech Republic and it is grounded at the Kotouc Stramberk company to the specific surface 420 m^2/kg. Limestone filler – originated from Mokra - is grounded by the Carmeuse company to different specific surfaces. The results for the specific surface 360 m^2/kg are presented in this paper. Fly ash f.a.450 (complying with EN 450 - Fly ash for concrete) and fly ash 12620 (complying with EN 12620 – Fillers for concrete) from the Chvaletice power station, which burns brown coal, were also used.

Concrete filler was obtained by crushing 1-year old cubes of SCC – 440kg CEM I 42.5R, 150 kg limestone, the water/(cement + limestone) ratio was 0.32, aggregates / paste volume ratio was 1.32. This concrete was grounded in a ball mill to specific surface – 450 m^2/kg.
A blend of sodium water glass and potassium hydroxide (50 % solution KOH) was used as activator. Silicate modulus of water glass M_s = 1.6, dry mass content 45 %.

For SCC production also ordinary portland cement CEM I 42.5 R and polycarboxylate-based superplasticizer were used. Besides the reported admixtures, a mechanically activated concrete filler (concrete filler FF) and an admixture based on mechanically activated fly ash (DASTIT®) were used., too.

3. EXPERIMENTAL METHODS

The concretes were prepared using drinking water, natural sand 0/4 mm and two narrow fractions of crushed aggregates 4/8 and 8/16 mm respectively. All concretes were prepared with the same grading of aggregates – the same is used for usual SCC concrete.

All mixtures were mixed in accordance with the composition shown in table 1 and 2 in a laboratory mixer in 30 litre volume. Immediately after the mixing, tests of workability (cone flow with reversed Abrams cone) and the content of entrained air were performed. After these tests the concrete was placed into steel moulds. For compressive tests 100 mm cubes were prepared which were unmoulded at the age of 24 hours and tested. Other specimens were stored in wet conditions (r.h. > 95% and t = (20 ± 2) °C) up until the tests at the age of 28 days.

Tab. 1 Composition and properties of SCAAC

	A	D	E	F
Σ [%]	10	10	10	10
(K+N)/S	60/40	60/40	60/40	60/40
w/(s+a)	0.51	0.46	0.46	0.46
GBFS 420 [kg]	450	300	300	300
f. a. 450 [kg]	-	150	-	-
Limestone [kg]	-	-	150	-
f. a. 12620 [kg]	-	-	-	150
Cone flow [mm]	580	740	610	520
Air content [%]	2.5	3.4	3.3	3.8
f_{c24} [MPa]	7.8	10.5	9.8	5.9
d_{24} [kg m^{-3}]	2261	2250	2271	2191
f_{c28} [MPa]	67.4	68.0	55.3	61.0
d_{28} [kg m^{-3}]	2255	2253	2280	2243
price [EUR]	87	76	79	76

Tab. 2 Composition and properties of OPC based SCC

	I	II	III	IV	V
w/(s+a)	0.42	0.42	0.42	0.42	0.42
CEM I 42.5 R [kg]	520	390	390	390	260
fly ash 450 [kg]	-	130	65	65	-
concrete filler 450 [kg]	-	-	65	-	-
concrete filler FF [kg]	-	-	-	65	-
DASTIT [kg]	-	-	-	-	260
superplasticizer [kg]	2.3	2.3	2.5	2.5	6.0
Cone flow [mm]	550	460	550	460	450
f_{c24} [MPa]	25.0	9.1	10.2	13.7	7.9
d_{24} [kg m^{-3}]	2300	2265	2266	2255	2227
f_{c28} [MPa]	67.5	58.8	51.2	54.2	65.3
d_{28} [kg m^{-3}]	2326	2313	2275	2297	2260
price [EUR]	61	49	49	49	55

4. DISCUSSION OF RESULTS

Both SCAACs and SCCs have nearly the same volume of paste – cca 0.345 m^3. The workability was much better for SCAACs – fresh concrete flows very smoothly. Cone flow loss proceeded continuously; concretes were workable for cca 30 minutes.

Also workability od SCCs was good – it was at the lower limit for SCC. It is possible to enhance it by the addition of superplasticizer. Especially the workability of concrete with a ternary binder – fly ash and concrete filler 450 was good.

The compressive strengths of SCAAC at the age of 24 hours were low, but they were nearly the same as those of OPC based SCC with admixture(s). The concretes with ternary binders showed better early strengths. Probably also some mechanical activation was reached by high speed centrifugal grinding, as concrete with concrete filler FF showed better strength than those with concrete filler 450 from a ball mill. At the age of 28 days all concretes showed relatively high strengths – but the strengths of SCAAC were higher. This was a consequence of a better reaction of mineral admixture in an alkaline environment – higher pH helps the decomposition of fly ash and this admixture takes part in strength development. Relatively high strengths were recorded also in the case of OPC based SCC.

The prices of SCAAc are significantly higher than those of OPC-based SCC, the reason being the high prices of alkaline compounds – especially KOH.

5. CONCLUSIONS

It is possible to produce SCAAC with such similar strengths as can be shown by usual SCC. Further properties (frost resistance, moduli of elasticity,...) of these concretes are reported in other papers.

The testing of durability in an aggressive environment of all above-mentioned concretes is being continued. An excellent durability of SCAAC was recorded in the previous paper. These properties will justify somewhat higher prices of SCAAC.

Another way would be the use of waste material(s) as part of activator; e.g. tests with cement kiln dust are proving rather promising.

6. ACKNOWLEDGEMENTS

This work was supported by Ministry of Industry and Business of Czech Republic, Project No: FR TI 1/004

7. REFERENCES

Bilek, V., Opravil, T., Soukal, F. (2010) Searching for practically applicable alkali-activated concretes, *1st Int. Conf. on Advances in Chemically-activated Materials (CAM´2010, China)*, Shi, C. and Shen, X. eds., RILEM Publications S.A.R.L., ISBN 978-2-35158-101-8, pp. 28-35

Pan, Z., Yang, N., (2010) Updated review on AAM in China, 1st International Conf. on Advances in Chemically-activated Materials (CAM´2010), RILEM publications S.A.R.L., China, Jinan, May 9-12, ISBN 978-2-35158-115-5, pp.45-57

Rostovskaya, G., Ilyin, V., Blazhis, A. (2007) The service properties of the slag alkaline concretes, Int. conf. Alkali Activated Materials – Research, Production and Utilization, Ceska rozvojova agentura, Prague, Czech Republic, ISBN 978-80-86742-18-2, 593-610

Szklorzová, H., Bílek, V. (2008) Influence of alkali ions in the activator on the performance of alkali activated mortars, *3rd Non-traditional Cement and Concrete Conf.*, Bilek, V. and Kersner, Z. eds., VUT Brno, 2011 Brno, Czech Republic,

van Deventer,J.S.J., Provis, L.J., Duxon, P. (2008) Update of the progress in the commercialisation of geopolymer technology in Australia, *3th Non-traditional Cement and Concrete conf.*, Bilek, V. and Kersner, Z. eds., VUT Brno, 2008 Brno, Czech Republic, ISBN 978-80-214-3642-8, pp.173-181

EXPERIMENTAL STUDY OF SHEAR BEHAVIOUR OF HIGH PERFORMANCE CONCRETE USING PUSH-OFF TESTS

Horia Constantinescu[1], Cornelia Măgureanu[1]
[1] Faculty of Civil Engineering
Technical University of Cluj Napoca
Str. G. Baritiu nr. 25, 400027 Cluj-Napoca, Romania

SUMMARY

The use of High Strength and High Performance Concretes is quickly being adopted by the construction industry world-wide. Research regarding the behaviour of elements cast using High Strength Concretes is therefore of paramount importance in order to ensure adequate design and construction of structures using this material.

This paper presents experimental results obtained from push-off tests performed on elements cast using concrete with a mean value of the compressive strength, determined on 150 mm cubes, of f_{cm}=100 MPa, reinforced with ϕ8 mm deformed bars (f_{yk}=500 MPa) in the form of stirrups crossing the shear zone. The distance between stirrups (s) and the number of stirrups was varied in order to determine the influence of reinforcement placement and of the mechanical reinforcement ratio ($\rho_v f_y$) on shear behaviour of reinforced High Strength Concrete elements.

1. INTRODUCTION

High Strength Concrete (HSC) is a relatively new material whose behaviour under different types of loading is not sufficiently understood. Behaviour in shear is of particular interest as HSC is known to exhibit fragile failures due to the strength of the cement matrix being as high as or higher than the strength of the aggregate. This leads to cracks passing through the aggregate rather than forming in the contact zone in between the matrix and the aggregate, taking the effect of aggregate interlock away from the shear resistance of elements. *(CEB-FIP 2008), (NISTIR 1996)*

This characteristic of HSC does not need to be a deterrent to the use of reinforced concrete elements cast using HSC as proper use of reinforcement could ensure adequate behaviour of elements subjected to shear *(Heghes 2009), (Letia 2010) (Negrutiu 2010).*

Shear in reinforced concrete elements is always coupled with bending but all major design codes around the world separate the design of elements in flexural/bending design and shear design, considering that the section designed in shear has a constant bending moment or ignoring the effect bending has (*Eurocode 2 2004), (ACI 318-08 2008).*

In order to study shear independently of bending, custom test specimens (push-off specimens) were designed, cast and tested. The results of this endeavour are presented in this paper.

2. EXPERIMENTAL PROGRAM

The concrete used to cast the three push-off specimens discussed in this paper had a mean value of compressive strength determined on 150 mm cubes f_{cm}=100 MPa (*RILEM 1994)*. The constituent materials used were Portland Cement CEM I 52.5R, grey silica fume with high content of SiO_2, commercially available as Elkem Microsilica Grade 940V, superplasticizer BASF ACE40, locally acquired aggregates river sand (particle size 0-4 mm), crushed quarry stone (dacite, particle size 4-16 mm).

HPC mix proportions were: cement (1 part), silica fume (0.1 parts), aggregates (3.3 parts), and superplasticizers (0.03 parts). The water/binder ratio was 0.26.

The reinforcing steel was size 8mm deformed bars with a characteristic yield strength of 500 MPa (f_{yk}=500 MPa). The distance between stirrups (s) and the number of stirrups was varied (s=100, 150, 200 mm) in order to determine the influence of reinforcement placement and of the mechanical reinforcement ratio ($\rho_v f_y$=4.2, 2.8, 2.1) on the shear behaviour of reinforced HSC elements. (Fig. 1)

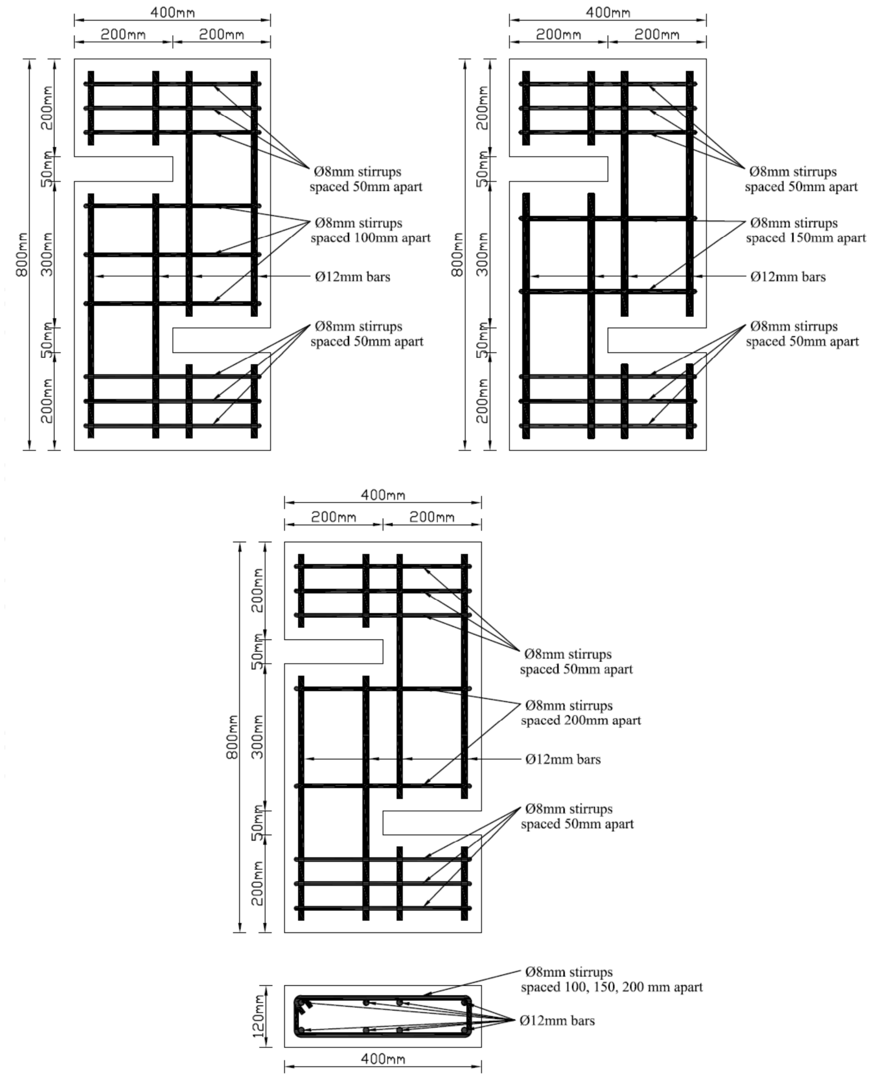

Fig. 1 Reinforcement details of push-off specimens

3. TESTING PROCEDURE

During testing the load was applied gradually. Each loading stage consisted in 100 kN increments, up to the failure of the elements. This test method was used in order to allow the necessary time for distribution of efforts throughout the element and visual inspection.

The load applied and the strains it produced in the elements were recorded using force and displacement transducers and strain gauges, connected to a data acquisition system (Fig. 2).

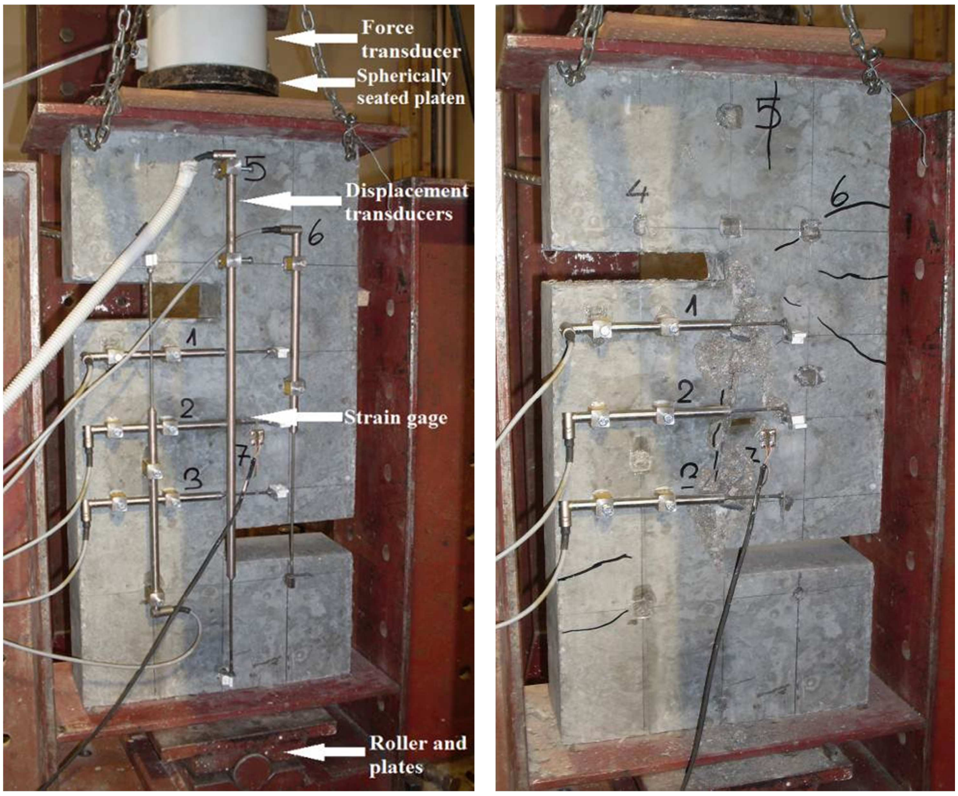

Fig. 2 Test setup of push-off specimens (left) push-off specimen after failure (right)

4. TEST RESULTS AND CONCLUSIONS

As expected, behaviour of the test specimens varied due to stirrup spacing (s=100, 150, 200 mm) and mechanical reinforcement ratio ($\rho_v f_y$=4.2, 2.8, 2.1) (Fig. 3).

In two of the elements, in which the distance s between stirrups was 100mm and 150mm, shear cracks formed at the same value of the load, namely 700 kN while in the third element tested with a distance between stirrups of 200 mm, the load at which shear cracking occurred was slightly higher, 800 kN. The formation of shear cracks in all specimens was sudden. In the first two elements the cracks had the same initial width while in the third element it was three times as wide. It could be said that in the third element the more even distribution of tensile efforts in the concrete led to the 100 kN increase of the load at which shear cracking occurred.

The failure load of the elements was 1150 kN, 1100 kN, 1000 kN. The values are very close to one another thus showing only a slight influence of stirrup spacing and mechanical reinforcement ratio on the ultimate load of the elements.

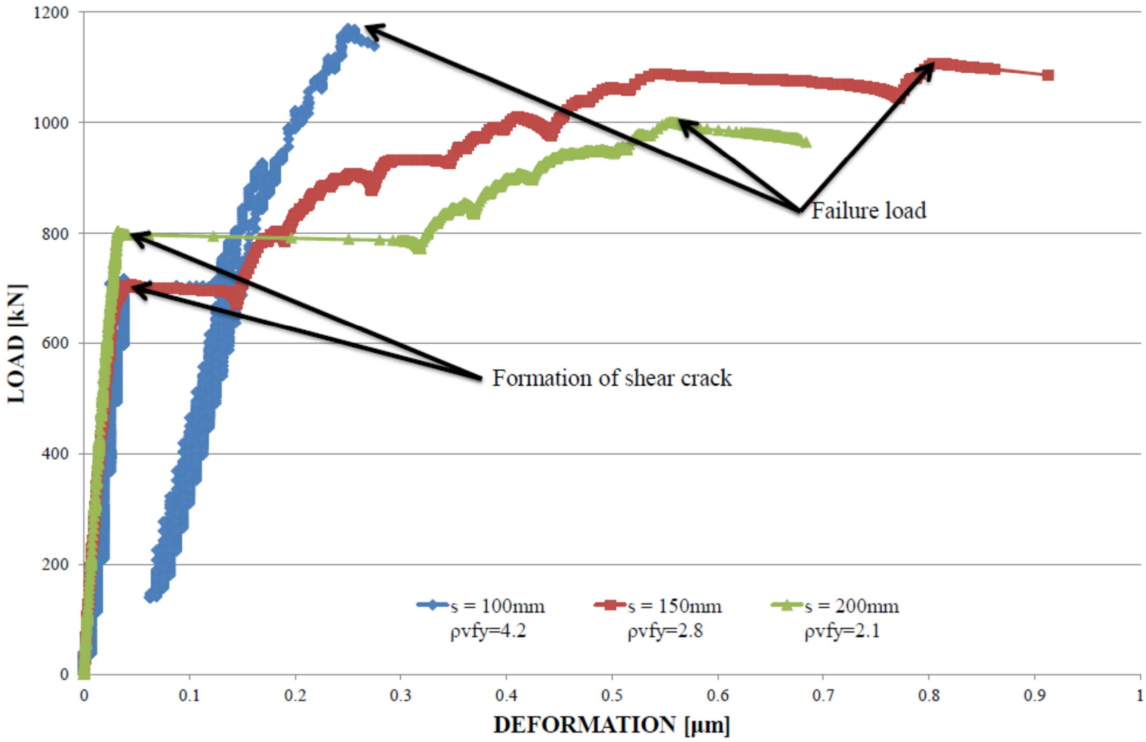

Fig. 3 Load – Transverse deformation at mid height for tested specimens

5. ACKNOWLEDGEMENTS

This paper was supported by the project "Doctoral studies in engineering sciences for developing the knowledge based society-SIDOC" contract no. POSDRU/88/1.5/S/60078, project co-funded from European Social Fund through Sectorial Operational Program Human Resources 2007-2013. Also, the authors would like to express their gratitude to CNCSIS for financing the research program within the PCE-PN II-IDEI Program, code 1053/2007.

6. REFERENCES

American Concrete Institute (2008), Specification ACI 318-08.

CEB-FIP (2008), "Constitutive modelling of high strength/high performance concrete", Task Group 8.2, International Federation for Structural Concrete, Sprint-Digital-Druck, ISSN 1562-3610.

Eurocode 2 (2004): Design of concrete structures – Part 1.1: "General rules and rules for buildings", European Committee for Standardisation

Heghes B. (2009), "Ductility of high strength - high performance concrete", PhD. Thesis, Technical University of Cluj Napoca, UT Press.

Letia C. (2010), "Elemente din Betoane de Înaltă Rezistență – Contribuții la Studiul Stărilor Limită de Fisurare", PhD. Thesis, Technical University of Cluj Napoca, UT Press.

Negrutiu C. (2010), "Durability of high strength and high performance concrete", PhD. Thesis, Technical University of Cluj Napoca, UT Press.

NISTIR (1996), "Shear Design of High-Strength Concrete Beams: A Review of the State-of-the-Art", NISTIR 5870.

RILEM (1994) "Technical Recommendations for the Testing and Use of Construction Materials", E & FN SPOON, ISBN 0419 18810X.

APPLYING ACOUSTIC EMISSION METHOD AT MONITORING OF LIFETIME CONCRETE STRUCTURE

Libor Topolář[1], Luboš Pazdera[1], Vlastimil Bílek[2], Jaroslav Smutný[1]
[1] *Department of Physics and Department of Railway Structures and Construction*
Brno University of Technology, Faculty of Civil Engineering
602 00 Brno, Veveri 331/95, Czech Republic
[2] *ZPSV a.s.*
Ostroh, Czech Republic

SUMMARY

Non Destructive Testing is a powerful tool for determination of technical structures lifetime. Acoustic Emission Method is an unusual technique which describes only active defects or changes into structure, consequently dangerous tension into structure *(Janseen, 1994)*. The method is appropriate to be used in homogenous structures as metal structures and then cracks are highly active (generates sound). Its application in civil engineering is not so much applied. This article shows possible application of Acoustic Emission Method for monitoring concrete structure changes during its lifetime. It is believed that early age of concrete structure is very important for its quality. Common concrete prism specimens have been tested after the production by Acoustic Emission Method *(Aitcin 2005)*.

1. INTRODUCTION

Acoustic emission is the term for the noise emitted by material and structures when they are subjected to stress. Types of stresses can be mechanical, thermal or chemical *(Shuling Gao, Wenling Tian, Ling Wang, Pei Chen, Xiaowei Wang, and Jinli Qiao, 2010)*. This emission is caused by the rapid release of energy within a material due to events such as crack formation, and the subsequent extension occurring under an applied stress, generating transient elastic waves which can be detected by piezoelectric sensors *(Mazal 2000), (Metacoustic Pty. Limited, Australia's First and Leading Acoustic Emission and Structural Integrity Evaluation Research and Application Group, 1978).*

Acoustic emission method can monitor changes in materials behaviour over a long time and without moving one of its components i.e. sensors. This makes the technique quite unique along with the ability to detect crack propagations occurring not only on the surface but also deep inside the material. The acoustic emission method is considered to be a "passive" non-destructive technique, because usually identifies defects while they develop during the test. The acoustic emission method is often used to detect a failure at a very early stage of damage long before a structure completely fails *(Grosse, Ohtsu, 2008), (Metacoustic Pty. Limited, Australia's First and Leading Acoustic Emission and Structural Integrity Evaluation Research and Application Group,1978).*

Fracture in a material takes place with the release of stored strain energy, which is consumed by nucleating new external surfaces (cracks) and emitting elastic waves, which are defined as acoustic emission waves. The elastic waves propagate inside a material and are detected by an acoustic emission sensor. Except for contactless sensors, acoustic emission sensors are directly attached on the surface *(Grosse, Ohtsu, 2008), (Blitz, Jack; Simpson 1991).*

The setting and hardening process of concrete can be considered as the most critical time period during the life of a concrete structure. To assure high quality and avoid problems in performance throughout the life of the material, it is essential to have reliable information about the early age properties of the concrete *(Popovics, 1971).* The properties of concrete are solely determined by the composition of its ingredients and the conditions during the setting and hardening process *(Ozturk, Rapoport, Popvics and Shah, 1999).*

There are many techniques to determine concrete properties. Their application during early age is very complicated or even impossible *(Struble, Zhang, Sun and Lei 2000).*

2. EXPERIMENTAL SETUP

Two samples of length, 400 mm, height, 100 mm, and width, 100 mm, were measured simultaneously. Four acoustic emission sensors were placed on the surface of both samples. (Fig. 1) Two sensors were placed on the first sample and the other two ones on the second sample *(Pazdera, Topolar, Bilek, Smutny, Kusak, Lunak 2010).* Each sensor was kept by specially made holder, so that the contact between sensor and sample surface was easy to achieve.

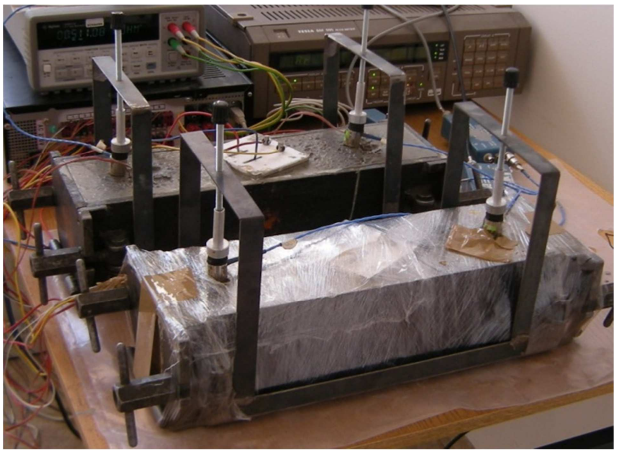

Fig. 1 Mounting acoustic emission sensors

3. RESULTS

During hardening one of the blocks was wrapped up to prevent it from spontaneous drying, whereas the other was left without protection to hardening in open air.

The following diagrams (Fig. 2) show a cumulative overshoot count (N_C) versus time (t) plot.

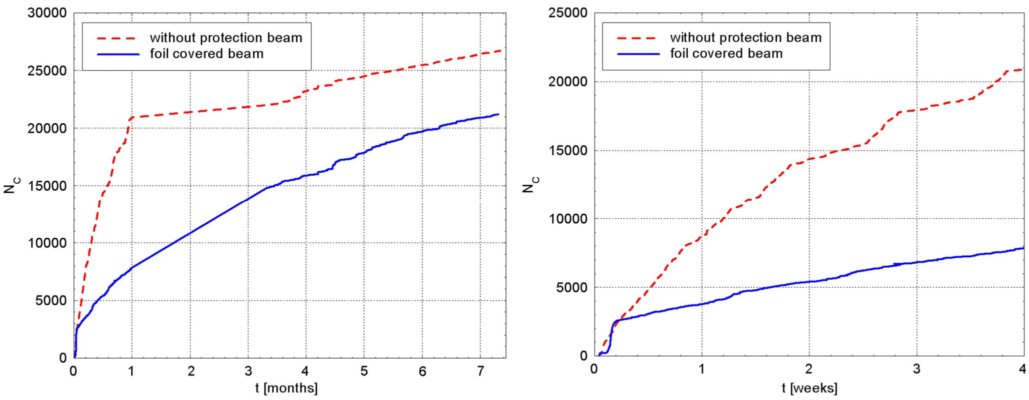

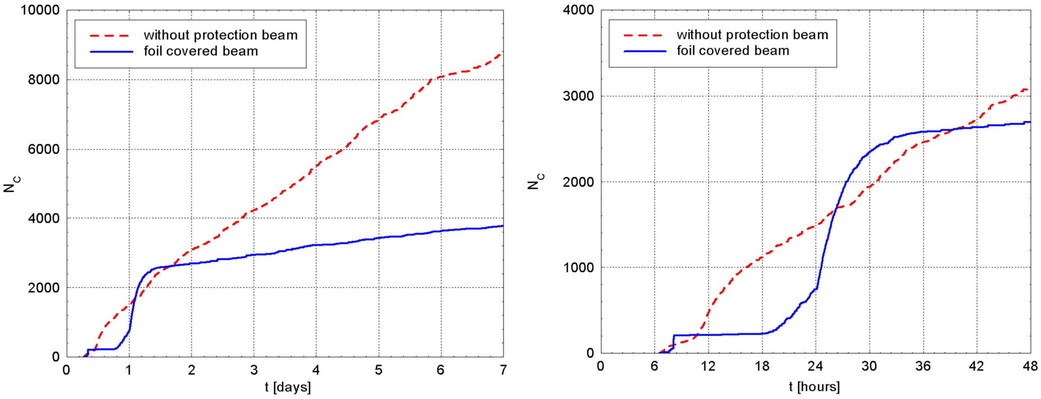

Fig. 2 Comparison of the wrapped specimen and specimen without protection at different time

It is evident from the shape of the curves that the specimen without protection features a substantially higher acoustic emission activity, from which a higher number of micro-cracks in the specimen can be inferred. It is clear from the detailed view of the diagrams that the specimen without protection shows a more acoustic emission event counts during the first 4 months (Fig. 3) (from the acoustic emission measurement starting point) and, consequently, larger phase changes.

The sharp increase in the acoustic emission event at the wrapped specimen at about 24 hours (Fig. 2 – in the bottom right) is connected with the unmolding of specimen so-called "exhale".

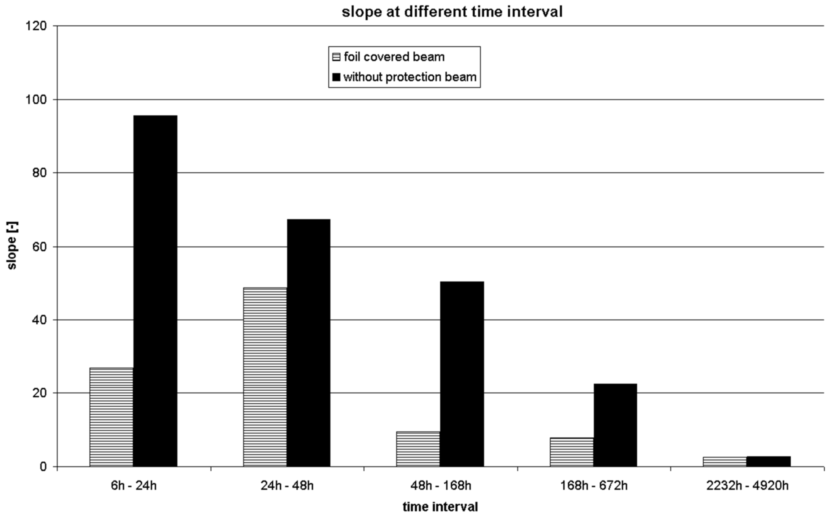

Fig. 3 The change in the slope during the hardening of concrete

4. CONCLUSIONS

Acoustic Emission Method as non-destructive technique shows advantages in the protection of concrete specimens. Cumulative curves of acoustic emission activity (Fig. 2 and Fig. 3) clearly show steeper slope of non-protected concrete sample. Number of micro cracks can be higher in the non-protected sample mainly during the early age.

Application acoustic emission method during hardening and setting concrete structure can help to create a better procedure for the protection of concrete structure.

5. ACKNOWLEDGEMENTS

This research has been supported by the project of GACR No. P104/10/0535 and by the part of the research project MSM 0021630519.

6. REFERENCES

Aitcin P C, (2005): "High Performance Concrete", Informační centrum CKAIT, Prague, ISBN 80-86769-39-9

Blitz, Jack; G. Simpson (1991). Ultrasonic Methods of Non-Destructive Testing. Springer-Verlag New York, LLC. ISBN 9780412604706

Grosse, Ch. U., Ohtsu, M., (2008) „Acoustic Emission Testing“, Springer-Verlag, Berlin 2008. ISBN 978-3-540-69895-1

Janseen J.D. (1994): Resistance of Concrete to Freezing and Thawing, Washington, DC

Mazal P, (2000)"Acoustic emission method using in evaluation of fatigue properties of materials", in Proceedings of European Conference on Advances in Mechanical Behaviour, Plasticity and Damage (EUROMAT 2000), eds Miannay D; Costa P; Francois D; Pineau A, Tours, France, pp. 1137-1142, ISBN 0-08-042815-0

Metacoustic Pty. Limited, Australia's First and Leading Acoustic Emission and Structural Integrity Evaluation Research and Application Group (Est 1978) URL: < http://metacoustics.com.au/whatisAE.cfm> [cit.2011-06-01]

Ozturk, T., Rapoport, J., Popvics, J.S. and Shah, S.P. (1999). Monitoring the setting and hardening of cement-based materials with ultrasound, Concrete Science and Engineering, Vol. 1, No. 2, pp. 83-91

Pazdera L., Topolar L., Bilek V., Smutny J., Kusak I., Lunak M. (2010): Measuring of Concrete Properties during Hardening, in Proceedings of the 48th International Scientific Conference on Experimental Stress Analysis, Velke Losiny, Czech Republic

Popovics, S. (1971). Physical aspects of the setting of Portland cement concrete, Journal of Materials, Vol. 6, No. 1, pp. 150-162

Shuling Gao, Wenling Tian, Ling Wang, Pei Chen, Xiaowei Wang, and Jinli Qiao (2010): Comparison of the Mechanics and Durability of Hybrid Fibre Reinforced Concrete and Frost Resistant Concrete in Bridge Deck Pavement, in Proceedings of the 10th International Conference of Chinese Transportation, Chinese

Struble, L.J., Zhang, H., Sun, G.-K., and Lei., W.-G. (2000). "Oscillatory shear behavior of Portland cement paste during early hydration," Concrete Science and Engineering, Vol. 2, No. 9, pp. 141-149

STEEL FIBER SCC HIGH STRENGTH LIGHTWEIGHT CONCRETE WITH LOCAL AVAILABLE MATERIALS

Sherif Yehia, Mohammad AlHamaydeh, Rashid Alhajri, Aly Abdelsalam, and Ayman Farid
American University of Sharjah
P.O. Box 26666 Sharjah, UAE

SUMMARY

Several mechanical properties are usually improved when steel fiber is added to a concrete mixture. However, volumetric ratio of the steel fiber affects the workability of the mixture. This adverse effect should be avoided during the development of self consolidating mixes especially with lightweight aggregate. The objective of this experimental investigation is to determine the volumetric ratio of the steel fiber which could be used while maintaining the unit weight, workability, and strength requirements. Three ratios of 0.5%, 1.0% and 1.5% were used during the evaluation. Slump flow test, unit weight, compressive strength, and flexural strength were used as evaluation criteria during the development stage. Followability and dry unit weight were met by the 0.5% and 1% fiber ratios but not by the 1.5% ratio. However, compressive strength in excess of 50 MPa was achieved by all ratios.

1. INTRODUCTION

Development of a steel fiber high strength light weight aggregate mix requires knowledge about advantages and limitations of each material and its impact on the fresh and hardened stages of the concrete. The main highlights are provided in the subsequent sections.

1.1 Lightweight Aggregate

Natural lightweight (LWT) aggregates were formed from volcanic eruption such as pumice and scoria. In Germany, the industrial use of LWT aggregates (pumice) started in 1845. In the 20th century, manufactured LWT aggregates were introduced to the market. As a result, it became possible to produce concrete with a high strength and low density at the same time. In 1917, Hayde of the U.S developed a process to expand clay using tubular kiln. During the world war two, the development of the LWT aggregate concrete increased. Several buildings were completely built using lightweight aggregates such as the 42-floor Prudential Life Building in Chicago.

Manufactured aggregates gain their reduced weight due to the entrained air during the production. Gained porosity affects concrete produced using LWT aggregate in two aspects. First, higher absorption capacity leads to strength reduction if more water to be added to reach the needed workability. The second impact which is also related to higher absorption capacity: it could serve a self-curing function (OR "it could be utilized for self-curing"). This will help improve the compressive strength by increasing the bond at the interfacial zone between the hydrated cement and aggregate surface (*Beaucour, Y., et. al. 2009).*

1.2 Steel Fiber

Improving crack resistance, crack propagation, tensile strength, impact resistance, in addition, to controlling shrinkage are some of the advantages of utilizing steel fiber in concrete mixtures. However, some limitations such as loss of workability and not maintaining a homogenous distribution of the fiber might affect achieving full benefits of this addition *(MacDonald et. al 2009),(Johnston 2001).*

1.3 Self Consolidated

Originating in Japan during the mid-1980s, self consolidating concrete is a highly workable concrete mix that needs little or no vibration when casting (*Holt, 2011)*. It allows concrete to self compact and can allow it to fill spaces which would be otherwise difficult to fill. It requires a sensitive balance between creating more deformability while ensuring good stability, including an adequate resistance to segregation and bleeding. This is done by adjusting the water cement ratio, adding certain admixtures, and selecting appropriate aggregates based on density, shape, size, and gradation (*Yang, 2004)*.

There are many advantages to using self consolidating concrete. It can potentially reduce the cost of a project by reducing the labor requirements for casting and allowing it to be done fast and easily as well as less noisily. Complex projects can be accomplished by allowing the concrete to be cast in places that are hard to reach or places with congested steel reinforcement. There are drawbacks to its use though, especially since it’s a very young technology. There is a lack of guidelines and specifications regarding the topic, as well as need for an accurate mix design (*Holt, 2011),* (*Yang, 2004),* (*Yehia, et. al., 2009)*. Bleeding and segregation is another problem that must be kept in mind when proportioning the mix (*Yang, 2004)*. The durability and strength of the concrete might also be affected due to the reduction of coarse aggregates and their interlocking feature. Creep and shrinkage at the early stages can also be a problem (*Khayat, 1999)*. There has also been a slight noticeable reduction in the modulus of elasticity of the mix (*Felekoglu, et. al., 2007)*.

The research herein deals with the development of a self consolidated high strength lightweight mix utilizing lightweight aggregate available in the United Arab Emirates.

2. EXPERIMENTAL INVESTIGATION

The main objective of the experimental investigation is to determine the optimum steel fiber percentage per volume which could be used to achieve the development of a self consolidated high strength lightweight concrete mix. Three percentages of 0.5%, 1.0% and 1.5% were used in the study. The evaluation criteria during the development stage were slump flow test and wet unit weight for fresh stage, while compressive strength and flexural strength were used for hardened stage. The target compressive strength is 40 MPa or higher and dry unit weight less than 2000 kg/m^3. Tests were conducted at 3, 7, 14, 21, and 28 days according to ASTM standard specifications.

3. RESULTS AND DISCUSSION

Mixes with 0.5% and 1.0% steel fiber per volume showed SCC characteristics and met the target flowability, however, the higher steel fiber weight in the 1.5% ratio reduced the workability and did not exhibit SCC characteristics. Fig.1 shows slump flow test for 0.5 and 1 % steel fiber, 550 mm and 510 mm spread were measured, respectively, with no sign of segregation. Wet and hardened unit weight were also calculated and found to be within the acceptable range defined by the ACI213R-03. All mixes with different steel fiber percentage achieved compressive strength higher than 50 MPa. Fig. 2 shows a typical failure mode during compression tests. The fiber improved the crack resistance and crack propagation. The flexural strength was higher than that calculated by the ACI Equation [$0.62\text{-}0.82\sqrt{f_c^`}$] (MPa) for the 1% and 1.5% as summarized in Table 1.

a) 0.5% steel fiber per volume

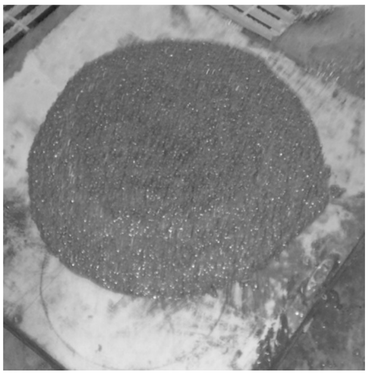

b) 1% steel fiber per volume

Fig. 1 Flow slump test

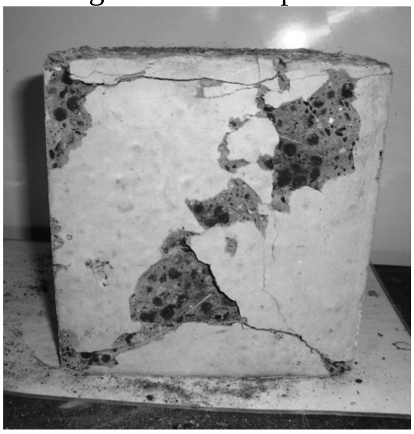

Fig. 2 Typical failure mode at 3-day test

Tab. 1 Summary of the test results

	Fiber Percentage		
	0.50%	1%	1.50%
28- Day Compressive Strength (MPa)	50.69	52.165	54.55
Theoretical Flexural Strength [$0.62\text{-}0.82\sqrt{f_c^`}$] (MPa) for Plain Concrete	4.14-5.83	4.47-5.92	4.57-6.05
28- Day Flexural Strength (MPa)	5.445	9.11	13.295
Fresh Unit Weight (Kg/m^3)	2001	2042.5	2071

4. CONCLUSIONS

Phase I of the experimental program presented in this paper discussed the development of a self consolidated high strength lightweight concrete mix utilizing available lightweight coarse aggregate source in the United Arab Emirates. The test results showed that all ratios of steel fibers used in the investigation met the evaluation criteria expect the 1.5% showed reduced workability because of the increased weight of the fiber. Therefore, this ratio will not be included in further stages of this investigation.

5. REFERENCES

Beaucour, Y., Ortula, S., Dumontet, H., and Cabrillac, R. (2009) "Influence of volume fraction and characteristics of lightweight aggregates on the mechanical properties of concrete," Construction and Building Materials, 23., 2821–2828.

Felekoglu, B., Turkel, S., Baradan B. (2007) "Effect of water/cement ratio on the fresh and hardened properties of self-compacting concrete," Building and Environment, Vol. 42, pp.1795-1802.

MacDonald, C. N., Ballou, M. L., and Biddle, D. T. (2009) "Case histories using synthetic fiber reinforced concrete," Eci conference on shotcrete for underground support, Conference 6.

Johnston, C. D. (2001) "Fiber reinforced cements and concretes," Advances in concrete technology Vol. 3 – Gordon and Breach Science publishes..

Yang, F. (2004) "Self-Consolidating Concrete," Civil and Environmental Engineering, University of California, Berkley, United States of America, Tech. Rep. 1..

Khayat, K. H. (1999) "Workability, Testing, and Performance of Self-Consolidating Concrete", ACI Materials Journal, Vol. 96, no.3, pp.346-354, May-June.

Holt, R. (2011) "Self-Consolidating Concrete", 2011, http://www.fhwa.dot.gov/hfl/innovations/scc.cfm

Yehia, S., Abudayyeh, O., Bhusan, B., Maurovich, M., and Zalt, A. (2009) "Concrete Materials: Properties, Performance and Applications" New York: Nova Science Publishers..

ACI213R-2003 "Guide for Structural Lightweight-Aggregate Concrete"

EXPERIMENTAL STUDIES ON MECHANICAL PROCESS OF RPC ARCH MODELS UNDER IN-PLANE LOAD

Baochun Chen[1], Renyuan Du[1],Zlatko Savor[2]
[1] *College of Civil Engineering of Fuzhou University*
350108 Fuzhou Fujian China
[2] *Faculty of Civil Engineering*
University of Zagreb Croatia

SUMMARY

Results of experiments on two reactive powder concrete (RPC) arch models, carried out with concentrated loads at quarter-span are discussed in the paper. Load-displacement curves, cracks, failure modes and ultimate load-carrying capacity of the arches were analyzed and compared with results obtained on reinforced concrete (RC) arch models. Experimental results show that the behaviour of RPC arches is similar to those of RC arches. The RPC arches also fail due to the mechanism formed by four plastic hinges caused by cracks in tensile areas. But the initial crack load, reinforcement yielding load and ultimate load of RPC arches are 2 to 3 times as high as those of RC arches; and the largest crack width in RPC arches is only forty percent of that of RC arches.

1. INTRODUCTION

Reactive powder concrete (RPC) is a relatively new concrete that is higher strength, better toughness and durability than normal concrete and high performance concrete. Its compressive strength is as high as 200 MPa (*Pierre et al 1995)*. But RPC without steel fiber should be chosen for using carefully, because it prone to brittle. It can be used in arch bridge which the compression is the dominant forces to reduce section size and structure self weight, enhance its span capacity and improve structure durability. The researcher from Croatia proposed design project of PRC arch bridge whose main arch span was 432 m×500 m and 1000 m, and considered that RPC would lighten self-weight of the arch *(Candrlic et al 2004, Chen et al 2005).* A research conducted trial design of RPC arch bridge, taking the Wanzhou Yangtze River Bridge as prototype, also counted that RPC could reduce self-weight of the main arch by about 40%, and decrease consumption of steel by 72% *(Yu 2008)*. However, the application of long-span RPC arch bridge has not been achieved yet. The main reasons may include high price of RPC and RPC arch research not enough. So far, Experimental study on the RPC arch has not been reported *(Yan et al 2009, Wang 2008, Tang 2004)*. Experiments on two RPC arch models are described in the paper in an effort to remedy this deficiency.

2. EXPERIMENTAL PROGRAMME

For adequate comparison, the two RPC arch models in this paper (R1 and R2) were designed as similar to the two RC arch models (C1 and C2) *(Chen 1986)*. Except the materials of the models, all other parameters were kept the same for R1 corresponding to C1, and R2 corresponding to C2. The span of the models is 400 cm; and cross section is rectangle, 15 cm high, 40 cm wide (Fig.1); diameter of steel bars is 10 mm. Other geometric parameters can be found in Tab. 1. Testing photos are presented in Fig. 2 and Fig. 3.

Tab. 1 The geometric parameters of arch models

Specimen	Arch axis coefficient	Arch span(cm)	Rise to span ratio	Arch rise (cm)
R1、C1	2.24	407.566	1/8	51.024
R2、C2	1.756	409.961	1/5	81.893

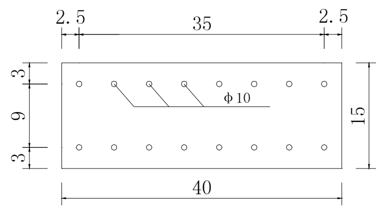

Fig. 1 The section and arrangement of reinforcement of RPC arch models (unit: cm)

Fig. 2 The test photo of R1   Fig. 3 The test photo of R2

RPC compositions: cement 833.8 kg/m^3, sand 975.5 kg/m^3, silica fume 250.1 kg/m^3, steel fibers 234 kg/m^3, super-plasticizer 20.9 kg/m^3, water 196.1 kg/m^3. The curing system of the arch models contained natural curing (2d), steam curing (8h, 180℃) and natural curing 14d.

From the material tests, the RPC compression strength is 150 MPa; tensile strength is 21.6MPa; the Young modulus is 3.9×10^4 MPa; and the peak strain is 0.0035. The yield strength of steel bar is 411 MPa; ultimate tensile strength is 567 MPa; and the Young modulus is 2.05×10^5 MPa.

3. TEST RESULTS AND ANSYSIS

The maximum out-plane displacement of Model R1 was about 0.35mm, just 1/11429 of the span; and about 0.46 mm of Model R2, just 1/8913 of the span. Therefore; the test is considered ideal in an in-plane loading condition.

The test process of RPC arch can also be divided into three phases as in the general RC arch, i.e., elastic phase, crack developing phase, and reinforcement yielding phase. The section at quarter span L/4 was chosen as representative due to the highest stresses for the introduction of these three phases, depicted in Fig. 4.

In elastic phase there is no crack on the arch model, and the load-displacement curve is totally straight. The second phase is the crack developing phase, in which the first crack appears and the load-displacement curve develops nonlinearly. In the third phase, the reinforcement bar yields and the displacement develops rapidly with small load increment. By comparing with

RC arch, it can be found that the ultimate load-carrying capacity of RPC arch is much larger, flexural rigidity improves obviously and drops slowly. Load comparison of each phase between R1, R2, C1 and C2 are presented in Tab. 5.

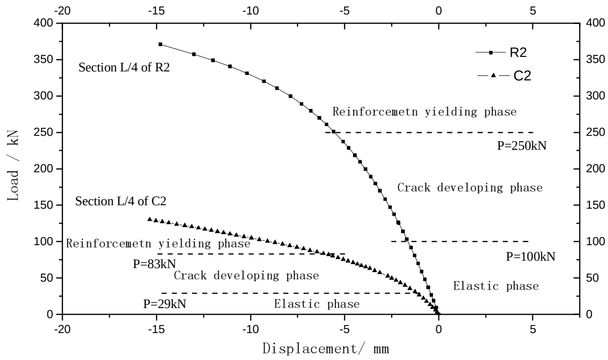

Fig. 4 The comparison between load-displacement curves of R2 and C2

Tab. 2 The load comparison of each phase among R1, R2, C1 and C2

category	R1	R2	C1	C2	R1/C1	R2/C2
Initial crack load（kN）	55	100	40	30	1.4	3.3
Reinforced yielding load（kN）	205	250	85	83	2.4	3.0
Ultimate load（kN）	375	373	140	130	2.7	2.9

First cracks appeared at the section of L/4, 3L/4 and two arch springs of R1 when the loading reached up to 80 kN, 55 kN, 80 kN, 90 kN, respectively. The cracks widened and developed as the testing continued, and even almost passed though the whole depth from the bottom or the top of the section. The cracks just concentrated at L/4, 3L/4 and two arch springings. The largest crack was about 3 mm wide, located at bottom of the loading area. The largest crack region was located at top of 3L/4, about 112 cm long (Fig. 5).

Cracks in C2 shown in Fig. 6 are similar to R1 (Fig. 5). But the first crack appeared in RPC arches when the load was much larger than that of RC arches as listed in Table 2. The largest cracks width in RPC arches is only forty percent of that of RC arches at the same load level. It is obvious that the crack-resistant capability of RPC arches is better than RC arches.

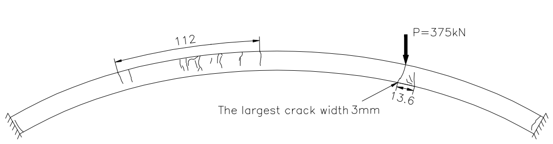

Fig. 5 The crack pattern of R1 (unit: cm)

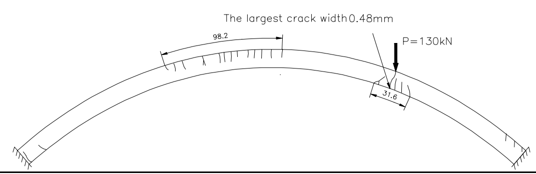

Fig. 6 The crack pattern of C2 (unit: cm)

The deflections of R1 are presented in Fig. 7. Deflection of each section increased almost by the same amount in the elastic phase; while those in section L/4 and 3L/4 increased quickly in the second phase due to reduction of their rigidity. When thin layer of crushed RPC was observed and crack depth of the section was very deep in the four key sections which means that plastic hinge has formed; no load increament was possible, the model arch was considered as failed due to four plastic hinges formed and behavor like a mechanism. Compared to deflection of RC arch model C2 in Fig. 8, it can be seen that the failed mode of RPC arch is similar to the RC arch.

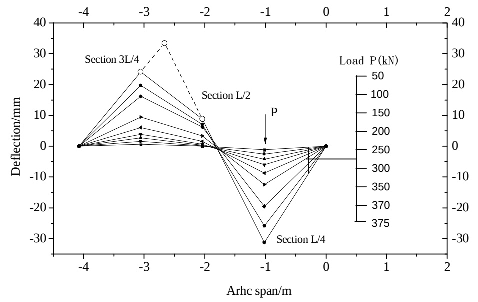

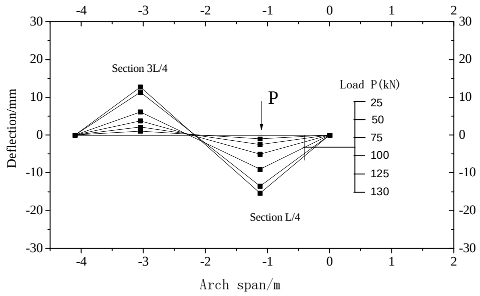

Fig.7 The deflection of R1	Fig.8 The deflection of C2

4. CONCLUSIONS

The behaviour of RPC arches is similar to those of RC arches. The RPC arches also fail due to the mechanism formed by four plastic hinges caused by cracks in tensile areas

The crack-resistant capability of RPC arch enhances significantly. The largest cracks width of RPC arches is only forty percent of that of RC arches.

The ultimate carrying capacity of RPC arches increases obviously. In the experiments, it is about 2 to 3 times as high as the ultimate capacity of RC arches.

5. REFERENCES

Candrlic, V., Radic, J., Gukov, I., (2004),, Research of Concrete Arch Bridges up to 1000m in Span[C], Arch Bridge IV, Advances in Assessment, Structural Design and Construction, Proceedings of the Fourth International Conference on Arch Bridge, 17-19, Nov. 2004, Barcelona, Spain, 538-547.

Chen, Y. M., Chen, B. C., Wu, Y. H., Huang, Q. W.,(2005),,Trail design of 432m RPC arch bridge. World bridge, 1, 2005: 1-4. (in Chinese)

Chen, B. C.,(1986),,Nonlinear Plane Finite Element Analysis on Reinforced Concrete without Hinge Arch. Fuzhou: Fuzhou University, 1986. (in Chinese)

Pierre, R., Marcel, C., (1995),,Composition of Reactive Powder Concrete. Cement and Concrete Research, 1995, 25 (7) : 1501-1511.

Tang, G. d.,(2004),,Experimental Study on Flexural Behavior of PRPC Box Girder. Beijing: Beijing JiaoTong University, 2004. (in Chinese)

Wang Z.N.,(2008),,Research on Flexural Behavior of Reactive Powder Concrete Reetangular Beam with Steel Bars. Beijing: Beijing JiaoTong University, 2008. (in Chin ese)

Yan, Z. G., Ji, W. Y., An, M. Z.,(2009),,Experimental Study and Full-Range Analysis of Reactive Powder Concrete T. Beams. Journal of Beijing Jiaotong University, 2009, 33(1): 86—90. (in Chinese)

Yu, J.,(2008),, Trial-design Research on Reactive Powder Concrete (RPC) Arch Bridge. Fuzhou: Fuzhou University, 2008. (in Chinese.)

VIBRATION AND FLEXURAL PROPERTIES OF RUBBERISED CONCRETE BEAMS

Mujib Rahman[1], Ali Al-Ghalib [1], Fouad Mohammad[1]
[1] *School of Architecture, Design and the Built Environment, Nottingham Trent University, Nottingham, NG1 4BU, United Kingdom*
Phone:+44(0)1158486502, Fax: +44(0)1158486140
E-mail: mujib.rahman@ntu.ac.uk

SUMMARY

To evaluate the potentiality of using as an anti-vibration system, rubber modified reinforced concrete was investigated in this study. The rubberised mixtures were produced by replacing 5%, 7.5%, and 10% by mass of aggregate with 1 to 4mm scrap truck tyre crumb rubber particles. A series of beams (1200 mm X 135 mm X 90 mm) were tested in a free vibration mode and then subsequently in a four point flexural tests. The input and output signals from vibration tests were utilised to calculate various dynamic parameters such as natural frequencies, frequency response function (FRF) and dynamic modulus of elasticity. The results showed that compared to control mixture, gradual reductions of natural frequencies in first six modes of all rubberised beams with highest being in the mixture with 10% rubber contents. In addition, despite the reduction in overall strength, rubberised mixture showed flexibility under loading possibly due to higher energy absorption capacity of rubber particles. Compared to control mixture, the results also showed a uniform global decrease in dynamic modulus over the span with as high as 26% reduction in the mixture with 10% rubber content. The results indicate rubberised concrete have better anti-vibration properties and could be viable alternative to use as a vibration attenuation material.

1. WHY RUBBERISED CONCRETE?

Scrap tyres form a major part of the world's solid waste management problem and will continue in coming years. Each year the UK alone produces around 30 million waste tyres with 1 billion being produced globally. Almost half of them are landfilled or stockpiled with the rest being recycled, exported, and disposed of illegally. Since 2006, the EU's Landfill Directive has barred disposal of most tyres as a landfill material. As a result, if alternatives to landfill disposal are not found, disposal costs will increase and illegal dumping or inadequate storage will continue to worsen. The fire risk associated with illegal dumps has the potential to cause significant environmental harm. In the last two decades, utilisation of scrap tyres as a construction material, especially in concrete and asphalt mixtures, has gained significant popularity in the research community as an alternative use of waste material to consume a large quantity in a most environmental friendly way (*Eldin and Senouci 1993, Dieb et al 2001, Airey et al 2003, Ganjian et al 2009*). However, in reality, usage of waste tyres in civil engineering is currently low because of concern over reduction in strength and long term durability.

Recent research (*Zheng 2008*) has demonstrated that rubberised concrete may provide a distinct advantage to absorb vibration and could possibly be used where vibration damping is needed, such as in foundation pad for rotating machinery and in railway stations; for trench filling and pipe bedding, pile heads, and paving slabs. In addition, it can also be used where resistance to impact or blast is required such as in railway buffers, jersey barriers (a protective concrete barrier used as a highway divider and a means of preventing access to a prohibited area) and bunkers. However, the study was conducted on mass concrete with as high as 45% rubber in the mixture compromising strength and durability significantly. In addition, as reinforcements are added in most of these above applications, it was felt that studying the vibration properties of rubberised reinforced concrete structures would simulate field application better.

2. VIBRATION TESTING

There is increasing acceptance that compared to other complementary localised static methods; vibration technique can be an efficient non-destructive technique to measure global response of a structural system from relatively inexpensive easily deployable sensors. In essence, the global assessment includes dynamic characteristics of the structures such as natural frequencies, mode shapes, and modal damping. These responses are a function of spatial physical properties of the structure (mass, damping, and stiffness) and therefore, changes in physical properties determined by geometry, distribution of mass, changes in stiffness, and boundary conditions will induce changes in its modal properties (*Farrar et al., 2001*).

In this study, results from a laboratory study on vibrational and flexural properties of reinforced concrete mixtures containing 5%, 7.5%, and 10% rubber are presented. The proportion of the rubber content in the mixtures was kept at a level so that strength and durability of the mixtures are not compromised adversely. The objectives of the research were to investigate: 1) the difference in the dynamic properties between reinforced concrete beam using control and rubberised mixtures. 2) The dynamic properties of rubberised reinforced concrete beam in free vibration mode 3) the effect of rubber contents on the flexural behaviour of the mixtures.

3. MIXTURE DESIGN AND EXPERIMENTATION

Depending on the purpose, concrete with strength 20-40 N/mm^2 are typically used in the infrastructure application and, therefore, to meet a target compressive strength of 20-25 N/mm^2 of rubberised concrete mixture, a control mixture with a compressive strength of 30 N/mm^2 was selected. The results were then compared with control mixtures of 25 N/mm^2. The coarse aggregate used in this study was crushed stone with maximum nominal size 20mm. Prior to mixing rubber particles, a sieve analysis was conducted to separate material retains in 5mm sieve. Once separated, 5%, 7.5% and 10% of the material was replaced by mass with 1-4mm sized crumb rubber particles where 80% of the rubber particles were between 2.36mm to 4mm. After mixing, each mixture went through a slum test to evaluate their consistently.

One beam (1200mm X 135mm X 90mm) and six cubes (100 mm X 100 mm X 100 mm) were produced for each mixture type. The reinforcement ratio, which was kept an acceptable level of 1.3%, was placed in the tension zone with 25mm clear cover. The mixture specifications and properties are listed in Tab. 1. The results showed overall slumps between 39 mm to 80 mm for all mixtures, indicating moist type mixture. However, it is interesting to note that the mixture becomes dryer as with increasing rubber content. This is because the jagged surface of the crumb rubber increases the friction between the particles**,** and hence reduces the flow. Finally, as expected, the density and strength of a mixture decreases with increasing amount of low density rubber particles.
After 28 days, each beam was tested in a simply support testing arrangement to investigate the dynamic properties in free vibration mode (Fig. 1). As shown in Figure 1, the beam was

divided, based on the theoretical analysis, into five sections to measure the modal response in multi reference points to capture all possible modes.

Tab. 1 Mixture specification and properties

Mixture type with % rubber	Mass/ beam (kg)	Density (kg/m^3)	Slump (mm)	Compressive strength (N/mm^2)	
				7 days	28 days
0%	35.0	2401	80	17	26
5%	34.5	2366	60	15	25
7.5%	33.8	2318	42	14	21
10%	33.0	2263	39	11	18

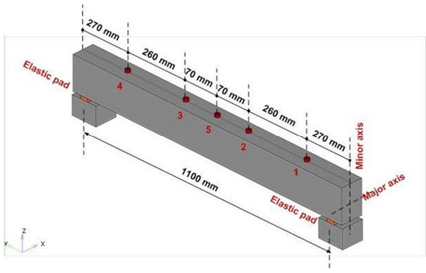

Fig. 1 Testing reference

4. MIXTURE DESIGN AND EXPERIMENTATION

Natural frequencies

A natural frequency is the frequency at which the structure would oscillate if it were disturbed from its rest position and then allowed to vibrate freely. The natural frequencies for first six modes are shown in Tab. 2. These values show gradual reduction of frequencies with increasing rubber contents, which indicates a uniform global decrease in strength over the span of the tested beam. The results also demonstrate the regular distribution of these frequencies and indicate consistent decrement in strength over the span.

Tab. 2 Natural frequencies

Mode	**Frequency (Hz)**			
	control	**5% rubber**	**7.5% rubber**	**10% rubber**
f_1	372	361	351	331
f_2	954	912	882	842
f_3	1705	1663	1573	1503
f_4	2521	2515	2395	2315
f_5	3326	3437	3267	3176
f_6	4061	3918	3737	3647

Frequency Response Function (FRF)

The FRF are normally used to describe the input-output relationship of any system for localising and quantifying the amount of change in material properties or lose of strength at the successive loading. The FRF can be expressed in terms of system properties such as mass, stiffness, and damping and as in most realistic structures, mass, stiffness, and damping are constant, it can be considered that FRF to be constant. Therefore, any change in material properties will be reflected in FRFs. The FRF for all four mixtures are shown in Fig. 2. It can be seen that compared to control mixture, approximatley 11% reduction in FRF in mixtures with 10% rubber content indicating higher changes in material properties.

Flexural response

After free vibration trials, each beam was tested in a four-point bending setup to investigate their flexural behaviour. The load deflection behaviour is shown in Fig. 3. As expected, the reduction in load bearing capacity was noted with increasing rubber content, although beam with 10% rubber contents show greater flexibility (more deflection) with high number of cracks before failure. This increase in flexibility could be due to greater energy absorption capacity of rubber particles.

Dynamic Modulus

Natural frequencies of a beam supported on flexible pads are extremely sensitive to the displacement, rotation and damping of the boundary conditions. Hense, the relationship between the natural frequencies of conventional ideal Euler-Bernoulli simply supported beam model was found not suitable in this case study. Therefore, dynamic modulus of elasticity (E_d) was determined numerically.

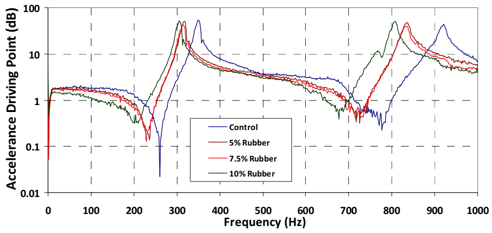

Fig. 2 FRFs for rubber contents

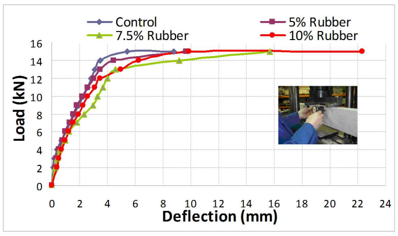

Fig. 3 Load deflection behaviour

The proposed model (as shown in Figure 4) along with the induced spring stiffness are employed to create a backward eigen-problem analysis. In this case, the measured fundamental modal frequency of each rubber content beam was fed and the corresponding dynamic stiffness was determined. The adopted model has a vertical displacement spring constant (K) which allows a certain amount of vertical deformation over support point. Points of support are assumed to be vertically suppressed by elastic springs. For this situation, the frequency equation includes a new stiffness ratio (δ), can be defined as,

$$\delta = \frac{KL}{E_d I}$$ where, I=sccond moment of area, L= span

The extracted dynamic modulus of elasticity are shown in Table 3. It can be seen that the dynamic modulus of elasticity decreases with increasing rubber contents with reduction being as high as 26% in mixture with 10% rubber content. Additionally, as damping is inversely proportional to the stiffness, lower dynamic modulus in the rubber modified mixtures is an indication of higher damping in the system.

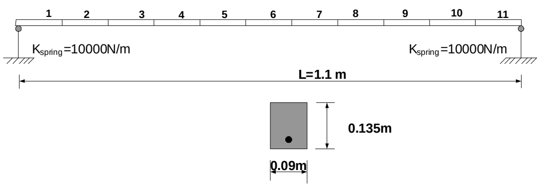

Fig 4. Simply supported beam with elastic springs

Tab. 3 Dynamic modulus of elasticity for beams with different rubber contents

Mixture with rubber content	**Frequency (Hz)**	**Dynamic modulus E_d (GPa)**	**% reduction E_d compared to control mixture**
0%	372	27	0.0%
5%	361	25	5.7%
7.5%	351	24	9.4%
10%	331	21	26.2%

5. CONCLUSIONS

This laboratory study gave some preliminary results on the dynamic properties of rubberised reinforced concrete beam. The results showed a reduction in natural frequencies and higher vibration absorption with increasing rubber contents without compromising strength significantly. If the durability issues were tackled appropriately, the rubberised concrete would have a high potential to be used where vibration damping is desirable. Further investigations are underway to determine damping and the changes in dynamic properties under successive loading.

6. REFERENCES

Airey, G.D., Collop, A.C. and Rahman, M.M., *Mechanical properties of crumb rubber modified asphalt mixtures*, Proceedings of the 3rd Eurasphalt and Eurobitume Congress, Vol. 1, pp 800-812, Vienna, 2004.

Eldin, N.N., and Senouci, A.B., *Rubber tire particles as concrete aggregate*, Journal of materials in Civil Engineering, 5(4), pp 478-496, 1993

Ei-dieb, A. S., Abdelw, M. M. and Abdel-hameed, M. E., *Concrete using tyre particles as aggregate*, Proceedings of the International Symposium organised by the Concrete Technology Unit. ISBN: 0 7277 2995 0: Thomas Telford Publishing, pp 251-259, 2001

Farrar,C. Doebling, S and Nix, D., *Vibration-based structural damage identification*, Philosophy Transactions Royal Society, Vol. 359., 2001

Ganjian E, Khorami M and Maghsoudi A, *Scrap-tyre-rubber replacement for aggregate and filler in concrete*, Construction and Building Materials 23, pp. 1828-1836, 2009

Zheng L., X. Sharon Huo , Y. Yuan , *Experimental investigation on dynamic properties of rubberized concrete*, Journal of Construction and Building Materials, pp 939–947, 2008

UTILIZATION OF PETROCHEMICAL INCENARATOR BOTTOM ASH (PI-BA) AS PARTIAL REPACEMENT OF FINE AGGREGATE

A. A. Ramezanianpour[1], Morteza Nikravan[2], R. Maknoon[2], N. NasherAhkami[2], M. Mahdikhani[2] R. Mousavi[2]*
[1]Head of Concrete Technology & Durability Research Center, Amirkabir University of Technology, Tehran, Iran,
[2]Department of Civil and Environmental Engineering, Amirkabir University of Technology, Tehran, Iran, m_nikravan@aut.ac.ir (to correspond)

SUMMARY
In this present study, the feasibility of recycling Petrochemical Incinerator Bottom Ash (PI-BA) was investigated in cementitious systems using cement (Type II42.5N) and silica fume in various additions. The percentages of PI-BA that replace fine aggregate are 0%, 15%, 30%, 45% and 60% by volume in cement-mortars. Then, Compressive strength, Capillary water absorption were carried out to evaluate solidified wastes. Generally, the physical and permeability characteristics of specimens were improved with silica fume additives. Furthermore, results show that 45% PI-BA with 10% Silica-fume has the potential of reuse PI-BA, as fine aggregate in cement-based construction and it could be economically and environmentally considerable.

1. Introduction

Incineration is one of the options used practice in petrochemical waste management *(Abduli, Abbasi et al. 2006*). An incinerator facility was established in 2009 to incinerate waste at M.B. Complex in South of Iran for decreasing amounts of waste volume as well as meeting environmental regulations. The waste volume reduction in the incinerator can reach up to 90% but it has the disadvantages of concentrating persistent pollutants in combustion residues (*Ferraris, Salvo et al. 2009*). Although bottom ash is less toxic than fly ash *(Park, Park et al. 2007*) the amount of bottom ash is significant more than that of fly ash and the composition is more heterogeneous *(Muller and Rubner 2006*). Usually, in developing countries, the industrial waste incineration bottom ash is sent to landfills (*Razak, Naganathan et al. 2009*). However, utilization of bottom ash is generally preferred over landfilling in accordance with Europe union waste policy *(Chen, Chu et al. 2008*) and landfilling is not a sustainable solution (*Ferraris, Salvo et al. 2009*). In several countries, the use of bottom ash (BA) is allowed for civil engineering application and many studies were performed in order to find possibilities for incorporating BA as partial replacement of fine aggregate in construction activities (*Filipponi, Polettini et al. 2003; Chen, Chu et al. 2008; Ferraris, Salvo et al. 2009; Gines, Chimenos et al. 2009*). It is due to demand for natural raw materials as well as saving landfill spaces. This paper presents an investigation on the behavior of the mortar produced with PI-BA used as a substitution for natural fine sand, evaluated by compressive strength and water transport property.

2. MATERIALS AND METHODS

2.1. Petrochemical Incineration Bottom ash

200 kg of waste material was collected from the incinerator bottom ash plant in this investigation. Three composite samples were taken and mixed homogenously. The grading of PI-BA was obtained according to ASTM C136 standard. The SSD Specific Gravity (Gs) and Absorption of samples were obtained in accordance with ASTM C128 standard test procedure (Tab. 2). The main Oxides of PI-BA samples were analyzed with XRF (Philips X'UNIQUE II) and reported in Tab. 2.

Tab. 1 grading, Fineness Modulus, Water Absorption and Specific Gravity of samples

Standard Mesh	Sieve size	Percent Passing (%)				
		Sample No.1	Sample No.2	Sample No.3	Mean	Standard deviation
4	4.76	98.84	99.60	99.68	99.37	0.464
8	2.38	88.15	94.21	93.51	91.96	3.315
16	1.19	67.80	70.09	71.43	69.77	1.836
30	0.595	47.97	50.12	44.16	47.42	3.018
40	0.42	32.77	35.75	30.84	33.12	2.474
50	0.297	20.98	23.19	23.38	22.52	1.334
100	0.149	11.01	15.12	13.31	13.15	2.060
200	0.074	7.77	9.08	8.77	8.54	0.685
FM		2.653	2.477	2.545	2.56	0.089
Gs		3.12	3.29	3.21	3.21	0.085
Water absorption (%)		12.40	13.12	12.95	12.82	0.38

Tab. 2 chemical composition of Petrochemical Incineration Bottom Ash samples

Component	L.O.I (%)	Fe_2O_3	Al_2O_3	CaO	MgO	P_2O_5	SO_3	TiO_2	ZnO
Sample No.1	7.50	56.40	0.87	15.70	4.50	0.76	8.10	1.04	2.04
Sample No.2	9.07	53.40	1.03	15.40	3.70	1.04	7.40	0.92	4.80
Sample No.3	8.24	49.80	4.45	17.60	3.90	1.03	7.20	2.24	3.80
Mean	8.27	53.20	2.12	16.23	4.03	0.94	7.57	1.40	3.55
Standard Deviation	0.785	3.305	2.022	1.193	0.416	0.159	0.473	0.730	1.397
Component	**SiO_2**	**Cl**	**K_2O**	**Na_2O**	**Cr_2O_3**	**MnO**	**NiO**	**MoO_3**	**CuO**
Sample No.1	<	0.02	<	<	1.34	0.26	0.04	0.02	1.19
Sample No.2	0.3	0.01	0.10	0.12	1.72	0.50	0.02	0.03	1.49
Sample No.3	<	0.02	0.20	0.05	2.26	0.36	0.04	0.02	1.95
Mean	-	0.02	0.15	0.09	1.77	0.37	0.03	0.02	1.54
Standard Deviation	<	0.006	0.071	0.049	0.459	0.121	0.012	0.005	0.381

The average of fineness modulus of the PI-BA is 2.56, indicating a rather fine grading. Moreover, the SSD specific gravity of PI-BA was 3.21, which is significantly higher than that of fine aggregates (2.50–2.65), probably due to the high iron content.

2.2. Cement, water and water reducer

Type II Portland cement and Tap water were used for the production of the cement mortar. In addition, GELENIUM 110 a carboxylic base superplasticizer was applied to maintain a constant slump flow using slump table test.

3. EXPERIMENTAL PROGRAM

In order to study the effect of the use of PI-BA as fine aggregates, cement mortar specimens were prepared according to ASTM C305 and tested in the laboratory. The percentages of PI-BA that replace fine aggregate are 0%, 15%, 30%, 45% and 60% by volume in cement-mortars and silica fume substitution 5 and 10 percent of cement. To evaluate solidified wastes, the compressive strength of cement mortar cubes were determined according to ASTM C109 after curing for 1, 3, 7, 28, and 90 days in curing room. Three specimens were prepared for each ages point and an average value was reported. Furthermore, the sorptivity was measured on mortar cubes specimens at age of 3, 7 and 28 days, which were dried in a 50 C° oven for 10 days (Ramezanianpour, Ghiasvand et al. 2009). After mass stabilization, specimen was rested on rods to allow free access of water to the surface. The masses of the specimens were measured after 0, 3, 6, 24 and 72 hr of absorption. The sorptivity coefficient (S) according to BS EN-480-5:1997 was obtained using the following expression:

$$\frac{Q}{A} = C + S\sqrt{t}$$

Where Q is the amount of water adsorbed; A is the cross section of specimen that was in contact with water; t is the time (second); c is the constant coefficient; and S is the sorptivity coefficient of the specimen (m/s$^{1/2}$).

3. RESULT AND DISCUSSION

3.1 Compressive Strength

The compressive strengths of the mortar cubes containing various percentage of Bottom ash and silica fume at different time periods up to 90 days are shown in Fig. 1 and Fig.2. ("A" and "SF" stand for PI-BA and Silica Fume, respectively).

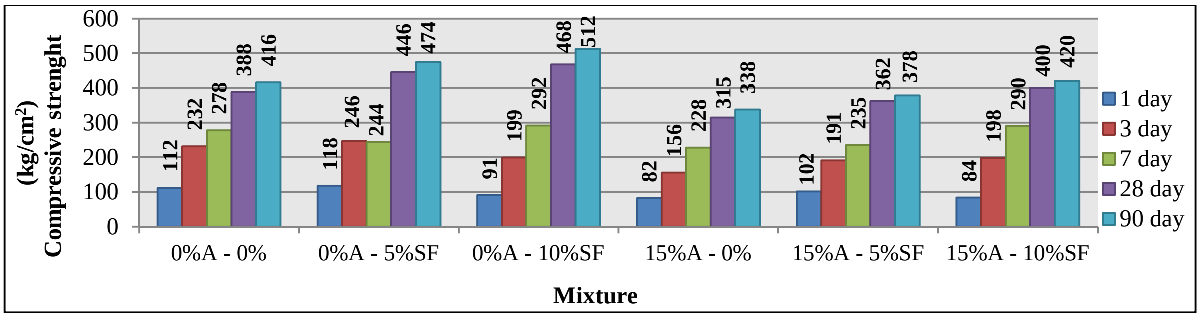

Fig. 1 Compressive strength at various ages for different mixtures with percentage of PI-BA and silica fume.

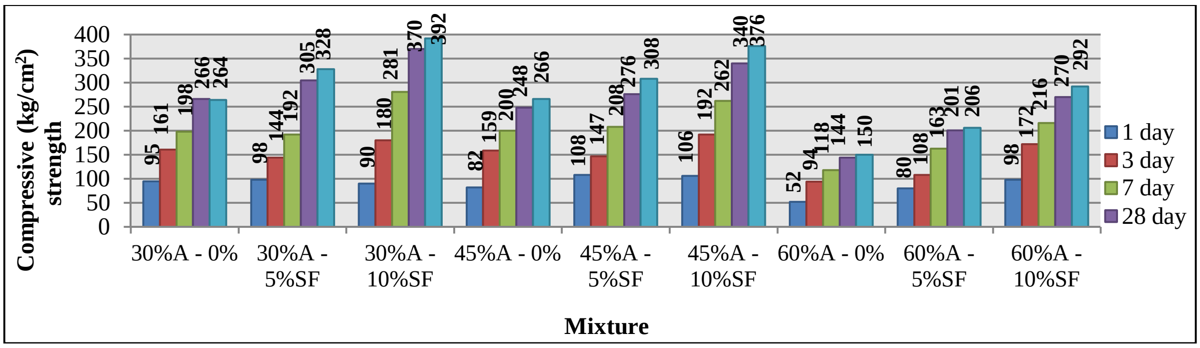

Fig. 2 Compressive strength at various ages for different mixtures with percentage of PI-BA and silica fume.

Generally, the mortar cubes PI-BA containing show lower compressive strength at all ages, which is attributed to the low instinct strength of bottom ash particles compare with natural sand and presence of heavy metallic contents in these materials, which interfere in cement hydration products (*Malviya and Chaudhary 2006*). Nevertheless, Silica fume accounts for the increase in compressive strength due to reactions with lime byproduct made by hydrating cement to produce more CSH and less calcium hydroxide in the cement matrix *(Gines, Chimenos et al. 2009*).

Fig. 4 shows the influence of the PI-BA ratio on the sorptivity of cement-mortars containing different amounts of silica-fume at the age of 3, 7 and 28 days. In all specimens, sorptivity decreases with the period of curing and increases with PI-BA replacement. A possible explanation could be that the bottom ash was finer than natural sand which absorbs more water. Furthermore, increasing the amount of PI-BA causes an increase porosity and reduction the compressive strength.

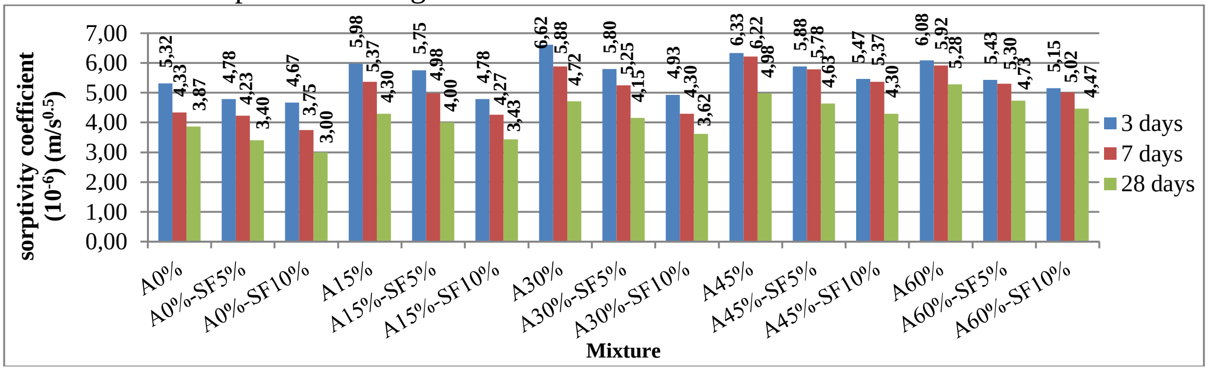

Fig. 4 The effect of PI-BA and Silica fume on the sorptivity coefficient at various ages

4. CONCLUSION

The results show that the PI-BA is suitable to be used in cement production due to their particles distribution which is similar to that of fine natural sand. As examples it can be used as a sand replacement in non-structural precast concrete pavers, masonry block production and parking lot. The results show that by increasing the PI-BA percents in mortar specimens, the compressive strength decreased and sorptivity increased. The mechanical properties of mortars were improved with silica fume addition. Consequently, results show that the use of 45% PI-BA with 10% Silica-fume replacement has the potential of reuse PI-BA as fine aggregate in the construction building and it could be considered as economical and environmental solutions for petrochemical plants disposal problem. This might be beneficial due to significant reduction the amount of residues for landfilling and partial substitution of raw materials in industrial applications.

5. ACKNOWLEDGMENT

The authors would like to thanks “Iranian National Elite Foundation” for their financial support of this paper.

6. REFRENCES

Abduli, M. A., M. Abbasi, et al. (2006). "Solid waste management in Tabriz petrochemical complex." Iranian Journal of Environmental Health Science & Engineering **3**(3): 185-192.

Chen, J. S., P. Y. Chu, et al. (2008). "Engineering and environmental characterization of municipal solid waste bottom ash as an aggregate substitute utilized for asphalt concrete." Journal of Materials in Civil Engineering **20**(6): 432-439.

Ferraris, M., M. Salvo, et al. (2009). "Use of vitrified MSWI bottom ashes for concrete production." Waste Management **29**(3): 1041-1047.

Filipponi, P., A. Polettini, et al. (2003). "Physical and mechanical properties of cement-based products containing incineration bottom ash." Waste Management **23**(2): 145-156.

Gines, O., J. M. Chimenos, et al. (2009). "Combined use of MSWI bottom ash and fly ash as aggregate in concrete formulation: Environmental and mechanical considerations." Journal of Hazardous Materials **169**(1-3): 643-650.

Malviya, R. and R. Chaudhary (2006). "Factors affecting hazardous waste solidification/stabilization: A review." Journal of Hazardous Materials **137**(1): 267-276.

Muller, U. and K. Rubner (2006). "The microstructure of concrete made with municipal waste incinerator bottom ash as an aggregate component." Cement and Concrete Research **36**(8): 1434-1443.

Park, J. S., Y. J. Park, et al. (2007). "Solidification and recycling of incinerator bottom ash through the addition of colloidal silica (SiO2) solution." Waste Management **27**(9): 1207-1212.

Ramezanianpour, A. A., E. Ghiasvand, et al. (2009). "Influence of various amounts of limestone powder on performance of Portland limestone cement concretes." Cement & Concrete Composites **31**(10): 715-720.

Razak, H. A., S. Naganathan, et al. (2009). "Performance appraisal of industrial waste incineration bottom ash as controlled low-strength material." Journal of Hazardous Materials **172**(2-3): 862-867.

EXPERIMENTAL AND PREDICTED COMPRESSIVE STRENGTH AND DENSITY USING THE NEURAL NETWORK MODEL OF NOVEL AER-TECH MATERIAL

F.G. Dan-Jumbo[1], M. Saidani and S. George[1]
[1] *Faculty of Engineering and Computing, Department of Built Environment, Coventry University, Priory Street, Coventry CV1 5FB, United Kingdom*
E-mail: fubarajumbo@yahoo.co.uk , m.saidani@coventry.ac.uk and samgeorge@orange.net

SUMMARY

Aer-Tech material is defined as a cementitiouse material with more than 10% of foam entrained in a plastic mortar. The Aer-Tech material is a special lightweight material, that outweigh the performance of conventional concrete, particularly in the areas of overlaying weight of concrete on earth mass and production cost.

This paper is aimed at showing potential application of neural network to predict compressive strength and density. The NN model is constructed by running about 300 experimental data of Aer-Tech material through an NN Mat lab programme. The NN model is then trained with input data of cement , sand , foam ,water , catalyst and water and its corresponding target data of compressive strength and density. The result show that the Aer-Tech NN-model can simulate inputs data and predicts their corresponding out put data.

Ultimately, the Aer-Tech NN model have proved its tool as a formidable tool in predicting compressive strength and density.

1. INTRODUCTION

1.1 Neural Network Model For Aer-Tech Material

In order to find the best combinations of materials and their relative proportions, an experimental laboratory programme was carried out. Mixes with different proportions of Aer-Tech material was carried out. Their respective compressive strength and density for 56 days test was taken for design of an effective model using the neural network.

The neural network tool tested to optimize the mixture ingredients to achieve the highest compressive strength. In order to obtain the final proportion for each binary or ternary binder, a simple but effective experimental design was made. The compressive strength and density of several mixes with different proportions was evaluated to ascertain the influence of various proportions on the strength.

1.2 Describing The Neural Network Model

An Artificial Neural Network (ANN) is one of the artificial intelligence techniques used as information processing systems, capable of learning complex cause and effect relationships between input and output data (Demuth, Beale and Hagan, 2008). It was further defined by

(Fanchou S and Pellinen TK, 2005) that neural network is a functional abstraction of the biological neural structures of the central nervous system.
Apparently the NN as its often known can exhibit a surprising number of human brains characteristics, for example, learning from experience and generalizing from previous examples to new problems. The neural network can provide meaningful answers even when the data to be processed include errors or are incomplete, and can process information extremely rapidly when applied to solve real world problems.

What happens in Neural network software is that the neural computing architect had built into the physical hardware (or machine) a neural software languages that can think and act intelligently like human beings. Which conforms to the analogy by (Yeh .IC,1998) that the processing element of neural network are similar to the neuron in the brain, which consist of many simple computational elements arranged in layers.

Comparatively, the neural network approach had widely been used to predict properties of conventional concrete and high performance concrete by researchers like (Kasperkiewics .J, 1995) ,(Lai.S,1997) and (Lee .SC,2003). Whilst, works by (Bai .J, 2003) has developed NN model that can effectively predicts the workability of concrete incorporating metakaolin (MK) and fly ash (FA).

Intrinsically, neural network approach to modelling process involves five main aspects: (a) data acquisition, analysis and problem representation; (b) architecture determination; (c) learning process determination; (d) training of the networks; and (e) testing of the trained network for generalization evaluation (Ahmet .O, Murat P. And M. A. Bhatti, 2004).

1.3 The Basic Strategy Of Neural Network

The basic strategy for developing a neural network model for material behavior is to train a neural network on the results of a series of experiments using that material. If the experimental results contain the relevant information about the material behavior, then the trained neural network will contain sufficient information about material behavior to qualify as a material model, these strategy conforms to works of (Lee S.C,2003).

Consequently, training a network with fewer samples often lead to early convergence.

1.4 Procedure For Aer-Tech Neural Network

With a clear objective of producing an effective ANN model of Aer-Tech material. The researcher had focus on training the network properly.

Appreciably, In the training of an ANN model, a function is mapped from known inputs to known outputs. This process is classified as a supervised learning. The training process involves passing a reasonable input of experimental data(mix constituent of Aer-Tech material) and their respective resultant compressive strength and density for training.

In addition, to minimise errors weights between the neurons are adjusted.

Specifically, the researcher had used the Matlab Neural Network Toolbox to construct and train the networks.

Interestingly, the Matlab toolbox has preprogrammed training functions. The Matlab tool box is different from other computational software because its operation is not programmed but is taught.

Primarily, the network is trained on the relationship between mix proportions of Aer-Tech material, its compressive strength and density.

Besides, the Aer-Tech material neural network model can be describe as mapping function represented in simple mathematical models defining a function F: X→Y. Each type of ANN model corresponds to a class of such functions.

The Aer-Tech neural network F consist of the nodes in which data are transmitted from one neuron to another and second also consists of a set of rules upon which the transformation of data within each neuron is based. The behavior of an ANN depends on both the weights and the input–output function (transfer function) that is specified for the units. In all the layers in the present study there are i inputs, j outputs, and k neurons. Inside each neuron, a weighted sum of the inputs is calculated and this value, called NET, is transformed by a hyperbolic tangent function. The transformed result is sent to neurons in the next layer. The input values are forwarded after multiplying by the weights associated with each neuron that diagram of neuron in ANN is shown in Fig.1.

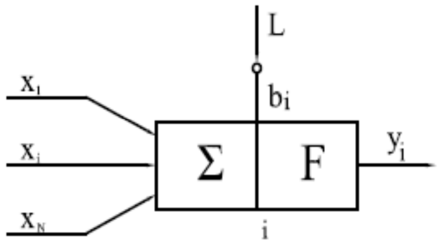

Fig. 1 A diagram of neuron in ANN.

Each training pattern contains an input vector of 5 elements viz. cement content, sand, water, foam, catalyst ratios and two output data compressive strength and density. Furthermore, ANN are highly non-linear, and can capture complex interactions among input and output variables. This characteristics is Liken to what happens in human brains. In the case of ANN the neuron is connected to other neurons through links that produce a stimulus to the entry and exit as a response, in addition, they have the ability to communicate among themselves. Whilst, the ANN has a finite number of neurons distributed in the input layer for input data and a corresponding output layer for the target out put data, also it has the intermediary layers called hidden layers, which establishes a network of relationships between layers of input and output values.

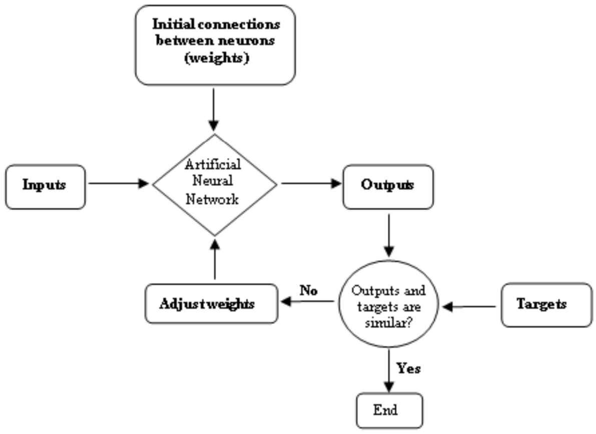

Fig. 2 Training back-propagation algorithm of the neural network method

From Fig. 2 one can deduce what happens in the neural network, it is obvious that entrance to a neuron is a numeric value defined as a scalar p, which in turn is multiplied by a weight w and finally generate a product wp, which is scalar as well. In order to generate a scalar output in a neuron, it is necessary to evaluate a function known as transfer function f, which may sometimes be influenced by a bias defined by a scalar b. The transfer function f, usually corresponds to a step, linear or sinusoidal function, which uses n as an argument and generates a scalar output.

1.5 Experimental Design

The Aer-Tech neural network model is developed by training matlab programme with experimental results of material composition, compressive strength and density. Which is obtained from about 81 different mix ratio of Aer-Tech material. More so after the network had been trained by the said experimental result, the model is simulated to predict compressive strength of Aer-Tech material and density for 56 days.

Whilst, the predicted results are compared with experimental result to verify the effectiveness of the neural network model. The error incurred during the learning can be expressed as root-mean-squared (RMS) one and is calculated.

$$RMS = \sqrt{(1/p)*\sum_j |t_j-o_j|^2}$$

Also, for a more holistic look on error, the absolute fraction of variance (R^2), the mean absolute percentage error (MAPE) and sum of the squares error (SSE) are calculated
Using the equation below

$$R^2=1-(\sum_j(t_j-o_j)^2/\sum_j (o_j)^2$$
$$MAPE=(o-t /o)*100$$
$$SSE =\sum_j (o_j-t_j)^2$$

Where t is the target value, o is the output value and p is the pattern.

1.6 Material and mixture composition

The constituent material used to produce Aer-tech material were comprised of: Pro-chem cement conforming to BS8110, pulverized river sand finer than 300μ (specific gravity 2.5), Aer-Tech catalyst and foam produced by aerating a foaming agent (Aer-Tech Sol) (dilution ratio 1:5 by weight) using an indigenously Aer-tech machine calibrated to a density of

1810kg/m^3. Fig. 3 give the linear value of constituent material composition that was transform to a nonlinear value into the matlab.

The values of parameters used in this model is as follows;

- Number of input layer = 5
- Number of hidden layer = 2
- Number of first hidden layer unites=4
- Number of second hidden layer unites= 1
- Number of output layer unites=2

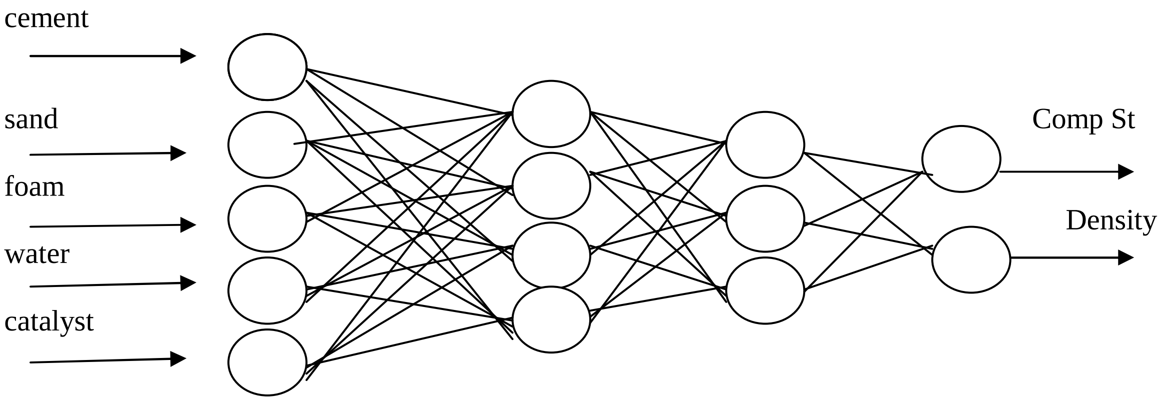

Fig. 3 Proposed Aer-Tech Neural Network Model

The Aer-Tech neural network model was constructed and trained using the neural network tool box of Matlab®. To train the network the numerical physical model was run several times in order to obtain enough input vectors and the corresponding target vectors.

Consequently, for effective and accurate training, all the inputs and outputs were normalized between -1 and +1 in order to avoid the influence of the scale of the physical quantities. In the same way, to feed the neural network it is necessary to normalize the data. A linear relationship was used to find the equivalence between the real coordinate system and the natural system (-1 to +1).

Below is Fig. 4 which shows the relationship between real and normalized scales Vi corresponds to the physical parameter i, and _ correspond to the same parameter but in the natural scale. The corresponding constants to normalize the input experimental data are:

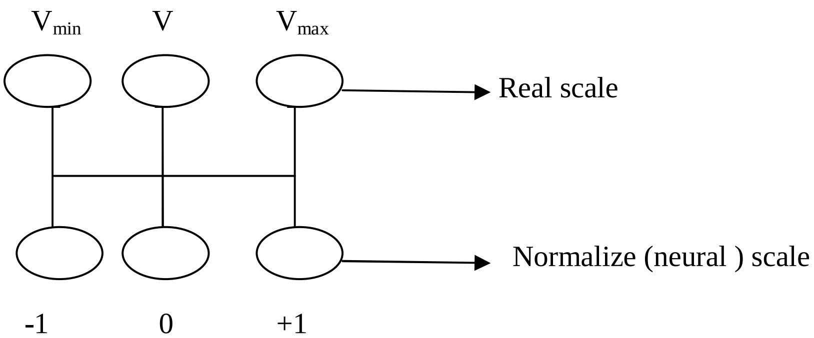

Fig. 4 Relationship between real and normalized scales

$U= 2(V_i - V_{avg})/(V_{max} - V_{min})$

1.7 Analysis Of Results

The Aer-Tech neural network developed in this research is used to predict compressive strength and density values of 300 Aer-Tech material mix design values. During this process a total of 300 specimen values for 56days compressive strength and density is pass through the matlab with 280 of them classified as training input and target values. where as the remaining are graded as testing input and target values. The overall performance of the training values and the corresponding testing set are seen in fig 3.11.

At the end of the training process, the neural network consisted of 2 hidden layers, one input layer and one output layer.

More so, the trained network is used to simulate some variable data's of cement, sand, foam , catalyst, and water, in order to subsequently predict the compressive strength and density.

The results of these simulation and the general performance of the Aer-Tech neural network has given rise to the following conclusion.

2. CONCLUSIONS

- The simulation analysis has demonstrated the Aer-Tech neural network can effectively be used to predict target compressive strength and density. The simulation process has also pickup some major dependencies of Aer-tech material, which indicate that the binder/water ratio was a key factor influencing strength of Aer-Tech material.
- The trained Aer-Tech neural network model, which was trained with about 150 experimental data's of Aer-Tech constituent material and corresponding output of compressive strength and density, can make better and realistic prediction of varying mix compressive strength and density.

3. CONCLUSIONS

Consequently, the distinctive features of neural network has made the approach different from other analytical methods. Since the system uses its training approach to solve complex problem easily.

The neural network based model is developed for predicting Aer-Tech material compressive strength and density. The Aer-Tech NN- model had shown strong potential as a feasible tool for predicting compressive strength and density. This model will clearly save an enormous amount of time, spent in the laboratory trying to optimize the best mix ratio for Aer-Tech material mix in order to achieve an acceptable compressive strength of the material.

More so, the Aer-Tech NN- model has predicted reasonable results for compressive strength and density, which again reduce the material waste and design cost required in achieving experimental compressive strength and density of Aer-Tech material.

Appreciably, the Aer-Tech NN model had made findings in this novel material more result oriented.

3. ACKNOWLEDGEMENT

This study forms part of a research programme supported by Aer-Tech development Ltd.

4. REFERENCES

British Standards BS8110 (2000). Testing Hardened Concrete: Part 14.

Cebeci, O.Z. (1981). "Pore structure of air-entrained hardened cement paste". *Cement and Concrete Research* **11**, pp. 257–265.

Cox, L. and Van Dijk, S. (2002). "Foam concrete: a different kind of mix". CONCRETE, Vol.36, No.2, pp.54-55.

Hoff, G.C. (1972). "Porosity–strength considerations for cellular concrete". *Cement and Concrete Research* **2**, pp. 91–100.

Keasel, E. P. and Visagie, M. (1999). "Micro-properties of foamed concrete". *R.K. Dhir, N.A. Handerson (Eds.), Specialist techniques and material for construction, Thomas Telford*.

Nambiar, E. K. K. and Ramamurthy, K. (2006). "Air-void characterization of foam concrete". *Elsevier,* 37 221-230.

Narayanan, N. and Ramamurthy, K. (2000). "Structure and properties of aerated concrete: a review". *Elsevier Science Ltd*.

Neville, A.M. and J.J. Brooks, J.J. (2004). "*Concrete Technology*", Pearson Education Pvt. Ltd., Singapore.

Saucier, F., Pigeon, M. and Cameron, G. (1991). "Air-Void Stability, Part V: Temperature, General Analysis and Performance Index," ACI Materials Journal, V. 88, No. 1, pp.25-36.

CONSIDERATION OF THE CO_2 UPTAKE THROUGH CARBONATION IN THE LIFE-CYCLE ASSESSMENT OF RC STRUCTURES

Tamas Dencsak[1], Corneliu Bob[1]
[1]"Politehnica" University of Timisoara, Department of Civil Engineering, 2nd T. Lalescu 300223 Timisoara, ROMANIA

SUMMARY

Concrete in form of plain, reinforced, or pre-stressed concrete, is the world's leading construction material, but it is considered non – ecologic due to the great amount of CO_2 emissions arising mainly from the manufacturing of the concrete components. On the other hand, concrete has the property to chemically react with airborne carbon dioxide, absorbing a part of it during primary and secondary life.

Although it is an important aspect, carbonation is not included in LCA models of RC structures. LCA models of built concrete focus mainly on the CO_2 emissions related to manufacturing, construction, operation and demolition phases. The aim of this paper is to perform a LCA study on a built RC structure, including the effect of carbon capture during the primary life of 75 years. The results can lead to a positive influence on the carbon footprint of concrete.

1. INTRODUCTION

The life cycle of RC structures can be divided into primary and secondary life. The primary life starts with the extraction and manufacturing of the raw materials for concrete production and ends with the demolition of the built structure. The secondary life commences when the demolished concrete is recycled and re-used in different applications as recycled concrete aggregate, road base, etc. It ends when the built construction reaches the end of its service life.

During the entire life cycle, the construction related processes contributes to great amount of CO_2 emissions, but there are also stages where carbon can be saved or captured through carbonation. Figure 1 presents summarized the carbon life cycle of a RC structure.

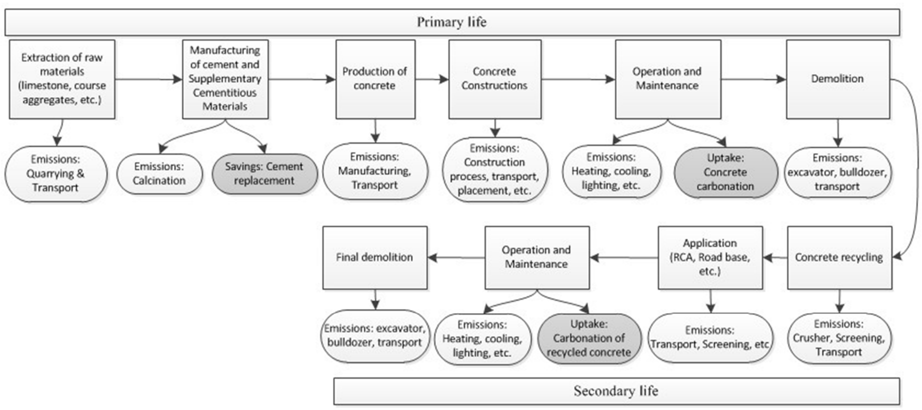

Fig. 1 Life cycle consideration of CO_2 emissions and uptake in RC structures *(Collins, 2010)*

Although concrete has the chemical ability to absorb and bind atmospheric CO_2, concrete carbonation has been previously researched only to consider the issues related to the corrosion of the reinforcement embedded in the concrete elements. The contribution of concrete carbonation to the life cycle CO_2 emissions has not been addressed in LCA. The objective of this paper is to include the effect of carbonation in the primary life of a RC structure.

2. CALCULATION METHODS AND MATERIALS

The calculations have been performed on a typical residential building in Romania, built of precast RC elements. The Precast Reinforced Concrete Large Panel structural system was extensively used in Romania primarily for 5-storey flat blocks. A rough approximation indicates that more than 40000 buildings of this type were constructed during the 1960-1990 period *(Demeter, 2005).* The study focused on the carbon cycle during the primary life of the structure. The calculation includes the CO_2 equivalent emissions arising from the production of the precast concrete elements in a cradle to gate assessment and the CO_2 uptake during the service life due to the carbonation of the exposed concrete areas. Because few data of embodied CO_2-eqv. are avaible for Romania, the „Inventory of Carbon & Energy V2.0" database has been used for the evaluation of the emissions.

2.1. Calculation of the carbonation depth

Carbonation models are based on Fick's first law of diffusion, whereby the carbonation depth of concrete, x, is the product between a carbonation rate coefficient and the squareroof of the exposure time. For the present study the formula proposed by C.Bob has been used for the calculation of the carbonation depth *(Bob, 1990)*. It takes in consideration the physical and chemical characteristics of the concrete and of the environment.

$$x = \frac{150 \cdot c \cdot k \cdot d}{f_c} \cdot \sqrt{t} \ \text{[mm]} \tag{1}$$

where:
x – carbonation depth;
c – correction factor for binder type;
k – correction factor for environmental conditions;
d – correction factor for CO_2 concentration;
f_c – concrete compressive strength;
t – exposure time.

2.2. Calculation of the CO_2 uptake

For the calculation of the CO_2 uptake the following formula has been used *(Pade, 2007)*:

$$a = r \cdot C \cdot CaO \cdot \frac{M_{CO2}}{M_{CaO}} \ [\text{kg/m}^3] \tag{2}$$

where:
r – the amount of CaO within fully carbonated OPC that converts to $CaCO_3$ (r = 0.75);
C – the quantity of OPC within the binder;
CaO – calcium oxide content within OPC;
M – the molar mass of the oxides

3. RESULTS

The data regardind the configuration, geometrie and concrete properties of the building are taken from the original project, type 770 – 81, Pb2, MM. The structure has been divided into the following parts:

- Exterior walls, of concrete C16/20, cement type CEM II A – S, 32.5R, 350kg/m^3;
- Interior walls, of concrete C12/15, cement type CEM II A – S, 32.5R, 300kg/m^3;
- Slabs, of concrete C16, cement type CEM II A – S, 32.5R, 350kg/m^3;
- Stairs, of concrete C16, cement type CEM II A – S, 32.5R, 350kg/m^3.

The total amount of concrete and reinforcement has been calculated for each part, in order to estimate the initial embodied CO_2- eqv., using the ICE V2.0 database *(ICE V2.0, 2010).*

For the calculation of the carbonation depth, using formula (1), the following assumptions have been considered:

- For all elements, the correction factor for binder type: c=1.2;
- For the interior elements, the correction factors for realtive humidity and CO_2 concentration: k=1, d=1;
- For the exterior elements, considering a higher relative humidity and CO_2 concentration, k=0.7 and d=1.2;
- Additional correction factor has been considerd for cover, paint, etc. For indoor concrete 0.7 and for outdoor concrete 0.9 *(Lagerblad, 2005)*;
- The exposure time has been considered 75 years.

The assumptions for the calculation of the CO_2 uptake are the following:

- Cement type CEM II A-S, with 15% slag and 85% OPC;
- The CaO content of OPC is 65%;
- Conversion coefficient of CaO to $CaCO_3$ is 75%;

All the results are summarized in Tab. 1.

Tab.1 Estimation of life cycle CO_2 in a RC Structures

Element	Concrete [m^3]	Steel [kg]	Total embodied CO_2 – eqv. [kg]	Exposed Area [m^2]	Carbonation Depth [mm]	Uptake [kg]
Ext. Walls	57.8	2751	21914.0	413	59	-5545.7
Int. Walls	147.6	4144.9	44424.4	1054.2	73	-14981.7
Slabs	151.3	7491.4	58146.5	1163.7	55	-14469.5
Stairs	16.9	1348.1	7920.7	94.6	70	-1512.0
Total			**132405.5**			**-36508.9**

During primary life the effect of carbonation on the life cycel of CO_2 emissions is considered smaller, because the exposed surface area, relative to volume of the built concrete structure, is much smaller then in the secondary life, where the concrete is crushed and used as RCA, with a greater area exposed to CO_2 for carbonation. Even so, the uptake is significant, because according to the performed life cycle estimations about 28% of the initial embodied CO_2 can be reabsorbed by the exposed concrete elements over their service life of 75 years. If we would consider the embodied CO_2 only in concrete, the uptake would represent about 42%. The high value of CO_2 absorption during primary life may have the following explanations:

- low quality of the concrete, which permit a good carbonation;

- high exposed area of the concrete elements relative to volume, in comparison to other type of elements (beams, coloumns, etc.).

On the other hand this phenomena can lead to the corrosion of the reinforcement, which will require some protection measures.

4. CONCLUSIONS

This paper has re-examined the life cycle carbon footprint of a typical residential building in Romania, built of large precast RC panels, specifically focusing on the contribution of carbon capture trough carbonation during the primary life.

Performing a LCA study, considering the initial CO_2 emissions arising from the production of the precast elements and the effect of carbon uptake during the primary life of 75 years, it resulted the about 28% of the initial CO_2 can be reabsorbed. Considering only the emissions for the production of the concrete, the uptake would be about 42%. If carbonation is ignored, emissions in LCA of concrete structures can lead to serious overestimations.

Considering also the secondary life, the CO_2 uptake can be much higher, because the surface area of the crushed concrete, re-used as RCA, is much greater exposed to CO_2 and carbonates.

Due to the high number of such building types in Romania, it is recommended to improve LCA models, including the effect of both primary and secondary life.

5. ACKNOWLEDGEMENTS

This work was partially supported by the strategic grant POSDRU/88/1.5/S/50783, Project ID50783 (2009), co-financed by the European Social Fund – Investing in People, within the Sectoral Operational Programme Human Resources Development 2007 – 2013.

6. REFERENCES

F. Collins (2010) „Inclusion of carbonation during the life cycle of built and recycled concrete: influence on their carbon footprint“, International Journal on Life Cycle Assessment, pp. 549-556

Demeter, I. (2005). "Short history of large panel structures in Romania." Scientific Bulletin of The "Politehnica" University of Timişoara, Vol. 51(65), No. 1, 87-94.

Prof G. Hammond & C. Jones: “Inventory of carbon & energy (ICE) version 2.0”.(2011) www.bath.ac.uk/mech-eng/sert/embodied/

Bob, C. “Some aspects concerning corrosion of reinforcement”, Proceedings of the International Conference “ The Protection of Concrete”, Dundee, Sept.1990

Pade C., Guimaraes, M. „The CO2 uptake of concrete in a 100 year perspective” Cem. Concr. Res. 2007, 37, 1384–1356.

B. Lagerblad (2005) „Carbon dioxide uptake during concrete life cycle – State of the art” Swedish Cement and Concrete Research Institute, CBI.

METHODS AND CRITERIA FOR CONCRETE DURABILITY EVALUATION

Dan Georgescu[1], Adelina Apostu[1], Radu Gavrilescu[2]
[1] *Technical University of Civil Engineering Bucharest, Faculty of Civil, Industrial and Agricultural Engineering, 124 Lacul Tei Blvd., Bucharest 2*
[2] *S.C. CARPATCEMENT HOLDING S.A., 1A Bucharest - Ploiesti Str., Bucharest Business Park, Bucharest 1*

SUMMARY

The article is showing the results of experimental researches, in order to study the possibility to apply in Romania new evaluation criteria of concretes freeze-thaw and sulfate resistance for concrete mixes with different cement types. Applications will be presented regarding the performance approach in order to evaluate the freeze-thaw resistance of certain concretes prepared with cements with additions, type CEM II/B-M (S-LL) 32.5R with different percent of slag and limestone and for sulfate resistance for concretes prepared with cements type CEM II/A-S 32.5N-LH ($C_3A \leq 6\%$) and CEM III/A 42.5N-LH. The application of experimental methods in accordance with the European standards and certain specific assessment criteria create the premises of elaborating at the national level a methodology for establishing the performance levels of concrete prepared with cements with additions.

1. INTRODUCTION

This article put in the evidence important aspects regarding the provision of concrete's durability based on modern approaches, mainly descriptive, and performance.

Currently, based on European and Romanian national regulations, the assurance of durability is accomplished through a descriptive approach, specifying the requirements related to composition and compressive strength of concrete depending of the classification of structural elements in certain exposure classes. This approach is not enough sensitive especially for the establishment of the necessary criteria of the new cement type's utilization fields.

2. EXPERIMENTAL PROCEDURES AND CRITERIA

The verification of concrete's composition for a certain application or establishing the utilization fields of cements must be performed based on a unitary methodology. In Fig. 1, it is evidenced the authors' proposal regarding the necessary stages in order to apply the performance criteria.

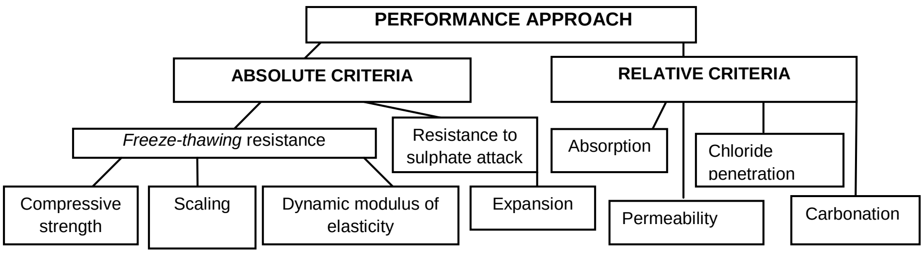

Fig. 1 The methodology application chart

This methodology will be applied in order to evaluate the freeze-thaw resistance of certain concretes prepared with cements with additions, type CEM II/B-M (S-LL) 32.5R with different percent of slag and limestone and for sulfate resistance of concretes prepared with cements type CEM II/A-S 32.5N-LH ($C_3A \leq 6\%$) and CEM III/A 42.5N-LH.

2.1 The testing methods used in freeze-thaw evaluations are standardized on European level in the documents: CEN/TS 12390-9 and CEN/TR 15177.

2.1.1 Evaluations criteria for concrete freeze-thaw resistance

- **Evaluations criteria for scaling:**
  - **Cube test :**
    - XF1 Exposure class (cement dosage 300 kg/m^3 and W/C ratio = 0.6)
      The quantity of scaled material does not have to produce a reduction more than 5% of concrete sample mass for 56 cycles and respective more than 10% for 100 cycles
    - XF3 Exposure class (cement dosage 300 kg/m^3 and W/C ratio = 0.6)
      The quantity of scaled material does not have to produce a reduction more than 3% of concrete sample mass for 56 cycles and respective more than 5% for 100 cycles
  - **Slab test**:
    - XF4 Exposure class (cement dosage 320 kg/m^3 and W/C ratio = 0.5)
      The quantity of scaled material from the surface of the sample does not have to be over 1Kg/m^2 after 56 freeze-thaw cycles (air entrained concrete)
- **Dynamic elasticity modulus:**
    - XF3 Exposure class (cement dosage 320 kg/m^3 and W/C ratio = 0.5)
      After 28 freeze-thaw cycles, the concrete sample does not have to show a reduction of dynamic modulus more than 25%.

After 56 freeze-thaw cycles, the concrete samples prepared with “experimental cement” type (studied for evaluation of the freeze-thaw resistance of concrete) does not have to show a reduction of dynamic modulus of elasticity more than 5% beside the value obtained for samples prepared with “standard cement” witch behaviour in specific circumstances is known as being favourable.

2.2. Evaluation of the sulphate resistance was performed measuring the expansion values on mortar samples, especially after 90 days of storage in aggressive sulphate environment (4,4% Na_2SO_4 solution)

2.2.1 Evaluation criteria for sulphate resistance

The expansion value does not have to be over 0.5 mm/m after 90 days of storage in aggressive environment (solution).

3. EVALUATION OF FREEZE-THAW RESISTANCE. APPLICATION FOR CEM II/B-M (S-LL) 32.5R

3.1. Cement compositions and codes:

1. CEM II/ B-M (S-LL) 32.5R – slag 15,5%, limestone 7.4% - code CEM 1;
2. CEM II/ B-M (S-LL) 32.5R – slag 14,5%, limestone 13.9% - code CEM 2;
3. CEM II/ B-M (S-LL) 32.5R – slag 14,4%, limestone 17.3% - code CEM 3;
4. CEM II/ B-M (S-LL) 32.5R – slag 14%, limestone 11.4% - code CEM 4;
5. CEM II/ B-M (S-LL) 32.5R – slag 16%, limestone 14.1% - code CEM 5;
6. CEM II/ B-M (S-LL) 32.5R – slag 16%, limestone 18.1% - code CEM 6.

3.2. Presentation of the results

An overview of the results, obtained after the evaluation of freeze-thaw resistance of cements according to the different acceptance criteria from international technical literature in XF exposure classes, are presented in the Tab. 1.

Tab. 1: Synthesis of the results

Exposure class		XF1	XF3		XF4
Method		Cube	Cube	Modulus	Slab
Cement code	CEM 1	OX	O	X	XO
	CEM 2	O	O	XO	O
	CEM 3	X	OX	X	XO
	CEM 4	X	X	X	X
	CEM 5	X	X	X	X
	CEM 6	O	O	X	XO

X = fulfilled criteria; O = not fulfilled criteria; XO = “on boundary” fulfilled criteria; OX = “on boundary” not fulfilled criteria.

4. EVALUATION OF SULFATE RESISTANCE OF CONCRETES PREPARED WITH CEMENTS TYPE CEM II/A-S 32.5N-LH ($C_3A \leq 6\%$), CEM III/A 42.5N-LH

The experimental research program are following the sulfate resistance of mortars prepared with CEM III/A 42.5R (36% slag), respectively two CEM II/A-S 32.5 N-LH types, measuring the expansion especially on 90 days. The results are presented in Fig. 2 showing the admissible level of expansion according to the previous presented criteria.

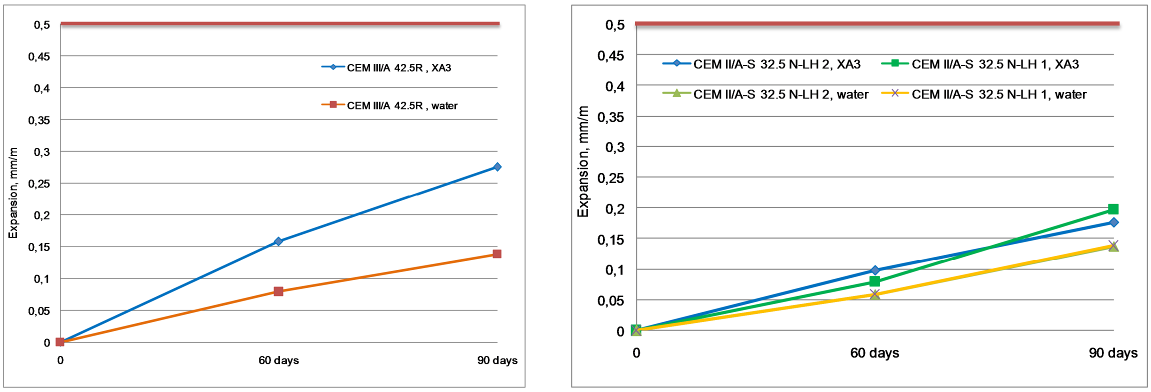

Fig. 2 Evolution of the mortar samples expansion prepared with CEM III/A 42.5R and CEM II/A-S 32.5 N-LH ($C_3A \leq 6\%$), stored in aggressive sulphate environment

5. CONCLUSIONS

- The paper presented a methodological proposal in order to determine the long-time behavior of concrete, related to the XF and XA exposure environment classes, based on performance approaches;
- The scientific research indicate that is possible to obtain different experimental results and conclusions regarding long time behavior of the concrete, depending on admixtures quantity and combinations, including for the same cement types;
- Taking into consideration the multiple combinations between the percentages additions and types and the manner in which they influence the cement and concrete characteristics, the proposed methodology must be applied for each type of cement for which there is no utilization experience in the country.

6. REFERENCES

European Committee for Standardization (2006), CEN / TS 12390-9: Testing hardened concrete - Part 9: Freeze-thaw resistance. Scaling

European Committee for Standardization (2006), CEN/TR 15177: Testing the freeze-thaw resistance of concrete - Internal structural damage

Muller C. (2008): Durability of concrete with CEM X cements, VDZ Germany, Düsseldorf

ONORM - B3303 – Betonprüfung, 2002

Romanian Standards Association, CP 012/1-2007: Code of practice for the manufacturing of concrete

Siebel, E. (1992-94): Frost- und Frost-Tausalz-Widerstand von Beton. Beton 42 (1992) H. 9, S. 496-501, ebenso Betontechnische Berichte

BEHAVIOR AND SHEAR STRENGTH OF REINFORCED HIGH-STRENGTH CONCRTE DEEP BEAMS

R. Aghayari [1] ,A. Arabzadeh [2],
1. Assistant Professor of Civil Engineering Dept, Razi University, Kermanshah, IRAN, Tel: 0831-4283264, Email: r.aghayari@gmail.com
2. Assistant Professor of Structural Engineering Dept., Tarbiat Modarres University, Tehran, IRAN, Tel: 021-82883323, Email: arabzade.a@gmail.com

SUMMARY

An experimental-analytical investigation was conducted to study the behavior of high-strength RC deep beams; a total of sixteen reinforced concrete deep beams with compressive strength in range of $59\ \text{MPa} \leq f'_c \leq 65\ \text{MPa}$ were tested under two-point top loading. The tested specimens were simply supported and the shear span-to-effective depth ratio was 1.10 and reinforced by vertical, horizontal and orthogonal steel bars in various arrangements. The test results indicated that both vertical and horizontal web reinforcement are efficient in shear capacity of deep beams, also the orthogonal shear reinforcement was the most efficient when placed perpendicular to major axis of diagonal crack. Concentrating of shear reinforcement within middle region of shear span can improve the ultimate shear strength of deep beam.

1. INTRODUCTION

The reinforced concrete deep beams have become an important structural elements having small span-to-depth ratio. The investigation of their behavior is a subject of considerable interest in RC structures researches. In deep beams, according to shear span-to-depth ratio and web reinforcement the ultimate strength is generally controlled by shear rather than flexure, if the sufficient amount of longitudinal reinforcement is used. Several different failure modes have been identified from experimental studies, due to variability in failure, the determination of their shear strength and identification of failure mechanism are very complicated. A number of significant or impressive parameters on shear behavior of deep beams have been identified; including concrete compressive strength, span-to-depth ratio, amount and arrangement of shear reinforcement and amount of main reinforcement. Several experimental studies were performed to investigate the efficiency of web reinforcement in shear behavior of deep beams. The objective of current study is to evaluate behavior and shear strength of RC deep beams. As the test variables are amount and arrangement of web reinforcement.

2. EXPERIMENTAL PROGRAM

2.1. Specimen details

Test specimens consisted of sixteen simply supported concrete deep beams with different properties. They were classified in four series according to type of their web reinforcing:

Series A consist of six deep beams with variable vertical steel bars and uniform spacing, **Series B** consist of three deep beams with variable vertical steel bars concentrated at center of shear span, **Series C** consist of four deep beams reinforced by both variable horizontal and constant vertical web reinforcement and **Series D** consist of three deep beams reinforced by diagonal steel bars which are placed perpendicular to diagonal cracks (Fig. 1).

All specimens had a rectangular cross-section with 80×400 **mm²**. their overall and effective spans wee 1600 **mm** and 1200 **mm,** respectively. Fig. 1 and Tab.1 gives the additional details of specimens.

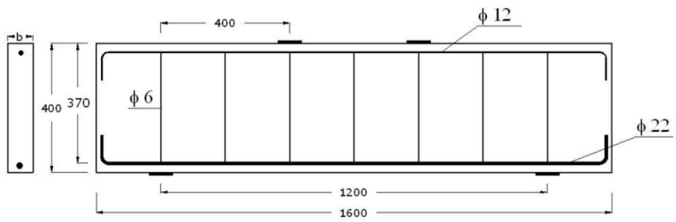

Fig. 1. a. Dimension of specimens

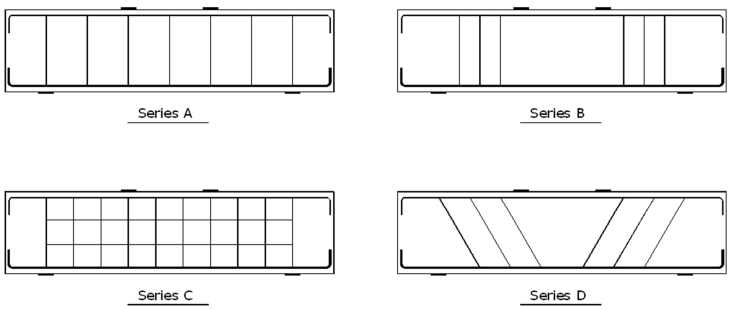

Fig. 1. b. The typical schema of specimens

2.2. Material properties

The longitudinal steel reinforcements consist of 12D (12 **mm** diameter), 22D and 25D deformed steel bars, and also steel shear reinforcement include 6D (6 **mm** dia.) smooth round bars. The concrete was prepared by Type II Portland cement and river fine aggregate. Maximum aggregate size was 12.5 mm and the slump was measured 90 mm. The concrete strength was defined based on the average value of three standard cylinders (300×150 mm) which obtained in range of $59\ \text{MPa} \leq f'_c \leq 65\ \text{MPa}$.

2.3. Test setup and loading

The hardened specimens were white-washed to observe explicitly the cracks and failure throughout the tests. The beams were tested in setup as shown in Fig. 2. All specimens were simply supported by using restrained and free roller and were loaded on the top face. The load was applied through a hydraulic jack to the center of a strong girder and divided to two-symmetric loads via its supports located on top face of specimens. The applied load and the reaction forces of specimens were distributed on top and bottom surfaces of beams through rectangular 130×80 mm^2 steel plates.

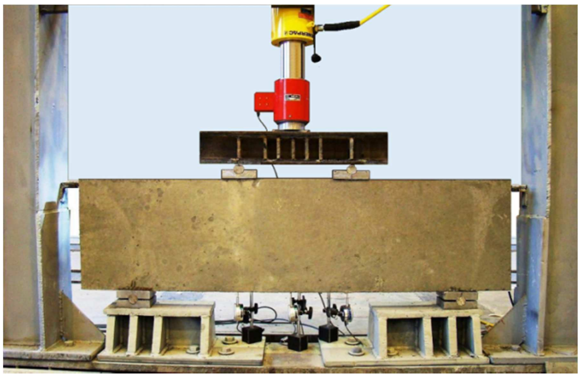

Fig. 2. Testing setup

3. EVALUATION OF TEST RESULTS

3.1. General behavior

All the beam specimens showed a same response up to failure. In the early steps of loading, few vertical flexural cracks formed in the pure-bending region. As the load increased approximately to 30-50% ultimate load, generally the diagonal cracks appeared at the mid-height of beam within the clear shear span in the direction of the main strut and propagated rapidly toward the outside edge of the loaded point and the inside edge of the support. While the diagonal cracks were developing across length, their widths were propagating in the center of shear span. Failure for all specimens was brittle and their failing mechanism is identified as follows:

a) Diagonal splitting along the direction of main strut.
b) Strut crushing failure due to forming of several parallel diagonal cracks.
c) Shear-compression near the support or loading point, this failure only observed in A-1 specimen (without shear reinforcement) after forming of diagonal cracks at mid-height of the beam and propagating toward the supports or loading points.
d) Shear-flexure failure, only one of the specimens failed due to excessive opening of propagated flexural cracks and yielding of main longitudinal reinforcement.

3.2. Effect of shear reinforcement

As observed during the tests, by increasing the ratio of shear reinforcement from 0 to 0.84 percent, the ultimate shear strength tends to increase about 80 percent. On the other hand, in specimens of series D, the shear reinforcement was more efficient than those of other series with same amount of shear reinforcement; it means that, when the web orthogonal reinforcing is placed perpendicular to direction of main strut, its efficiency on the ultimate shear strength is more significant than when it is placed in vertical or horizontal direction. Moreover, because of high concrete confinement next to supports and loading points, the initial cracks form at the mid-height of beam within the shear span. Consequently, concentrating the shear reinforcement at central region of shear span is more efficient than uniform spacing of them, but with the same amount of shear reinforcement, the shear strength for specimens of series B is greater than of series A. in addition, It was resulted that the effect of horizontal shear reinforcement is less than vertical shear reinforcement. Moreover, at a shear span-to-effective depth ratio closer to 1.0 the resistance of horizontal shear reinforcement occurs due to dowel action, but this has a very small effect compared to effect of main longitudinal reinforcement.

3.3. Strain in web reinforcement

Through the test of all specimens, strain of web steel bars was recorded via attached strain-gauges. Measurement and observation show the significant effectiveness of web reinforcing on preventing the cracks opening. The strain response of shear reinforcement for all beams was the same, and can be summarized to:

a) Strains of web reinforcement at middle region of shear span were higher than those which were near the supports or loading point.
b) Strains of horizontal web bars were lower than of vertical reinforcement.
c) Strain of shear reinforcements increases significantly beyond the formation of diagonal cracks.
d) Strain of shear reinforcement in specimens with small ratio of shear reinforcing was bigger than those which were reinforced heavily.

4. CONCLUSION

The behavior of sixteen tested deep beams was investigated. According to performed study following conclusion can be made:

a. The shear reinforcement are subjected to variable strains depends on their location in the span of the beams. The steel bars placed in central zone of shear span are subjected to higher strain than those placed near the support. Consequently it is probable that the shear reinforcement cannot attain their yielding force, it shall be considered in equilibrium conditions of strut-and-tie model.
b. Amount and arrangement of shear reinforcement are effective on ultimate strength of deep beams and the concentrated bars in central region of shear span have higher efficiency on strengthening of deep beams.
c. The horizontal shear reinforcement can improve the shear strength of reinforced concrete deep beams as well as the vertical reinforcement. The efficiency of horizontal reinforcing decreases due to increasing of shear span-to-depth ratio and can be vanished by setting inclination angle of strut, closer to 25˙
d. The inclined shear bars becomes the most efficient when are placed perpendicular to diagonal cracks.

5. REFERENCES

A. Arabzadeh, A. R. Rahaei, R. Aghayari, (2009), A simple strut-and-tie model for prediction of ultimate shear strength of RC deep beams, *International journal of civil engineering*, IRAN, Vol. 7, No.3, pp. 141-154

A. Arabzadeh, (2001), Analysis of some experimental results of simply supported deep beams using truss analogy method, *Iranian Journal of Science & Technology*, Vol. 25, No. 1, Shiraz University, IRAN, pp.115-128.

INNOVATIVE GREEN CONCRETE MIXES BY USE OF GLASS BY-PRODUCTS

Ofelia Corbu[1], Cornelia Măgureanu[2], Dumitru Moldovan[2], Henriette Szilágyi[3], Oana Cazac[2]
[1] *Central Laboratory*
Technical University of Cluj-Napoca
40027 Cluj-Napoca Bariţiu 25
[2] *Department of Reinforced Concrete and Steel Structures*
Technical University of Cluj-Napoca
40027 Cluj-Napoca Bariţiu 25
[3] *„URBAN –INCERC" National Research Institute Cluj-Napoca Branch*
400524 Cluj-Napoca Calea Floresti 117

SUMMARY

Present study will present a green concrete mix developed as part of a PhD research programme aiming (among other objectives) at finding value added uses for by-products such as glass; after crushing in standard grain sizes, ranging from [16 mm] down to glass powder and completely or partially replacing traditional types of aggregates (coarse and sand) and even (in given ratios) part of the cement, the mechanical properties of the concrete was investigated.

1. INTRODUCTION

Concrete is by far the primary construction material due to its improved properties that come often in environmental unfriendly packages. It is therefore the researchers' duty to find alternatives, such as by use of by-products or supplementary cementitous materials, to achieve friendly concrete and to decrease the energy consumption (*O.Corbu et al 2010)*. This in turn will lead to less materials becoming part of an industrial production lead flow and thus improve the overall quality of the surrounding environment.

General gain of experience started with the research programme Grant A, CNCSIS 1036/2007-2009, "Green Concrete" – ECOLOGY & SUSTENAIBILITY coord. by Prof.dr.ing.Cornelia MĂGUREANU aiming at finding new usage for various by-products as concrete constituents. Further experimental results were collected in the research programme for a PhD thesis by O. Corbu aiming at using glass by-products as partial aggregate and cement replacements.

2. RESEARCH PROGRAMME

2.1 Concrete constituents

Materials used in present study are commercially available at local producers or licensed construction materials suppliers.

2.1.1 Aggregates

Various types of aggregates such as quartz sand (0/0,3 mm), coarse (0/4 mm), crushed glass grains (0/4, 4/8, 8/16 mm) and GP (Glass Powder) were investigated in present study (for the last two, see Fig.1 and Fig. 2).

Fig. 1. Glass aggregates & powder

Fig. 2. Bulk glass by-product

2.1.2 Cement

Cement grade of 52.5, commercially available as RAPIDCEM ®/PORTLAND Cement type CEM I 52,5R supplied by the mill in Hoghiz Braşov county of LAFARGE CEMENT Romania S.A was used in present study.

2.1.3 Silica fume (SF)

Admixture type II (pozzolanic or retarded hydraulic) commercially available as Elkem Microsilica Grade 940-U supplied by BASF Romania, the national dealer of the Dutch based chemical group Elkem was used in present study.

2.1.4 Glass Powder (GP)

Admixture type II (fine grained glass powder) is another pozzolanic constituent that improves mix properties.

2.1.5 Superplasticizer

Polymer eter-policarboxilate brand new generation type superplasticizer commercially available as GLENIUM ACE 30, a high water dosage reduction agent, supplied by BASF Chemical Company was used in present study.

2.1.6 Water

Tap water was considered to be satisfactory for present study.

2.2 RESULTS

2.2.1 Fresh and hardened concrete properties

Mixes under study are listed in Tab. 1 as ratios of the cement dosage used in the reference mix named S7. Starting from this mix, the cement, SF and GP proportions were varied resulting in the S8-1, S8-2 and S8-3 mixes.
The most successful mix S8-1 was then further improved by varying SF and GP proportions and thus developing the final S8-1,A (best behaviour) and S8-1,B, mixes.

Tab. 1 Mix proportions

Mix	Proportions %								
	CEM Lafarge	SF Elkem	GP	Glass grain size 0/4	Coarse agg. 0/4	Glass grain size 4/8	Glass grain size 8/16	Super-plasticizer BASF	W/C
S7	1	0.1	-		45%	25%	30%	0.02	0.35
S8-1	0.8	0.125	0.250		45%	25%	30%	0.02	0.35
S8-2	1	0.1	-	45%		25%	30%	0.02	0.35
S8-3	0.8	0.125	0.250	45%		25%	30%	0.02	0.35
S8-1,A	0.8	0.125	0.250	-	45%	25%	30%	0.025	0.36
S8-1,B	0.8	-	0.375	-	45%	25%	30%	0.025	0.36
Mr	0.8	0.1			45%	25%	30%	0.02	0.35
M	0.8	0.1			45%	25%	30%	0.02	0.35

Tab. 2 Fresh concrete properties

Characteristics	Mixes under study					
	S7	S8-1	S8-2	S8-3	S8-1,A	S8-1,B
W/C	0.35	0.35	0.35	0.35	0.36	0.36
W/B	0.25	0.25	0.25	0.25	0.26	0.26
Superplasticizer dosage	0.02	0.02	0.02	0,02	0.025	0.025
Slump Flow [mm]	S5- 255 F4- 525	0	0	S2- 53	S4- 188	S4- 165
Temperature [ºC]	21.6	21.8	21.0	22.7	22.7	23.3
Entrained air [%]	2.00	1.75	0.40	1.62	2.50	2.00
Density [kg/m^3]	2313	2346	2265	2295	2338	2337

Tab. 3 Hardened concrete properties

Characteristics	Mixes under study							
	S7	S8-1	S8-2	S8-3	M	Mr	S8-1,A	S8-1,B
W/C	0.35	0.35	0.35	0.35	0.35	0.35	0,36	0,36
W/B	0.25	0.25	0.25	0.25	0,31	0,31	0,26	0,26
CEM dosage	1	0.8	1	0.8	0.8	0.8	0.8	0.8
SF dosage	0.1	0.1	0.1	0.1	0.1	0.1	0.1	-
GP dosage	-	0.2	-	0.2	-	-	0.2	0.3
f_{cm} 7 days	61.1	66.3	59.2	69.1	80.4	74.2	71.9	48.4
f_{cm} 28 days	69.6	70.3	68.0	79.6	87.9	79.7	83.0	50.3
f_{cm} 56 days	76.5	82.9	73.8	79.6	92.8	80.3	83.7	50.7
f_{cm} 90 days	79.9	83.2	74.4	83.7	101.7	80.7	85.6	52.3
f_{cm} 120 days	86.8	85.5	74.7	89.9	116.5	89.6	88.4	54.2
$f_{ct,fl}$ 270 days	4.0	3.1	2.7	3.2	5.8	-	-	-
$f_{ct,sp}$ 28 days	3.7	6.1	4.5	4.5	5.7	-	3.7	1.7
MOE [GPa] 28 days	47	50	50	52	48	-	54	-
Abrasion [mm^3/5000 mm^2]	8482	7684	12216	14204	6913	7068	7517	5632
Strength loss η	-	-	-	-	-	5.52	5.54	9.87

(%) at G100								
Permeability at 12 atm. [mm]	-	-	-	-	-	-	10	-
Carbonation at 360 days [mm]	0	0	0	0	0	0	0	0
Shrinkage [mm/m]	0,20	-	-	-	-	-	0.30	-

3. CONCLUSIONS

The fresh and hardened properties of the S8-1,A may be considered outstanding. Compressive strength development, abrasion resistance, modulus of elasticity and freeze-thawing strength are similar to the reference mixes using either crushed (M) or coarse aggregates (Mr). S8-1,A exhibits excellent shrinkage behaviour (recorded up to 120 days) which soften after about 56 days (RH 65±5%; T 20±2°C). Permeability is at a maximum of 10% of the minimum allowed in the corresponding national code provisions.

The strength of the glass grains is less than the one for coarse or crushed aggregates but may still be used successfully in combination with alkaline reaction inhibitors *(Ahmad Shayan 2002),* than cause swelling of concrete and thus lead to cracking. In the present study silica fume (improved workability, increased density and better compressive strength) and glass powder (improved abrasion resistance) were used as inhibitors.

Since the chemical properties of the glass by-products are primordially to any result, primary mixes are a must to establish the specific influence on mix properties.

4. ACKNOWLEDGEMENTS

This outcome has been achieved with an extensive material support by Lafarge Romania. Another party contributing to this study is BASF Romania. All support is gratefully acknowledged.

5. REFERENCES

Corbu, O., Măgureanu, C., Oneţ, T., Szilágyi, H., (2010) „Economia De Energie La Realizarea Betoanelor Performante“, Conferinţa Stiinţă Modernă şi Energia, 20-21 Mai, Cluj-Napoca, 2010

Corbu, O., Măgureanu, C., Szilágyi, H., (2010) „Performance Concrete“, Proc. of Contel, Sibiu, 2010.

Shayan A., (2002). „Value-added Utilisation of Waste Glass in Concrete“ IABSE SYMPOSIUM MELBOURNE, 2002

SR EN 206-1: 2002 Concrete-Part1: Specification, performance, production and conforming, Conforming European Standard EN 206-1: 2002

TOPIC 2
ADVANCED REINFORCING AND PRESTRESSING MATERIALS AND TECHNOLOGIES

A CONFINEMENT REINFORCING ELEMENT (TUBE) FOR REINFORCED AND PRE-STRESSED CONCRETE MEMBERS

U. Mayer[1], J. Ožbolt[2], A. Toth[3], J. Varga[4]
[1] *nolasoft, Augustenstrasse 39a, D-70178 Stuttgart*
[2] *IWB, Universität Stuttgart, Pfaffenwaldring 4, D-70569 Stuttgart*
[3] *EPFL, CH-1015 Lausanne*
[4] *Keller AG Ziegeleien, CH-8422 Pfungen*

INTRODUCTION

Reinforced concrete as a structural load-bearing material has a long tradition. The working principle is simple; concrete should carry the compressive stresses, the reinforcement takes up the resulting tensile stresses. The connection between concrete and reinforcement is ensured by the bond, which is described by a so-called bond-slip law. Today's reinforced concrete is based on this age-old principle; however, the manufacturing of components and a computational description of the resulting composite have developed a great deal over time.

1. HISTORICAL OVERVIEW – THE PASSIVE CONFINEMENT

If ribbed bars carry tensile load, the bond stress is the longitudinal component of the inclined interactional force. The radial component of the stress produces hoop tensile stresses in the concrete which may lead to splitting cracks so decreasing the stiffness of the concrete matrix. In 1989 J. Varga investigated the nature of this radial stress field and used a wire mesh around an individual ribbed bar to it (*Varga, 1990*) However, this confinement proved to be effective it has practically failed as it is impossible to bundle a mesh around each individual rebar.

2. THE ACTIVE CONFINEMENT

The confinement reinforcement (Patent Number EP 1795667) is made of smooth reinforcing bars (see prototype in Fig. 1). The single bars, up to 16 altogether, are interwoven forming a circular tube having a specific diameter.

Fig. 1 The prototype of the confinement reinforcement in the workshop

If this reinforcing element is put under tension, the elongation of the element leads to a contraction in radial direction and therefore to an "internal" confinement of the "inner" concrete. The result is that the overall behaviour of, and the stress distribution within, the structural element changes. The concrete volume stays compressed while the steel bars in the tube are always under tension, regardless of the type and place of the load and the actual function of the structural member.

3. EXPERIMENTAL AND NUMERICAL INVESTIGATIONS

In the past years experimental investigations and finite element modelling were carried out to verify theoretical ideas and the effectiveness of such confinement reinforcement.

3.1 Initial tests with a column and short beams

At first a cylindrical specimen d/h = 150/300 mm was cast with a centric tube reinforcement from 4xϕ6 wires in 45 degree angles. Two strain gauges were also glued at the middle of the tube reinforcement onto the bars in both directions to monitor the stress in the wires if the cylinder is compressed. Both strain gauges indicated tensile stresses in the tube's steel. In the second comparative test series beams with different reinforcements were cast LxBxH=750x100x200 mm (Fig. 2). Beam (1) was without any reinforcement, beam (2) was reinforced with 4xϕ8 bars and 4xϕ6 stirrups along the length and beam (3) with two tube reinforcements with 4xϕ6 wires along the length. The weight of reinforcement in beams 2 and 3 were 2200 g for both. Beam (1) had a bending crack in the middle, beam (2) showed shear failure, cracks ran from supports 45 degree up and beam (3) showed a bending failure with fine cracks in the middle region. Both beam (1) and (2) were disintegrated after reaching the ultimate load while for beam (3) the displacement transducer ran out of range.

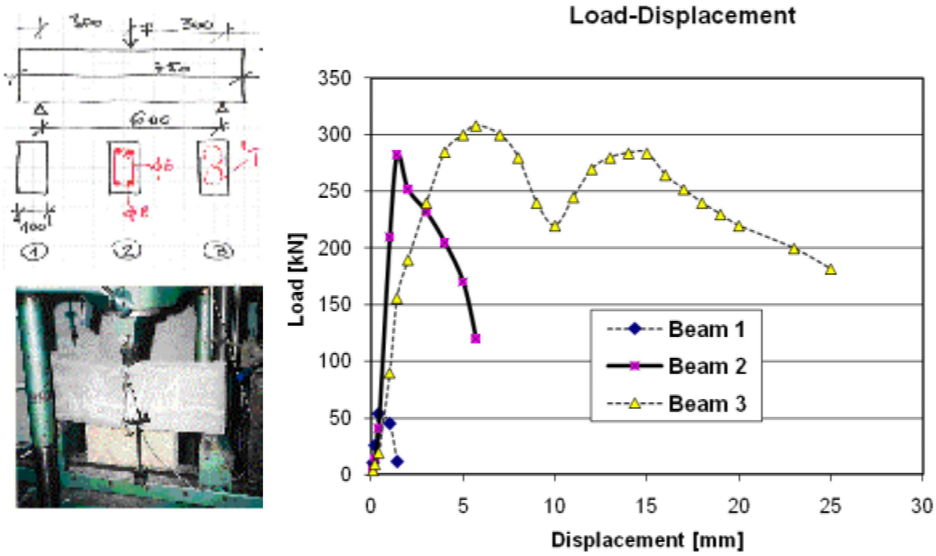

Fig. 2 Beam tests (Geometry / Test Arrangement / Load – Displacement curves)

3.2 Slab - punching through resistance

After many years and a successful patent application, Nolasoft nominated A. Toth to test the tubes as punching through reinforcement in full size slabs at the Széchényi University in Györ. The following results are extracted from *(Toth, 2006)* and *(Nolasoft, 2007*).

The dimensions of the standard reference specimen are as follows: BxWxH =3.0x3.0x0.28 m, circular support (12 single supports at d = 2.4m), 200 mm column head for punching through, C20/25, 0.8% reinforcement ratio with high strength bending reinforcement. The enclosed figures here are with test 4 (b) red), as shown in Fig. 4.

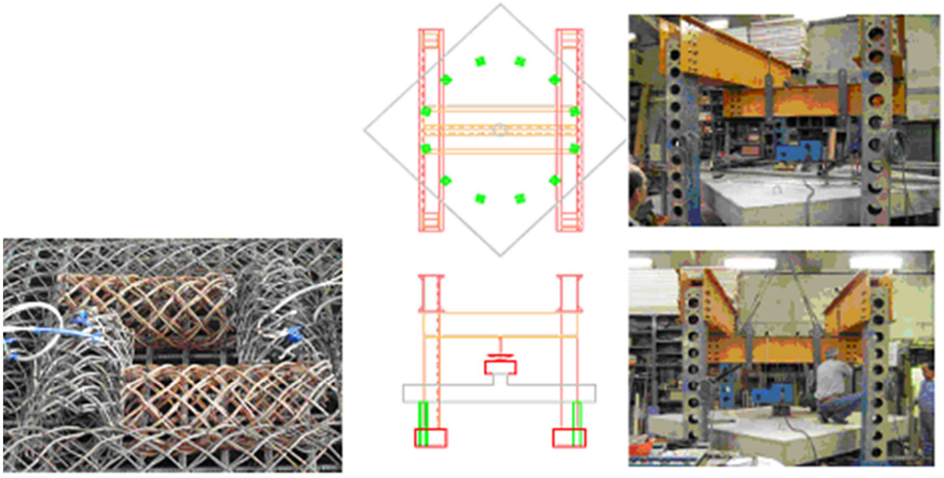

Fig. 3 Punching tests (Geometry / Tube Arrangement / Test setup)

Parallel to full size testing, Nolasoft investigated the load bearing behaviour using FE analysis (MASA 3). Fig. 4 shows test and FEM results, with an identical 0.8% reinforcement ratio. The load-displacement curves are: a) the specimen without punching reinforcement (black), b) specimen (Test 4) with Tubes, with the strengthened area for punching kept identical to test Z3 (red), c) specimen (Test Z3) tested at the University of Aachen, Germany using current practice, 60 x headed stud solution (blue) and d) specimen (FEM) reinforced with Tubes enforced to fail locally in punching shear (green).

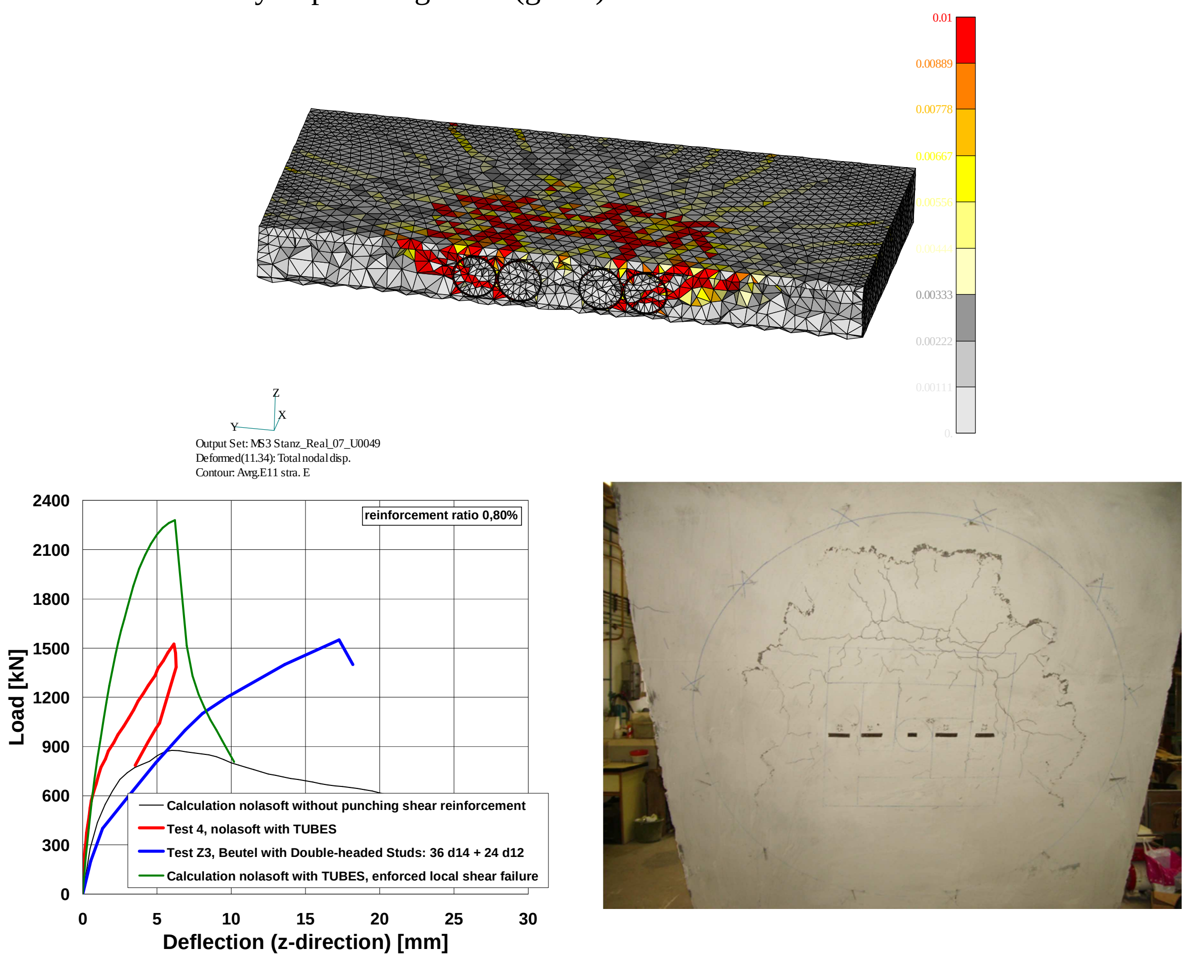

Fig. 4 Experimental and numerical results of punching tests (FE principal strains (cracks) / Load-Displacement curves / top view of test specimen (cracks))

3.3 Pullout of cast in place headed studs

The influence of the confinement reinforcement on the load-bearing behaviour of cast in place headed studs under centric tension in a thin slab was numerically invesigated (see [4]). The use of the „Tube“ leads to an increase of the ultimate load by a factor of 2. Furthermore a more ductile behaviour is recognized (see Fig. 5).

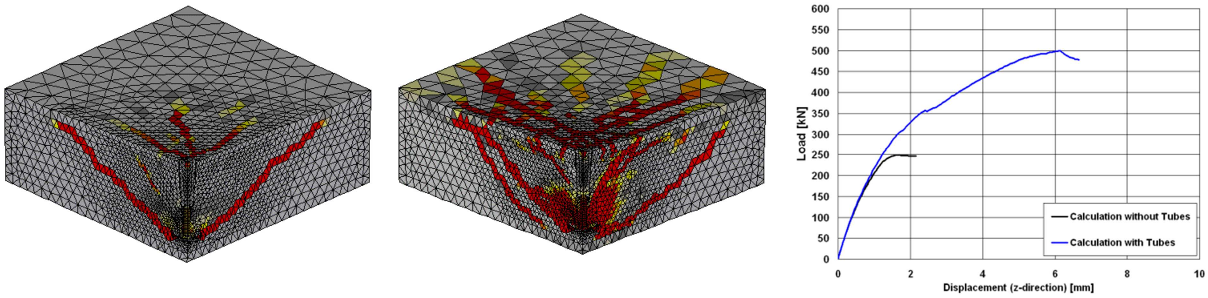

Fig. 5 Numerical results of headed stud pullout (FE principal strains (cracks) without and with “Tube” / Load-Displacement curves without and with “Tube”)

4. CONCLUSIONS

In structural concrete elements use of confinement reinforcement results in a spectacular increase in the shear capacity and resistance against buckling, and in a strong reduction of crack widths. The Tubes can be combined with the traditional reinforcing bars and using swell-cement the concrete can be pre-stressed without any hydraulic devices and cables. The use of this reinforcing element opens opportunities for reinforced concrete where tensile and shear loads dominate, such as earthquake load and where a tight crack-control is also required.

5. ACKNOWLEDGEMENTS

The authors are extremely grateful to Prof. Zoltàn Toth and his colleagues in the Civil Engineering test laboratories of the Széchényi University in Györ, Hungary and to Mr. Peter Toth and his colleagues of Motto KFT in Györ, Hungary for the many years of moral and financial support with the experimental work.

6. REFERENCES

Nolasoft, The Tubes – a New Reinforcing Element for Reinforced and Pre-stressed Concrete Members (Patent No. EP 1 795 667), 2007

Toth A., Diploma Munka, Punching failure of flat slabs, Model and test of confinement reinforcement, Technical University of Budapest, 2006

Varga J., Vasbeton Gabonasilo Falak Optimàlis Méretezése, Egytemi Doktori Ertekezés, BME Epitömérnöki Kar, Epitöanyagok Tanszéke 1990

Varga J., Microcrack-free Reinforced Concrete Structures, Exploiting the Innovative Potential of Concrete, Concrete Society of Southern Africa, Cape Town 1992, Pages 1–10

SHEAR DESIGN OF RC/FRC CONCRETE FOR BRIDGE DECK SLAB

Paola Rita Marcantonio[1], *Marco Petrangeli*[1]
[1] *Department of Engineering*
University of Pescara
65121 Pescara v.le Pindaro 42

SUMMARY

Fibre reinforcement significantly increase shear and punching resistance of concrete elements. For certain type of applications the use of fibre allows the complete elimination and/or substantial reduction of traditional reinforcement. The use of Fibre Reinforced Concrete is therefore particularly suited for structural elements with limited thickness subjected to punching loads such as concrete bridge slabs.
The paper summarize the research carried out towards the definition of a reliable set of formulae for the evaluation of shear capacity of RC and FRC deck slabs. The research started with a review of the available models and strength prediction formulae. Subsequently, a physical model for the evaluation of shear capacity in reinforced and fibre reinforced concrete elements is proposed. The proposed shear model is based on the insight of the shear resisting mechanisms provided by the shear enhanced fibre beam element developed by the authors.
The strength prediction using the various approaches and formulae are then compared as a function of a set of relevant parameters such as span to depth ratio, longitudinal and transverse reinforcing, axial force, etc. Finally, the technical and economic advantages of using fibre reinforced concrete slabs for large span composite girders is discussed with some simulations applied to recent structures designed by the authors.

1. INTRODUCTION

It has been demonstrated that the use of fibre reinforcement in concrete elements can lead to a substantial increase of the mechanical properties, especially shear and punching resistance; for certain type of application fibre reinforcement allows the complete eliminations and/or substantial reduction traditional reinforcement.
For this reason, the use of Fibre Reinforced Concrete (FRC) is particularly suited for structural elements, such as concrete bridge slabs, where the position of wheel loading is not spatially fixed. The use of FRC can be therefore competitive since can lead to a substantial reduction of slab thickness without the need to insert additional shear reinforcement. Furthermore, the increase in slab manufacturing cost can be easily offset by the reduction in steel girder weight.

The expressions proposed by major international norms and guidelines for the evaluation of shear strength of RC and FRC elements will be compared to the new one proposed by the authors. Based on these formulae, the advantage of using FRC slabs over RC ones shall be discussed with respect to bridge deck geometry configurations.

2. SHEAR STRENGTH OF REINFORCED CONCRETE

Shear modelling and strength prediction, although being extensively investigated, have not consolidated yet. The different proposals and national codes available in literature still provide a large scatter in the predictions of shear capacity for members with and without transverse (shear) reinforcement. In the paper a new rational approach to shear strength prediction shall be discussed and compared with all other major formulations available in literature.

2.1 An overview of design equations for RC shear strength

In the **MODELCODE 2010** the shear strength is a sum of the contributions of concrete resistance ($V_{Rd,c}$) and truss mechanism ($V_{Rd,s}$). There are three level of Approximation differing in the complexity of the applied methods and the accuracy of the results. In the Level III or Higher level of Approximation, steel and concrete contribution depends on the average longitudinal strain at mid-depth of the member (ε_x), calculated by

$$\varepsilon_x = \frac{M_{Ed}/z + V_{Ed} + 0.5N_{Ed} - A_p f_{po}}{2(E_s A_s + E_p A_p)} \tag{2.1.a}$$

In the last issue of **EUROCODE 2**, contrary to the previous ones, concrete and transverse steel contributions are not added. Either the concrete or the steel one must be used for the design of new structures. In members not requiring design shear reinforcement the design value for the shear resistance $V_{Rd,c}$ is given only by concrete contribution. While in members requiring shear reinforcement the design value for the shear resistance $V_{Rd,s}$ is provided by shear reinforcement only. In both formulations, shear resistance is increased by a factor $\beta = 2d/a$, if the loads is applied within a distance $0.5d < a < 2.0d$, where a is a span ratio.

In the **PRIESTLEY's** proposed formula [6], the shear strength is a sum of concrete resistance (V_c), inclined strut mechanism due to axial load (V_p) and transverse steel truss mechanism (V_s). Since the Priestley formula was mainly developed for seismic applications, the concrete contribution varies according to flexural ductility reached by the element via he *k* parameter. In this paper the value of *k* will has been set to the maximum (0.29) since shear resistance under static loading is considered. Despite the axial load contribution being hardly applicable to deck slabs – although arching actions do develop in deck slab as well – it will be kept as a parameter so as to compare the proposed formulae across a wider range of applications. The contribution of shear reinforcement in Priestly formula is based on the truss analogy with a 30° angle between the compression diagonals and the element axis.

2.2 A proposed equation for RC shear strength

In the proposed formula, concrete and transverse steel contributions are added similarly to the Model Code. The main difference with respect to all other formulations is with the definition and evaluation of the concrete resistance. In the proposed model we identify a concrete cohesive contribution (V_{CH}) and a concrete frictional contribution (V_{CF}). The concrete cohesive component can only be exploited before diagonal cracking of concrete and therefore cannot to be added to the transverse steel mechanisms (V_S) that kicks in only in cracked members. The rational beyond this approach is that the concrete contribution is made of two parts, a mode I (tensile) resistance and a friction component carried out by the section portion under compression. When RC structures develop shear cracks, the loss of this cohesive (mode I) contribution must be taken over by the transverse steel. A significant concrete contributions remain there though, that is the one carried by friction by the uncracked portion of the section. With reference to the model depicted in Fig. 1 the following contributions to shear capacity can therefore be singled out.

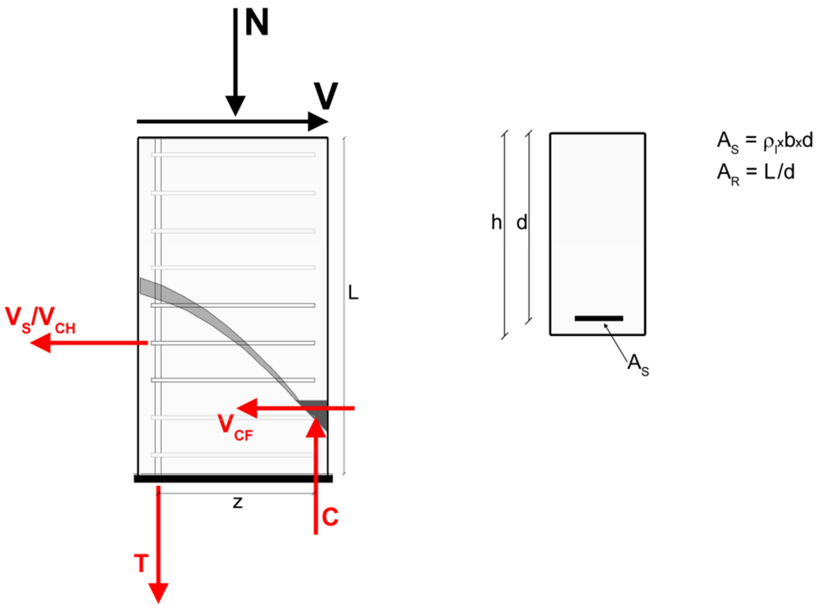

Fig. 1 Forces acting in the RC concrete element under shear load

The contribution of transverse reinforcement to shear strength is based on the same truss mechanism used by all other formulations and does not need to be repeated here. Finally we have the following two expression for uncracked and cracked members:

$$V_{Rd(uncracked)} = V_{CF} + V_{CH} \quad (2.1.b)$$

$$V_{Rd(cracked)} = V_{CF} + V_S \quad (2.1.c)$$

2.3 Comparison of RC shear design strength

The different formulae will be compared with reference to the RC section depicted in Fig. 1 where d=450mm, b=200mm, f_y=430MPa, f_{cu}=3.5MPa. Comparisons are carried varying the following parameters: aspect ratio (A_R), longitudinal reinforcement (ρ_l), transverse (hoop) reinforcement (ρ_t) and axial load (N). The inclination (θ) of the compression strut has been fixed according to the MC2010 so as to obtain comparable results for the various formulations.

$$\theta = 29^\circ + 7000 \cdot \varepsilon_x$$

The first comparison is carried out plotting the different shear strength predictions as a function of the aspect ratio for two different values of axial load while keeping all other parameters constant to the specified values.

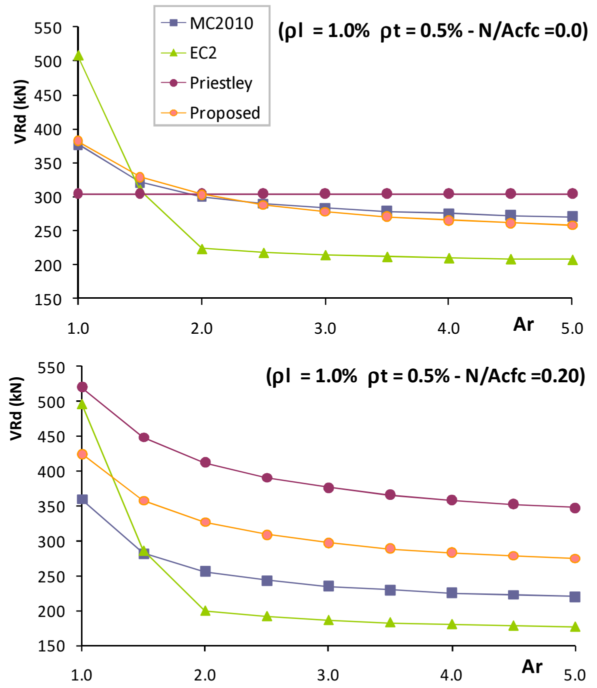

Fig. 2 Shear strength (V_{Rd}) as a function of Aspect Ratio (Ar)

The proposed formulation yield results that are very close to the MC2010 ones except for axially loaded members where it yield values intermediate between the MC2010 and the Priestly formula.
The second comparison is carried out plotting the different shear strength predictions as a function of the longitudinal reinforcement ratio for two different values of axial load.

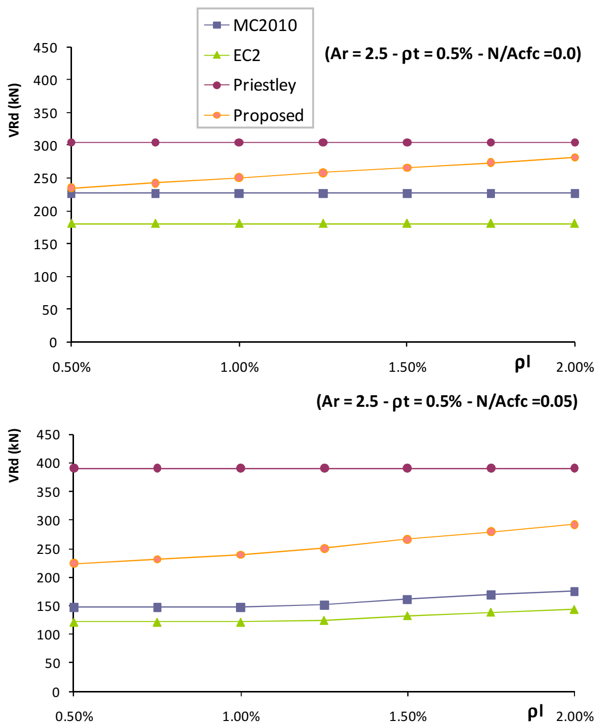

Fig. 3 Shear design strength (V_{Rd}) as a function of longitudinal reinforcement (ρ_l)

Since the expression used to calculate θ is independent of the longitudinal reinforcement, all formulations provide a constant shear resistance (as a matter of fact the EC2 concrete contribution does change but only the steel truss mechanism is used). The propose formulation is therefore the only one yielding an increase of shear resistance via the concrete fiction component (increase of internal compression in concrete).The third comparison is carried out plotting the different shear strength predictions as a function of the transverse (hoop) reinforcement for two different values of axial load.

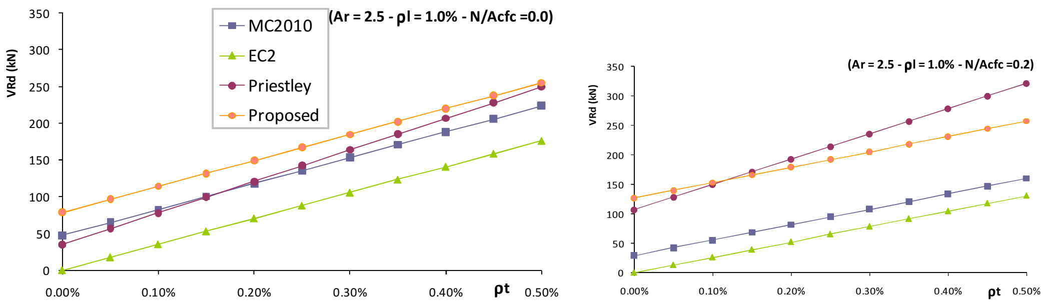

Fig. 4 Shear design strength (V_{Rd}) as a function of transverse reinforcement (ρ_t)

The fourth comparison is carried out plotting the different shear strength predictions as a function of the axial load for two different values of aspect ratio while keeping all other parameters constant to the specified values.

All the proposed example clearly shows the proposed formula to be very consistent despite of its simplicity. The effect of the various parameters are properly accounted for with the resulting shear predictions always very closet o the one proposed by the new MC2010 but improving with respect to the former as far as longitudinal reinforcement and axial load are concerned.

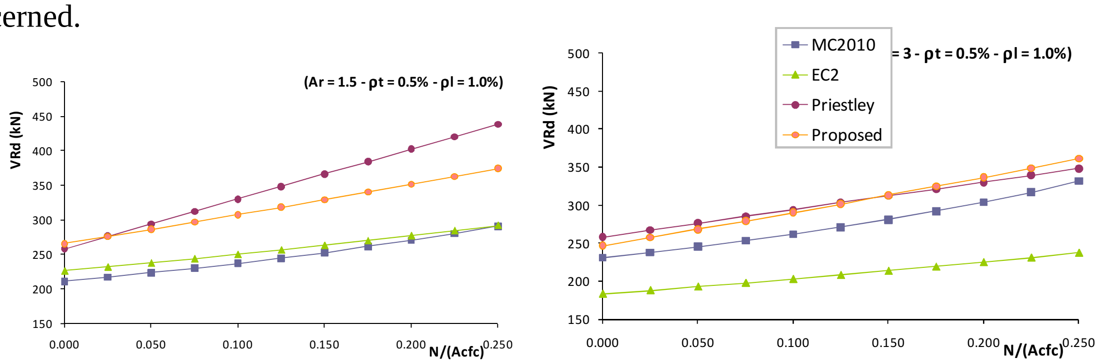

Fig. 5 Shear design strength (V_{Rd}) as a function of axial load (N)

3. SHEAR STRENGTH OF FIBRE REINFORCED CONCRETE

Fibres act as a randomly distributed reinforcement, bridging the cracks and allowing the transmission of significant stresses even with considerable crack widths. Although the shear resistance of FRC concrete elements has been extensively investigated in the last 10 years, the specific formulae for the shear strength evaluation have not consolidated yet. In fact, the different proposals give predictions of shear capacity of FRC concrete elements that significantly differ to each other. The main issue being how to include the fibre contribution. Some authors add the fibre contribution modifying the concrete component of the shear mechanism while other add the fibre shear resistance to the resisting mechanisms (concrete and truss mechanism) already defined for reinforced concrete.

In this work, the proposed formula is compared to the one proposed by the MODEL CODE 2010.

3.1 An overview of design equations for FRC shear strength

In the new Model Code the design value in members without shear reinforcement is given by an equation where the contribution of fibre is supposed to modify the longitudinal reinforcement ratio. This is calculated using the toughness properties of the fibres, namely, the equivalent strength relevant for the ultimate state. This parameter is evaluated by a three point bending and is used to classify the performance of material with regard to the behaviour in tension. For fibre reinforced concrete with Vf<2% this value can be change between 1 to 4 MPa.

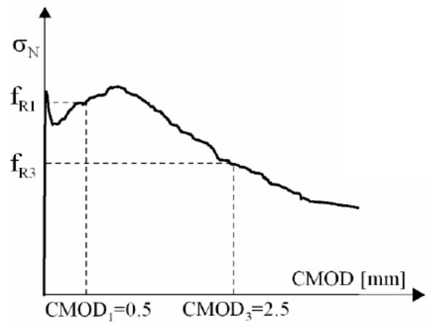

Fig. 6 Typical results from a bending test on a softening material

In order to classify the post-cracking strength of FRC a linear elastic behaviour can be assumed, by considering the characteristic residual strengths significant for service (f_{R1k}) and ultimate (f_{R3k}) conditions (see fig. 6). In members without shear reinforcement the design value is given by the following formula:

$$V_{Rd,FRC} = \left\{ \frac{0.18}{\gamma_C} \cdot k \cdot \left[100 \cdot \rho_l \cdot \left(1 + 7.5 \cdot \frac{f_{Ftuk}}{f_{ctk}} \right) \cdot f_{ck} \right]^{1/3} + 0.15 \cdot \sigma_{cp} \right\} \cdot b_w \cdot d$$

3.2 A proposed of design equations for FRC shear strength

The proposed formula for shear prediction of RC elements can be easily modified and used for FRC elements too. The modification is simple and consistent. When FRC structures develops shear cracks, because of the available ductility, the cohesive contribution remain and is added to the one carried by friction by the uncracked portion of the section. In other words, the concrete mode I contribution, is prolonged into the cracked state because of the post peak ductility provided by the fibres. Therefore, the cohesive concrete component is added to the ones due to friction and by transverse steel. Elastic properties are not significantly affected by fibres, unless a high percentage of fibres is used (>2%). This researches focus only FRC concrete with percentage of fibres less or equal to 2%. For this reason, the concrete cohesive component, before crack, is the same used for RC concrete element (2.1.f). After cracks, this component is still effective and it is function of the equivalent strength f_{Ftuk}. Finally we have the following two expression for uncracked and cracked members:

$$V_{Rd,FRC(uncracked)} = V_{CF(uncracked)} + V_{CH(uncracked)} \tag{3.2.a}$$

$$V_{Rd,FRC(cracked)} = V_{CF(cracked)} + V_{CH(cracked)} + V_S \tag{3.2.b}$$

3.3 Comparison of FRC strength prediction

In the following, shear strength prediction of the proposed formula is compared to the one obtained with MC2010. Calculation have been carried out with reference to the same section and same material parameters used for the RC elements. When looking at the proposed comparisons one should notice that in the current version of the MC2010 there is no provision for aspect ratio effects in transversally unreinforced FRC members. This will be possibly modified in later versions as already proposed by the Italian norms on FRC design [8]. To all accounts, in the aspect ratio range of 2 to 3, where most of the experimental tests have been carried out, both formulae yield similar results that closely match the experimental findings.

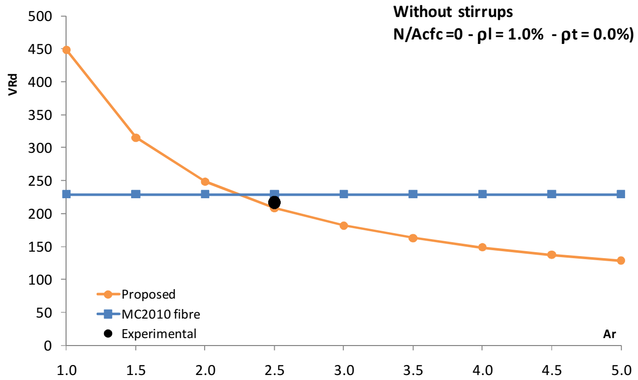

Fig. 7 Shear design strength as a function of Aspect Ratio (Ar)

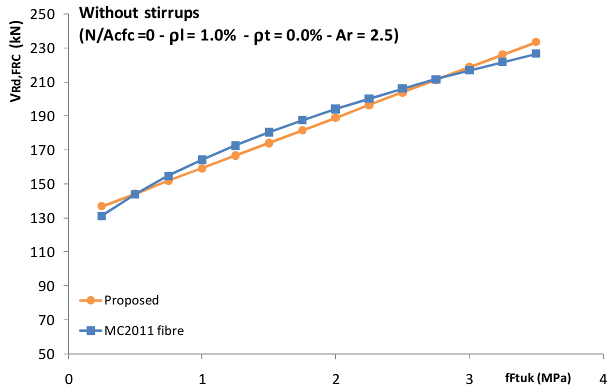

Fig. 8 Shear design strength as a function of FRC equivalent strength (f_{Ftuk})

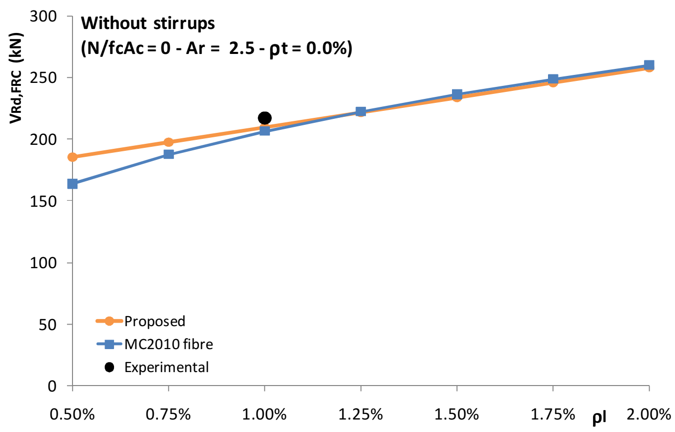

Fig. 9 Shear design strength as a function of longitudinal reinforcement (ρ_l)

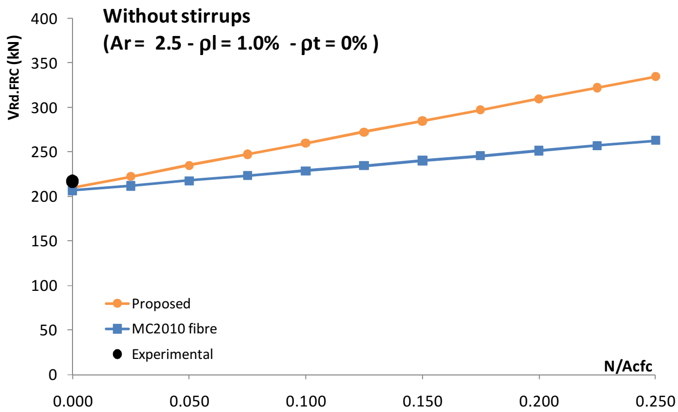

Fig. 10 Shear design strength as a function of Axial Load (N/f_cA_c)

4. DECK SLAB NUMERICAL SIMULATION

In order to assess the shear demand due to concentrated axel loads on bridge deck slab, a parametric set of numerical simulations have been carried out using linear elastic plate elements.A typical configuration of a deck slab supported on 4 longitudinal beams has been modelled varying the beams spacing from 2 to 6 metres. Plate element size has been fixed at 10x10cm. The concentrated tandem load of Eurocode 1 (UNI EN1991-2:2005) has been used with a total weight of 200 kN applied onto a 35x60 footprint. The longitudinal beams have been assumed to provide a knife type rigid support. This configuration obviously disregards the effect of the beams top flange width and flexural stiffness and the vertical compliance of the beams itself. For each configuration (beam spacing) maximum shear in the slab has been calculated averaging the finite element values over a 100cm long section. The shear force calculated this way has been compared with the slab capacity calculated according to the formulae discussed in the previous chapters.The authors are obviously aware of the fact that this approach disregards the two following fundamental factors:

1. The shear resisting mechanisms in a slab are bi-dimensional. Although the beam supports tends to concentrate the shear demand along a line the non-linear behaviour of the slab redistributes forces and generally leads to a punching type of failure. The mono-dimensional parameterisation of demand and capacity is still considered to provide meaningful results
2. Typical shear failures of deck slabs involve a great deal of fatigue effects. If anything, fatigue is more severe in RC members than FRC ones due to the ductility provided by the fibres that reduce crack propagation. In the graphs plotted in the following paragraph both the shear static demand (the one found with the FE analysis described above) and a fatigue shear demand equal to the previous one increased by 50% have been plotted and compared to the slab capacity for the various beam spacing.

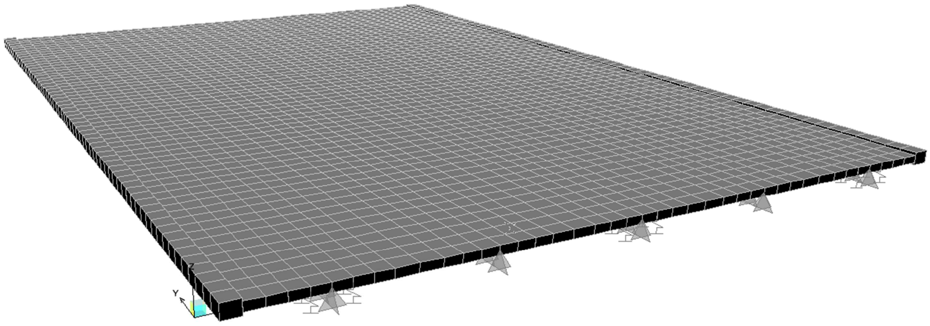

Fig. 11 FEM Model

The shear resistance of RC and FRC slabs have been calculated using the proposed formulae for different longitudinal reinforcement ratio (from 0.2% to 1.0%) and beam spacing of 2 and 4 metres respectively as a function of the slab thickness (slabs have been assumed to be without transverse reinforcement). The shear capacity to shear demand ratio for the 6 configurations (3 reinforcement ratios each for RC and FRC) has been plotted in the two following graphs, the first one for transverse beams spacing of 2 metres, typically used for prestressed concrete beam decks and the second one, for transverse beams spacing equal to 4 metres, more customary in composite deck design.The curves are all bending compatible that is they have been traced only for thickness providing a bending capacity greater than the demand, as found with the finite element model discussed in the previous chapter.The two graphs clearly shows that, independently of the actual accuracy of the shear demand and capacity prediction and fatigue effects, there exist an obvious range of application for FRC slabs, in the 20-15 cm range that will most probably be exploited in future bridge deck slab design. Assuming a 100% safety factor for shear to account for fatigue effects, the graphs shows that RC slabs are limited by their shear resistance when thickness falls below 20-25cm. The available increase in shear resistance when using FRC does open up the possibility to significantly reduce slab thickness over a wide range of deck configurations.

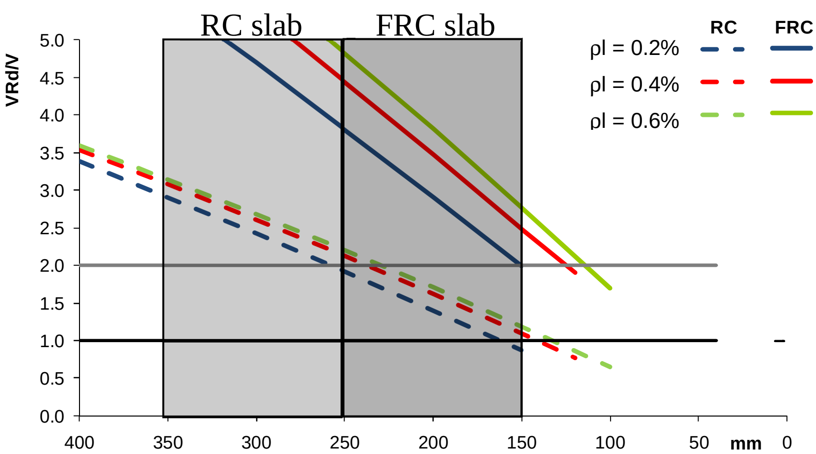

Fig. 12 Shear resistance of RC/FRC concrete slabs (L=2m)

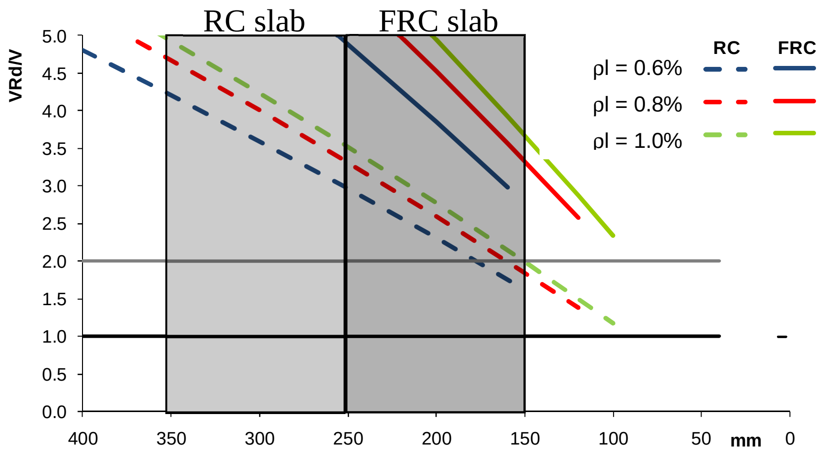

Fig. 13 Shear resistance of RC/FRC concrete slabs (L=4m)

5. CONCLUSIONS

Composite bridge design has been steadily increasing its range of application; today composite girders spanning more than 100 metres are standard practice with few examples spanning over 150 metres. For these bridges, weight of the RC slab becomes significant and its reduction economically interesting. Even more so if we take into the picture the new cable supported (stayed, arch, etc..) composite girders that are being extensively used up to the 500 metre span range. The most logical and technologically ready solution seems to be the use of FRC slabs for this type of structures. With FRC the slab thickness can be reduced to 15cm circa with significant saving in the self weight of the structure. 10 cm of concrete amount to 240 kg/m^2 which is roughly half the weight of the steel carpentry in medium to large span composite girders. The use of FRC does require special provisions when casting these elements, so much that use of precasted slabs seems almost compulsory. Luckily enough, FRC does simplify the use of precast elements because it strongly reduce the rebar anchorage length and thus the joint dimensions between slab panels and the weight of the precast slab elements itself thus making precasting very competitive and structurally sound.

6. REFERENCES

Fib Bulletin 55: Model Code 2010 – First complete draft, Volume 1

Fib Bulletin 56: Model Code 2010 – First complete draft, Volume 2

Petrangeli M., Pinto P.E., Ciampi V. (1999) *Fiber Element for Cyclic Bending and Shear of RC Structures. I:Theory*. Journal of Engineering Mechanics Vol.125 No.9, pp. 994-1001.

Petrangeli M. (1999). *Fiber Element for Cyclic Bending and Shear of RC Structures. II:Verification*. Journal of Engineering Mechanics Vol.125 No.9, pp. 1002-1009

Petrangeli M., Ožbolt J. (1996) *Smeared Crack Approaches – Material modeling* Journal of Engineering mechanics Vol.122 No6, pp. 545-554.

Priestley M.J.N., Verma R., Xiao Y. (1994) Seismic shear strength of reinforced concrete columns. J. Struct. Engrg. Volume 120, Issue 8, pp. 2310-2329 (August 1994)

UNI EN 1992-1-1:2005 Eurocode 2. Design of reinforced concrete. Part 1-1: Generals Rules for building

CNR204/2006. Guide for the Design and Construction of Fibre –Reinforced Concrete Structures

SUSTAINABLE, COMPOSITE, AND THERMALLY EFFICIENT PRECAST CONCRETE LOAD BEARING AND ARCHITECTURAL PANELS USING CFRP GRID

William Greg Bunn[1], Sami Rizkalla[1], Greg Lucier[1], & Larbi Sennour[2]
[1]North Carolina State University, Raleigh, NC USA
[2]The Consulting Engineers Group, Inc., San Antonio , TX USA

SUMMARY

This paper investigated the use of a carbon fiber reinforced polymer (CFRP) material, configured as a grid and placed in composite action with rigid foam insulation, as the main shear transfer mechanism for precast prestressed sandwich load bearing and architectural wall panels. The CFRP/rigid insulation shear transfer mechanism provides composite action between the two concrete wythes in sandwich wall panels, allowing for greater structural capacity, higher thermal efficiency, and a longer service life. The program examined various parameters believed to affect the shear transfer including the type of rigid insulation, the insulation thickness, and the spacing between the rows of CFRP grid. The program was designed to determine the characteristics of the shear transfer mechanism of the grid/insulation as affected by these parameters.

1. PRECAST CONCRETE SANDWICH PANEL SYSTEM

For the last fifty years, precast prestressed concrete sandwich wall panels have been used as building envelopes for various applications including schools, office buildings, and warehouses. Panels are constructed with two outer concrete layers separated by rigid foam insulating core, providing for better thermal efficiency. In place, sandwich wall panels can provide the dual function of transferring load and insulating the structure (PCI Committee on Precast Sandwich Wall Panels, 2011). They are designed to behave either in full composite, non-composite, or partially-composite action. At least a partial degree of composite action is typically desirable, as it allows for thinner panels, affords a weight savings, and results in an all-around more efficient structural system. Composite action between concrete wythes is achieved by connecting them through the core insulation material to transfer shear forces, which can be accomplished by using one of several techniques. Traditional shear connectors include steel trusses, bent wire connectors, or solid concrete zones cast between the concrete wythes. Although these techniques have been shown to produce the desired composite action they also create several unwanted side-effects such as thermal bridging, increased weight, and vulnerability to corrosion, to name a few. This study investigated the use of the carbon fiber reinforced polymer (CFRP) grid shown in Fig. 14 as a shear transfer mechanism. One feature that makes CFRP grid a desirable option for shear transfer in sandwich wall panels is its inherent lack of thermal conductivity. A core of rigid foam insulation crossed only by CFRP grid has been shown to provide full composite action without any thermal bridging, which cannot be accomplished with traditional steel and concrete alternatives.

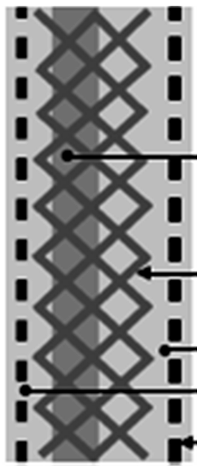

Fig. 14 Schematic of Grid and Insulation

2. EXPERIMENTAL PROGRAM

The extensive experimental program completed at North Carolina State University consisted of sixty-six concrete sandwich wall panel specimens, representative of a section of a full scale wall. The specimens are referred to as "push-out" specimens due to the testing configuration described below. All panels were tested to evaluate the different parameters believed to affect the performance and strength of the CFRP grid in direct shear. The testing parameters considered in the program were the type and thickness of the rigid foam insulation, the spacing between lines of grid, the effect of the concrete-foam bond, the transverse strength of grid, the presence of gaps in the lines of grid.

3. TEST SETUP

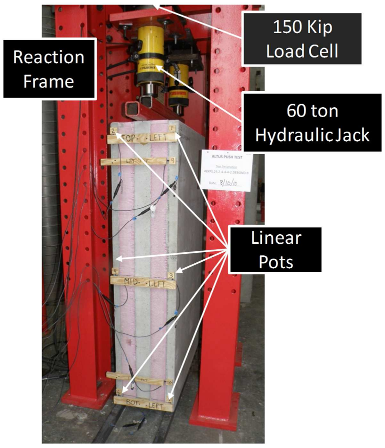

Fig. 15 Test Setup

The test setup used for all push-out specimens is shown in Fig. 15. Panels were tested in a double shear configuration to eliminate eccentric shear forces. The panel specimens were constructed with three wythes of concrete to allow for this double-shear configuration. Each specimen was supported vertically at the bottom edge of the two outer concrete wythes by 2" square steel bar stock. Load was applied by two 60-ton hydraulic jacks through two HSS steel beams to distribute the load evenly through the inner concrete wythe. As load was applied, the center wythe was forced downward with respect to the outer wythes. The applied load was measured along with relative vertical displacements between the concrete wythes at eight locations. Relative horizontal motion between the outer wythes was also measured at two locations.

4. TEST RESULTS

The load deflection relationship measured for a typical panel is shown in Fig. **16**. Test results indicate that the parameters have a pronounced effect on shear flow. The use of expanded polystyrene foam (EPS) provides greater shear resistance in comparison to extruded polystyrene foam (XPS), due to its superior bond characteristics, for a given amount of CFRP grid. Results showed that an increase in the thickness of the EPS insulation reduced shear flow capacity; a result not clearly observed for XPS insulation. Increasing the grid spacing had little effect on the capacity of XPS panels; however it was increased capacities in EPS panels. Several panels were tested with no grid to isolate the effect of the concrete-foam bond on the transfer of shear forces. Two panels with no grid and EPS foam exhibited a high degree of strength as a result of the excellent EPS bond characteristics. On the other hand, XPS panels with no grid illustrated the weak bond developed between standard XPS and concrete.

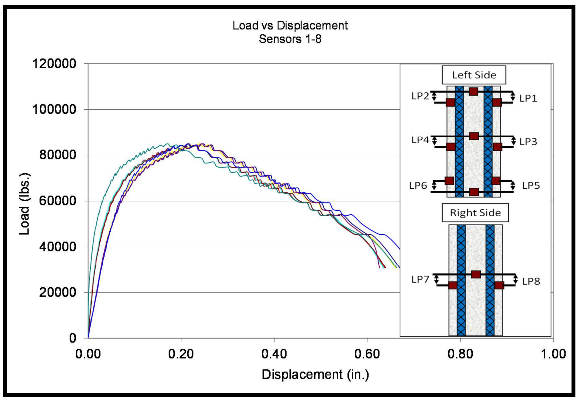

Fig. 16 Typical Load Deflection Data

5. FAILURE MODE

It was observed that all tested panels exhibited rupturing of the grid tension cords and buckling of the compression cords, as shown in Fig. 17. Several panels also showed signs of the grid pulling out from the concrete due to insufficient embedment length. The photographs in Fig. 17 were taken after testing with the insulation removed down to the depth of the grid. Post-test inspections of the panels showed that XPS insulation was easily removed from the concrete wythes and left smooth clean surfaces, while particles from the EPS insulation remained bonded to both concrete faces after they were pried apart, as shown in Fig. 18.

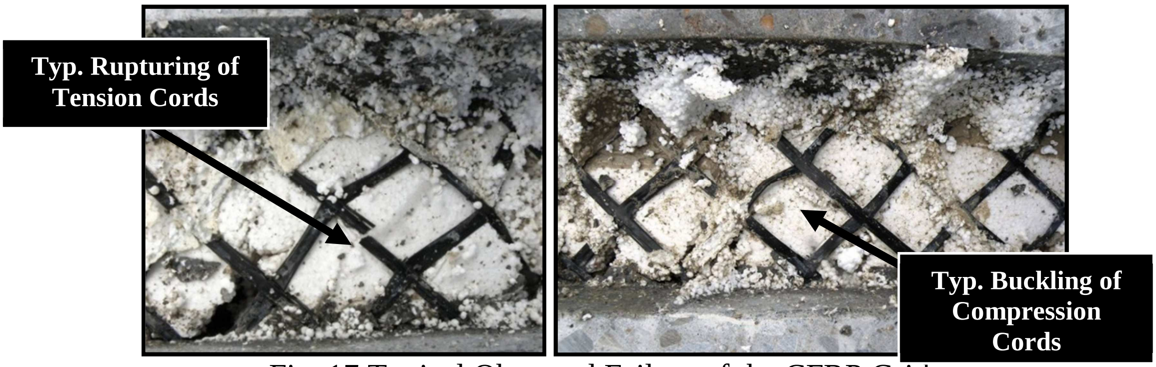

Fig. 17 Typical Observed Failure of the CFRP Grids

Fig. 18 Surface of Concrete Wythes after Testing

6. CONCLUSIONS

Panels produced with EPS foam insulation developed higher shear strengths in comparison to panels insulated with XPS foam when the same quantity of CFRP grid is used. When using EPS foam, increasing the spacing between vertical lines of grid tends to increase the shear flow strength for a row of grid and its given tributary area, likely due to the high bond strength of EPS foam. Increasing the spacing between grids for the XPS foam did not increase the shear flow strength for a given line of grid and its associated tributary area. The tests indicated that increasing the thickness of EPS insulation foam decreases the shear flow strength while changes in the thickness of XPS foam insulation (up to 4”) had minimal effect in shear transfer behavior. Results indicate that CFRP grid oriented in the transverse direction can provide considerable shear strength, perpendicular to the applied load. Results further indicate the presence of gaps along the length of the grid do not affect the shear flow strength of the grids.

7. DESIGN EXAMPLE

The following example illustrates the shear grid required to achieve composite action. The design value selected for the grid is based on tests similar to those presented above. The design value was chosen by performing a statistical analysis prescribed by the building code.

Given the typical example:
L=9 m; a=1 m; h=10 m; f_c'=35 MPa & 2400 Kg/m^3; EPS Insulation; Wind Load w=1.2kN/m^2
b=3.5 m; t=250 mm; $t_{top\_wythe}=t_t$=75 mm; $t_{insulation}=t_i$=100 mm; $t_{bottom\_wythe}=t_b$=75 mm ;
Moment of Inertia=I=4.38 10^9 mm^4; First moment=Q=2.44 10^7 mm^3

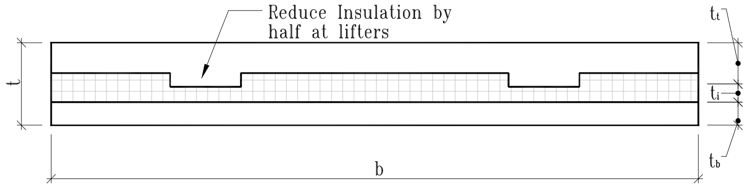

→Determine the shear demands (see diagram)
→Using US Codes (ASCE 7-05 and ACI 318-08); V_{1u}=1.6wbh/L(L-h/2)=29.9 kN;
V_{2u}=1.6wbh/L(h/2) – 1.6wba=30.6 kN; V_{3u}=1.6 wba=6.7 kN; Max. Shear=V_u=30.6 kN
→The corresponding shear flow = $q_u = V_uQ/I$; q_u = 170.5 kN/m
→The shear flow capacity of a single row of shear grid for a 100 mm thick EPS insulation is
q_n = 42 kN/m; The design capacity with a Φ=0.75; Φq_n = 0.75 x 42 = 31.5 kN/m
→Number of rows of shear grid required is $N = q_u/\Phi q_n$ = 170.5/31.5 = 5.4 rows
→Use **6** rows of shear grid

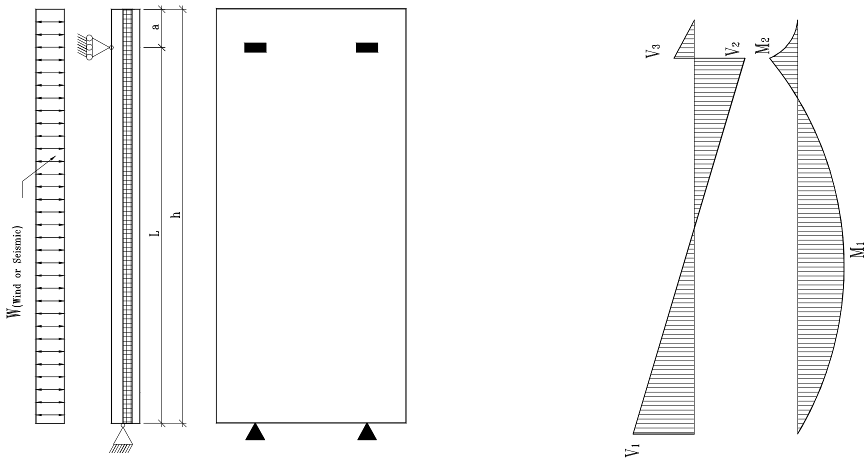

8. ACKNOWLEDGEMENTS

The authors would like to recognize AltusGroup for their support of this project.

9. REFERENCES IN TEXT:

PCI Committee on Precast Sandwich Wall Panels. (2011). State of the art of Precast/Prestressed concrete sandwich wall panels. *PCI Journal*, *56*(2), 131-176.

REPAIR AND PROTECTION OF KRK BRIDGE

Jovo Beslac[1], Mario Ille[1], Jelena Bleiziffer[1]
[1] *Structure Management Department*
INSTITUT IGH, d.d.
10000 Zagreb, Janka Rakuse 1

SUMMARY

Krk bridge consists of two large reinforced concrete arch spans. The bridge set in harsh environment has substantially deteriorated over its 30 years of service, and many repairs have been carried out. Many deficiencies are associated to the very thin concrete cover. The paper focuses on currently on-going research into design and application of an efficient protective system for reinforced concrete structure in maritime environment.

1. INTRODUCTION

Fig. 1: Krk Bridge connecting island of Krk (left) and the mainland (right).

Krk Bridge connects the island of Krk – the largest and the northernmost of the inhabitated Croatian islands, with the mainland. The bridge was constructed from 1976 to 1980. The total length of the bridge amounts to 1,430 m. The bridge consists of the two reinforced concrete arch bridges: the „larger" arch spanning 390 m and the „smaller" arch spanning 244 m. The 390-m span is not founded on shore, instead arch springs from supports formed by an inclined strut and horizontal beam and located around 35 m away from the shoreline. The inclined struts on both sides of the sea strait are founded 19 m below the sea level. When completed, the Krk Bridge was the world record concrete arch span in the world, surpassing the Gladesville Bridge in Sydney, Australia by 85 m (*Savor and Bleiziffer, 2008*). To achieve this exceptionally large span it was necessary to reduce the dead load as much as possible. The structural members of minimum statically admissible size were utilized, with very small concrete cover of 2.5 cm for the bridge superstructure. Krk Bridge design and construction has been focus of many professional papers and has found way into most bridge engineering handbooks as one of the greatest engineering achievements. The bridge maintenance over the past 30 years proved to be just as challenging.

2. MAINTENANCE MEASURES

Extensive maintenance measures were taken on the Krk Bridge during its 30 years of service life. The bridge is located in aggressive maritime environment (*Radic et al., 2005*), with its main members like foundation elements and lower parts of the arches being most exposed.

The adverse impact on bridge durability may be summarized as follows: (1) too low designed concrete cover (of only 2.5 cm), (2) relatively high salinity of the Adriatic Sea (approximately 3.5 %), (3) maritime environment with very frequent changes of strong southern and northern winds spraying sea-salt on exposed concrete members during winter months and (4) the winter drops of temperature below freezing point (10 to 15 cycles).

What concerns the low thickness of the concrete cover, the design and construction engineers were explaining later that it was designed so because it had been planned to apply protective coating to the entire concrete structure. Only some parts were protected: some with epoxy (not physically compatible with concrete) and some with brittle polymer cement mortar (porous coat increased the penetration).

In 1990, very complex multipurpose moveable scaffolding was constructed specifically for the Krk Bridge to solve the problem of inspection and repair and protection of inaccessible parts of the bridge structure. From that moment, the maintenance measures could truly start to be effectively planned and executed. Furthermore, the technology for the protection of reinforced concrete has improved over the past years, especially by the pure polymer coats impermeable for chloride ingress.

For columns and lower parts of the arches the following measures were anticipated:

- concrete cover must be partly or totally (depending on the chloride concentration) hydro demolished by the water pressure of 2500 bar
- hydro demolished concrete cover must be impregnated with penetration reinforcement corrosion inhibitor
- hydro demolished concrete cover must be renewed by high quality cement mortar, 1 or 2 cm thicker, with 50 MPa compressive strength and 2.0 MPa adhesion to concrete substrate
- repair mortar and concrete must be protected by pure polymer coat 1.5 mm thick with the adhesion to mortar 0.8 MPa and capillary absorption below 0,01 $kg/m^2/h^{0.5}$.

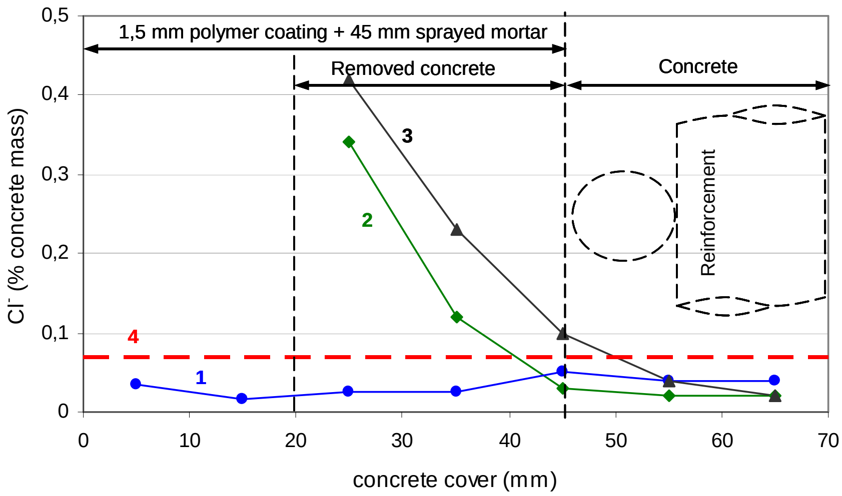

Fig. 2: Chloride ingress in the protective system after 7 years (1) and in concrete after 10 years (2) and 20 years (3); (4) is threshold value for the Krk Bridge

For upper parts of the structure (with lower chloride ingress):

- concrete surface must be washed by water pressure of 1500 bar, impregnated by penetration reinforcement corrosion inhibitor and protected by pure polymer coat as described before.

Nearly all columns and lower parts of the arches have been protected. The efficiency of the system has been tested after 7 years of use and assessed as satisfactory (Fig. 2). There is even some redistribution of chlorides that have remained in the concrete. Cathodic protection is currently being executed for the submerged elements that support the larger arch.

3. FURTHER RESEARCH

As already described, concrete surfaces of the bridge that are 25 m above the sea will be protected by pure polymer coat (this comprises 40,000 m^2 of the arch surfaces and underside of the superstructure). During 2010 an investigation into the efficiency of coatings available on the market was carried out (*INSTITUT IGH, 2010*). This included laboratory and on-site testing. Manufacturers were invited to apply coating on "trial" surfaces at three locations on the bridge. The decision to apply protective coating only and not to remove the existing concrete cover was based on the following facts: (1) most of the structural members are extremely thin (11-13 cm), thus hydrodemolition is not a suitable option; (2) adding any thickness to the existing concrete cover would result in major increase in deadload (approximately 1,000 tonnes for an increase of 1 cm in thickness) and (3) chloride concentration at the level of reinforcement is below the threshold value.

Total of 13 trial surfaces have been prepared of 9 protective systems. Testing was carried out in accordance to the EN 1504-2. Control (reference substrate) samples were prepared in accordance to the EN 1766. Six protective systems were assessed as inadequate, due to one or combination of the following deficiencies: cracking and delamination observed on site, low adhesion, low thickness, low resistance to freeze/thaw in chloride aggressive environment, low crack bridging ability and/or discoloration in UV resistance test. The remaining three protective systems were assessed as provisionally adequate, as improvements are required to increase the adhesion to fully meet design specifications.

The works on the Krk Bridge initiated a further research into durability design of reinforced concrete structures in aggressive maritime environment. Experience gained on several large reinforced concrete bridges in Croatia in maritime environment has revealed that to achieve adequate durability and specified service life, usual measures prescribed in standards (*Radic et al., 2010*) such as concrete mixture properties and concrete cover thickness should be combined with surface protection systems. Research is focused on the efficiency of reinforced concrete surface protection systems in preventing the ingress of aggressive substances into concrete, and development of models to predict service life of reinforced concrete members where resistance is represented by the integration of a protective system and concrete cover.

The European standard EN 1992-1-1 for design of concrete structures specifies that minimum concrete cover, $c_{\min}$, shall be provided in order to ensure: (1) the safe transmission of bond forces; (2) the protection of steel against corrosion (durability); and (3) an adequate fire resistance. The greater value for $c_{\min}$ satisfying the requirements for both bond and environmental conditions shall be used. The standard gives recommendations for minimum admissible thickness of concrete cover due to environmental conditions, depending on exposure conditions, design working life, concrete strength, member geometry and quality control measures. The standard also specifies that for concrete with additional protection (e.g. coating) the minimum cover may be reduced. The standard recommends the reduction value to be zero. One of the goals of this research is to provide further specifications on determining the reduction value, depending on type and properties of the protective system. The outline of the experimental part of the research is shown in Figure 3.

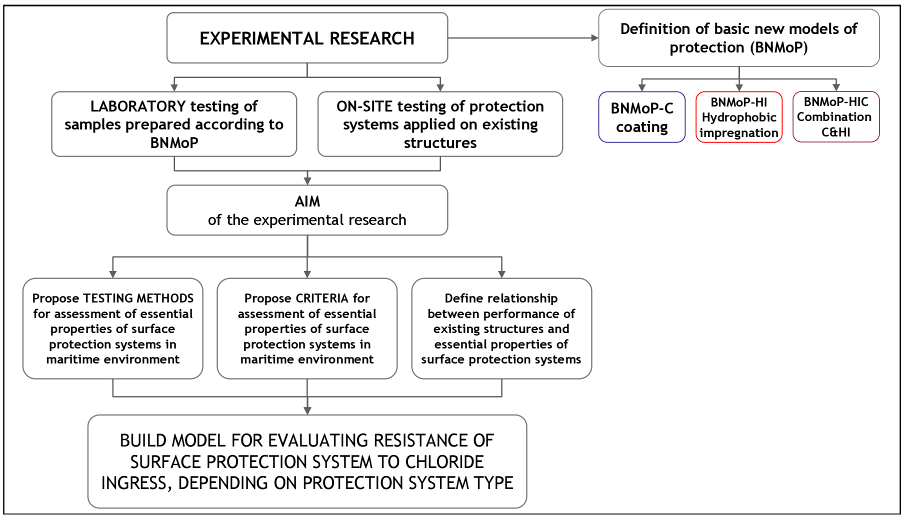

Fig. 3: Outline of the research into efficiency of protective systems for RC structures in maritime environment

The results of the testing performed so far (laboratory testing and on-site testing of protection system on existing structures in maritime environment) show that essential properties of dense (organic) coatings and chloride ingress protection may be achieved by protection system consisting of around 2.5 mm thick long-lasting elasto-plastic polymer coating (long-lasting elasto-plastic bonding and leveling layer of polymer-cement at least 2 mm thick and elasto-plastic polymer (acrylic or epoxy-polyurethane) wearing layer 0.7 mm thick). This system ensures ingress protection in accordance to the EN 1504-2 (capillary absorption ≤ 0.01 $kg/m^2/h^{0.5}$, adhesion ≥ 0.8 MPa and crack bridging ability > 1.0 mm. The on-going testing should provide information on time-dependence of the properties of concrete surface protection systems due to weathering and environmental conditions.

4. CONCLUSIONS

Design and construction of the Krk Bridge was very delicate and bold engineering introducing many innovations and breaking records. Its maintenance during last 30 years in very aggressive maritime environment was equally challenging. The works on the Krk Bridge initiated an ongoing research into durability design of reinforced concrete structures in aggressive maritime environment, namely in developing further specifications for application of surface protection systems on damaged structures as well as integrating surface protection systems with concrete cover in the design of new structures in aggressive maritime environment.

5. REFERENCES

INSTITUT IGH, d.d. (2010) „Report on testing and assessment of efficiency of surface protective systems for the remaining unprotected parts of RC Krk Bridge“.

Radic, J., Bleiziffer, J., Kalafatic, I. (2010) „New approach to ensuring durability of structures“, Građevinar 62 (11), pp. 971-980.

Radic, J., Bleiziffer, J., Tkalcic, D. (2005) „Maintaining Safety and Serviceability of Concrete Bridges in Croatia“, Bridge Structures Assessment, Design and Construction (1) 3, pp. 327-344.

Savor, Z., Bleiziffer, J. (2008) „Long Span Concrete Arch Bridges of Europe“, In J. Radić & B. Chen (eds) Long Arch Bridges, SECON, pp. 171-180.

TESTING OF HIGH STRENGTH CONCRETE BEAMS AND COLUMNS WITH HIGH STRENGTH REINFORCEMENT

Norbert Randl, Csaba Simon, Joachim Juhart, Michael Wirnsberger, Friedrich Däuber
School of Civil Engineering & Architecture
Carinthia University of Applied Sciences
9800 Spittal an der Drau, Villacher Straße 1, Austria

SUMMARY

In the frame of a research project funded by the Austrian Research Foundation (FFG) reinforced concrete elements made out of high strength concrete in combination with different types of high performance reinforcements have been tested. For a better understanding of high performance materials working together in combination and of the differences to conventional reinforced concrete, several specimens have been produced in a first step. Four-point bending tests have been carried out on beams. To examine the buckling behaviour, several slender columns have been tested as well. The bond properties between the concrete and the different types of reinforcement have been determined by pull out tests in order to get a consistent approach for the overall behaviour.

1. RESEARCH SIGNIFICANCE

During the last three decades in the field of reinforced concrete, the production methods have been optimized and tailor-made high performance materials have been developed, in terms of improved durability, sustainability and strength properties. These researches and developments open the door for the construction industry to use reduced resources and to produce more environmentally friendly and sustainable structures. Although these materials have already industrial applications, most of the standards do not yet contain recommendations about their design since the differences in their behaviour compared to conventional concrete and conventional reinforcement have not been investigated sufficiently. The ongoing research project “HiPerComp” with the major aim of bringing high performance materials into the practice of civil engineering and architecture is being carried out at Carinthia University of Applied Sciences (CUAS) and funded by the Austrian Research Foundation (FFG). The behaviour of these high performance materials in combination is investigated, thereby providing necessary knowledge for the realisation of new applications in structural engineering and architecture.

2. MATERIAL PROPERTIES

2.1 Concrete

For the first test series a high strength concrete was developed with the precondition to use locally available components in Southern Austria, especially conventional local aggregates (no hard stone). The water binder ratio was 0,25. Cement CEM I 52,5 R and silica fume as well as superplasticizer on PCE-basis were used. The fresh and hardened concrete properties were tested according to the Austrian technical standard ONR 23303 *(ASI 2010)*. The concrete had a spread of 55 cm determined by flow-table test and an air pore content of 2%. A rapid decrease of the workability over a short period of time was observed, therefore further development is ongoing. The mean value of the 28 days compressive strength measured on cubes with a side length of 100 mm was 113 N/mm^2. They were cured under water until the 7th day and under room conditions until the 28th day according to ÖNORM B 4710-1 *(ASI 2007)*. The mean value of the splitting tensile strength measured on cylinders was 6.5 N/mm^2. Since the development of the concrete recipes for the project is not yet finished, variations of the components and further determination of material properties (e.g. modulus of elasticity) is ongoing.

2.2 Reinforcements

Tab. 1 shows the material properties of the different types of reinforcement that were used for the test series. BSt 550 is a commonly used steel in Austria for RC structures and it was used for the production of stirrups for the columns and for the steel reinforced beams. S670/800 is used in practice for soil anchors and also has advantages for RC-columns *(Falkner et al 2008)*. The high strength steel St 900/1100 is mainly used for prestressing. The last two were used as longitudinal reinforcement in both columns and beams.

Glass Fibre Reinforced Polymer (GFRP) bars are used for structures in aggressive environments, where corrosion of the steel can be a significant problem. Examples of structures that may be particularly at risk include marine structures, bridges subjected to de-icing salts and sometimes industrial buildings. In these cases Fibre Reinforced Polymer (FRP) elements can serve as an alternative to reinforcing and prestressing steel, since they are not susceptible to the classical types of corrosion. Moreover, they have high tensile strength, low density and are non-magnetic *(Luc, T. and Stijn, M. 2011)*. In Tab. 1 it is shown that the GFRP bar has different material properties compared to steel, it has no yield strength and the modulus of elasticity is much lower. For the tests GFRP bars were used as reinforcement in one beam.

Tab. 1 Material properties of reinforcements *(Falkner et al 2008, Schöck 2010)*

Material properties of the different type of reinforcements				
properties	**BSt 550**	**S 670/800**	**St S900/1100**	**GFRP bar**
Ultimate tensile strength f_{tk} [N/mm^2]	550	800	1100	>1000
Characteristic yield strength f_{yk} [N/mm^2]	500	670	900	no yielding
Design yield strength f_{yd} [N/mm^2]	435	583	783	445
Design yield strain	2,18‰	3,27‰	3,82‰	7,4‰
Tension modulus of elasticity [N/mm^2]	200000	205000	205000	60000
Minimum concrete cover	acc. EC-2	acc. EC-2	acc. EC-2	d_s + 10mm
Density γ [g/cm^3]	7,85	7,85	7,85	2,2

3. COLUMN TESTS

3.1 Test setup

Four slender columns (λ=69) have been produced with the dimensions of 100 mm x 100 mm x 2000 mm. The columns were reinforced with two types of high strength steel bars: S670/800 and St 900/1100. For all the columns normal steel (BSt 550) stirrups have been used. The columns were designed in a way that buckling failure becomes decisive. Fig. 1 shows the designed cross-sections of the columns and Fig. 2 presents the test setup. During the tests the applied load, the vertical displacement at the top of the column, the horizontal displacement at the middle as well as the vertical and horizontal strains at the mid-section have been recorded.

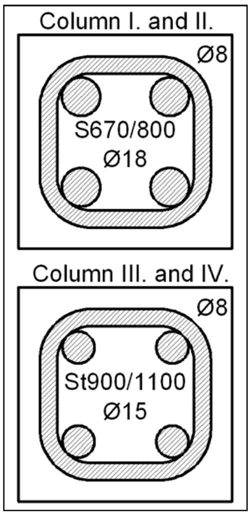

Fig. 1 Column cross-section

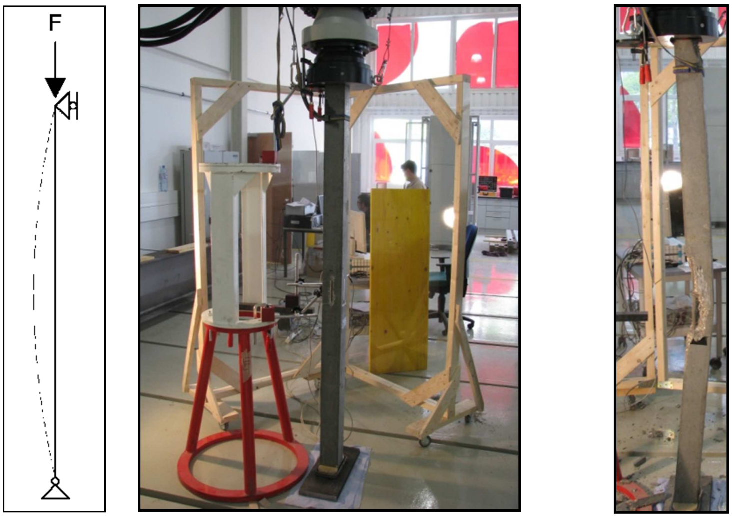

Fig. 2 Test setup and failure mode

3.2 Test results

The evaluation of the tests focused on the failure load, the failure mechanism and the vertical strains at failure. Tab. 2 shows the test results.

Tab. 2 Column buckling test results

	Calc. ult. load [kN]	Failure load [kN]	Vertical strains at failure[‰]				Mean value of strains [‰]
			DMS1	DMS2	DMS3	DMS4	
Column 1 (S670/800)	1043	1155	2,45	1,16	3,37	1,99	2,24
Column 2 (S670/800)		1082	2,25	0,28	3,59	1,80	1,98
Column 3 (St900/1100)	946	835	1,88	1,78	1,18	1,37	1,55
Column 4 (St900/1100)		727	1,06	0,63	1,61	2,03	1,33

In the cases of column 1 and 2 the failure mode was buckling. The mean measured vertical strain was between 1.98 ‰ and 2.24 ‰. The tests of column 3 and 4 ended up in premature failure with the splitting of the concrete cover at the load introduction zone where the compressive stress in the cross-section was between 73 N/mm^2 and 84 N/mm^2. A possible reason – currently being investigated – might be the non-satisfying bond properties with the St 900/1100 reinforcement.

4. BEAM TESTS

4.1 Test setup

Three beams have been produced with the dimensions of 150 mm x 250 mm x 3500 mm. The dimensioning was derived on the basis of EC2 with the application of the mean values of the material properties and without safety factors. The target was to reach a ductile failure mechanism so that during the tests the crack propagation and the deflections at different load levels could be observed.

It is generally accepted that in most structural applications with FRP, over-reinforced concrete sections will be inevitable *(fib 2007)*. Therefore in the case of the GFRP reinforced beam, the target was to design an over reinforced cross-section which is still close to “balance”. The reinforcement ratio for the “balanced-section” was calculated according to a formula derived from EC2 *(Pilakoutas et al 2002)*. The result was 0.81 %. The reinforcement ratio of the tested beam was 1.6 %. The applied load, the deflection, the compressive strains at the top of the beams and the crack patterns were recorded. Fig. 3 shows the cross-sections and Fig. 4 the test setup of the beams.

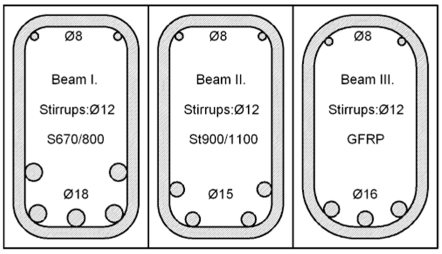

Fig. 3 Beam cross-sections

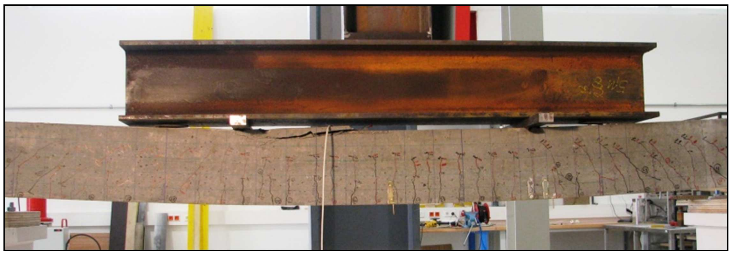

Fig. 4 Test setup

4.2 Test results

For all three beams the calculations agree with the test results. Fig. 5 shows the calculated and measured load-deflection curves and Fig. 6 presents the relation between the calculated and observed crack widths at different load levels.

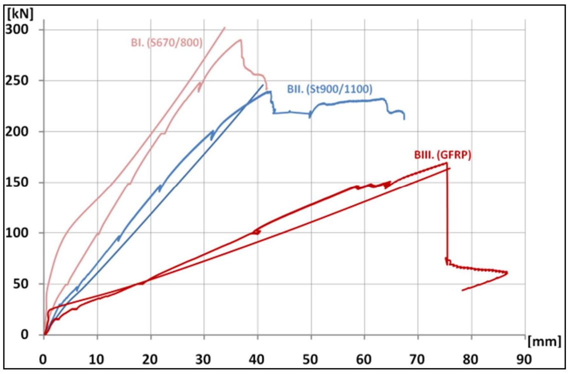

Fig. 5 Load – Deflection

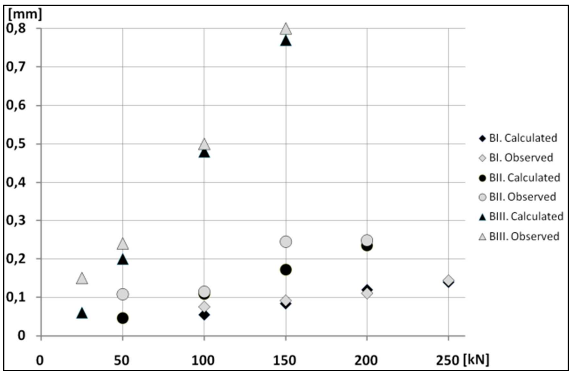

Fig. 6 Crack width – Load

It can be seen in Fig. 5, that the failure mode differs between the beams with steel reinforcements and the beam with GFRP reinforcement. In the case of steel reinforcement first the reinforcement yielded and after that the concrete crushed at the compressed zone. Therefore the failure mechanism was rather ductile.

The gradient of the load - deflection curve of the GFRP-beam is much lower than that of the steel-reinforced beams. The deflections at the same load level are 2-3 times higher and the same with the crack width. At the end the beam failed by the crushing of the compressed zone in a rather brittle way. Possible solutions for increasing the ductility of the FRP reinforced concrete elements would be to increase the confinement of the compressed concrete zone or to use the FRP reinforcement in combination with steel bars.

Tab. 3 contains the calculated and measured failure loads, the measured deflections at failure and the strains in the compressed concrete zone and in the reinforcements at failure.

Tab. 3 Beam test results

	Calc. ult. load [kN]	Failure load	Calculated def. [mm]	Measured def. [mm]	Max. strain in concrete [‰]	Max strain in reinf. [‰]
Beam I. (S670/800)	302	292	36,6	36,8	3,2	6,3
Beam II. (St900/1100)	246	232	40,6	57,8	3,1	6,8
Beam III. (GFRP)	164	169	78,3	75,3	3,2	12,0

5. PULL-OUT TESTS

5.1 Test setup

Several pull-out tests have been carried out to determine the bond properties between the high strength concrete and the different types of high performance reinforcements used for the production of the columns and beams. The test setup was prepared according to the RILEM recommendation *(RILEM TC 1994)*. The side lengths of the specimens were 10 times the reinforcement diameter and the bond lengths were 5 times the diameter. Fig. 7 shows the test setup for the pull-out tests.

Fig. 7 Pull-out test setup

5.2 Test results

The derived bond strength between the high strength steel (S670/800) and the high strength concrete based on the results of the pull-out tests was higher than expected: the estimated value based on the extrapolation of f_{bm} values given in TR 023 *(EOTA 2006)* is less than 25 N/mm^2. After slip of the reinforcement (>0.1 mm) measured on the back side of the pull-out specimen, the failure occurred finally by splitting of the concrete. Tab. 4 shows the test results with the calculated bond strength at 0.1 mm slip. Concerning the other types of reinforcement the tests are currently ongoing with reduced embedment depth to avoid premature failure of the rebar.

Tab. 4 Test results and calculated bond strength

	Φ [mm]	Bond length [mm]	Surface [mm^2]	Ultimate force [kN]	Force at 0,1mm slip [kN]	Bond strength [N/mm^2]	Average [N/mm^2]	Remarks
S670/800	18	90,7	5129	203	194	37,8	**37,8**	After slip, conc. splitting
	18	91,7	5186	208	196	37,8		After slip, conc. splitting
	18	89,7	5072	205	192	37,9		After slip, conc. splitting

6. CONCLUSIONS

The structural behaviour of high strength concrete members with high performance reinforcement has been investigated by means of beam bending tests, column buckling tests and pull-out tests. In the pull-out tests it turned out that with certain types of high performance reinforcement like S670, a very high bond strength can be achieved. The failure mode of the columns depends on the detailing and the bond properties of the reinforcement. The test results of the column reinforced with S670/800 are satisfactory. Concerning the beams, the design principles given in Eurocode 2 work relatively well in the case of high performance materials provided the bond behaviour is comparable or better than that of standard reinforcement.

In conclusion, the working together of several combinations of high strength concrete and high performance reinforcement is promising. However, the research project is ongoing and other topics like serviceability and fatigue behaviour are going to be investigated.

7. REFERENCES

Austrian Standard Institute (ASI) (2007), “Concrete - Part 1: Specification, production, use and verification of conformity (Rules for the implementation of ÖNORM EN 206-1 for normal and heavy concrete)”, ÖNORM B 4710-1 (2007 10 01) (in German)

Austrian Standard Institute (ASI) (2009), “Eurocode 2: Design of concrete structures – Part 1-1: General rules and rules for buildings”, ÖNORM EN 1992-1-1 (in German)

Austrian Standard Institute (ASI) (2010), “Test methods for concrete - National application of testing standards for concrete and its source materials” ONR 23303 (2010-09-01) (in German)

European Organization for Technical Approvals (EOTA) (2006), “Assessment of post-installed rebar connections”, TR 023, EOTA Technical Report, 20 p. (in English)

Falkner, H., Gerritzen, D., Jungwirth, D., Sparowitz, L. (2008), „Das neue Bewehrungssystem – Druckglieder mit hochfestem Betonstahl SAS 670/800“, Beton- und Stahlbetonbau, Vol. 103, 05/2008, pp. 304-317 (in German)

fib (2007), “FRP reinforcement in RC structures”, technical report bulletin 40, 147 p. (in English)

Luc, T. and Stijn, M. (2011), “Use of FRP in concrete structures: trends and challenges”, Keynote Lecture, *fib* Symposium PRAGUE 2011, pp. 1071-1084 (in English)

Pilakoutas, K., Neocleous, K. and Guadagini, M. (2002), “Design philosophy issues of fibres reinforced polymer reinforced concrete structures”, Journal of Composites for Construction, 6(3), pp. 154-161 (in English)

RILEM TC (1994), “AAC 8.1 Pull-out test for reinforcement, 1992”, RILEM Recommendations for the Testing and Use of Constructions Materials, p. 140 (in English)

Schöck (2010), “Technical Information”, Shöck ComBAR® (in English)

PROPOSAL FOR A METAL-CONCRETE-COMPOSITE-SLAB ELEMENT

Stephan Pirringer, Johann Kollegger
Institute for Structural Engineering
Vienna University of Technology
Karlsplatz 13 / 212
1040 Vienna, Austria

SUMMARY

For common reinforced concrete slabs, regardless of size, a concrete cover is needed that cannot be utilized for the load-bearing capacity. A higher thickness and weight and thus increased costs of the slab are a consequence of the concrete cover. By replacing the reinforcement with a perforated steel sheet that is arranged on one side of the slab, the concrete cover can be saved and the slab thickness can be reduced.

This new approach to composite slabs can be used for small formatted, constructive elements, as for example covers for cable channels, deck slabs for pedestrian bridges and prefabricated parts for short spans.

1. INTRODUCTION

There is a wide range of areas of application for small reinforced concrete slabs. Covers for cable channels, for example in tunnels and on bridges, is one of the common fields of application, and therefore a matter of prefabricated, mass-produced articles.

The contribution of the mild steel reinforcement to the load-bearing capacity can only be ensured if a concrete cover exists, that can establish a sufficient bond between those two basic materials. In small formatted concrete slabs this coverage can amount from 10% to 20% of the overall weight and material consumption.

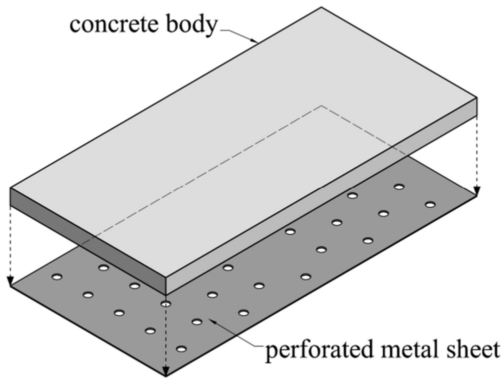

Fig. 1 Schematic assembly of a MCC-slab

With an approach that is currently under development at Vienna University of Technology the concrete cover can be saved. By replacing the mild steel reinforcement with a perforated metal sheet (Fig. 1), it is possible not only to reduce thickness and weight and thus the costs of the slab, but also to reduce the effort and complexity of formworks. The bond between the two basic materials of the metal-concrete-composite-slab (MCC-slab) is established by the concrete filling the punched holes of the perforated metal sheet.

For a proper fabrication of the slabs, the metal sheet can simply be put on the bottom of the formwork. One further advantage of this system is the possibility of using commercially available perforated metal sheets that are available in different configurations, without any further treatment. Also the costs of recycling are estimated to be low.

2. TECHNICAL BACKGROUND OF THE MCC-SLAB

In contrast to some common composite slabs, this approach means working without any of the usual mild steel reinforcement, and using only a perforated metal sheet instead. Since this method tends to be only used for small slabs with thicknesses down to 5 to 10 centimeters and even less, the end anchorage poses the major problem. Due to the low construction height no end anchorage as known from common composite slabs, e.g. shear studs and/or dovetailed deformations of the profiled (trapezoidal) sheet at the bearing, can be used. Therefore we have to accomplish an anchorage just by a load transfer through the concrete dowels placed in the perforation of the metal sheet (Fig. 2). In addition of proving the resistance to bending and lateral force, the structural stability of the concrete dowels plays a significant role.

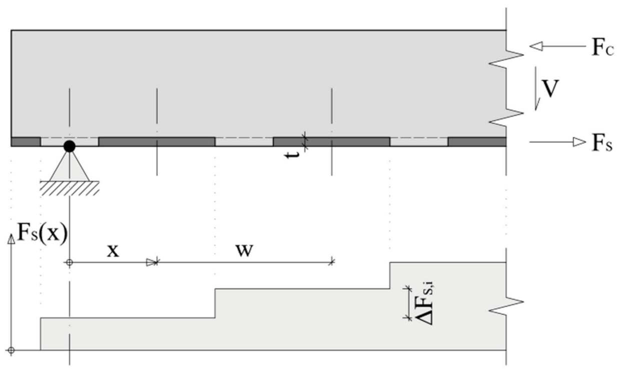

Fig. 2 Schematically, longitudinal cut of a MCC-slab

For a first approximation of the bending capacity, a linear distribution of strains over the whole cross section, according to Eurocode 2, was used. An approach of a fully plasticized cross section is also possible *(Eurocode 4)*, but for prefabricated small slabs with dimensions of practical relevance, the difference of those two methods is negligible. The resistance due to shear forces was calculated in the same manner as for composite slabs in general.

The load bearing capacity of the concrete dowels was approximately calculated by formulas based upon the bearing pressure *(Berger, 1994)* and the bending stresses that result from the bending moment due to an offset t/2 of the dowel force $\Delta F_{s,i}$.

3. PREPARATION OF THE SPECIMENS

For a first impression of the functional efficiency of the small composite slabs, especially the bond behavior in the joint, we decided to carry out a preliminary series of tests. Five specimens with the same overall dimensions (L/W/H = 100.0/20.0/5.0 [cm]), same self-compacting concrete and same material for the reinforcement were investigated. Sendzimir galvanized, perforated metal sheets with an arrangement of round holes in a rectangular grid were used for all specimens.

In this first series of tests we decided to apply two different types of perforated metal sheets. Since the punching of the perforation forms burrs along the cutting edges on the one side and rounded edges on the other side, we expected a difference to occur concerning the orientation of the metal sheet towards the concrete body. Furthermore, a plastic foil was applied on the bottom side of the perforated metal sheet of two specimens (VK1 & VK3). During the concreting process, the foil becomes deformed and thereby increases the concrete dowel. In addition, the foil prevents the cement laitance from leaking under the metal sheet.

The five specimens were arranged as shown in Tab. 1:

Tab. 1 Assembly of specimens

Specimen	**Perforated metal sheet**						
	t [mm]	Ø [mm]	w [mm]	A_{eff}/A [%]	A_{eff} [cm²]	Orientation concrete facing side	Foil used
VK 1	2.0	20.0	48.5	41.2	2.35	burr edges	+
VK 2	2.0	20.0	48.5	41.2	2.35	burr edges	-
VK 3	1.5	10.0	20.0	50.0	1.50	burr edges	+
VK 4	1.5	10.0	20.0	50.0	1.50	rounded edges	-
VK 5	1.5	10.0	20.0	50.0	1.50	burr edges	-

4. PERFORMANCE AND RESULTS OF THE PRETEST

4.1 Test set-up

For all five specimens a 4-point bending test was carried out. We used a slightly modified test set-up than recommended in Eurocode 4 for investigations of the composite action. The initial bearing distance in the test set-up amounted to 90.0 cm, and the loads were located in the third points of the MCC-slab. While the displacement-controlled load was applied, the deflection at the midspan of the slab, as well as the vertical and longitudinal relative displacement between the concrete and the metal sheet at the corners were measured continuously (8 displacement transducers, WI1 – WI8).

Plastic bending deformations occurred at specimens VK3 and VK5. In these two cases the test was interrupted and repeated with an alternative test set-up. For the second test cycle the span was reduced to 80.0 cm and the loads were applied at a distance of 20 cm from the bearing.

4.2 Results

In accordance to the precalculations, VK1 and VK2 collapsed under smaller loads than all the other specimens, even though a higher steel cross section was used. During the load application no noticeable cracks could be observed. Except VK4, in all the tests the final collapse was pre-announced by increasing relative displacements. VK1 and VK2 collapsed in sudden bursts at deflections of about 3.8 and 3.5 mm, whereas vertical displacements up to 0,2 mm and longitudinal displacements up to 0,1 mm occurred. Unlike VK3 and VK5, VK4 broke without plastic bending deformations. That the reason might have been the different metal sheet orientation can only be assumed.

As mentioned above, plastic bending deformations occurred at the first load cycle of VK3 and VK5 (Fig. 3), accompanied by some minor relative displacements of the metal sheet up to 0,01 mm. While the test set-up was modified for the second load cycle, sudden relative displacements occurred. At the second load cycle the MCC-slabs VK3 and VK5 collapsed in sudden bursts as well.

In general, different failure mechanisms caused the specimens to collapse depending on the configuration of the perforation and the degree of shear connection.

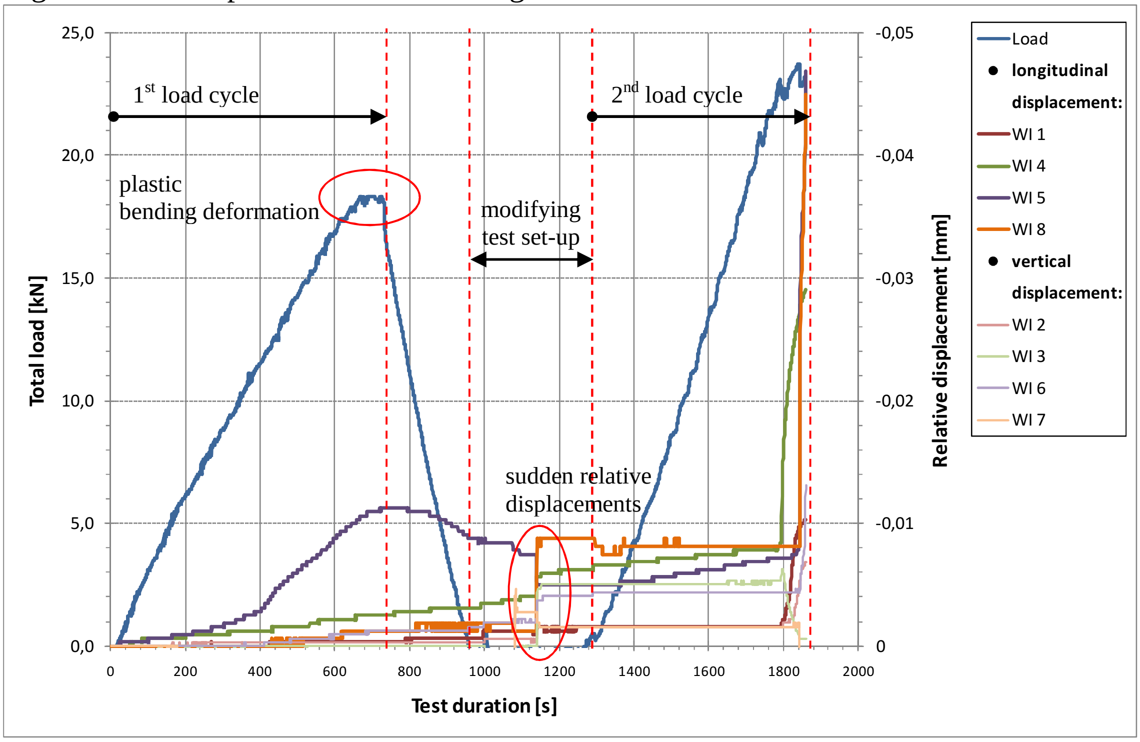

Fig. 3 Test results of specimen VK5 of both test set-ups and load cycles

5. CONCLUSIONS

Contrary to the general apprehension, no detaching of the perforated metal sheet could be detected at any specimen before the tests had been performed. Furthermore, it could be shown that with the correct selection of size (diameter) and layout of the concrete dowels, in short the perforation of the metal sheet, the bond within the MCC-slab is strong enough to resist loads up to the bending loading capacity. The results of the preliminary series of tests suggest that the application of a plastic foil does not increase the load bearing capacity, whereas the orientation of the metal sheet is of importance.

Based upon the actual results, further tests of the contact surface with its concrete dowels, tests with dynamic loading and tests with a freeze-thaw attack are in the planning stage.

6. REFERENCES

Berger, J. (1994), “Technische Mechanik für Ingenieure. Band 2: Festigkeitslehre”, Braunschweig; Wiesbaden: Vieweg

ÖNORM EN 1992-1-1 (2009), “Eurocode 2: Bemessung und Konstruktion von Stahlbeton und Spannbetontragkwerken, Teil 1-1: Allgemeine Bemessungsregeln und Regeln für den Hochbau”

ÖNORM EN 1994-1-1 (2009), “Eurocode 4: Bemessung und Konstruktion von Verbund-tragwerken aus Stahl und Beton, Teil 1-1: Allgemeine Bemessungsregeln und Anwendungsregeln für den Hochbau

„REVIVAL" OF CEMENT CONCRETE PAVEMENT IN HUNGARY

Mrs. Katalin dr Karsai [1], Mrs. Éva Szántó[2], Mr Zoltán Vörös[3]
[1]Institute for Transport Sciences Non Profit Ltd., Budapest, Hungary
[2]National Infrastructure Developing Private Co. Ltd., Budapest, Hungary
[3]UTIBER Ltd., Budapest, Hungary

1. SUMMARY

The first concrete pavement was built in Hungary on motorway M7 between Budapest and Lake Balaton. After 30 years, concrete pavement was built again on the Motorway M0 around Budapest. The limited performance capacity of asphalt pavements on expressways and motorways made it necessary to turn to the concrete pavements again. The development of the last 30 years up in design, technology and regulations was followed.
When Hungary became member of the European Union, it updated its regulations, renewed the technology for concrete pavements. Before starting with the construction of a concrete pavement, experiences were collected on construction of test sections with different surface finish techniques used for the preparation of the Construction Technical Permission (ÉME). The new Road Technical Directives was introduced in 2006 and based on a 28 km-long new motorway section built on motorway M0. In 2008, the specification for concrete pavements with exposed aggregate was introduced. The reconstruction and extension of the existing motorway M0 to 2*3 lanes will be carried out using this technology.

2. THE FIRST CONCRETE MOTORWAY IN HUNGARY M7

Construction of the first Hungarian motorway M7 between Budapest and Lake Balaton started in 1963 applying Portland cement concrete pavement. The pavement thickness and width had been increased in the sections between 1967 and 1975. Expansion joints were not used yet. Thickness and material of the base course changed more or less together with that of the pavement. Some sections of this 110 km long motorway section had shown the signs of early deterioration because of various construction (technological) failures. Typical failures have been cracks due to un-sufficient support of the slabs, height difference between two slabs at the joints due to lack of dowel bars and anchors in the joints, ravelling of the pavement surface because of using salt for de-icing in winter period.

3. REGULATIONS

A separate volume for construction of concrete pavements named ÉKSZ were published in 1963, the revised edition of it in 1971. These technical prescriptions supplemented by the rules of detailed Company Specifications about technology, quality requirements, testing and control, etc. had to be taken into consideration during construction.
In 1981 the ÉKSZ regulation was followed by the Hungarian standard *MSZ 07-3212*.
Important changes in regulations happened about 2000, when the previous Road Technical Prescription was replaced by the *UT 2-3.201:2000* based on the results of recent research and development activity in Europe. Development of the last 30 years had to be followed up in design, technology and regulations. Hungarian government decided in 2003 to develop the motorway and expressway network. The new standards for cement concrete pavements, materials, laboratory testing had to be introduced as harmonised standards. The 1/2004 ÉME – Construction Technical Permit was the first regulation issued according to this. New Road Technical Prescription *(UT 2-3.201:2006 Construction of Concrete Pavements,*

Specifications, Requirements) was introduced in 2006. Based on the latest European experiences and standards another Road Technical Prescription *(UT 2-3.211:2006)* has been issued for structural design of rigid and composite pavement structures. Prescription for cement concrete pavements with exposed aggregate *(UT 2-3.213:2008* Construction of Two Courses Doweled Concrete Pavement with exposed aggregate) was introduced in 2008.

4. TEST SECTIONS

Road No 7538.

The first test section, a heavily trafficked (above 1110 heavy vehicles/day) secondary road No 7538 between Lenti and Letenye (close to the Hungarian and Slovenian border) was selected and constructed in summer of 1999.On 100 mm mixed-in-place cement stabilisation base and 150 mm mixed-in-plant cement stabilisation base 220 mm jointed cement concrete pavement or 220 mm jointed cement-concretepavement with exposed aggregate or 170 mm continuously reinforced concrete pavement or 30 mm stone mastic asphalt+80 mm high modulus binder course+90 mm high modulus base course were built in. The continuously reinforced cement concrete pavement with a thickness of 170 mm and 0.67 % reinforcement was constructed without transversal joints. The 6 m wide cement concrete pavement was built as a single layer in two phases of 3 m width each.

Road No 44.

In 2003, a test section was built on road No 44. (AADT=9804 unit vehicles/day with 1981 heavy vehicles/day.) The pavement structure variants had been tested on a length of 350 m each.

Road No 4.

Another test section was built in 2003 on road No 4. (AADT = 16 651 unit vehicles/day with 2154 heavy vehicles/day). The 8.25 m wide cement concrete pavement was laid in a single pass with a slip-form paver. The concrete pavement structure and the reference asphalt section had been tested in a length of 500 m each.In order to evaluate and to compare the performance of the various pavement types, the monitoring of the different subsections was decided with a frequency of 6 months, later of 12 months. The evaluation methodology contained the theoretically possible failure types for the different pavement variants. *Table 1* shows the different types and condition parameters evaluated for each pavement type.

Tab.1. Possible failure types of the different pavement variants and their parameters.

Failure type	**Condition parameter**	**Asphalt**	**Concrete**
		pavement	
Longitudinal deformation	Unevenness	X	
Slab faulting	Unevenness		X
Rutting	Transverse profile	X	
Loss of skid resistance	Skid resistance	X	X
Wear of aggregate grains	Macro roughness	X	X
Surface defects	Visual evaluation of surface defects	X	X

5. CONSTRUCTION OF CEMENT CONCRETE PAVEMENT

Based on earlier traffic data and experiences cement concrete pavement was proposed for the next coming sections of M0. Before starting with construction of motorway projects with rigid pavement structure experiences collected on construction of test sections with different surface finish techniques, like artificial grass, exposed aggregate and broom were thoroughly evaluated.

The first cement concrete pavement in a length of 12.5 km of M0 East section was opened in December 2005. Construction of the next 26.5 km of M0 was realized according to this regulation and opened to traffic in September 2008. The East section of M0 motorway between M5 and M3 motorways was completed. The reconstruction and extension of the existing M0 motorway to 2*3 lanes in the South section between the M1 and M5 motorways shall be executed with exposed aggregate.

The pavement structure is as follows: 20 cm Ckt-4 cement bound base course, bitumen emulsion as an intermediate layer and 26 cm CP4/2,7-32 cement concrete layer.
The standard cross section of the concrete pavement between motorways M5 and M31 have 2*2 lanes with 3,75 m width of each, and a 3 m wide emergency lane. On section between motorways M31 and M3 it is 3,5m. In interchanges the lane width is generally 6 m, while on collectors 7,5 m.

The ø 25 mm and 50 cm long round dowel bars with Teflon protective layer were placed into the transversal joints of the main carriageway by a special device installed on the slip form paver. In all other cases, the dowel bars were fastened on a special steel wire supporting structure. The dowel bars were placed every 25 cm in the middle of the concrete layer. The ø16 mm and 60-80 cm long anchors installed every 1 m were also placed by the slip form paver in the main carriageway, but for emergency lanes it had to be glued in bored holes. The anchors had 20 cm long special protective layer against corrosion.

The concrete mixture had to be designed for different weather conditions. CEM II/A-S 42,5 N and CEM II/B-S 32,5 R type cements were used. In summer periods, the CEM II/B-S 32,5, in colder periods CEM II/A-S 42,5 N type cements were chosen. For both cement types, the laboratory tests were made before starting with the construction. Basalt or andesite were used for the mixture with D_{max} = 32 mm or 22 mm.

Plastifyer and air pore former were added to the mixture to assure the necessary consistency for compaction and to protect the layer against corrosion (negative effects of de-icing salt).
Concrete was produced by 2 batching plants with a mixing capacity of 3 m^3 each installed very close to the relevant sections. The mixing plants were fitted with moisture measurement devices for the sand fraction. The output of the mixing plant was designed for 1 m/minute construction speed +20% reserve, which meant practically 200 m^3/hour output with 1 minute mixing time after all components were already added to the mixture. The approved recipe was tested in the mixing plant, and the test results were approved by the Engineer.

Before starting with construction test sections had to be built by the Contractor with Wirtgen SP1600 slip form pavers to test and harmonise the whole procedure (mixing, transport, building in, surface treatment, aftercare etc.) which were evaluated and approved by the Engineer.

The main carriageway and the collectors were built with 2 pc with “fresh on fresh” technology 21 cm thick followed by the 8 cm upper layer. Emergency lanes were built with Wirtgen SP 500 slip form paver in full depth. After the longitudinal smoother the surface was sprayed with 200 g/m^2 curing material to protect it against drying out, warming up and formation of wild cracks. Construction of the cement concrete pavement on bridges required special technology and mixture because of the reinforcement of the slabs (steel mesh 10*10 cm, ø 10 mm).

On sections of motorway M0 different types of surface finish were used: artificial grass, steel brush. Concrete pavement with exposed aggregate will be built on M0 between M1-M5.
Transversal joints were cut every 5 m, depth of the initial cut was 25-33% of the layer thickness to keep cracking process under control, longitudinal joints were cut in 33-45% of the layer thickness. Later the joints were widened up 25-35 mm deep to 10-12 mm. Hereafter the joint edges were grinded in 45º slope. Cleaning was followed by placing of joint sealant string and spraying of primer. The joints were filled up with hot bituminous joint sealing material.

6. CONCLUSIONS

In the last 6 years managed in Hungary to update the technology and prescriptions to the latest European standards. Preparation of the relevant standards and prescriptions was running nearly parallel with tendering and application of these new specifications. The implemented project sections of the M0 motorway were executed by well trained European contractors. Due to the long intervals between preparation of tender documents and the realisation, furthermore the EU financing procedure determined the contract conditions. Nevertheless cement concrete pavements became real alternatives to asphalt pavements especially on motorways, expressways with extremely high traffic volume and heavy traffic portion.
For the future Hungary has to focus on monitoring of the existing cement concrete pavements have been built in the last decade to collect experiences both for future projects and for operation and maintenance of such pavement types.

REFERENCES

Concrete Committee of the Hungarian Road Association lead by Mr Dr Imre Keleti:
Elaboration of the Specifications for construction of jointed concrete pavements
ÚT 2-3.201 Construction of concrete pavements. Construction requirements
ÚT 2-3.211 Dimensioning of concrete and composite pavements
ÚT 2-3.213 Construction of jointed concrete pavement with exposed aggregate
ÚT 2-3.210 Recycling of concrete pavement
Dr András Liptay: New specification of concrete pavements and direction of the development Közúti és Mélyépítéstudományi Szemle 50/12
Dr habil. László Gáspár- Ágnes Görgényi -Dr Imre Keleti: Proposals for renewal of the domestic quality control system Közúti és Mélyépítéstudományi Szemle 55/3
Dr. András Liptay: Construction and development of concrete roads int he last 60 years
Dr. András Liptay: Regulations of the concrete pavements, Presentation held on 31st May 2007 organised by the Hungarian Concrete Association

EXTERNAL SHEAR STRENGTHENING WITH CFRP FOR BEAMS WITH INSUFFICIENT INTERNAL SHEAR REINFORCEMENT

Mazen Al Makt – György L. Balázs
Budapest University of Technologies and Economics
Faculty of Civil Engineering
Műegyetem rkp.3.
H-1111 Budapest

SUMMARY

An external shear strengthening technique is introduced in this research work using CFRP strips. A series of tests were carried out in order to study the behaviour of concrete beams strengthened by this technique. The strengthening technique is based on inserting CFRP strips inside slots near to the surface on the two sides of the beams, the slots are cut first, then the CFRP strips are glued by resin into the slots from both sides. The results indicated considerable increase in shear capacity as well as increase in stiffness and better crack distribution. The strengthened beams failed in flexural instead of shear.

1. INTRODUCTION

An experimental study was carried out to increase the shear capacity of reinforced concrete beams by applying strengthening with near surface mounted technique, as this technology is becoming an efficient way of strengthening for concrete structures (*Blaschko, 2001; fib, 2001; fib, 2006; Hollaway, Leeming,1999*). The beams were tested in four-point bending. The load was applied at a constant rate under deflection control up to failure of the beams. In one part of the test series beams were tested without strengthening. They failed in shear as the shear failure was the expected failure mode as it was designed. The test results for these beams were considered to be as references to analyze the results. In other part of the test series, beams were strengthened with four CFRP strips on each side of the beams (Fig. 1). These beams were not precracked before strengthening. The capacities of these beams were expected to be the upper limit for these type of beams fore both cases uncracked or precracked. The strengthening technique is based on inserting CFRP strips inside slots near to the surface on the two sides of the beam.

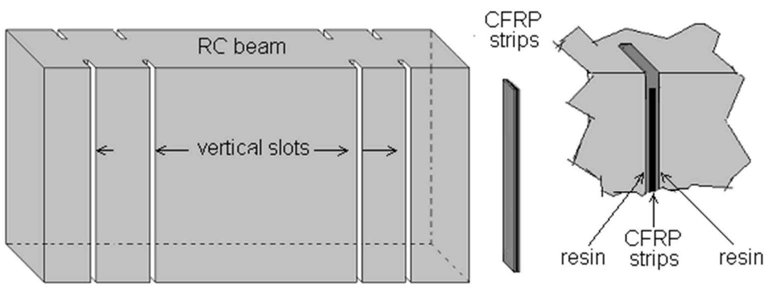

Fig. 1 View of the specimens with external shear strengthening

2. BEAM DETAILS AND MATERIAL PROPERTIES

As the aim of the research work is to evaluate a shear strengthening method the beam dimensions were chosen to have relatively high depth as shown in Fig. 2. to clearly distinguish the shear cracks and shear failure more. The mixing of concrete was carried out in a concrete mixer in the laboratory of the Dept. of Construction Materials and Engineering Geology at Budapest University for Technology and Economics with design strength of C35. Cubes and prisms were cast with each individual beam and used as control specimens for determining the compressive and flexural strengths of concrete.

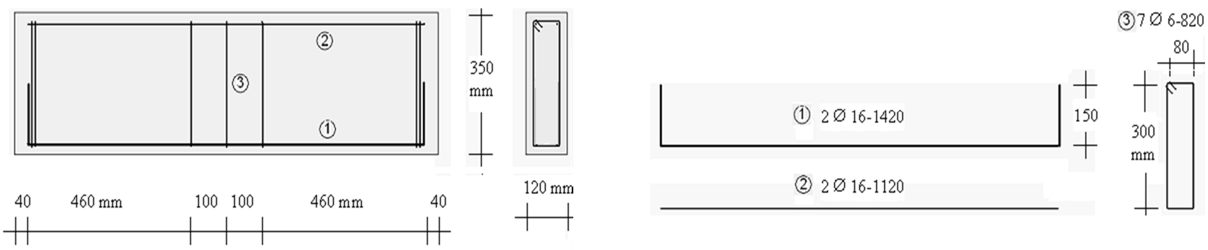

Fig. 2 Beam dimensions and reinforcement details

CFRP roll of 10 m length and 50 mm width was supplied by Sika Hungary Ltd. industrial sponsor. The roll was chopped off by cutter to 300 mm length strips; the strips were longitudinally cut by cutting machine to two pieces of 24 mm wide each, as the cutting disk has 2 mm width. The two components adhesive was developed especially for bonding process of structural concrete and Sika CarboDur CFRP strips. Mixing ratio by volume for part A (clear amber resin) and part B (black hardener) is 3:1.

3. EXPERIMENTAL RESULTS

As it was expected, all three unstrengthened beams failed in shear, the three beams behave in a similar manner. They had little number of cracks, max. 7 cracks. The crack patterns clearly confirmed the minimal shear reserve of the beams as shown in the left part of Fig. 3.

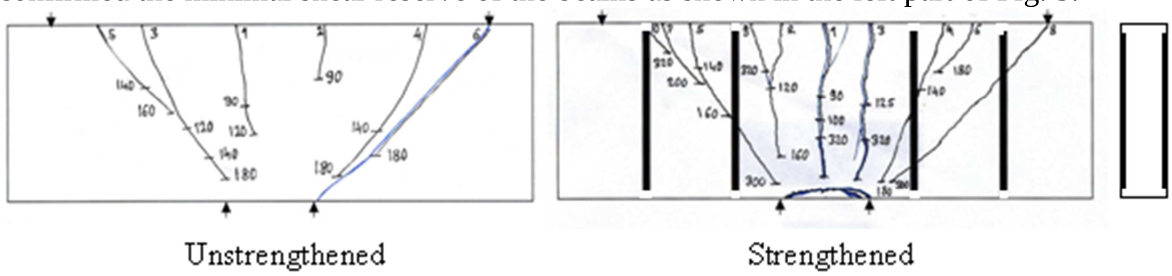

Fig. 3 Typical observed crack patterns for unstrengthened beams and for strengthened beams

For the strengthened beams the crack patterns show an increase of the number of cracks by 40 % comparing with the crack patterns of unstrengthened beams. The strengthened beams had better crack distributions and more symmetrical arrangements of the cracks along the beams as shown in the right part of Fig. 3.

The load versus crack width diagram for the unstrengthened beams shows that the shear reserve was minimal, hence crack widths of shear cracks 3, 4, 5 and 6 were increasing more effectively than widths of flexural cracks 1 and 2. This implies that shear failure was most likely to occur. For the strengthened beam the diagram shows that, the crack width for all cracks continuously and gradually increased as the load increased including flexural cracks. It is clearly seen that in reverse for unstrengthened beams the flexural cracks were present more actively for strengthened beams hence crack widths of flexural cracks were increasing more effectively than widths of shear cracks, so flexural failure was most likely to occur (Fig 4).

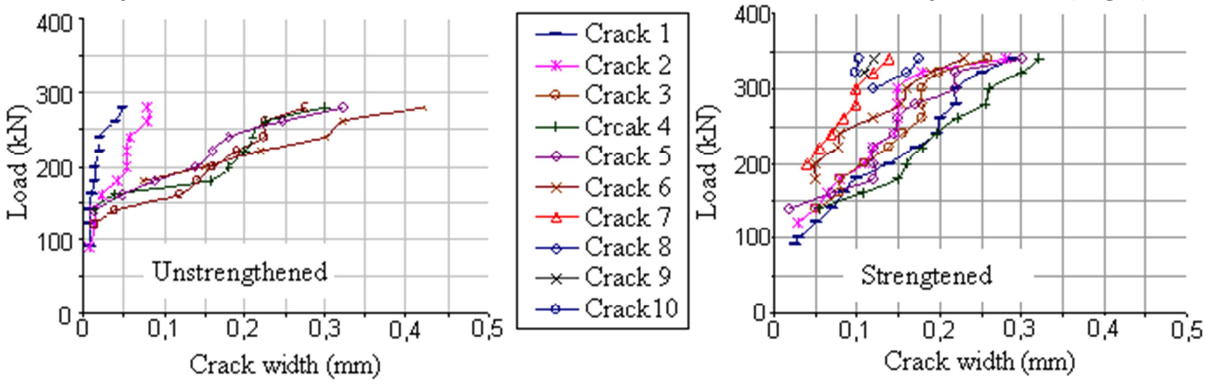

Fig. 4 Typical load versus crack width for unstrengthened beams and for strengthened beams

Comparison of load versus deflection diagrams for strengthened and unstrengthened beams show that the deflection of strengthened beams was significantly decreased more and more as the load level increased comparing to the deflection of the unstrengthened beams (Fig 5). The diagram also shows that the maximum loads reached for strengthened beams are higher than the average maximum load for unstrengthened beams by up to 17%.

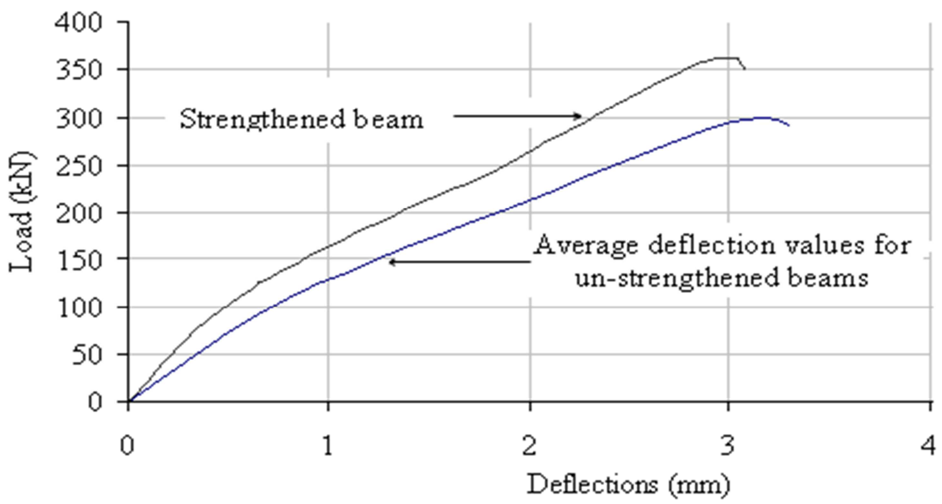

Fig. 5 Comparison of deflection versus load for unstrengthened and strengthened beams

4. CONCLUSIONS

The near surface mounting technique for shear strengthening used in this research prevented the reinforced concrete beams from shear failure, and the beams were stimulated to go through flexural failure. Thus the strengthening strips successfully enhanced the shear bearing capacity of the beams (Table 1).
The near surface mounting technique for shear strengthening used produced better crack distribution indicating higher number of cracks and lower value of total crack width.
The near surface mounting technique for shear strengthening used significantly improved the stiffness of the beams, hence the deflection versus load graphs of the strengthened beams show higher gradient comparing with same graphs of the unstrengthened beams.

The strengthening strips actively participated as stirrups in control of crack width and load bearing capacity. Debonding of strengthening strips was not observed until failure especially because non of the crack which crossed the strips became the failure crack.

Tab. 1 Comparison of deflection values at some load levels for all beams

Beam description	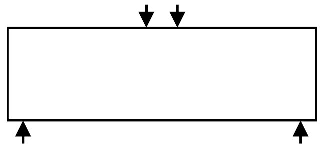			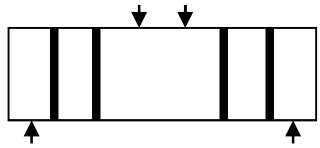		
	Unstrengthened beams			Strengthened beams		
Beam group number	1	2	3	1	2	3
Deflection (mm) at 100 kN	0.691	0.682	0.754	0.636	0.480	0.489
Ratio to average value of Unstrengthened beams	Average value = 0.709			10%	32 %	31%
Deflection (mm) at 200 kN	1.789	1.864	1.914	1.620	1.495	1.373
Ratio to average value of Unstrengthened beams	Average value = 2.433			13%	13%	22%
Deflection (mm) at 300 kN	~3.080	2.985	~3.177	2.629	2.871	2.327
Ratio to average value of Unstrengthened beams	Average value = 3.081			15%	7%	24%
Failure load (kN)	299.35	301.75	297.55	347.79	326.33	362.09
Ratio to average value of Unstrengthened beams	Average value = 299.55			14%	8%	17%
Failure mode	Shear			Flexural	Flexural	Flexural

5. ACKNOWLEDGEMENTS

The authors are grateful to Sika Hungary Ltd. industrial sponsor for their kind interest and their support of the research.

6. REFERENCES

Blaschko, M. A. (2001), Load bearing capacity of concrete elements with CFRP strips glued into grooves, PhD Thesis, TU Munich, in German.

fib, (2001), Externally bonded FRP reinforcement for RC strectures, *fib* bulletin 14, ISBN 2-88394-054-1, Laussane.

fib, (2006), Retrofitting of concrete structeres by externally bonded FRP with emphasis on seimic application. f*ib* bulletin 35, ISBN 2-88394-075-4, Laussane

Hollaway, L. C., Leeming, M. B. (eds.), (1999), Strengthening of reinforced concrete structures using externally bonded FRP composites in structural engineering. CRC Press ISBN 1855733781.

CREEP TESTS ON CONCRETE MADE OF DIFFERENT ACTIVE ADDITIVES

A. Sprince, L. Pakrastinsh, A. Korjakins, G. Shakhmenko and G. Bumanis
Riga Technical University
16 Azenes Str., Riga, LV-1048, Latvia

SUMMARY

This paper introduces the recent state of research on creep of new concrete made by replacing the cement with a utilizing recycled active additive coming from waste glass and adding a montmorillonite mineral nano particles and comparing it to a control concrete. Several kind of concrete mixes using unconventional additives have been developed and prepared. Specimens were tested in two extreme environments: in one case there was 100% humidity provided by protecting the specimens from desiccation and in the other case specimens were air-dried and protected from any moisture. Concrete specimens were loaded in a constant room temperature and with a constant level of moisture and the properties of the concrete were examined. The properties investigated include compression strength, modulus of elasticity, elastic and creep strain, creep recovery, creep coefficient.

1. INTRODUCTION

One of the main constituents of reference concrete is cement. Every year approximately 2.35 billion tons of cement is produced — that is almost 1 m^3 of cement for every person in the world. The carbon dioxide released into the atmosphere during the cement production process. Its release into the atmosphere contributes to the global warming and the development of holes in the ozone layer. (*Sprince, et al., 2011*). In the last few years it has been recognized that one of the main sources of environmental pollution is waste. It has become a major environmental problem because many types of waste do not break down. One of the possibilities of utilizing waste is recycling, which would not only save natural resources, but also decrease the amount of deposited waste. Glass waste requires recycling. (*Sprince, et al., 2011).* One of the solutions would be to recycle the lamp glass by using it in concrete production, where it can partly replace fine sand or cement and thus help create a new construction material. *(Mageswari et al., 2010).*

Nowadays nano-particles of clay minerals are used in production of polymeric nanocomposite in order to improve mechanical characteristics. Investigations on modifying concrete compositions by nano particles are carried out in present time in different countries. It is proved that nanosized silicium dioxide particles allow to achieve very dense microstructure and to improve performance characteristics of concrete (*Maksimovs R.D.et al., 2006*).

In the design of concrete structures, the two main design objectives are strength and serviceability. A structure must be strong enough and sufficiently ductile to resist, without collapsing, the overloads and environmental extremes that may be imposed on it *(Gilbert et al., 2011).* One type of strain that plays a major role in successful and continuous use of structures is creep – deformations that appear due to long-term loading of the structural element (*Rilem TC 107-CSP, 1998*). Creep can be defined as a time-dependent part of the strain resulting from stress (*Neville et al., 1983).*

2. MATERIALS AND METHODS

One of the goals of the experiment was to find out whether the new concrete compositions can be competitive and whether its physical and mechanical properties are equivalent to those of ordinary concrete. The object of this experimental study was concrete made with lamp glass powder (LGP) obtained from fluorescent lamp waste and montmorillonite clay mineral nano particles (MNP). The experiment consisted of replacing cement with lamp glass powder (LGP) in amounts of 0, 20 and 40 per cent and montmorillonite clay mineral nano particles (MNP) in amounts of 1per cent of the total cement volume. Other raw materials used for this study were natural coarse diabase aggregate, fine aggregate quartz sand and normal portlandecement CEM I 42.5 N. Standard sample cubes 100x100x100 mm and prisms 40x40x160 mm were produced in order to investigate the mechanical characteristics of the material (Sprince, et al., 2011). At the beginning of the test, the samples were 51 and 57 days old and they were kept under constant load for 90 days and for creep recovery they were kept without load for 30 days. The tests were conducted in two extreme conditions. In one case no moisture exchange with the environment was permitted, which was ensured by protecting the specimens against desiccation, and in the other case drying was permitted under conventional conditions, by protecting the specimens against moisture. They were kept in a dry atmosphere of controlled relative humidity in standard conditions: temperature 23 ± 1ºC and relative humidity 25 ± 3% (*Sprince, et al., 2011).*

The creep was measured in hardened concrete specimens subjected to a uniform, constant compressive stress σ_{c0} applied at time τ_0 and equal to 40 per cent of the characteristic compressive strength of concrete, i.e. σ_{c0}= 0.4 *f* (*Rilem TC 107-CSP, 1998).*

3. RESULTS AND DISCUSSION

Strength tests were carried out on the cubes after 7, 28, 42 and 58 days of hardening in standard conditions.

The modulus of elasticity was determined by measuring the deformations on the sides of the specimens according to Hooke's law.

Tab. 1 Mechanical properties of concrete compositions

Specimen	Age, days	Modulus of elastisy, GPa	Elastic strain $\varepsilon\,(\cdot 10^{-3})$	Basic creep $\varepsilon\,(\cdot 10^{-3})$	Creep coefficient (90 days)	Recoverable creep $\varepsilon_{r,e}\,(\cdot 10^{-3})$ (30 days)	Recoverable creep $\varepsilon_{r,c}\,(\cdot 10^{-3})$ (30 days)
Reference	51	32,5 (dry)	0,8 (dry)	2,4 (dry)	3 (dry)	1,2 (dry)	1,1 (dry)
Reference	51	31,6 (moist)	0,8 (moist)	3,8 (moist)	5,0 (moist)	3,2 (moist)	3,2 (moist)
20% LGP	51	21,9 (dry)	0,9 (dry)	3,5 (dry)	4,0 (dry)	2,6 (dry)	2,6 (dry)
20% LGP	51	27,9 (moist)	0,8 (moist)	2,3 (moist)	2,9 (moist)	1,5 (moist)	1,4 (moist)
40% LGP	51	27,2 (dry)	0,7 (dry)	1,9 (dry)	2,7 (dry)	1,2 (dry)	1,1 (dry)
40% LGP	51	30,7 (moist)	0,9 (moist)	2,4 (moist)	2,7 (moist)	1,7 (moist)	1,6 (moist)
Reference	57	42,3 (dry)	0,6 (dry)	2,4 (dry)	4,2 (dry)	1,8 (dry)	1,8 (dry)
Reference	57	36,5 (moist)	0,7 (moist)	3,0 (moist)	4,6 (moist)	2,7 (moist)	2,7 (moist)
MNP	57	32,2 (dry)	0,8 (dry)	2,9 (dry)	3,9 (dry)	2,4 (dry)	2,4 (dry)
MNP	57	37,7 (moist)	0,6 (moist)	3,4 (moist)	5,3 (moist)	2,6 (moist)	2,7 (moist)

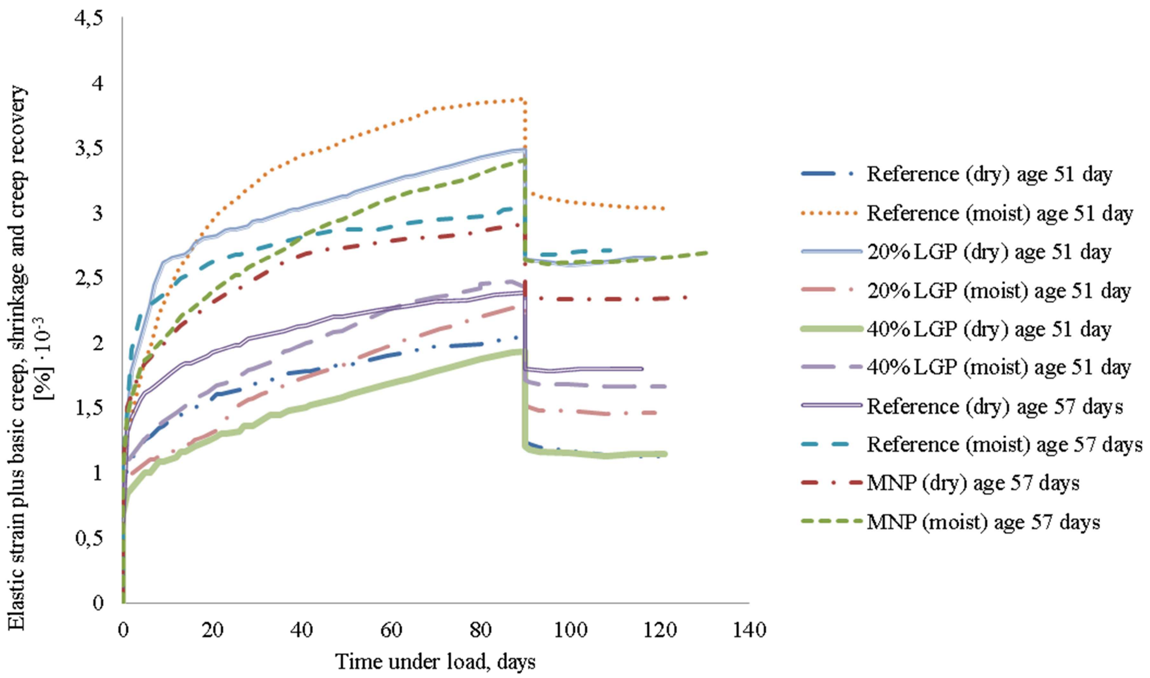

Fig. 1 Elastic strain and basic creep of new concrete mixtures

When concrete is subjected to a sustained stress, creep strain develops gradually in time as shown in Figure 1. Creep increases with time at a decreasing rate. In the period immediately after initial loading, creep develops rapidly, but with time the rate of increase slows considerably. Figure 2 shows recoverable and irrecoverable creep as well.

The final creep coefficient is a useful measure of the creeping capacity of concrete. The results of the experiments are presented in Table 1.

4. CONCLUSIONS

This experimental study proves that lamp glass powder and montmorillonite mineral nano particles can be successfully in the production of concrete thus potentially decreasing the amount of deposited waste and the use of cement, which would lead to a reduction of carbon dioxide release into the atmosphere.

In the future, the physical and mechanical properties of this new concrete containing lamp glass powder and montmorillonite mineral nano particles should be investigated in a more detailed way. In order to decrease the dispersion of results, the number of specimens and tests should be increased. The results of this experiment can be used to predict creep deformations.
Elastic, long-term deformations (creep) and creep recovery testing was carried out, and the modulus of elasticity, the compression strength of ordinary concrete and of concrete containing lamp glass powder and montmorillonite mineral nano particles were determined. Basic creep test results were summarized on the 90th day and creep recovery on the 30th day.
Fine lamp glass powder and montmorillonite mineral nano particles caused a long-term hardening effect. Specimens in which cement was partially replaced with lamp glass powder showed a larger increase of compression strength than reference concrete specimens, and the compression strength of 58 days old concrete specimens containing LGP was larger than that of reference concrete specimens. Reference concrete specimens and specimens containing MNP showed a similar increase of compression strength at both ages.

The modulus of elasticity in dry conditions was larger for reference concrete specimens. For specimens containing LGP the larger modulus of elasticity was achieved by hardening in moist conditions. The modulus of elasticity in dry conditions was larger for reference concrete specimens but in moist conditions the larger modulus of elasticity was for specimens containing MNP.

Under constant mechanical loading, the strain of concrete increases significantly with the loading duration. Creep strain increases with time at a decreasing rate. In the period immediately after initial loading, creep develops rapidly, but with time the rate of increase slows significantly. Concrete specimens cured in moist conditions showed larger increase of basic creep deformations. Recoverable and irrecoverable creep deformations were determined.

The creep coefficient increases with time at an ever-decreasing rate. The final creep coefficient is a useful measure of the creep capacity of concrete. On the 90th day of testing the value of the basic creep coefficient reaches 2.7 to 5.0 times the value of the instantaneous strain.

5. ACKNOWLEDGEMENT

This work has been supported by the European Social Fund within the scope of the project “Support for the Implementation of Doctoral Studies at Riga Technical University”.

6. REFERENCES

Gilbert R.I., Ranzi G. Time-Dependent Behaviour of Concrete Structures (2011) *Span Press*, London and New York, pp.11, 25- 27,29,30.

Mageswari M. and Vidivelli B. (2010) The Use of Sheet Glass Powder as Fine Aggregate Replacement in Concrete. The Open Civil Engineering Journal, 4, pp. 65-71.

Maksimovs R.D., Gaidukovs S., Zicans J., Kalnins M., Plume E., Spacek V., Sviglerova P. (2006) Nanocomposites based on styrene-acrylate copolymer and organically modified montmorillonite. Mechanical properties. Mechanics of Composite Materials, Riga, Latvia.

Neville, A.M., Dilger, W.H. and Brooks, J.J. (1983) Creep of Plain and Structural Concrete. *Construction Pres*s, 1983, London and New York.

Rilem TC 107-CSP (1998): Creep and shrinkage prediction models: principles of their formation. Measurement of time-dependent strains of concrete.Materials and Structure, Vol. 31, pp. 507-512.

Sprince A., Pakrastinsh L., Korjakins A., Shakhmenko G. (2011) Effect of Montmorillonite Nano Admixture on Long-term Deformations of Concrete. Scientific Journal of Riga Technical University, Construction Science, Vol.12, Riga Technical University, Riga, Latvia.

Sprince A., Korjakins A., Pakrastinsh L. (2011) Creep behaviour of concrete with glass waste microfiller, Proceeding of 8th International scientific conference Environment. Technology. Resources. Rezekne University, Rezekne, Latvia.

Sprince A., Pakrastinsh L., Korjakins A. (2011) Experimental study on creep of new concrete mixtures, Proceeding of International scientific conference Civil Engineering’11, Latvian University of Agriculture, Jelgava, Latvia.

BASALT FIBER REBAR IN CONCRETE – EXPERIMENTS AND CONCLUSIONS

Ferenc Zámolyi,
Bautechnisches Institut (BTI)
AUSTRIA, 4048 Puchenau (bei LINZ), Karl Leitl Strasse 2

SUMMARY

The basalt rebar is capable of reinforcing constructive concrete components; however, the method for determining the load bearing ultimate limit state for steel reinforced beams, cannot be used in this case. This article describes the need for a simple calculation method and tries to construct one, in which a serviceability limit state (width of the cracks) converts into a load bearing limit state.

1. INTRODUCTION: Rock fiber rebar reinforced concrete

Mineral fiber rebars were used in the USA since a decade for reinforcing concrete motorways at the expansion joints, on account of the need for corrosion resistance. For example, in 2010, in North-Ireland (*County Fermanagh*), a 22 m concrete-deck of a bridge was built, with a basalt fiber reinforcement. (*see Today´s Concrete Technology – Internet home page).* The material was sourced from Cheboksary, Chuvash Republic, Russia. The „Technobasalt" company sells basalt rebar, textile rowing and fiber in Europe made of raw material from Russia. Other Countries, as for instance Austria, are trying to use the basalt rebar for reinforcing constructive parts of concrete buildings.

Our laboratory (BTI) is carriyng out tests since a decade on different fiber-reinforced concrete trial samples by Austrian companies. The only kind, which is capable of building load bearing components, is the basalt reinforced polymer rebar (since 2010 tested). This rebar has a higher ultimate strength, than normal rebars. Furthermore, it is corrosion resistant, like stainless steel, whereas it is about 40% cheaper. The fire resistance seems to bee much better than any other rebars used before. Its alkali resistance is better than this feature of the AR-glass fiber. The specific weight of the basalt rebar is almost 3 times less than the density of steel. The BTI tested some concrete beams (span length about 5 m) and made pullout tests on rebars, produced with different materials.

2. ACCORDANCES AND DIFFERENCES: Calculation - Measurement

Several tests must start with a prediction of the load bearing capacity of the specimen. As the first part of Fig. 1 (blue frame) demonstrates, the calculation of the maximum moment of the 5 m normal reinforced beam with a well known approximation method, was in accordance with the measured value.

In the second part (violet, dashed line and frame) we took in account, that the strain-stress curve of the basalt fiber has a linear behavior almost up to the ultimate strength and it has a Young modulus which is 4 times less than steel (Fig. 2).

The calculation for the specimen with 2x11 mm basalt rebar, revealed the same load bearing moment, than for the beam with a 3x10 mm normal rebar. Yet, the measured ultimate moment for the basalt reinforced beam was 30% less! Neither the compressed concrete, nor the basalt rebar was destroyed. The cracks were bigger and we could hear the movement of the basalt rebar in the beam.At the end, the concrete coverage of the basalt rebar jumped down and the deflection became very large. The beam could not be loaded anymore (Fig. 3).
Therefore, this conclusion can be drawn: probably the bond stress is very low for the basalt rebar. Pullout tests were carried out and they indicated, that the bond stress is indeed less; however, the difference is not significant! (Fig. 5). It is more likely, that the minor Young modulus is responsible for the great cracks.

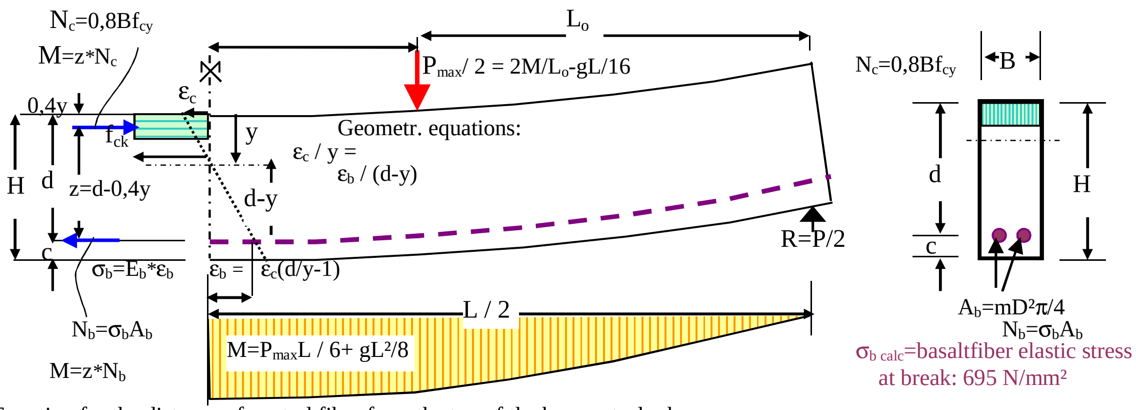

Equation for the distance of neutral fibre from the top of the beam, steel rebar :

I. $N_c = 0{,}8Bf_{cy} = N_s = f_{yk} A_s$; --> $y_s = f_{yk}A_s / (0{,}8B*f_c)$

M_{calc}= 32,1 kNm = $M_{measured}$

Equation for the distance of neutral fibre from the top of the beam, mineralfiber rebar (Eq I.): M_{calc}=32kNm=1,3$M_{measured}$

Equlibrium equations: I. $N_c = 0{,}8Bf_{cy} = N_b = s_b A_b = E_b\varepsilon_c(d/y-1)A_b$; II. $M = P_{max}L / 6 + gL^2/8 = z*N_c$

$y^2\, 0{,}8Bf_c + y*A_bE_b\varepsilon_c - d*A_bE_b\varepsilon_c = 0$; --> $y_b = d*k*[\,(1+4/k)^{1/2}-1]/2$ where $k = \rho_{bc}k_{bc} /0{,}8$ and $\rho_{bc}=A_b/(Bd)$; $k_{bc}=E_b/(f_c/\varepsilon_c)$

Fig. 1 .Simplified calculation of load bearing capacity

Concrete	Steel rebar:		Basalt rebar:	
f_{ck}= 30 N/mm²	f_{yk}= 550 N/mm²		f_{bk}= 700 N/mm²	
B = 100 mm	m_sD_s = 3*10 mm	measured moment	M_bD_b = 2*11 mm	measured moment Basalt fiber reinforced
H = 300 mm	$M_{s\ calc}$=32,1 kNm	=$M_{s\ meas}$=32,1 kNm	$M_{b\ calc}$=32 kNm >>	$M_{b\ meas}$=23,4 kNm !!!

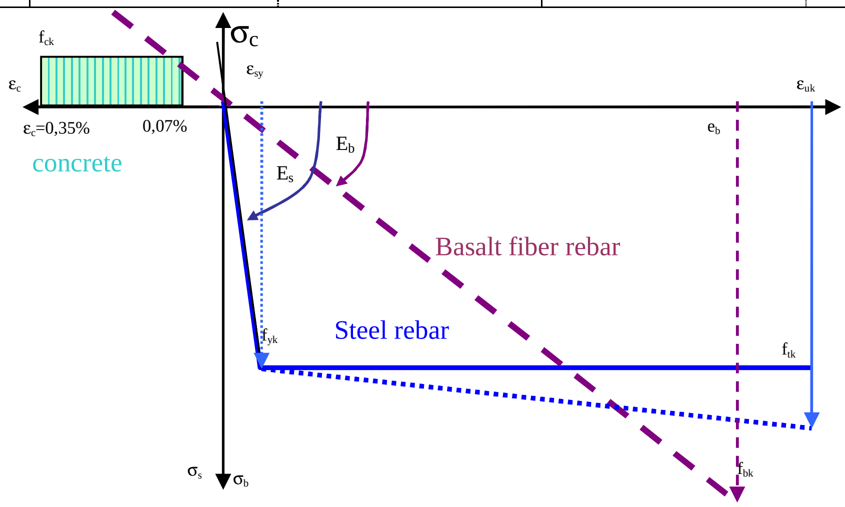

Fig. 2 Simplified Material Curves

Fig. 3 Limit state (beam with basalt rebar)

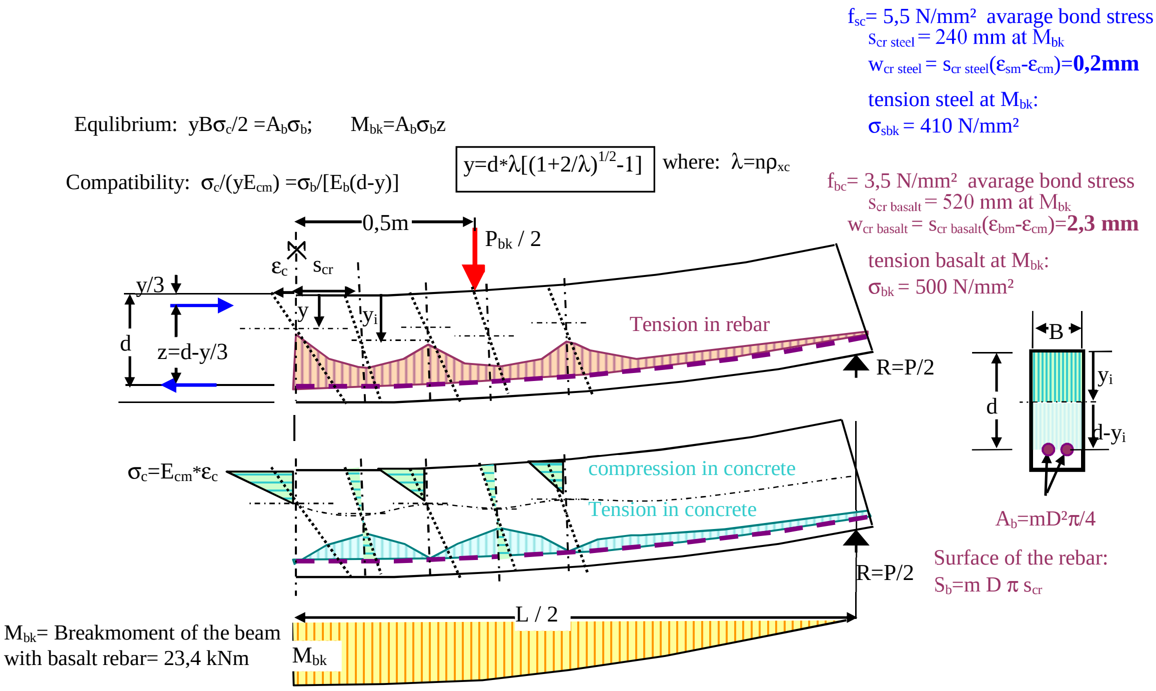

Fig. 4 Calculation of crack width and crack distance

Concrete and rebar are in elastic state

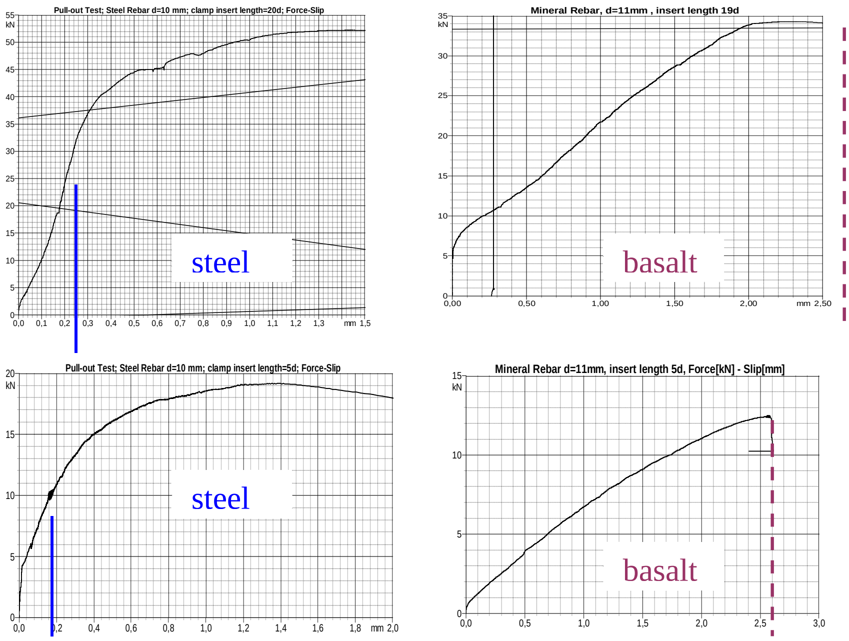

Fig. 5 Bond force – slip diagrams

Fig. 6 Slip Measurement
on the test beam with steel rebars

3. A SERVICEABILITY LIMIT STATE CONVERTS INTO AN ULTIMATE LIMIT STATE

The limitation of the crack width is normally a serviceability limit state. In order to reduce the corrosion of normal steel rebars, it is necessary to control the crack width with artificially defined crack width values, according to the environment. The corrosion is no problem for the basalt fiber, but due to the great cracks, the load bearing capability is vanishing before reaching the ultimate compressive strain of concrete, or the ultimate tensile strength of the basalt fiber rebar. The model (Fig. 4.) displays, that the predicted (and as well observed) crack widths during the destroying moment of the beam with basalt fiber, are only approximately 0,2mm wide, at the beam with normal steel. The calculation takes into account the bond stress and the **Young modulus** of reinforcement.

The predicted approx. 2.3 mm crack width at the basalt fiber reinforced beam, causes the vanishing of bond forces: the maximum of the bond shear stress is achieved at this slip value (Fig. 5: bond force-slip diagrams at the pullout tests and Fig. 6: measurement of slip on the beams). We can create a “physical” criterion for the crack width, based on the Young modulus of the basalt fiber, as well as the bond stress and slip from the pullout tests. This gives a simple method to predict the load bearing capacity of basalt fiber rebar reinforced concrete beams. The normal force/surface shear force ratio is better for rebars with small diameter: we suggest to use several thin rebars instead of one thick rebar (the same advice as for the normal steel reinforcement for keeping the cracks small).

4. CONCLUSION

The basalt fiber rebar is a very useful reinforcement for concrete in case of the need for light weight, corrosion- and fire resistance. The load bearing limit for constructive components must be calculated from the “physical” ultimate crack width. This signifies that the high ultimate strength of the basalt fiber rebars cannot be reached and more rebars with small diameter have to be used.

Development objectives in the near future:
- improving the bond strength between concrete and basalt fiber rebar
- improving the Young modulus of the basalt fiber rebar
- controlling of the alkali resistance and durability of the basalt fiber rebar
- standardizing the calculation of the load bearing limit state for constructive components

5. REFERENCES

Balázs, G. L. at all 1985 – Dolgozat a beton repedéstágasság számításáról. UVATERV

Leutbecher, T. (2007) „Rissbildung und Zugtragverhalten von mit Stabstahl und Fasern bewehrtem Ultrahochfesten Beton (UHPC)“, zur Erlangung des akademischen Grades eines Doktors der Ingenieurwissenschaften genehmigte Dissertation

Wei-Chong Liao, Han-Yang Lin, Meng-Chang Lee and Pai-Heng Hung, Department of Civil Engineering, Feng Chia University, Taiwan: „The Pullout Test of a FRP Rebar within a Nanoclay/Concrete Block“

Ibell, T. University of Bath; Pedro Silva, University of Missouri-Rolle, USA: „Design of Continuous FRP-Strengthened Concrete Structures allowing Moment Redistribution“

MODULUS OF ELASTICITY AND COMPRESSIVE STRENGTH - STATISTICAL ANALYSIS OF CONCRETE C45/55 XF2 FOR PRESTRESSED PRECAST BEAMS

Petr Huňka[1], Miroslav Vokáč[1], Karel Kolář[2], Petr Bouška[1], Stanislav Řeháček[1], Jiří Kolísko[1], Pavel Reiterman[2],

[1] *Klokner Institute, CTU in Prague*
Experimental Department
166 08 Prague, Solinova 7

[2] *Faculty of Civil Engineering, CTU in Prague*
166 08 Prague, Thakurova 7

SUMMARY

Random behavior of concrete C45/55 XF2 used for prefabricated pre-stressed bridge beams is described on the basis of evaluating of vast set of measurements. Detailed statistical analysis is carried out on 141 cylinders with sizes 150×300 mm, produced from October 2010 to June 2011. Only one worker took all specimens during the whole period and the following measuring of modulus of elasticity and compressive strength of concrete was carried out in Klokner Institute laboratories. The measuring takes place at the age of 28 days, only one testing machine with the same capping method is used. Suitable theoretical models of division are determined on the basis of tests in good congruence, with the use of $\chi^2$and Bernstein's criterion.

1. INTRODUCTION

Apart from the compressive strength which is a basic parameter for design of concrete structures, we can more often meet with the requirement to determine the value of static modulus of elasticity of concrete and its development in time. Justification of increased interest in monitoring the elastic modulus is obvious, because one of the main characteristics of each material is the modulus of elasticity E_c. Modulus of elasticity describes the ability of concrete to act flexibly to a certain degree under a given load. Modulus also determines how much the concrete (material) will be deformed under load. Modulus enters the static calculations and is closely related to many other physical and mechanical properties of concrete such as creep, shrinkage, frost resistance, etc.

In the paper, 141 results of tests of concrete C45/55 XF2 are presented, which have been running in laboratories of Klokner Institute in the long term (October 2010 to June 2011). These tests are a part of the check of the production of precast prestressed bridge beams produced by Skanska, division Prefa. The beams are tested for the compressive strength of concrete and particularly static modulus of elasticity. The prefabricated beams are used in bridges under the management of The Road and Motorway Directorate of the Czech Republic (RSD). For each beam, the test of modulus of elasticity is always carried out on two cylinders (size 150x300mm) produced at the same time as the beam *(Huňka, Kolísko, 2008).* Test specimens were made into steel moulds, compacted on vibratory table, were demoulded after 24 hours and the samples are stored in water according to ČSN EN 12390-2 up to the test, which takes place within 28 days. Compressive surfaces are capped by a mixture of sulphur, ash and sand. The measurement of the static modulus of elasticity is conducted in accordance with ČSN ISO 6784.

2. STATISTICAL ASSESSMENT

Elementary concepts and techniques of the theory of probability and mathematical statistics applicable to civil engineering are available in a number of standards *(Huňka, Jung, Kolář, Řeháček, 2010).* The sample characteristics – mean, standard deviation, coefficient of variation and skewness – are then estimated by the classical method.

Compressive strength:
The sample mean $m = (\Sigma\, x_i) / n$ = **61.1 MPa**
The sample standard deviation $s = (\Sigma\, (x_i - m)^2) / (n - 1))^{0,5}$ = **6.5 MPa**
The sample coefficient of skewness $\omega = [n\, (\Sigma\, (x_i - m)^3) / (n\text{-}1) / (n\text{-}2)] / s^3$ = **-0.23**
The coefficient of variation is **10.6%.**

Modulus of elasticity:
The sample mean $m = (\Sigma\, x_i) / n$ = **41.0 GPa**
The sample standard deviation $s = (\Sigma\, (x_i - m)^2) / (n - 1))^{0,5}$ = **2.2 GPa**
The sample coefficient of skewness $\omega = [n\, (\Sigma\, (x_i - m)^3) / (n\text{-}1) / (n\text{-}2)] / s^3$ = **+0.21**
The coefficient of variation is **5.4%**.

Density of harden concrete:
The sample mean $m = (\Sigma\, x_i) / n$ = **2432 kg/m^3**
The sample standard deviation $s = (\Sigma\, (x_i - m)^2) / (n - 1))^{0,5}$ = **29,8 kg/m^3**
The sample coefficient of skewness $\omega = [n\, (\Sigma\, (x_i - m)^3) / (n\text{-}1) / (n\text{-}2)] / s^3$ = **-0.18**
The coefficient of variation is **1.2%**.

Generally, the consideration of asymmetry to determine properties is recommended whenever the coefficient of variation is greater than 0,1 or the coefficient of skewness is outside the interval <-0.5, 0.5>. Due to higher skewness, the sample should be tested for outliers. Testing for outliers is a very delicate subject, because outliers should be identified by other than statistical reason. In general, true outliers can distort the results considerably for small samples. Histograms of the obtained measurements are indicated in Fig. 1 - 3.

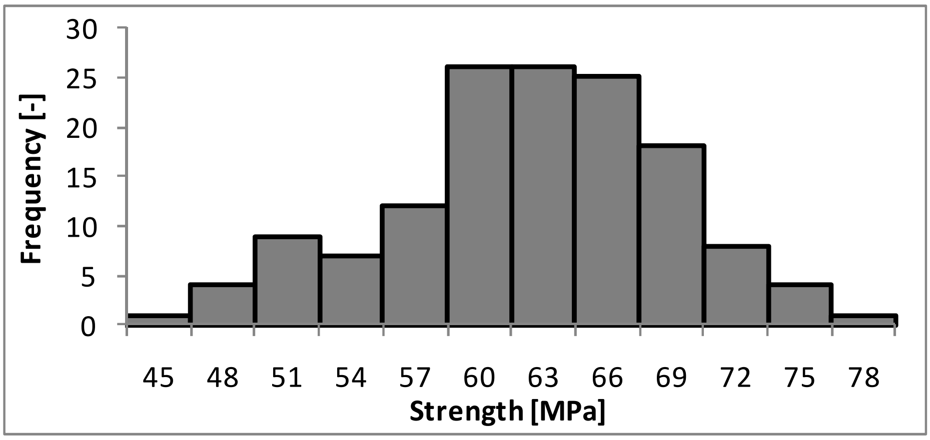

Fig. 1 Histogram of compressive strength

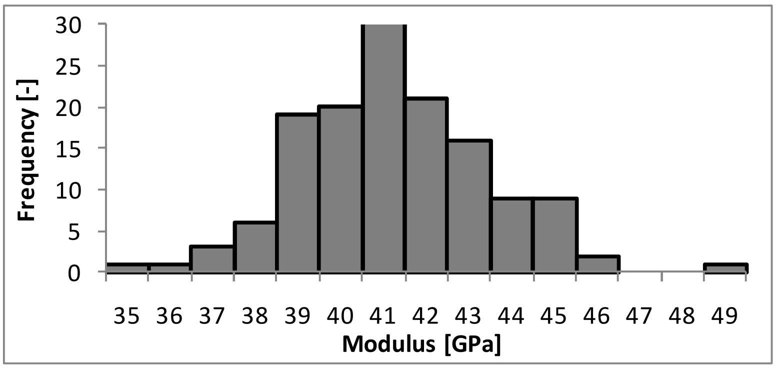

Fig. 2 Histogram of modulus of elasticity

3. GOODNESS OF FIT TEST FOR DISTRIBUTION FUNCTIONS - STRENGTH

The software Statrel and EasyFit was used for the calculation. Distribution tests are also very sensitive to outliers. This again implies some iteration with respect to outliers. Three types of distribution test are considered in this paper see tab 1:

Tab. 1 Results of goodness fit test - strength

Test / Distribution	Kolmogorov-Smirnov	Anderson-Darling	Chi-Squared
Beta	0,05276	0,36095	7,69633
Normal	0,05508	0,44101	6,36351
Lognormal (3P)	0,05837	0,56446	6,78809
Gamma	0,06343	0,76435	6,96808
Lognormal	0,07199	0,98133	8,37016

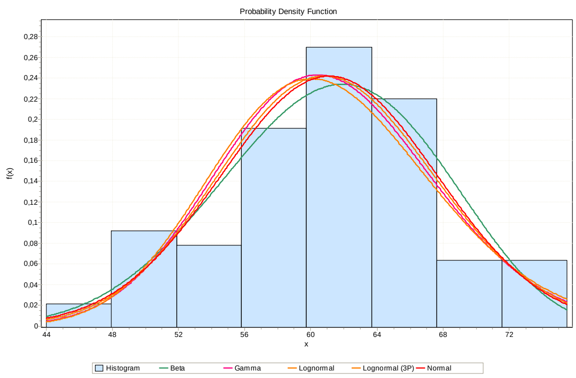

Fig. 3 Histogram of concrete strength and the considered theoretical models

4. GOODNESS OF FIT TEST FOR DISTRIBUTION FUNCTIONS – MODULUS

Tab. 2 Results of goodness fit test - modulus

Test / Distribution	Kolmogorov-Smirnov	Anderson-Darling	Chi-Squared
Beta	0,07958	0,55997	23,78889
Normal	0,08542	0,61317	29,47595
Lognormal (3P)	0,07419	0,54010	14,40501
Gamma	0,07831	0,55903	14,42329
Lognormal	0,07478	0,54163	14,40617

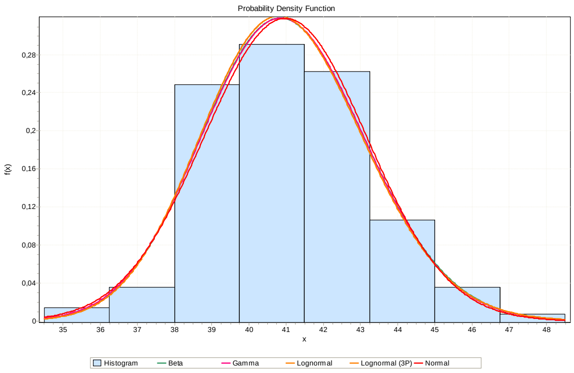

Fig. 4 Histogram of modulus of elasticity and the considered theoretical models

5. CONCLUSIONS

Concrete strength:

- Beta and normal distributions have the lower bound at the origin may be a suitable model for concrete strength.
- The sample has a relatively high skewness. This is one of the reasons why the design value of the material property should be preferably determined on the basis of the characteristic value which is not significantly sensitive to the distribution asymmetry.

Modulus of elasticity:

- Mean value m = 41.0 GPa, standard deviation s = 2.2 GPa, coefficient of skewness $\omega = +0.21$.
- In the case of modulus of elasticity, the mean value is the design value of the material property for structure design. This is the main difference in comparison with compressive strength.
- It seems that all distributions are close together. Of course, the mean value is independent of the choice of distribution function.

6. ACKNOWLEDGEMENTS

The research work presented in this paper has been supported by the CTU SGS10/228/OHK1/2T/31 “The Study of Testing and Technological Influences on Test Results of Moduls of Elasticity of Modern Concrete

6. REFERENCES

Huňka P., Kolísko J., (2008), The Study of Specimen Shape and Size on Test Result of Modulus Elasticity. Conference 15. Concrete days 2008. ČBS Servis. s.r.o... pp. 386–381.

Huňka P., Jung K., Kolář K., Řeháček S., (2010) Statistical Analysis of Modulus of Elasticity and Compressive Strength of Concrete C45/55 for Presstresed Precast Beams Testing and Quality in Civil Engineering. ISBN 978-80-214-4144-6. Brno University of Technology. pp. 65-72

EN 1990 Eurocode - Basis of structural design. CEN 2002.

EN 1991-1-1 Eurocode 1 Actions on structures. Part 1-1 General actions. Densities. self-weight. imposed loads for buildings. CEN 2002.

RECOMMENDED CONCRETE PROPERTIES FOR HIGH STRENGTH STEEL REINFORCEMENT

Sherif Yehia, Mohammad AlHamaydeh, Shahinaz El Kalie, Yasmien Ibrahim
American University of Sharjah
Sharjah, United Arab Emirates

SUMMARY

The use of high-strength steel (HSR) as reinforcement in concrete structures has advanced significantly in the last 40 years. Ductile high strength steel which has a yield strength ranging from 520 to 1000 MPa is commercially available due advances in nontechnology. However, The ACI-318-08 building code requirements for structural concrete specifies that the yield strength must be taken as the stress corresponding to a strain of 0.35% when high strength rebars [f_y more than 410MPa] are to be used. This condition limits the yield strength to be less than 680MPa. In addition, a recent study concluded that for serviceability and cracking control, stresses in steel should be limited to 50% of the yield strength to have similar performance of Grade 60 steel. Therefore, this paper provides a discussion about concrete properties considered necessary to fully utilize high strength steel in design.

1. INTRODUCTION

The behavior of a concrete member with HSR must be evaluated to ensure that the concrete strain does not exceed 0.003 before adequate member ductility is achieved. In addition, considerations for preventing brittle or premature failure are at the same level of importance.

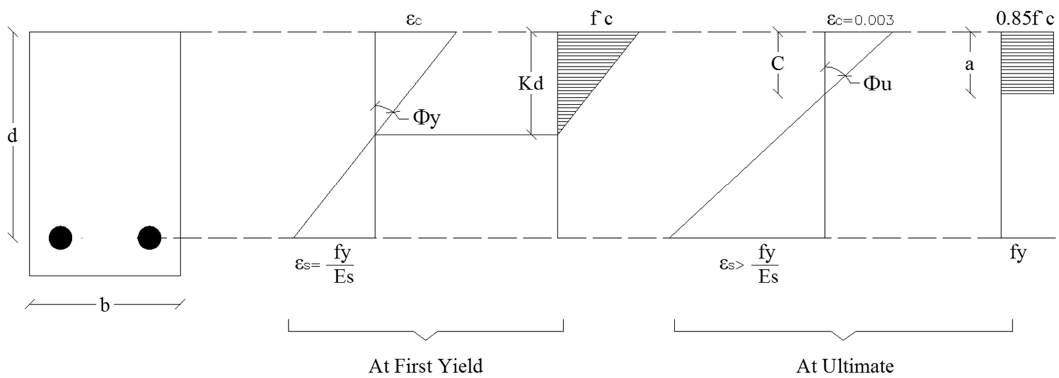

Fig. 1 Strain and stress diagrams at first yield and at ultimate

Strain and stress diagrams at first yield of tension steel and at ultimate are illustrated in Figure 1. Ductility behavior of a concrete section in the limit state design is defined as the ratio of the ultimate curvature to the curvature at first yield.

$$\frac{\phi_u}{\phi_y} = \frac{\varepsilon_{cu}}{f_y/E_s}\,\frac{d(1-k)}{c} = \frac{0.003}{f_y/E_s}\,\frac{d(1-k)}{a/\beta_1} \tag{1}$$

where φ_y is the curvature at first yield, f_y = yield strength of steel, E_S= modulus of elasticity of steel, d = effective depth of tension steel, and k = neutral axis depth factor, $\varphi_u$is the ultimate curvature, ε_{cu}= concrete strain in the extreme fiber at ultimate, a = depth of the equivalent rectangular stress block, c = the neutral axis depth, and $\frac{a}{c} = \beta_1$

The influence of the section and material properties on the $\frac{\varphi_u}{\varphi_y}$ can be summarized [refer to Equation (1)] as follows:

- An increase of yield strength decreases the ductility because it increases the yield strain ($\frac{f_y}{E_S}$) therefore, $\frac{\varphi_u}{\varphi_y}$ is decreased.

- An increase of the concrete strength will increase the ductility because k and a are decreased, therefore, φ_y is decreased and $\frac{\varphi_u}{\varphi_y}$ and is increased.

The above discussion shows that the current design concept and procedures may not be applicable with the use of high strength steel as reinforcement unless special concrete properties are specified. In addition, serviceability and cracking control are the main concern when high strength steel is considered in reinforced concrete design. Number, spacing, and width of cracks and bond between steel and concrete are all durability related issues. Stress level in steel after concrete cracking is the main factor affecting crack width. Other parameters such as compressive strength, bond properties, shape of strain distribution, and reinforcement details (bar diameter, spacing, arrangement, and concrete cover) also contribute and influence crack width (*Ghali, et. al. 2002*). Control of cracking could be partially achieved by improving concrete properties. High performance, steel fiber, high strength, and ultra-high strength are different concrete types which could be considered with high strength steel. Improving the tensile strength of concrete is another approach for cracking control. The main objective of this paper is to formulate, through an extensive literature search, an answer for the following question: "is there recommended concrete properties for high strength steel reinforcement?" Therefore, characteristics of different concrete types and properties of high strength steel reinforcement (*ASTM-A1035*) will be presented. In addition, considerations when high strength steel to be used in the design will be briefly discussed.

2. MATERIAL PROPERTIES

2.1 Concrete

2.1.1 High performance concrete (HPC)

High Performance Concrete (HPC) is a specialized series of concretes designed to provide performance benefits and cost benefits in the construction of concrete structures. The performance benefits is the longer life in severe environments, better volume stability, high degree of toughness, high early strength, and long-term mechanical properties; in addition to, ease of placement and consolidation without affecting strength. The cost benefit is achieved by less material used, fewer beams, reduced maintenance, extended life cycle and aesthetics. HPC is usually evaluated based on two criteria, strength and durability. Strength criteria include compressive strength, modulus of elasticity, shrinkage, creep, whereas durability criteria deal with freeze-thaw, scaling, abrasion, chloride permeability. Four types of HPC were developed; very early strength (VES), high early strength (HES), very high strength (VHS), fiber reinforced (HES + fiber). These types were classified based on minimum strength criteria, water-cementitious ratio, and minimum durability factor (*U.S Department of transportation Federal Highway Administration, 2011).*

2.1.2 High strength concrete (HSC)

High-strength concrete mixtures were achieved by reducing porosity, inhomogeneity, and microcracks in the hydrated cement paste and the transition zone. Compressive strength is in the range of 50 to 100 MPa (7 to 14 ksi), in addition, the strain corresponding to the maximum stress increases with strength *(Mehta and Monteiro 2006*). However, for design purposes, it is found that for compressive strength up to 124 MPa (18ksi), compressive strain limit (ε_{cu}) of 0.003 is applicable (*Rizkalla, et. al. 2007*)

2.1.3 Ultra-High performance concrete (UHPC)

UHPC has high compressive strength, obtained through dense particle packing, implying high durability, improved freezing-and-thawing resistance, increased resistance against various chemicals, and higher penetration resistance. UHPC has a compressive strength that can be more than 150 MPa (22ksi), in addition, UHPC could be produced with or without fiber. Special curing and heat treatment were required at early development (*Graybeal 2006*); however, Wille et. al. (*2011*) produced UHPC without the need of heat treatment or special materials. Compressive strain at peak stress was found to be in the range of 0.0035 to 0.0041 depending on the curing conditions (*Graybeal 2006*).

2.2 Steel

2.2.1 Conventional Steel

Deformed reinforcing bars which are commonly used in the construction industry meet the following ASTM specifications; (a) Carbon steel: ASTM A615; (b) Low-alloy steel: ASTM A706; (c) Stainless steel: ASTM A955; (d) Rail steel and axle steel: ASTM A996. Bars from rail steel shall be Type R. Specified yield strength is 410 MPa (60 ksi) and yield strain is defined by $\varepsilon_y = \frac{f_y}{E_s}$. In case of f_y exceeding 410 MPa (60 ksi), the yield strength shall be taken as the stress corresponding to a strain of 0.35 percent (*ACI 318-08:3.5.3.2*).

2.2.2 High strength steel reinforcement (HSR)

HSR technically known as ASTM-A1035 has a yield strength ranging from 75 to 150 ksi and has a high corrosion resistant which consequently enhances the long-term durability of the structure. ASTM-A1035 steel bars have a corrosion resistance 5 to 6 times greater than that of conventional carbon steel bars based on the critical chloride threshold level (CCTL) (Faza, et. al. 2008). However, ACI 318-08 limits yield strength to that corresponds to a strain of 0.35 percent. Furthermore, ACI 318-08:9.4 specifies for flexural design strength of reinforcement that f_y and f_{yt} not to exceed 550 MPa (80 ksi), while f_y and f_{yt} should be taken equal 410 MPa (60 ksi) for shear, torsion, shear friction method, shells, folded plates, special moment frames, and special structural walls reinforcement. f_y and f_{yt} could be used equal to 680 MPa (100 ksi) as transverse reinforcement or spiral reinforcement

3. DISCUSSION

The recent study by Shahrooz et. al. (*2011*) which concluded that if HSR with f_y equals 680 MPa (100 ksi) to be used in flexural design a change of the tension control and compression control limits from 0.005 and 0.002 to 0.009 and 0.004, respectively. This change will ensure that the cross section will have ductility behavior concrete thus controlling the failure due to concrete crushing. In addition, several other recommendations were presented in their report to limit f_y to 410 MPa (60 ksi) for shear-friction design. However, for crack control and reinforcement spacing, it is recommended to use stresses in steel at service loads (f_s) to $0.5f_y$ [340 MPa (50 ksi)]. The finding by Shahrooz et. al. (*2011*) and other available literature suggest that the compressive strain should be improved by utilizing steel fiber or by the addition of steel in the compression zone to allow the HSR to reach an acceptable level of stress before concrete crushes.

4. CONCLUDING REMARKS

This paper, through an extensive literature search, provides some highlights about the limitations of utilizing HSR in the construction industry. The emphasis was given to concrete properties to improve the compressive and tensile strengths. The use of steel fiber or high strength concrete could provide a solution to improve compressive strain and concrete tensile strength. The authors believe that the HRS has a good potential in the market if a clear design procedure which satisfies strength and serviceability requirements is adopted.

5. REFERENCES

Faza, S, Kwok. J and Salah, O. (2008),"Application of High-Strength and Corrosion-Resistant ASTM A1035 Steel Reinforcing Bar in Concrete High-Rise Construction", CTBUH 8th World Congress

Shahrooz, B.H., Miller, R.A., Harries, K.A., Russel, H.G., (2011)," Design of Concrete Structures using High Strength Steel Reinforcement", *National Cooperative Highway Research Program Report 679*

Federal Highway Administration, What is High Performance Concrete (2011). Retrieved June 24, 2011 from, U.S Department of transportation Federal Highway Administration Web site: http://www.fhwa.dot.gov/bridge/hpcwhat.htm

Ghali, A., Favre, R., El-Badry, (2002) Concrete Structures: Stresses and Deformation, 3rd Edition, London; New York : Spon Press, pp 584.

Mehta, P. K., and Monteiro, P.J.M., (2006) Concrete: Microstructure, Properties and Materials," New York : McGraw-Hill, pp 659.

Rizkalla, S., Mirmiran, A., Zia, P., Russell, P., and Robert Mast (2007) Application of the LRFD Bridge Design Specifications to High-Strength Structural Concrete: Flexure and Compression Provisions, *National Cooperative Highway Research Program Report 595*

Graybeal, B. A., (2006) "Material Property Characterization of Ultra-High Performance Concrete," FHWA-HRT-06-103, August, pp 188.

Wille, K., Naaman, A.E., and Parra-montesinos, G. J. (2011). "Ultra-High Performance Concrete with Compressive Strength Exceeding 150 MPa (22 ksi): A Simpler Way," ACI Materials Journal, V. 108, No. 1, January-February, pp. 46-54.

ACI 318.08 - Building Code Requirements for Structural Concrete (ACI 318-08)

ASTM Standard A615, 2009, "Standard Specification for Deformed and Plain Carbon-Steel Bars for Concrete Reinforcement," ASTM International, West Conshohocken, PA, 2009, DOI: 10.1520/A0615_A0615M-09B, www.astm.org.

ASTM Standard A706, 2009, "Standard Specification for Low-Alloy Steel Deformed and Plain Bars for Concrete Reinforcement," ASTM International, West Conshohocken, PA, 2009, DOI: 10.1520/A0706_A0706M-09B, www.astm.org.

ASTM Standard A955, 2011, "Standard Specification for Deformed and Plain Stainless-Steel Bars for Concrete Reinforcement," ASTM International, West Conshohocken, PA, 2011, DOI: 10.1520/A0955_A0955M-11, www.astm.org.

ASTM Standard A996, 2009, "Standard Specification for Rail-Steel and Axle-Steel Deformed Bars for Concrete Reinforcement," ASTM International, West Conshohocken, PA, 2009, DOI: 10.1520/A0996_A0996M-09B, www.astm.org.

IMPACT RESISTANCE OF FIBRE REINFORCED CEMENTITIOUS COMPOSITES

Stanislav Rehacek, Ivo Simunek, Petr Hunka, Jiri Kolisko
Klokner Institute, Czech Technical University in Prague, Czech Republic
Solinova 7, 166 08 Prague, Czech Republic

SUMARY

Fiber-reinforced composite materials are becoming important in many areas of technological application. In addition to the static load, such structures may be stressed with short-term dynamic loads or even dynamic impact loads during their lifespan. Dynamic effects can be significant especially for thin-walled shell structures and barrier constructions. Impact loading of construction components produces a complex process, where both the characteristics of the design itself and the material parameters influence the resultant behavior. It is clear that reinforced concrete with fibers has a positive impact on increasing the resistance to impact loads. However, the assessment of the increase of this resistance has not been sufficiently verified experimentally. Laboratory load tests and first results of impact loads tests are presented.

1. INTRODUCTION - PROJECT OBJECTIVES AND PROGRESS

The goal of the project is to establish new procedures for evaluating the impact resistance of cementitious composites. An appropriate shape of test specimens, ways to support the test specimens and the method of measurement were chosen on the basis of experiments. A suitable form of test specimens was selected on the basis of static load tests of unreinforced test specimens.

The load tests of specimens reinforced with different fibre content of reinforcement were made afterwards.

2. CHOOSE OF THE APPROPRIATE SHAPE OF TEST SPECIMENS

Based on the literature search, two types of specimens were selected for testing. The first one is a square plate of side 500 mm and the second one is a circular plate with a diameter of 500 mm. In both cases, the thicknesses of the specimens were 50 mm. The test results were subsequently verified by the statical analysis. The specimens were supported along the perimeter. The surface area on which the load was applied was circa 7850 mm^2. The specimens in shape of a circular plate with a diameter of 500 mm and 50 mm thickness were selected for further examination on bases of the tests results.

3. STATIC TESTS OF REINFORCED SPECIMENS

The next step was to determine the static load of the specimens with different amounts of reinforcement. Each recipe, with different amounts of reinforcement is given in Tab. 1. The steel wire Fibers with hooked ends (KrampeHarex DE50/1,0 N) of diameter 1,0 mm and length of 50 mm were used.

Tab. 1 Mixtures A, B and C

MIXTURE		A	B	C
Concrete component		[kg/m³]	[kg/m³]	[kg/m³]
CEM II/A-S 42,5 R – Čížkovice		350	350	350
Aggregate:	Fine 0 - 4mm, Kazňějov	1195	1189	1181
	Coarse 4 - 8mm, Kazňějov	644	641	636
Superplasticizer, Chysofluid Optima 208		8,75	8,75	8,75
Steel wire Fibers KrampeHarex DE50/1,0 N		20	40	80
Water		157,5	157,5	157,5

The test results of reinforced specimens in the form of a dependency graph between deflection and applied force are shown in Fig. 1. Marking of specimens A, B, C corresponds to the mixture in Tab. 1.

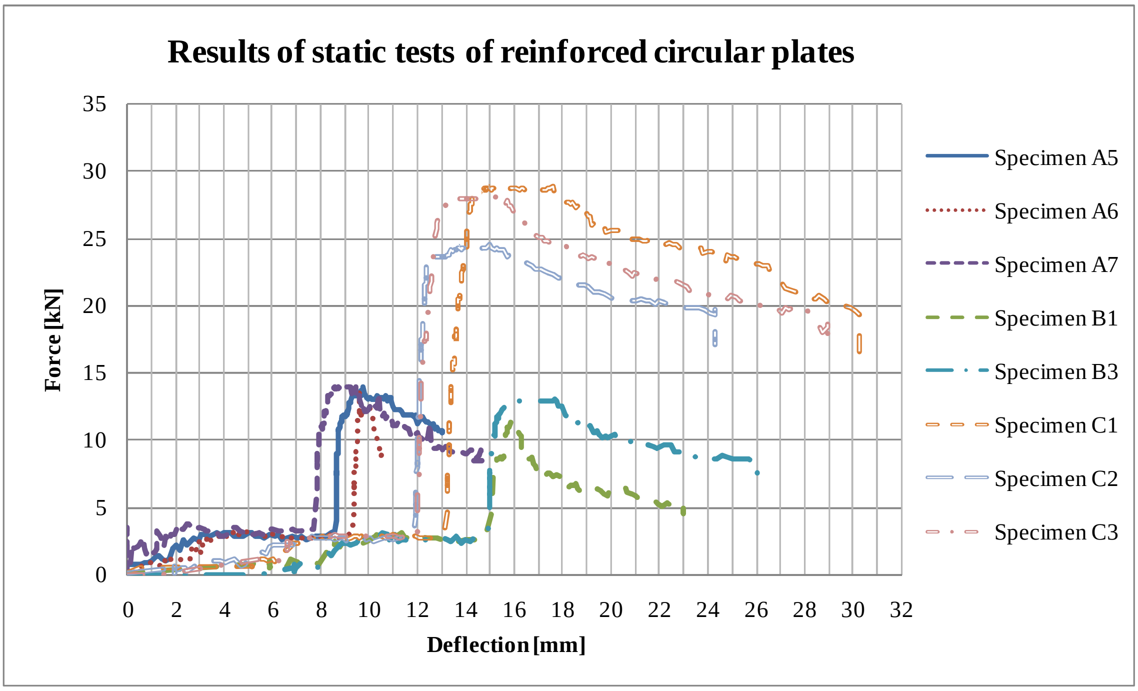

Fig. 1: Results of static tests of reinforced circular plates

4. DYNAMIC TESTS OF REINFORCED SPECIMENS

Dynamic load test was carried out at loading speed 70 mm/s. The maximum force at the failure and deflection were monitored. The specimens in shape of a circular plate with a diameter of 500 mm and 50 mm thickness were supported along the perimeter.

The test results of reinforced specimens in the form of a dependency graph between deflection and applied force are shown in Fig. 2 and Fig. 3. Due the limited space of this paper only the A and C mixtures are presented.

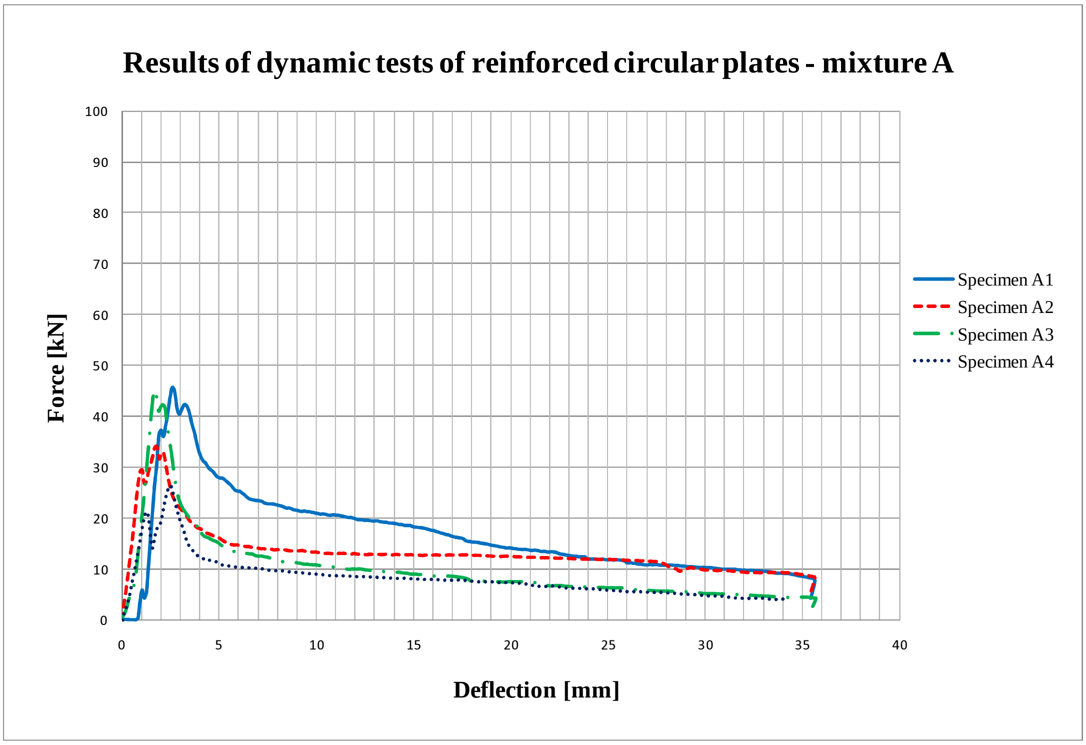

Fig. 2 Results of dynamic tests of reinforced circular plates – mixture A

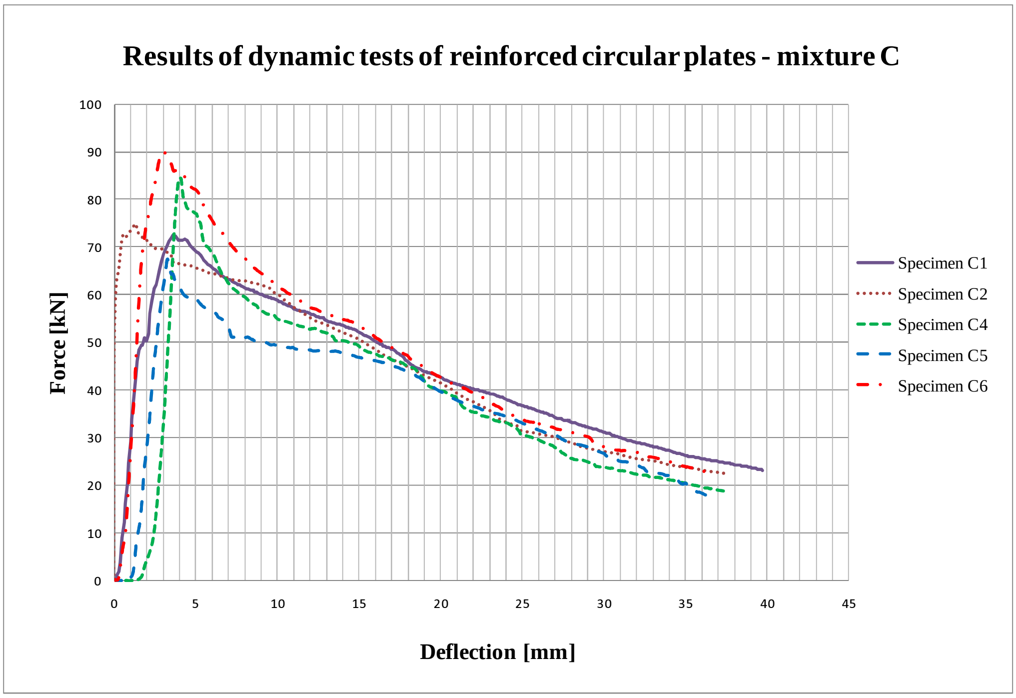

Fig. 3 Results of dynamic tests of reinforced circular plates – mixture C

5. CONCLUSION

The percentage increase of the different ways of loads and different mixtures are shown in Tab. 2. As a basis for comparison, mixture A is chosen.

Tab. 2 Comparing the tests results

Type of test	**Parametr**	**Mixture**		
		A	**B**	**C**
Static load test - circular plates	Max. Force [kN]	12,91	13,2	27,05
	Increse [%]	**-**	**2,2**	**109**
Dynamic load test - circular plates	Max. Force [kN]	37,8	54,0	76,6
	Increse [%]	**-**	**42,7**	**102,6**
Dynamic load test - circular plates	Energy [kNm]	0,430	1,092	1,711
	Increse [%]	**-**	**154,0**	**297,9**

The results obtained so far can be summarized as follows:

- Circular plate of diameter 500 mm and 50 mm thickness was selected as the optimum form of the specimen.
- Increase of the fibre reinforcement 40 kg/m^3 does not affect the increase in static load, but allows further increase in deflection. It also significantly increased dynamic load resistance of the specimens.
- Increase of the fibre reinforcement 80 kg/m^3 leads to a significant increase in static load. It also significantly increased dynamic load resistance of the specimens. The overall increase of strength ranges from 70 - 110%, compared to specimens with reinforcement around 20 kg/m^3.
- The energy needed to reach deflection 35 mm was evaluated from the force-displacement relationship. The overall increase of energy for specimens with reinforcement 40 kg/m^3 is around 150%, compared to specimens with reinforcement 20 kg/m^3. The overall increase of energy for specimens with reinforcement 80 kg/m^3 is around 300%, compared to specimens with reinforcement 20 kg/m^2.

The impact resistance testes with different amounts of reinforcement will be followed. Impact resistance of concrete with different degrees of reinforcement will be evaluated by setting the shock energy in failure of the specimens.

6. ACKNOWLEDGEMENTS

The research work presented in this paper has been supported by the GAČR 103/09/0055 and GAČR P104/10/2359.

7. REFERENCES

Bentur A, Mindess S, Banthia N, 'The behaviour of concrete under impact loading: Experimental procedures and method of analysis', Matériaux et Constructions, Vol. 19, No 113, pp 371 – 378

Kolisko J, Dudikova M, Klecka T, 'Bending test fiber reinforced concrete with polypropylene fibers. Effect of the shape of the test beam', In: 6 Conference Special Concrete, Sekurkon Prague, Beroun 2009, pp. 186-193, ISBN 978-80-86604-42-8

Bentur A, Mufti A, Banthia N, 'Fibre reinforced concrete, Present and future', Canadian Society for Civil Engineering, October 1998

Banthia N, Mindess S, Bentur A, Pigeon M, 'Impact testing of concrete using a drop-weight impact machine', Experimental Mechanics 29 1 (1989), pp. 63–69.

FIBRE REINFORCED CONCRETE CALCULATIONS IN ULTIMATE AND SERVICEABILITY LIMIT STATE

Karoly Peter Juhasz
Department of Mechanics, Materials & Structures
Budapest University of Technology and Economics
1111 Budapest, Műegyetem rakpart 1-3. K.II.42.

SUMMARY

Macro fibres have been well accepted for the reinforcement of sprayed concrete in mining and tunnelling applications, and today are starting to be used in other structural elements either in combination with existing steel bars, reducing the size of the steel bars or replacing the steel altogether. Although the use of fibre-reinforced concrete in the building industry is already common practice, generally accepted design methods are still lacking. Due to this many engineers are hesitant to use fibre-reinforced concrete. This paper describes a calculation method for the use of fibre-reinforced concrete for the ultimate limit state (ULS) and serviceability limit state (SLS) using the modification of the latest Austrian guideline - Österreichusche Vereinigung für Beton- und Bautechnik 2008 (*OVBB*).

1. INTRODUCTION

FRC beams reinforced with a low-dose of macro fibres show a reduction in the load-displacement diagram which means that the moment after first crack is less than before cracking in the elastic situation. This indicates that the failure will occur in statically determinate structures (e.g. simple supported beam) when it reaches and exceeds the elastic moment limit. For this reason low-dose FRC is used for statically indeterminate secondary structures (e.g. industrial floors), or primary structures if the risk to human life is small or economic consequences are either not significant or negligible (e.g. some house bases, cellar walls, pools). FRC can only be used for statically determinate primary structures if a high-dose of fibre or a combination of fibre and steel bars is used. The fibres could reduce the area of the reinforcement, the crack width and the deflection of the structure.

2. CALCULATION METHODS

The designs of RC structures are calculated in three stress states: (i) elastic, uncracked, (ii) elastic, cracked; and (iii) plastic (fig. 1). (i) and (ii) are used for the serviceability limit state and (iii) for the ultimate limit state. The serviceability requirements of the structure are determined by the crack width and the deflection criteria of the concrete.

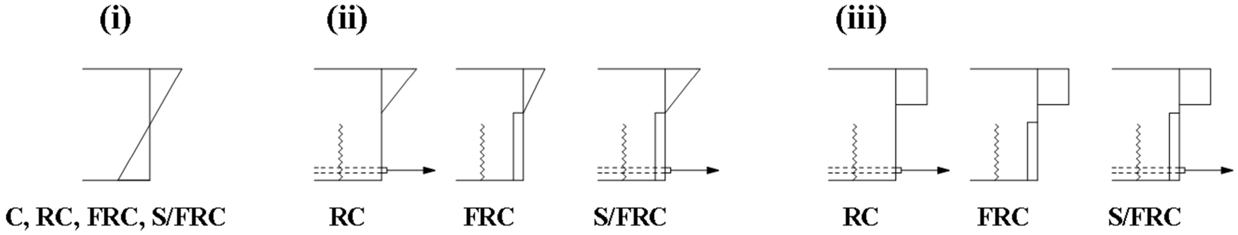

Fig. 1 Stress states

3. MATERIALS

The effect of the fibre to the FRC, S/FRC highly depends on the dosage, shape and material of the fibre. There is a minimum dosage of fibre under which there is no effect on performance (similar to a minimum steel ratio). The maximum fibre dosage is determined by the ability of the fibres to mix with the concrete. The paper focuses on a low dosage (0.1-2 V%) FRC (*Balázs, 1999*).

FRC is a cement-based composite material reinforced with randomly distributed, short fibres. The main benefit of the fibre is the post-cracking properties i.e. concrete becomes a more ductile material. Development of the post-crack stress is due to the ability of the fibres to transfer tensile stress across a cracked section, potentially leading to a reduction in crack widths.

A modified version of the Austrian guideline *(OBVV)* has been used to calculate the FRC beam. The stress-strain diagram was simplified for hand-calculations (L), non-linear calculations (NL), which are presented in the guideline. The calculation with diagram (L) is easy to use, however gives less accurate results. The (NL) diagram is not suitable for hand calculations. I recommend the (NLM) diagram which gives a better result than (L), presumably closer to reality, but still could be used for hand calculations (Fig. 2).

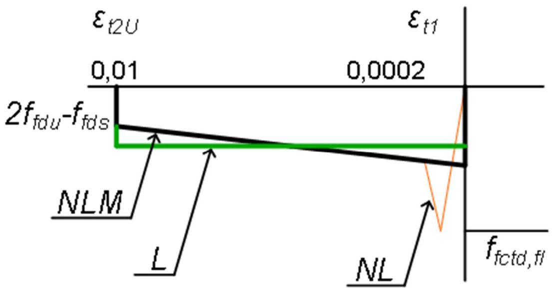

Fig. 2 Stress-strain diagrams for FRC

The steel reinforcement elastic-plastic diagram is as recommended by the Eurocode (*EC*) and only the tensioned bars are taken into consideration.

4. THE CALCULATIONS

In the elastic non-cracked stress state (i) the effect of the macro fibres, as for other reinforcement, is negligible. We need to use this state for the deflection calculations.

We need to take into consideration further conditions at the (ii) stress state. Concrete as well as FRC could be at the maximum strain condition when we are at the limit of the stress state, and the steel could be elastic or plastic. The moment-curvature diagram has been calculated from the formulas (Fig. 3). This is the basis for the maximum moment and deflection calculations.

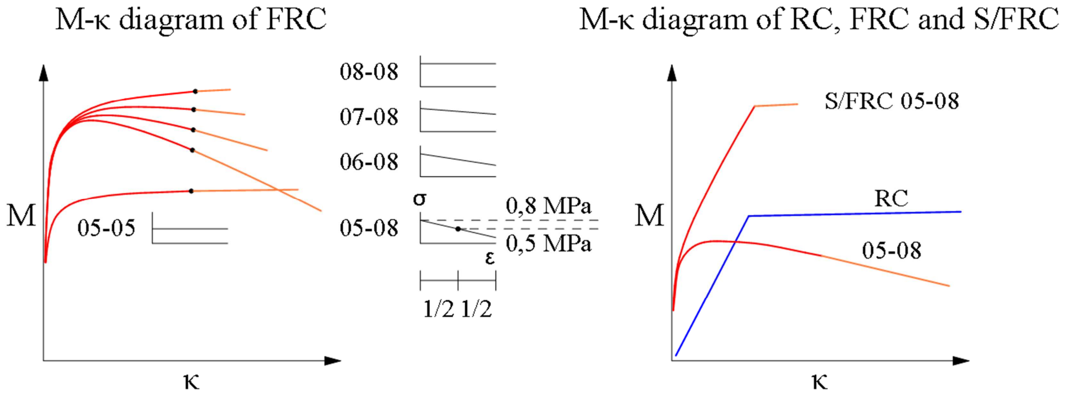

Fig. 3 Moment-curvature diagram from different stress-strain relationships

5. ULTIMATE LIMIT STATE

The moment-slope diagram shows the maximum moment for the ultimate limit state which could be calculated in the (ii) stress state for FRC and (ii) or (iii) stress state for S/FRC which depends on the steel/concrete ratio. Only the moment capacity calculation was taken into account.

6. SERVICEABILITY LIMIT STATE

6.1. Deflection

Deflection of RC structures is calculated from the curvature, so the moment-curvature relationship is required. This relationship is linear in the (ii) stress state for RC and non-linear for FRC and S/FRC.

The formula for curvature in EC is as follows (taking into consideration the „tension-stiffening”):

$$\kappa = (1-\varsigma)\kappa_I + \varsigma\,\kappa_{II} \qquad (1)$$

The deflection is the double integral of the curvature.

If we change the curvature of RC to the curvature of S/FRC we get the following function that is used for the calculation of deflection.

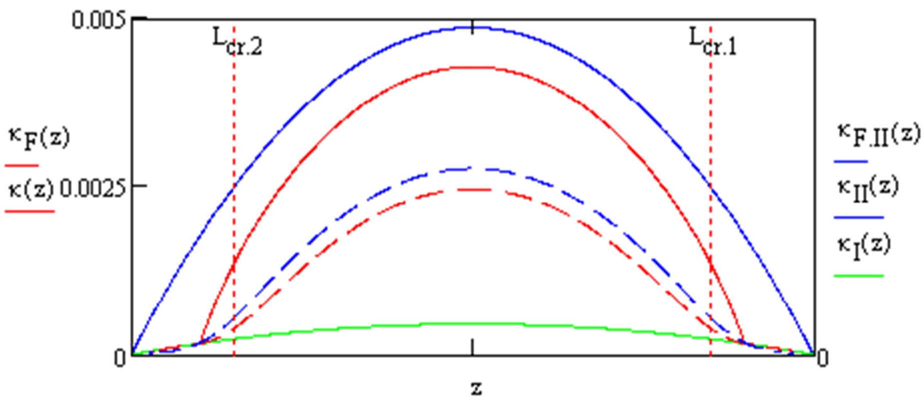

Fig. 4 Function of curvature of a two support beam

blue line: curvature according to (ii) stress state, green line: curvature according to (i) stress state, red line: curvature for deflection calculations, solid line: RC, dashed line: S/FRC

According to the improved calculation the displacement are reduced, however we have to take into consideration the following:

a) The steel is in elastic state, but the FRC in „plastic". For this reason I recommend to calculate the loads with the frequent combination instead of quasi-permanent combination.
b) Further research is needed to determine how the fibre modifies the tension-stiffening.
c) Research on the creep of FRC continues.

6.2. Crack control

The EC gives the following formula for the calculation of crack widths:

$$w_k = \beta s_{rm} \varepsilon_{sm} \text{ [mm]} \tag{2}$$

where s_{rm} is the distance of the cracks. The Italian guideline for *FRC CNR-DT 204/2006* (2006), changes only the calculation of s_{rm} with ξ. This dimensionless coefficient takes into consideration the fibres by their diameter and length ratio, but not the dosage. This coefficient could reduce the s_{rm} by upto 50%.

The RILEM 162-TDF gives a calculation method for both FRC and S/FRC. The recommendation for S/FRC is very simple - that a reduction of the stress in the steel bar by the fibres has to be taken into consideration for the EC calculation. It gives a simple and easy to use formula:

$$w = \varepsilon_{fc,t} (h - x) \tag{3}$$

7. CONCLUSION

A FRC section has the biggest moment in (ii) stress state, so both the ULS and SLS must be verified here. Because of this FRC can be used economically in situations where both the ULS and SLS have a similar value, for example a quasi-permanent value is high and the safety factor is low, the load is permanent (e.g. industrial floor, hydrostatic pressure tanks).

As for S/FRC the fibre will reduce the deflection, the amount of steel reinforcing area required and the crack width. Where steel reinforcing is designed for crack control or the reduction of deflection and not for load bearing reasons the fibre could succeed (e.g. watertight products).

9. REFERENCES

Balázs, L. Gy. (1999), „A szálerősítésű betonok múltja, jelene és jövője", *fib Magyar Tagozata, Szálerősítésű Betonok konferenciakiadvány*

CNR-DT 204/2006 (2006), „Guide for the Design and Construction of Fiber-Reinforced Concrete Structures", design recommendation, *Advisory Committee on Technical Recommendations for Construction, Rome*

Österreichusche Vereinigung für Beton- und Bautechnik (2008), „Richtlinie Faserbeton, Ausgabe Juli 2008"

RILEM TC 162-TDF (2003), „σ-ε design method", design recommendation, *Materials and Structures, Vol. 36, October 2003, pp. 560-567*

TOPIC 3
ADVANCED PRODUTION AND CONSTRUCTION TECHNOLOGIES

STRENGTHENING OF THE LOWER RING OF THE RIBBED REINFORCED CONCRETE DOME OF THE CENTENNIAL HALL IN WROCŁAW

Jerzy Onysyk[1,2], Przemysław Prabucki[2], Krzysztof Sadowski[2], Jan Biliszczuk[1,2]
[1] *Wrocław University of Technology*
Wybrzeże Wyspiańskiego 27, 50-370 Wrocław, Poland
[2] *Research & Design Office MOSTY-WROCŁAW*
Strzegomska 42a, 53-611 Wrocław, Poland

SUMMARY

The Centennial Hall in Wrocław (Poland) was constructed in 1911-1913. The dome of the Centennial Hall with the lower ring diameter 65,0 m was the greatest concrete dome in the world since the ancient times.The subject of this paper is strengthening of the lower reinforced concrete ring by presstressing tendons. The paper presents the structure of the Centennial Hall, results of the calculations, details of the strengthening and final results of the renovation.

1. SHORT HISTORY OF THE CENTENNIAL HALL IN WROCŁAW

The Centennial Hall in Wrocław is a unique structure in terms of architectural and structural solutions. It was constructed in 1911-1913. Initially, it was called *Festhalle (Trauer, Gehler 1914)*, but later it was given the name of *Die Jahrhunderthalle* to commemorate the 100th anniversary of King Frederick William III of Prussia's proclamation "An Mein Volk" calling upon the people to rise up against Napoleon *(Beuth Verlag GmbH, 2007)*. It was an early period of mature reinforced concrete, the rules of which, after minor amendments and supplements, are still valid nowadays. The Centennial Hall was constructed by Dyckerhoff&Widmann company from Dresden (current name: DYWIDAG). The Centennial Hall has been exploited for almost 100 years without any significant repairs of the most important structural elements. In 2006, this monumental Centennial Hall was listed as a UNESCO World Heritage Site for its pioneering reinforced concrete structure constructed in the style of modernism *(Beuth Verlag GmbH, 2007)*. The dome of the Centennial Hall with the lower ring diameter of 65.0 m was the greatest concrete dome in the world since the ancient times, considerably surpassing the 44.0 m high Pantheon dome (a diameter of 44 m), the domes of Hagia Sophia in Istanbul and of St. Peter's Basilica in Rome, and other domes of structures built during the Renaissance. In 2009, the renovation works of the Centennial Hall's elevation, window joinery and roofs covering were started. The renovation design was preceded by conducting a building survey report *(Persona, M.)*. In consequence, it was decided that the dome ring be strengthened.

2. STRUCTURE OF THE HALL

A general plan and a cross-section of the Centennial Hall showing its shape are presented in Fig. 1. The structure of the Centennial Hall consists of two fundamental parts: the upper and the lower one. The upper structure is a ribbed dome made up of a compressed upper ring with an internal diameter of 14.40 m, of tensioned lower ring with an internal diameter of 65.00 m, of ribs (32 items) connecting both rings and of transoms connecting the ribs (32 items) along the circumference of the dome. The structure of the dome is supported by means of steel movable bearings by the lower structure, with a cylinder layout. The bearings are placed radially according to the dome's ribs. Such shape of the external elevation of the Centennial Hall makes the sophisticated superstructure, visible inside the building, a surprising element used sometimes in architecture.

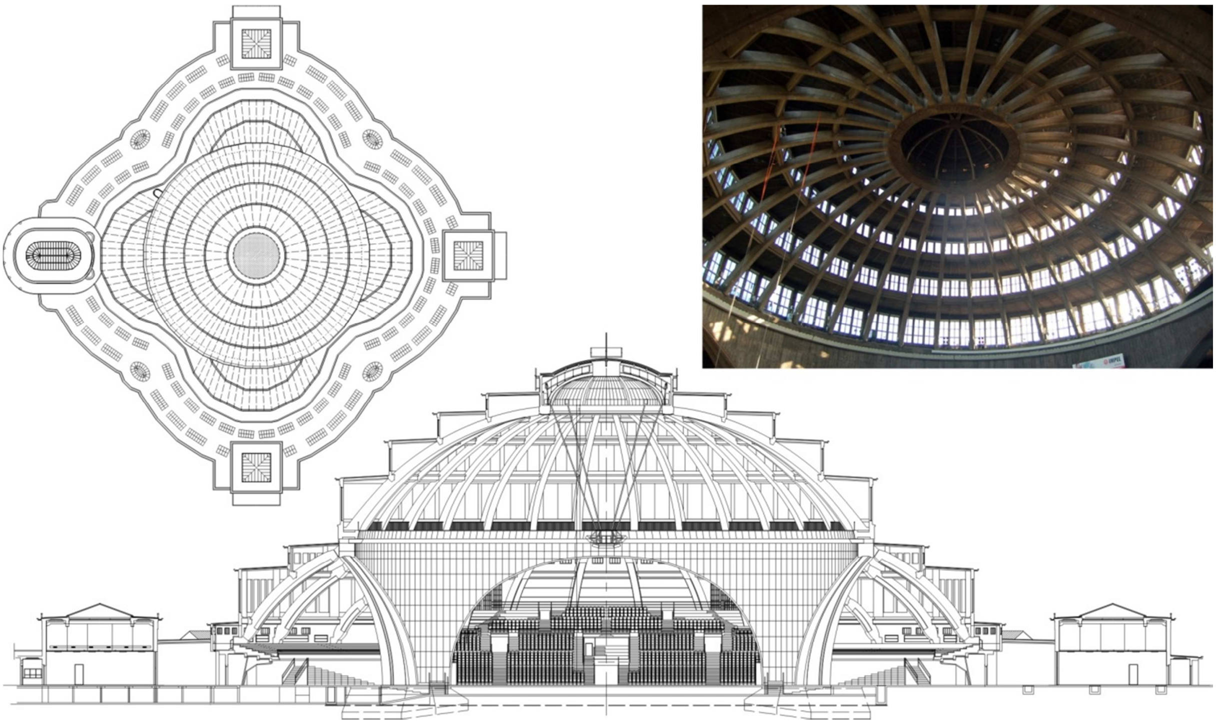

Fig.1 The Centennial Hall in Wrocław. General drawings *(Trauer, Gehler 1914),* (Zementverlag, 1937)

All elements of the structure and elevation of the Centennial Hall are made of reinforced concrete. It should be emphasized that some of the elements of the Centennial Hall, weighing up to 2.5 t, were prefabricated. They are considered the first use of prefabrication in Europe.

2.1. Structure of the lower ring of the dome. Technical condition

Fig. 2 Vertical cracks on the surface of the lower (tensioned) ring. Condition after sandblasting; a fragment of the truss.

The authors were familiar with the original calculations of the ribbed dome *(Trauer, G.)*. The most significant element of the dome is the lower ring since the axial tensile force, as always inconveniently transferable in reinforced concrete, definitely dominates in it. The lower ring determines safety of this part of the structure.A cross-section of the lower ring of the Centennial Hall's dome and its steel rocker bearings; are presented in Fig. 3.The ring is a reinforced concrete element with stiff reinforcement. The reinforcement is constituted by two trusses placed horizontally. Vertical cracks were noticed at regular spacing on the surface of the ring, along its circumference (Fig. 2). Without going into much detail of the technical condition of the structure in this paper, it should be said that the conclusion of the building survey report *(Persona, M.)* stated the necessity to strengthen the ring. Uncovering allowed also stating that the truss chords and the connections between elements did not corrode (Fig. 2).

3. STRENGTHENING OF THE RING

3.1 Assumptions

The designed strengthening was based on a system of cables, the same as in prestressed concrete elements. The design assumptions were the following:

1. The strengthening cannot interfere in the dome's structure. It should be hidden within the horizontal plane of the dome and it can minimally change the Hall's elevation.
2. Big forces must not be applied to the dome's structure, therefore the strengthening should be a passive strengthening, using cables tensioned to 15% of their characteristic strength (0.15 x 1860 MPa); such level of tensioning ensures proper anchorage of the cables in the anchor blocks.
3. The number of the cables should be enough to guarantee transference of the whole tensile force present in the ring.

3.2. Calculations

To design the dome's strengthening it was necessary to conduct static calculations determining the internal forces in the dome's elements. Class (e_1+e_2; p_3)[1] model was used for the calculations. The calculations showed that the most strained element of the dome is the tensioned lower ring, and the biggest tensile strength, being an unfavorable combination of loads, is at the level of ca. 6000 kN. The calculations included in *(Trauer, Gehler 1914)* defined that force at less than 5000 kN. Current calculations show that the force had been underestimated at the stage of designing of the Centennial Hall.

3.3. Construction of the strengthening

The strengthening of the lower ring was designed in the form of 27 cables Ø15.7 mm, grouped in 9 cables and placed in HDPE tubes. 140 mm spacing of the cables resulted from the placing of the anchorages. There arose a problem with hiding of the X-anchorages which are of grater dimensions than the cables placed in the tubes. The solution to this was placing of the anchorages in a staircase (technological passage), built in the 1920s independently of

[1] e_1 – one-dimensional rod elements,
e_2 – surface elements (two-dimensional)
p_3 – three-dimensional space of the model

the whole structure of the dome. On the side surface of the ring, the HDPE tubes were covered with a layer of mortar with reinforcement grid, which altogether gave 90 mm and managed to be kept under the throat of the ring. Structural details of the applied strengthening are presented in Fig. 3.

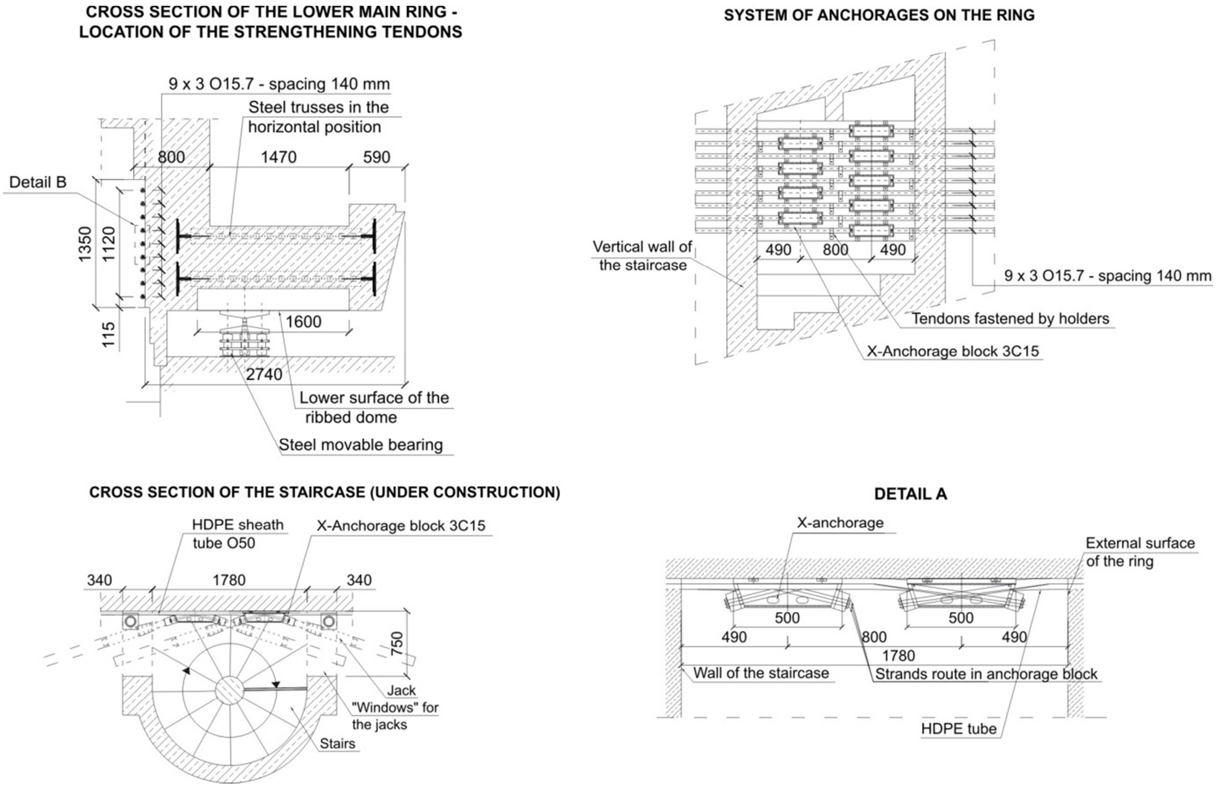

Fig. 3 Structural details of the strengthening.

Fig. 4 Stages of the works and the final effect; Centennial Hall after renovation.

Next photographs (Fig. 4) show the stages of the performed works and the final effect of the renovation of the Centennial Hall's elevation. The paint finish of the concrete was made in the glazing technique which used to be applied in the Renaissance in artistic painting. Currently, the second stage of works is taking place.

4. CONCLUSIONS

The applied strengthening proved effective at the stage of the works which were not dependent on the temperature and other weather conditions. After two years since the accomplishment of the renovation works, no undesirable effects has been reported.

5. REFERENCES

Beuth Verlag GmbH, (2007) Gebaute Visionen. 100 Jahre Deutscher Ausschuss für Stahlbeton

MOSTY-WROCŁAW Research and Design Office (2009). Projekt remontu elewacji, stolarki okiennej i pokrycia dachów Budynku Hali Stulecia we Wrocławiu; Projekt wykonawczy w zakresie zmiany sposobu wzmocnienia głównego pierścienia rozciąganego kopuły żebrowej Hali [transl.: Design of the Renovation Works of the Elevation, Window Joinery and Roof Coverings of the Centennial Hall in Wrocław; Working Design for a Change of Strengthening of the Main Tensioned Ring of the Ribbed Dome of the Centennial hall]. Wrocław, September.

Persona, M. Ekspertyza stanu technicznego konstrukcji budynku Hali Ludowej we Wrocławiu [transl.: A Building Survey Report of the structure of the Centennial Hall in Wrocław]. MBM Sp. z o.o., Wrocław.

Trauer, Gehler (1914): Die Jahrhunderthalle in Breslau; Berlin: Julius Springer,; a copy.

Trauer, G.: Festhalle in Breslau. Berechnung der Kuppel. Original Material preserved in the Museum of Architecture in Wrocław.

Zementverlag, (1937): Neues Bauen in Eisenbetone.

STRUCTURAL DESIGN OF REINFORCEMENT IN TAILOR-MADE CONCRETE STRUCTURES

D. Fall, K. Lundgren, R. Rempling, K. Gylltoft
Chalmers University of Technology
Department of Civil and Environmental Engineering, Division of Structural Engineering
Sven Hultins gata 8
412 96 Gothenburg, Sweden

SUMMARY

The ability of making tailor-made concrete structures, utilizing the formability of concrete, in an effective manner is the aim of the ongoing European project TailorCrete. With modern tools, such as industry robots, it is possible to mill a concrete formwork in Styrofoam or molding sand directly from a 3D-modell. A fully developed automated production enables irregular shaped concrete at a lower cost than current production methods; this has until today been examined only for non-load-carrying concrete elements. This article presents possible reinforcement alternatives for implementation in such production process. Each solution is associated with certain advantages and disadvantages. Furthermore, this article discusses the importance of developing rational design methods while working with tailor-made concrete elements.

1. INTRODUCTION

Automated production of concrete elements is a very wide expression. It covers everything between machinery performing single production steps to advanced fully automated systems for production of e.g. façade elements or concrete bricks. Most of the automated production seen today is developed for large production series. Each machine is designed and programmed to perform a few steps in the production e.g. reinforcement bending or welding. Generally, these machines only produce one type of element with very limited variations between series. The project TailorCrete the aims at general automation of all steps from 3D-model to finalized concrete structures. Such general solution would allow unique elements to be produced while retaining the economic benefits seen in large scale automated production; hence, tailor-made concrete structures could be used more commonly than as today, only in prestigious projects. More information about the project can be found at www.tailorcrete.com.

2. REINFORCEMENT ALTERNATIVES

The relatively high compressive stress capacity of concrete is well-known and the main reason for the wide use of concrete as a building material. However, tensile stress and shrinkage tends to cause cracks in the unreinforced material. Therefore, reinforcement is used to provide structural integrity post cracking. In the initial phase of the project different reinforcement alternatives were studied in order to evaluate which is suitable for automated production. The study is presented in (*Fall and Nielsen, 2010*). Conventional steel reinforcement has been widely used during the last century. During the last decades many alternative or complements have been developed e.g. fibre reinforcement, fibre reinforced polymer bars and textile reinforcement.

Conventional reinforcement provides the concrete element with high loading capacity and a well-established design procedure. Thereby, the use of conventional steel reinforcement simplifies the implementation of tailor-made concrete elements with regards to regulations and standards. It is, however, important to stress that the need for development of the production method development is large. In order to fulfil the project aims the reinforcement bars must be formed, in an automated fashion, in arbitrary geometries and assembled with sufficient precision and robustness.

Fibre reinforcement is often described as short discontinuous fibres of varying length, thickness and material. Reinforcing fibres can be made of steel, glass, various synthetic materials (coal, polymer, etc.) or organic materials. Steel fibres can be used as primary reinforcement and have good durability with regards to corrosion. Glass fibres are most commonly used in thin, non-structural, concrete elements e.g. façade elements. The tensile strength of glass fibres is very high; however, it is heavily influenced of deterioration. Synthetic fibres can be produced from several materials with widely differing properties e.g. polyethylene, polypropylene, coal or aramid. The main benefit of using fibre reinforcement is that, in carefully chosen amounts, it offers a simple and rational production process well suitable for application in concrete elements of complex shape. Fibre reinforcement is mainly used as secondary reinforcement. However, in some applications it has been used as primary reinforcement with good result (*Oslejs, 2008*). Further research is needed for such use to a larger extent. Furthermore, it is desirable to distribute and orient the fibres throughout the concrete structure in order to improve and optimize the reinforcing effect.

Bars made of fibre reinforced polymers (FRP-bars) could be a good alternative in tailor-made concrete structures, especially in thin parts where the concrete cover demanded for conventional reinforcement could not be fulfilled. FRP-bars are made by continuous aramid, coal or glass fibres incorporated in a polymer matrix (e.g. polyester, epoxy or vinyl ester). The properties of the composite is affected by the fibre and matrix materials, but are generally characterized by lower weight, lower elastic modulus and higher tensile strength than conventional steel reinforcement. Although FRP does not corrode, other deteriorating mechanisms affect the composite. Sea salt, de-icing salt, freeze-thaw cycles, UV – light and fresh water could all influence the durability (*Dejke, 2001*). In general the fracture is brittle; however, a more ductile material behaviour could be obtained by combining several fibre materials within the matrix (*Karlsson, 1998*). The big disadvantage with FRP-bars is the generally limited formability, i.e. the composite cannot be reshaped.

Textile reinforcement is made of continuous fibres arranged in several directions (e.g. nets or mats). In these textiles the fibre material is more effectively utilized than if the same material is scattered randomly in the concrete, as in the common case of fibre reinforced concrete. However, the production and application process are very complex. Common fibre materials are AR-glass, coal or aramid but also thin steel or polymer threads can be used. The textile composites can be produced through hand lay-up, pultrusion or extrusion. While hand lay-up is a manual craftsmanship based production, pultrusion and extrusion techniques are more suitable to industrial production with large series. Textile reinforcement offers great flexibility and could therefore be considered as an alternative for tailor-made concrete elements; however, the production methods used today demands extensive development in order to be implemented in a fully automated production process.

Additionally, it should be mentioned that many of the presented alternatives can be used in combinations, e.g. conventional steel reinforcement and fibre reinforcement. The identified advantages and disadvantages of the discussed reinforcement types are summarized in Tab. 1. In this table all fibre materials are generalized under the category fibre reinforcement. As mentioned, the fibre material influences the composite behaviour; however, the general features tabulated are common for all fibre materials.

Tab. 1 Summary of advantages and disadvantages with different reinforcement systems.

	+	-
Conventional reinforcement steel	Provides structural integrity. Conventionally used, i.e. easy to implement with regard to guidelines and design codes. Inexpensive	Might be difficult to produce effectively in arbitrary geometries. Certain concrete cover needed, i.e. not suitable for very thin concrete elements.
Fibre reinforcement	Can be added to the concrete during mixing.	Rarely used as primary reinforcement.
Fibre reinforced polymer	Good durability. Could be used in thin concrete members.	Rare technology which might lead to high costs. Fixed shape once produced.
Textile reinforcement	Could be applied in arbitrary geometries	Rare technology which might lead to high costs. Production method might need development

2. DESIGN METHODOLOGY

As previously mentioned, enabling the use of unique concrete elements at normal price levels is the purpose of developing an automated production process. For this to be used in practice, it is also important to improve the links between architects, structural engineers and producers. Furthermore, there is a need for a rational method for reinforcement design in complex geometries.

The process would start with creation of a 3D-model of the building. The structure can then be subdivided into producible concrete elements and analyzed to design a reinforcement layout or establish the amount and type of fibres needed. Design is commonly performed on basis of linear elastic analysis. The engineer can then, through sectional design, make sure that equilibrium is fulfilled utilizing plastic redistribution of stresses in the structure. Examples of design methods can be found in the literature *(Lourenco and Figueiras, 1993; Tomás and Martí, 2010)*; however, complex geometries introduces challenges with regards to e.g. reinforcement direction. Once the reinforcement has been defined in the model, the final layout could be verified by additional analyses and then be produced (Fig. 1, middle). The automated production, with great possibilities of producing concrete elements with complex geometries, also allows for geometrical optimization. By adjusting the geometry, the material consumption could be decreased. Today, the process is divided in steps between architects, structural engineers and producers. One important possibility with the more automated process is that it enables a more easy-going interaction between the involved competences.

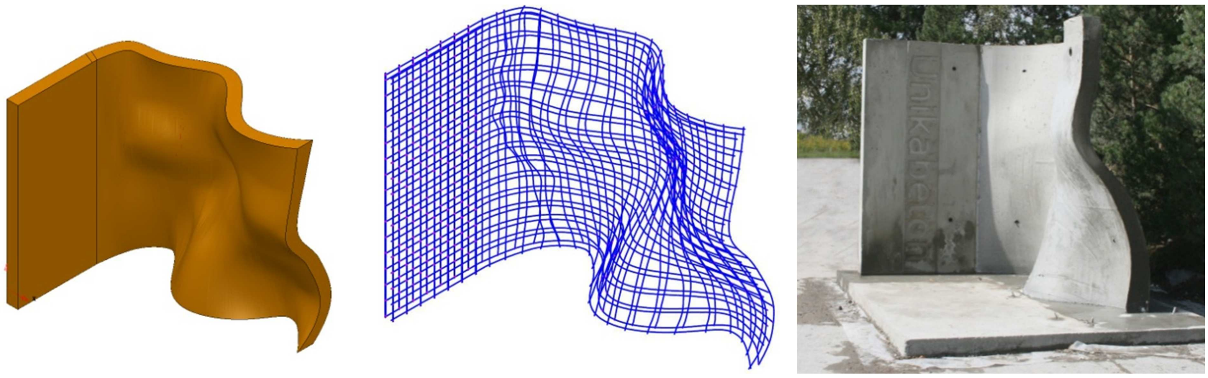

Fig. 1 Architectural model of prototype element (left) and the corresponding reinforcement modell (middle). Manufactured (unreinforced) prototype (right). Photo: Thomas Juul Andersen, Teknologisk Institut (DTI)

In order to simplify the production, the design shall aim at reinforcement bars bent only in one plane, even if the concrete element is double curved. While assembling it is likely that the bars will bend down by the self-weight. This change in position must be accounted for when the production is planned.

3. CONCLUSIONS

Good solutions to the problems associated with automated production of concrete structures are needed. The increased demand for unique concrete elements will also put demands on the production methods to be more cost effective than the time consuming and complex methods used, only in prestigious projects, today. Possibilities of using the formability of concrete fully will not only make building more aesthetically attractive but also open up for utilizing the structural advantages with complex geometries.

4. ACKNOWLEDGEMENTS

This research has received funding from the European Community´s Seventh Framework Programme under grant agreement NMP2-LA-2009-228663.

5. REFERENCES

Dejke, V. (2001), "Durability of FRP Reinforcement in Concrete", Department of Civil Engineering. Göteborg, Chalmers University of Technology, Vol., 211 p.

Fall, D. and C. Nielsen (2010), "Concrete reinforcement solutions". Gothenburg, Chalmers University of Technology, Vol. 2010:7, 27 p.

Karlsson, M. (1998), "Fiberkompositarmering", FoU-Väst, Vol. 9803, 42 p.

Lourenco, P. and J. Figueiras (1993), "Automatic Design of Reinforcement in Concrete Plates and Shells", Engineering Computations, 10: 519-541.

Oslejs, J. (2008), "New Frontiers for Steel Fiber-Reinforced Concrete", Concrete International, May (1): 45-50.

Tomás, A. and P. Martí (2010), "Design of reinforcement for concrete co-planar shell structures using optimization techniques", Meccanica, 45(5): 657-669.

BROWN BASINS – AN INNOVATIVE AND ECONOMIC METHOD FOR SEALING CONCRETE STRUCTURES AGAINST GROUND WATER

DDI Paul Brünner
Eisner ZT-GmbH, 8010 Graz, Austria

SUMMARY

The Brown Basin (BB) is a new technology for sealing concrete structures and offers an economic alternative to the commonly known and used systems "Black Basin" and "White Basin" (WB). In order to regulate the design and implementation of the system, the Austrian Society for Concrete and Construction Technology ("Österreichische Vereinigung für Beton- und Bautechnik", ÖVBB) has published a guideline *(Österreichische Vereinigung für Beton- und Bautechnik 2010)*. The main aspects of it are presented in this article.

1. INTRODUCTION

Several methods for sealing a building are known today: Brown Basin, White Basin, Black Basin, Diaphragm Wall. For each building, the optimal system has to be chosen by considering the special requirements and boundary conditions as well as economic aspects. Durability and maintenance have to be taken in consideration as well: accessibility, consequences of leaks and moisture damages, possibility to check the sealing. Especially for Black Basins, the finding of leaks is very difficult. White Basins are a very efficient method for sealing, but require high reinforcement percentages, larger dimensions of the components and a relatively small joint distance to limit crack formation.

The Brown Basin is a sealing system that can be used against ground water and leak water. Those parts of the concrete structure coming into contact with water are covered with Bentonite-layers on the complete wetted surface. The structural function is carried over by the concrete, the sealing is taken by the bentonite, which is bound between two textile layers. The term "Brown Basin" is derived from the brown colour of the bentonite, a highly swellable clay mineral.

The system has been developed about ten to fifteen years ago and is more and more demanded by clients, but the design and implementation was not regulated yet. As a consequence, the ÖVBB has published a new guideline to support engineers and construction companies in the realisation of this new technology. The guideline treats the design and construction, recommendations for calls for tender, the material and the implementation of Brown Basins.

2. THE SYSTEM

Bentonite is named after the Benton-Formation, Fort Benton / Montana. It is a rock made up of a mixture of several clay minerals with montmorillonite being the main component (60% to 80%). The high percentage of montmorillonite is the reason for the high water absorbing capacity and the swelling capacity of about 600%. Only natrium bentonite shall be used for Brown Basins. The bentonite is bound between to layers of geotextiles and attached on the concrete structure. The bentonite can be installed either before casting the concrete ("composite system") or after concreting ("non-composite system"). In the first case, the bentonite mats are inserted in the formwork and thus inseperably bound to the concrete. In the second case, the bentonite mats are mechanically fixed on the concrete structure after removal of the formwork. The soil pressure of the backfilling material (> 200 kg/m²) prevents the bentonite from expanding. Thus, a waterproof ($k=5*10^{-11}$ m/s according to ASTM D5887) layer is generated.

The fields of application of Brown Basins are:
- sealing against impounded seepage water and phreatic water
- sealing of buildings of all types (high-rise buildings, industrial buildings etc.)
- changing phreatic levels are controllable
- The guideline deals with water pressure up to 10 m (buildings with higher water pressures have been erected already).

Brown Basins are not suitable for:
- sealing and rehabilitation of masonry

Brown Basins can be used with special proof of swelling capacity of the bentonite in:
- saliferous phreatic and seepage water
- aggressive phreatic water

3. CLASSIFICATION AND DESIGN

According to the guideline for White Basins, the same requirement categories[2] were defined. So Brown Basins and White Basins can be directly compared:

Tab. 1: Requirement categories

Requirement Category	Description	Example	Brown Basin	White Basin	Diaphragm Wall
A_s	Completely dry: no visually detectable moisture signs (dark coloured spots)	Storage buildings for very moisture-sensitive goods.	✓	✓	
A_1	Widely dry: Single moisture spots, visibly detectable (max. mat, dark coloured spots)	Traffic buildings with high requirements. Habitable rooms, storage buildings, cellars (storage rooms), building service rooms with special requirements.	✓	✓	✓
A_2	Slightly moist: Visually and manually detectable, single shining moisture spots on the concrete surface	Garages, building service rooms (central heating rooms, collectors, e.g.), traffic buildings.		✓	✓
A_3	Moist: Dropwise water influx with generation of water cords	Garages (with additional measures: channel drains, e.g.) etc.		(✓)	✓
A_4	Wet: single leaking water influx spots for foundation slabs, walls and diaphragm walls	Outer part of double wall construction.			✓

[2] Requirement Category means in German "**A**nforderungsklasse" (thus A)

The definition of the Requirement Category is a task of the client. He has to decide how dry his building should be. The category is independent of the method of sealing (BB, WB, DW). Depending on the Requirement Category and the expected water pressure (W_0 – W_2), a Construction Class is defined, which regulates further details of the construction.

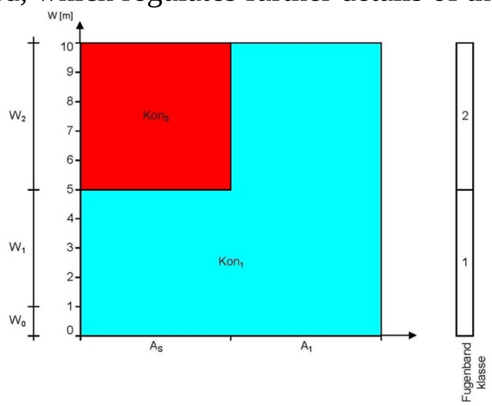

Fig. 1 Relation between water pressure, Requirement Class, Construction Class, Joint Class

Tab. 2: Construction class

Construction Class	Minimum component thickness	Limitation of cracks	Minimum concrete requirement	Recommended max. joint distance
Con_S	0,3 m	0,3 mm	XC3/XD2/XF1/XA1L/SB(A)	≤ 30 m
Con_1	0,25 m	0,3 mm	XC3/XD2/XF1/XA1L/SB(A)	≤ 60 m

It has to be distinguished between working joints and expansion joints. Depending on the water pressure class, different design for the joints is allowed. For working joints, the bentonite mats are the primary sealing, waterbars the secondary sealing. For expansion joints, waterbars represent the primary sealing.

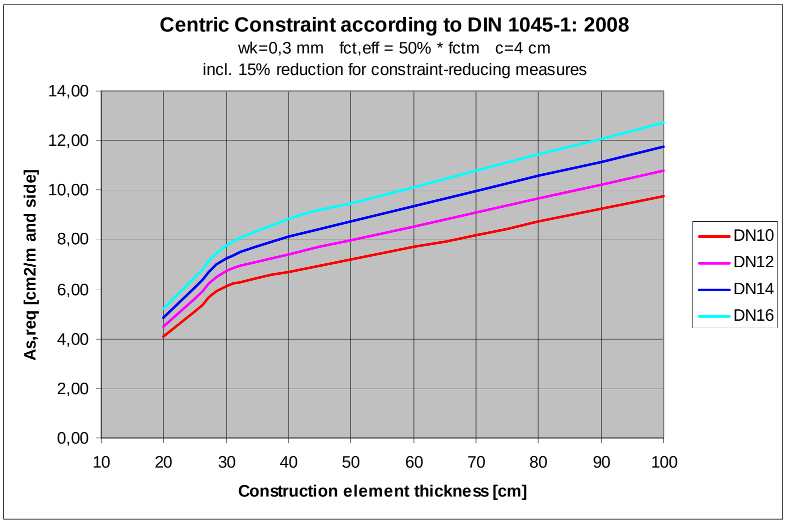

Fig. 2 Required Reinforcement for central constraint acc. to DIN 1045-1:2008

In the design, loads have to be determined according to EN 1991 and to be combined according to the rules of EN 1990. Based on the boundary conditions of Tab. 2, the Ultimate Limit State and the Serviceability Limit State have to be investigated and proofed according to EN 1992. For the dimensioning against centric constraint due to early cracking, the diagram in Fig. 2 has been developed. The calculations are based on DIN 1045-1:2008. The regulations currently valid in Austria (ÖNORM B 1992-1-1:2007) would require slightly more reinforcement for the load case “centric constraint”. Additionally, the required reinforcement for the load case “centric constraint” (crack width limitation: w_k = 0,3 mm) according to ÖNORM B 1992-1-1 is exceeding that according to the Guideline for White Basins *(Österreichische Vereinigung für Beton- und Bautechnik 2009)* (with crack width limitation for w_k = 0,2 mm). Actually, a new draft of ÖNORM B 1992-1-1 is in progress, where the more favourable values of the DIN 1045-1 shall be adopted. Up to then, the engineer has to decide himself whether to use the more favourable values of the DIN 1045-1:2008 or not.

4. REALISATION

When applying bentonite mats horizontally, the underground has to be even and clear of snow and ice. Moist or wet underground is admissible, standing water not. After the installation of the mats, the reinforcement and the concrete have to be placed immediately in order to prevent penetration of moisture into the mats. In case of swelling of the bentonite before casting, the contractor has to consult the producer and, when indicated, replace the bentonite mat. In the joint area, the mats have to be bond in interspaces of 25 to 30 cm, the overlapping has to be at least 10 cm. For vertical application, the above is valid analogously. Special attention has to be paid to the evenness of the underground when bentonite mats shall be used with jet grouting, bored pile walls and diaphragm walls. Edged noses > 3 cm have to be removed, indentations > 3 cm have to be filled up. Punctual noses and indentations are not admissible.

Mechanical damages of the bentonite mats which are recognized before casting have to be covered with an additional layer of bentonite with an overlapping of at least 10 cm. Leaking construction elements (cracks, moist spots on the surface etc.) have to be injected according to the guideline “Injection Techniques, Part 1” of the ÖVBB *(Österreichische Vereinigung für Beton- und Bautechnik 2008).*

5. CONCLUSIONS

Brown Basins are an economic and technically high grade alternative to White Basins. Their main advantages compared to White Basins are a less complicated design, the larger admissible crack widths and the larger admissible joint distances. Nevertheless, accurate design and construction are essential for the success of the system, as for all other sealing methods as well. By now, many buildings in Austria (Underground parking Kastner & Öhler Graz, water pressure 16m/ Thermal springs Bad Mitterndorf, water pressure 3,20m etc.) have already been successfully sealed against groundwater by this technology. In the future, Brown Basins will become a serious alternative to the conventional methods “White Basin” and “Black Basin”.

6. REFERENCES

Österreichische Vereinigung für Beton- und Bautechnik (2010): Merkblatt Bentonitgeschützte Betonbauwerke – Braune Wannen

Österreichische Vereinigung für Beton- und Bautechnik (2009): Richtlinie Wasserundurchlässige Betonbauwerke – Weiße Wannen

Österreichische Vereinigung für Beton- und Bautechnik (2008): Richtlinie Injektionstechnik, Teil 1: Bauten aus Beton und Stahlbeton“

Martin Schramböck (2010): Calculation of Centric Constraint

EXPERIMENTAL INVESTIGATION OF THE UPPER LIMIT OF THE SHEAR STRENGTH OF SPUN-CAST CONCRETE ELEMENTS

István Völgyi[1], György Farkas[1]

[1] *Department of Structural Engineering*
Budapest University of Technology and Economics
1111 Budapest Műegyetem rakpart 1-3

SUMMARY

A parametric experimental study was carried out to analyse the local load carrying capacity and behaviour of hollow cylindrical RC specimens. This topic is part of a research program of shear-bending behaviour of hollow cylindrical members. The parameters of loading setup and specimens under research were: the loaded area, distance between support elements, angle of loading/support elements, wall thickness, length of specimen, transversal and longitudinal reinforcement.

Local failure modes of specimens were analysed through crack patterns and load-displacement diagrams. A mechanical model was created for calculation of the local behaviour of members.

1 INTRODUCTION

The topic of this research is the shear behaviour of hollow cylindrical members without a diaphragm. This paper examines the local behaviour of partially loaded members under shear-bending loading.

Shear resistance models used today are based on the shear truss analogy or the modified compression field theory. Hollow cylindrical specimens do not have a grid parallel to the load. It is not easy to imagine which way are compressed struts able to work in this “curved grid”. Do these specimens have another load carrying mode?

An important difference for the typical cross sections is the local behaviour. Spun cast concrete members are usually produced without diaphragms. In the case of partial loading, global behaviour of the member may be affected by the local stresses.

2 LOADING SETUP, SPECIMEN PARAMETERS

The test setup is shown in Fig. 1. Stiff steel elements were used in the load zone and in the support zones. Relative displacements of the upper to lower and of the left to right extreme fibers of the central cross section of the specimen were measured using LEDT-s. Deformation in direction x vs y is called ovalization in this paper.

The wall thickness of the 24 specimens in the research was v = 55 or 90 mm. Specimens were made without spiral, respectively Ø5/75 or /150 helical transversal reinforcement were used. 12Ø10 of Ø 14 longitudinal bars were used. The applied specimen lengths were 330, 630, 930 or 1230 mm. The angle of centre of support and of loading elements were chosen at ω = 30°, 60° or 90°. The angle of centre assigns the type of the local behaviour. The number of loading surface elements and distance between support elements (L) were changed.

It is known that the structural behaviour of specimens depends on the type of loading. Both setups tested in research are shown in Fig. 1. The first loading setup is able to show the specialties of clear local behaviour. The second loading setup is a model of the typical member under shear and bending. Interaction of the local and global behaviour can be shown through these specimens.

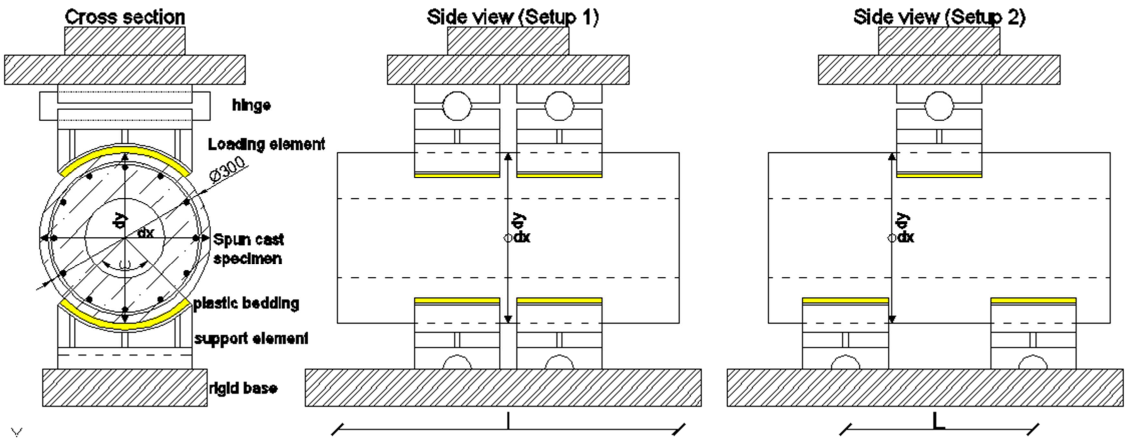

Fig. 1 Loading setup

Specimens are made of normal strength spun-cast concrete. The mixture was made of siliceous aggregate (m=6.0), CEM I 52.5N type cement and had a w/c ratio of 0.3. Mechanical properties of the concrete are reported in (*Völgyi et al 2009. and Völgyi et al 2010.*).

3 FAILURE MODES

Three different failure characterities were detected according to the combination of the parameters:

a., frame failure mode **b.,** crump **c.,** shear failure.

Topic of this paper are the local failure mode types (a, b).

Frame failure mode (Fig. 2) is the typical failure mode of specimens with a low angle of centre of loading element. The phenomenon is similar to the collapse of the RC pipes at standard quality control after EN 1916:2003. The differences of the phenomenon detected in the tests are caused by loading the specimen partially in the longitudinal direction and by the variation of the angle of centre of loading element. The crack pattern of short specimens is very similar to the pipes in literature. Specimens are simple reinforced. Transversal reinforcement is installed, but only in the outer region of the wall. After crack upper and lower points of cross section (at 12 and 6 o'clock) do not have any bending moment resistance. Specimens without transversal reinforcement collapse at the moment of first cracking. Helical reinforcement in the middle height of the specimen works as longitudinal reinforcement of a rectangular axial wall section.

The crack pattern of the long specimens shows that the ovalization, as well as the effectiveness of cross sections far from the loading element is even lower. This means that the function of length to load bearing capacity is not linear.

The stiffness of the cross section is lower after the appearance of cracks. The ductility of behaviour mode is considerable. The ratio is increasing up to the failure of the specimen. This increment is caused by the degradation of bending stiffness at 3 and 9 o'clock in the cross section.

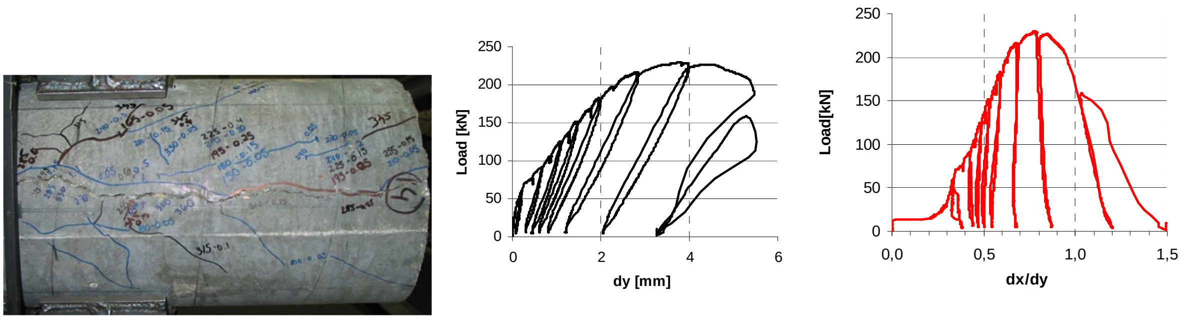

Fig. 2 Crack pattern and diagrams of transversally reinforced specimens with frame failure mode

The failure mode of the specimens of group **b** is the failure of concrete around the loading element (Fig. 3). Crump is the typical failure mode of specimens with a large angle of centre of loading element. The failure mode is similar to the punching of RC slabs in technical literature. The failure mode has also differences to punching. That is why a new expression is adopted. Crump is a traditional expression of mining, it is the collapse of a tunnel. The difference to punching is caused by the curved shape of the cross section. The thickness of the "slab" varies along the critical perimeter.

First cracks appear at 6 and 12 o' clock at the inner extreme fiber of the wall. Additional cracks appear on the outer side at 3 and 9 o' clock later. The length and width of the cracks grow. The behaviour of the specimen is quasi bilinear in this phase.

After the first phase, a quasi brittle failure mode appears with a dislocation on the inner surface of the specimens around the loading element(s). The failure mode is brittle, plastic deformation is very small before the failure of the specimen. Critical cracks appear just before the failure of the specimen.

The load-ovalization diagram of the sample specimen (Fig. 3) clearly shows the difference of the character of the punching failure mode to the frame failure mode. The first phase of the diagram is very similar to the frame failure mode. At the ultimate load level, the direction of the curve changes. It shows the development of the new, brittle failure mode. In the case of crump, deformation in the y direction grows quickly. At the same time, x deformation does not increase significantly.

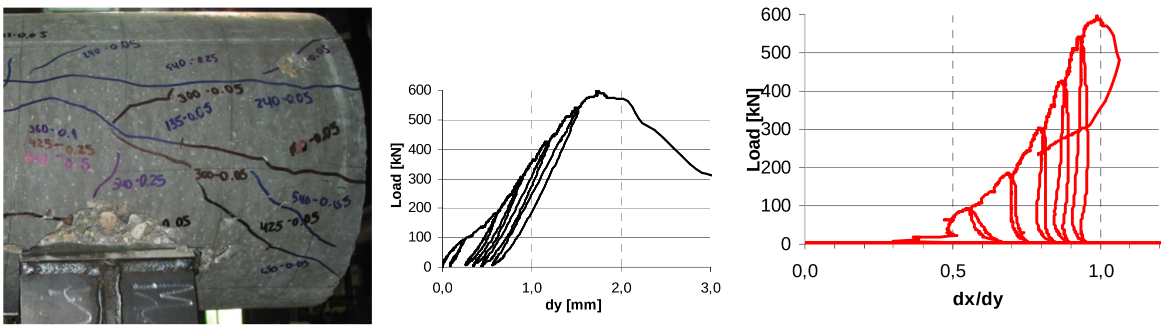

Fig. 3 Crack pattern and typical diagrams of specimens with failure mode "b"

4. MECHANICAL MODEL

The local load carrying capacity of hollow circular RC specimens is a minimum of the resistance of the frame load carrying mode and of punching resistance. Two separate mechanical models are also created for approximation of the local resistance of the specimens. The mean values of the material properties and of the geometrical dimensions are applied in the models. The models are also able to approximate the mean value of the local resistance.

4.1 Frame failure mode

The frame failure mode is a bending failure of the rectangular longitudinal section at 3 and 9 o' clock due to eccentric compression. After cracking this curved frame opens at the upper and the lower point, see Fig. 4. A hinge is also placed into the extreme fiber at 6 and 12 o' clock.

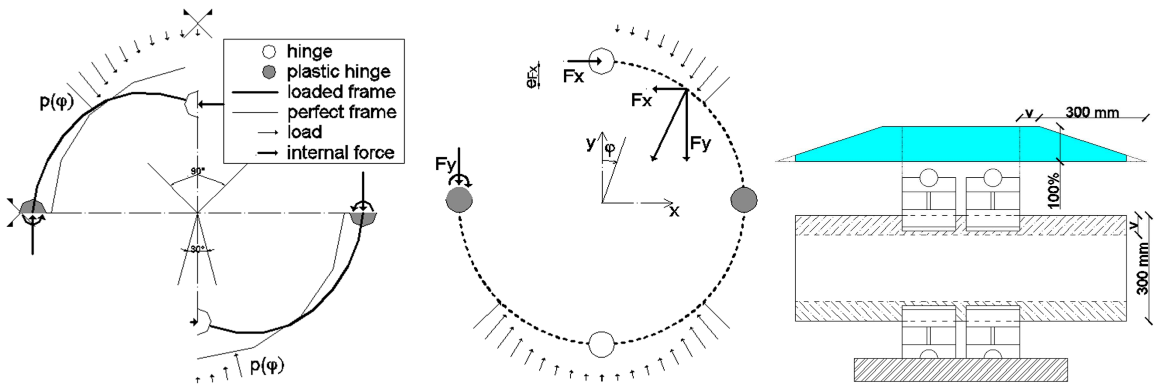

Fig. 4 Stress distribution under the loading element, calculation of bending moment reduction in plastic hinge due to the eccentricity of horizontal forces, respectively explanation of effectiveness factor (ζ).

Stress distribution under the loading element (p) is not constant because of the ovalization of the specimen. The assumption of the model is a triangular distribution of stress under the rigid loading element. The consequence of this stress distribution is a significantly higher horizontal joint load in the hinge at the same load level in the case of a large angle of centre at the loading element.

The effectiveness of the cross sections under the loading element is unity. This zone is expanded in a distance equal to the wall thickness because of the solid wall. It is assumed that effectiveness (ζ) builds down linearly to a distance equal to the diameter of the specimen, see Fig. 4.

4.2 Crump

The mechanical model of this behaviour mode is an equivalent slab projected onto a plane, explained in Fig. 5. The thickness of the slab is a function of the angle from the direction of the load. The control perimeter to the loading elements distance is half of the wall thickness of the specimen. The effective thickness of the "slab" at the control perimeter is equal to the vertical projection of the wall thickness (Equation 1). The shear stress along the control perimeter is taken to be uniformly distributed. The load transmitted by the loading elements is also taken to be concentric.

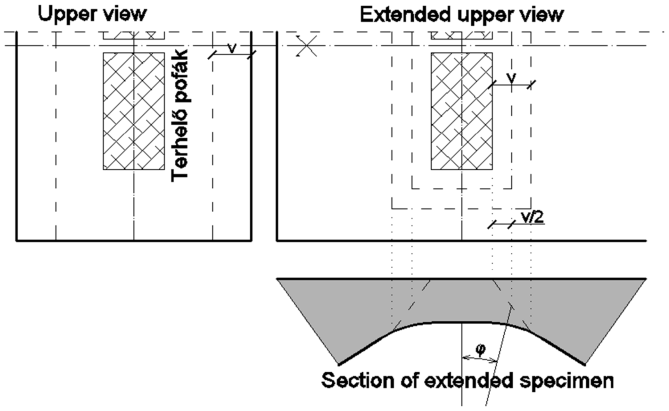

Fig. 5 Explanation of projected specimen and control perimeter

No “punching shear reinforcement” is installed in the specimens. Both types of reinforcement applied in the specimens are orthogonal to the control surface. Both reinforcements are also compatible to the tension steel in the orthogonal direction of the usual plane slabs, see Equation 2. The proposed formula for calculation of crump resistance is Equation 3.

$$v^*(\varphi) = \frac{v}{\cos\varphi} \quad \textbf{(1)} \qquad \rho_l = \sqrt{\rho_{lx} \cdot \rho_{ly}} \quad \textbf{(2)} \qquad F_b = \oint v^*(\varphi) \cdot f_{ct} \cdot \left(1 + \rho_l \cdot \frac{f_{uw}}{f_c}\right)$$

(3)

The results of the proposed model are reliable. The average of the calculated/measured resistance ratio is 95%. The standard variation of the ratio is under 10%.

5 CONCLUSIONS

Local failure modes of partially loaded hollow cylindrical RC members can be divided in two groups, named frame failure mode and crump. Crack patterns and characterites of load-displacement diagrams were analysed.

A proposed model has been created to calculate the local load carrying capacity of members in the case of idealized loading tested in research.

6 REFERENCES

Völgyi, *I. and Farkas, G. (2009),* “ Determination of strength of spun-cast concrete elements”*, Fifth International PhD DLA Symposium in Engineering 2009.* Pécs*, pp.70-71.*

Völgyi, I., Farkas, G and Nehme, S. G., (2010)“*Concrete Strength Tendency in the Wall of Cylind-rical Spun-Cast Concrete Elements”*, Periodica Polytechnica Civil Engineering 54/1, pp.23-30.

SHEAR STRENGTH OF PREFABRICATED AND PRESTRESSED HOLLOW CORE SLABS FOR RESIDENTIAL BUILDINGS WITH A DEPTH LESS THAN 300 MM

Gábor Kovács[1], Gábor Alajos Molnár[1], István Bódi[2]
[1] *ASA Construction Ltd.*
HU-1036 Budapest, Lajos u. 160-162
[2] *Department of Structural Engineering*
Budapest University of Technology and Economics
1111 Budapest Műegyetemrakpart 1-3

SUMMARY

Voids of the hollow core slabs made by slipformer technology are rather oval, than circular. Production technology restrict the use of shear reinforcement, therefore web shear is an important failure mode. Shear resistance depends on the critical point where the first crack appears. This is well-investigated in the case of circular voids, but there can be differences with mainly constant vertical web width. Shear tests were presented under industrial circumstances to compare the shear resistance of slabs with a depth less than 300 mm and with the calculations according to the Hungarian standard MSZ EN 1992-1-1 and MC 2010.

1. HOLLOW-CORE SLABS WITH SLIPFORMER TECHNOLOGY

Prefabricated hollow-core slabs are widely used in Hungarian industrial buildings. Most of the local producers operate with the well-known extruder technology with circle voids. With slipformer technology the tubes are rather oval, than circular with a mainly constant vertical web width. Both technologies restrict the placement of shear reinforcement, this makes the units sensitive to shear especially with shorter spans in residential buildings.

Most common slipformer cross-sections and spans in Hungary can be seen in Fig.1, Tab. 1.

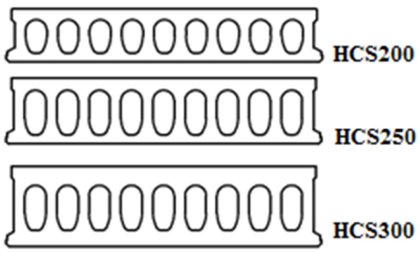

Fig.1 Slipformer cross-sections

Type	Height (mm)	Nominal width (mm)	Span (m)	Max strand number	Self weight (kN/m2)
HCS-200	200	1200	4-10	10xY1860-12.5	3,08
HCS-250	250	1200	6-12	10xY1860-12.5	3,57
HCS-300	300	1200	8-15	14xY1860-12.5	4,72

Tab.1 Hollow core cross-section's data

2. WEB SHEAR FAILURE

Heavily prestressed or short span hollow-core slabs subjected to a high shear force typically fail as shown in Fig. 2. When an inclined crack appears in the web close to the support, its immediate propagation cannot be prevented, the shear crack grows towards the flanges and results a brittle web shear failure.

The meaning of the unexplained symbols in the following equations can be found in the given codes.

2.1 MSZ EN 1992-1-1:2005 (EC2)

In regions uncracked in bending the shear resistance is given by MSZ EN 1992-1-1:2005:

$$V_{Rd,c} = \frac{I \cdot b_w}{S} \sqrt{\left(f_{ctd}\right)^2 + \alpha_1 \cdot \sigma_{cp} \cdot f_{ctd}} \qquad (1)$$

where S is the first moment of area above and about the centroidal axis, σ_{cp} is the concrete compressive stress at the centroidal axis due to axial loading and prestressing ($\sigma_{cp} = N_{Ed}/A_c$).

This formula bases on the traditional criterion for shear tension failure in the webs:

$$\sigma_I = \frac{\sigma}{2} + \sqrt{\left(\frac{\sigma}{2}\right)^2 + \tau^2} = f_{ct} \qquad (2)$$

where σ_I is the maximum principal stress, σ is the horizontal normal stress at the centroidal axis, τ is the shear stress due to imposed loads and f_{ct} is the tensile strength of the concrete.
In the near of the support the vertical normal stress has a positive effect on the failure load, but it is not explicitly included in Eq.1. It is implicitly taken into account by considering only the zone where the positive effect due to the vertical stresses is weak or non-existing. It follows that the failure is only considered at the centroidal axis or very close to it with a result of 45° inclination for the cracks.
An axial stress can be the same as σ_{cp}, where N_{Ed} is the prestressing force, which increases from zero to full force within the transmission length.
Shear stress can be calculated according to the well-known shear formula from elementary beam theory.

According to their test results, *Walraven* and *Mercx (1983)* suggested to reduce the shear resistance by 25%, *Pajari (2009)* wrote about an overestimate of 10% for slabs with more than 300 mm depth. Although this traditional calculation method seems to be nonconservative for higher slabs this method was taken to EC2. The problem with the method is that it does not take into account shear stresses due to the transfer of the prestressing force which results that principal stress and the critical point is not in the middle of the higher slabs, especially in a case of oval voids with a mainly constant vertical web width and therefore the principal stress is higher.

2.2 Model Code 2010 and MSZ EN 1168:2005

In 2011 fib has published the first draft of the New Model Code. The meaningful change to the shear provisions is the inclusion of “Levels of approximation”. Level I provides the least accurate results, but also the quickest to calculate. Level I approximation corresponds to the calculation method of MSZ EN 1992-1-1:2005. The same conclusions can be done as previously. In Level II the shear tension capacity is calculated from (the same method can be found in MSZ EN 1168:2005):

$$V_{Rd,c} = \frac{I \cdot b_w(y)}{S(y)} \left[\sqrt{\left(f_{ctd}\right)^2 + \alpha_1 \cdot \sigma_{cp}(y) \cdot f_{ctd}} - \tau_{cp}(y)\right] \qquad (3)$$

where τ_{cp} is concrete shear stress due to transmission of prestress at height y and distance l_x, estimated according Eq. 6., and σ_{cp} is concrete compressive stress in the same place and estimated according Eq.7.:

$$\tau_{cp} = \frac{1}{b_w}\left[\left(\frac{A_c(y)}{A} - \frac{S_c(y)\cdot(Y_c - Y_{pt})}{I}\right)\frac{dP_t(l_y)}{dx}\right] \tag{4}$$

where A_c is the concrete area above height y, Y_c is height of concrete centroidal axis, Y_{pt} is height of centroidal axis of prestressing steel.

$$\sigma_{cp}(y) = \left(\frac{1}{A_c} + \frac{(Y_c - y)}{I}\right)F_p(l_x) \tag{5}$$

where F_p is the not fully developed prestressing force in the distance l_x from the support.

The formulas given in Level II correspond to *Yang*'s *(1994)* method and take into account shear stresses due to the transfer of the prestressing force. *Yang* has proposed that the critical stresses can be found on the thick line in Fig. 3. In the hatched zone to the left from this line the support reduces the principal stress, to the right the increasing prestress does the same. The position of the critical point is not self-evident, the web shear failure is affected both by the shear force and bending moment, hence it is not completely correct to talk about shear resistance, because not only the shear force but also the bending moment contributes to the web shear failure. Critical stresses tend to be at the depth where the web width is narrowest and where both the shear stress due to transfer of prestressing force and normal stress due to the bending are close to zero.

Slipformer machines make oval cores. This means the weakest width is not only a point but constant line in the cross-section, see grey zone in Fig. 3. The most likely location is the lowest part of the constant web and an inclination of 35° can be supposed for the cracks.

Fig. 2 Web shear failure

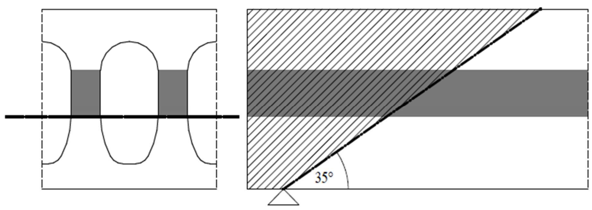

Fig. 3 Possible location of the critical point

2.3. Shear tests

3 pieces test slabs were produced with the maximal number of strands for each three cross-sections. The theoretical strength of the concrete was C40/50-XC1-16-F4 (MSZ 4798-1:2004), the adequate strength was measured. The strand type is EN 10138-3-Y1860S7-12.9-I-F1-C1 with an initial prestressing stress of 1100 N/mm^2. Those slabs were chosen from production which suits best the required strength and geometrical sizes.

Even lighter concrete blocks were used for loading in the near of the suspected shear resistance: 1 piece 10 ton, 1 piece 5 ton, and several 2,5 ton, this calibrates the accuracy of the measure.

Web shear tests were done according to MSZ EN 1168:2005. Two line load method suits for industrial circumstances. 10 cm x 10 cm wooden logs were used to concentrate the loads and a 5 cm wide 1 cm thick neoprene strip was put 5 cm from the end of the slab to absorb the bumps of the support.

2.4. Results

Tab. 2 Results of the tests and calculation in kN

Test slab	Break load	Resistance	EC2-MC2010 Level I	MC2010 Level II
HCS-200/10 (TS01)	200	175	185	181
HCS-200/10 (TS02)	200	175	185	181
HCS-200/10 (TS03)	200	175	185	181
HCS-250/10 (TS04)	225	200	220	210
HCS-250/10 (TS05)	225	200	220	210
HCS-250/10 (TS06)	225	200	220	210
HCS-300/14 (TS07)	325	300	312	296
HCS-300/14 (TS08)	325	300	312	296
HCS-300/14 (TS09)	325	300	312	296

3 pieces of hollow core slabs were tested for each cross-section. The depth of the slabs was less than 300 mm. The accuracy of the shear test is 2.5 ton (25kN). Resistance means the weight of the last step in the loading which cause breaking in the web minus 2.5 ton. Shear resistance was calculated according to MSZ EN 1992-1-1:2005 (EC2) and ModelCode 2010 Level I and Level II as can be seen in Tab. 2. Safety factor for the materials and for the loads were 1.0. Geometrical sizes were measured and the produced cross-sections were tested, although there were not significant differences with the theoretical values.

5. CONCLUSIONS

Significant differences between theoretical approximation of Level I, EC2 and Level II can only be found in the case of HCS-300/14, so Level I, EC2 can be used for conceptual design for all examined cross-sections. A computer program with a calculation method of Level II was made for each cross-section, more precise approximation does not extend run time.
It can been seen on Tab. 2, the accuracy of the measured values in industrial circumstances (25 kN) is higher than the difference between the results of two calculation methods, but the break loads are always higher than Level II values, therefore the most accurate calculation method is suggested to use for industrial needs.

7. REFERENCES

Pajari, M., (2005) „Resistance of prestressed hollow core slabs against web shear failure“, Espoo.VTT Technical Research centre of Finland 2005. VTT Research Notes, pp. 2292.

Pajari, M., (2009) „Web shear failure in prestressed hollow core slabs“, Journal of Structural Mechanics 2009. Vol. 42, No 4. pp. 207-217.

Yang, L., (1994) „Design of Prestressed Hollow core Slabs with Reference to Web Shear Failure“, ASCE Journal of Structural Engineering 1994. Vol. 120, No.9, pp. 2675-2696

Walraven, J.C., Mercx, W.P.M (1983) „The bearing capacity for prestressed hollow core slabs“, Heron 1983. No. 3. pp. 3-46

TIMBER-CONCRETE COMPOSITE FLOOR STRUCTURES - ENVIRONMENTAL STUDY AND EXPERIMENTAL VERIFICATION

Magdaléna Kynčlová [1], Ctislav Fiala[1], Petr Hájek[1]
[1] *Faculty of Civil Engineering*
Czech Technical University in Prague
166 29 Prague, Thákurova 7

SUMMARY

The composite structures based on high performance silicates and wood represent the beneficial alternative to the timber floor structures. Proposed timber-concrete composite floor structure benefits from lower weight of slender HPC or UHPC deck (compared to common RC slab) while improving acoustic parameters and fire safety of the structure (compared to timber floor structure). More over the combination of thin silicate slab and timber beam represents the effective cross-section from the perspective of bending stress. An essential role in the design of structure is played by the connection system between timber and silicate slab. The experimental investigation focuses on different types of timber-concrete glued connections. The comparison of complex LCA of the timber-concrete floor structure with three various floor structures shows the environmental effectiveness of the proposed solution.

1. INTRODUCTION

The construction and operation of buildings in EU consume 40% of all produced energy, emit 30% of overall CO_2 and contribute by 40% to total waste production. These numbers can be decreased only by changing the attitude to building technologies and techniques. Development of new materials, structures and construction technologies for construction of buildings should be thus based on the struggle for the reduction of primary non-renewable material and energy resources, while keeping performance quality, safety and durability on a high performance level.

The composite structures based on high performance silicates and wood represent the beneficial alternative to the timber floor structures. The timber structures have problems to achieve sufficient stiffness; the lack of mass causes troubles with acoustics, inflammability of wood limits the use from the perspective of fire safety. These disadvantages can be reduced by utilizing timber-silicate composites.

2. EXPERIMENTAL VERIFICATION OF TIMBER-CONCRETE GLUED CONNECTIONS

The first step in the research of the timber-concrete composite floor structures was to verify the possibility of glued connection. The shear test was proposed. Both sides of concrete prism 100/100/400 were glued to two timber prisms 80/160/320. The arrangement of the test is apparent from figure 1. In the first set of experiments there were tested two types of concrete (OPC – ordinary portland cement concrete and HPC – high performance concrete) and three various glues (Sikadur 30, Sikadur 330, SikaFloor 156). Timber prisms were from glued laminated wood. Eventhough, there were quite high variances in results, trend was obvious. Difference between OPC and HPC timber composites was in the type of failure – the rapture in timber-OPC composites was mainly in concrete while in HPC-timber composite the rapture was in the timber. The best results were achieved with SikaFloor 156 despite having the worst workability. This type of glue is too liquid for that type of application. Therefore, for the second set of experiments a specific filler (3% and 5% by mass) into the SikaFloor 156 was introduced. The glue with 5% of filler proved well both from the point of workability and shear strength.


Figs. 1,2 Shear test of timber - OPC concrete composite

3. CASE STUDY – LCA OF FOUR VARIOUS CONCRETE FLOOR STRUCTURE

A set of environmental information data on concrete components and related processes has been collected and determined within the research performed at the CIDEAS centre of the Czech Technical University in Prague. These data are based on regionally available materials and on source data provided by companies producing and/or selling their products mainly on the Czech market. Energy and emission factors were taken from GEMIS.

The analysis was performed for four various RC floor structures (three are from HPC), that were designed for four-storey residential building with ground plan 14.2 x 22.3 m. This analysis focuses primarily on floor structures and does not cover concrete beams and supporting structures. The analysis covers all significant life cycle stages: transport of the raw material to the concrete plant, concrete production, and transport to the building site, pumping of fresh concrete, formwork and demolition of structures. All assessed variants V1-V4 were designed for following conditions: theoretical span 4.4 m (simply supported), dead load (excluding self weight of the floor structure) g_k = 4.0 kN/m^2 and live load q_k = 2.0 kN/m^2. Variants V1, V2 and V4 were designed as one way slab, variant V3 as two way slab then.

3.1 Description of floor structures variants

The four alternatives were designed from three different concrete mixtures – ordinary concrete C30/37, high performance fibre concrete HPC105 and HPC140. The HPC105 mixture was fibre concrete with 25 mm long steel fibres Fibrex A1. These fibres have tensile strength of only 350 MPa. The HPC140 mixture was designed as fine-grained with 13 mm long steel microfibres. The tensile strength of these fibres is 2400 MPa. The amount of steel fibres in both mixtures was 1% by volume. As suggested in designation, HPC105 has compressive strength of 105 MPa, HPC140 has 140 MPa then.

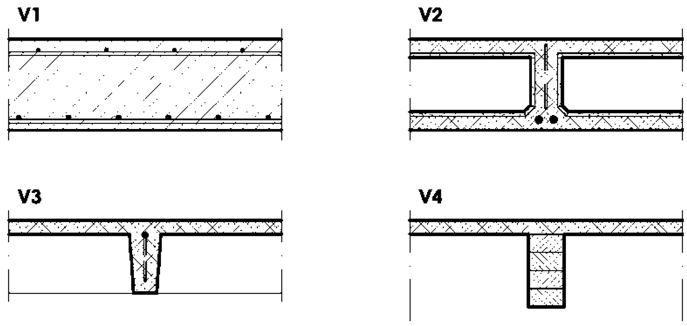

Fig. 3 Schematic sections of four floor structures alternatives

V1 full RC slab C30/37 – thickness 200 mm, main reinforcement R10 ā 110 mm at the bottom surface, distributive reinforcement R8 ā 200 mm and reinforcing mesh W8/150/150 at the upper surface, ring beams reinforced by 4 R12 with stirrups R6 ā 200 mm.

V2 prefab concrete panels HPC105 with fillers from recycled laminated drink cartons - thickness 200 mm, high performance fibre concrete with compressive strength of 105MPa, upper and bottom deck 30 mm without conventional reinforcement, reinforced only by fibres Fibrex A1 1% by volume, width of ribs 50 mm, ribs spacing 500 mm, main reinforcement 2 R16 ā 500 mm, filigree shear reinforcement R5 ā 250 mm, ring beams from C30/37 on external walls reinforced by 4 R12 with stirrups R6 ā 200 mm, ring beams on inner walls reinforced by 2 R12 with stirrups R6 ā 200 mm.

V3 waffle floor structure HPC105 – thickness 160 mm, upper deck 30 mm, width of ribs in both directions 50-70 mm, rib's spacing 600 mm, rib's reinforcement at the bottom surface R8 and R14 at upper surface in both directions, filigree shear reinforcement R5 ā 200 mm and R5 ā 180 mm, ring beams from HPC105 on external walls reinforced by 4 R12 with stirrups R6 ā 200 mm, ring beams on inner walls reinforced by 2 R12 with stirrups R6 ā 200 mm.

V4 timber-concrete composite floor structure - thickness 190 mm, upper deck 30 mm from HPC140 reinforced by steel microfibers 13 mm long, timber beam 80/160, timber-concrete connection by gluing, ring beams from C30/37 on external walls reinforced by 4 R12 with stirrups R6 ā 200 mm, ring beams on inner walls were reinforced by 2 R12 with stirrups.

3.2 Analysis results

Three alternatives of floor structures from HPC V2, V3 and V4 were analyzed and compared with reference solid RC slab from standard concrete C30/37 – V1. Graph in the Figure 4 shows for all four alternatives detailed primary energy flows associated with particular material components, transport and construction processes. It is evident that the highest energy consumption is associated with cement production and steel use. The best results reaches alternative V4 – composite timber - HPC floor structure, due to the use of timber beams with significantly lower primary energy demands. Top slab was made from very thin HPC140 slab precast elements. Variants V2 and V3 from HPC105 show lower primary energy consumption in comparison with reference solid slab (V1) due to more effective optimized hollow core and ribbed shape of floor cross section.

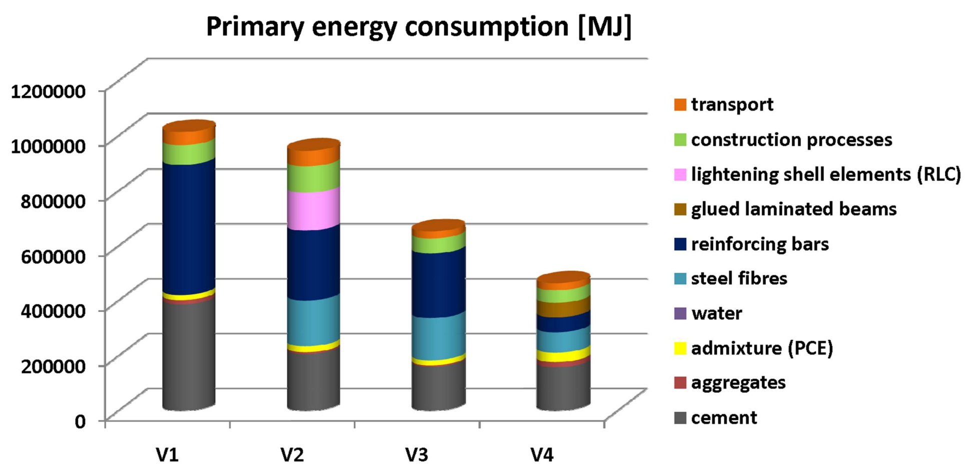

Fig. 4 Aggregated data – primary energy consumption

4. CONCLUSIONS

New types of high performance silicate composites enable design of ultra thin decks with thickness less than 30 mm. Some applications use even 15 – 20 mm thin UHPC decks. That thickness disables to use ordinary mechanical kinds of connection. Glued connection represents an effective option.

Presented experimental results of timber-concrete composite shear test proved the possibility of timber-concrete glued connection. Therefore, there is a chance to design the timber-concrete composite with HPC or UHPC slender deck with thickness of only 30 mm or less. Environmental efficiency of such composite structure was shown in the LCA case study. The research of timber-concrete composite floor structures is continuing with the large scale bending tests of composite beams with HPC slender slab.

5. ACKNOWLEDGEMENTS

This outcome has been achieved with the financial support of the research project granted by Czech Grant Agency GACR P104/10/2153. All support is gratefully acknowledged.

6. REFERENCES

GEMIS (Global Emission Model for Integrated Systems) - version 4.6, database CZ, D 2010, www.oeko.de/service/gemis/, 2010.

Hájek, P., Fiala, C., Kynčlová, M. (2011) Life cycle assessments of concrete structures – a step towards environmental savings, Structural Concrete, Journal of the fib, Vol 12/1, March 2011, ISSN 1464-4177, pp. 13-22

Fiala, C., Kynčlová, M., Hájek, P., (2011) Potentials for Reduction of Environmental Impacts of Construction Using High Performance Concrete, in Proc. fib Symposium Concrete engineering for excellence and efficiency, 2011 Prague, June 2011

INCREASE OF LOAD BEARING CAPACITY OF REINFORCED CONCRETE INSTALLATIONS SLABS BY SHEAR REINFORCEMENT

Christian Albrecht, Jürgen Schnell
Technische Universität Kaiserslautern
Institute of concrete structures and structural engineering
Paul-Ehrlich-Straße, Gebäude 14
D-67663 Kaiserslautern

SUMMARY

In building construction, reinforced concrete floors with integrated ducts are increasingly executed. In case of the installation of larger duct cross sections as well as in case of the accumulation of small tubes, the shear force resistance of reinforced concrete floors drops down strongly. In such cases shear reinforcement is required. So far, there have been no design rules for the dimension of local reinforcement in the area of ducting. This often leads to a refusal of such systems. Due to these reasons, the shear force bearing capacity of one-way reinforced concrete floor slabs with different types of ducting were analysed. The experiments demonstrate the increase in shear force bearing capacity of floor slabs with integrated service ducts by the use of local shear reinforcing elements.

1. PREAMBLE

In addition to tubes for electrical installations, both liquid and air-leading ducts are embedded into structures. Circular ducts but also rectangular (flat) channels are installed. In general, reinforced concrete cross sections outside the bending pressure zone are not fully exploited. Therefore, the cross section can be utilized in this area for duct lining, provided that the shear force resistance is not reduced inadmissibly. Related to the load bearing capacity of one-way floor slab systems without shear reinforcement Schnell and Thiele could develop design rules, which were also included in the reprint of DAfStb volume 525 (*DAfStb Heft 525, 2010; Schnell, J., Thiele, C. 2006)*. In case of installation of larger duct cross sections as well as in case of accumulation of small tubes the shear force resistance of reinforced concrete floors drops down so strongly, that in such cases shear reinforcement is getting required. So far however, design rules according to which a local reinforcement in the area of ducting could be dimensioned are missing. In practice, this often leads to refusal and prevention of such systems by structural engineers and checking engineers. Therefore, looking on the load bearing behaviour of one-way reinforced concrete floor slabs with different types of ducting, the present research project should examine the increase of shear force bearing capacity provided by local shear reinforcing elements (*Schnell, J., Albrecht, C., 2011*). The project was financed by the Federal Office for Building and Regional Planning in Germany (BBR).

2. TESTING PROGRAM

In due course of the research project a testing program was developed, which should provide insight views on the loading leading to failure, the modes of failure and the influence of shear reinforcement on the load-bearing capacity of the building elements. After previous trial testing a total of 14 tests at slab elements were carried out. There were circular and rectangular shaped single ducts and groups of circular shaped tubes tested, joined with a reference study for each geometry without shear reinforcing elements inside. For better comparability an equal opening height of d_O / d = 0.5 was given in all testing arrangements. In addition to the opening geometry, the type and the amount of shear reinforcement were varied. In this respect, a shear concentration factor ($S_{V,Rm,ct}$) was introduced. It describes the ratio between the load-bearing capacity of shear reinforcement as resulting with characteristic material properties to the average shear force resistance. For the testings, the shear concentration factor was chosen to 1.0, 0.75 and 0.5. For each test body two three-point bending tests were conducted under modified positions of bearings (see Fig. 1).

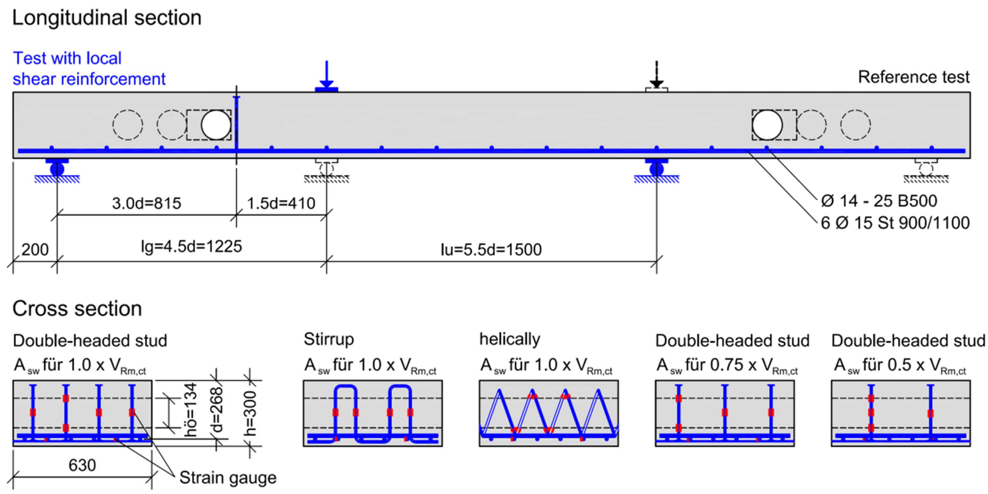

Fig. 1 Longitudinal section and cross sections of tested elements

3. TESTING RESULTS

Tab. 1 lists the achieved shear forces in the ultimate limit state in comparison with the results of reference tests and the theoretical load bearing capacity of a slab under the same boundary conditions for the tests with single circular ducts. The indicated shear forces had been converted into a cylinder strength of f_{cm} = 25 N/mm² ($V_{u,25}$). The calculation of the theoretical capacity of an identical slab element, not impaired by embedded ducts, has been done as per equation 70, DIN 1045 (2008) using a prefactor of 0.2 and with $f_{cm} = f_{cm,test}$ = 25 N / mm² ($V_{Rm,ct}$). The overview can clarify what effective influence do local shear reinforcing elements exert on the shear resistance of installation floors. The comparison with the expected load bearing capacity according to (*DAfStb Heft 525, 2010*) ($V_{o,Rm,ct}$) clearly indicates that the design approach based on (*DAfStb Heft 525, 2010*) is kept on the safe side. The increase in load-bearing capacity turns out percentagewise accordingly. The shear forces topped in the state of failure and the failure modes of all testings become available within the final report (*Schnell, J., Albrecht, C., 2011*). The following compares only the tested elements with circular ducts. The loading at failure and the modes of failure are shown in Fi. 2 and a comparison of the strength deformation-diagrams is depicted in Fig. 3. The test no. V-R-4 with $S_{V,Rm,ct}$ = 0.5 achieved a shear force at 136%, compared with the reference test. The shear crack at failure ran through the opening as like to the reference test. The test no. V-R-3 with $S_{V,Rm,ct}$ = 0.75 achieved a shear force at 149%, compared with the reference test. The shear crack at failure did not run, otherwise as to the reference test, across the opening, but first above the opening and then below the opening down to the tension area. During test no. V-R-2 with $S_{V,Rm,ct}$ = 1.0 the shear force could be increased to 165%, compared with the reference test. The shear crack at failure did no longer run through the opening like in the reference test. A shear crack occurred above the opening. A compare-son of testings with shear concentration factor $S_{V,Rm,ct}$ = 1.0 (V-R-2, V-R-5 and V-R-6) yield that the load-bearing capacity evidently can be increased not only by shear rails, but also by helically formed bars or regular stirrups.

Tab. 1 Shear forces of single circular ducts under ultimate loading

test no.	ducting	type of shear reinforcing element	$S_{V,Rm,ct}$ [-]	$V_{u,25}$ [kN]	$V_{u,25}$ / $V_{u,25,Referenz}$	$V_{u,25}$ / $V_{Rm,ct}$	$V_{u,25}$ / $V_{Rm,ct,o}$ [1] mit c=0,2
V-R-1	circular dØ = 0.5d	reference test – none	---	94.25	---	59.9%	119,7%
V-R-2		shear rail – on one side	1.00	155.66	165.2%	98.8%	197.7%
V-R-3		shear rail – on one side	0.75	140.59	149.2%	89.3%	178.5%
V-R-4		shear rail – on one side	0.50	128.10	135.9%	81.4%	162.7%
V-R-5		stirrup – on one side	1.00	149.10	158.2%	94.7%	189.4%
V-R-6		helical	1.00	146.14	155.1%	92.8%	185.6%

* $V_{Rm,ct} = V_{cal,25,not\ impaired\ by\ ducts} = 157.5$ kN

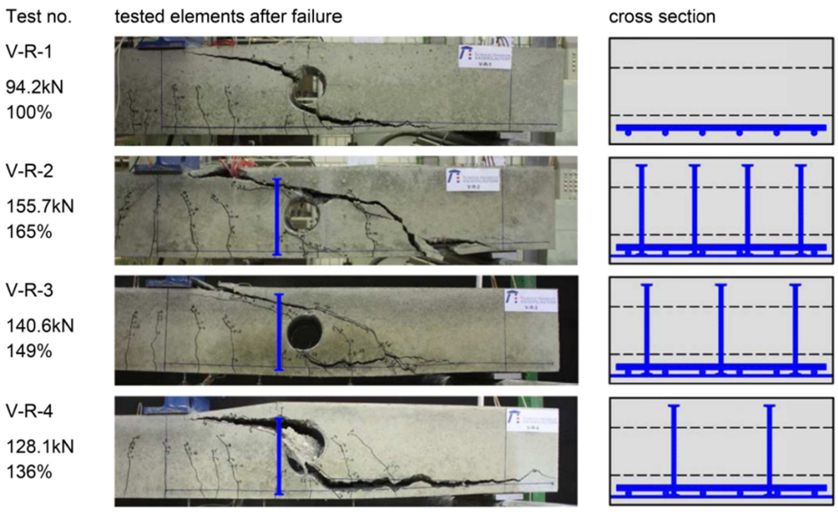

Fig. 2 Ultimate shear force and modes of failure at building elements with single circular ducts and shear rails at the side of the loading input

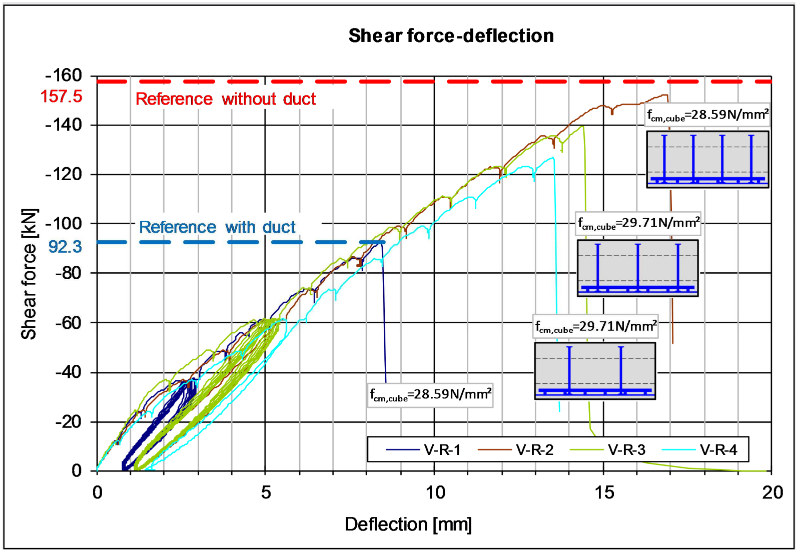

Fig. 3 Shear force-deflection-diagram – circular ducts: reference test and tests with shear rails located at the side of the loading input

4. PRELIMINARY DESIGN CONCEPT

A preliminary design concept was proposed for circular ducts with shear rails, which however still must be verified before application in practice. The design concept shall cover the limitation of the shear force resistance by $V_{Rd,ct}$ resulting from a cross section not impaired by ducts, the impact of the opening on the shear force resistance and the effectiveness of the studs.

It is recommended, that the design assessment for floor slabs with embedded circular ducts ($V_{Rd,ct,o+Dü}$) is based on the equation proposed in (*DAfStb Heft 525, 2010*) ($V_{Rd,ct,o}$) and to adjust the shear force such like calculated by an additive value depending on the effectiveness of the studs ($\Delta V_{Rd,shear\ rail}$). The shear resistance of the floor slabs with ducts should be limited by slaps without ducts - see (*DIN 1045-1-1, 2008*), equation 70 ($V_{Rd,ct}$).

$$v_{Rd,ct,o+Dü} = v_{Rd,ct,o} + \Delta v_{Rd,shear\,rail} \leq v_{Rd,ct}$$

With regard to the testings performed, the effectiveness of studs was limited by the anchoring. In case of smaller ducts embedded and in case the studs can sufficiently be anchored, the effectiveness of the studs must be limited by the capacity of the steel. The design of the anchor is based on the design of headed studs *(DIN 1045-1-1, 2008)* and is listed in the final report of the research project *(Pregartner T., 2009)*.

5. SUMMARY OF RESULTS

The research project carried out could show that the load-bearing capacity of installation floors can effectively be increased by local shear reinforcing elements. Depending on the size and geometry of ducts, as well as on the built-in reinforcement quantity, even the level of load-bearing capacity of floor slabs the cross section of which are not impaired by ducts can be faced or exceeded without shear reinforcement.

The anchoring of the utilized shear reinforcing elements exhibits a decisive influence on the load-bearing capacity. Looking on this subject it is not only essential, whether shear rails or regular reinforcing bars are built in. It is also essential in which vertical and horizontal distance to the ducts the reinforcement is installed and whether the longitudinal reinforcement is enclosed.

A preliminary design concept for installation floors comprising circular ducts and local shear rails has been developed, which must however be verified through further testings and parametric studies. The research based on the performed testing program will continue at the Technische Universität Kaiserslautern.

6. REFERENCES

DAfStb Heft 525 (2010), “Erläuterungen zu DIN 1045-1”, Beuth Verlag, Berlin, 2. überarbeitete Auflage

DIN 1045-1-1 (2008), “Tragwerke aus Beton, Stahlbeton und Spannbeton Teil 1: Bemessung und Konstruktion”, Beuth-Verlag, Berlin

Pregartner T. (2009), “Bemessung von Befestigungen im Beton”, Ernst & Sohn

Schnell, J., Albrecht, C. (2011), „Tragfähigkeitssteigerung von Installationsdecken durch Querkraft-Bewehrungselemente”, Abschlussbericht BBR-Forschung Z6-10.08.18.7-08.39.

Schnell, J., Thiele, C. (2006), " Anwendungsgrenzen für Luftkanäle in Stahlbetonplatten ohne Querkraftbewehrung”, Abschlussbericht DBV-Vorhaben 250 und 259

TESTING OF A WIDE REINFORCED CONCRETE BEAM

Attila Puskás[1], Zoltán Kiss[1]

[1] *Department of Reinforced Concrete and Steel Structures*
Tehnical University of Cluj-Napoca
Cluj-Napoca, 400027, Str. G.Baritiu nr. 25

SUMMARY

Due to the few information and poor literature about wide beams testing of a wide pre-stressed concrete beam is performed in order to compare the behavior of the beam under the design loads with the presumed behavior taken into consideration in the design phase. Loading of the three beams until failure permitted good observance of the beam behavior. The results of the tests are emphasizing the real behavior of the beams, with transversal deflections not even considered in the design provisions of beams but remarked in the test results.

1. INTRODUCTION

Buildings with wide concrete beams were used in the last decades in area with no or moderate seismicity. Due to the reduced floor height and the relatively simple technology of realization multistory buildings with wide concrete beams were realized in Europe in the Mediterranean area (Spain, Italy, Portugal), but also in Germany and Hungary. These structure are characterized by concrete beams having width larger than of the columns they are supported. Typical structural systems are frame structures having wide concrete beams in one direction with concrete slab having the bearing reinforced in the perpendicular direction to the wide beam direction or frames with wide concrete beams in both directions, with concrete slab laid over the wide concrete beams.

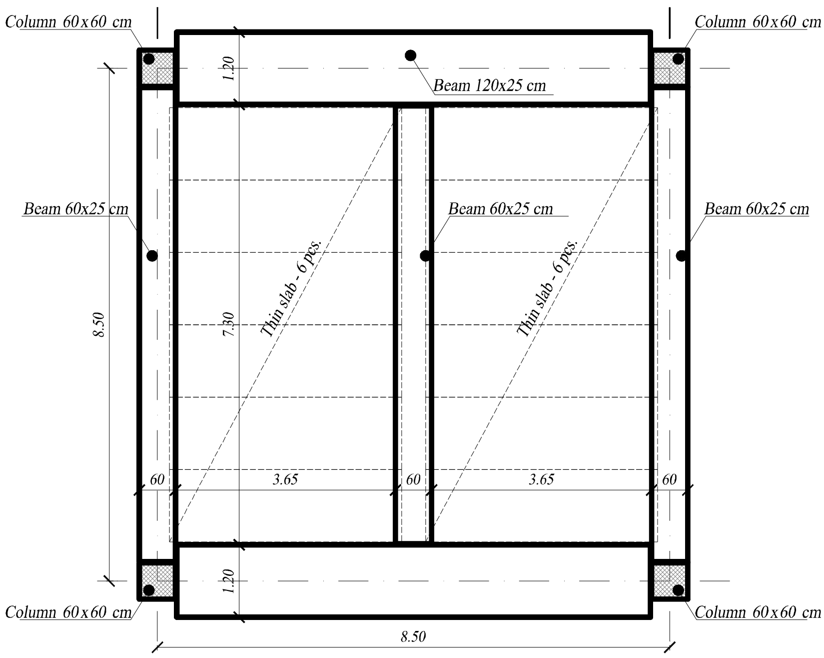

Fig. 1 Layout of structural elements

Beside the relatively reduced energy dissipation capacity of these structures the lateral rigidity is also reduced, similar to those with flat slabs. Due to these characteristics there are several studies about structures with wide concrete beams acted by seismic loads. These studies made on beams with different width ratio according to the support (column) width are revealing the vulnerability of the nodes loaded by cyclic loads, increased lateral flexibility of structures using wide beams and hence limited applicability of the wide beam frame structures in seismic area. It has to be noticed that beside the tests made on the nodes of wide beam-supporting column, there are very limited number of studies dealing with the specific behavior of the wide beams according to the behavior of the usual ones.

According the existing code provisions the width of the wide beams is limited to (b_c+$1.5h_b$) in ACI-318, based on the existing experience regarding design, execution and behavior of wide concrete beams. The norm NZS3101 from New Zeeland is limiting the width of the beams to the smaller value from (b_c+$0.5h_c$) și ($2b_c$). SR EN 1992-1-1 does not include any specification for wide beams, but limitations of the strips at the internal columns of $0.25l_y$ (l_y representing the width of the flat slab panel) and (b_c+y) for the marginal columns could be considered as informative value for the slab strip being intensively loaded, assimilated to a wide beam.

2. SLAB SYSTEM OF A MULTISTOREY BUILDING

Imposed short term execution period of a multistory building obliged the design team to use prefabricated structure in order to fulfill the requirements of the client regarding the short execution time. In case of considerable openings (column layout of 8.50x8.50 m) for such a prefabricated structure the typical solution means use of inverted T type main girders. For the studied building, due to the limitations of the free height, the only acceptable good solution seemed to be use of prefabricated wide concrete beams. In such a way main girders of 120x25 cm were prefabricated, the height after overtopping becoming 45 cm. The secondary beams of 60x25 cm also have to be mentioned; these beams are taking over the effective weight of the slab built up by prefabricated thin-slabs and over-concreting, transmitting the loads to the main beams (Figure 1). Thus the main beams are loaded by the distributed loads from the area above the beam and the concentrated loads given by the secondary beams, in the middle of the span, on both sides of the main beam.

3. TEST MODEL FOR THE WIDE BEAMS

In order to follow the behavior of the beams supposed to the presented loading, deformation and strain measurements were performed for three almost identical pre-stressed concrete wide beams. PA-G1 and PA-G2 were two identical beams to those designed and built in the multistory building, while PA-G3 had the transversal reinforcement on the top of the beam closed inside the prefabricated part. Before concreting of beam PA-G3, strain gauges were placed on the longitudinal reinforcements (12 measurement points realized by LY11-0.6/120 type micro strain gauges on the pre-stressing tendons and 8 measurement points realized by LY11-3/120 type micro strain gauges on the passive reinforcement), in order to track the strain variation in the reinforcements during the test.

At the testing the beam was considered simple supported, placed on metallic support with rubber strip, having a clear span of 7.60 m. Concentrated loads were induced in the middle of the opening, close to the side of the beam, by 2 double acted hydraulic cylinders of 120 to for PA-G1 and PA-G2 and 1 for PA-G3, acted by a electric motor pump of 400. The exact value of the force produced by the hydraulic cylinder was measured by a 2 MN force transducer. The beams were supposed to cyclic loading, the maximum load for each cycle being reached in steps. Deformation of the beam was permanently tracked by displacement transducers.

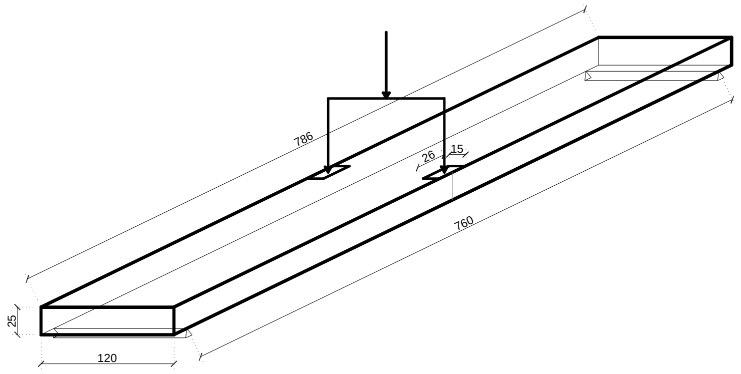

Fig. 2 Load scheme of the beam

For PAG1 and PAG2 the displacements were measured in 14 points as follows: 2 displacement transducers measuring the displacement of the beam near the support, and 3 displacement transducers at the middle of beam and on the sides in each of the following sections: at ¼ of the beam length in the left side, at ¼ of the beam length in the right side and at 20 and 40 cm from the middle of the span to the left and to the right hand side. For beam PAG3 due to the large number of strain transducers measured in the same time the deformation of the beam was measured in 9 points, in the following sections: near the support, at ¼ of the beam length and at 20 cm from the middle of the span. By measuring the transversal deformation of the beam we intended to put into evidence the importance of the transversal deformation of the wide beam, if the measured values will be considerable.

4. DEFORMATION OF THE BEAM DURING THE TESTS

In order to follow the behavior of the beams the cyclic loading was applied in steps.

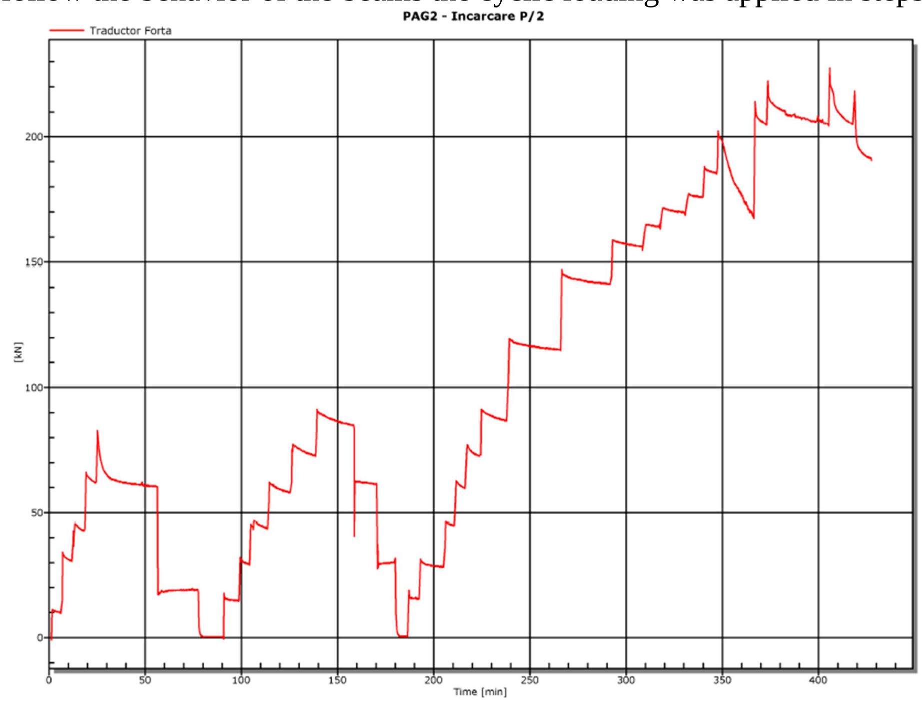

Fig. 3 Load steps for PAG2

The deformation of the beams put into evidence the difference in the deformations in several cross sections: in the middle of the span the deformed shape of the beam was convex, the difference of the deflection on the sides to the middle being more than 3% while at the support area (measured for beam PAG3) the deformed shape of the cross section was concave, similar to effect at the simple supported slabs, but presenting difference on the deflection from the sides to the middle of the cross section less than 2%.

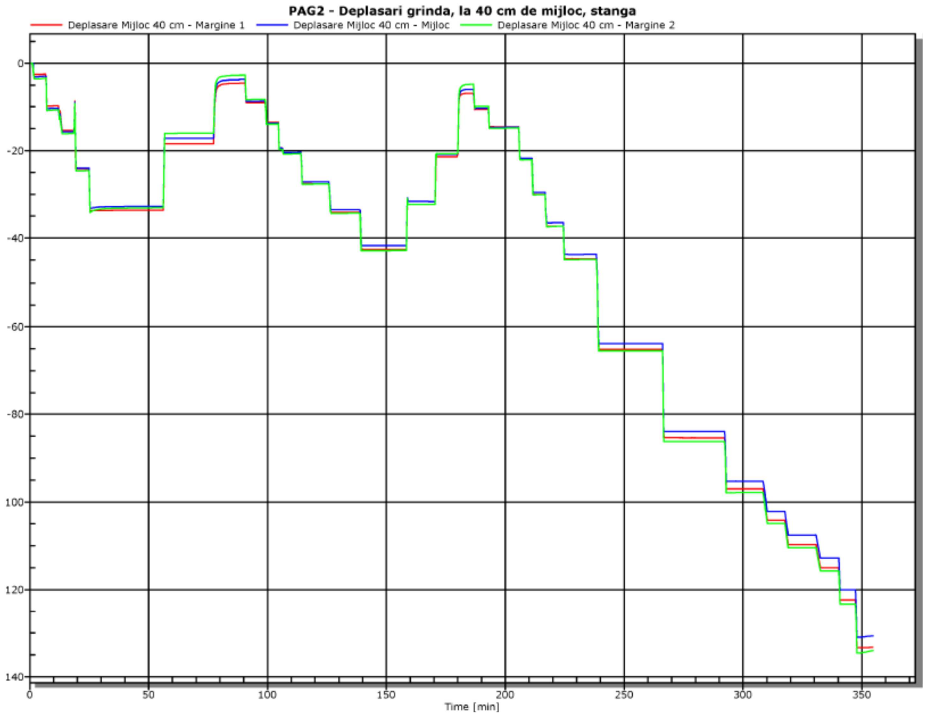

Fig. 3 Typical deformation of PAG2 at the middle of the opening

5. CONCLUSIONS

In case of wide concrete beams transversal deformation has to be considered. The transversal deformation depends on the way the loading is acting on the beam.

6. REFERENCES

***, SR EN 1992-1-1 (2004), "Reguli generale și reguli pentru clădiri"

***, ACI-318. Building code requirements. Michigan, USA: American Concrete Institute; 1999.

***, NZS3101. The New Zealand standard for the design of concrete structures. Wellington, New Zealand: Standards New Zealand; 1995.

Kiss Z., Oneț T. (2008) "Proiectarea structurilor de beton armat după SR EN 1992-1", Ed. Abel, Cluj-Napoca 2008

Quintero-Febres CG, Wight JK. Investigation on the seismic behavior of RC interior wide beam–column connections. USA: University of Michigan, 1997 [Report no. UMCEE 97-15].

Popov EP, Cohen E, Koso-Thomas K, Kasai K. Behavior of interior narrow and wide beams. ACI Struct J 1992;89(6):607–16.

W.L. Siah, J.S. Stehle, P. Mendis, H. Goldsworthy: Interior wide beam connections subjected to lateral earthquake loading, Engineering Structures 25 (2003) 281–291

A. Benavent-Climent: Shaking table tests of reinforced concrete wide beam–column connections, Earthquake Engng Struct. Dyn. 2005; 34:1833–1839

USE OF PREFABRICATED ELEMENTS IN STRUCTURAL AND ARCHITECTURAL DESIGNING OF CONCRETE BRIDGE SUPERSTRUCTURES

Jan Biliszczuk[1, 2], Wojciech Barcik[2], Jerzy Onysyk[1, 2], Krzysztof Sadowski[1], Robert Toczkiewicz[2], Kamil Tukendorf [2]
[1] *Wrocław University of Technology*
Wybrzeże Wyspiańskiego 27, 50-370 Wrocław, Poland
[2] *Research & Design Office MOSTY-WROCŁAW*
Strzegomska 42a, 53-611 Wrocław, Poland

SUMMARY

The paper concerns the use of prefabricated concrete and steel elements in constructing prestressed concrete box girders. A few selected examples of such structures (beam bridges and cable-stayed bridge) built recently in Poland are presented.

1. INTRODUCTION

Nowadays, great attention is paid to the aesthetics and architectural quality of bridge structures. Particularly high aesthetic demands should be fulfilled by urban structures, as their appearance is often critical to the architectural expression of a city. Elegant form of a bridge can be attained by constructing box girders within which the drainage system can be hidden. To achieve this, cross-section of a superstructure should be a two- or three-cell box girder. In the case of a three-cell cross-section, to optimize the construction of a superstructure, side prefabricated concrete or steel elements are often used. These may be either nonstructural or load bearing elements, as in the examples given below.

2. „GĄDOWSKA" FLYOVER

"Gądowska" flyover in Wrocław (*Biliszczuk et al. 2002*), built in 2000-2002 along the city ring road, consists of two parallel, curved in plan 15-span box structures, made of prestressed concrete class C50/60 (see Fig. 1). Side junctions (beam-plate structures) are joined to both superstructures. Span lengths of the flyover vary from: 33.0 to 52.0 m. The structure was erected by longitudinal incremental launching method, only a part of it was cast on scaffolding.

Fig. 1 View of the completed „Gądowska" flyover

Assembly of precast, curved elements (Fig. 2), forming side parts of the three-cell box cross-section, proceeded as follows:

- placing of steel anchors in the holes drilled near the bottom edge of the web;
- lifting and positioning of the precast elements (weight of each: approx. 3.5 tons);
- connecting of the precast element with the deck plate cantilever by welding steel sheets embedded in the rib of the precast element and in the concrete deck plate;
- in-situ casting of bottom and top joints after assembling of all precast elements.

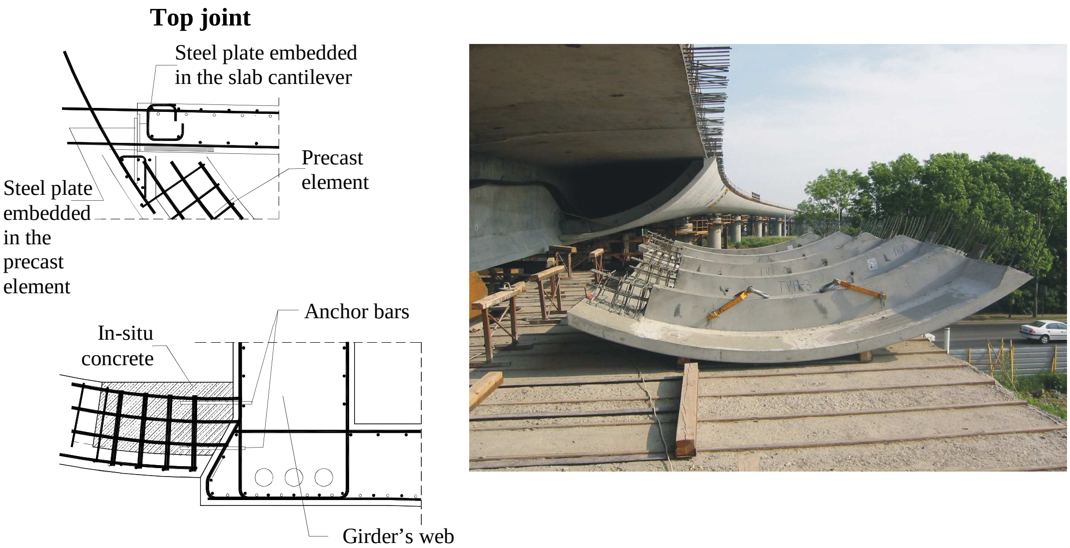

Fig. 2 Details of joints and view of the precast elements

3. STRUCTURES ALONG THE MOTORWAY RINGROAD OF WROCŁAW

3.1. Bridge over the Odra River

Bridge over the Odra River (see Fig. 3) consists of three structures (*Biliszczuk et al. 2011*):

- southern flyover E1, total length 610 m: 11-span prestressed concrete beam, span lengths: 40.0 + 2 x 52.0 + 56.0 + 60.0 + 6 x 50.0 m;
- main bridge M2, total length 612 m: cable-stayed bridge consisting of two parallel prestressed concrete decks, suspended to one 122 m high pylon, span lengths: 50.0 + 2 x 256.0 + 50.0 m;
- northern flyover E3, total length 520 m: 9-span prestressed concrete beam, span lengths 50.0 + 60.0 + 7 x 50.0 m.

Fig. 3 View of the bridge crossing the Odra River (*photo W. Kluczewski*)

The main bridge and the northern flyover were constructed by means of longitudinal launching method. The southern flyover was erected span by span, using movable scaffolding system. Both the main bridge and the flyovers have similar configuration of the main girder. In the cross-section, it is a three-cell box made of prestressed concrete. Side, inclined webs of the box were designed as thin-walled precast elements made of reinforced concrete. In the suspended spans the precast elements are in tension, while in the spans of flyovers they are in compression.

Fabrication of superstructure segments (incremental launching method) proceeded in the following stages:

- placing of precast side elements (weight up to 8 tons);
- casting of the bottom plate and webs;
- casting of the deck plate;
- post-tensioning and launching the segment.

Fig. 4 shows the installation of prefabricated segments during construction of the superstructure. In the main (cable-stayed) bridge, seams of the adjacent panels were cast in-situ, while in the flyovers there are no joints between them. View of the completed northern E3 flyover after assembling of prefabricated edge parapets is presented in Fig. 5.

Fig. 4 Use of side precast elements in erection of the main bridge superstructure

Fig. 5 View of the E3 flyover after assembling of prefabricated edge parapets

3.2. Multi-span WA-19 and WA-17 flyovers

Two long flyovers, WA-19 and WA-17 (*Biliszczuk et al. 2008*), in which preassembled steel elements forming the superstructure are used, were built along the ring road of Wrocław.
WA-19 flyover consists of two structures curved in plan, separate for each carriageway. Each of them is a 16-span continuous beam made of prestressed concrete class C50/60. In the

cross-section, it is a single box structure. The superstructure was cast in-situ on scaffolding in 5 sections. Span lengths of both parallel structures are identical: 35.0 + 40.0 + 3 x 45.0 + 50.0 + 2 x 55.0 + 44.0 + 58.0 + 2 x 50.0 + 40.0 + 50.0 + 48.0 + 40.0 m. The total length of the flyover is 750.0 m. Due to the significant length of the deck plate cantilevers, they are supported by steel tube struts, forming a "V" shape in side view (see Fig. 6). The struts carry the load in the transverse and longitudinal direction, and also dominate the architectural reception of the flyover.

Structural configuration of the WA-17 flyover is similar to the previous, but it was erected by means of incremental launching. The total length is 300.0 m, the span lengths are: 30.0 + 40.0 + 50.0 + 60.0 + 57.0 + 34.0 + 29.0 m. Fig. 6 shows the structure during the construction stage.

Fig. 6 Erection of the WA-19 (left photo) and WA-17 (right photo) flyovers

4. CONCLUSIONS

Analysis of the presented examples provides the following conclusions:

- use of precast concrete or preassembled steel elements in designing of bridge superstructures enables achieving interesting architectural effects;
- prefabricated elements can be used both in straight and curved bridge spans;
- use of precast elements, supporting bridge deck cantilevers, reduces width of the box girder, thus minimizing the width of the pier and the costs of its erection;
- application of prefabricated elements reduces the time of bridge construction,
- prefabricated elements can be used in spans built in any construction technology,
- present technolgy allows manufacturing of thin-walled and complex-shaped prefabricated elements, and ensures high material quality and geometrical accuracy.

5. REFERENCES

Biliszczuk J. et al.: „Rozwiązania konstrukcyjne zastosowane w projekcie estakady w ciągu Obwodnicy Śródmiejskiej Wrocławia", Inżynieria i Budownictwo, 9/2002, pp. 498-510

Biliszczuk J. et al.: „Bridges along highway ring road of Wrocław", Proc. of IABSE Symposium Imporoving Infrastructure Worldwide, Weimar 2007, pp. 280-281

Biliszczuk J. et al.: „Technological aspects of construction of a concrete cable-stayed bridge along the highway ring road of Wrocław", Proc. of *fib* Symposium Prague 2011, pp. 427-430

TYPICAL DAMAGES AND PROTECTIONS OF CONCRETE BRIDGES LOCATED ON AREAS WITH GROUND DEFORMATIONS

Marek Salamak
Silesian University of Technology, Road and Bridge Dep.
ul. Akademicka 5, 44-100 Gliwice, Poland

SUMMARY

The construction of bridges in the Silesian urban agglomeration, in the operation area of a number of coal mines, is a specific task. This is mainly because of the need to take into account in the design the necessity of protection against strong ground surface deformation. The reasons of such deformations can come also from shallow tunnelling, groundwater withdrawal or post-seismic phenomena. Concrete bridges with their heavy and rigid solids are sensitive to the irregular subsidence, the horizontal strain in a subsoil and the inclination of previously horizontal surface. The paper shows examples and the list with typical damage categories of concrete bridges which are located on areas with ground deformations. It suggests also some methods of rectification and protection.

1. INTRODUCTION

The Upper Silesian Agglomeration is a cluster of neighbouring cities forming a strip about 70 km wide with highly concentrated industrial and business activities. The Agglomeration is inhabited by ca. 10 % of the population of Poland, and the average population density is over 1900 persons/km^2. It is also a large transportation centre. It is an important component of the European transport network. The predominant traffic direction is east-west (Berlin-Cracow-Lvov) along the existing A4 motorway and the local thoroughfare (DTS). The total traffic flow along this direction may in the near future reach 200 thousand vehicles per day. The other traffic direction, north-south, comprises mainly the A1 motorway under construction, part of the transeuropean north-south route, which links Scandinavia with the South of Europe.

All these transport routes run across areas of intensive underground mining activities. There are nearly 40 coal mines in the region. Total output of these mines is close to 100 million tonnes of coal per year. One of the effects of these activities are ground surface deformations which cause damage to the infrastructure.

This calls for the taking into account of protection against strong effects of ground surface deformation in the design of civil engineering structures and for continuous monitoring of the condition of the latter (*Salamak 2005*). That is one of the factors, which contribute to the high cost of motorway construction here, amounting to nearly 15 million Euro for 1 km, which is about three times as high as in other regions of Poland.

2. DAMAGES OF BUILDING STRUCTURES

In the scheme of building structural damage, according to the proposal given by (*Bien 2010*), three groups of criteria for classification may be used:

- causal criteria - relating to the cause or causes of the damage,
- effect criteria - connected with the impact (effects) of damage,
- cause-effect criteria - trying to connect causes and effects.

In the first approach ground deformation will always be the primary cause, which may be due to various influences: the operation of mining, tunnelling, or changes in ground conditions. Secondary causes are associated with the nature of these deformities. This can be a continuous and discontinuous deformations or ground vibrations. Continuous deformations to which this paper is limited, are associated with different vertical and horizontal displacements, slopes of the terrain and ground strains. Displacements and slopes have a significant impact on mutual motions of bridge solids (the swing supports, displacements spans) and the strains cause additional stress in the foundation and retaining elements (tangential stresses under the foundation, changes of the pressure on the wall abutments)

As the causes of bridge failures encountered in practice are often not evident, and it happens that they are composed of many causes, most rational seems to be adopting the effect as a criterion for classification damages. This approach is commonly used in Bridge Management Systems. This is especially true of objects in the areas of ground deformation, where the usual primary and main cause is the deformation of the land on which the object is erected. Distortion caused by the mutual displacement of bridge solids as a consequence may cause further damages, already delayed in time, such as changes in material properties as a result of deterioration in their corrosion resistance, for example, by cracking.

The overall impact of mining and related ground deformation in the structural objects can be found in (*Kwiatek 2007*). For example bridges, according to him include the effects of overloading statically indeterminate structures, clamping joints and excessive movements of the sliding bearings. Note, however, that given in the same spot possible damages to buildings, and thus inclinations, cracks, walls shape deformation and user discomfort apply equally to the bridges. Bridges as linear objects (roads, railways) are also sensitive to change declines, faulty drainage and excessive damage to the roadway on the approach. The range of damage is so very big and covers most of the observed defects in both the cubature and line objects.

Departments of Mining Claims themselves and to varying degrees of accuracy, try to keep a record of damaged buildings cubature for estimating the damage caused. The most common form is a sheet-damaged building, developed by the Central Mining Institute in Poland. There hasn't been similar model form for the bridges so far. It can be assumed that the reason for this is that the number of bridges in relation to the cubature objects, until recently, was significantly lower. There wasn't also ambiguously defined responsibility for them. But the situation changed after the reform of road administration and implementation of an extensive road construction program in Poland. With each year the number of bridges is increasing rapidly. Especially large and important bridges, located in passageways of main routes. The awareness and responsibility of their respective owners also increases, which include in addition to the State Treasury, local government units. Hence, it would be a useful introduction to the use of a uniform format form, documenting damage to the bridge associated with the deformation of the terrain. It would complement currently used in the economy of bridge maintenance systems and methods of a general description of damage.

3. SYSTEMATICS OF BRIDGE DAMAGE

Assuming the systematic failures of bridges with the effect criterion, damages in Bridge management Systems may divided into the following types:

1. Changes of the position of bridge elements - inconsistent with the design the object or its part displacement, at which the mutual distances of all points of displaced structure element do not change (also the restriction of the movements).
2. Deformation - inconsistent with the design the geometry change, causing changes in the mutual distances of the points of the object or its part (eg, bending, twisting).
3. Loss of material continuity - not compatible with the project breakdown structure of the material (such as cracks, breaks).4
4. Failures - the loss of serviceability of the object or its part (isolation, lighting, drainage, etc.).
5. Damage to corrosion protection - a partial or complete dysfunction of material protections.
6. Losses of material - reducing the amount of construction material relative to the design.
7. Destruction of material - the deterioration of physical and chemical characteristics of the material in relation to the design.
8. Pollution - the presence of all kinds of dirt, runs, raids, and unforeseen in the project plant vegetation.

In the case of objects that are affected by terrain deformation direct relation of cause and effect can be speak for damage to type 1 to 4 Other damages are not directly related to the displacements and deformations of the ground, but may arise as a consequence of deformation, repositioning, cracks or failure of the bridge elements. Their origin is not so clear. Especially in the case of long used objects where there is already material aging and the effects of poorly maintenance and the lack of casual repairs. For this reason, these types of damage have been omitted from the further damage systematic.

Changes in the location of the bridge elements include:

- Displacements of supports (in the foreground, vertical, rotating, swinging).
- Displacements of approaching slabs.
- Displacements of spans (in the plan, the vertical breaking, declinations, contactless tracks).
- Displacements of bearings (in the plan, detachment, eject).
- Changes in expansion joints (tightening, gaping, shearing).

Deformations of the bridge elements include:

- Bends of the support elements (frame columns and wing abutments deformation).
- Bends and torsions of spans (strains in indeterminate spans, oblique and curved spans).
- Deformations of bearings (roller jam, elastomeric deformation, breaking of anchorages and bearing slides, exceeding the displacement range).
- Deformation of the carriageway on the approaches (bumps, humps, depressions on pavement and sidewalks, tracks deformation in the plan).

Loss of the material continuity is mainly cracks and breaks in the structure spans (due to bending, compression, torsion) and supports (cracks in the body, disruption of the wings, sheared of back walls). Failures are related to the change in the roadway declinations (change of traction parameters, the problems with waste water), gaping of expansion joints, damages of external facilities (pipelines, water supply, power cables, telecommunication and traffic control).

4. BRIDGE PROTECTIONS AGAINST GROUND DEFORMATIONS

The primary and original way to protect the bridge to the influence of terrain deformation is to use simple, statically determinate structural systems. Because in such schemes, the mutual movement of solids, for example due to uneven settlements or inclinations, will not generate additional internal forces in the superstructure. Much it limits the designer, who is not able to use, especially for larger and more exposed objects, contemporary design solutions. Other security methods include:

- the use of sand bags under the foundations,
- reducing the friction of the soil through their bodies, smoothing abutments,
- division into smaller segments by dividing large supports,
- special bearing system which allows easy deflection,
- adopt appropriate range for large displacements in the expansion joints and bearings.

In addition, prediction should be made at the design stage of both bearings, the possibility of rectification of span and potential multiple increasing the height of supports and embankments. All these treatments are mainly aimed at extending the life of functional object in a situation of excessive and uneven ground movement.

5. CONCLUSION

Damages of bridges located in areas of ground deformations, and this area is the Upper Silesian Industrial District in Poland, have a specific nature and require some experience and knowledge in their identification and assessment. This is mainly associated with the kinematics of solids components of the bridge and the lack of adequate security for the construction of old objects built before the planning of mining activities in its vicinity. Gathered experience and the systematic of damage will develop effective ways of protection of new bridges and eliminate a number of problems that are seen at their current operation.

6. ACKNOWLEDGMENTS

The paper was prepared under financial support from the research project no N N524 166835 from Polish Ministry of Science and Higher Education.

7. REFERENCES

Bien J. (2010), ”Uszkodzenia i diagnostyka obiektów mostowych”, WKŁ, Warszawa

Kwiatek J. (2007), ”Obiekty budowlane na terenach górniczych”, GIG, Katowice

Salamak M., Weseli J., Radziecki R. (2005), Monitoring of highway bridges in areas under mining exploitation influence, 5th International Conference on Current and Future Trends in Bridge Design, Construction and Maintenance, 17 – 18 September, Beijing, China, p. 469-478

STUDY OF THE ADHERENCE AMONG MORTAR OF REPAIR WITH CIMENTO GEOPOLIMÉRICO APPLIED IN SUBSTRATUM OF CONCRETE WITH CIMENTO PORTLAND.

Silvio de C. Mazza[1]; Vanessa S. Silva[2]; Dylmar D. Penteado[3]; Marcos M. Silvoso[4]

[1] *Departamento de Ciências e Tecnologia dos Materiais, Pesquisador Mestre.*
Escola Politécnica. Universidade Federal da Bahia.
Rua Alm. Carlos Parag. de Sá, 140, sl. 101. Pituba. 41.810-660 - Salvador, BA - Brasil
email: scmazza@ig.com.br
[2] *Professora Doutora, Departamento de Ciências e Tecnologia dos Materiais.*
Escola Politécnica. Universidade Federal da Bahia.
Rua Aristides Novis, 02, DCTM. Federação. 40210-910 - Salvador, BA - Brasil
[3] *Professor Doutor, Laboratório de Engenharia Civil.*
Universidade Estadual do Norte Fluminense Darcy Ribeiro,
Av. A.Lamego, 2000.Pq Califórnia. 28013-602 - Campos dos Goytacazes, RJ – Brasil
[4] *Professor Doutor e Pesquisador, Programa de Engenharia Civil/COPPE.*
Universidade Federal do Rio de Janeiro. FAU. Dep.de Tecnologia da Construção.
Av. Pedro Calmon, 550. 21941-901 - Rio de Janeiro, RJ - Brasil

SUMMARY

This work is the result of the behavior of geopolymer mortar adhesion of the repair in the slot, pulled the stringer beams of concrete, looking for a better knowledge of the geopolymer and the adhesion between these materials. The experimental program consisted of checking the mechanical behavior of concrete repair and verification of adherence behavior repair to the concrete substrate. From the analysis of the results obtained, it can be concluded that the geopolymer mortar improved part performance repaired and secured increased tensile strength of beams in the reference, indicating it as a good technique for repair of structures.

1. INTRODUCTION

Research involving the use of geopolymer cement in construction are being conducted in several countries, to example of France, Spain, Portugal, Australia, United States, South Africa and Brazil, with the highest scientific and technological advances achieved to date occurred in the latter. Those progresses come from research conducted mainly in the Military Engineering Institute, where they were studied some important properties of geopolymer such as microstructure, adhesion to steel in concrete armed, when applied in industrial flooring, paving, ballistic protection, and maritime and port works other performance requirements that are more severe with regard to durability to chemical aggressive.

2. EVOLUTION OF STUDIES ON GEOPOLYMERS

Historically, this type of ligand has been the subject of intense analysis by researchers in various parts of the world, but only in 1978, Joseph Davidovits introduced and patented the term "geopolymer". Several other works on the collection, characterization and employment of geopolymers are under development in several places in the world (*Roy, 1999*), following the example of Korea (*Yang et al., 2007*), Portugal (*Torgal et al, 2008*) and USA (*Sakulich, 2009*).

In Brazil, one can trace the evolution in studies of this type of material (Tab. 1) starting in the middle of the decade of 90.

Tab. 1 Chronology on some events concerning the cement geopolimérico in Brazil.

Autor	Ano	Descrição
Costa Jr., A. M.	1996	Resistance of Composite Materials to the Ballistic Impact geopolymer concrete
Barbosa V. F. F	1999	Synthesis and Characterization of Polissialatos
Thomaz, E. C. S	2000	geopolymer concrete
Dias, D. P.	2001	Cements Geopoliméricos: Study of Adherence and Tenacity to the Fracture Geopolymer cements: Study of adhesion and fracture toughness
Cuiabano, J. L. S. P.	2002	Effect of Temperature on the Properties of geopolymer cement
Lima, F. T.	2004	Micro and nanostructural characterization of geopolymer composites Metacauliníticos
Souza, L.G	2005	Geopolymers-Based Industrial Waste
Silva, A. C. R.	2006	Behavior of Concrete Floor for geopolymer Under Cyclic Loading
Pinto, E. N. M. G.	2007	Activation Folder geopolymer for Cementing Oil Wells
Dias, A. A.	2008	Study of Degradation of geopolymer mortar for Acetic Acid and Sulfuric
Mauri, J.	2009	Study of Degradation of geopolymer mortar
Mazza, S.C.	2010	Study of mechanical properties and adhesion of the system geopolymer mortar / concrete

3. USE OF NEW MATERIALS FOR REPAIR

Research involving repair mortars, in most cases did not address one of the most important properties: the adherence between the substrate and repair

4. METHODOLOGY OF EVALUATION

The methods of adopted rehearsals were AFNOR NF P 18-851:1992 (dependent of the rupture type) and ABNT NBR 12142:1994 (determination of the resistance to the traction in the flexing). In the first, the rupture can in the following ways: just of the concrete, without compromising of the repair system (Type C); with the breaking of the repair and propagation for the concrete prism (Type M), with the detachment of the sloping part and development of the fissure for the concrete (Types I-1 and I-2) - in these cases the rupture occurs in the region of the inclined groove, and to release the break and subsequent repair of the concrete (Type D). In the second case, through the load versus vertical deflection behavior.

5. ADHESION BEHAVIOR OF SHEAR ON THE BENDING BEAM MONOLITHIC AND REPAIR (AFNOR NF P 18-851:1992)

Concrete beam – Monolithic

In Fig.1, we see the result of testing of monolithic concrete (unnotched) to serve as a reference for looking at the type of rupture.

a) Monolithic concrete Beam. b) Break the concrete beam type M - Monolithic..

Fig. 1 Configuration of the test and break the monolithic beam. AFNOR NF P 18-851:1992.

It appears that the body-of-proof concrete prism, receiving efforts during the tensile test in the four-point bending, split in its middle third. It was also observed that, at fracture, the crack spread from bottom to top, like the rupture of type M - Monolithic prescribed in the AFNOR NF P 18-851:1992.

Concrete beam - Repaired with the reference mortar (Grout)
In Fig. 2, we see the result of bending test four points in the body-of-proof concrete prismatic slot filled with the reference mortar (grout) to verify the type of rupture.

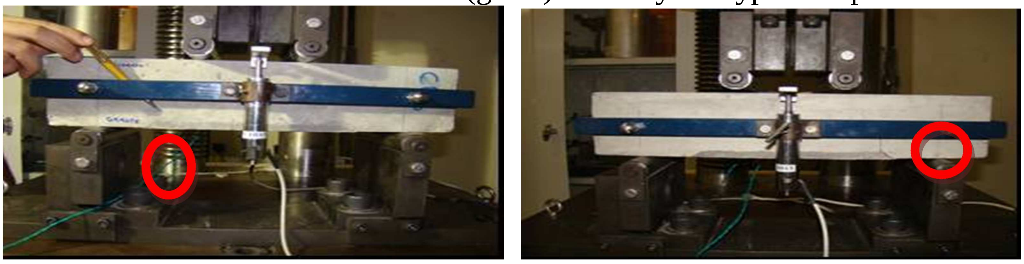

a) Beam with grout repair. b) Rupture of the beam repaired with grout, type I-2.

Fig. 2 Configuration of the test and the rupture of two Type I-beam with grout (AFNOR NF P 18-851:1992

In the body of the test piece prismatic concrete repaired with grout, it is observed that the repair material is away on the slope of repair, with the development of the concrete to crack. Note, then, that the form of rupture was of Type I-2, based on French standard, which prescribes how this type of break for body repair.

***Concrete beam - Repaired with* geopolymer**
In Fig. 3, we see the result of bending test within four points of slot filled with concrete with a geopolymer mortar, to check the type of rupture.

a) Configuration of beam with geopolímero b) Rupture of the beam with repair, type M.

Fig. 3 Setting up the test and rupture Type M - Monolithic. AFNOR NF P 18-851:1992 test.

The test performed, it appears that the body-of-proof prismatic concrete repaired with the geopolymer, upon receiving the efforts during the trial, presented with early cleft repair, located in the middle third of the body-of-proof . Later, with the disruption of the repair, there was the crack propagation for concrete prism, acting monolithically (Type M).

6. MECHANICAL BEHAVIOR OF THE SYSTEM REPAIR / SUBSTRATE THROUGH THE FLEXING REHEARSAL TO FOUR POINTS (ABNT NBR 12142:1994)

Behavior Load versus Vertical Deformation

In Fig. 4, the curves meet "potential" and details of the monolithic concrete beams and the beams repaired.

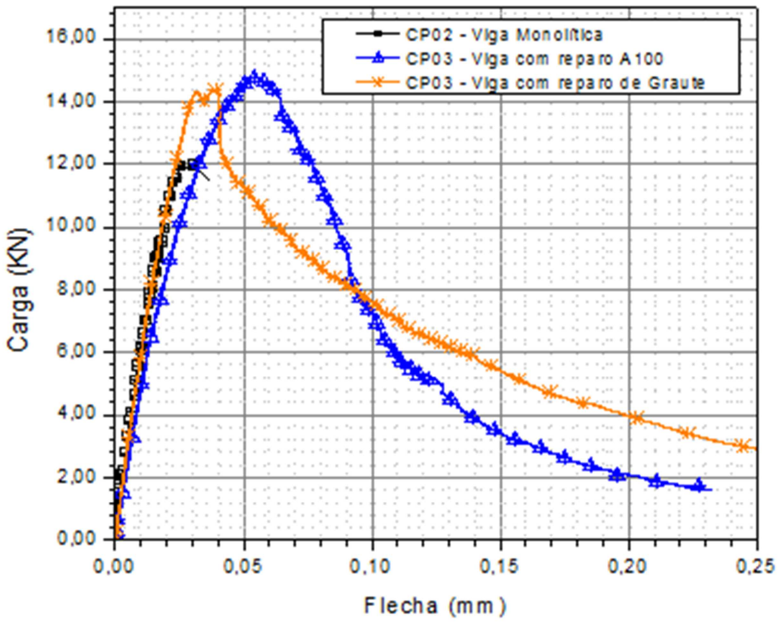

Fig. 4 Load versus displacement curves of the beams (curves with the greatest potential) tested.

It is observed that the deflections read in the vertical beams in the middle of the curves will have very close. This fact indicates perfect adherence to concrete repair, allowing the solidarity of the system substrate / repair system

7. CONCLUSION

From the experimental results, we can consider that there was an increase of strength and stiffness provided by the repair adopted, concluding that the reconstitution and strengthening of stringer slot pulled the beams repaired with geopolymers are effective not only in terms of cargo capacity, for the resistance increment to the system, as well as in terms of adherence.

8. REFERENCES

Association Française de Normalisation. AFNOR NFP 18-851: Produits ou systèmes de produits à base de résines synthétiques ou de liants hydrauliques destinés aux réparations de surface du béton durci. - Essai de flexion sur éprouvette évidée et reconstituée. Bruxelas, 1992.

Brazilian Association Of Technical Standards. NBR 12142: Traction in the flexing. prismatic. BATS. 1994.

Roy, D. M. 1999. Alcali – activated cements. Opportunities and challenges. Cement and Concrete Research v.29, p. 249-254.

Sakulich, A.R., Anderson, E., Schauer, C., Barsoum, M.W., 2009, Mechanical and microstructural characterization of an alkali-activated slag/limestone fine aggregate concrete, Construction and Building Materials, v. 23, pp. 2951-2957.

Yang, K. H.; Song, J. K., Ashour, A. F., Lee, Eun-Taik., 2007, Properties of cementless mortars activated by sodium silicate, Construction and Building Materials 22 (2008) 1981–1989.

Torgal, F.P., Castro-Gomes J. P., Jalali, S.. Properties of tungsten mine waste geopolymeric binder. Construction and Building Materials Vol.22, pp.1201-1211. 2008.

DESIGN AND USES OF FIBER COMPOSITE MATERIAL IN INSULATED CONCRETE WALLS

Venkatesh Seshappa, P.E & S.E.
Composite Technologies Corporation
1000 Technology Drive, P.O. Box 950, Boone, IA 50036 USA

SUMMARY

This paper discusses the design and uses of fiber composite material in the insulated concrete walls. This paper discusses some of the newer load transfer devices developed for multiple applications including the double wall applications and walls for Zero Energy structures.

1. INTRODUCTION

Integrally insulated wall panels known as sandwich panels have been around for four decades. However, new challenges are faced with thicker insulation required due to the change in building codes, which requires innovative devices for different applications. These applications could be precast or site-cast walls of different sizes and shapes.

2. X-SHAPED LOAD TRANSFER DEVICE

Thermomass has developed an X-shaped load transfer device (LTD) (worldwide patent pending) to use in the sandwich wall panels for use in multitude of applications. Figure 1 shows such a device. As discussed in the introduction, thicker insulation layers (125 mm to 200 mm) are required by the codes as sustainable design is adopted. 200 mm insulation thickness is quite common for zero energy buildings. X-shaped LTD is made from glass fibre composite material which has a very low thermal conductivity and hence does not create a thermal bridge between the wythes.

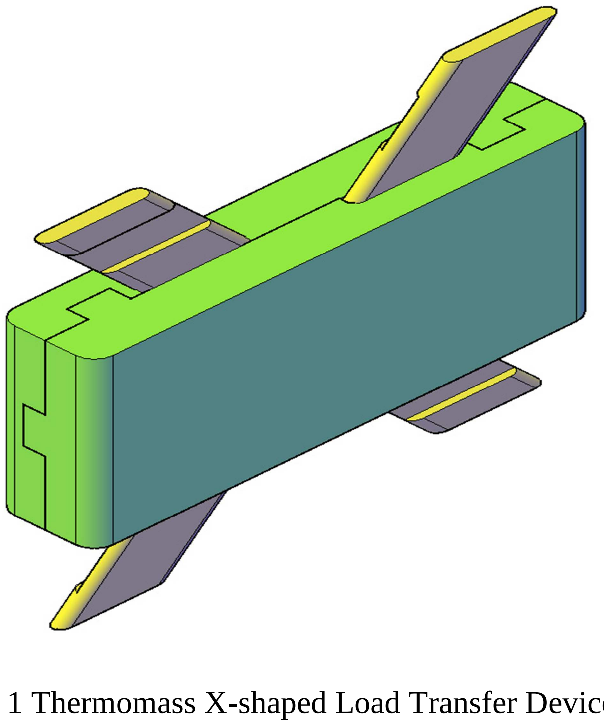

Fig. 1 Thermomass X-shaped Load Transfer Device

3. APPLICATIONS FOR X-SHAPED LOAD TRANSFER DEVICE

There are several applications for such device. They are:

1. To support the free hanging fascia wythe in a structurally non-composite insulated wall panels with insulation thicker than 125 mm.
2. To provide additional shear transfer capacity at the ends of the structurally composite panels where a solid through concrete section was required otherwise and thus eliminating thermal bridge due to solid zones of concrete. In this application, the X-shaped LTD is used in conjunction with other types of Thermomass connectors.
3. To manufacture a structurally composite panel with thicker insulation, thus reducing the concrete wythe thickness required as compared to structurally non-composite panels.
4. To provide torsional resistance for the fascia wythe in a spandrel (horizontal) panel.
5. To provide support at localized areas for signage and canopies in insulated wall applications.

A cross section of the panel with the X-shaped LTD is shown in Figure 2.

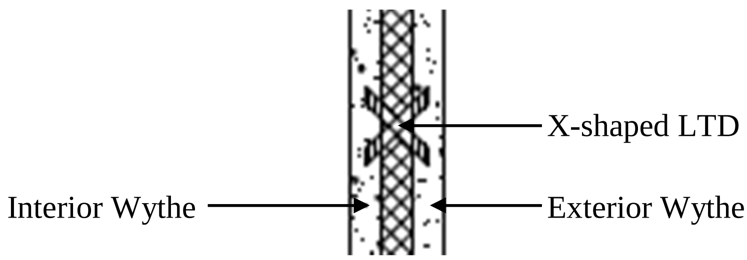

Fig. 2 Cross section of a wall panel with X-shaped LTD

4. TESTING PROGRAM

The testing program consisted of determining the shear capacity of these LTD's and the shear stiffness of the LTD's. To test these properties, it was decided to cast sample panels of 0.6m x 1.2 m with four (4) LTD's in each panel. The concrete wythe thickness for the testing program was 100 mm and insulation thickness of 100, 150 and 200 mm were tested. The test setup is shown in Figure 3. The samples were tested in horizontal orientation due to size of the test sample. The load was applied using a hydraulic ram to the top wythe with help of a spreader beam. Load and displacement of the top wythe was measured continuously using data acquisition system. Displacement was measured at both left and right end and average displacement was used in load-displacement curves. The ultimate average shear load per LTD was determined by taking the average of 4 test specimens and dividing by number of LTD's per specimen (four). The ultimate shear values of LTD's are given Table 1. The load displacement curve for 200 mm insulation thickness is given in Figure 4. Typical failure modes of all specimens were pull-out of LTD from concrete.

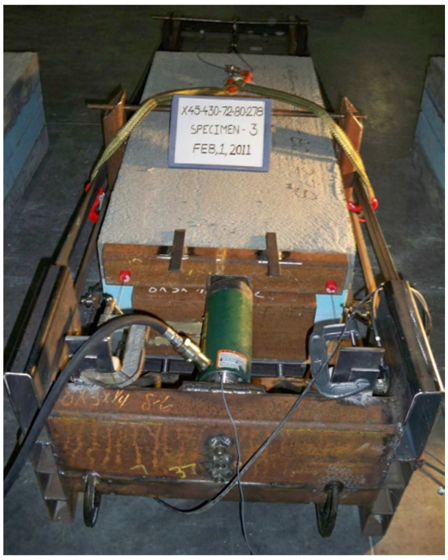

Fig. 3 Photograph of test setup

Insulation Thickness (mm)	Ultimate Load per LTD (kN)
100	35.0
150	26.3
200	35.1

Table 1 Ultimate shear load capacities

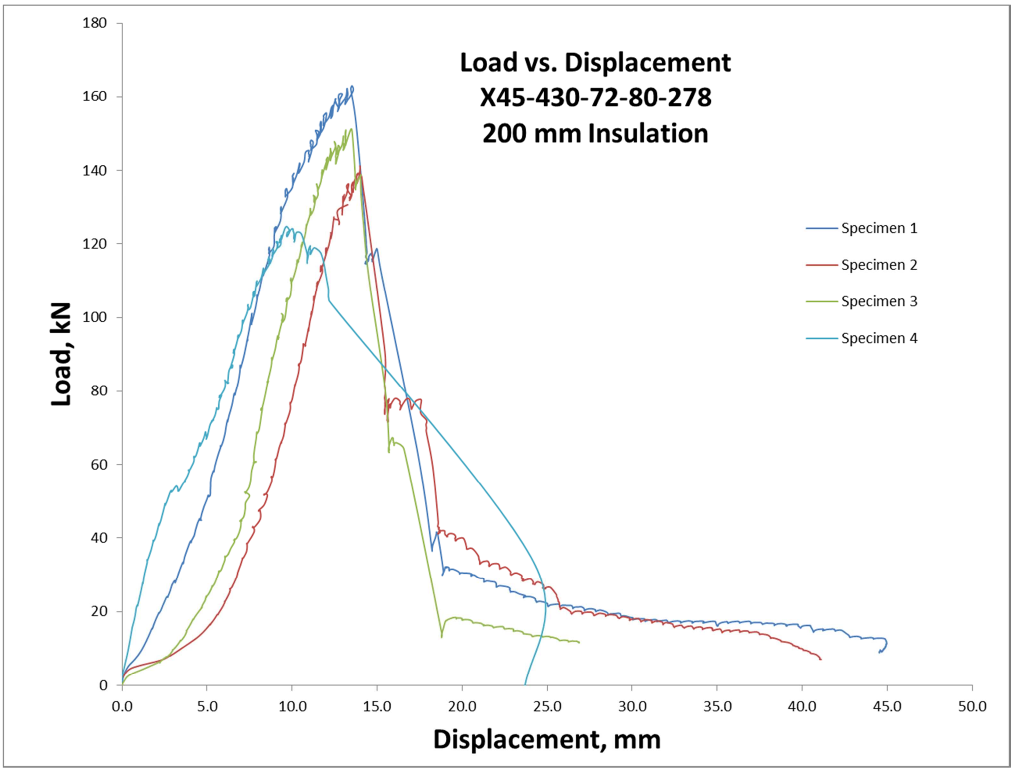

Fig. 4 Load vs. Displacement Curves for 200 mm insulation thickness

5. DESIGN METHOD

The design of wall panels using Thermomass LTD's can be carried out by following classical approaches or any other rational method. The space limitation in this paper does not allow discussing the design methods in detail.

6. PANEL CONSTRUCTION PROCESS

The manufacture of wall panels using Thermomass LTD's is similar to other horizontally cast sandwich wall panels. It involves in the placing an exterior wythe of suitable thickness, placing rigid foam insulation boards with pre-drilled holes for LTD's and other connectors as required. The LTD's and connectors are then placed in plastic concrete and vibrated to achieve proper consolidation around the LTD's and connectors. The reinforcement for the interior wythe is then placed on top of the rigid foam insulation and interior wythe concrete is then placed. Once the concrete wythes are hardened, the wall panel is stored or erected in place by cranes.

7. CONCLUSIONS

Thermomass LTD's can be effectively used in manufacture of sandwich wall panels for different applications which eliminates significant thermal bridge between the wythes. The applications shown in section 3 are only a few of the applications and there are several other applications in which this type of Load Transfer Device can be used.

8. REFERENCES

Wade, G.T., Porter, M.L., Jacobs, D.R. (1988), "Glass-Fiber Composite Connectors for Insulated Concrete Sandwich Walls", Iowa State University, Ames, IA.

ASTM E-488, Standard Test Methods for Strength of Anchors in Concrete and Masonry Elements, ASTM International, West Conshohocken, PA.

STUDY OF THE CO-OPERATION BETWEN PERFOBOUND CONTINOUS CONNECTORS AND CONCRETE SLAB

Filip-Văcărescu Florin[1], Köllo Gavril[2]
[1] *Department of Civil & Materials Engineering and Earth Science*
North University of Baia Mare
Romania, Maramureş, 430092-Baia Mare, 62/Ath Dr. V. Babeş str.
[2] *Faculty of Civil Engineering-Department of Railwais, Roads & Bridges*
Technical University of Cluj-Napoca
Romania, Cluj, 400500- Cluj-Napoca, 72th Observator str.

SUMMARY

The use of perfobound continuous connectors is an upcoming solution in composite steel-concrete for bridges and civil structures. With high initial stiffness, bearing capacity and ductility made them a new and economic solution. This paper represent the first two stages of an comprehensive research on continuous connectors and revel the results obtained by mean of original laboratory tests, regarding the co-operation of concrete slab and connectors constructed from rolled steel plate cut longitudinally in rectangular strips with various cutting shapes

1. INTRODUCTION

SR EN 1994-1-1:2004 in Annex B, stipulate that if design rules from 6.6 could not be applied, then laboratory tests are needed to determine the proprieties and the behaviour of the connectors. Two major problems occurred in this case:

-this type of tests (standard push-out test) are suitable only for headed studs connectors.

-performing this kind of tests need large testing machines and costly samples.

Clearely this type of tests will not solve the problem of this study. However material specification (steel, concrete) whas taken in acount.

This paper represent the first stage of an comprehensive research on the behaviour of the continuous connectors also the co-operation with concrete slab and focus on two major problems:

-defining a faster, costless but reliable test method, suitable for relative small testing equipment (max load for tensile tests = 500 KN). Taken account of this constraints the test method used in this research was: SIGLE PUSH-OUT TEST. A wild range of testing equipment was designed and manufactured for this purpose, the tests where performed at the "LabCon" witch is an North University lab, specialised in building material testing with recognised national competences in domain.

-defining an optimal geometry for this type of connectors from point of view of behaviour and manufacture costs. Two major types of connectors was considered for this study. The first one with holes intersecting one edge of the steel stripe (Fig. 2 a.), designate as: K(± 35) where 35 represent the circle radius of the hole and the sign ±

the indication that the hole intersect the material and the edge of the stripe. The other one with holes inside the edges of the strip (Fig. 2 b) designate as K(-25).

2. TESTING ARRANGEMENTS

2.1. Defining the push-out technique

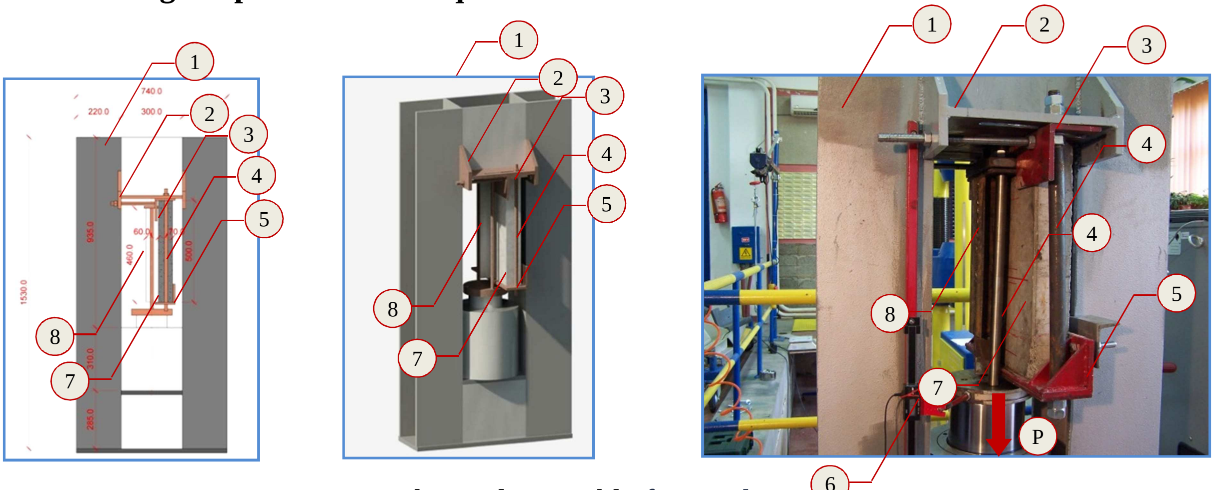

Fig. 1 Mechanical ensemble for single push-out test
1:TEHNOTEST F50 Universal Testing Machine, 2:Console, 3:Upper sample support, 4:Steel tension rod, 5:Lower sample support, 6:Digital mesuring tool with USB cable connection for data aquisition, 7:Concrete slab, 8:Steel connector

2.2. Definindg the tests specimens for single push-out tests

Connectors (Fig. 2): cutted fom steel sheet plate S235 with f_y=240N/mm^2 (f_y whas taken as the mean value of tree specimens)

Two basic types of connectors whas taken in consideration for this study:

- type K(±35): with holes intersecting the boundaries of the steel stripe (Fig. 3 a)
- type K(-25):with holes inside the boundaries of the steel stripe t6(Fig. 3b)

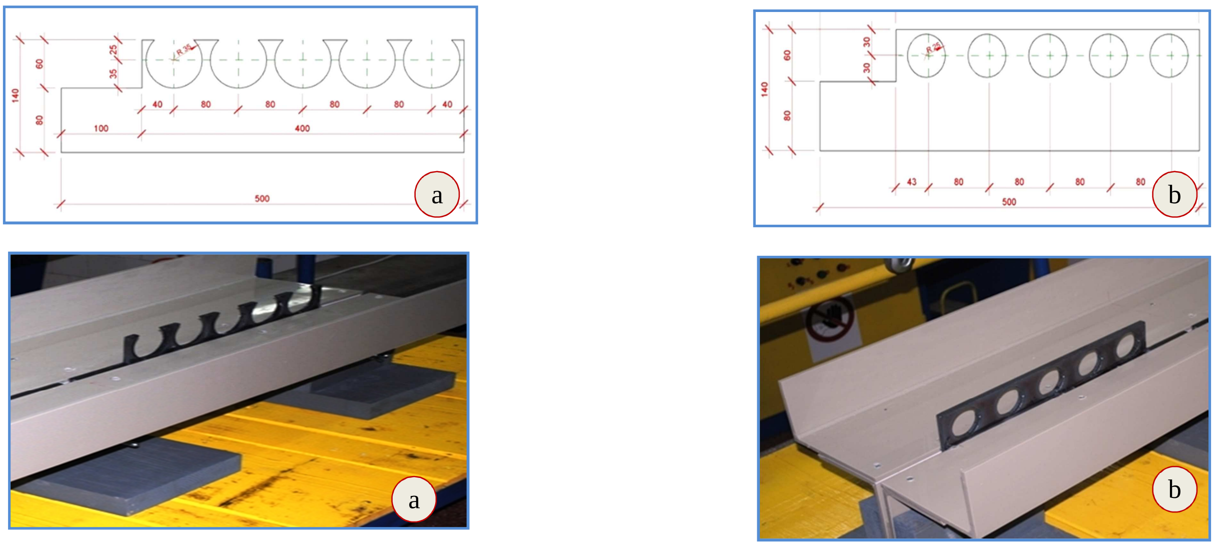

Fig. 2 Connectors types
a: K(± 35):connector with holes intersecting the boundaries of the steel stripe,
b:K(-25): connector with holes inside the boundaries of the steel stripe

Concrete slabs (Fig. 3) : l=500; b=350; h=75; f_{cm}=30 N/mm2 (f_{cm} whas taken as the mean value of four concrete specimens prepared at the time of casting the push specimens)

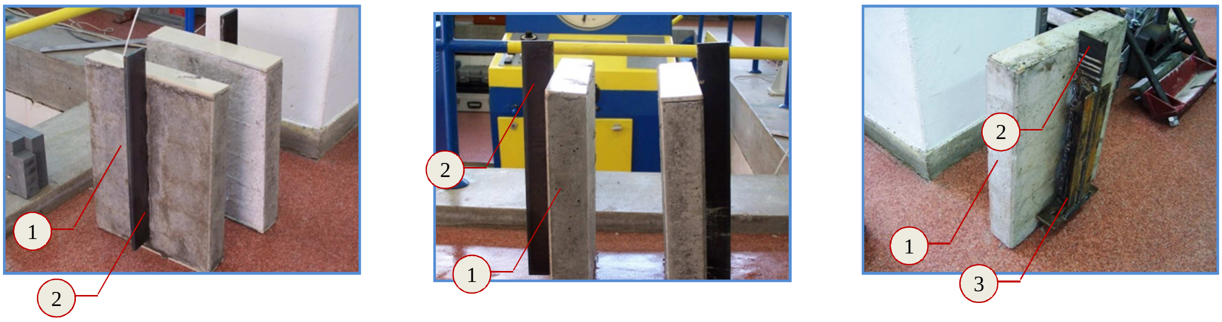

Fig. 3 Specimens for single push-out tests
1: concrete slab reiforced with ribbed bars, 2: connectors type: K(±35) & K(-25), 3:connector reiforcements

Reinforcement (Fig. 4): ribbed bars Ø8 mm with $450 \leq f_{sk} \leq 550$ N/mm^2 (Fig. 4)

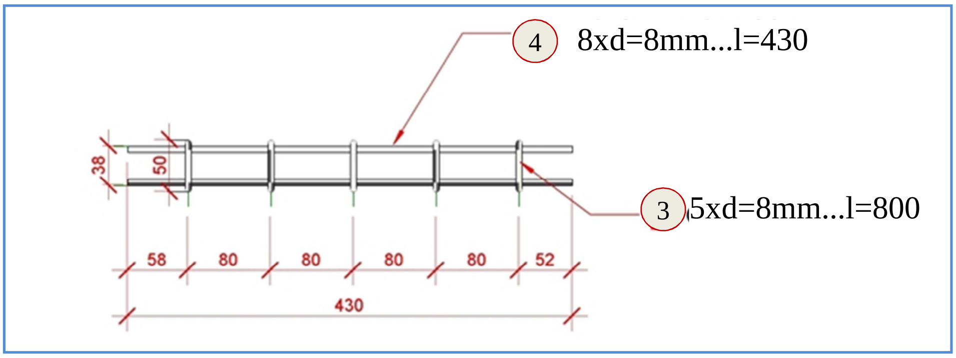

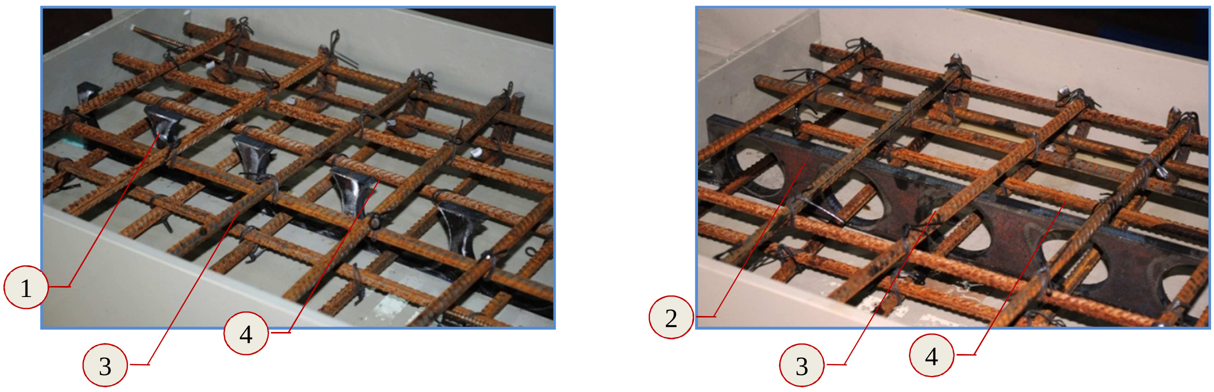

Fig. 4 Reinforcement in the case of two type of connectors
1:connector type K(± 35), 2: connector type K(-25), 3: reebars Ø8, 4: logitudinal bars Ø8

4. CONCLUSIONS

The tests whas considered finish at 320 KN load force, due to partial distruction of the concrete slab as the result of co-operation betveen connectors and the slab in the side where load force whas applied on the specimens (Fig. 5). However no desplacements could be observe between connectors, regardless the geometry, and the concrete slab which meen an etreme rigid coportament of the connectors. This behaviour impose a redimension of the connectors for a more ductile one in the next stage of tests.

Fig. 5 Tests results
a): slab with K(± 35) connector, b): slab with K(- 25) connector

5. REFERENCES

Bertalan. S.,Influence of shear coneectors on the elastic behavior of composite girders-Doctoral disertation

Ciutina, A. : Comportarea Structurilor in Cadre Compuse din Oterl-Beton si a Imbinarilor Acestora Editura Orizonturi Universitare Timisoara 2007

Dischhger, F.,Elastic and plastic deformations of reinforced concrete load-carryng structures and especially that of arch bridges,

Hawranek, A. & Steinhard, O., Teory and analysis of steel bridges

Hechler, O., Wojciech L.,Gunter S., Eva Viefhues : Continuus Sheear Conectors in Bridge Constructions,

Hechler,, O.,Wojciech. L.,Gunter.S.,Eva. V.,Continous shear connectors in bridge constructions

Hoischen, A., Composite girder with discrete elastic connectors,

Köllö, G., Moga, P. , Gutiu, St., Kiss, Z. : Calculul Structurilor dupa Eurocod Cluj Napoca 2008,

Michel. T.,Jean-paul. L.,A mechanical model for connections by adherence for steel-concrete composite beams,

SR EN 1994-1/2006 Eurocod 4: Proiectatrea Structurilor Compozite de otel si Beton Partea a 1 si 2 Reguli Generale ; (Anexa B)

DATABASE OF RC STRUCTURAL WALL SEISMIC TEST PROGRAMS

István Demeter, Tamás Nagy-György, Valeriu Stoian
Politehnica University of Timisoara
2nd T. Lalescu street, 300223 – Timisoara, Romania

SUMMARY

Experimental campaigns further corroborated the post-earthquake field observations regarding the good seismic performance of RC structural walls however undesirable failure modes were also identified. A series of seismic design principles were devised based on laboratory investigations performed primarily on wall elements and wall building systems subjected to quasi-static cyclic or monotonic lateral loads. As the number of experiments increases in time, an overview of the field becomes more cumbersome and time-consuming. In this paper a database of the experimental programs on RC structural wall seismic tests is presented.

1. INTRODUCTION

Laboratory tests on structural elements are aimed to reproduce the as-built loading and boundary conditions and observe the behaviour mode and measure the response. The experiments are excellent for checking the accuracy of theoretical predictions and/or to assess the behaviour for devising explanatory theories. As the number of experimental investigations increases continuously the need for the data to be ordered emerged also.

Three types of ordered information on lab tests were identified: reference list, catalogue and database. Reference list documents are the most widespread, in fact each experimental investigation report includes a review of the literature regarding other previous works in the field. Extended reference list documents are works dedicated especially to the review of the literature on a specific field. A catalogue type document furnishes more detailed tabulated information on the experiments, mostly on specimen basis. As the number of data lines increases in a catalogue it can be used for statistical evaluations employing specialised computer programs featuring filtering, sorting and searching functions and it can be referred to as database. RC wall cyclic test databases were assembled by Wood, Stanic et al., and Gulec and Whittaker. Online databases are the most easily accessible sources of test information and there is an increasing number of projects in this direction, for example Shear wall database of Palermo, University of Minho’s DABASUM on FRP-based shear strengthening of RC beams, and RILEM’s MSC Data warehouse on masonry strengthening with composite materials. It is important to note that a significant portion of the test data is not available, for language barrier reasons, proprietary issues or not in mainstream publications. The most important data sources are conference proceedings, journals and research reports.

2. DATABASE CHARACTERISTICS

The database described in the following sections was assembled with the aim of a general overview of the cyclic tests carried out on RC walls. Generally, a database or catalogue has its unit commonly a specimen. The present database differs from this by having its unit a test program, for reasons of reducing the collection time and bearing in mind the scope of focusing on the boundary conditions, which are in most cases invariables for a program. In general a database has two major clusters of data columns: specimen data and results. In the present phase the database contains information pertaining to the first cluster of program data. In these conditions it can be referred to as a condensed program database.

The data columns were grouped in three sets: program identification, specimen data and boundary conditions. The first set of data columns contains information regarding the laboratory the tests were performed at, year of publication and country name. As a convention, the year of reference was assumed to be corresponding to the earliest publication that contains detailed information on the program. Specimen data columns refers to designation, construction, specimen type, concrete technology, opening condition, strengthening condition, number of specimens, scale and web thickness. The third set of data columns includes information on the test-set-up, loading and boundary conditions.

It is noteworthy that most of the data columns represented a constant parameter for a specific program, therefore suitable for data processing. A few exceptions were represented by the wall thickness and specimen type, par example, which in many cases were variable inside a program, causing an effect of multiplication of the program. This was resolved by dividing the program in smaller units in order to have unique values for the data columns. This explains why other, more detailed information was excluded from the database. As of March 2011, the database contains 151 data lines and 222 reference lines. The discrepancy is owing to the fact that a certain test program commonly is published more than once at different stages of data processing.

3. GENERAL OVERVIEW

Early laboratory investigations on RC walls subjected to in-plane lateral loads were conducted starting from the 1950s in USA, Japan, Canada and New-Zealand. This early period can be considered until the end of the 1970s (Fig. 1). A significant increase in the number of tested specimens in the 1980s and onward can be observed. It is important to mention that the actual content of the database is limited to the available literature in English language and consequently is not exhaustive. It would be of great importance to obtain country-level reports on this topic by resident researchers who have more in-depth view of the situation in their own country. The geographic distribution of the actual content indicates an approximately one-quarter share of the experimental work between USA, Japan, Europe and other countries. The tested walls were representative of prototypes pertaining to civil constructions and to Nuclear Power Plants (NPP), the first case being more common. In the following discussions the NPP-walls were not considered. According to the present content of the database the Romanian contribution to the RC wall experimental investigations is represented by 7 programs conducted at 4 laboratories, the earliest being dated from 1992. This should be also reviewed by researchers from each university centre in order obtain a more accurate view of the situation.

4. SPECIMEN DATA

The experimental specimens modelling prototype walls of civil structures were classified in component, element and building system types (Fig. 1). Components are web-isolated panels or joint of precast elements. Wall elements are 1-storey, 1-plane and 1-bay structural members not framed by columns and beams. Wall building systems are multi-storey, multi-plane or multi-bay or frame-wall assemblages. A generic loading type data column was also introduced at this stage in order to separate quasi-static tests from dynamic ones. Complex programs featuring both loading types were divided in two uniform groups so as to comply with this criterion. Subsequent discussions are restricted to wall elements and building systems (components excluded) tested in quasi-static manner (dynamic tests excluded). The distribution of storey numbers amongst the wall building system specimens is also indicated.

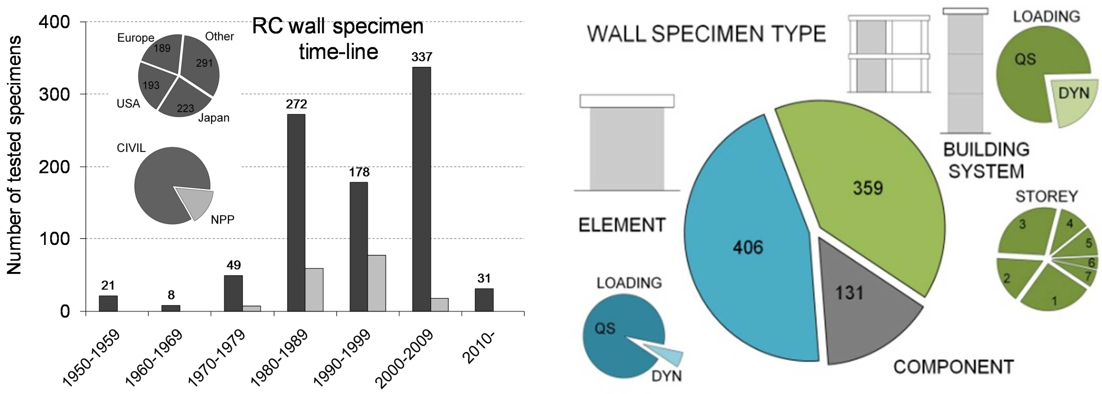

Fig. 1 Review of the laboratory tests

Two further data columns referring to model-to-prototype scale and web thickness of the specimens were considered. These parameters exhibited different distribution according to the type of the specimens. The scale of the wall elements was chose to belong to the 0.25÷0.4 or 0.8÷1 ranges, while for the wall building systems the 0.2÷0.33 scale factor range was preferred. As for the web thickness, the 50, 80 and 100 mm values were representative of wall elements and wall building systems too.

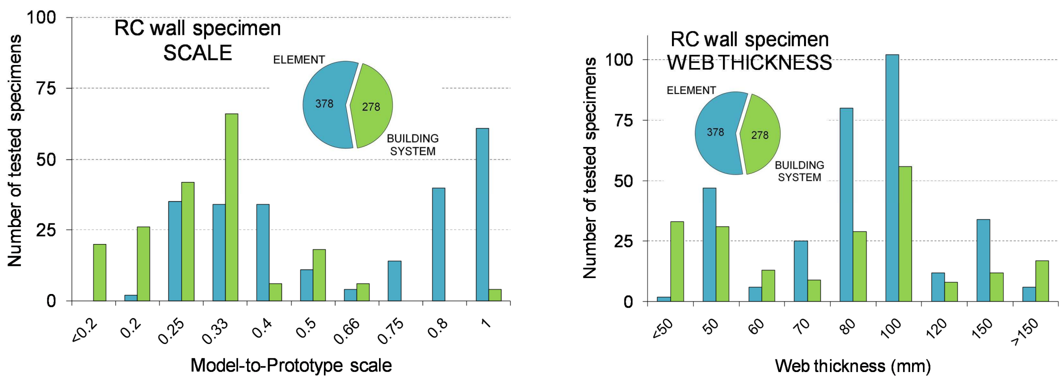

Fig. 2 RC walls scale and wall thickness

A series of three data columns were taken referring to concrete technology, opening condition and strengthening condition. As it can be seen in Fig. 3 the monolithic, solid and non-strengthened specimens prevailed over test programs including precast, solid with opening or slitted and strengthened specimens, respectively. Amongst the latter category three groups were according to the employed strengthening technique: conventional, FRP-EBR and other. Conventional techniques mean repair of the damaged walls by replacing of the crushed concrete and fractured reinforcements, FRP-EBR (Fiber Reinforced Polymers Externally Bonded on concrete surface), while other techniques included Steel Plates bonded, selective weakening, frame infill or wing walls. The restricted database contains 16 programs that included precast walls, 14 programs that included walls with openings and 16 programs that included walls strengthened by FRP-EBR technique.

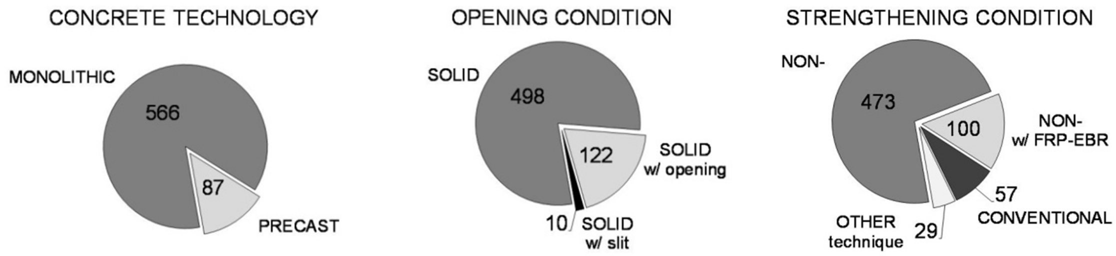

Fig. 3 Data on concrete technologies, openings and strengthening conditions

Tab. 1 Tests on FRP strengthened walls

PROGRAM ID		**SPECIMEN**					
Laboratory-Year	Country	Designation	Type	Concrete techn	Opening	Strengthening	No. of spec.
CARLT-2000	Canada	wall	wall element	monolithic	solid	non; FRP-EBR	7
TOKYU-2000	Japan	T; U; RC; CF; CFR; /	column wing-wall	monolithic	n/a	non; FRP-EBR	15
TUSJ-2000	Japan	Specimen	wall-frame syster	monolithic	solid; door; windo	non; FRP-EBR	10
AUTH-2003	Greece	MSW; LSW; FRPM	wall element	monolithic	solid	non; FRP-EBR	11
MGILL-2003	Canada	W	wall system	monolithic	solid	non; FRP-EBR; RC;	4
UUTAH-2003	USA	Specimen; wall as	wall system	precast	solid	FRP-EBR connecti	9
HOKU-2004	Japan	WA	wall-frame syster	monolithic	door; window	non; FRP-EBR	3
MMCAN-2004	Canada	CW; RW	wall element	monolithic	solid	non; FRP-EBR	3
NCREE-2004b	Taiwan	PF; WF	wall-frame syster	monolithic	solid; frame	non; FRP-EBR	6
UFUK-2005	Japan	W; specimen	wall-frame syster	monolithic	solid	non; FRP-EBR	6
UPT-2005	Romania	SW; RW	wall system	monolithic	solid; door	non; FRP-EBR	5
NTUSG-2010	Singapore		wall element	monolithic		FRP-EBR	4
UPT-2010	Romania	PRCWP	wall element	precast	solid; door cut-ou	non; FRP-EBR	5
UPT-2011	Romania	CSRCW	wall system	monolithic	solid	non; FRP-EBR	6

5. DATA ON TEST SET-UP, LOADING AND BOUNDARY CONDITIONS

In this chapter several data should be discussed and explained, but due to space limitation only those are mentioned which were considered in the conception of this database. These important informations refer to the:

- test set-up: fixing of the specimen; loading elements; type, number, position of the loading devices.
- loading strategies: direction, rate and control of the loads; monotonic, cyclic or dynamic; displacement or load controlled; failure criteria.
- boundary conditions: base fixing; the loading elements' degree of freedom; the shear span.

6. REFERENCES

DABASUM - Database for FRP-Based Shear Strengthening of Reinforced Concrete Beams. < http://dabasum.civil.uminho.pt/index.php>, University of Minho (May 05, 2011).

Demeter, I. (2011), "Seismic retrofit of Precast RC Walls by FRP Composites", PhD thesis, Politehnica University of Timișoara, Romania.

Gulec, C. K. and Whittaker, A. S. (2009). "Performance-based assessment and design of squat reinforced concrete shear walls." Technical Report MCEER-09-0010.

RILEM TC 223-MSC Data warehouse, MSC: masonry strengthening with composite materials < https://rilem223dwh.isqweb.it/ > (May 05, 2011).

Stanic, A., Sigmund, V. and Guljas, I. (2003). "Behavior of the walls under in-plane horizontal loadings." Proc., fib-Symposium, Athens, Greece.

Shear wall database of Palermo. < http://by.genie.uottawa.ca/~palermo/Wall.htm > (May 05, 2011).

Wood, S. L. (1990). "Shear strength of low-rise reinforced concrete walls." ACI Struct. J., 87(1), 99-107.

JOINT SEALING PRINCIPLES OF WATERTIGHT STRUCTURES AND THEIR COMBINATION

Tamás Simon[1], Dávid Szabó-Turák[2]
[1] *Department of Construction Materials and Engineering Geology*
Budapest University of Technology and Economics
1111 Budapest Műegyetemrakpart 1-3
[2] *Bau-Haus Kft.*
1016 Budapest, Csalogány u. 6-10

SUMMARY
The expression „watertight concrete" may be misinterpreted several ways, it is more precise to say: the concrete mixture is suitable to prepare a watertight structure. We would like to present with this paper that the watertightness does not only depend on the mixture in the laboratory, but also on the construction circumstances, on the after-care (curing), and the sealing of the construction joints, expansion joints, pipe- and cable penetrations.

1. INTRODUCTION

One of the definitions says that the technology of watertight concrete production is based on the principle that crack-free concrete can be called watertight if the volume of water filtering through is lower than the minimum vaporisable amount of water on the opposite side. This interpretation can be questioned, because the amount of the evaporating water depends on the moisture content and the temperature of the medium on the opposite side.

The earlier Hungarian standard (*MSZ 4715/39-82*) and the valid European standard (*EN 12390-8:2009*) focuses only on the material of the concrete, testing how much can it resist the water pressure. These definitions raise also several questions, because knowing just the behaviour of concrete under a given pressure is not enough. The fact, that the whole structure cannot be prepared at the same time offer dozens of problems to be solved, the sealing in the joints, and the problems of the formworks.

During dealing with these questions inevitably will appear the different movements of bigger structures, the spontaneous deformations of concrete which destroy homogeneity. Incorrectly designed movement joints, will make the watertightness of the structure questionable in whole.

2. CURRENT QUESTIONS OF THE WATERTIGHT IN SITU CONCRETE CONSTRUCTIONS

If the requirement on the saved side is known, and we know the claimed watertightness, then the outside waterpressure should be analyzed, and the structure serves to protect the saved environment from the moisture under this water pressure. The EN 206-1:2002 standard orders only that the partners have to agree in the watertightness and the testing method. Further help may be found in the Hungarian MSZ 4798-1:2004 standard, which also orders the usage of the EN 206-1:2002 in Hungary. The MSZ 4798-1:2004 identifies three types of watertight concrete within the environmental classes:

XV1(H): which allows 0,4 l/m^2/day to filtrate through the wall under "small" water pressure, when the wall thickness is more than 300 mm.XV2(H): which allows 0,2 l/m^2/day to filtrate through the wall under ”small” water pressure, when the wall thickness is less than 300 mm; or near ”big” water pressure, when the wall thickness is more than 300 mm.XV3(H): which lets 0,1 l/m^2/day to filtrate through the wall under ”big” water pressure, when the wall thickness is less than 300 mm.

These definitions may be difficulty interpreted. The “small” and the ”big” water pressure cannot be considered as an exact definition, and the standard does not give any more exact definition. On the other hand for the concrete mixtures it is not defined, how these requirements can be achieved. To solve these, a specialist in concrete technology must be involved.MSZ 4719-1:1982, and also the EN 12390-8:2009 standards order the test specimens and the test procedure differently. The Hungarian standard studies that how high water pressure is needed for a certain penetration, the European one studies that how deep penetration is achieved under constatnt water pressure. The MSZ 4798-1:2004 standard does not specify concrete, gives only requirements about the targeted conditions on the saved side of the structure *(Simon, Szabó-Turák, 2010).* Watertight structures should be concreted continuously, but due to organisational reasons and some expected or unexpected situations construction joints are avoidless *(Janzó, 2004).* The watertight joint preparation must be kept in hand during the design phase.

3. PRINCIPLES OF JOINT TYPES

The joint of the concrete construction always means a break in the material-continuity. This break can be intended or spontaneous. In case of watertight constructions, it is always important, that spontaneous cracks must not lead through the structure, or they should not emerge. If such cracks evolve, the watertightness of the structure will be questionable.

The concrete structures cannot be concreted in one due to the previously mentioned reasons, so all concrete constructions go hand in hand with joints. The distance between the joints depends on several factors.
We will introduce the assortment of the DBV-Merkblatt (among the several assortments of the literature). This assortment identifies three main joint types: construction joints, expansion joints and crack joints.

Tab. 1 The review of the joint types (DBV-Merkblatt, 2001)

Joint type	Illustration	Comment
Construction joint	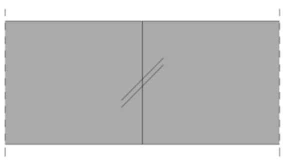	- borderline of the previously and later concreted parts - due to stress which is caused by the thermal expansion
Crack joint	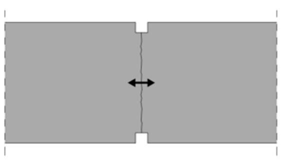	- made by weakened section - movement possibility nearby structural shrinkage - possibility to forward shear loads - the reinforcement runs through the joint
Expansion joint	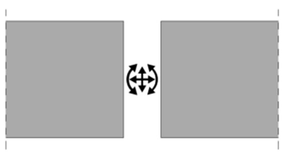	- there is a possibility to move or turn in all directions

The *construction joint* is the most typical one, which takes shape between two part of the concrete construction. The construction joint will develop, if the accepting part starts to harden, when newly poured side is concreted. It is a usual requirement for them to work together. The place and the shape of the construction joint should be marked on the final drawings. *(Janzó, 2004)* The reinforcement is continuous, but the break in the concreting effects civil engineering behaviour. The shear load can be transferred by the concrete only with special shape (for example: by indented construction joint: *EN 1992-1-1:2010*), but tensile loads cannot be (by the concrete) forwarded. Most frequent is, when the arrival of the concrete to the construction site is delayed. Some hours delay can mean the start of the concrete's setting, and an undesigned construction joint emerges. For these cases those may have correct solution, who will be prepared for the possibility.

The *crack* joint's design is made to handle the high tensile stresses, which makes cracks through the cross section. These locations of cracks can be designed, and so the in one time concreted parts might be greater. If the places of these cracks are not previously designed, then they might cause serious damages to the watertightness of the structure. Through the crack joint can pass all or a part of the reinforcement.

*Expansion joint*s are designed by reason of frameworks, or they are prepared to separate two part of the building. Usually there is no load transfer over the joint. The joint comes to the surface, so there must be enough concrete covering, and the reinforcement is to be broken. Movement is possible to every direction.

4. JOINT SEALING PRINCIPLES OF THE IN SITU CONCRETE CONSTRUCTIONS

There are four main principles for the joint sealing, the *labyrinth*-, the *filling*, the *cohesion*- and the *adhesion* principle.

Expansion joint means structural separation between buildings, or building parts. The constructions on the two sides of the joint can move separately to each other, and the joint requires a relatively big space. The joint sealing has to work during these conditions, and therefore further types and principles cannot be used for sealing of expansion joints according to our present knowledge.

The *labyrinth* principle based on that the longer is the way of the water to pass, the less will be the pressure which water will force through. All types of the joints can be sealed by using this principle. We may count on the *embed* principle here, but it is written as a separated principle in some of the literatures. This principle is based on that between a metal and the concrete an adhesion force will occour, and that adhesion (always together with the labyrinth) obstructs the passage of water. This adhesion contact forms during the hardening of the concrete, and a chemical connection occurs between the concrete and the metal The Wan der Waals forces between the molecules are perpendicular to the surface. *(Balázs, 2002)*

The *filling* principle cannot be used in expansion (opened) joints, but in closed joints (construction joint) it is the most effective joint sealing. It works so, that the gaps near the joint (which can be cracks, pores, voids, capillaries and so on) are filled up with a sealing material. The advantage of this method is that all of the concrete's voids will be filled up. At the same time by mail usage, much of the material may be lost, and the structure (due to the high pressure) can be destroyed.

Tab. 2 The working of the joint sealing principles (Hohmann, 2004)

Sealing principle	**Effect**		**Example**
Labyrinth principle	Makes longer the length of the waters passing way	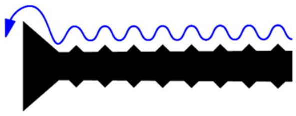	- PVC or rubber waterstops - metal waterstops - shrinkage tubes
Filling principle	To fill all the capillaries, and hollows	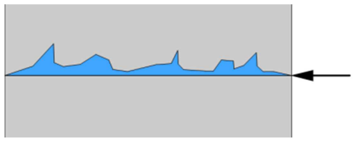	- Injection systems under pressure - Self injected seals - after-crystallizing materials
Compression principle	Pressure of the profile to the concrete structure	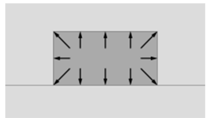	- Polymer expansion seals
	Pressure to both sides of the joint	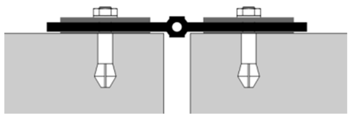	- Clammed construction
Adhesion principle	Adhesive band along the joint of the structure	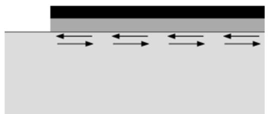	- Adhesive systems

Using the *compression* principle on the surface initiates such a high protection, which cannot be overdrawn by the water pressure, and that makes a border for water penetration. This principle assumes that the concrete is so dense, that the water cannot pass around the sealing, or the joint cannot be removed by the water pressure. This method is used by the shape-retaining expansion seals (polymer expansion seals), there are compression bands too, which are used for repair of expansion joints.

The *adhesion* principle needs an adhesive material, which is to be used between the sealing and the concrete structure, or glues together the two structural parts. The water pressure should not be able to overcome the adhesive force, and pass through the joint. This principle assumes that too the concrete is so dense, that the water cannot pass around the sealing.
These principles can be combined, to make the sealant more secure. The using of labyrinth principle is the most frequent. There are waterstops (sealants) with injection hose (labyrinth principle combined with filling principle), the metal waterstops are combined often with special coatings. There are sodium-bentonite coatings (labyrinth + filling priciples), butyl and bitumen coatings (labyrinth + adhesion principles).

5. CONCLUSIONS

The expression „watertight concrete" can cause several misunderstandings because the definition may referr to the concrete material and the structure itself as well. If the concrete mixture is watertight, still the structure may have problems due to the joints.
There are three main type of the joints: construction joints , expansion joints and crack joints.
There are four main principles to the joint sealing: he *labyrinth*-, the *filling*, the *cohesion*- and the *adhesion* principle. These principles can be used alone and they can be combined in the practice.

6. REFERENCES

Janzó József (2004): Vasbeton és feszített beton ivóvíztárolók tervezése, építése és üzemeltetése; Kézirat, Budapest

Simon Tamás, Szabó-Turák Dávid (2010): Vízzáró beton a szabványok tükrében, Vasbetonépítés, 2010/2

Balázs György (2002): Építőanyagok és kémia, Műegyetemi kiadó, pp. 291

Rainer Hohmann et al (2004): Fugenabdichtunge bei wasserunddurchlässigen Bauwerken aus Beton; Fraunhofer IRB Verlag, 19-36. oldal

Fugenausbildung für ausgewählte Baukörper aus Beton 2001, DBV-Merkblatt

EN 1992-1-1 (2005): Eurocode 2: Design of concrete structures. Part 1-1: General rules and rules for buildings

EN 12390-8:2009: Testing hardened concrete – Part 8: Depth penetration of water under pressure

MSZ 4798-1 (2004) „Műszaki feltételek, teljesítőképesség, készítés és megfelelőség. Az MSZ EN 206-1 és alkalmazási feltételei Magyarországon”

TEMPERATURE DEPENDANT SLIDE JOINTS FOR CRACKING ELIMINATION IN CONCRETE FOUNDATION

Radim Čajka[1], Kamil Burkovič[2], Vladimir Gřunděl[2], Martina Janulíková[1], Pavlína Matečková[1], Marie Stará[1]
[1] *Faculty of Civil engineering, VSB-Technical University of Ostrava*
17. listopadu 15/2172, Ostrava, 708 33, Czech Republic
[2] *Arming Ltd., design and building company*
Ocelarska 6/338, Ostrava, 703 00, Czech Republic

SUMMARY

In the paper utilization of slide joint is presented in case of horizontal deformation of subsoil (undermining) or horizontal deformation of foundation structure (e.g. pre-stressing). Contemporary experiments of slide joint temperature dependant shear resistance are described and partial test results are introduced. The test results are used for calculation of slide joint shear stress for particular subsoil deformation rate.

1. INTRODUCTION

Slide joints are effective tool for elimination of friction in footing bottom caused by horizontal deformation of foundation structure owing to shrinkage, creep, pre-stressing and temperature variation or by subsoil deformation, owing to e.g. undermining, Fig. 1. Material of slide joint is mainly bitumen asphalt belt.

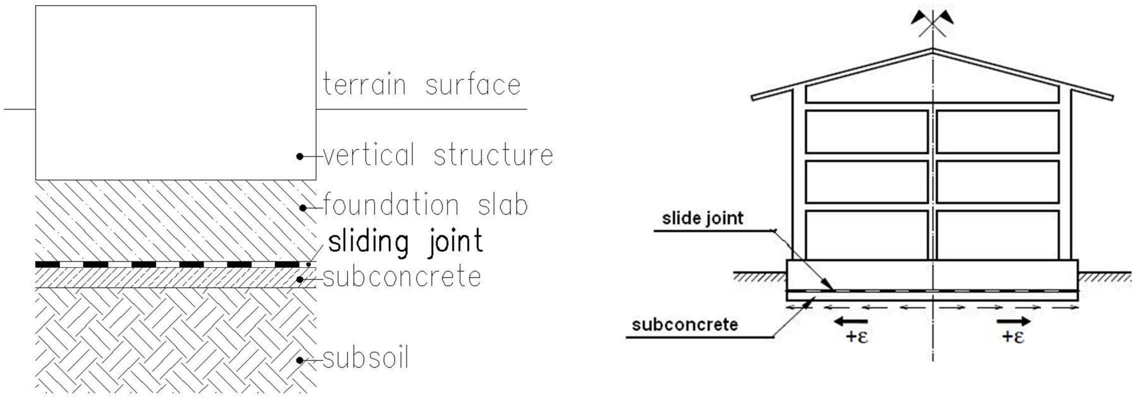

Fig. 1 Schematic drawing of slide joint

Shear resistance of slide joints is primarily dependant on the deformation rate. First sliding joints tests were focused on this fact and were made in 80th of last century for asphalt belt common in that time *(Balcarek, Bradac, 1982)*. Material characteristic of bitumen belt has been changed significantly since that time and this fact demanded new experiments. At VSB – Technical University of Ostrava unique equipment was designed for shear resistance measuring. Renewed experiments for different types of bitumen belts passed in 2008. *(Maňásek,2008)*. One of the important factor which affect the shear resistance is the temperature and that is way the experiments continues with measuring the shear resistance of slide joint as a function of temperature in air-conditioned room.

2. PARTIAL EXPERIMENT RESULTS

2.1 Experiment description

At VSB – Technical University of Ostrava unique equipment was designed for slide joint shear resistance measuring. In between concrete blocks with dimension 300 x 300 x 100 mm 2 asphalt belt specimens are placed, vertical load is applied and after one day delay also horizontal load is applied, Fig. 2. Displacement *u* of middle concrete block is measured for 6 days. Experiments for different types of bitumen belts at laboratory temperature passed in 2008, test results were presented in several papers, e.g. *(Čajka, Maňásek, 2007).*

New experiments are focused on influence of temperature to shear resistance of sliding joint. Whole experimental equipment is placed in air conditioned room. The experiments are in the progress in 2011.

Fig. 2 New testing method of slide joint shear resistance

2.2 Partial experiment results

In the Fig. 3 partial experiment results are presented. Specimens of common IPA™ asphalt belt are imposed to vertical load 0.5 Mpa and horizontal load 2.0 kN and 0.95 kN. The experiment results are presented for the temperature 20°C and 10°C. Temperature 20°C represents the laboratory temperature and temperature 10°C represents approximately average temperature in footing bottom. In the chart, Fig. 3, it is perceptible that the influence of temperature to shear resistance is significant.

3. APPLICATION OF EXPERIMET RESULTS

3.1 Expected horizontal deformation

Underground mining affects also buildings at the surface. Terrain deformation comprises subsidence, declination, curvature and also horizontal deformation. Expected horizontal deformation of subsoil in the Ostrava-Karviná district affected with underground coal mining is approximately $\varepsilon \cong 10^{-3}$. In dependence on the depth of working coal seam and speed of mining it is possible to estimate the horizontal deformation rate. Deformation passes over after several months.

Horizontal deformation of pre-stressed foundation comprises instant elastic deformation of concrete cross-section and creep and shrinkage. Expected horizontal deformation of foundation structure is approximately $\varepsilon \cong 10^{-4}$. Deformation is developed throughout years.

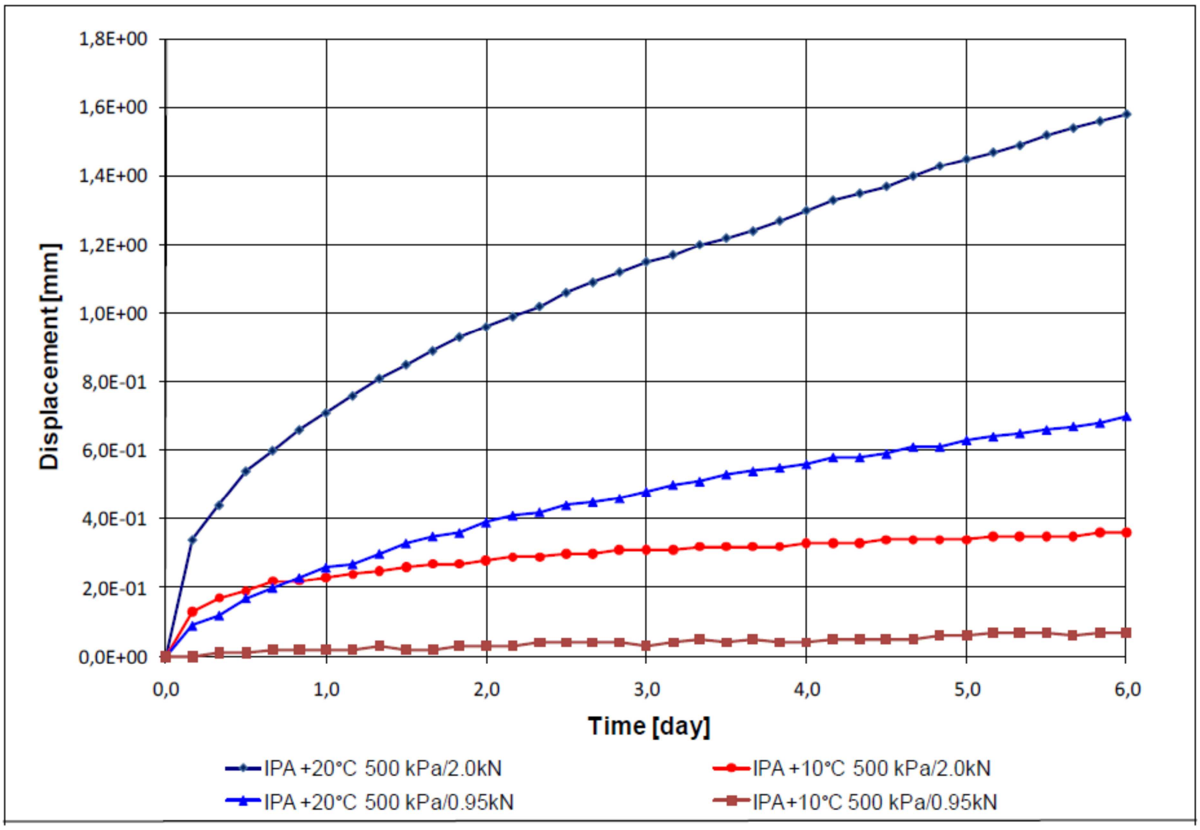

Fig. 3 Partial experiment results

3.2 Shear resistance of slide joint

As it was proved with primary testing in 80th of last century, the lower is the horizontal deformation rate the lower is the shear resistance of slid joint, *(Balcarek, Bradac, 1982)*. Taking measurement of shear resistance for particular deformation rate is problematic. It was therefore decided to appoint experimentally the deformation rate for different shear stress, Tab 1. Using linear regression it is possible to appoint the shear resistance of slide joint τ as function of deformation rate *v*, Fig.4.

Tab. 1 Steady deformation rate for arbitrary shear stress

		Temperature 20°C		Temperature 10°C	
Shear stress τ	kPa	11.11	5.28	11.11	5.28
Deformation rate *v*	$m.s^{-1}$	1.5E-06	2.31E-07	8.1E-07	1.16E-07
Linear regression		$\tau = 5.10^6.v + 4{,}22$		$\tau = 8.10^6.v + 4{,}31$	

3.3 Discussion

The subsoil deformation is considered with value $\varepsilon = 5.0 \times 10^{-3}$, which is common on areas affected with underground mining, deformation passes over after 40 months. Maximum deformation rate in the margin part of the strip foundation with length 20 m is according to code *(CSN 730039, 1990)* $v = 4.10^{-9}\,m.s^{-1}$. This deformation rate responds to shear stress

$\tau = 4.24$ kPa for 20°C and $\tau = 4.34$ kPa for 10°C. Shear stress in slide joint is calculated with linear extrapolation. It is possible to complement the experiments with one more shear stress values and thus verify or specify the calculated regression.

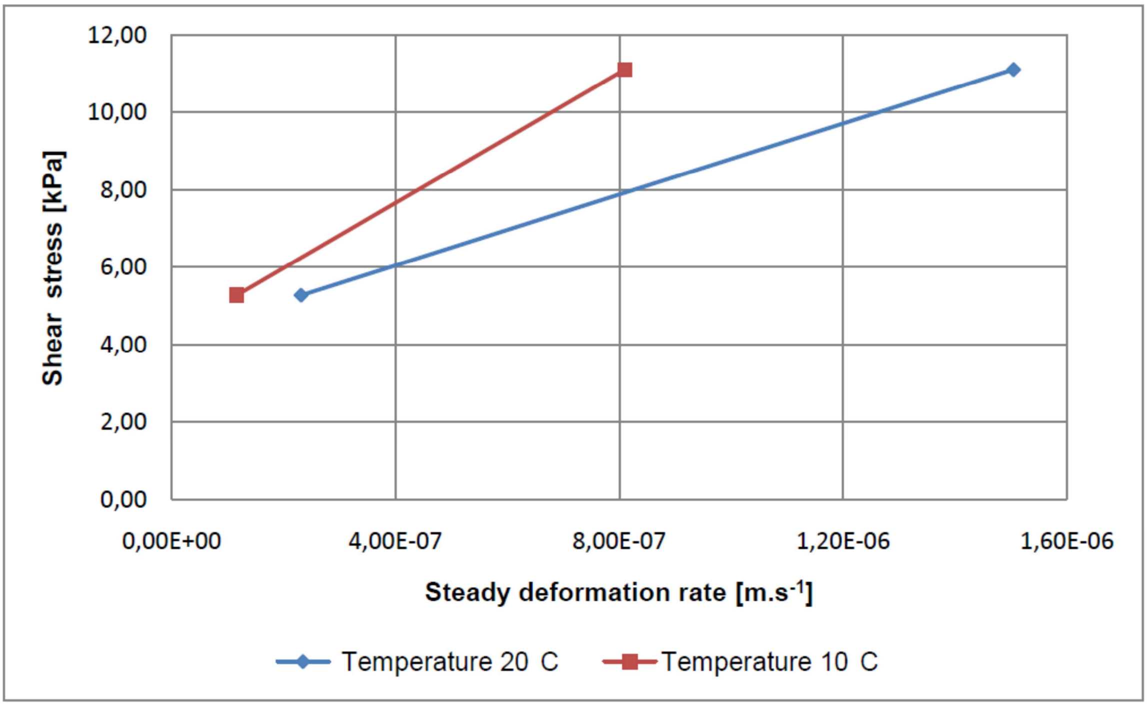

Fig. 4 Shear stress as a function of deformation rate

4. CONCLUSION

In the paper utilization and experimental testing method of slide joint is presented. Test result for common asphalt belt IPA™ and for the temperature of 10°C and 20°C are introduced. Using linear regression and extrapolation it is possible to calculate the shear resistance of slide joint for arbitrary deformation rate.

5. ACKNOWLEDGEMENTS

This outcome has been achieved with the financial support of the Ministry of Industry and Trade of the Czech Republic, program TIP, project No. FR-TI2/746 Rheological sliding joint with thermo-controlled viscoelastic properties.

6. REFERENCES

Balcarek, V., Bradac, J. (1982): “Utilization of bitumen insulating stripes as sliding joints for buildings on undermined area”, Civil Engineering, 1982,in Czech

Čajka, R. , Maňásek, P. (2007): “FEM analysis of the structure with sliding joint affected by deformation loading” In The Eleventh International Conference on Civil, Structural and Environmental Engineering Computing, St. Julians, Malta, ISBN 978-1-905088-15-7.

ČSN 730039 (1990): “Design constructed facilities in mining subsidence areas. Basic requirements”, UNMZ Prague, 1990, in Czech

Maňásek, P. (2008): “Foundation structure with slide joint”, Ph.D. thesis, VSB TU Ostrava, 2008, in Czech

IDENTIFICATION OF COMPUTATIONAL MODELS IN LOAD CARRYING STRUCTURES OF CONCRETE BRIDGES ON THE BASIS OF MAKING LOAD TESTS

Piotr Łaziński[1], *Marek Salamak*[1]
[1] *Silesian University of Technology, Road and Bridge Dep.*
ul. Akademicka 5, 44-100 Gliwice, Poland

SUMMARY

A load test is an identifying experience where a computational model should reflect the real work of the construction. The paper presents, gained during tests, differences of deflections with relation to computational model results. It shows that smaller real deflections are not the reserve of the load capacity construction but the computational model. That is why load tests should be made on the basis of the adequate theoretical model eliminating differences of rigidity between the real object and the computational one. The factors influencing the increase of the whole rigidity of the span with relation to assumptions while modelling were described.

1. INTRODUCTION

Load tests of new bridge objects due to accompanying them measurements and observations can create the whole picture of real behaviour of constructions and verify a computational model.

While analysing the results of the load test the results are often much smaller than the theoretical ones and are treated as the reserve of load capacity. It is not a correct idea. Significant discrepancy between the theory and tests is the result of taking the wrong model to be tested.

In situ tests of concrete bridge objects are made on the basis of the project of the load tests. In the study we theoretically know deflections of tested spans calculated on the basis of norm features of concrete according to EC2. The calculations do not contain real features of concrete at the age function and equipment influence which in some cases are of great importance. The approach is justified because a project leader of the object and its project team can compare results calculated theoretically before the test load. Comparison of the results at the same norm assumption verifies computational models accepted by two independent sides.

In order to interpret results of in situ researches there was introduced division of a computational model depending on the stage of its building into three models. The Model of Building Project (MBP) is made by a project leader on the basis of material features according to norms in force. Model of Introducing Test Load is made at the same norm assumption as MBP at the stage of project of test load by project team. Model of Verified Test Load contains results of test load and real values of concrete features on the basis of destructive researches received from the laboratory of concrete and the influence of object equipment.

From 2002 to 2010 a group of people from Roads and Bridges Department Silesian University of Technology made about 300 test loads of bridges. They were most objects situated on the A1,A2,A4,A18 motorways and S1, S3, S7,S69 fast way in Poland. Results and experience made us analyse conformities between calculated during test loads deflections of spans and values gained in calculations on the basis of accepted theoretical models. It is important while discussing about built object if it got a required and assumed load capacity by a project leader.

Received results from field researches and destructive concrete researches show discrepancy which occur systematically between computational models and results of real bridge constructions. Due to analyse of changing features of concrete for some time and cooperation of flag stones there was described the influence of the factors on differences in rigidity of motorway flyovers of some types.

Carried out researches of 65 objects about six types of constructions confirmed a discrepancy of real rigidity of spans and received from theoretical analyses. Tested spans of steel construction and steel- concrete show a great harmony of theoretical results (Uo) with the measured ones in test loads (approximately 85%). There is a different situation with concrete bridges where regardless of the kind of superstructure there is a great difference of theoretical (Us) and measured ones (Uo) where rigidity El is responsible for particularly resilience module (approximately 53%). If theoretical test results are much smaller they cannot be treated like the reserve of superstructure. The discrepancies are the sign of taking inappropriate model to be tested.

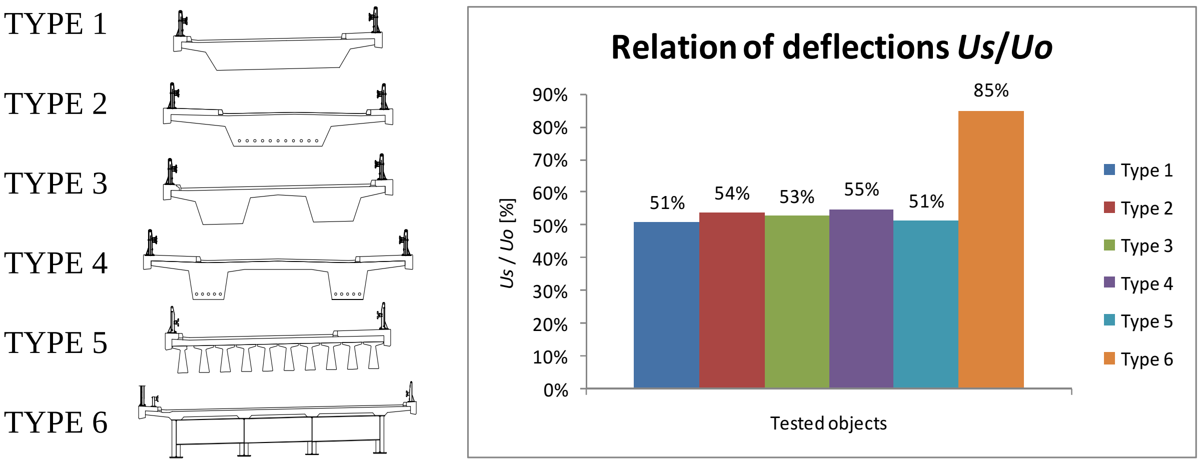

Fig. 1 Relation of deflections Us / Uo in six types of tested bridge objects

2. COMPUTATIONAL MODELS

Contemporary bridge construction require modern techniques of theoretical analyse. Virtual numerical models are today the base to carry out analyses. In practice effective analytical methods are replaced by numerical methods and we can analyse any engineer structures due to them.

In the process of carrying out project, with the help of computer, bridge constructions are made with the use of discreet computational models. There are three basic elements of computational models:

1. Model of geometry: way of remodeling geometry object.

2. Model of material: profile of construction material.
3. Model of loads: way of presenting loads.

In the researches at the stage of project of test load we deal with a computational model where two components (model of geometry and model of load) are known to eliminating degree significant discrepancies during the test and model of material in case of concrete construction is changeable and depends on time influence and kind of used aggregate. What is more, every study is accepted by a project leader before the test. That is why in the project of test load I suggest taking norm features of concrete in the model (MITL) what follows verification of results of computational model accepted by a designer and test team. The approach makes computational mistakes possible to correct. Just only in the summary of test load discrepancies of measured and theoretical deflections should be verified on the model (MVTL). In the model real values of concrete features are taken into consideration on the basis of received from the laboratory durability researches after 28 days of maturing. The influence of equipment will be changeable every time depending on movement parameters of bridge and that is why in the paper the influence was described only for a certain type of superstructures. The suggested chart of adequate modeling procedure of real objects is presented below.

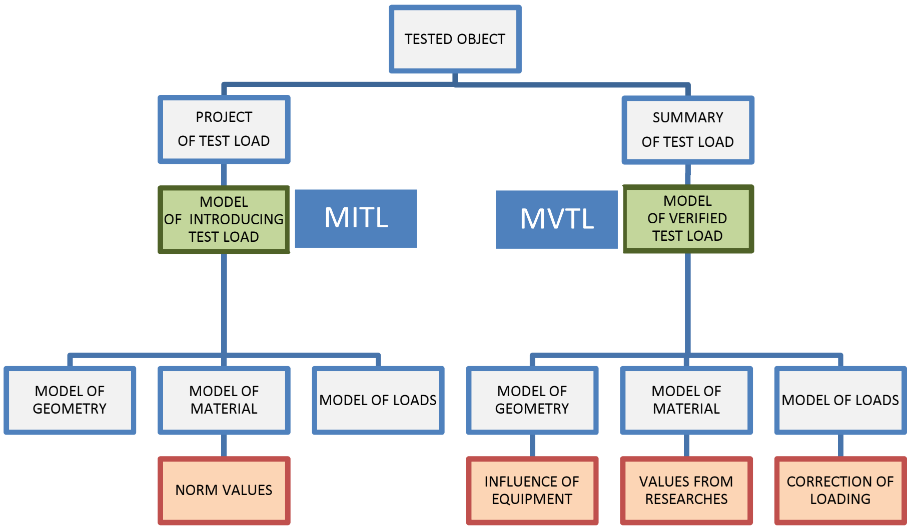

Fig. 2 The chart of modeling procedure of real objects in test loads.

3. ANALYSE OF CHANGING CONCRETE FEATURES

Structural transformations occurring in the process of cement hydration influence on the change of material profile of concrete with decreasing intensity while staling material. Time to achieve maturity of concrete and stabilization of its physical characteristic is not permanent and depends both on the composition of mixture and environmental conditions of material work. In practice as far as researches of concrete bridges are concerned there is only a report from researches concerning durability of concrete. Changes of resilience module during hardening concrete we can connect with changes of durability concerning squeeze after 28 days of maturity.

We can consider value of EC2 resilience module of concrete at the age function with taking into consideration used aggregate.

$$E_{cm}(t) = 22 \cdot \left(\frac{f_{cm}}{10} \cdot e^{s \cdot \left(1 - \sqrt{\frac{28}{t}}\right)} \right)^{0,3} \cdot \alpha_E \qquad [GPa]$$

4. ANALYSE OF INFLUENCE OF BRIDGE EQUIPMENT

Footway construction is partly responsible for differences of rigidity of real superstructure, which in practice, is connected with superstructure through footway slab bars. The ways of connecting often occur in new objects and cause that in usable states start to cooperate while carrying short-lived loads. On the basis of my own in situ researches at two stages of building object there is presented a real cooperation of the element with superstructure of type 4.

Suggested value of effective coefficient of joining footway slab with superstructure equals 0,72.

5. CONCLUSION

Carried out researches and analyses show that in the case of concrete superstructures age and kind of used aggregate (basaltic aggregate - increase of module by 25%) have influence on conformity of measured girder deflections with calculated theoretically. The influence of joining footway slabs with superstructure is important depending on participation of surface area. In the whole cross section (increase of rigidity by 20%). The results of researches were used to create adequate modeling procedures and planning tests while taking into consideration elements causing increase of real rigidity of concrete spans.

6. ACKNOWLEDGMENTS

The paper was prepared under financial support from the research project no N506 396235 from Polish Ministry of Science and Higher Education.

7. REFERENCES

Łaziński P. (2009), „Procedura modelowania obiektów rzeczywistych w postaci pewnego typu konstrukcji mostowych", Praca doktorska, Politechnika Śląska, Gliwice

Łaziński P., Weseli J. (2008), "Wyznaczenie rzeczywistych czasowych rozkładów cech betonu dla modelowania I planowania badań odbiorczych mostów autostradowych", Projekt badawczy promotorski N506 396235

EN 1992. Eurocode 2:"Design of concrete structures"

NEW TECHNIQUES USED TO COST APPRAISAL FOR CONSTRUCTION DESIGN PROJECTS

Katalin-Éva Kiss
Budapest Business School
1, Eroilor Str, Cluj-Napoca, RO

SUMMARY

Any developing country must focus on the small firm strategies in order to keep the interest of investors and attract new financing sources. An architect manager posseds all kind of specific instruments to validate the efficiency of labor. Knowledge and practical experience helps him to offer economical evaluations, numerical ones, about the solutions used, related to dynamic technological and economical changes on the market. Having in view all the factors that may show in a competition based environment, it assures an optimistic compromise and the way to success. So far, the statistical prognosis seems to be the most fair and appreciated method, it lets the firm's strategy to be placed in time limits given by the transitional economies. Rational thinking and following methodology instructions are essential in expertising, so that economists could reveal well-fitted appreciations and competitive decisions.

1. STATISTICAL PROCESS CONTROL

1.1 Introduction

Technological firm strategies gain more interest recently in the construction industries, especially because of the high-quality performances achieved by professional estimators. Expert systems are complex and handy instruments that store encoded data about the construction market and offer the highest human expertise that could never been obtained with usual analyses.

1.2 Study of processes

1.2.1 The initial research

Success requires mastery of statistical process control methods and data collection techniques, among which stands out as important the observation, the experiment (test) and the investigation (survey). Information collected are used in a qualitative and quantitative data analyses, developing models like cause and effect diagrams, marketing models, expert systems and marketing information systems. By these means, the research results are made available to company management in order to substantiate the most appropriate decisions that are taken on present or future work.

Rehabilitation projects of old buildings form an important part of counselling to architects and design engineers. In this case, specialists solve conservation projects for construction or rehabilitation of historical objectives, a specific risk situation, by doing a grading of 1 to 5 – depending on the frequency of errors and their impact on the construction. Divergent perceptions of the differences appear when we have major different trainings and experience of interface backgrounds. Resolving differences may be through statistical measurements.

1.2.2 Analyses of collected data

Researcher W. M. Kohen *(1996)* describes the long-term effects of innovations. In his interpretations there's never too much motivation, nor additionality, in fact companies often contribute with more than 50% of their reserves to Research & Design Projects. R&D Projects are naturally efficient and innovative investments, but however questionable at certain times, because the business market failure can be almost inevitable in certain situations.

On their web-site, the American Society of Professional Estimators makes public their demands to be met by persons responsible for process control, members of the association, and specifies that there are no codes, laws or standards applicable in economical engineering or professional cost estimating. By surveying, it appears that the individual estimators, practicing in constructions, are 58%, among these 17% work for companies that operate manually and 25% elsewhere. The beneficiaries of these services may be managers or owners of businesses, members of groups of professional design, construction investors.

1.3 The economic purpose of the method

From the perspective of the beneficiary, cost estimates can be used to determine whether the project should be processed. In constructions, the contractor estimates his costs and decides whether or not to bid for auction. Costs are estimated in all phases of design and execution. The consumer is fully satisfied when the best solution was found to fit the requirements: regulations, technical feasibility, environmental standards, site conditions, costs or any possible comparisons (eg. excessive noise and high initial costs).

Economic side of th project provides information on initial and future costs, so designers can make decisions depending on cost implication. The economist will make his contribution in the design team, too. Team structure will be carefully planned, as final decisions being taken by its members. The economist will be an active member, providing useful information at the right moment, when making important decisions in the firm strategy planning. He will have the techniques, knowledge and experience to give answers to questions about the cost of each project phase. The point is to understand the mentality of the architect – how to think and work -, more accurately, the methods of design, so he may select the lowest cost method, adapted to specific situations. The economical engineer will not take upon himself the full responsibility, but will share it with the architect, who has cooperated in planning costs.

2. TECHNIQUES USED TO COST APPRAISAL FOR DESIGN PROJECTS

2.1 Description of the investment

Cost models are usually calculated in the stage of finishing the building and detailed on structure components, so prices are ready in the final stage. However, they are not based on economic principles. When dealing with worldwide economical regressions, modelling techniques for constructions may be even sophisticated, if not explicited enough in the functional-relational sense.

In time, existence and relationships among selected variables represent actually a stable and measureable hypothesis. At the time being, at data measurement, most regression models fail, because of failing to represent aspects of the process and does not simulate reality.

2.2 Appraisal of the investment

John Raftery *(1984)*, british researcher, has expressed interest in the possibility of modelling the needs depending on the market, design complexity and involvement of the builder. Information source and nature of data taken are questioned and many other aspects too, such as the model-data interface (if data are matched to the model chosen), the impact of this modelling technique on it’s validity, interpretation of results found, the decision procedure (facilitated), etc. His help in designing structures, to follow the context for performance models, is based on rational and unified criterias.

3. EXPERT SYSTEMS

3.1 Presentation

Brandon *(1984)* stated that the use of IT, and particulary expert systems, will have a major impact on construction professionals. Problems are going to become more explicit in the program, using human power to create them and the computer will reach a similar conclusion with the expert.

Another expert, Naylor *(1983)* considers IT a component able to provide expertise based on real knowledge so that the system would provide intelligent advice or make intelligent decisions about processing a function. The acquisition will be based on the system's ability to justify their own "line of cause and effect". These computer programs contain such an expert system that provides information in the following cases:

a. Database for management theories, the phase being put into practice
b. Transparency and explanations of its functions and answers to questions about its capabilities
c. Flexibility and integration of new technologies based on existing knowledge

The fundamental concept of flexibility is defined by separating the knowledge of major relevance, to the excent accepted, from the interactive procedures used.

Newton *(1984)* defines an expert system as being based on: knowledge (database) and user interface. The database is essential for a realistic expertise. Interface refers to dynamic decisions processed by the program, in other words, means the relationship between input data and control data optimized production. But, it justifies to focus on selected components of the issued data. Obviously, there are alternative systems, based on existing documentation. The user is seen as an applicant in this case, who can be an ignorant person or an expert in the field, requiring a more sophisticated approach.

3.2 Operating strategies

If you set the goal first, then must continue to develop strategies and opportunities to achieve its intended purpose. We arrive to a conclusion, based on predefined information. By interacting with the operator, we find new rules for decision making on tracking IT-s.

Lansdown *(1982)* describes such expert programs:

a. They know a lot, on a limited area of interest, and they are important
b. They can work within conversations, when providing advice
c. Their science consists not only in the variety of programs used, but in better production and market rules interpretation. Thus we use the same interface for database updates.
d. If uncertainty persists, solutions are developednin more probabilistic manners
e. Questions launched by the system are relevant to the cause-effect relationship and will not continue to the operator, if he already has enough information to complete
f. Expert systems can explain their reasoning and justify their decisions, so that professionals recognize the quality and beneficiaries understand the reliabitity of output data.

Due to the development of the private sector in economy, the application is about to develop a new technique for estimating variables such as: rent, location of construction, exterior and interior design,decorations. As a matter of fact, all combinations of the above factors contribute to different values of the size of rent. Projects include planning and management proposals for the auction, value analyses, ensuring investment in construction financing. Newton has designed interfaces – along with the database and operations performed by the controller – that will solve viability calls for projects in the construction business sector development.

4. CONCLUSIONS

Oligopolistic firms with national market position accept estimates of construction costs using their own databases. These data are continuously adjusted according to fluctuations of the local labor or capital resources. There is the except for schools constructions, which requires evaluation of simplified procedures, substantially reduces costs in all phase but especially in the early stages of drafting. These projects for schools are unique and published in details in newspapers and magazines, featuring resource planning for future constructions of schools or university centers. Approximately 70% of resources are allocated to brand new facilities in this aea. Of course, it will be still charged 1% of the total cost for “pocket costs” or unpredictable costs.

In our country, we can find success motivation, developed project planning software and statistical expertise. At the moment we save money on costs at the design stage and lose much of its products sale, companies are characterized by centralized techniques, the use of databases to improve business management and marketing.

Economic science offered algorithms solve the motivation of the ones with low-income wages and simultaneously the entrepreneur’s found in “hunger” for major gains.

5. REFERENCES

Belbin, R. M. (1992), “Management Teams, Why they Succeed or Fail”, Heinemann Ltd, London

Hillebrandt, P. M. and Cannon, J. (1990), “The Modern Construction Firm”, Macmillan, London

Ferry, D. J. and Brandon, P. S. (1991), “Cost Planning of Buildings”, Blackwell Scientific Publications, Oxford

Sonea, S. (2004), “Gestiunea dinamica a firmelor mici si mijlocii”, UTPRES, Cluj Napoca

Chiorean, T. (2004), “Pretul lucrarilor de constructii”, UTPRES, Cluj Napoca

Klette, J. and Moen, J. (1998), “R&D investment responses to R&D subsidies: A theoretical analysis and a microeconometric study”, NBER Summer Institute

www.asce.org

http://www.ncef.org/

http://bgm.stanford.edu/newsletter_archive

TOPIC 4
ADVANCED CONCRETE STRUCTURES

BRIDGE OVER "PRIEMYSELNÁ" STREET ON R1 EXPRESSWAY SECTION "NITRA – SELENEC"

Adrián Sedlák[1], Jaroslav Halvonik[2], Róbert Magyar[1], Ľubomír Placek[1]

[1] *DOPRAVOPROJEKT a.s*
Kominárska 2,4
832 03 Bratislava, Slovak Republic
[2] *Slovak University of Technology in Bratislava, Faculty of Civil Engineering*
Radlinského 11
813 68 Bratislava, Slovak Republic

ABSTRACT

The bridge forming a flyover along "Priemyselná" Street is a dominant structure on the R1 southern bypass of the town Nitra. Due to complexity of site conditions the bridge with the overall length of 1,165 m is formed of two separate structures built by two different construction methods: first structure 806 m long is being constructed by incremental launching method, second one with length of 359 m by cast-in-situ balanced cantilever construction method.

1. INTRODUCTION

The bridge is a part of the R1 Expressway section Nitra, West – Selenec. The structure is situated within the urban area of the town Nitra and is crossing (bridging) both the railway track and the river Nitra.

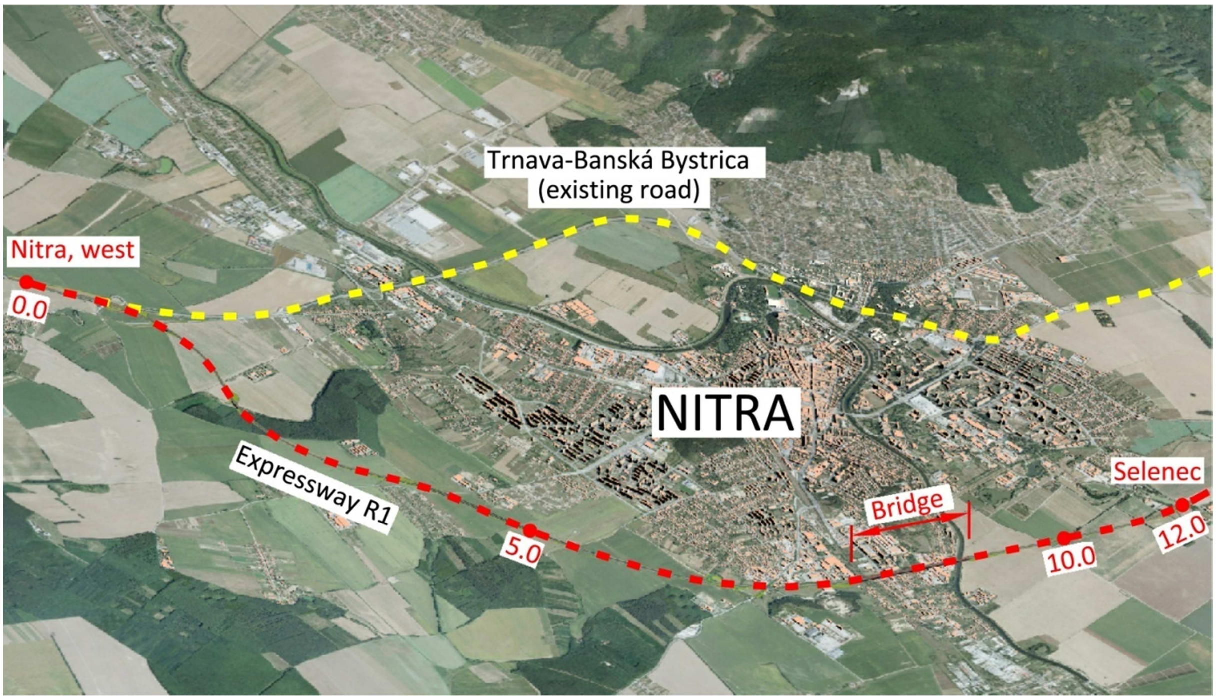

Fig.1 Bridge location

The bridge consists of two structures – construction units – with different shape and constructed by different construction methods. Construction unit N°1 (CU1) has been designed as two separate parallel bridges with single-cell box-section superstructure to be constructed by incremental launching method. Construction unit N°2 (CU2) has been designed as one superstructure for full expressway profile, i.e for both traffic directions. The CU2 cross section is formed by 3-cell structure with lower haunch above each pier. The bridge superstructure has been constructed by cast-in-situ free cantilevering.

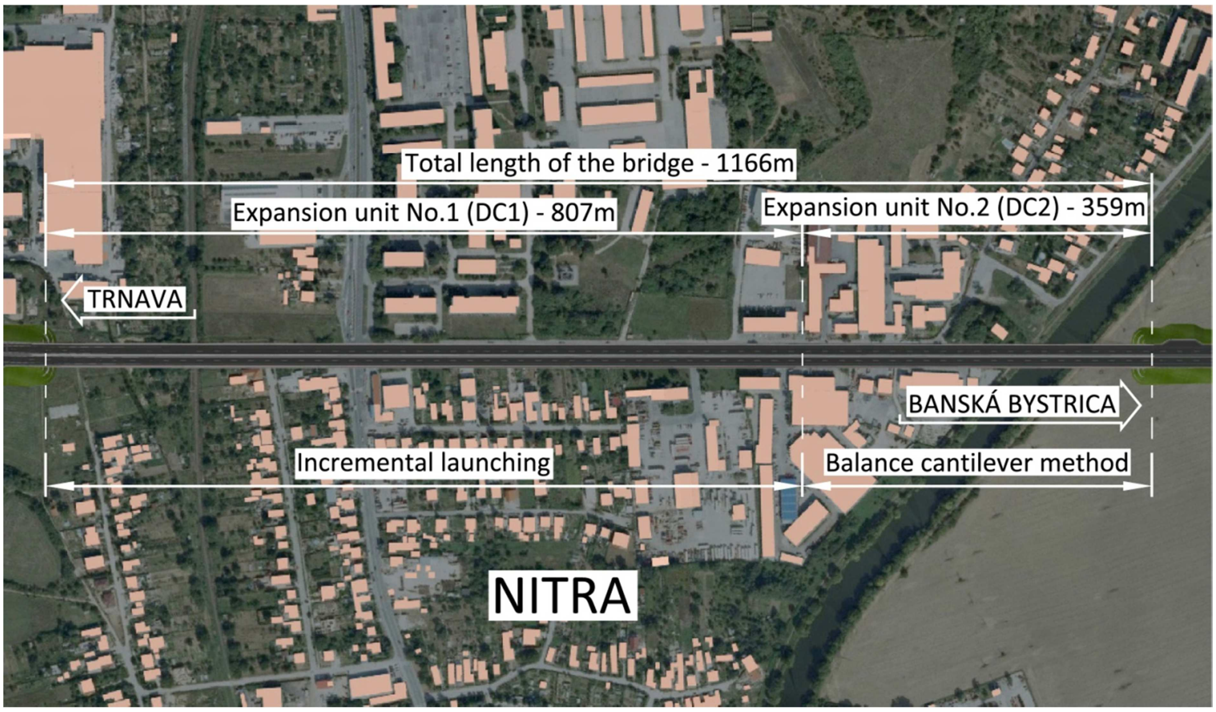

Fig. 2 Bridge two superstructures

2. DESIGN CONCEPT OF BRIDGE SUPERSTRUCTURE

Final design of the bridge superstructure was significantly influenced by the site conditions. The bridge crosses the railway track, the I/64 road, various in-town roads and streets and the river Nitra. The R1 expressway in km 8.4-8.7 is situated in the town's industrial zone with a number of plants. Within the given locality the precondition was to minimize the land required, which resulted in increasing the bridge spans. Due to this reason the bridge was divided into two separate structures with different length of spans in km 8.47 of the R1 expressway.

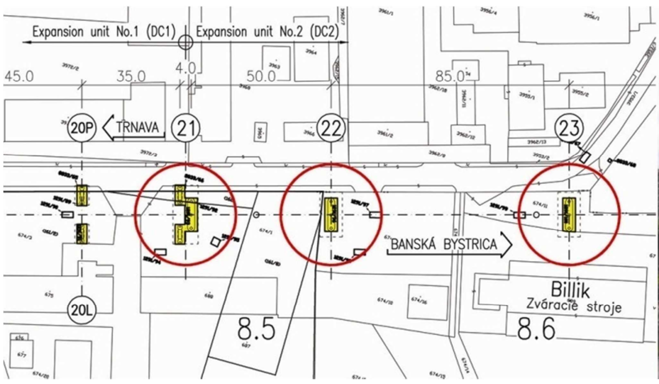

Fig. 3 and 4 Land required in the industrial zone

Spacing of piers for construction unit N°1 (CU1) was influenced by the site conditions; length of superstructure spans varies from 40 to 45 m. Spacing of piers for construction unit N°2 (CU2) was given by the site conditions (the industrial zone) and the bridging of the river

Nitra; the length of superstructure spans is 85 m. The form of the bridge substructure was influenced by the lack of space for the bridge foundations within the river Nitra flood protection dykes and necessity to minimize the land required within the industrial zone. The resulting permanent land required at the given locality is “only” outline of the piers.
In km 8.47 of the R1 expressway a joint pier with expansion joint is situated in order to enable movement of two different superstructures. Design of cross sections of the aforementioned structures was influenced by aesthetic reasons so as their junction would not form a “disturbing feature”.

3. CONSTRUCTION UNIT N°1 (CU1)

The unit N°1 (CU1) has been designed as two separate parallel bridges. The superstructure of each of them is formed by a single-cell prestressed cast-in-situ structure with constant cross section strengthened above the piers and in the places of deviators and fixing devices. From the structural point of view the superstructure represents a continuous 20-span girder (with depth of 2.67 m) constructed by the incremental launching method altogether in 40 segments with their length varying from 12.0 – 22.5 m. The bridge substructure consists of abutment N°1, piers and the joint pier N°21. The bridge foundations are designed to be resting on piles with diameter of 0.90 m. The bridge superstructure rests on “calotte” bearings (spherical knuckle bearing).

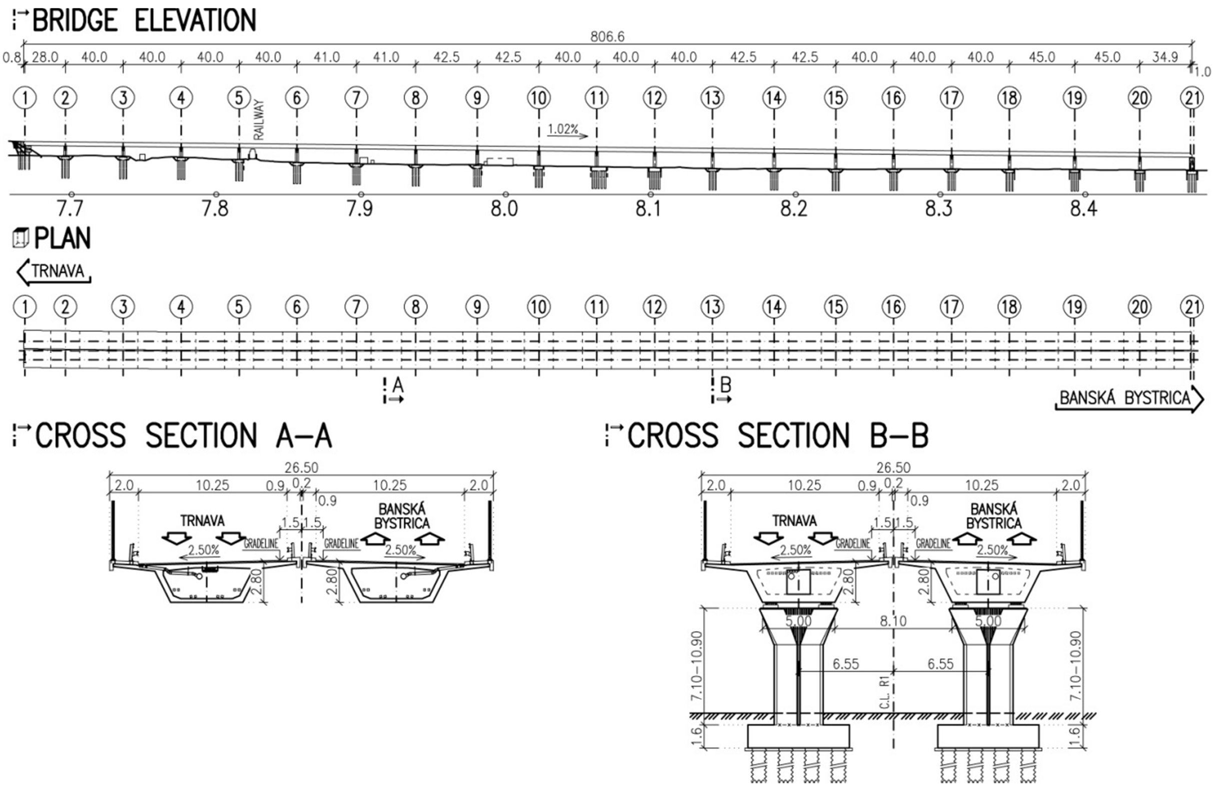

Fig. 5 Longitudinal section and cross sections

Casting of superstructure (its individual segments) is carried out in the concrete-casting plant situated behind the abutment N°1. Casting is performed in two stages: the bottom slab and webs and then the top slab. The length of individual segments varies from 12.0 – 22.5 m and depends on the section position within the bridge superstructure. Due to technological reasons the length of the first two segments is 12.0 m. The incremental launching of bridge superstructure is carried out by means of two hydraulic jacks situated at the abutment N°1 and on the auxiliary construction at the pier N°11. Due to the structural and the technological reasons the 32 m long steel launching noses are firmly fixed with the first segment of bridge superstructure.

The superstructure prestressing includes 3 basic types of tendons:

I.) longitudinal bonded tendons (prestressing during superstructure launching)
II.) longitudinal unbonded tendons inside the bridge box
III.) prestressing bars and bonded tendons for fixing the launching nose.

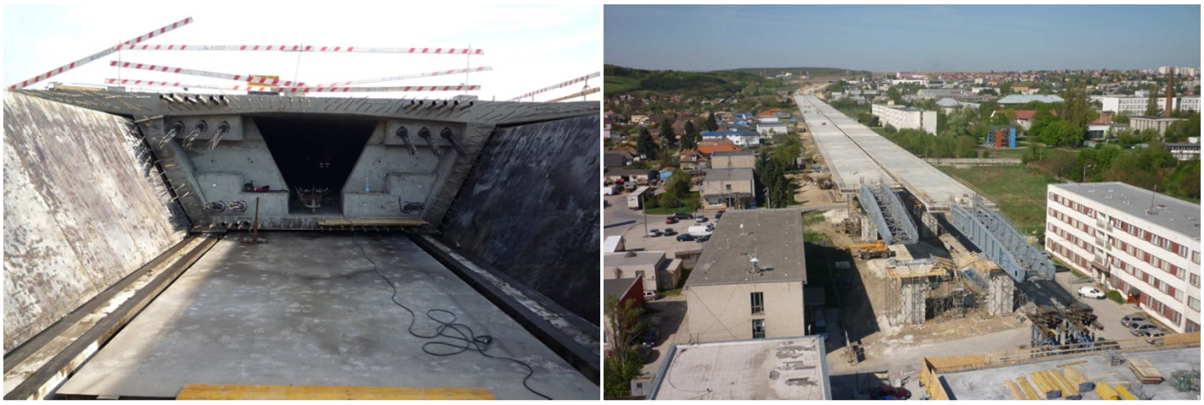

Fig. 6 and 7 Bridge superstructure construction

After launching the bridge superstructure into final position the unbonded tendons inside the bridge box are prestressed as first and then the temporary slide plates are replaced with permanent bridge bearings. By the contractor's decision there are larger slide plates used on the bridge in consequence of which the superstructure is constructed 60 mm higher compared to the design level. The replacement of slide plates and seating of superstructure on permanent bearings is carried out in several stages by phased structure settlement, provided that the uneven settlement of bridge superstructure at adjacent piers shall not exceed the value of 20 mm.

When deciding on construction method for the superstructure of construction unit N°1, the time factor was crucial; due to this reason the most suitable construction method was the incremental launching. By using this method the superstructure of the unit N°1 was completed in 320 days.

4. CONSTRUCTION UNIT N°2 (CU2)

The unit N°2 (CU2) has been designed as a single bridge (single superstructure) for both R1 expressway directions. The bridge superstructure is formed by 3-cell prestressed cast-in-situ structure with variable depth and lower haunches above piers. From the structural point of view it represents a 5-span continuous girder (with the depth varying from 2.80 m to 4.50 m), constructed by the balanced cantilever construction method for the whole cross section width (26.0 m). The bridge superstructure consists of four balanced cantilevers and two end spans constructed on stationary scaffolding. The bridge substructure consists of the joint pier N°21, piers N°22-25 and abutment N°26. The bridge foundations are designed to be resting on piles with diameter of 0.90 m. The bridge superstructure rests on "calotte" bearings (spherical knuckle bearing).

The in-situ cantilever construction is being carried out by means of three pairs of form travelers (6 pcs in total); the balanced cantilevers over the river Nitra were constructed as first, then those over industrial zone of "Priemyselná" street. Each balanced cantilever is formed by 12.5 m long base segment and 7 pairs of typical segments with the length of 4.75 – 5.00 m; its overall length is 82 m, the maximum cantilever overhang during the superstructure construction is 41.50 m. Casting of individual segments is carried out completely in one pour; except for the deviators for unbonded tendons, which are being carried out subsequently through construction openings in the deck slab.

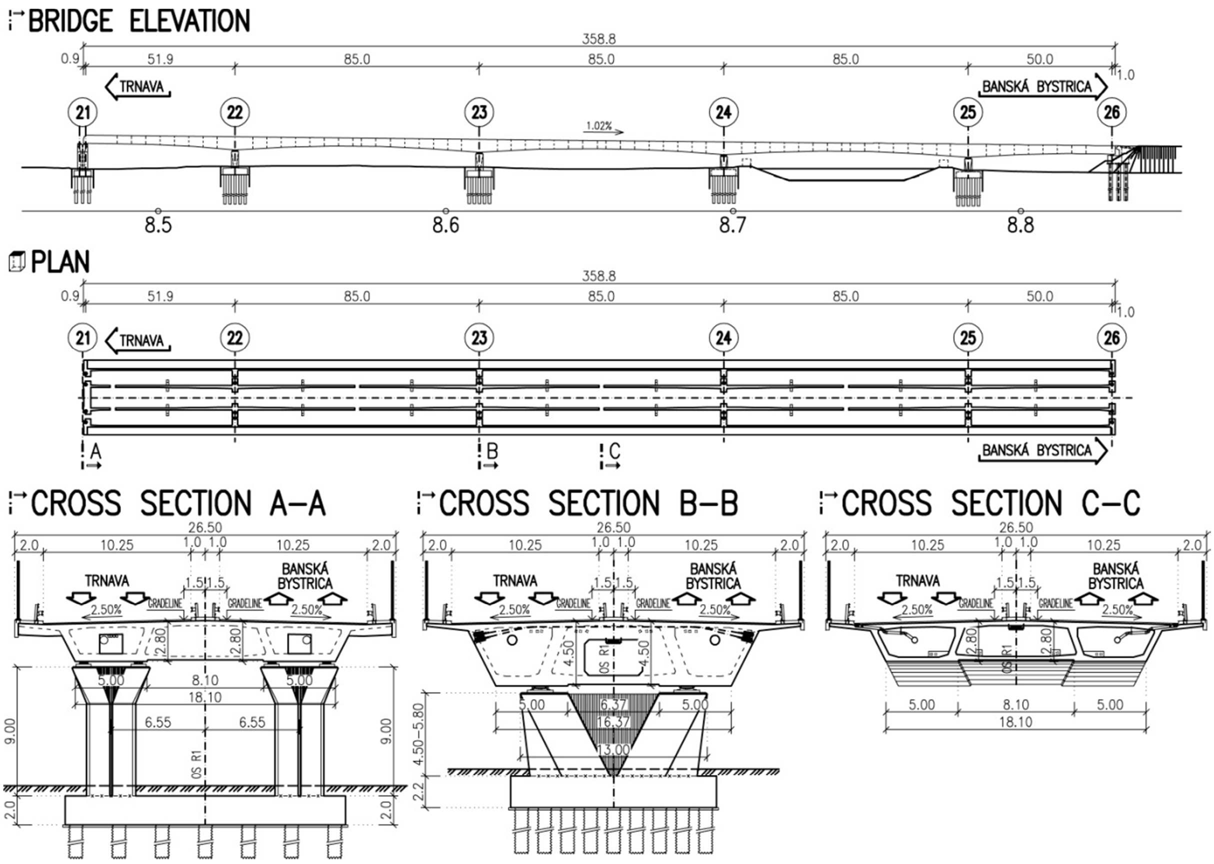

Fig. 8 Longitudinal section and cross sections

The design of superstructure prestressing includes 3 basic types:

I.) longitudinal bonded prestressing (the top slab, webs and the bottom slab)
II.) transverse bonded prestressing at diaphragms over the pier
III.) longitudinal prestressing with unbonded tendons inside the bridge box cells.


Fig. 9 and 10 Bridge superstructure construction

At each pier the bridge superstructure rests on the pair of bearings. The result of this is an indirect support of the outer webs; for the transfer of resulting shear forces at the diaphragm it was necessary to use the transverse bonded tendons, which were prestressed gradually in 2 stages, depending on the intensity of shear forces in the diaphragm area.

Stability of the balanced cantilevers during construction was provided for by means of temporary concrete walls erected on piers footings which will be removed after completing the superstructure.

The site conditions, the need to minimize land required during construction works and the crossing of the river Nitra are the main reasons for using the balanced cantilever construction method for construction of the unit N°2. The total time for the superstructure completion is 250 days.

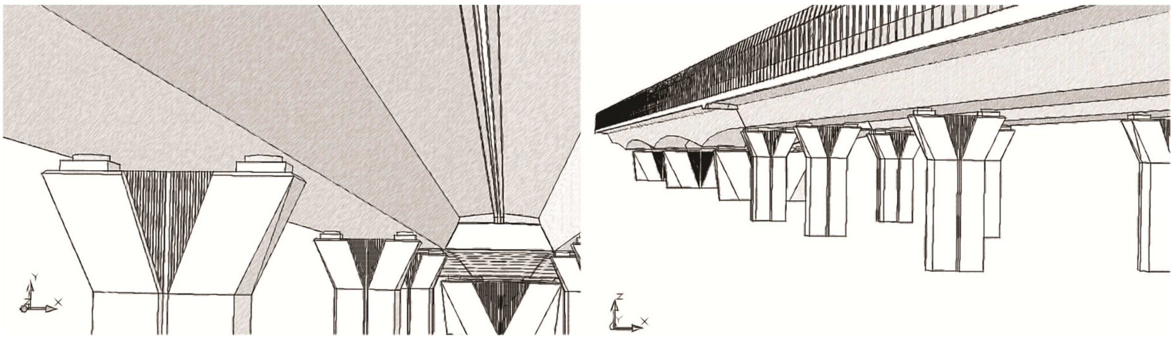

Fig. 11 and 12 Visualisation

5. CONCLUSIONS

The introduced bridge is a part of the R1 Expressway in section Nitra, west – Selenec which belongs to the second package of PPP projects in Slovakia. General Contractor of the Project is GRANVIA CONSTRUCTION Ltd. Contractor for the bridge is the Hungarian company A-HÍD ÉPÍTŐ ZRT. Construction works started in 12/2009 and the bridge will be completed during the year 2011.

6. REFERENCES

Guidance for good bridge design *fib* Task Group 1.2 Bridges, Bulletin 9, July 2000

FIRST APPLICATION OF THE BALANCED LIFT METHOD FOR BRIDGES ON THE S7 MOTORWAY IN AUSTRIA

Thomas Pils[1], David Wimmer[2], Susanne Gmainer[2], Johann Kollegger[2]
[1] *ASFINAG BAU MANAGMENT GmbH*
Modecenterstraße 16/3; A-1030 Vienna, Austria
[2] *Vienna University of Technology - Department of Structural Engineering*
Karlsplatz 13/E212-2; A-1040 Vienna, Austria

SUMMARY

The Austrian highway management company ASFINAG intends to build two bridges on the S7 motorway in Austria using the balanced lift method. In the course of a research project on the usage of thin precast concrete plate elements for bridge construction, it became possible to carry out a full-scale test of a bridge erection according to the balanced lift method. The full-scale test structure is similar to the bridges planned for the S7 motorway. Using the balanced lift method for building a bridge involves vertical assembly of compression struts and bridge girders. The bridge girders are rotated into the final horizontal position by either a vertical lift of the lower end points of the compression struts or by lowering the upper end points of the bridge girders. Cost comparisons with bridge projects built by the balanced cantilever method or incremental launching show a 30 % potential of saving costs.

1. PROJECT AREA

In the course of the new S7 motorway “Fürstenfelder Schnellstraße” between Riegersdorf and Staatsgrenze the section crosses the rivers “Lafnitz” and “Lahnbach”. The total length of the S7.21 Lafnitz-bridge is about 120 metres and the S7.22 Lahnbach-bridge about 100 metres. The cross section (Fig. 1) of the S7 motorway in this line section is traced out for two separate directed lanes, therefore the bridges across the rivers should be erected separately, regarding prospective reconstruction measures. Both areas are ecological sensitive and part of the nature reserve „Natura 2000”.

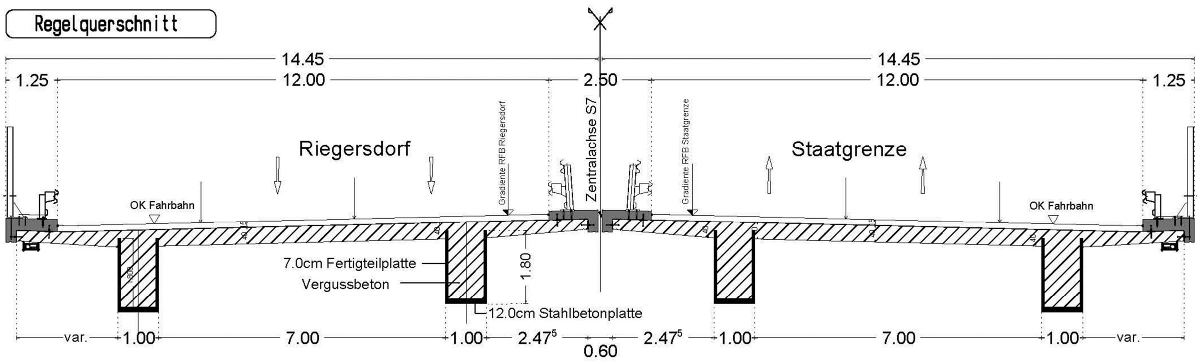

Fig. 1 Cross section of S7.21 and S7.22

The bridges are basically nessesary to afford the meander of the rivers and to provide options for the deer pass. To avoid encroachment in nature habitats, an erection on a falsework is not desired on the part of the owner. The manipulation areas of the building yard should be as small as possible, so the access to the construction site is only permitted at the central pier and at the abutments. For this reason only free cantilever, incremental launching or the balanced lift method are possible manufacturing technologies to build these bridges.

2. BALANCED LIFT METHOD

The balanced lift method was conceived at Vienna University of Technology in 2006. International patent applications have been filed (*Kollegger, 2007*), (*Kollegger, 2009*). The application of the balanced lift method for building valley bridges with high piers is shown in Fig. 2. Compression struts are assembled adjacent to the pier and subsequently the bridge girders are built in a vertical position preferably using climbforming. By lifting the lower end points of the compression struts, the bridge girders are rotated from the vertical position into the final horizontal position. If the topographical situation requires a design with piers of small or medium height, an auxiliary pier is used for the lowering process of the bridge girders as shown in Fig. 3.

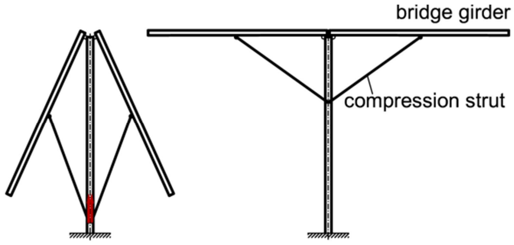

Fig. 2 Balanced lift method for bridges with high piers

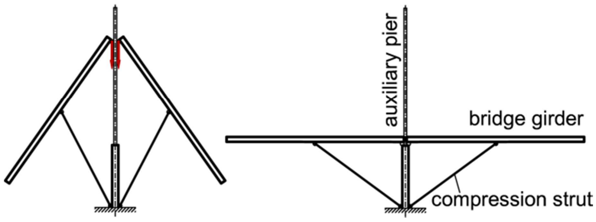

Fig. 3 Balanced lift method for bridges with piers of small or medium height

3. S7.21 AND S7.22 BRIDGES

The ASFINAG has ordered in addition to an original design, which was done for steel-concrete-composite bridges, an alternative design using the balanced lift method. The planned erection procedure for the original design was incremental launching, so the cross section has to be rather high to adjust the bending moments during the launching process. Compared to the composite construction, the superstructure of a bridge erected by the balanced lift method can be much lighter because the compression struts reduce the span lengths significantly. It could be shown that the construction costs for the post-tensioned concrete bridges erected with the balanced lift method amounted to only 70 % of the calculated costs for the composite bridges.

For this reason the S7.21 and S7.22 bridges will each be built using the balanced lift method for bridges with piers of small height (Fig. 3) to produce the central sections of the bridges (Fig. 7). This central section consists of two bridge girders with lengths of 35 m and two 18 m long compression struts and will be built eight times, two for every separate directed lane. Therefore a high pre-fabrication-level is suitable for recurring construction sections. The cross sections of the bridge girders are U-shaped pre-cast-elements with 70 mm thick wall elements and 200 mm bottom plates. The wall elements are generally used as pre-cast slab elements in combination with in-situ concrete for buildings. The prefabricated compression struts have a box-profile with a wall thickness of 120 mm. The pre-cast elements are designed as light as possible for a better handling during the lowering and assembling operations and for lower forces during the transport. However, the U-shaped prefabricated elements, which are basically developed as formwork for the webs, have to offer enough stiffness to carry the load of in-situ concrete (Fig 4). Therefore every necessary pre-stressing cable and anchor will be already casted in during the prefabrication. For further details on the production process of the prefabricated elements we refer you to (Kollegger, Gmainer, Wimmer, 2011), where an explicit description can be found.

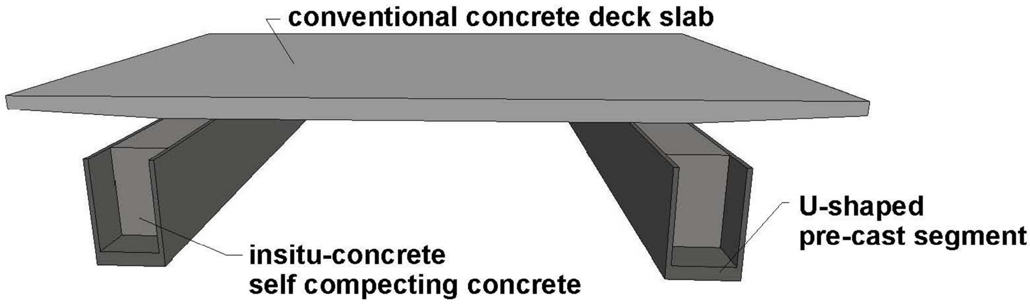

Fig. 4 Schedule of the construction process

The schedule of the construction process is based on mounting the pre-cast-elements and cast in-situ concrete subsequently. The newly formed square-section girder will be completed with a conventional reinforced concrete deck slab, just like in a composite bridge. All things considered the construction period at the building yard can be minimised significantly, because of the high pre-fabrication-level.

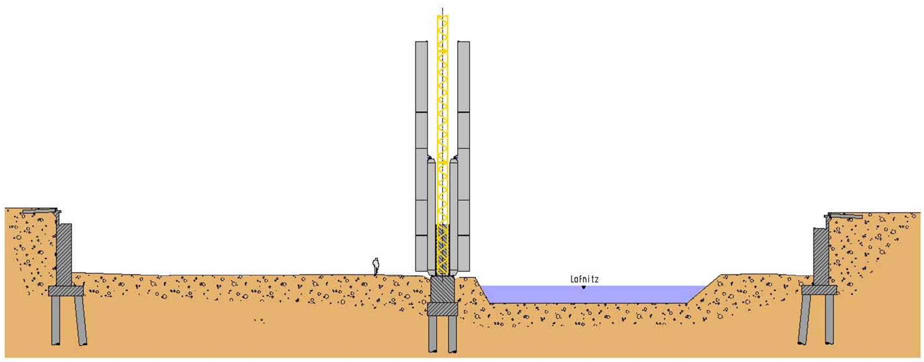

Fig. 5 Mounting auxiliary piers and pre-cast elements in vertical position

In the first step of the assembling operation the abutments, the central pier and the associated foundations will be erected. Then two auxiliary piers, which are equipped with guiding rails, can be assembled. These temporarily fixed supporting pylons are needed to install the pre-cast bridge elements in a vertical position and to adjust horizontal forces during the lowering operation (Fig. 5). All connections between the construction elements have to allow a rotation, in case of the connection between compression strut and bridge girder exceeding 155°. During a full-scale test, realised in September 2010, economic hinge connections could be developed. (*Kollegger, Gmainer, Wimmer, 2011*). Each end of the two bridge girders is connected by high tensile pre-stressing strands with a heavy lifting strand system, which is fixed on the top of the auxiliary piers. The heavy lifting system is needed to lower the construction from the vertical into the final horizontal position (Fig. 6). The superstructure of both bridges should offer a longitudinal gradient of 1.25 %. This decline can be achieved by stressing or relaxing the monostrands, which connect the two bridge girders, and by raising or lowering the end points of the bridge girders at the pier.

The next step of the assembling operation is to fill the compression struts and the bridge girders with cast in situ concrete and to adjust the deflections of dead load by stressing separate monostrands for each casting section. After hardening of the central section, the distance from the end points of the cantilevers to the abutments will be spanned by means of prefabricated beams with the same cross-section as the balanced lift part (Fig. 7). To connect these suspension beams with the central section a continuous tendon will be attached. These tendons reinforce the two newly formed square-section beams, so that the girders can carry the load of the subsequently cast in situ concrete deck slab. Based on the application of the balanced lift method and the high prefabrication level the construction period can be minimised significantly and a T-beam bridge can be erected without using area under the bridge, which means less encroachment in natural environment.

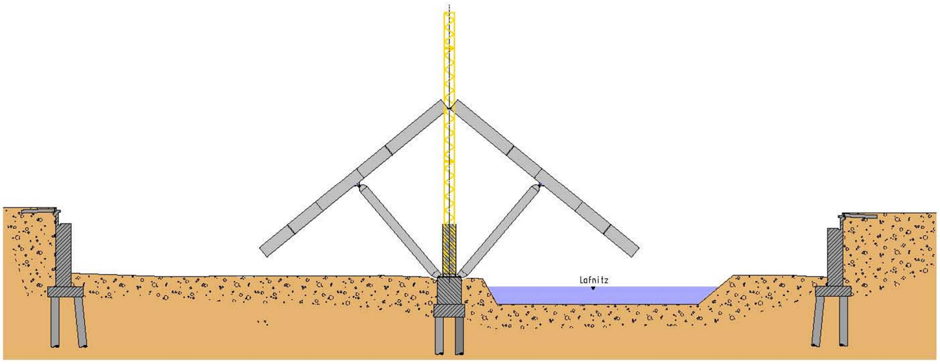

Fig. 6 lowering operation

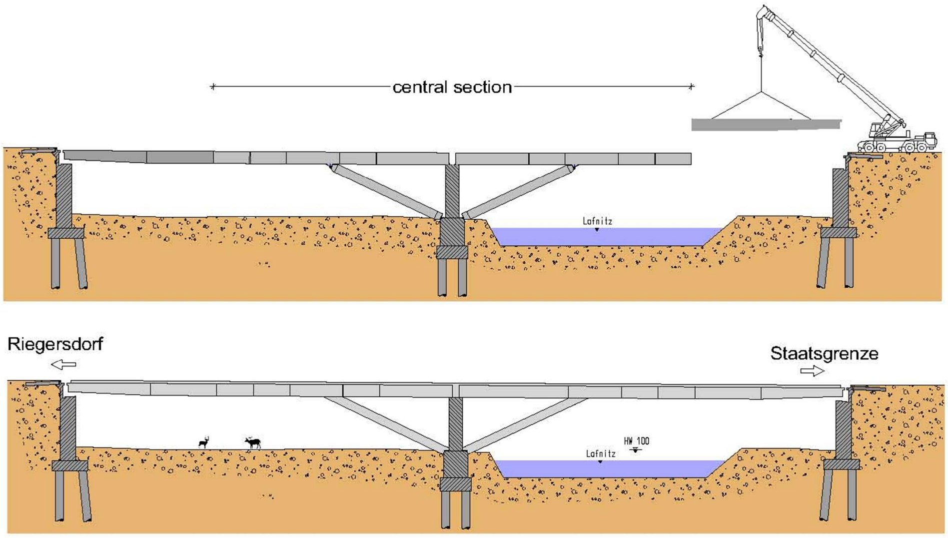

Fig. 7 Complement with suspension beam and deck slab

5. CONCLUSIONS

The full-scale test, which was carried out in September 2010, has impressively demonstrated the rapidity of the construction method. Using prefabricated construction elements in conjunction with the balanced lift method is an attractive alternative option compared to steel-girders, which are used for steel-concrete-composite bridges. Other areas of application can be highway and road structures with spans of 20-70 m, and tunnel ceilings in an open design.

6. REFERENCES

Kollegger, J. (2007), “Brückenklappverfahren“, German patent Nr.10 2006 039551, 2007

Kollegger, J. (2009), “Tilt-lift method for erecting a bridge”, WO 2008/022359, 2009

Kollegger, J., Gmainer, S., Wimmer, D. (2011) “Full-scale test of building a bridge by the balanced lift method“, Proceedings fib Symposium Prague, 2011, pp.471-474

REINFORCED CONCRETE CONSTRUCTIONS ON THE M6/M60 MOTORWAY - IS IT A HUNGARICUM?

Edina Éva Bechtel,Éva Szántó
National Infrastructure Developing Co., Budapest
1134 Budapest, Váci út 45.

SUMMARY

The M6/M60 motorway between Szekszárd and Pécs (M6 motorway phase III) is part of a 203 km long motorway section from Budapest to South of Hungary, built in the last years in Public-Private Partnership.The preparation was the task of NIF (National Infrastructure Developing Co.), and the Concession Contract was concluded with the Consortium as a Concessionaire, which was the legal predecessor of the MAK Mecsek Autópálya Koncessziós Zrt. on 21st November 2007.

Based on the previous PPP project experiences, NIF as the technical representative of the State had a defined task on the project.

As a result of geographical and geological circumstances there were planned and constructed 4 tunnels, 9 viaducts and 74 other large structures, which made it a special section of Hungarian motorways.

The site works were started in February 2008 and the section was opened to traffic on 31st March 2010. The very short deadline made it necessary to organize and construct the 79.4 km long section very accurately and roundly.Our presentation gives an overview of the preparation, the organization and the implementation of the reinforced concrete constructions and introduces two special and interesting constructions: a viaduct and the first motorway tunnels in Hungary.

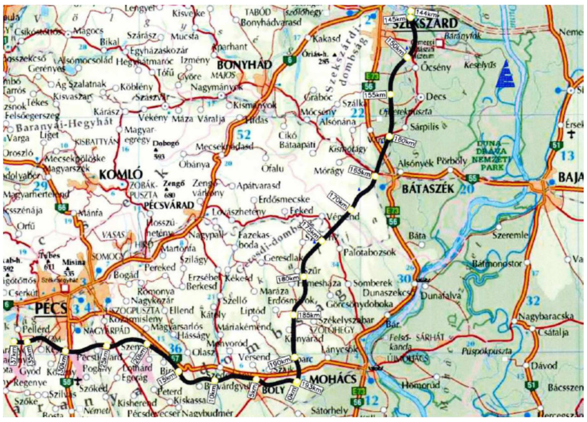

Fig. 1 The track of the M6/M60 motorway section

1. INTRODUCTION

In about two years there were built 49.2 km of dual carriageway for the M6 motorway and 30.2 km of dual carriageway for the M60 motorway, including 10 interchanges, 3 rest areas and 2 O&M centres. Also, there were built many other public roads in connection of the project.

The main structural works comprise 9 viaducts (8 from these are reinforced concrete structures), 4 tunnels, and 74 other large structures.

The partners:

Concession Company:	MAK Mecsek Autópálya Koncessziós Zrt.
Contractor:	Mecsek Construction Group
Independent Engineer:	Ove Arup & Partners International Limited in cooperation with EUROUT Mérnöki, Tanácsadó, Szervező és Kereskedelmi Kft
General Designer:	UNITEF ’83 Zrt.

2. VIADUCT 1693 ABOVE BELSŐRÉT STREAM BRANCH AND GAME CROSSING

The bridge is located between the tunnel A and the tunnel B. The only bridge on the site built with incremental launching method. It was cast and longitudinally prestressed on fix formwork and then launched into its final position.

Fig. 2 The viaduct 1693

General data of the bridge:
Nomination: M6 motorway   Segment: 169+322.55 km   Number of supports: 7
Main sizes of the bridge (measured of the radius of R=4750 m):
Length of the superstructure: 278.6 m (measured in the road axis)
Spans: 37.8-4x50.0-39.0 m
Total bridge width: 13.45 m
Width of the car track: 10.32 m
Block length: left track: 26.20+25.00+7x25.00+26.20+26.20 m
right track: 25.64+25.00+7x25.00+26.20+25.37 m
Total width of the bridge: 37.95 m

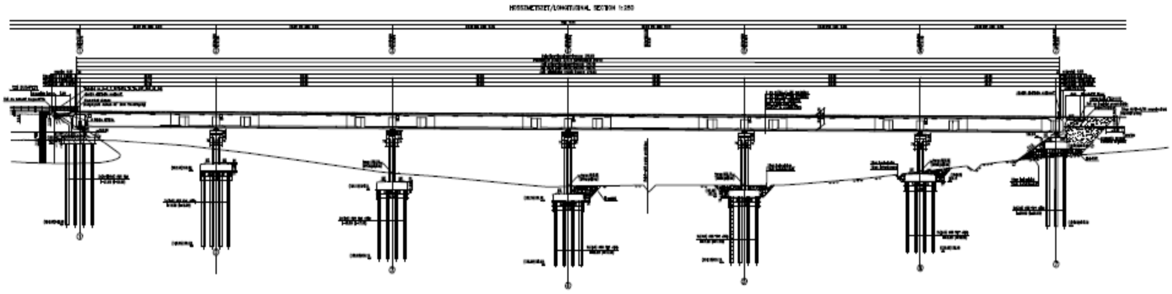

Fig. 3 The longitudinal section of the viaduct 1693

The structure of the bridge is: 6 spanned, continuous bridge girder. The superstructure is containing 2 identical wide box profiled deck slabs made out of pre-stressed reinforced concrete separated by a 11.05 m wide air-gap.The structure of the bridge is pre-stressed reinforced concrete, with adhesive deposite pre-stress led in the lower and upper slab and in the rib. It was built by incremental launching method. The wall of the abutments are solid, the intermediate supports have solid pillar structure. The bridge is shouldered on the abutments and on the intermediate piers on hinged supports. There were planned expansion jointed structures with pointing sill, provided with test field. The bridge is based on 80 cm bored reinforced concrete piles.

The construction of the bridge had begun with the piling in July of 2008. The construction of the substructures, adjusting to the incremental launching method, were built from the abutment No. 1 as on the abutment No. 7.The on-site precast units were erected from the production bench behind the abutment No. 1 by cyclic casting. The reinforcement assembly, the casting, the prestressing and the launching of the units were made of a one week cycle.
There were made 11 units, each 25-26 m long both the right-side and the left-side. The launching took place in downward direction along 0,5 % slope by the use of a 32 m long, steel launching nose. The prestressing was made of inside, grouted post-tensioned cables. The launching process lasted 6 months, the whole construction of the bridge lasted 22 months.

<u>The concrete specifications:</u>

Structural elements of abutment and wing wall: C35/45-16/K f50 vz5
Pier column: C35/45-16/K f50 vz5
Cross beam on pier: C35/45-16/K f50 vz5
Prestressed concrete deck: C40/50 -16/K f50 vz5

3. THE TUNNELS

The speciality of these tunnels is, that these are the first tunnels on motorway in Hungary. There were built four tunnels in a length of 1321 m, 399 m, 855 m, 418 m.

Fig. 4 The temporary lining

Fig. 5 Shotcrete

According of the building method, the temporary lining of the tunnels was made of shotcrete.
The invert arch of the tunnels is a 60-cm-thick reinforced concrete structure, it is made of water-tight concrete.The inner lining is a typically 35 cm thick structure made of reinforced concrete.

Around the inner lining there is a 2-mm-thick PVC water-proofing with a 900g/m^2 geotextile cover.

<u>The quality of materials:</u>
Invert arch: C30/37-XA1-XV2(H)-24-F3
Inner lining: C30/37-XF2-24-F4
Reinforcement bar: B500B

The pavements in the tunnels – contrary to the other section of the motorway section - were also built of concrete.

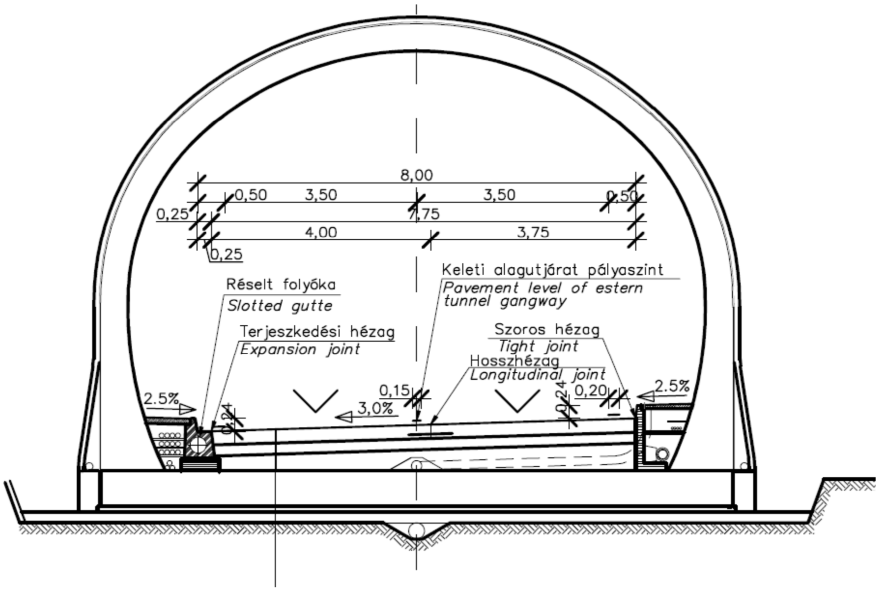

Fig. 6 Design cross section, running tunnel built with open construction

<u>The pavement structure:</u>
25 cm CP 4/2,7 dowel jointed concrete pavement
20 cm Ckt-4 road base+500gr/sqm spec. mass geotextile separating layer on it
FZKA32 fill in variable thickness

4. ORGANIZATION

The short deadline and the great number of large structures made it necessary to organize the contraction very punctual.In order to serve the tunnel contraction there were erected a whole “city” near of the tunnel A with offices, accommodations for employees, restaurant, and also a mixing plant only to serve the tunnel construction and the viaduct 1693.The concrete supply was organized by 10 mixing plants in a distance from several km to 35 km.

5. SUMMARY

The concrete structures of our presentation are not unique in themselves, the applied technologies, construction methods and materials have been widely known. The speciality of the presented motorway section lies in the quantity and capacity used within the short deadlines and distance in the scope of one project, for the first time in Hungary.

VIADUKT ŠKURDA – MOTORWAY RING AROUND THE ANCIENT CITY OF KOTOR

Damir Tkalčić, Stela Dubravac
Institut IGH d.d.
Croatia, 10000 Zagreb, Janka Rakuše 1

ABSTRACT

The viaduct is situated on the ring road around the ancient city of Kotor, declared by the UNESCO as a World Heritage Site. Considering the terrain configuration, the planned construction method and environmental protection measures defined by the Regional Institute for Protection of Cultural Monuments in Kotor, a continuous girder was selected as the load bearing structure over three spans, with a box type cross section and variable height, executed by free cantilevering method. This way, the motorway alignment is nestled along the plateau surface and the canyon cliffs remain untouched. The harmony of design of the Škurda Viaduct offers a notable view of the City of Kotor in the untouched natural environment, and as such it becomes a part of the surroundings.

1. INTRODUCTION

The Bay of Kotor is a branchy and outspread bay on the southern part of the Adriatic East Coast in Montenegro. The City of Kotor, and the region as well, is under the UNESCO Cultural Heritage Protection since 1979, which obliges to very prudential interventions in space. The ring road around the Ancient City of Kotor presents a very complex problem because all large scale building operations, especially roads, leave a permanent trace in the area, changing its overall appearance for ever. Precisely because of this, the ring road project is a big challenge for the builders and experts in the field of cultural heritage protection.

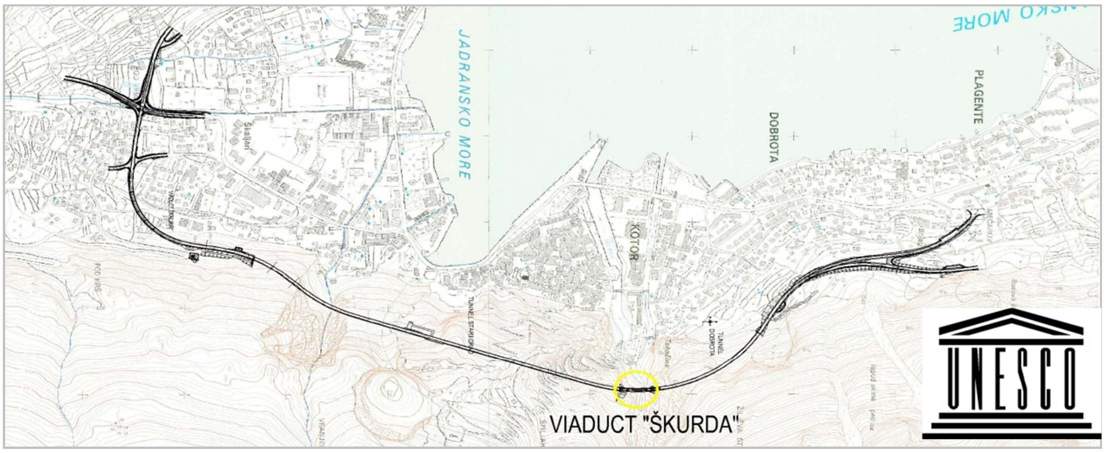

Fig. 1 The Bay of Kotor

2. DESCRIPTION OF THE STRUCTURE

The Škurda River canyon is a nature complex under the UNESCO protection, which imposes significant limitations with regard to building activities. Also, the Tunnels Stari Grad and Dobrota are situated on the canyon sides, forming a part of the ring road. Their portal structures partially overlap with the viaduct structure.

The obstacle that had to be overcome, as well as the potential construction method had to be considered during the definition of the viaduct structure. An arch bridge imposed itself as a logical solution, considering the high bearing capacity of rock mass. However, since the main task during design development was to maximally preserve the natural beauty of the Škurda River canyon, and since no works were allowed on the canyon sides and edges during construction, this solution was considered unacceptable.

2.1 Viaduct superstructure

As a result of all above mentioned, a continuous girder with three spans length 16.0 m + 60.0 m + 16.0 m imposes itself as the logical bearing structure, with a box type cross section and variable height. Overall length of the structure is 99.2 m.

The gradient is ascending by 2.5%. In plan view, the viaduct is in a left curve, radius R = 350.0 m. Its height over the canyon reaches 30 m on the average.
Lengths of side spans (short in relation to the central span 16.0/60.0 m) are defined by the shape of the obstacle, but also by the fact that they interfere into the portal structures of both tunnels. Therefore, free cantilever method imposes itself as the ultimate construction method, where the continuity, i.e. fixity of the main span is ensured by short boundary fields (which are counterweights in the static sense) fixed into the supporting structure consisting of posts and abutments.

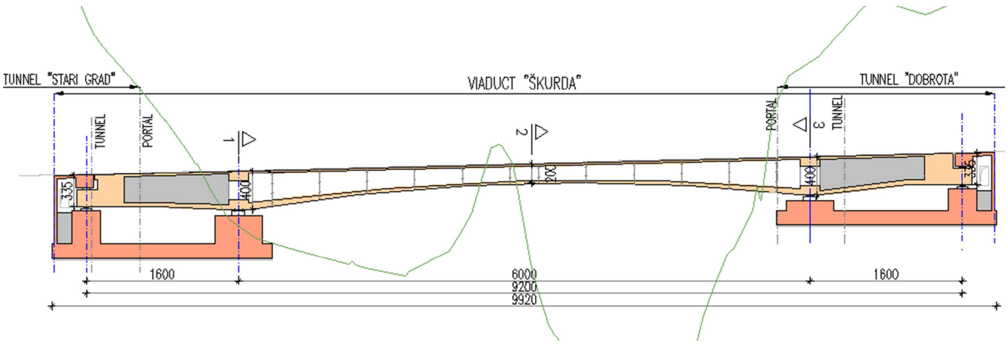

Fig. 2 Longitudinal section of the viaduct

The bridge superstructure leans on the side supports on a bearing over an abutment (first construction stage compression bearing), to prevent the superstructure from uplifting. It is therefore supported by consoles on abutments from above, which intake the permanent, uplifting reaction of the second, final viaduct construction stage.

For the same reason, the hollow boxes in the end fields are filled with low strength non reinforced concrete. This type of structural design of abutments and posts ensures the fixity of the central span through the bracing of forces post-abutment.

Box girder with one chamber has a very strong geometry, and considering that the side spans partially interfere into the tunnels, at places where the tunnel and viaduct „overlap“, the width of the upper flange plates (consoles) decreases, while the lower flange plate width remains constant.
Lower flange plate of the girder is executed horizontally in the transverse direction while the carriageway slab is inclining. In plan view they follow the road curve. Change in the girder height is achieved by the change of the inclination of the lower flange plate.

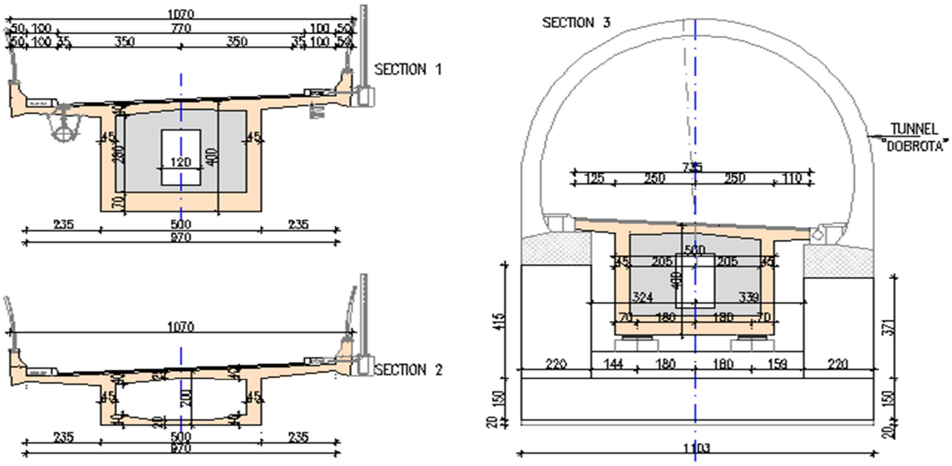

Fig. 3 Cross sections

The ratio between the length and structural height of the beam in the central field over the post is 60.0/4.0 = 15, i.e. 60.0/2.0 = 30 in the span center.

Transverse walls within the boxes are planned on the posts – diaphragm walls with openings. Viaduct design and analysis are done in accordance with EUROCODE and national regulations of Montenegro.

Main construction material of the bearing structure is prestressed concrete, tensioned reinforcing steel B500A, and cables 1570/1770 N/mm2.

2.2 Viaduct substructure

Massive reinforced concrete abutments are planned, designed to accept the uplifting reaction of the symmetrical superstructure. The walls on the foundation slab form a box like cross section in plan view. A transverse girder is constructed near the abutment top, which intakes the uplifting reaction. The superstructure end is wedged between the abutment wall from beneath and a girder from above, forming space for an expansion joint at the end of the transverse girder.

The posts are massive with a full cross section. Viaduct foundation works are executed in hard carbonate rock, on shallow, large surface area footings (as a result of the selected bearing structure).Since the left viaduct side is in Tunnel Stari Grad, and the right viaduct side is in Tunnel Dobrota, portal structures of both tunnels lean on the foundation slab by way of a massive wall. The slab connects the posts and abutment structure on both tunnels. During excavation of foundation pit for the abutment structures, the number and arrangement of possible anchors will be defined in agreement with the Soil Mechanics Engineer engineer, which will serve to anchor the massive walls into the rock mass.

2.3 Viaduct equipment

Bearings – The superstructure leans on the abutments and posts over the pot bearings, two on each support. Fixed bearings are on post S2. Pot bearings are planned on abutments, to control the uplifting reaction, and are placed on the superstructure under the shear beam of abutment. Apart from this, elastomere bearings are also installed on the central abutment wall, to intake the reaction during bridge construction.

Expansion joints – The viaduct is planned as one wing, with expansion joints installed at the position of abutments.

Concrete guard rail and noise protection elements – Concrete guard rail type New Jersey is executed as a series of monolith elements, tightly connected to the box bearing. The viaduct will also have a steel structure with safety transparent panels made of polycarbonate glass. Steel structure posts are executed with an externally inclined radius curvature, and are anchored into the concrete guard rail.

Electrical and Telecommunication installations –Electrical and telecommunication installations on the viaduct outside of the portal structures are to be conducted through PVC pipes in the inspection paths, and on installation racks, anchored under the beam. Manholes are planned in the vicinity of lighting posts, for installation of lighting cables.

3. CONSTRUCTION METHOD

The viaducts is to be constructed by free cantilevering, in 5,0 m long segments, except the central segment in the crown.

According to design, the viaduct will be constructed as follows:

1. Construction of abutments
2. Construction of reinforced concrete posts
3. Construction of the base on the scaffolding (3,5 m) and mounting of mobile scaffold on it – form traveller to be used in construction of further segments (5 m) by cantilevering
4. Connection of span structure is to be done by concreting of the last 2m long segment
5. Dismantling of form traveller
6. Construction of passageways, kerbs, etc.
7. Waterproofing and asphalt works

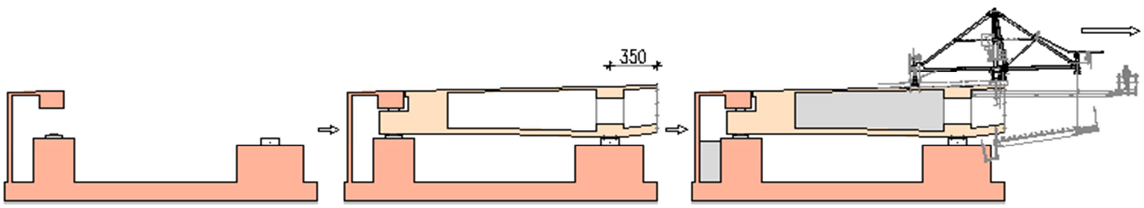

Fig. 4 Construction stages

This construction method tries to keep negative influences on the surroundings at a minimum, therefore free cantilevering is applied, except on the construction of abutments with counterweights. After completion of excavation works, works on the construction of foundation slab, sills, longitudinal walls and cross beams of the rear abutment side must be executed simultaneously on both sides of the canyon.

This is followed by construction of consoles on the scaffold and completion of rear frames, after which symmetrical free cantilevering in segments can begin.

4. REFERENCES

http://whc.unesco.org/en/list/125

Tkalčić D., 2010. Zaobilaznica Kotora, Dionica oko Starog Grada – Glavni građevinski projekat Vijadukta Škurda / , Motorway ring around the Ancient City of Kotor, Section around Stari Grad – Detailed Construction Design of the Škurda Viaduct; Institut IGH d.d., Zagreb

ADVANCED MODELLING OF FIBRE REINFORCED CONCRETE STRUCTURES

Radomír Pukl, Petr Havlásek, Tereza Sajdlová, Vladimír Červenka
Červenka Consulting
150 00 Praha 5, Na Hřebenkách 55, Czech Republic

SUMMARY

Experience with nonlinear numerical modelling of fibre reinforced concrete (FRC) structures is presented. Possible levels of FRC material modelling, inverse analysis of appropriate FRC material parameters and selected practical examples are shown. Issues regarding reliability, durability and global safety of FRC structures are sketched.

1. INTRODUCTION

Fibre reinforced concrete (FRC) is extensively used composite construction material. It is structural material having a base of plain concrete supplemented by fibres that brace the structure of material. The fibres can be made of various materials, shapes and dimensions. The FRC technology was initiated in order to improve relevant mechanical properties of concrete. A significant desired feature is the avoidance of negative effects of volume changes of concrete during its maturation and avoidance of shrinkage cracks. Addition of steel fibres also results in increased tensile strength and ductility of the material. The fibre reinforced concrete becomes to be used also for design and construction of load carrying structural members, but the recent design codes doesn't cover the design of the FRC-based structures sufficiently.

The nonlinear finite element simulation is well-established advanced method for analysis and modelling of concrete and reinforced concrete structures *(Červenka et al. 2002)*. Behavior of the structure under service or ultimate loading conditions can be realistically simulated. Crack initiation and development, load carrying capacity and post-critical behavior of the structures, structural parts or experimental specimens can be traced and investigated. Nonlinear fracture analysis accounting tensile capacity of material enables to exploit reserves, which are usually neglected or diminished in codes or in linear analysis. Such an advanced numerical analysis can be also efficiently used for structures made from the fibre reinforced concrete. In particular, it can help in cases not sufficiently supported by design codes. Since the improved tensile behavior and ductility in the FRC is a dominating feature, the potential profit from the nonlinear analysis of FRC-based structures is much higher than in standard reinforced concrete structures. Furthermore, higher spatial variability of material properties occurring in the FRC can be accounted in the numerical models and utilized for evaluation of structural safety and reliability.

2. MODELLING OF FIBRE REINFORCED CONCRETE MATERIALS

Special constitutive material models were developed for description of FRC-material in the nonlinear finite element analysis *(Pukl et al. 2005)*. They account the high toughness and ductility of FRC as well as possible uncertainties and spatial variability of the material properties. Several levels of FRC modelling at the material levels can be utilized in the nonlinear numerical analysis. The first approach is utilization of the material models developed for plain concrete with appropriately adjusted material parameters (tensile strength, fracture energy). The form of the tensile descending branch is exponential function which not optimal for the description of FRC response, but its use is rather pragmatic – it is of advantage that the models for plain concrete are very well verified and exhibit stable behaviour.

In order to improve the modelling of the FRC tensile behavior material laws with special forms of the tensile descending branch more suitable for FRC were formulated and implemented. Two models are designed especially for steel fibre reinforced concrete (SFRC). They are derived from plane stress material law for plain concrete. If the fracture energy is known, an objective material law based on the crack band approach can be used. After cracking, the tensile stress drops to certain fraction of the tensile strength. In practical cases the fracture energy value is often difficult to evaluate since in tests it is a hard task to follow the long-persisting descending branch until the zero tensile stress. In such a case a local formulation of the tensile material law is available. It is similar to the previous model but it is formulated directly in terms of strains and does not employ the fracture energy and crack band approach.

The most sophisticated and most general model of FRC material represents an extension to the fracture-plastic constitutive law called CC3-User model. It describes the tensile behavior according to the material response measured in tests point-wise in terms of the stress-strain relationship. The first part of the diagram is the usual stress-strain constitutive law. After exceeding the localization strain the material law assumed for the prescribed characteristic crack band width is adjusted to the actual crack band width. All these models were successfully applied in numerical simulations of experimental specimens. The FRC material can be also combined with the conventional reinforcement.

3. RANDOMNESS AND SPATIAL VARIABILITY OF FRC PROPERTIES

Accounting uncertainties in FRC-materials is of extreme importance since the scatter of experimental response is generally much higher comparing conventional concrete. The classical statistical and reliability approach is to model material parameters as random variables with prescribed distribution function. The stochastic response requires repeated analyses of the structure with these random input parameters, which reflects randomness and uncertainties in the input values. As the nonlinear structural analysis is computationally very demanding, a suitable technique of statistical sampling should be used, which allows a relatively small number of simulations *(Pukl et al. 2010)*. Results of the stochastic analysis are statistical characteristics of structural response – ultimate load or deflection, stresses, crack width etc., information on dominating and non-dominating variables (sensitivity analysis), and estimation of reliability or failure probability. It can be used for evaluation of the global structural safety *(Červenka 2011)*. Using degradation stochastic modules also the durability of the structure can be assessed.

Since the heterogeneity of the FRC-material is due to the fibre contents rather high, an improved approach to reality (e.g. in crack location and direction) can be achieved using special methods taking into account spatial variability of the material properties. The spatial variability of material properties is introduced by a special envelope for the basic material models, which initiates material values in specified points *(Pukl et al. 2010)*. The spatial distribution of a particular material property can originate from two alternative sources: it can be really measured values along the modelled specimen, or the spatial distribution of the local values can be generated by advanced stochastic methods. The models based on random fields approach were implemented in the integrated system for probabilistic assessment of engineering structures.

4. IDENTIFICATION OF FRC MATERIAL PARAMETERS

Properties of the composite material vary with the character of fibres, specific geometrics, distribution, orientation and densities together with the degree of concrete consolidation. Testing of the material properties is a complex task which is not satisfactorily solved until now. Therefore, the knowledge about material properties of the FRC in a particular case can be often poor or uncertain. The appropriate values (mainly of the tensile material properties – tensile strength f_t and fracture energy G_f) can be adjusted by inverse analysis from results of available tests on simple structures such as three-point or four-point bending beams. This procedure has been successfully developed, verified and applied for steel fibre reinforced concrete with various contents of fibres using various above mentioned material models *(Pukl, Sajdlová 2011)*. Some general rules were derived for determination of appropriate tensile properties of SFRC based on concrete class and fibre contents. To support the identification procedure, also the above mentioned randomization of the deterministic model was employed for the inverse analysis, using regular distribution of the investigated material parameters. From evaluation of the stochastic results the optimal parameters were confirmed.

5. APPLICATION EXAMPLE

Response and ultimate load carrying capacity of tunnel tubings used in tunnel boring method (TBM) was investigated. These tubings are usually designed and produced from reinforced concrete with steel rebars. Such tubings were tested in Klokner institute of CTU in Prague until destruction; nonlinear numerical model of the tests of RC tubing was investigated to support the experiments. An alternative design by fibre reinforced concrete without rebars was investigated only numerically. Selected results – crack patterns, comparison of the response curves and ductility – are presented in following figures. The behavior of FRC structure was found to be superior to RC tubing. Crack patterns shown in the Figure 1 exhibits larger local crack width for the RC tubing. In the SFRC model the cracks are less localized and they are formed in a wider band; crack opening is lower. Resistance of the SFRC specimens against the acting load is higher and the post peak behaviour is more ductile (Fig. 2). The alternative design by SFRC has better performance, and in the same time it can save up time and reduce labour.

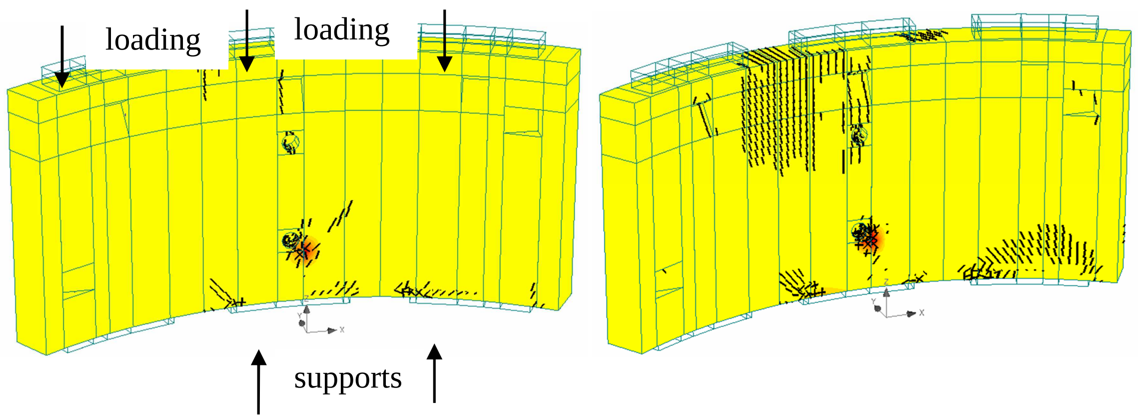

Fig. 1 Crack patterns for RC tubing (left) and FRC tubing (right)

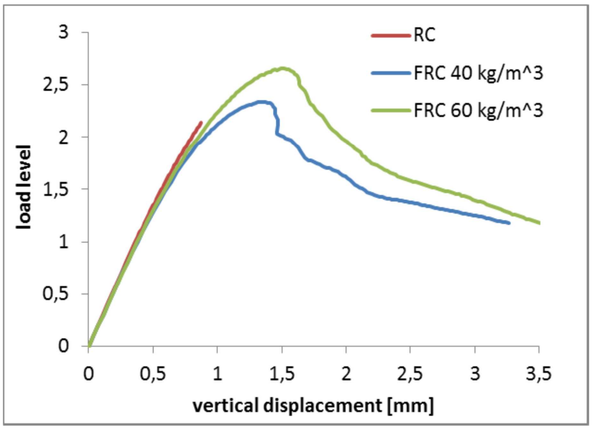

Fig. 2 Load-displacement diagram from numerical simulation of tubing – comparison of reinforced concrete and fibre reinforced concrete

RC = standard reinforced concrete with mild reinforcing steel rebars,
FRC 40 or 60 kg/m^3 = fibre reinforced concrete without rebars, with content of 40 or 60 kg of steel fibres in one cubic meter of concrete mixture

6. CONCLUSIONS

In the fibre reinforced concrete the tensile behavior and ductility is a dominating feature. For that reason the potential profit from the nonlinear analysis of FRC-based structures is much higher than in standard reinforced concrete structures. Advanced material models for numerical simulation of fibre reinforced concrete were developed and utilized in practical applications. Sophisticated techniques for accounting uncertainties, randomness, spatial variability and identification of material parameters are available. The described methodology is implemented into integrated software tools for nonlinear analysis of FRC-based structures, which can be utilized in practice. Global safety of the structure as well as its durability can be assessed using these tools.

7. ACKNOWLEDGEMENT

The presented research was performed within the project FR-TI1/612 CERHYD and the grant No. P105/10/1156 "COMOCOS - Complex modelling of concrete structures". Authors gratefully acknowledge this support.

8. REFERENCES

Červenka, V., Červenka, J., Pukl, R. (2002): „ATENA – A tool for engineering analysis of fracture in concrete“, Sadhaná 27(4), pp. 485-492

Pukl, R. et al. (2005): „ Deterministic and statistical models for nonlinear FE analysis of FRC-based structures“, In: CCC 2005, Graz, Austria, pp. 130-133

Pukl, R. et al. (2010): „Advanced tools for numerical analysis and life-cycle assessment of reinforced concrete structures“, In: IALCCE 2010, Taipei, Taiwan, p. 141

Červenka V. (2011) „Design of fibre reinforced concrete structures based on nonlinear analysis“, submitted to Fibre Concrete 2011, Prague, September 2011

Pukl, R., Sajdlová, T. (2011) „Identification of material parameters for nonlinear modeling of fibre reinforced concrete structures“, submitted to Fibre Concrete 2011, Prague, September 2011

OPTIMIZATION AND ASSESSMENT IN STRUCTURAL ENGINEERING USING ADVANCED MONITORING CONCEPTS

Alfred Strauss, Roman Wendner, Alexander Krawtschuk and Konrad Bergmeister
Department of Civil Engineering and Natural Hazards,
University of Natural Resources and Life Sciences,
Vienna, A-1190, Austria.

SUMMARY

Nowadays, bridge owners and planners tend to include life-cycle cost analyses in order to optimize structural reliability and durability within financial constraints. In order to reduce these risks, smart permanent and short term monitoring concepts can be used to observe the performance of structural components during prescribed time period. The objectives of this paper are discussing concepts for (a) the effective incorporation of monitoring data in model updating procedures by means of influence lines, (b) the investigation of the functionality of monitoring systems including error tracking, and (c) the inverse identification and evaluation of sensor properties and monitoring values. The proposed methodology will be applied to an existing three-span joint less bridge structure, instrumented with an integrative monitoring system.

1. INTRODUCTION

Recently, a shift in civil engineering philosophy toward life-cycle cost analysis can be observed. The key element of this performance oriented design philosophy is monitoring. “Monitoring” includes all types of direct acquisition, observation and supervision of an activity or a process and as a consequence of this the corrective intervention. The overall objective is to determine systematically and analyse any potential failure causes, as well as failure effects and worst case scenarios. Furthermore this concept includes the definition of performance indicators based on influence lines and model correction factors.

2. PROOF LOADING BASED INFLUENCE LINE CONCEPT

Proof load tests on the Marktwasser bridge have been performed on Friday, Feb. 19th 2010 with temperatures between 0°-2°C. The results serve for calibrating static linear model and the verification of the assumed structural behavior. Firstly defined load situations were considered to ensure a proper model calibration, taking into account the boundary conditions. Then three 40 to trucks with known axle loads were positioned in 16 static scenarios. The trucks were positioned independently in the most unfavorable configurations on lanes 1-3 (Fig. 1(a)). For the model calibration nine static load situations with a single truck of 41.55 to in lane 1 were considered only (Fig. 1(b)).

2.1 General interpretation of Fiber optical sensor- and LVDT- associated influence lines

In general stress/strain as well as deformations contain contributions from dead load, temperature loads, earth pressure, partial settlements and the time dependent processes creep and shrinkage. In order to account for these effects during data analysis all the mentioned load situations are analyzed in a finite element model. In total 17 load cases are considered including the nine proof loading scenarios.

However, during the proof loading procedure stress/strain as well as deformation contributions caused by other loads than the proof loading vehicle can be assumed to remain constant and thus can be neglected. In general, a good agreement between the numerically generated influence lines for horizontal strain (stress) at the location of the fiber optical sensors and the experimentally obtained values can be observed, see Fig. 2. This figure portrays the simulated influence lines for sensors d_{7u} and d_{9o} of the full initial finite element model bedded drilling piles (solid line) as well as idealized models (soil-structure interaction is substituted by rotational springs; dashed, dash-dotted and dotted line) in comparison to the extracted sensor readings during the experimental proof loading procedure (vertical bars).

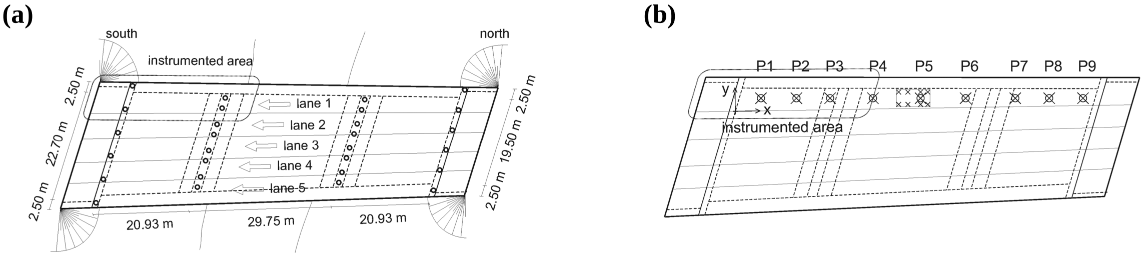

Fig. 1 (a) top view indicating the traffic lanes and isntrumented area. (b) model points for static load scenarios.

2.3 Interpretation of IL with respect to modeling and monitoring

The span by span comparison between simulated influence lines and experimental influence values shows deviations of 10 % to 45 % with respect to the initial finite element model, see Figs. 2(a-b). Apart from divergences between model and reality (degrees of restraint, stiffness distribution, local stress trajectories not covered by the model) the reasons for the observed deviations may be contributed to (a) an inaccurate determination of truck positions during the proof loading procedure, or (b) an insufficiently well calibrated monitoring systems. A single monitoring system does not allow a statement regarding the true nature of the deviation.

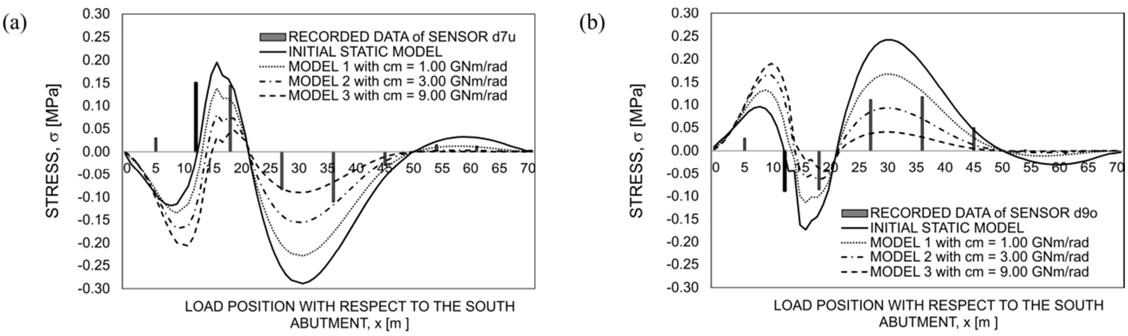

Fig. 2 Influence lines (IL) extracted from the Finite Element Model of the bridge system S33.24 with respect to the measured values of the nine proof loading positions: (a) IL of stresses associated with the fiber optical sensor d_{7u}; and (b) IL of stresses associated with the fiber optical sensor d_{9o}

As the LVDT influence lines related to sensors w_1 and w_2 presented in Figs. 3(a) and (b) show qualitatively similar deviations, it can be concluded that (a) the calibration of both monitoring systems is adequate, (b) no severe or systematic error is present in the measurements, and (c) the likely cause has to be contributed to modeling.

2.4 Interpretation of influence lines with respect to load position and stiffness distribution

Reasons for differences in structural response between model and reality such as boundary conditions or stiffness distributions are best investigated by simplified models. Therefore, in a first approach abutment walls and columns have been substituted by idealized translational and rotational springs. This simplification allows an effective investigation of the impact of uncertain modeling parameters on the shape of the observed influence lines. Here the effects of the uncertain stiffness of the substructure and especially the structure – soil – interaction are directly accessible for qualitative interpretation and quantitative assessment.

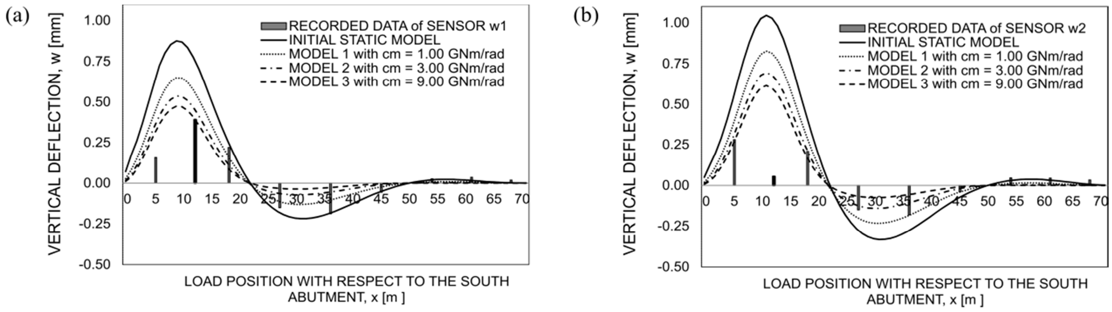

Fig. 3 Influence lines (IL) extracted from the Finite Element Model of the bridge system S33.24 with respect to the measured values of the nine proof loading positions: (a) IL of vertical deflections associated with the LVDT sensor w_1; and (b) IL of vertical deflections associated with the LVDT sensor w_2

2.5 Truck positioned in the northern lateral span

The comparably small experimental influence values for the FOS strain sensors d_{7u} and d_{9o} (Figs. 2) extracted for the truck positioned in the western part of northern lateral span indicate a stiffer structural system than accounted for in the initial model. However, the LVDT influence values for sensors w_1 and w_2 (see Fig. 3) show the opposite behavior with higher vertical deflections indicating a more flexible real structure. The opposing deviation from the respective numerically generated influence lines leads to the conclusion that the data of one of the monitoring systems has to be slightly erroneous or at least biased in its magnitudes. In case one of the monitoring systems can be determined to be more reliable, systematic errors in the other monitoring system can be identified.

2.6 Truck positioned in the main span

The experimental influence lines for the truck positioned in the main span show both for the FOS sensors d_{7u} and d_{9o} and the LVDT sensors w_1 and w_2 a decrease in the system stiffness (e.g., indicated by the possible assignment of proof loading measurements to numerical model quantities) by trend with increasing distance from column axis x = 20.93 m to 50.68 m. However, the deflection influence lines again show a lower system stiffness as already concluded for the truck positioned in the northern span.

2.7 Truck positioned in southern lateral span (instrumented span)

The three numerically obtained influence values for sensors d_{7u} and d_{9o} and the associated measurements for the truck within the southern span do not allow a satisfactory interpretation. For the load position of x = 5.05 m the strain sensors indicate a more flexible system as compared to simulation results for the initial model whereas for the load position of 11.86 m an extremely stiff real system has to be concluded. However, the LVDT influence lines for sensors w_1 and w_2 indicate a stiffer real system as compared to the initial finite element model which is in disagreement with the interpretation of the strain sensor data. Again the opposing indications by both monitoring systems have to be evaluated with respect to the systems' reliability.

Due to the global design of the structure (inclined abutment and column axis; haunches near the column axes) local deviations in the stress and strain trajectories from the ideal assumptions have to be considered. These influence stress/ strain recordings by the fiber optic monitoring system in two ways. First, the sensors themselves might not be aligned with the trajectories. In this case the sensor readings would underestimate structural response. Considering the locations of sensors d_{7u} and d_{9o} near haunches of the column axis this effect might explain the comparably small measured response. Second, if the sensors are aligned perfectly, the recorded quantities represent the real structural response at the sensor' locations. However, local (spatial) effects at the load positions, which are not accounted for in the model, still could lead to an underestimation/ deviation in the measured values (e.g. due to a direct load transfer to the abutment and reduced use of system bending carrying capacity).

3. CONCLUSIONS

The objective of this article was the investigation of monitoring concepts based on influence lines for the evaluation of the real behavior of engineering structures. The concepts of influence lines have been theoretically presented and combined to an efficient procedure for the incorporation of monitoring data during the processes of modeling and subsequently assessing a structure's real behavior. The presented methodology was successfully applied to a three-span jointless bridge structure utilizing monitoring data of a proof loading procedure obtained by a fiber optic strain and LVDT based deflection monitoring system. The determination of influence lines based on local monitoring quantities such as strain or deflection enhance the sensor importance in space, which is otherwise restricted to local properties of e.g. system characteristics. Within the presented case study the influence line concept was successfully used to investigate the real stiffness ratio between bridge deck slab and substructure as well as the soil structure interaction by the comparison between model variations and experiment. Furthermore, the comparison between the different investigated models and reality allows the identification of deficiencies in the current model approach and thus the definition of requirements for modeling. Although the idealized models showed partially a good agreement with the measurements the complexity of reality seems only to be representable by more detailed modeling concepts including the modeling of the foundation piles.

4. ACKNOWLEDGEMENTS

This research was conducted with the financial support of ASFINAG and BMVIT within the research project "Monitoring and analysis of integral bridge structures" and with the financial support of the Austrian research funding agency FFG within the EUREKA Eurostar research project "Risk Lifetime Assessment of Concrete Structures". The opinions and conclusions presented in this paper are those of the authors and do not necessarily reflect the views of the sponsoring organizations.

5. REFERENCES

Vrouwenvelder, T., *The JCSS probabilistic model code.* Structural Safety, 1997. **19**(3): p. 245-251.

JCSS Probabilistic Model Code Part 1: Basis of Design. 2001.

Ang, A.H.-S. and W.H. Tang, *Probability concepts in engineering planning and design, basic principles*. 2007: Wiley & Son.

Okasha, N.M. and D.M. Frangopol, *Integration of Structural Health Monitoring in a System Performance Based Life Cycle Bridge Management Framework.* Structure and Infrastructure Engineering, 2011: p. (in press).

CONCRETE HIGH-RISE GREEN BUILDINGS FOR CENTRAL EUROPE

Peter Lenkei
Pécs University, Hungary
len980@t-online.hu

Motto

"On Spaceship Earth there are no passengers, everybody is a member of the crew.

We have moved into an age in which everybody's activity affected everybody else."

Marshall McLuhan (1911-1980)

SUMMARY

The paper shows the possibility and the importance of high-rise green concrete buildings in Central Europe. At the same time necessary to deal with the different structural demands due to the sustainability of these buildings. These are shown for diverse solutions. Finally the city development approaches are treated.

1.INTRODUCTION

During the last 10-20 years several interesting trends could be observed in the construction of high-rise buildings.

First of all concrete are more and more increasingly used as basic structural material for high-rise buildings of different heights. For example the structure of the present-day highest building of the world, the Burj Kalifa (previously called Burj Dubai) is formed from concrete almost up to the top. The Petronas twin towers were built from concrete, except the outrigger beams. Even the steel structures of high-rise buildings are often encased in concrete.

The second and may be the most important change was brought about by the sustainability principle. Nowadays the concept of green building, eco building, net-zero energy building, thermos building e.g. double-skin façade system Fig. 1 (*Strabala 2011*), etc. are the most frequently mentioned subjects in the related journals.

By all means such concepts besides the important advantages could increase the construction and the maintenance costs. Unfortunately the state support for such buildings only exists westwards and eastwards of Central Europe.

2.CHANGES DUE TO SUSTAINABILITY

There is a struggle for the title of the World Greenest Skyscraper, i.e. for the world's most environmentally friendly skyscraper. But this demands connected with serious structural changes. The changes are due to prospective energy savings in lighting, air conditioning and heating etc.

The changes could be formal e.g. double outer glass layers for air circulation with small fans, or supports for solar cells. These changes are not connected in substantial alterations of the structural system.

Fig. 1 Shanghai top high-rise buildings (from left): World Financial Center, Jin Mao Tower, the soon to be built Shanghai Tower with double skin façade system and with vertical-axis wind turbines (wind farm) on top of the building

There are changes forcing substantial alterations of such traditional systems like the core and shell or the multi tube systems.

One of the frequented solution is the big vertical ventilation tube in the middle of the building e.g. the Deutsche Bundespost building in Bonn Fig. 2 (H. Jahn and M. Jahn 2003) and the big "cigar" in London by Foster. In this case all the structural elements should be distributed around the perimeter. Such a solution is aimed for energy savings by more or less permanent temperature all around of the year. The functional problem is the bad acoustics due to the tube effect and the structural problem is the less economic sketch. But this solution requires operation several small ventilators for reliable air flow.

.

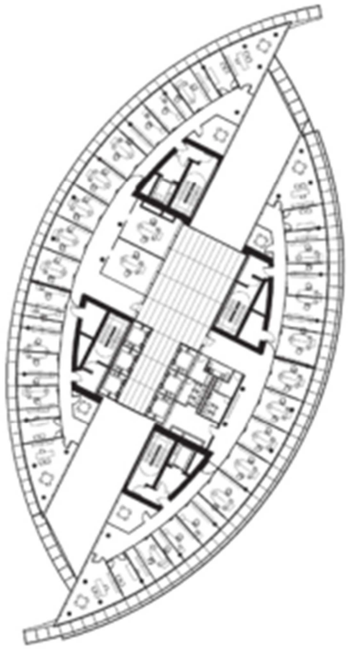

Fig. 2 The Bundespost building in Bonn: the building at night and the typical storey lay-out

There are lot of green buildings, but only few net-zero energy buildings

The implementation of a net-zero energy buildings possible only by means of energy producing equipments, like wind turbines, solar cells or use of geothermic energy.

The latest system is the use of wind turbines in-building, on the building or apart of the building.

One solution is the horizontal wind turbines, placed in traverse horizontal holes on several heights. These holes cause several changes, namely the width of the building should be limited, the vertical structural elements and the elevators should be placed only in the two far ends. In addition the outrigger beams should be heavy.

The other solution is the vertical wind turbines placed structurally apart from the buildings or placed on the top of the buildings. The reason for this is the wind turbine should be open to the wind. Here the problem is the two structures instead of one or the higher structure.

Both this systems could lead to serious architectural problems.

3.CITY DEVELOPMENTS

The other problem is the traditional principles of the town planning and development: “no high-rise buildings in our city”. This is true for capitals and lot of main cities in Central Europe which are on river banks and the townscapes include the old city centers of heritage value. But for new cities and for new parts of old cities the central part or the entrance to the city could/should be marked by high-rise buildings of 30-40 stories.

High rise buildings are usually built for mixed use of: office, entertainment, residence and commerce. There is another problem, the function of high-rise buildings and the demand on the presumed function, e.g. nowadays in Hungary new office buildings are utilized only by 30-40%.

4.CONCLUSIONS

The present and the future are for the concrete sustainable high-rise buildings. Sustainability could be achieved by energy savings and use of renewable energy sources during the construction and use of these high-rise buildings.

The vertical wind turbines are the mostly recommended renewable energy alternative. The high-rise towers outfitted with wind turbines could potentially bring in excess energy over own power needs.

High-rise buildings of 30-40 stories is a realty of recent and/or future city developments in some Central European cities.

5.ACKNOWLEDGEMENTS

The author acknowledge with thanks the support from the Hungarian Research Foundation (Grant K 69164) which made possible to carry out the research, part of which is reported herein.

6.REFERENCES

Jahn, H. and Jahn, M. (2003) “Post Tower, Bonn” Tall Building and Transparency Conference Proceedings Ed. W. Sobek,.ILEK Stuttgart, Session 1, p. 1-11

Strabala M. (2011), Urbanatomy (http//Shanghai urbanatomy.com/index php/i-ahaerts-shanghai/features/4474-the-master-builder)

PPFRC CORNICE AND WALL COVERING

J. Kozák[1], B. Magyari[2], G. Tassi[3],
[1]Argomex Ltd., H-5561 Békésszentandrás,
[2]Innoir Ltd., H-6000 Kecskemét,
[3]Budapest University of Technology and Economics, H-1521 Budapest

SUMMARY

Concerning the incidents of fire in various objects occurring in the last decades, the use of PPFRC (Polypropylene Fibre Reinforced Concrete) was aimed to reduce damages to concrete structures. In case of transparent constructions, the fire protection has not been subjected to scientific evaluation rigorously enough. - The József Attila Study and Information Centre of University of Szeged represents useful example a closing, dividing and fire protection cornice in a transparent building. - Ventilated PPFRC façades of residential and public buildings combined with thermal insulation have the principal function of blocking fire. - An experimental investigation of a PPFRC member is described.

1. INTRODUCTION

In Hungary, PPFRC cladding of building façades is widely used. The more than 20 years' research resulted in many advantages of fibre reinforced façade panels as of strength, durability and esthetical view.

As is well-known, the requirements of thermal insulation, and fire protection of structures *(Lublóy, Balázs, 2009, Fehérvári, 2008)* have recently been enhanced significantly, and all these resulted in strict expectations as façades are concerned.

Currently, the composition of façades on reinforced concrete structures is deemed up to date with the following ingredients: 160~200 mm thermal insulation of rock-wool, 30~40 mm ventilating space and, at last, the cover of stone or FRC. The increasing of the gap between the cover and the load carrying structure demands enhanced requirements from the parts of the connection of the covering.

2. THE MANUFACTURING OF MATERIAL

The prefabrication and use of FRC elements applied at façades began in the 1980s. In the beginning, the elements were flat and rectangular, with slight Oarchitectonic profiling. Organic architecture recognized the excellent formability of FRC at the beginning of the 1990s, and so, the creation of spatial, complex shapes soon prevailed in the application of PPFRC.

Manufacturing of the covering PPFRC façade elements is taking place in ready mixed condition. The reinforcing material is a polypropylene fibre and it is applied in 0.1~0.5 % of the mixed volume. The fibre is 40 mm long with a diameter of 0.18 mm. The plates are cast in steel moulds thus the correct sizes and a perfect surface is reached. Depending of the thickness of the plates, the maximal grain size of the material is 4.0~8.0 mm. With the mixture cement CEM I 52.5 N is used either in white or in grey colour. Beside the fibre reinforcement steel bars are added, furthermore fixation bolts. After 24 hours, the compressive strength of the PPFRC is higher than 14.0 N/mm^2, thus the moulds can be removed without thermal curing. When white cement is applied, the finishing of the elements can be made with diamond polishers, as well. After 28 days maturing 53.8 N/mm^2 is seen as a typical value of the compressive strength of PPFRC.

3. EXAMPLES OF PPFRC FAÇADE ELEMENTS FOR RESIDENTIAL AND PUBLIC BUILDINGS

Over many centuries, buildings were supplied by stone, brick, mortar or traditional concrete cladding. Recently FRC, in Hungary mainly PPFRC, façade elements are widely, used *(Kozák, Magyari, Tassi, 2008)*. Let us mention here a few examples.

Close to the Duna Plaza in Budapest, four buildings of 6~8 stories – “Prestige Towers” - have been erected. For cladding, 80 mm thick, generally of 4~6, at a max 9 m^2 size, altogether 1600 m^{2}self compacting PPFRC panels were applied in various colours.

A multi storey educational building was enlarged in Pécs. 30 mm thick, 0.70~1.50 m^2 white, PPFRC panels were applied to this structure. The full surface is 950 m^2.

The Education Centre of Semmelweis University in Budapest was cladded with terracotta colour PPFRC panels, their surface was 0.7 m^2 each, altogether 2100 m^2 with a thickness of 30 mm. Corner and window rim members were manufactured, as well.

Various special forms for a market hall cladding were produced by application of PPFRC at Lehel Square, Budapest. This material was used, among others, for ornamental building elements in the Auditorium Maximum of the Pázmány Péter University at Piliscsaba *(Magyari, Tassi, 2007)*.

4. THE TRANSPARENT BUILDING AND THE FIRE BLOCKING CORNICE

The mentioned cornice is to be seen on the façade of the József Attila Study and Information Centre of University of Szeged (Fig. 1). The architect is László Mikó.

The basic data of the building in question are as follows: ground area 25,000 m^2, the length of the cornice is 750 m.

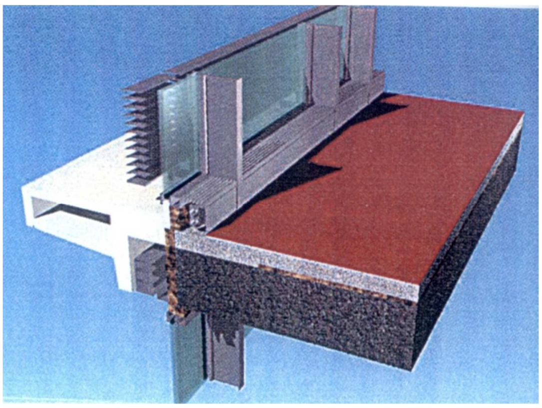

Fig. 1 Connection between the cornice and the glass-covered façade

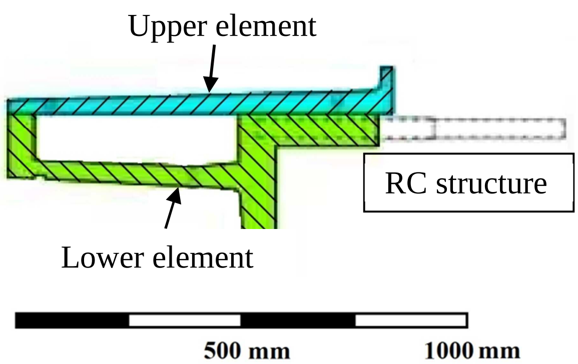

Fig. 2 Schema of a cornice element

The primary function of the applied cornice (Fig. 2) is the blocking of the vertical propagation of the fire between stories of separated fire protected areas furnished with glass façades but not with parapet walls (Fig. 1). Besides, the elements serve as an architectural division of the plain façade parts and with the grooves indented on their lower surface.

As for the manufacturing is concerned, materials and constructional details only should be applied so the elements of the cornice may contain no thermal bridges and they have to satisfy the requirement of fire blocking one hour time's long. Furthermore, they have to be fastened to the construction of the floor.

A typical length of the cornice elements is 1.80 m. These members are fastened to the floor structure with the aid of three cantilevers each. After the correct positioning and jointing of the façade elements they have to be welded to the steel plates laid in the concrete of the floor before casting.

The elements of the cornice are made of PPFRC. The concrete grade is C 35, the colour is faded white, the surface is polished.

The cornice consists of two parts (Fig. 2). The lower one carries the loads and this one is connected to the reinforced concrete floor structure. The upper one is self supporting and it conveys the loads to the lower part.

The basic sizes of a typical lower element are as follows: 1792×800×380 mm, while those of the upper elements are: 1792×825×35-60 "L" - shape heights is 120 mm. The lower elements are constructed with the mentioned steel cantilevers. These are made of three pieces, DV 90×50×4 mm box profile and they are welded to the steel reinforcement of the cornice elements.

Since the DV box profiles cross the thermal insulation of the façade, here the profiles must be coated with KATEPOX in two layers, furthermore 0.50 mm stainless steel protection is applied against corrosion, while a plastic sealing is needed at the ends.

The reinforcing bars, Ø 8 and Ø 10 mm are of grade B.60.50, Ø6 mm of C15.H. Type of the steel reinforcement is a mesh.

The covering element of the cornice is supported by the lower one and they are connected by bolts plugged to the lower element. For the lifting of the lower elements four hooks are embedded in the reinforced concrete structure while the upper elements are lifted by three bolts of M12 size. The weight of one element is 5.43 kN.

The composition of the concrete is the following:
CEM I 52,5 N white pc 350 kg/m^3; OK 4/8 sorted gravel 833 kg/m^3; 0/0.5 yellow limestone milling 416 kg/m^3; 0/4 TH sorted and washed sand 416 kg/m^3; Melment L-40 1.5 % 5,25 kg/m^3; water ~180 l; Politon BV 40-1 1 kg/m^3.

5. FIRE RESISTANCE TESTS

The propagation of the fire takes place at the openings. Thus, especially the details of the ledgers must be designed and constructed very carefully.

At the cases discussed, the elements of “L”-shape were provided with a glass-fibre reinforcement at the reveals and in a thickness of min. 20 mm.

For the fire resistance tests C 35 grade PPFRC, 1000×1000 mm size, 30 and 60 mm thick plates have been prepared. They were supplied by 200×200 mm mesh size ø 6 mm, respectively ø 8 mm reinforcing bars. The tests have been carried out in 60 days maturity of the specimens. The fire was simulated by a gas burner at a temperature of approx. 800 °C, and that of the concrete never raised above 500 °C. Both the temperature of the PPFRC (Fig. 3) and the deformation of the plates were measured at the beginning of the tests and at the end of them. The crack pattern was recorded, as well.

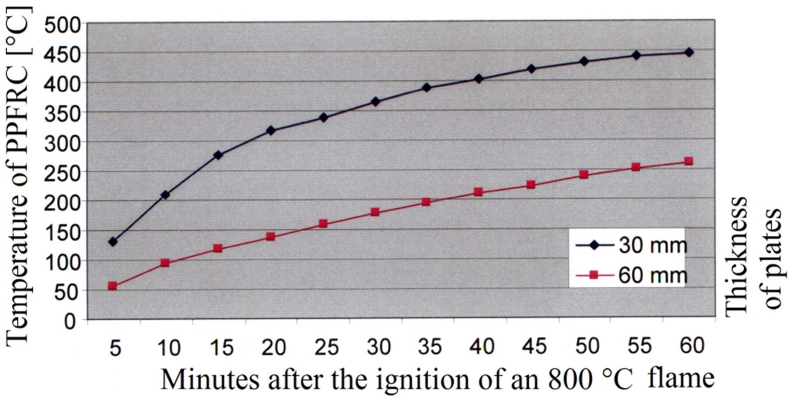

Fig. 3 Temperature chart of the PPFRC plate 800°C flame

The limited volume of this paper doesn’t allow to show more details. However, it may be concluded that PPFRC is very suitable for the covering of façades and it can serve fire resistance. surveyed in current literature *(Balázs, Lublóy, 2010).*

6. CONCLUSION

The examples shown confirm that PPFRC is suitable for the expectations raised by up-to-date requirements for façades. According to the experience, the PPFRC plates and cornices can be made easily, quickly and economically. The installation of the prefabricated PPFRC panels can take place in the final stage of construction, and these elements, based on the prime quality of prefabrication, may correspond with the highest architectural, physical, structural and fire resistance requirements.

7. REFERENCES

Balázs, L. G., Lublóy, É. (2010), „Survey of possibilities of fire effect design of reinforcedconcrete structures (In Hungarian), *Vasbetonépítés*, pp: 15-22.

Fehérvári, S. (2008): “Characteristics of tunnel fires”, *Concrete Structures*, pp. 56-60.

Kozák, J., Magyari, B., Tassi, G. (2008): „Fibre reinforced concrete elements for urban building façades”, *Proceedings, Central European Congress on Concrete Engineering,* Opatija, pp. 69-74.

Lublóy, É., Balázs, L. G., (2009), „Behaviour of reinforced concrete structures under high temperature” (In Hungarian), *Vasbetonépítés*, pp. 113-118,

Magyari, B., Tassi, G. (2007): „Effect of non-metallic fibres on the concrete properties”. *Proceedings of the fib Symposium, Dubrovnik*, pp. 367-374.

CONSTRUCTION OF THE BRIDGE 209 IN NYITRA

János Barta[1], *László Takács*[2]
[1] *M-HÍD C. LTd.*
H-1138 Budapest, Karikás Frigyes u. 20.
[2] *A-HÍD C. LTd.*
H-1138 Budapest, Karikás Frigyes u. 20.

SUMMARY

The R1 motorway, which at the moment ends at the city of Nyitra, branches off near Nagyszombat (Trnava) from the D1 highway which will connect Pozsony (Bratislava) and Kassa (Kosice) in the future. The next section of R1 towards Besztercebánya (Banska Bystrica) – including the section passing by the city of Nyitra from south – is under construction as a PPP project. A-Híd C. Ltd. is taking part in this work as the contractor for the largest, almost 1.2 km long structure, i.e. bridge No. 209.

1. INTRODUCTION

One of the most significant works to be performed by A-HÍD C. Ltd. in 2010-11, which is simultaneously its first real challenging work ordered from abroad, is bridge No. 209 in Nyitra. The first steps were taken as early as in December 2008 when Granvia Construction s.r.o. approached Hídépítő ZRt in connection with the construction of a substantial bridge. Hídépítő owed the invitation to its past history and considerable references well-known in the Czech Republic and Slovakia as well. The negotiations, which needed to clarify numerous technical and financial issues, began soon. As a result of these negotiations, which became successful in August 2009, an agreement was reached on the construction of the bridge in a value of EUR 30 million followed by the conclusion of the contract in early 2010.

2. THE PROJECT

The 4 separate sections of R1 motorway being under construction are implemented as a single PPP project in cooperation of the Government of Slovakia and Granvia Construction. The operating period of the PPP project is 30 years, i.e. the State has to pay operating charges to Granvia and the contractor undertakes a guarantee for the construction works for that period. The length of the 4 sections is 52 km, including 84 bridges in a total length of 6843 m, of which A-HÍD constructs 1166 m. The deadline for completion is 28 September 2011.

3. DESIGN

The substructures and the prestressed R/C superstructures of bridge No. 209 were designed by Dopravoprojekt while the temporary structures (necessitated by the special technologies) by the Technical Department of M-HÍD ZRt. The designers of Dopravoprojekt described the details of the bridge structure in a separate presentation, so such details are not specified herein.

4. THE TECHNOLOGIES

The complete bridge is divided into two separate dilatation units lengthwise (DC1 and DC2).

The 806 m long DC1 section (Fig. 1) was constructed by incremental launching. The segments were manufactured in the constructing deck behind abutment No. 1. They were fastened to the previously completed bridge section by prestressing and then pushed from the constructing deck onto the earlier completed piers. Important part of this construction technology is the launching nose, which serves for reducing the exceptional big stresses in the RC cantilever structure which arise when the structure has left the previous pier, but still has not reached the next one. As a result, the spans with maximum 45 m length could be bridged.

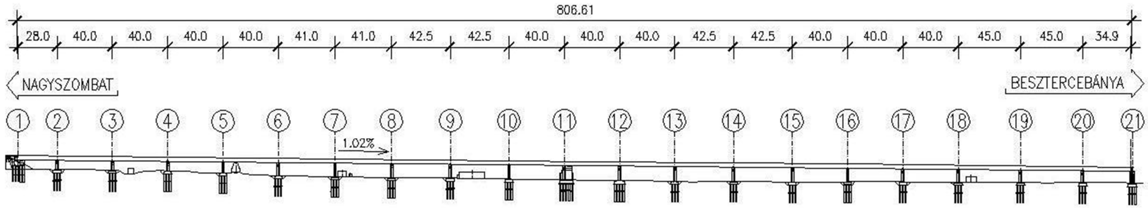

Fig. 1 Side view of the first dilatation unit of bridge No. 209 in Nyitra

The superstructure of the second, 360 m long dilatation unit DC2 (Fig. 2) was built by on-site concreting balanced cantilever method, started from the middle piers. The 4.75 and 5 m long segments were manufactured in one phase in form travellers supported on the ready superstructure. For the sake of the balance of the scales, the cantilever fabrication was going on simultaneously at both sides of the piers. The prestressing of the bridge took place in two phases. Immediately after the cantilever segments had been manufactured, they were stressed together using internal prestressing cables, and after the 3 m long closing segments connecting the arms of the bridge had been concreted and had hardened, the entire bridge was prestressed by external cables which were placed in the inside of the box.

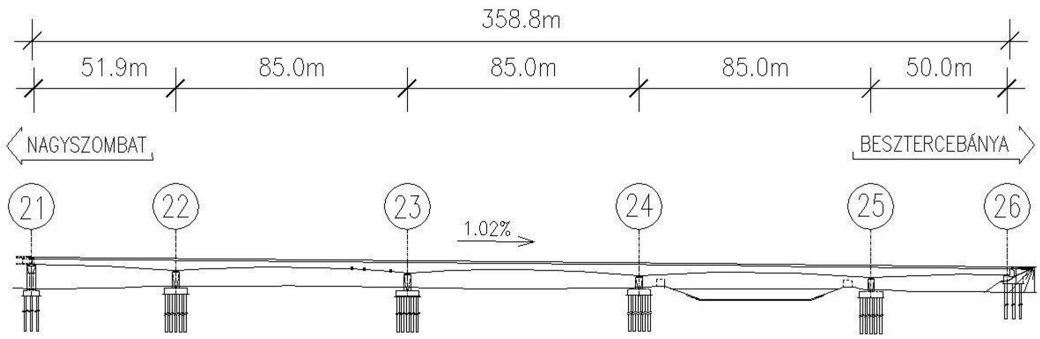

Fig. 2 Side view of the second dilatation unit of bridge No. 209 in Nyitra

5. CONSTRUCTING PROCESS

The worksite was handed over for starting construction works finally on 26 December 2009 instead of original planned September, later October, due to a protracted relocation of a 110kV electric aerial cable at the location of the bridge. Works could be started with the construction of the bored piles of the deep foundation in January 2010. In the subsoil, the quality of which varied but was nevertheless mostly inadequate for the purposes of foundation works, several boring methods needed to be used (Soil-Mec, CFA). Construction of the waterside supports necessitated making of an artificial peninsula supported by Larssen sheet piles. At DC1 works started with the constructing decks. The core of the two structures independent of each other was the movable RC grid and the droppable bottom, loaded on the R/C grating supported by piles and connected with the pilecap of abutment No. 1. The formwork of the constructing deck, supplied by PERI, was built on the RC grid (Fig. 3). The launching equipment (i.e. a classic lifting-pushing jack), due to move the bridge structure in its place, was placed on the abutment. Due to the substantial length of the bridge, two of these equipments needed to be used “from half way on”, so a temporary R/C structure, a launching-support, capable of taking up large horizontal loads, needed also to be built near pier 11. The moving superstructure only passed by the other substructures. To facilitate this, temporary launching structures – slides and lateral guides – were placed on the top of the pierheads.

Fig. 3 Constructing deck of DC1 with the launching nose ready for starting

One of the great advantages of this technology was seen when the superstructure passed above the crossed railway line and main road: the construction works of the bridge structure caused no disturbance in the traffic beneath at all (Fig. 4).

Fig. 4 Pushing of the DC1 bridge section above Érsekújvári (Nove Zamky) road

In line with the superstructure, the DC2 substructures are squatter and form a single structure but their design is in harmony with the slimmer piers of DC1. The first element of the superstructure, i.e. the 12.5 m long starting segment was built upon a steel platform mounted on two “blade” walls and on the pier body itself. From this point on, these blade walls were serving also to stabilize the bridge arms being built.

Construction of the superstructure was started above the two waterside piers at the same time. The formwork wagons were supplied by DOKA, compiled mostly from module units. Their structure consisted of four diamond shaped deck units (one above each web of the superstructure), of which the two outer ones travelled on longitudinal rails (Fig. 5).

Fig. 5 Formwork wagon of the DC2 bridge section

Using these wagons each 5 m long segment pair (7 pairs per arm) was constructed during 8 or 9 days (the segments are concreted in one phase). The last segment at the end of the bridge was constructed on scaffolds suspended at the free end of the bridge arm and on the abutment. The middle closing segments were built by the formwork wagon (Fig. 6) and the segment at the other end of DC2 was constructed on a classic heavy scaffold before the common pier.

Fig. 6 Connection of the two arms of the DC2 bridge section above the river

After the R/C structures have been completed, the works will be finished by the insulation of the deck with 2 layers of bituminous sheet covered by a 9 cm thick asphalt layer. The final form of the bridge is given by two inspection sidewalks at the two outer sides of the bridge provided with noise protection walls, and H3 safety protecting railing, while in the middle a H2 rail is installed on the bridge. After the load tests have been carried out to demonstrate the behaviour of the bridge structures being in compliance with the statical calculations, the bridge will be opened for traffic temporarily and then, after a 6-month test operation period, the technical hand-over process will be closed and the project will be finally completed.

6. CONCLUSIONS

As usually, Hídépítő ZRt (A-HÍD Építő ZRt) attempted a difficult task again constructing a more than 1 km long motorway bridge using two completely different technologies, moreover, outside the present borders of Hungary. Due to the above fact, it has to tackle not only the usual (engineering, technological) difficulties but also other difficulties arising from different labour, official and other conditions. We believe it will result in full success and we will be able to hand over the bridge to our Client in due date and in excellent quality.

REHABILITATION OF THE MUNICIPAL EMERGENCY HOSPITAL "DR. CONSTANTIN OPRIŞ" FROM BAIA MARE

Gelu Mugurel Zaharia[1], Radu Mircea Zoica[1]
Department of Civil & Materials Engineering and Earth Science
North University of Baia Mare
Romania, Maramures, 430092 – Baia Mare, 62/Ath Dr. V.Babes Street

SUMMARY

The building was designed and finalized in the 1970s, having the maximum height B+GF+12F, total area at basement level being of almost 7400 m^2. The standards, which were strictly obeyed in the design and execution phases, are nowadays outdated and also the building almost reached its designed life. The city hall decided to rehabilitate this symbol of the town in order to make it secure for the generations to come. In order to make the rehabilitation possible we first made an assessment in order to know the visible faults, and then made the GEO and nondestructive element studies that we had to do in order to have a clear overview of the structure and its faults.

We will present in the technical paper here, two comparative solutions for the rehabilitation, both of them being solved respecting the Eurocode standards. The first one presented is the reinforcing of the existent structure, beams and columns, and the second one is a carefully chosen set of concrete reinforced walls mounted through the building in several critical and important sections. Both of the solutions were analyzed taking into account the structural requirements for this type of building and from the cost point of view, also.

1. OVERVIEW OF THE STRUCTURE

The building was designed and finalized in the 1970s, having the maximum height B+GF+12F, total area at basement level being of almost 7400 m^2. The building is divided in 14 bodies with the following heights A with B+GF+2F, B with B+GF+2F, C with B+GF+2F, D with B+GF+2F, E with B+GF+2F, F with B+GF+11F, G with B+GF+11F, H with B+GF+12F, I with B+GF, K with B+GF, M with B+GF+11F, N with B+GF+11F and another two bodies with B+GF height regime.

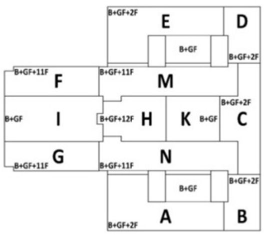

Fig. 3 Height regime

Due to the important changes in the standards area the city hall decided that the building has to be rehabilitated. Also the hospital has almost reached its designed life from the moment it has been finalized, meaning the 70's. In order to have a better overview of the problems and solutions for the rehabilitation an assessment has been made and a structural modeling using both computational and handwritten methods. The models studied with FEM were compared to Eurocode restrictions and also the results from the handwritten methods were subject to the same restrictions.

2. REHABILITATION PROPOSALS

Rehabilitation described in V1 model is the reinforced concrete covering of the columns measuring 20 cm, and for the girders the consolidation is made from 3 to 3 axis on the transversal direction with the same depth and on the longitudinal direction the model is rehabilitated with one meter high concrete walls on the façade beams, making thus the columns short columns.The rehabilitation solution

V2 with concrete reinforced walls in 11 transversal frames, concrete reinforced walls that reach from the underground level throughout the top level with variable width, from 35 in the basement to 30, 25, 20 cm to the top. Likewise, on the longitudinal direction 7 frames are to be rehabilitated in the same manner as described above.

The analysis consisted in calculating the seismic forces for each level and their distribution over the rehabilitated levels, as well as determining the structural rigidity in the two model of consolidation. The seismic force in the second model (V2) is greater, F_{bx}=397 tons, F_{by}=416 tons compared to values of the V1 model, i.e. F_{bx}=241 tons, F_{by}=157 tons. 60 % of the seismic forces in the first model (V1) are supported by the rehabilitated frames, respectively 85% in the second model (V2), in this case the columns are supporting only gravitational forces, the rehabilitation being therefore unnecessary due to the fact that the bending moments on the two directions are more reduced than the ones that these elements have been initially dimensioned.

The comparative results for both the methods studied are presented in the table below comparing the values θ_{max} for both of the cases and the existent situation:

A parallel in these two rehabilitated models can be reduced to the study of the relative and total level displacements. The seismic sensitivity is the factor that explains the best the structural solutions through habilitation, provided that the existent structure has values over the limit, $\theta > 0.3$, in the situation that the frames are covered with a layer of reinforced concrete (V1) the values drops to 0.13 which means that the bending moments are increased in order to take into consideration the 2nd order effects. In the V2 model, with reinforced concrete walls, θ does not exceed 0.05, meaning that the structure is more rigid.

3. CONCLUSIONS

The analysis of the structural rehabilitation methods generated two valid solutions and, in parallel, through a technical-economic analysis have been worked out both the values of the basic necessary materials and the value of the execution costs and the needed execution time. As regards the rehabilitation costs of the two solutions there are no significant differences. Both variants include a volume of circa 1500 m^3 of concrete in consolidations, 190 tons reinforced steel and 7300 sqm of formworks. There are differences only in the necessary execution time and in the localization of intervention works within the structure of model V2 which is more reduced. The beneficiary is to make the decision as concerns the final solution by also taking into account the heckling in the necessary workflow of the hospital generated by the rehabilitation process.

Tab.1. Θ_{max}

	Existent	V1	V2		Existent	V1	V2
Levels	Θ_{max}	Θ_{max}	Θ_{max}	Levels	Θ_{max}	Θ_{max}	Θ_{max}
Level 13. (SLS)	0.006	0.006	0.011	Level 6. (SLS)	0.033	0.008	0.023
(ULS)	0.022	0.021	0.023	(ULS)	0.124	0.031	0.047
(SLS)	0.002	0.028	0.011	(SLS)	0.067	0.033	0.021
(ULS)	0.007	0.105	0.022	(ULS)	0.251	0.124	0.042
Level 12. (SLS)	0.011	0.011	0.015	Level 5. (SLS)	0.037	0.008	0.020
(ULS)	0.042	0.042	0.030	(ULS)	0.140	0.032	0.040
(SLS)	0.003	0.035	0.013	(SLS)	0.063	0.034	0.020
(ULS)	0.011	0.132	0.026	(ULS)	0.237	0.129	0.040
Level 11. (SLS)	0.017	0.017	0.018	Level 4. (SLS)	0.043	0.010	0.013
(ULS)	0.062	0.063	0.036	(ULS)	0.16	0.039	0.026
(SLS)	0.035	0.035	0.015	(SLS)	0.075	0.034	0.018
(ULS)	0.132	0.132	0.030	(ULS)	0.280	0.129	0.036
Level 10. (SLS)	0.018	0.004	0.020	Level l 3. (SLS)	0.048	0.011	0.011
(ULS)	0.067	0.015	0.041	(ULS)	0.178	0.042	0.021
(SLS)	0.048	0.025	0.017	(SLS)	0.078	0.034	0.016
(ULS)	0.182	0.094	0.034	(ULS)	0.292	0.128	0.031
Level 9. (SLS)	0.023	0.005	0.022	Level l 2. (SLS)	0.112	0.024	0.006
(ULS)	0.085	0.020	0.045	(ULS)	0.420	0.091	0.013
(SLS)	0.066	0.026	0.019	(SLS)	0.081	0.034	0.012
(ULS)	0.249	0.099	0.038	(ULS)	0.305	0.127	0.023
Level 8. (SLS)	0.027	0.006	0.024	Level 1. (SLS)	0.101	0.022	0.002
(ULS)	0.100	0.023	0.047	(ULS)	0.377	0.081	0.004
(SLS)	0.071	0.026	0.020	(SLS)	0.047	0.019	0.001
(ULS)	0.264	0.097	0.041	(ULS)	0.176	0.070	0.003
Level 7. (SLS)	0.028	0.007	0.024	Groundlevel (SLS)	—	—	—
(ULS)	0.107	0.026	0.048	(ULS)	—	—	—
(SLS)	0.053	0.029	0.021	(SLS)	—	—	—
(ULS)	0.199	0.107	0.042	(ULS)	—	—	—

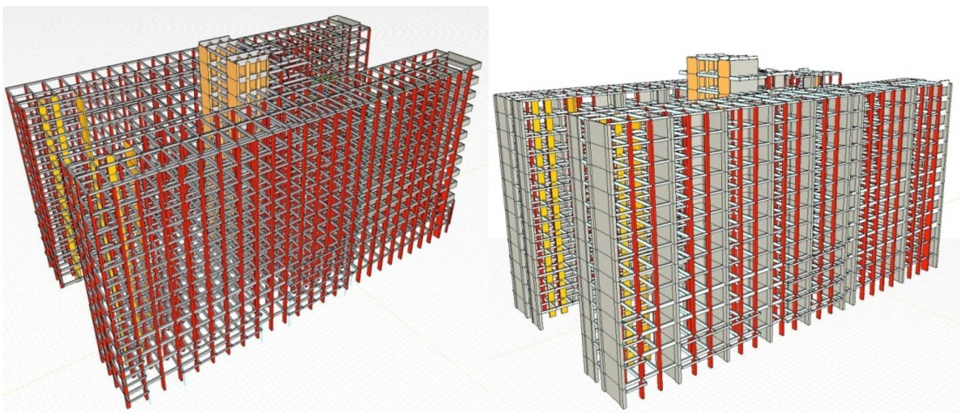

Fig. 2 Frame consolidation (V1) vs. concrete walls consolidation (V2)

4. REFERENCES

SREN 1992-1 (Eurocode 2)

SREN 1998-1 (Eurocode 8)

ME 003-1999 – Manual privind investigarea de urgenţă postseism şi stabilirea soluţiilor cadru de intervenţie imediată pentru punerea în siguranţă provizorie a construcţiilor avariate. Elaborat: IPCT.

GE 032-1997 – Normativ privind executarea lucrărilor de întreţinere şi reparaţii la clădiri şi construcţii speciale. Elaborator: INCERC

GV 001/0-1995 – Metodologia pentru evaluarea clădirilor şi construcţiilor speciale din grupele 1 şi 2

Fintel. M.. 1991. Shear walls – an answer for seismic resistance. Concrete International. July : pp.48-53

Hayashi. T.. Niwa. H.. Fukuhara. M.. 1980. The strengthening methods of the existing reinforced concrete buildings. Proceedings 7 WCEE. Istanbul. 7 : 89-96

Kahn. L.P.. Hanson. R.D. 1979. Infilled walls for earthquake strengthening. Journal of the Structural Division. 105 (2) : pp.283-297

Petrovici. R. 1995. Consolidarea structurilor în cadre prin introducerea panourilor de forfecare din beton armat monolit. Revista AICPS. : pp.27-39

TOPIC 5

MODELLING, DESIGN AND TESTING

NONLINEAR FINITE-ELEMENT-SIMULATION OF ULTIMATE SHEAR LOAD TESTS OF OLD POST-TENSIONED BRIDGE GIRDERS

Markus Vill[1], Anton Schweighofer[2] and Johann Kollegger[2]

[1] *ÖBB-Infrastructure, Bridge Department, 1020 Vienna, Austria, Praterstern 3*
[2] *Vienna University of Technology, Institute for Structural Engineering 1040 Vienna, Austria, Karlsplatz 13*

SUMMARY

At the beginning of the 1950s, the use of prestressed concrete for bridge structures rapidly increased. Many of these structures, which are still in use, have already reached their maximum service life. Therefore, the question arises whether sufficient load-carrying-capacity and serviceability (according to the state of the art) can still be ensured or not. In the course of the destruction of an underground railway station (Fig. 1) and a street bridge (Fig. 6), the ÖBB Bridge Department and the Institute for Structural Engineering at the Vienna University of Technology were given the opportunity to carry out tests concerning the shear load carrying capacity on six bridge girders, which were built between 1950 and 1960.The paper includes a short description of the bridge structures, a summary of the results and the results of non-linar finite- element simulations.

1. STRUCTURE 1: GIRDERS SÜDTIROLER PLATZ

The structure was designed with single-span girders and a supporting distance of 17.5 m. The girders (T-beams) were removed during the demolition work of the railway station. All T-beams had the original length of 17.5 m, a plate width of 3.3 m and a height of 1.15 m - 1.40 m. The slab was prestressed in the transverse direction at a distance of 75 cm with tendons St 75/105 Rg Ø 26 mm, the webs contained with 14 tendons St 75/105 Rg Ø 26 mm along the bridge axis.

In the center part of the girders transverse reinforcement (stirrups in web of T-beam) consisted of Ø 10 mm with a distance of 25 cm and close to the supports bars Ø 12 mm with a distance of 25 cm were placed (Fig. 1). A recalculation of the structure according to the current standard showed that the design load (dead and life load) is approximately 40% higher than the shear resistance according to EC 2 (*EN 1992-1-1, 2009).*

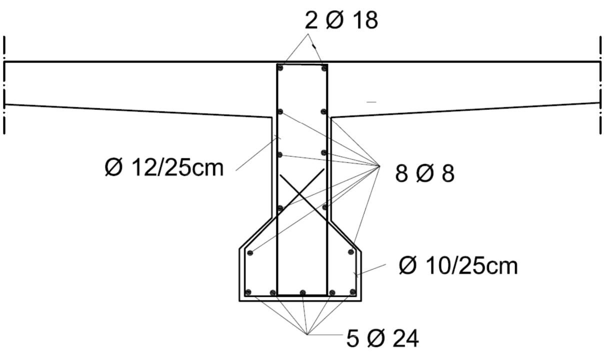

Fig. 1 left: Removing of the girders, right: Cross section and reinforcement near supports

Furthermore, to obtain information about the durability of the structure, the properties of the materials used – concrete, reinforcing steel, pre-stressing reinforcements– were analysed by testing samples of bridge material in the laboratory.

1.1 Test Setup “Load Tests”

In the load tests the bridge girders were supported on two wood bearings at intervals of 15 meters. On each side of the girders a bearing block with a height of 1.05 meters was concreted. Two steel girders were placed on these bearing blocks. The bridge and the steel girders were tensioned together with four traverses and 16 post-tensioned threaded bars with a diameter of 32mm, and thus a closed system without additional foundations was created. The schematic test setup is shown in Figure 2.

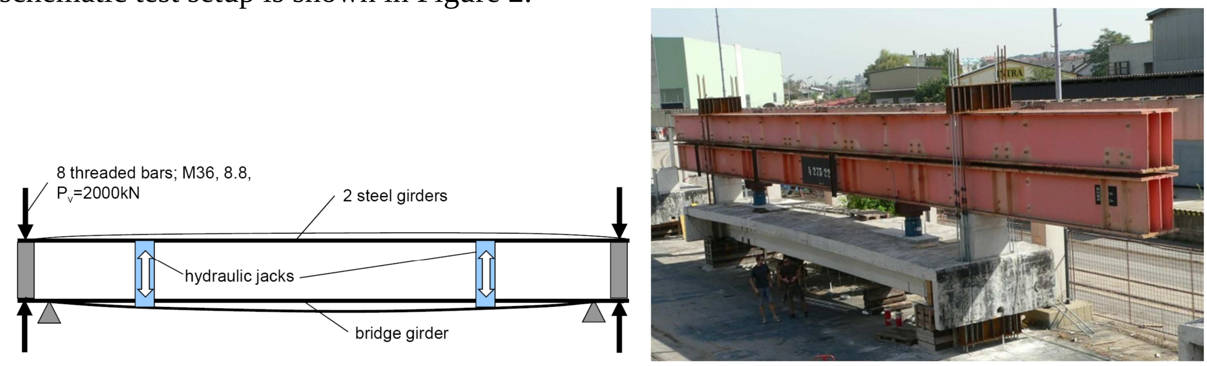

Fig. 2 Test setup

The bridge structure was subjected to a four point bending by applying two loads by hydraulic jacks, which were gradually increasing to maximum load. Three tests were carried out where the load distances were varied from 2.75 m up to 3.5 m distance to the bearings.

1.2 Nonlinear finite-element simulation

The calculations were made with the program ATENA (*ATENA, 2007*).

Concrete

For the concrete, the already implemented sBeta material model (*ATENA, 2007*) was used (Fig. 3). Drill bits were taken and tested for the calculation of the cube compressive strength. The result was a cube compressive strength of f_c=70 N/mm². The tensile strength f_t was calculated by the determined pretensioning force and the load during the onset of cracking and averaged about 2,7 N/mm². The elastic module was 38.000 N/mm². The type of tension softening model was exponential (see Fig. 3). The specific fracture energy G_f was calculated with 102N/mm. The compressive strain at the compressive strength in uniaxial compressive test ε_c amounted to 0,289%. The reduction of the compressive strength due to cracks was 0.8.

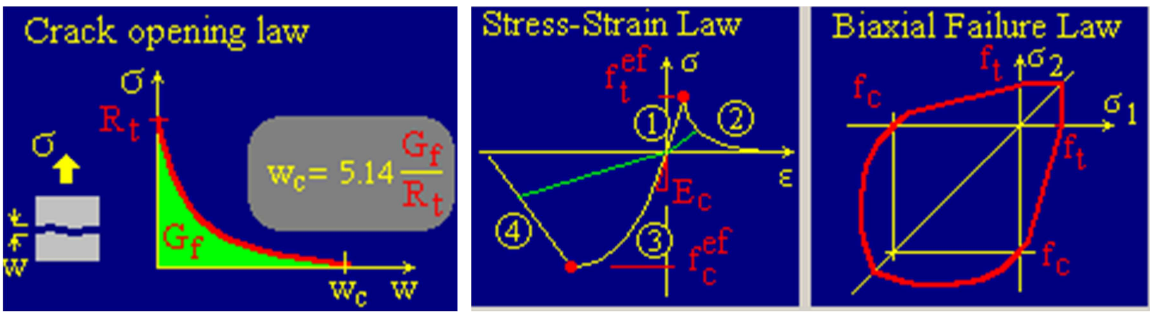

Fig. 3 Type of tension softening model (Picture by ATENA)

Prestressing steel

The 0.2% yield strenght was 780 N/mm² and the elastic modulus was 210000 N/mm². The material property of the prestressing steel was modeled with the stress – strain diagram. The tensile strength had a value of 1040 N/mm².

Reinforcement steel

For the modeling of the material behavior of the reinforcement steel a bilinear material model with hardening was used. A yield strength of f_y=450N/mm² and a elastic modulus of E_s=209500 N/mm² was chosen. The input of the reinforcement was made with individual bars and not with the option of a smeared reinforcement.

1.3 Results of the field tests and comparison with calculations

Fig. 5 shows the load – deflection – diagram of load test 3 and of the ATENA simulation. The ATENA simulation and the field tests correspond very well. The field tests as well as the numerical simulations show a bending failure and no shear failure.

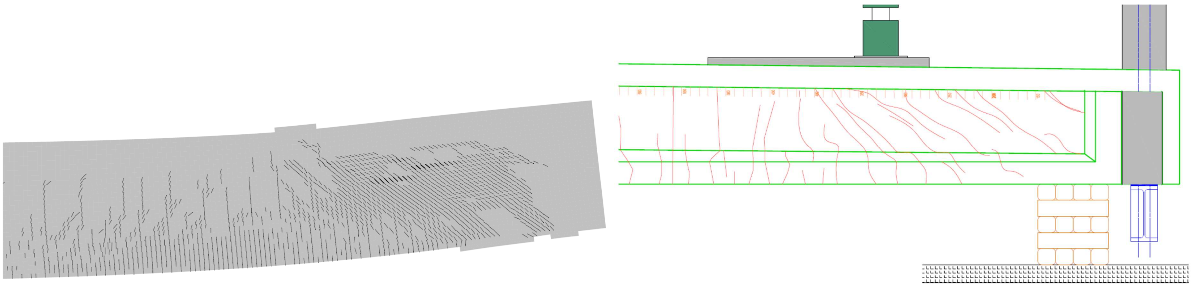

Fig. 4 left: crack pattern by ATENA; right: load test

Although the yield stress in the transverse reinforcement was achieved, the girder did not fail in shear due to the dowel effects of the prestressing steel and the shear transfer in the concrete. That agreed with the measured strain in the transverse reinforcement. The failure occurred when the yield stress of the longitudinal bars and the tendons was reached.

During the load tests maximum loads of two times 2.64 MN were measured before failure occurred. The load tests showed big deflections of 120 mm in the middle of the span, significant cracks widths of 4 mm, and a ductile behaviour of the T-beams.

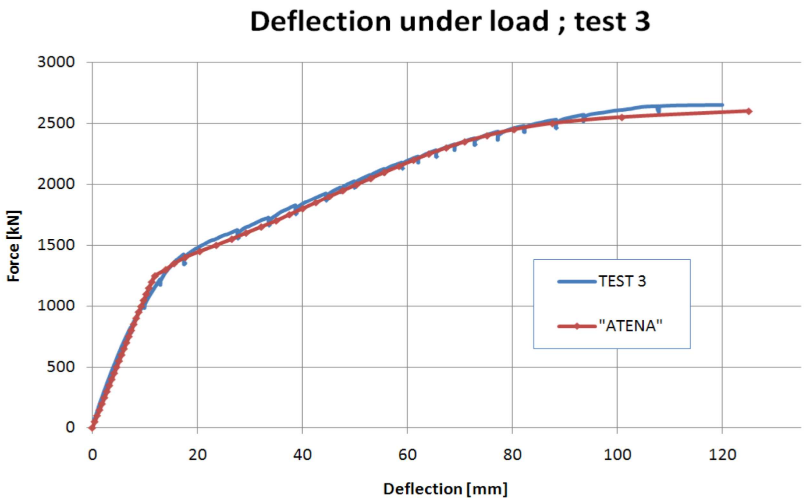

Fig. 5 Load-deflection diagram

Tab. 1 Relation of results

STANDARD	DESCRIPTION		[kN]	γ[-]
ÖN B4002	Shear force – Load model bridge class 1 – SLS	V_k	950	~1,0
ÖN B4002	Shear force – Load model bridge class 1 – ULS	V_{Ed}	1.332	~1,4
EC2	Shear resistance of transverse reinforcement	$V_{Rd,s}$	863	~0,9
EC2	Shear resistance of the concrete	$V_{Rd,max}$	2.300	~2,4
TEST	Shear force from load test 3	V_{test-3}	2.640	~2,8
ATENA	Shear force from ATENA "TEST 3"	V_{ATENA}	2.580	~2,7

Tab. 1 shows a comparison of the calculated loads to the measured loads. During the tests maximum loads of 2.64 MN were measured wheras the calculated resistance of the shear reinforcement according to Eurocode 2 is only 0,863 MN (*Hengl 2009*). Therefore, a global safety factor of 2,8 for this test was calculated.

2. STRUCTURE 2: PRESTRESSED STREET BRIDGE

In the course of the destruction of a bridge, which was built in the year 1952, the Institute for Structural Engineering at Vienna University of Technology got the possibility to carry out tests concerning the shear load carrying capacity. The bridge construction was designed as a continuous beam spanned over two fields with a respective supporting distance of 31.30 m. Within this research project, a test setup was developed, allowing getting information about the shear load carrying behavior of two separated tee beams. The beams were removed during the demolition work of the bridge. Both beams had a length of 14 m, a plate width of 1.05 m and a height of 1.57 m.

Fig. 6 left: bridge over river, right: removing

During the load test 2 a maximum load of 4.197 kN had been measured before failure occurred. The load tests showed big deflections, significant crack widths and a ductile behavior of the of tee beams. Details are shown in (*Vill, 2011*). The publication contains a detailed description of the bridge structure, the results of the load tests, a comparison of the calculated shear load capacity with the measured loads and the results of a nonlinear finite element calculation of the tests.

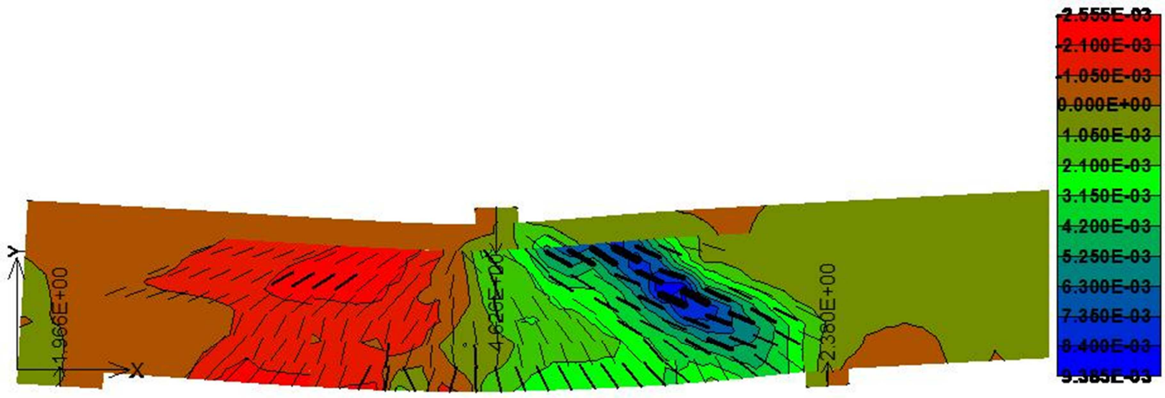

Fig. 7 Load step 226 at maximum load, strain γxy [-]

Fig. 7 shows the calculated strains $\gamma_{x\text{-}y}$ of load step 226 at maximum load when failure occured. Furthermore, the crack pattern in the web is shown in Figure 7 with maximum crack widhts of aprox. 3 mm which are similar to the measured crack widhts.

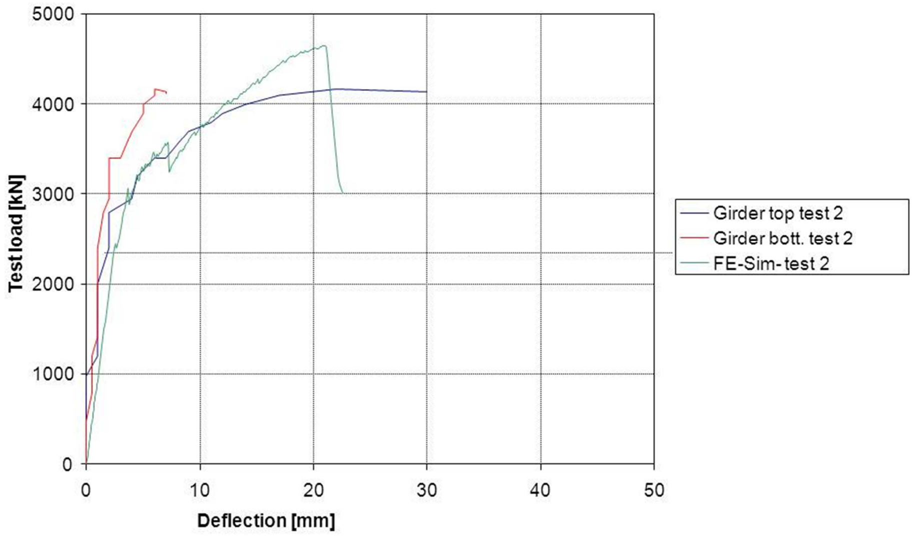

Fig. 8 Load-deflection diagram

A comparision of the measured and calculated load-displacement graphs are shown in Figure 8 which shows good accordance. A maximum load of 4.197 kN was measured, which results in a maximum shear force on the right part of the girder of aprox. 2.398 kN. The resistance V_{Rms}, calulated as resistance of the stirrup reinforcement (ϕ 10/25) according to EC2 is 502 kN, the vertical component of the calculated remaining prestressing force is 257 kN. Finally the test shows a ductile failure behavior with big crack widths and large deformations. The calculated load carrying capacity according to EC2 has a big coefficient of safety.

3. CONCLUSION

The numerical simulations with ATENA are in accordance with the load tests. During the load tests of structure 1 (Südtiroler Platz) a maximum load of two times 2.64 MN was measured before failure occurred. In the ATENA simulation the maximum load averages to 2.55 MN.

The load tests of structure 2 (Salzachbrücke) also showed good correlation with the results of the numerical simulation. The maximum load calculated by ATENA was 4,62 MN which was aprox. 10% more than the measured load. The reason for this difference can be illustrated by bond failure of longitudinal tendons which were cut thru on the end of the test girders.

The load tests as well as the simulation showed big deflections, significant crack widths and a ductile behavior of the T-beams. Finally, additional load bearing mechanism beside the part of the shear reinforcement like tensile strength of the concrete or dowel effects of the prestressing steel must be accountable for the high maximum loads measured during the tests.

The results of the test-series are an important basis for a goal-oriented maintenance planning for the ÖBB bridge stock, which includes many similar structures. Furthermore, similar structures, which are currently in use, showing good maintenance conditions must not be replaced due to calculated insufficient shear load resistance.

5. ACKNOWLEDGEMENTS

We thank ÖBB Infastruktur AG for providing funds for the accomplishment of these tests. Also we thank Ing. Dr. Radomir Pukl, from Cervenka Consulting, for the excellent support.

6. REFERENCES

ÖNORM EN 1992-1-1:2009: Bemessung und Konstruktion von Stahlbeton- und Spannbetontragwerken, Österreichisches Normungsinstitut, Wien, 2009.

ATENA. 2007. ATENA Program Documentation. Cervenka Consulting, Praha 2007.

Maurer, R. und Bäätjer,G. 2006, Entwicklung von Konstruktions- und Bemessungsgrundsätze in Deutschland im Hinblick auf die Tragsicherheit von Spannbetonbrücken, München Massivbau Seminar 2006.

Vill, M. Brunner, H., Torghele, H. and Kollegger, J. 2007, Schubversuche an ausgebauten Trägern einer Straßenbrücke aus Spannbeton, Heft 65, Schriftenreihe der österreichischen Vereinigung für Beton- und Bautechnik, Wien, 2007.

Hengl, H. 2009. Großversuche an Spannbetonträgern, Master’s thesis, TU - Wien.

Vill, M. Brunner, H., Torghele, H. and Kollegger, J. 2011, Zerstörende Belastungsversuche zur Untersuchung des Schubtragverhaltens von vorgespannten Trägern einer Straßenbrücke, Beton-und Stahlbetonbau, 106, 4, 241-249, WILEY-VCH Verlag.

ON FATIGUE RESISTANCE OF PAVEMENT CONCRETE SLABS

Ludvík Vébr[1], Petr Pánek[1], Bohuslav Novotný[2]
[1] *Department of Road Structures, Faculty of Civil Engineering*
Czech Technical University in Prague
Thákurova 7, 166 29 Prague 6
[2] *Expert Society for Science, Research and Counselling*
Czech Society of Civil Engineers
Komornická 15, 160 00 Prague 6

SUMMARY

The paper summarizes results of pilot testing of seven concrete slabs resting on granular base in testing box. The experimental project was intended to verify recent findings that fatigue resistance of concrete slabs is much higher than that predicted using concrete flexural characteristics derived from concrete beam testing. Results obtained confirm enhanced fatigue resistance of concrete slabs with (possible) far reaching consequences for concrete pavement design.

1. INTRODUCTION

The attention in this paper is focussed on fatigue cracking in concrete pavements that represents a key failure mechanism of the complex process of pavement exploitation (in-service pavements are subject to fluctuating stress range conditions due to changing temperature and moisture gradients and varying traffic loads). In order to develop a design procedure for jointed plain concrete pavements, Darter and Barenberg *(1977)* compiled fatigue beam results available at that time into equation

$$\log N_{lim} = 17.61 \times \left(1 - \frac{\sigma}{f_{fl,beam}} \right), \tag{1}$$

where N_{lim} is number of load application until failure, σ is applied maximum stress level, and $f_{fl,beam}$ is flexural strength (modulus of rupture) of the concrete. This beam fatigue equation predicts the allowable number of load applications with a 50 percent probability of failure.

Roesler et al *(2005)* conducted large scale slab fatigue testing to confirm previous research findings that concrete slabs exhibited a greater fatigue resistance than predicted by concrete beam fatigue curves. The main reason for this discrepancy was the inaccuracy in characterizing the slab's static strength using a beam flexural strength test. Their testing program resulted in finding that slab's flexural strength was approximately 2.8 times higher than the beam flexural strength, so that with fatigue equation for concrete slab rewritten as

$$\log N_{lim} = 17.61 \times \left(1 - \frac{\sigma}{\kappa \, f_{fl,beam}} \right), \tag{2}$$

the "slab fatigue resistance enhancement" factor κ equals 2.8. The aim of our present research was to prepare and conduct test program that would verify this information on concrete slab enhanced fatigue resistance.

2. TESTING PROGRAM

In order to explore the effect of enhanced fatigue resistance of concrete pavements, a total of eight slabs were cast for testing program. The slabs plan was 1.1m by 1.4m, seven slabs (reported here) were 10cm thick, the eight slab (to be tested) is 8cm thick. Slabs were cast in wooden forms and after curing they were placed on top of sand/gravel mix subgrade contained in a laboratory box (so that subgrade modulus $E_s \approx 60$ MPa). Slabs were instrumented with imbedded strain gauges to record strains induced by load and with linear variable differential transducers to monitor slab movements (deflections) during testing.

The load was transmitted to the slab instantaneously by hydraulic actuator over circular area having radius 5cm. The central transverse edge load position was chosen for first five slabs (Fig. 1), while the loading system position was changed to the central longitudinal edge position for slabs six and seven. For various technical reasons, the accelerated version of fatigue tests had to be conducted, frequency of cyclic loading (formed by single load pulse) ranging between 4.5 Hz and 7.2 Hz.

Fig. 1 Concrete slab in testing box, loading system.

The composition of the slab concrete: cement 390 kg/m^3, water 190 kg/m^3, aggregate 1785 kg/m^3 (fine aggregate 0-4: 830 kg/m^3, coarse aggregate 8-16: 955 kg/m^3), resulted in following mechanical properties (flexural strength being assessed by the thumb rule as 0.10 – 0.15 f_c):

strength in compression:	$f_c \approx 60$ MPa,
mass density:	$\rho_c \approx 2350$ kg/m^3 ,
flexural strength:	$f_{fl,beam} \approx 6$ MPa.

Process of slab testing preparation and evaluation was supported by the FEM analysis of the contact of concrete slab and elastic halfspace. The slab is analyzed (in the scope of the Kirchhoff plate theory) by the FEM procedure using triangular division of the slab plan – in each node deflection and its first two derivatives in both coordinate directions are to be determined. The contact of slab with supporting system is materialized through contact stresses that are linearly varying within limits of triangular FEM elements. Using standard values of pavement concrete characteristics according to Czech design specifications TP170 (*2004*), the FEM computation arrived at maximum load resultant value Q_{max}= 8.5 kN (Q_{min}= 0.5 kN) as the value at which the slab fatigue failure is to be expected after $N_{lim} \approx 10^5$ load repetition. This value was then chosen as starting value for cyclic loading of the first slab.

3. TEST RESULTS

The results of fatigue testing of first five slabs are summarized in Tab. 1. Presented are total load resultants Q_{max} ($Q_{min} \approx 0.5$ kN), load induced stresses σ^*, frequencies of the cycling loadings, numbers N^* of applied load repetitions and κ^* as fatigue resistance enhancement factors determined from equation (2) by substituting $N_{lim} = N^*$, $\sigma = \sigma^*$. The value $\kappa^* = 2.66$ for the fifth slab is already quite close to the value $\kappa = 2.8$ found by Roesler et al (2005) and it is to be noted that loading of the slab ended at 1×10^6 load repetitions without slab failure.

Tab. 1 Fatigue test results for slabs No. 1 - 5

Slab No.	force resultant Q_{max} [kN]	stress σ^* [MPa] FEM	frequency [Hz]	N^*	κ^*
1	8.5	2.65	4.5	1×10^6	-
2 – 4	17.0	5.28	7.2	1×10^6	1.33
5	34.0	10.55	7.0	1×10^6	2.66

Further increase in applied load was scheduled for slab number six. Shortly after start of the cycling loading, still in period of load intensity increase, the slab failed by cracking. The seventh slab was, therefore, loaded in a stepwise intensity increase pattern, as can be seen from Tab. 2.

Tab. 2 Fatigue test results for slabs No. 6 and 7 (+ indicating slab failure)

i	slab 6		slab 7	
	σ^*_i [MPa]	N^*_i	σ^*_i [MPa]	N^*_i
1	6.28	110	2.22	2.5×10^5
2	7.50	55^+	4.40	2.5×10^5
3			6.46	2.5×10^5
4			8.50	8.5×10^5
	$\hat{\kappa} = 1.387$		$\hat{\kappa} = 2.136$	

The required fatigue resistance enhancement factor $\hat{\kappa}$ is determined from the nonlinear equation expressing Miner law of damage accumulation in k successive loading processes

$$\sum_{i=1}^{k} \frac{N_i^*}{N_{lim,i}} = 1 \; , \qquad \log N_{lim,i} = 17.61 \times \left(1 - \frac{\sigma_i^*}{\hat{\kappa}\; f_{fl,beam}}\right), \qquad (3)$$

Results of Tab. 2 show, that even in the case of failed sixth slab, the fatigue resistance of the slab was higher than that predicted by classical fatigue curve (1). The results presented in Tab. 1 and 2 fully support findings of Roesler et al (2005) on slab enhanced flexural strength.

4. DESIGN CONSEQUENCES

Since fatigue properties play decisive role in pavement design procedures, the realized increase in concrete slab fatigue resistance may seem to bring about substantial savings in slab thicknesses. The implementation of this finding directly in the design procedures represents, however, much more involved problem. Required are additional and more elaborated testing programs with emphasis placed on concise simulation of the slab/subgrade interaction as well as of slab loading patterns. In concrete pavement design procedures allowance must be also made for weak zones in the concrete resulting from drying shrinkage, poor mix characteristics, etc. To account for microscopic damage at the slab surface, a non-zero initial damage or a slab strength reduction needs to be incorporated.

To illustrate, however, potential of incorporating (at least partially) enhanced fatigue resistance of concrete slabs in concrete pavement design, the catalogue pavement D0-T-1-S of the Czech design specifications TP170 (2004) was "redesigned" using several values of fatigue resistance enhancement factor κ (in very restricted version: κ = 1.1 and κ = 1.25). Results of standard TP170 (2004) design procedure are shown in Tab. 3, the pavement composition being:

CB I	27 cm	concrete slab,
KSC I	15 cm	cement treated aggregate base,
SD	15 cm	crushed stone,
PII		standard subgrade of deformation modulus 60 MPa.

Tab. 3 Thickness h_{CB} of concrete slab in dependence on value of factor κ

	fatigue resistance enhancement factor κ		
	1.0 (TP170)	1.1	1.25
h_{CB}	27 cm	25 cm	23 cm

5. CONCLUSIONS

The pilot testing program, presented in the paper, confirmed findings of Roesler et al (2005) on enhanced fatigue resistance of concrete slabs. Further research in this direction is needed to deepen our knowledge on limits of applicability of the observed fatigue resistance enhancement in order to use its potential in more effective concrete pavement design procedures.

6. ACKNOWLEDGEMENTS

The present paper was prepared as a part of research supported by the Czech Grant Agency project No. 103/09/1746.

7. REFERENCES

Darter, M. I., Barenberg, E. J. (1977), "Design of Zero-Maintenance Plain Jointed Concrete Pavement", Report No. FHWA-RD-77-111, Vol. 1; Federal Highway Administration.

Roesler, J.R., Hiller, J.E., Littleton, P.C. (2005), "Large-Scale Airfield Concrete Slab Fatigue Tests", Int. J. Concrete Pavements, 1, pp. 66-87.

TP170 (2004), "Pavement Design" [Technical Specifications], Ministry of Transport of the Czech Republic

FRACTURE PROPERTIES AND SIZE-EFFECT OF CEMENT COMPOSITE UHPC

Miroslav Vokáč[1], Petr Bouška[1], Jiří Kolísko[1], Jan Tichý[2]
[1] *Klokner Institute*
Czech Technical University in Prague
166 08 Prague, Šolínova 7
[2] *Skanska CZ, a.s.*
411 08 Štětí, Litoměřická 723

SUMMARY

At the present time, the applications of the cement composite called UHPC are increasingly used in the civil engineering structures. Klokner institute is engaged in research and testing of fracture parameters of such composites. The research work was focused to the geometrically similar specimens with the characteristic dimension of the cross section height from 40 to 150 mm. The dependence of the size-effect was described by the Bažant's law. The obtained result shows a significant dependence on the dimension. Therefore, the structural design should be based on the samples with the representative testing size.

1. INTRODUCTION

The investigated UHPC material consists of cement CEM I 42,5 R (656 kg), slag (81 kg), microsilica (101 kg), aggregate 0/4 mm (1157 kg), superplasticizer (39,8 l), water (156 l) and steel fibres ∅0,2/20 mm (101 kg). This type of composite is developing for thin-wall structure elements. The tensile and fracture properties ware investigated according to standard *EN 14651* and *RILEM Recommendations*, i.e., three point bending test with notched specimen with dimensions 150/150/600 mm. The test arrangement is drawn in fig. 1. The test results accomplished on the first beams made of UHPC shows dependence of tensile strength on element size. Therefore, the three sets of specimens with different size (*D* = 40, 100 and 150 mm) were tested and results were evaluated by Bažant's size effect law *(Bažant et al. 1998, 2002)*.

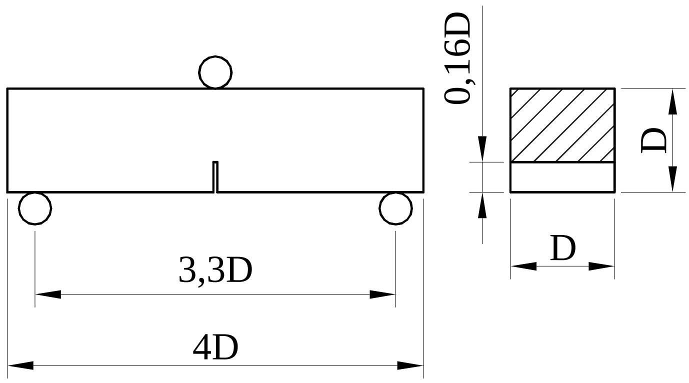

Fig. 1 Test arrangement of tree-point bending test with notched specimen – characteristic size of specimen *D* was equal to 40, 100 and 150 mm

2. SIZE EFFECT LAW

Bažant introduced size effect law for quasi-brittle materials by the relation

$$\sigma_N = \frac{B\,f_t'}{\sqrt{1+D/D_0}}\,, \qquad (1)$$

where σ_N is nominal strength, D is characteristic size of specimen (structure), D_0 is constant with dimension of length, B is dimensionless constant and f_t' is the tensile strength of material, introduced only for dimensional purposes. The regression constant $B\,f_t'$ and D_0 in equation (1) were solved by Linear Regression II (*Bažant et al., 2002*), i.e., by linear regression definited by

$$Y' = A'X' + C' \qquad (2)$$

where $X' = \frac{1}{D}$, $Y' = \frac{1}{\sigma_N^2 D}$, $B\,f_t' = \frac{1}{\sqrt{A'}}$ and $D_0 = \frac{A'}{C'}$.

3. RESULTS

The measured dependence of tensile stress on crack mouth opening displacement (CMOD) measured on several scaled specimens are presented on graphs, see Fig. 1 – 3. These graphs were evaluated according to the standard *EN 14651* and, furthermore, the nominal strength of each sample was taken into regression analysis of size effect law. The input data are presented in Tab. 1. The solved regression constant are $D_0 =$ 33,21 mm and $B\,f_t' =$ 39,84 MPa.

The size effect law could be plotted in graph with the *x* co-ordinate $\log(D/D_0)$ and the *y* co-ordinate $\log(\sigma_N / B\,f_t')$ as it is shown on Fig. 5. The curve corresponds to Bažant's size effect law, the horizontal dashed line to strength criteria (plastic behavior) and the oblique dashed line to the size effect law according to the linear elastic fracture mechanic (LEFM).

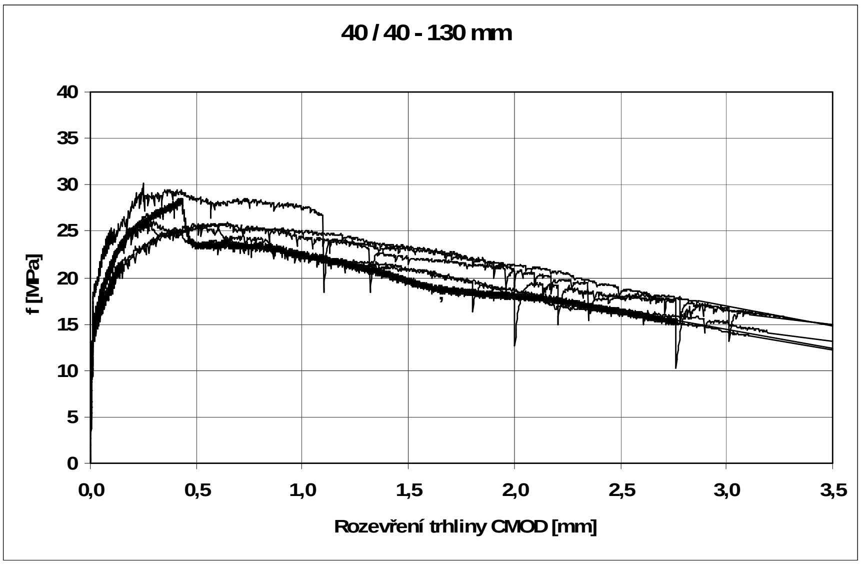

Fig. 2 Dependence of tensile stress on crack opening (CMOD) – samples 40/40/120 mm

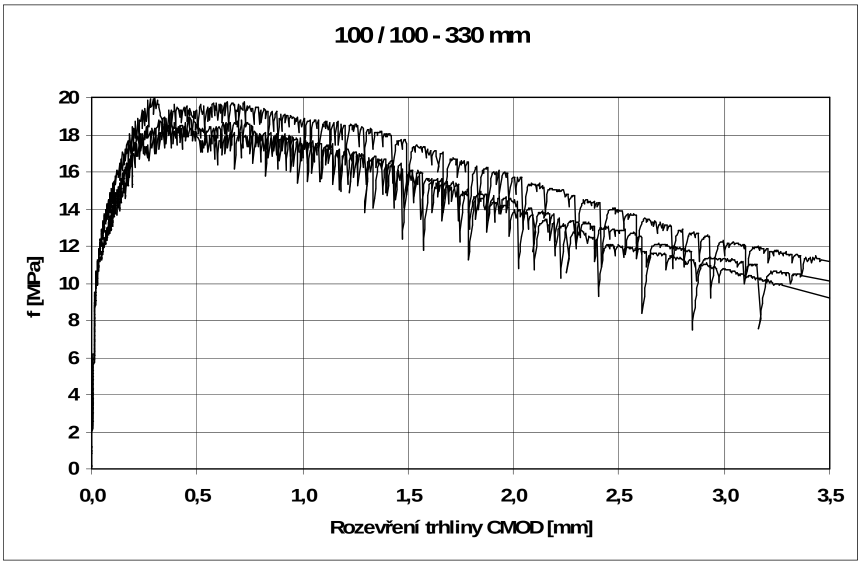

Fig. 3 Dependence of tensile stress on crack opening (CMOD) – samples 100/100/300 mm

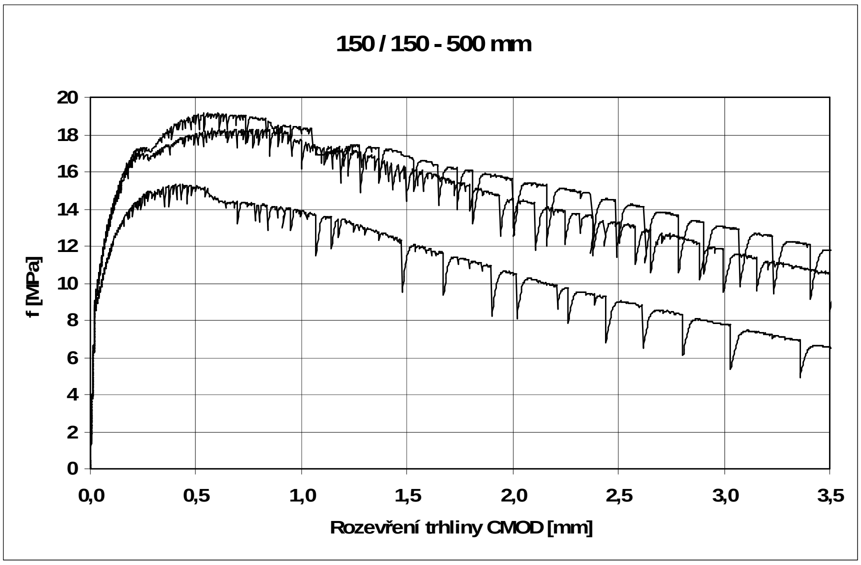

Fig. 4 Dependence of tensile stress on crack opening (CMOD) – samples 150/150/600 mm

Tab. 1 Input data for size effect law regression

D [mm]	Nominal strength σ_{Ni} [MPa]					
40	28.5	26.9	26.1	30.2	25.8	25.0
100	19.6	20.0	18.5			
150	15.3	19.2	18.3			

The suitable approach could be chosen depending on the parameter $\beta = D / D_0$ *(Bažant et al., 1998)*. If the size of structure element, resp. specimen, is small ($\beta <$ 0,1) than the strength criteria, resp. plastic design, could be used. If the size of structure is too big ($\beta >$ 10) than the LEFM is appropriate to design. If the characteristic dimension is between mentioned value, i.e., 0,1 $\leq \beta \leq$ 10, the non-linear fracture mechanics covering size effect law should be take into account.

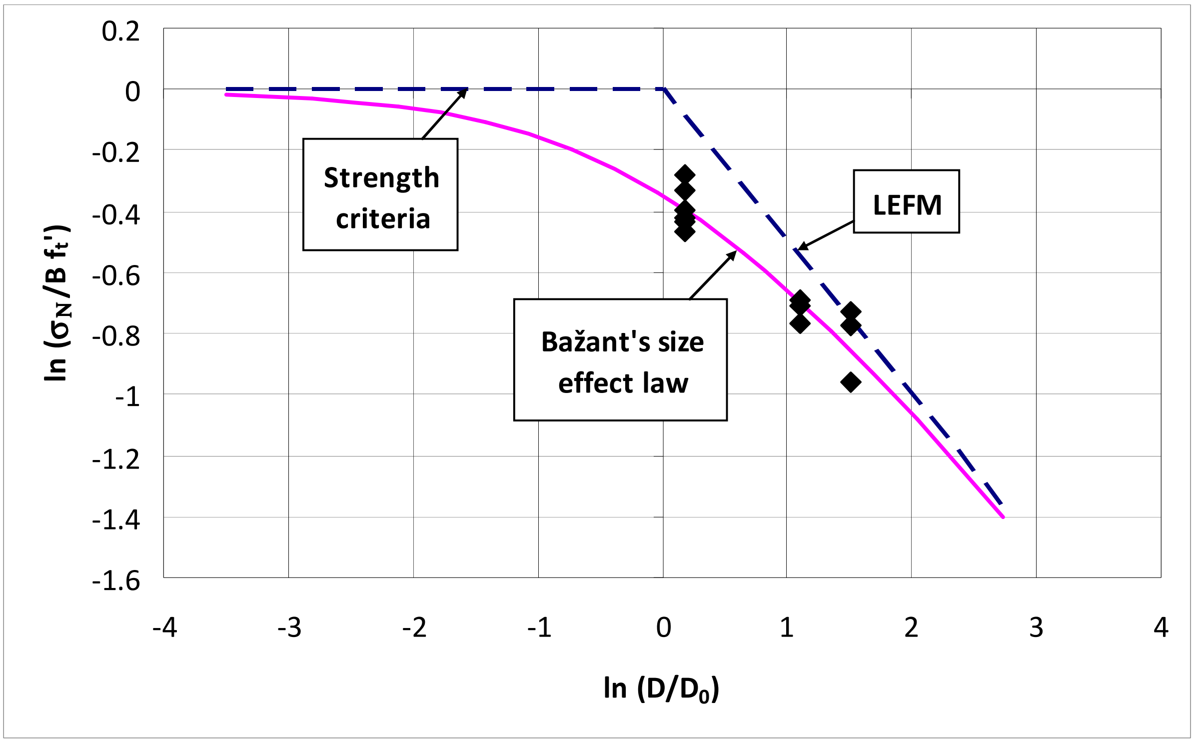

Fig. 5Size effect result – dependence of nominal strength on characteristic dimension in logarithmic scale

4. CONCLUSIONS

It was proved that the investigated UHPC material behaves according to size effect law. The dependence of nominal tensile strength on characteristic size is significant if UHPC composite is applied for structure elements. It was demonstrated that the common dimensions used for structure members belongs to the domain where the strength criteria (plastic behaviour) is not suitable for the reliable design of the structure. Therefore, the advanced methods which take into account the size effect shall be used.

5. ACKNOWLEDGEMENTS

This study was partially supported by the project GA ČR No. P104/10/2359 and partially by the project TA ČR No. TA01010269.

6. REFERENCES

Bažant, Z.P.; Planas, J. Fracture and Size Effect in Concrete and Other Quasibrittle Materials. London : CRC Press, 1998. 616 p. ISBN 0-8493-8284-X.

Bažant, Z.P. Concrete fracture models: testing and practice. In Engineering Fracture Mechanics. No. 69, 2002, pp. 165-205. ISSN 0013-7944.

EN 14651:2008 Test method for metallic fibered concrete - Measuring the flexural tensile strength (limit of proportionality (LOP), residual).

RILEM. RILEM Technical Recommendations for the Testing and Use of Construction Materials. London : E&FN Spon, 1994. ISBN 0 419 18810X.

EXPERIMENTAL EVALUATION OF FRP RETROFITTING SYSTEM FOR TWO-WAY RC SLABS

S. C. Floruţ, V. Stoian, T. Nagy-György, D. Dan, D. Diaconu
"Politehnica" University of Timisoara
Department of Civil Engineering
2nd T Lalescu, 300223 Timisoara, Romania

SUMMARY

The paper presents results obtained by experimental investigations on reinforced concrete (RC) slabs retrofitted using Fibre Reinforced Polymer (FRP) composite materials. Theoretical and experimental research have been performed in order to determine the effectiveness of these strengthening solutions in the particular case of cut-outs created in the corners and on the edges of the slabs. By performing the six experimental tests on the three slabs, the effectiveness of the proposed technique was evaluated, the results being quite encouraging.

1. INTRODUCTION

In today's world of civil engineering, specialists consider more and more the composite materials, especially the FRPs. The composite materials properties have made their use to prove a real success in a series of applications, starting with local strengthening up to highly complex works. One of the circumstances in which the use of FRP might be suitable refers to strengthening/retrofitting of reinforced concrete slabs with or without openings. In many situations, the need of creating new openings into existing buildings' slabs arises, mostly due to changes in functionality or in destination. Thus, one of the experimental programs that is in progress at the "Politehnica" University of Timisoara concerns the study of strengthening/retrofitting solutions that involve the use of FRPs for RC slabs, with and without cut-out openings. Similar studies were previously performed worldwide, on one-way and two-way slabs, with or without cut-out openings. However the amount of information on this topic is quite limited, the present research program being developed with the purpose of providing more data to interested research communities.

2. EXPERIMENTAL PROGRAM - SPECIMENS, MATERIALS, PROCEDURES

The experimental program involves tests on four large scale elements. All the elements were rectangular, with dimensions of 2650x3950x120 mm. They were tested in horizontal position, being simply supported along the edges and loaded gravitationally. The first specimen (denoted RCS-FS-01 standing for Reinforced Concrete Slab - Full Slab) was a full slab and served as reference. Into the second element (denoted RCS-RSC-01 standing for Reinforced Concrete Slab - Rectangular Small Cut-out) a rectangular cut-out of 960x1540 mm was created. The third element (denoted RCS-RLC-01 standing for Reinforced Concrete Slab - Rectangular Large Cut-out) had a rectangular cut-out of 1060x2650 mm inserted into it. The experimental results obtained on these three slabs are presented in this paper. In the first phase, each element is tested in its bare state (RC slab without any FRP retrofitting) up to a certain stage. Afterwards, a mixed strengthening solution that involves the use of both NSMR-FRP and EB-FRP techniques is applied. After allowing the materials to cure, the elements are retested up to failure. The geometrical characteristics of the three specimens are presented in Fig. 1.

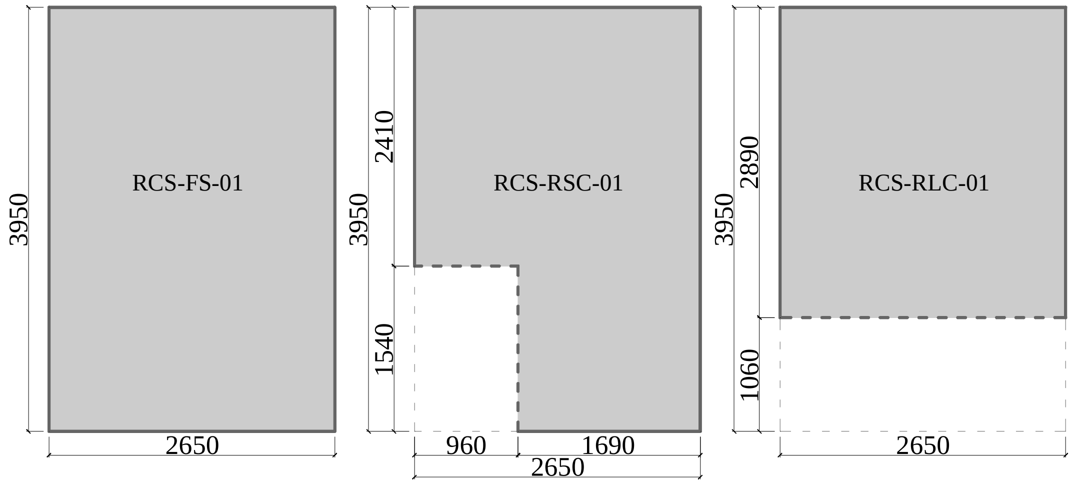

Fig. 1 Geometrical characteristics of the three specimens.

By performing experimental tests on samples, it was evaluated that elements were all cast using concrete with cubic compressive strength of 65 MPa (N/mm^2). The slabs were reinforced with steel welded wire meshes at the inferior side (4 mm in diameter with spacing of 100 mm) and with steel rebars at the superior one (6 mm and 10 mm bars). The bars in the steel welded wire meshes had average yield strength of 597 MPa, 537 MPa and 545 MPa for the RCS-FS-01, RCS-RSC-01 and RCS-RLC-01, respectively. The inferior reinforcement was laid on the entire surface of the slab, while the superior one was placed only along the edges, mainly due to constructive reasons.

It was decided to use a load distributed over a central patch of 600x1200 mm. For inducing the load, a hydraulic jack with a maximum load capacity of 500 kN and a maximum stroke of 160 mm was used. The load is applied in one single cycle at constant rate. The edges of the specimens rested with 125 mm on a series of supporting elements through a layer of mortar. The strategy is to test elements in their bare state up to a stage that would assume the need of retrofitting interventions. These tests were denoted RCS-FS-UU-01, RCS-RSC-UU-01 and RCS-RLC-UU-01. Afterwards, a mixed strengthening solution that involves the use of both NSMR-FRP and EB-FRP techniques is to be applied. Finally the retrofitted element is tested up to its complete failure. The tests on retrofitted specimens were denoted RCS-FS-DS-01, RCS-RSC-DS-01 and RCS-RLC-DS-01.

3. BEHAVIOUR DURING TESTS ON BARE ELEMENTS

The behaviour of the slab during RCS-FS-UU-01 test was as expected, four cracks appearing on the direction of the yield lines. The maximum load level reached during this test was 118.25 kN. Past this value, the strain in numerous reinforcement bars has reached yielding point, the cracking has stabilized and the vertical mid-span displacement has past the maximum allowable deflection as provided by EN 1992-1-1 (L/250=2400/250=9.60 mm). Moreover, deflection continued to increase without a substantial increase of load. During the test, the maximum vertical mid-span displacement had a value of 10.28 mm.

For the RCS-RSC-UU-01 test the maximum load level was 87 kN while the maximum vertical displacement had a value of 11.36 mm. The first crack was visible at a load of 60 kN.
During RCS-RLC-UU-01 test the maximum recorded load level was 74.5 kN while the maximum vertical displacement had a value of 9.59 mm. The first crack was visible at a load of 55 kN. The load-displacement curves are presented in Fig. 4.

4. STRENGTHENING PROCEDURES

For the full slab, the CFRP materials are bonded on the tension side of the slab in the directions parallel to both length and width of the slabs. In case of slabs with cut-outs, the CFRP materials are bonded at the bottom side, around the cut-out, parallel to its edges. For all specimens the CFRP materials were bonded to the concrete surface using two-component epoxy based resins.

For each specimen, a mixed (hybrid) retrofitting technique was used, involving the use of both Externally Bonded FRP (EB-FRP) and Near Surface Mounted Reinforcement-FRP (NSMR-FRP) systems. It was decided, that for all of the specimens, the CFRP components that are parallel to the width of the slab are to be mounted as NSMR while the CFRP components that are parallel to the length of the slab are to be mounted by EB-FRP technique. The configuration of the retrofitting CFRP components is presented in Fig. 2.

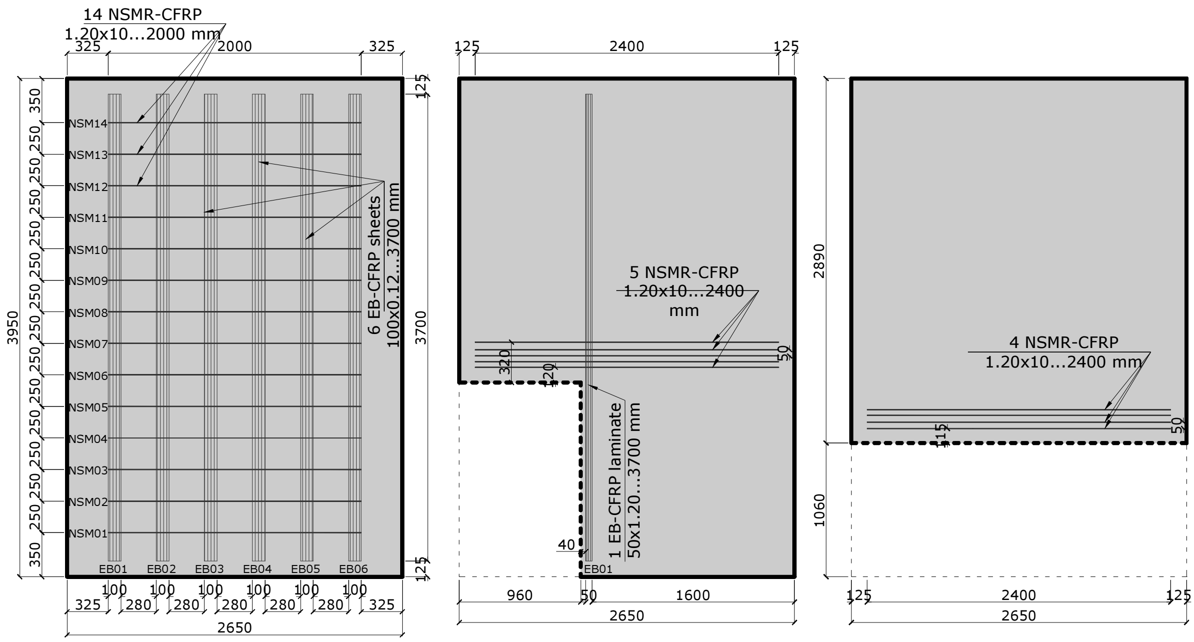

Fig. 2 Lay-out of the retrofitting CFRP components.

5. BEHAVIOUR DURING TESTS ON RETROFITTED ELEMENTS

The RCS-FS-DS-01 slab was tested up to failure, reaching a maximum load of 185.5 kN that corresponds to a vertical mid-span deflection of 50 mm. After this level, the deflection increased while the load diminished. The slab was able to deflect almost 110 mm before full failure. Both the EB-FRP sheets and the NSMR-FRP that were intersected by the principal cracks, have failed due to CFRP rupture, no type of premature failure being observed.

The RCS-RSC-DS-01 test reached a maximum load of 85.75 kN at a central deflection of 27 mm. Maximum deflection was of 33 mm. All of the five NSMR-FRPs have failed by fibre rupture, while the EB-FRP has debonded from the concrete surface at relatively low strain. The RCS-RLC-DS-01 test reached a maximum load of 74.75 kN at a central deflection of 8 mm. Maximum deflection was of 87 mm. All of the four NSMR-FRPs have failed by fibre rupture. The final crack patterns and the load-displacement curves are presented in Fig. 3 and Fig. 4 respectively.

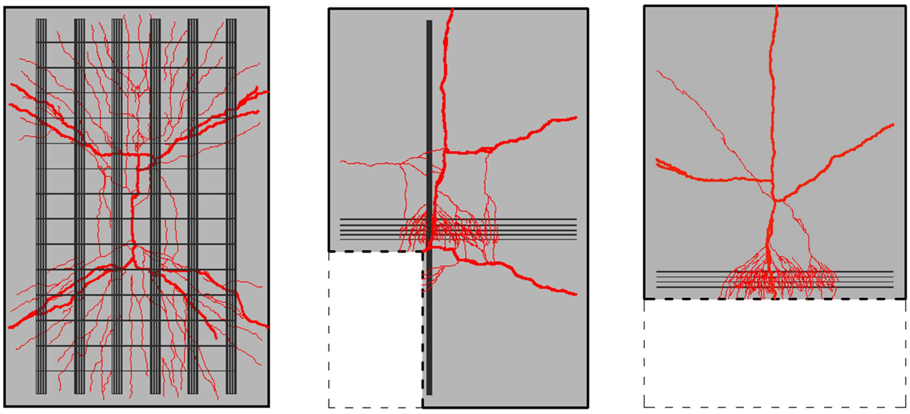

Fig. 3 The final crack patterns superopsed with the retrofitting system.

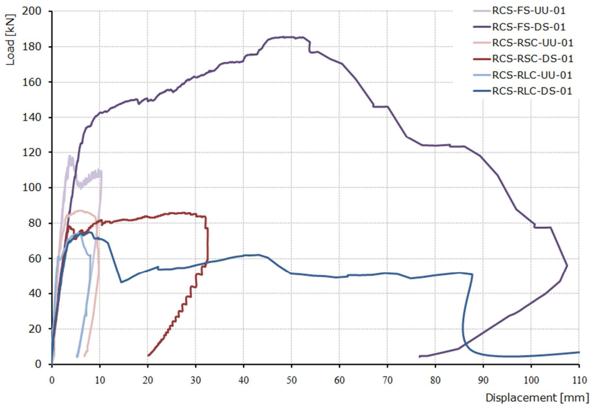

Fig. 4 Load-displacement diagrams.

6. CONCLUSIONS

The behavior of the full slab was improved quite significantly after applying the retrofitting system. The load capacity at U.L.S. is improved by 59.3%. However, if the allowable deflection at S.L.S. is considered, the load capacity is improved only by 37.3%, the corresponding load level being 102 kN and 140 kN, prior and after retrofitting, respectively. By applying the retrofitting systems, the capacity of the slabs with cut-outs was restored. The amount of CFRP laid-up around the cut-outs was insufficient for increasing the bearing capacity of the slabs. The failure of NSMR-FRP by fiber rupture along with the crack patterns, have proved the effectiveness of the CFRP elements.

7. ACKNOWLEDGEMENTS

The authors kindly acknowledge the Ministry of Education, Research, Youth and Sport in Romania as the research work was granted partially by this authority.

8. REFERENCES

S. C. Floruţ, V. Stoian, D. Diaconu, D. Dan „Experimental investigations of the behavior of RC slabs retrofitted by a mixed NSMR-FRP and EB-FRP technique“, SMAR 2011, 167/7e.

NONLINEAR ANALYSIS OF TIMBER-FIBRE CONCRETE COMPOSITE STRUCTURES

Vojtěch Petřík, Iva Broukalová, Vladimír Křístek, Martin Půlpán
OSVVP ČSSI
Komornická 15, 160 00 Praha 6, Czech Republic

SUMMARY

Numerical analysis of timber- fibre concrete structures must take into account the strong physical nonlinearity fibre concrete. The implementation of appropriate material models is requested. Modern computer programs based on finite element method enable analysis of structures including considering of physical and geometric non-linearity. Structural fibre concretes are known as quasi-ductile materials. Their behaviour in elements strained by tensile is characterised by softening behaviour after first crack occurs. Conditions for appropriate numerical simulation of real behaviour of the timber-fibre concrete composite structure are implementation of realistic material model, i.e. stress-strain relation, and appropriate simulation of the connection between the timber and fibre concrete parts of the composite structure.

1. INTRODUCTION

Composite structural systems that join advantageous properties of particular materials for given straining are utilised for various types of structures. Timber-concrete composites (TCC) with reinforced concrete slab are used both for strengthening and repair of existing timber floor structures and in newly built structures for dwelling, industry and bridges.

Fibre concrete with fibres distributed uniformly and in all directions in the matrix can resist tensile loads. This is a benefit in cases with complicated loading of the cement component caused by outer loading and volumetric changes and local extreme stresses in zones where connectors are anchored.

2. NONLINEAR ANALYSIS

Analytical and numerical methods based on assumptions of elastic theory can't be applied in analysis of behaviour of structural systems as for higher deformations the material behaviour is strongly non-linear. The modulus of slip of interconnection is not the liner function as well. The real behaviour of the composite structure with fibre-reinforced concrete slab can be described with non-linear numerical analysis whereas the knowledge of constitutive relations is inevitable.

2.1 Implementation of the material model of fibre reinforced concrete

The stress-strain diagram of fibre concrete is derived in inverse analysis. In the procedure of inverse analysis the curvature of the deflection line is determined, stress-strain diagram derived and material parameters of the implemented material model are identified and verified in a numerical simulation. Details about numerical simulation – see (*Petřík, 2004*), *(Vráblík, Křístek 2004)*.

The constitutive relations of fibre concrete were verified in numerical simulation of a four-point bending test in programs ANSYS and ATENA. The figure 1 shows approximation of analysis with the test result.

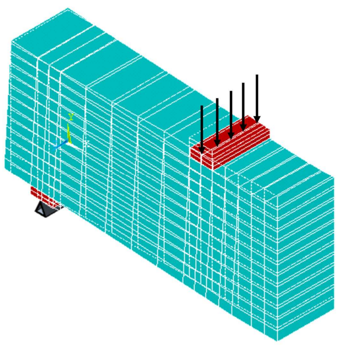

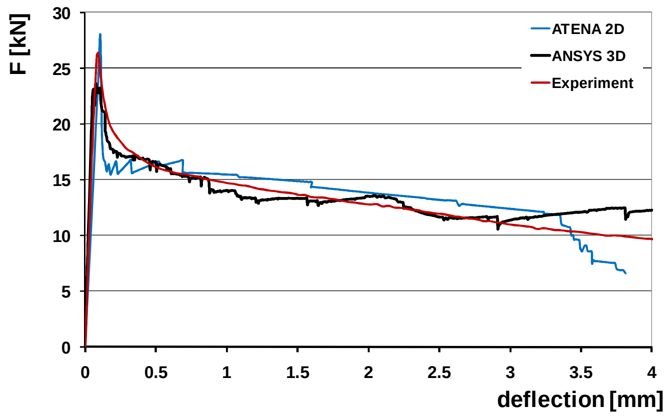

Fig. 1 Numerical model and results of the analysis

The numerical simulation was rather complicated because fibre concrete had pronounced tensile softening. Optimisation of material models parameters aimed to appropriate approximation of the test results and also to robust and convergent numerical analysis. Of course the curves in the Fig. 1 did not result from the first run of inverse analysis; many runs of inverse analysis had to be performed to obtain the favourable result. It shall be noted that sensitivity analysis showed rather high dependence of the result on the finite element size.

2.2 Implementation of the model of interconnection

The connection of the (fibre) concrete part with the timber beam is provided in most cases by pin-connection or by lamellas glued to timber beams, which have high slip modulus in initial phases of deformation – the interconnection is very rigid. Without other strengthening is the use of glued lamellas debatable as they decrease the section area and stiffness and restrict action of fibres in the most strained sections.

Discrete models of connection elements are suitable for analysis of the stress state of the continuum in their neighbourhood but their utilisation in numerical models of structural systems is practically impossible as such numerical model has too many finite elements and the numerical problem is unsolvable even for contemporary efficient computers. From the practical point of view it is more profitable to utilise the interconnecting gap between the timber beam and fibre concrete slab and to apply contact elements with appropriate material model.

To verify the material model of interconnection numerical simulations of extrusion test were performed in ATENA and ANSYS programs. The interconnection is based on model of Mohr-Coulomb friction with parameters tangential and normal stiffness, cohesion and angel of inner friction. Comparison of numerical simulations and test and a model of test specimen (*Kuklíková 2004, Koželouh 1975*) is depicted in the Fig. 2.

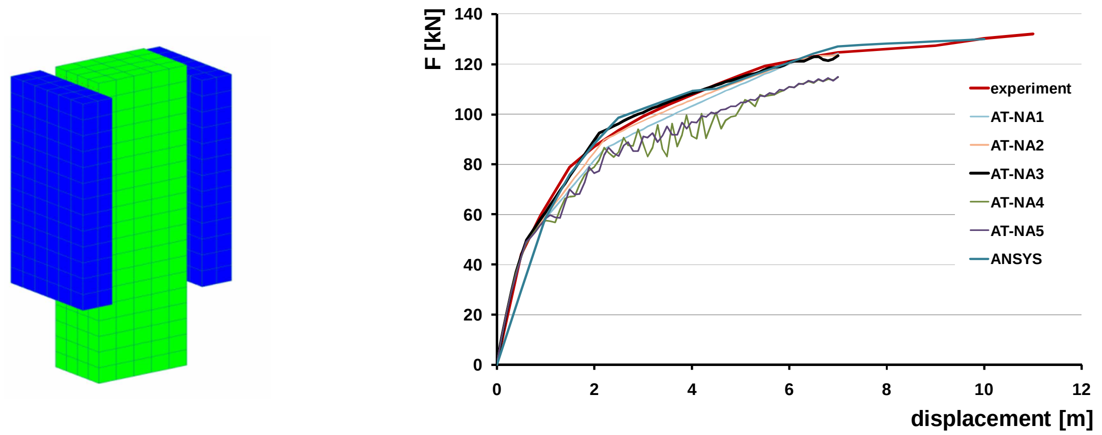

Fig. 2 Numerical model and results of the analysis

Deformation characteristics of the interconnection have the substantial importance for analysis of the stress state and load - deformation diagram. Therefore the real initial stiffness and the deformation softening must be described very accurately in the numerical simulation. The extrusion test was simulated very appropriately by both software tools. Curves designated AT-NA4 and AT-NA5 describe behaviour of the model with different size of finite elements.

2.3 Analysis of the combined beam

Material models of the contact and fibre concrete were applied in the numerical model of combined timber – fibre concrete T-section. A beam with span 6.5 m was modelled. Tth section of the timber beam is 0.14 x 0.24 m, width of the slab is 0.94 m and the thickness of the slab is 0.06 m. The timber material is assumed linear-elastic. Model and load-deflection curves are in the Fig. 3.

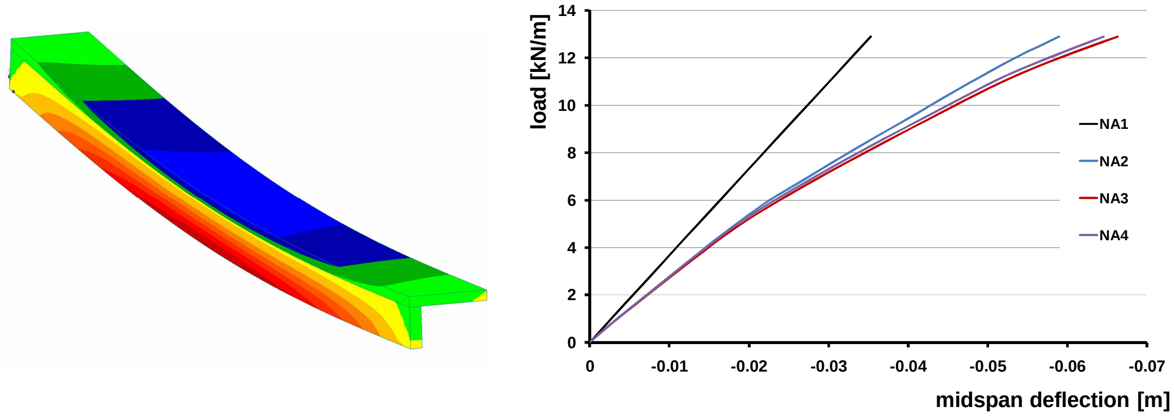

Fig. 3 Numerical model of composite beam and results of the analysis

The model was loaded with constant linear load; the load was applied in increments until the mean value of the tensile strength of timber was reached. The analysis was performed in alternatives according to Tab. 1.

The results of the numerical simulation show that value of the tangential slip modulus and the shape of the load-deformation curve of connecting elements according to the extrusion test have the fundamental importance for the layout of stresses in the composite section and development of deformations (load-deflection curves Fig. 3 – curve NA2). The increase of deformations in the tensile part of the concrete component is also evident. (Fig. 3, curve NA3). Application of fibre concrete may increase the stiffness of the bended composite beam as the beam resists tensile stresses even after cracking (Fig. 3, curve NA4). The increase of stiffness in bending depends on the value of residual tensile strength of fibre concrete; in analysis NA4 fibre concrete with high softening was used.

Tab. 1 Table of used materials

Numerical analysis	Contact	Concrete	Timber
NA1	rigid	elastic	elastic
NA2	nonlinear	elastic	elastic
NA3	nonlinear	plain concrete, nonlinear	elastic
NA4	nonlinear	fibre concrete, nonlinear	elastic

2.3 Analysis of the structural system

The effect of material properties of fibre concrete and deformation characteristics of connection on the behaviour of the structural system is now investigated in a case study of the model in Fig. 4. One parameter is the thickness of the fibre concrete component. The results of the numerical simulation will be verified in full-scale laboratory tests. The tests are scheduled for September 2011. If the schedule is kept, the results will be presented at the conference

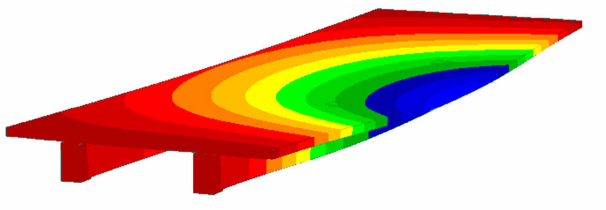

Fig. 4 Model of structural system

3. CONCLUSIONS

Corresponding analysis of behaviour of combined structural systems until the ultimate load-bearing capacity can be performed only if non-linear behaviour of materials and interconnection is taken into account. Verification of implemented material models by numerical analysis of experiments shall be an integral part of non-linear analysis of the structural system as it increases probability that the real behaviour of the combined system will be appropriately simulated. If it is to the contrary, the complex numerical model with many implemented non-linearities may become a “black box”.

4. ACKNOWLEDGEMENT

The contribution has been achieved within the project GAČR 103/09/2097.

7. REFERENCES

Kuklíková, A.: Kompozitní dřevobetonové konstrukce. Disertační práce, ČVUT Praha, 2004

Křístek, V.; Studnička, J.: Analysis of composite girders with deformable connectors. Proc. Instn. Civ.Engrs, Part2, Dec. 1982.

Petřík, V.: Materiálové modely a výpočtové analýzy vláknobetonových konstrukcí. Disertační práce, ČVUT Praha, 2004

Vráblík, L.;Křístek, V.: Vláknobeton- přibližná metoda inverzní analýzy. Beton 6/2004

NUMERICAL ANALYSIS OF BEHAVIOUR OF FRC PRESTRESSED ELEMENT

Alena Kohoutková[1], Iva Broukalová[1]
[1] Department of Concrete and Masonry Structures
Faculty of Civil Engineering, Czech Technical University in Prague
166 28 Praha, Thákurova 7

SUMMARY

The paper presents comparison of laboratory tests and numerical simulation of precast reinforced concrete and prestressed concrete element. The presented achievements are a part of collaboration of the research institute CTU in Prague Faculty of Civil Engineering Department of Concrete and Masonry Structures and the industrial plant SMP CZ a.s. that intends to design and provide more efficient concrete and fibre-concrete products.

1. INTRODUCTION

The government programme for science and research supports interconnecting of science and professions and the transfer of technologies and the stress on outcomes in a form of practical applications is laid. Shared projects of research centres and industrial and construction companies are supported by foundations and funds. In a project like this our Department of Concrete and Masonry Structures joints with construction and facilities company SMP CZ. The construction company expects that the partnership with research institute will introduce new procedures and production technologies, implementation of production of new products with enhanced properties – new products shall be cost effective, the manufacturing of the new products shall be more efficient and thus it will be more competitive in the market compared to presently manufactured products. Designing of thinner elements is considered what may reduce the cost of transport and possibly the price of the element, too.

2. USE OF FIBRE REINFORCED CONCRETE FOR THE PRECAST COLUMN

A certain part of the production of the company consists of precast elements of noise-barriers. Some precast elements show defects after transport to the site; the edges and corners are spalled out. Other elements exhibit defects after assembling. These defects are claimed by the contractor and the producer must repair them or replace the damaged element.

Modification of some elements to elements with higher impact resistance would decrease expenses related to the mentioned problem. It has been proved in previous research programmes that dispersed fibres added to concrete matrix increase toughness, durability and impact resistance. At the same time the decrease of traditional rebar reinforcement can be considered. It was demonstrated that use of dispersed fibre reinforcement enables reduction of shear reinforcement.

The noise barrier consists of columns fixed in the basement and horizontally spanning panels. First of all the investigations focused on columns. The columns have I-shaped section what enable supporting of horizontal panels. The connection detail is in a figure 1. The columns are manufactured in lengths from two to six meters according to local conditions and other requirements. Current precast columns are made from reinforced concrete with classical rebar reinforcement. The investigations enquired after possibilities of the reduction of rebar reinforcement in the element with combined (rebar – dispersed) reinforcement and if it would be cost-effective. The feasibility of production of prestressed columns with and without dispersed fibre reinforcement was verified too.

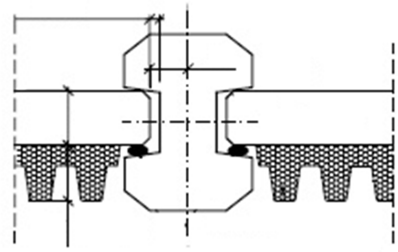

Fig. 1 Detail of the noise barrier – connection of the I shaped column and horizontal panels

The dispersed reinforcement was assumed in two variants – steel fibres and synthetic fibres. SFRC (Steel Fibre Reinforced Concrete) was chosen in cases where the increase of tensile strength and residual tensile strength were demanded, synthetic fibres were chosen for the increase of toughness and resistance to stroke damage.

Full-scale tests and numerical simulations of the precast columns were performed within the research project. The paper compares results of laboratory tests and numerical simulations. The other consequences of the research programme and laboratory testing of the element are discussed in of authors Jan Vodicka, Jiri Kratky and Hana Hanzlova "Influence of Shear Resistance on Ductility of Bended Fibre Concrete Element".

Tab. 1 Summary of types of specimens and measures cracking and peak loads

Labelling of column	Rebar reinforcement	Type of fibres	Anchoring length [mm]	Load at cracking	Peak load
S 11	Mild rebar + links	no fibres	600	9.8	36.1
				12.8	36.7
				14.5	36.1
S 12	Prestressing tendons	no fibres	600	30.0	44.2
				24.0	41.3
				30.0	42.6
S 13	Prestressing tendons	no fibres	800	30.0	42.0
				32.5	42.9
				28.0	40.2
S 14	Prestressing tendons	no fibres	1000	28.5	44.5
				30.3	43.6
				30.0	42.4
S 15	Prestressing tendons	Steel fibres	800	34.0	43.5
				33.0	43.4
				34.0	43.5
S 16	Prestressing tendons	Steel fibres	600	36.5	44.0
				32.4	43.0
				30.0	40.2
S 17	Prestressing tendons	Synthetic fibres	800	34.7	42.2
				33.7	42.0
				36.5	42.9

3. COMPARISON OF LABORATORY TESTS AND NUMERICAL SIMULATION

The numerical simulations were performed in a program for non-linear analysis of concrete structures ATENA 3D. Particular cases were modelled that corresponded to real laboratory tests. A reference reinforced concrete column with classical rebar reinforcement including shear reinforcement (links) was modelled to compare the new type of element to the current precast element and its behaviour. Furthermore a task with prestressed column was assembled. The prestressing is provided with two tendons placed in the axis of symmetry (see Fig. 2). The prestressed element has no other rebar reinforcement.

For the prestressed columns an effect of support length was investigated to verify the transfer length for prestressing. The tests had three types of supporting of the precast column: the columns are fixed in a rigid concrete body; the anchoring length was 600, 800 and 1000 mm. In the same lay-out the numerical models were prepared.

Fig. 2 End section of the column with two prestressing tendons during laboratory testing with strain gauges for measurement of the slip of tendons

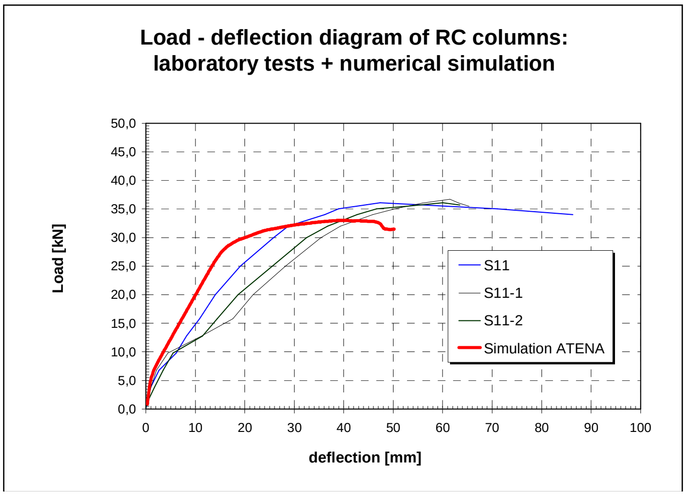

Fig. 3 Comparison of the Load-deflection curves of the precast column with classical rebar reinforcement

Loading in the laboratory was applied in five cycles. In each cycle the load increased by 5 kN, than the specimen was unloaded. In the sixth cycle the load increased until collapse. In the numerical simulation the load was applied by deformation of the specimen in small increments until the collapse was reached.
In laboratory loading a relation Load – deflection was recorded. To compare laboratory results and numerical simulation the load – deflection curve was determined also in the numerical modelling.

In addition a slip of the prestressing tendons was measured for both tendons.

The models were prepared in 3D modification of ATENA program. The shape of the body meets real features of the precast column. For description of material characteristics material models implemented in ATENA program were utilised that can describe non-linear behaviour in tensile and in compression including hardening and softening. The finite elements of the concrete body are solid tetrahedral elements; the reinforcement is modelled by truss elements.

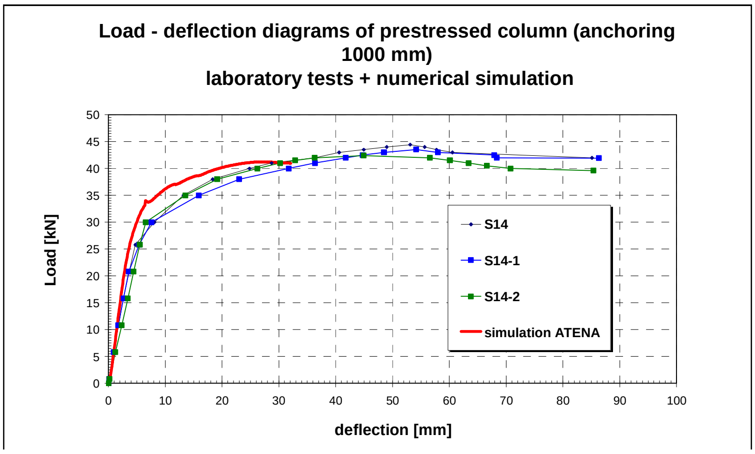

Fig. 4 Comparison of the Load-deflection curves of the prestressed column

4. CONCLUSIONS

Executed tests, performed calculations and simulations show that prestressed columns have higher resistance than the reinforced concrete columns; at the same time the failure mode is acceptable and safe. For the tested length of columns are the prestressed columns reliable even without additional shear reinforcement or dispersed reinforcement. Yet the fibre reinforcement is assumed to enhance toughness, reliability and resistance to damage during transport and manipulation.
The object of further investigations will be feasibility of columns with higher lengths. Utilisation of numerical simulation is anticipated for verification of resistance, reliability and failure mode.

5. ACKNOWLEDGEMENTS

This outcome has been achieved with the financial support of the Ministry of Industry and Trade of the Czech Republic program TIP FR—TI2/496; theoretical results gained in the project GACR 103/09/1788 were exploited .

6. REFERENCES

Červenka, V., Jendele, L., Červenka, J.: ATENA Program Documentation Červenka Consulting, 2005

REINFORCED CONCRETE AS STRENGTHENING MATERIAL FOR HISTORIC BUILDINGS

Ildikó Bucur-Horváth, Anca Genoveva Rab, Robert Ozsváth
Technical University of Cluj-Napoca
400020 Cluj-Napoca, C. Daicoviciu 15, Romania

SUMMARY

The paper deals with the opportunity of using reinforced concrete in strengthening structures or structural elements of old buildings belonging to the architectural heritage.
Due to its well-known qualities reinforced concrete can hardly be avoided as repairing or strengthening material. Then again, the use of reinforced concrete in the case of historic buildings is the subject of a controversial debate. Studies on structural reinforcing as well as our own professional experience show that in many cases the use of reinforced concrete is unavoidable, respecting international regulation in terms. The paper discusses the cases and conditions of using reinforced concrete as strengthening material for historic structures correctly.

1. INTRODUCTION

Any intervention on a historic building should carefully be made. Besides the general demands concerning the functionality as well as structural reliability (resistance and stability, serviceability, durability and maintenance), the rehabilitation process has to respond to some specific requirements regarding authenticity, aesthetics, structural, physical and chemical compatibilities etc.

Due to its well-known qualities, reinforced concrete proves to be a very useful strengthening material for reinforcing structures. However, the specialists approach the use of reinforced concrete in the case of historic buildings suspiciously, and rather with dislike. The main roots of this aversion are some unfortunate structural interventions on historic structures during the 20th century (especially in its first quarter) without respecting the basic rules (mostly unknown at that time) concerning the safeguarding of the architectural heritage. For that reason many strengthening works were compromised, especially those on masonry structures of marble, stone or brick. The most famous example is the Balanos intervention on the Acropolis monuments (1902-1930). Nicolaos Balanos restored – among others – nine columns of the northern peristyle colonnade of the Parthenon. In order to restore the shape of column drums, the missing pieces were replaced by reinforced concrete. The steel reinforcing rods were anchored in the marble. This intervention (and also others) seems to be very brutal. They indicate a lack of respect toward the original material and structural authenticity.

This experiment and similar another cases led those interested to lay down the guidelines of monument rehabilitation. Athens Charter was born this way (1931), followed by Venice Charter in 1964. Moreover, restorations of brick or stone masonry using Portland cement often give trying experiences. The main problems concern physical, chemical and mechanical incompatibilities and the undesirable water-tightness of the cement mortar applied on masonry.

2. GUIDING PRINCIPLES OF HISTORIC STRUCTURE RESTORATION AND CONSOLIDATION

The basic principles concerning restoration of historic monuments are laid down in the Venice Charter: the restoration of monuments must appeal to all the sciences and techniques, which can contribute to the study and safeguarding of the architectural heritage; the respect for the original materials; any necessary extra work must be distinct from the architectural composition and must bear a contemporary stamp; where traditional techniques prove inadequate, the consolidation of a monument can be achieved by the use of modern conservation and construction techniques, the efficiency of which has been shown by scientific data and proved by experience; the valid contributions of all periods to the building of a monument must be respected; replacements of missing parts must integrate harmoniously with the whole, but at the same time must be distinguishable from the original.

Structural interventions have to respect these guidelines, too. As far as the correctness of a strengthening intervention is concerned, it is not easy to make a right judgment. There are several criteria to be taken into account like structural conformation, the quality of the materials used, the details of architectural image etc. and the actual technical state can be so different that every case has to be studied substantially. However, one can point out the necessary proceedings and principles regarding structural interventions on historic buildings:

- To establish the different stages of the construction;
- To determine the technical state *(Bucur-Horváth 2001)* for every part of the building;
- To maintain the original structural form as much as possible;
- The consolidation material and technique have to be consistent with the original ones;
- It is recommended to use traditional techniques, but in certain cases they could be supplemented or changed by cautiously applied modern techniques;
- To make structural transformation when the change in use or the precarious technical state requires it;
- The added structural elements or subassemblies have to be of appropriate degree of reliability and they must be distinguishable from that original.
- To try and apply reversible solutions to allow further space for intervention as much as possible;

3. REINFORCED CONCRETE AS STRENGTHENING MATERIAL FOR HISTORIC STRUCTURES

Reinforced concrete as strengthening material for historic structures can fulfill almost all of the listed principles, except for the reversibility requirement. Thus, the choice of reinforced concrete as a strengthening material – like any modern construction technique – must be examined carefully. The need and efficiency of using it have been illustrated by scientific data and proved by experience.

Actually, one can ask certain questions: Which are the domains where reinforced concrete can be used properly for structural strengthening? Which are the cases when reinforced concrete is almost inevitable or just recommended as a strengthening material for historic structures? Which are the conditions of using reinforced concrete for strengthening stone and/or brick masonry structures?

Obviously, historic structures of reinforced concrete will be strengthened with reinforced concrete or metallic elements and subassemblies, compatible with the original structure. Foundation strengthening with reinforced concrete is the most usual solution for damages caused by unequal settlements, by underpinning the existing foundations and creating joining girders of reinforced concrete at a proper level.

Much more questions should be handled in the case of stone and/or brick masonry structures. Usually, they are structures with masonry piles and walls as vertical structural elements and different systems of masonry vaulted slabs or/and timber slabs as horizontal structural elements. Generally, one can identify at least three ways of structural intervention (Bucur-Horváth et al 2008). They are (in an increasing order of the degree of intervention): (1) structural interventions preserving the entire original structure; (2) structural strengthening by modifying the original structure with compatible structural elements; (3) indirect strengthening using additional bearing systems in order to discharge a historic structural subassembly or to diminish certain structural displacements.

The restoration of masonry structures with Portland cement (mortar or concrete) may present the following inconveniences:

(a) The intervention is hardly reversible; the demolition of the strengthening may cause damages.
(b) The properties of the strengthening material considerably differ from the properties of the original material. Its strength is high, its flexibility and deformation capacity is low compared to the original masonry. All these can induce undesirable internal stresses in the original structure.
(c) Its thermal expansion coefficient is well above the masonry's coefficient. Because of this, contact surface tensions arise resulting in the separation of the two materials. As a result capillary tubes may appear ensuring the rising of the capillary water and consequently moisture damages are caused.
(d) Its water vapor permeability is very low. Therefore, a continuous covering with mortar or concrete using Portland cement blocks the natural ventilation of the original wall, the moisture of masonry increases, with all its related consequences.
(e) Water-soluble salts can be formed and could damage the masonry.

The above findings present in fact the limits of using reinforced concrete. They also provide guidance on how to avoid the inconveniences listed above. That is very important because there are cases in which the use of reinforced concrete is almost unavoidable. It may happen that any other applicable technique is hard to find.

It could happen when the old brick structure is in a very bad technical condition and we are almost forced to use covering with reinforced mortar or concrete (1). In these cases, in order to ensure vapor permeability, i.e. the ventilation of the wall, it is recommended to use other cements with lower content of clinker like Pozzolanic cement (45-64% clinker and 36-55% pozzolana) or Composite cements (40-64% clinker, 18-30% dross and 18-30 % pozzolana, respectively 31-5o% clinker, 31-50% dross and 31-50% pozzolana) instead of Portland cement. Obviously, the lower allowed clinker contents are strictly related to the strength class. In this case, the mechanical properties of concrete are much closer to the mechanical properties of the masonry as far as strength, flexibility and deformations are concerned.

Another method to ensure the masonry ventilation is the partial covering. The concrete layer does not cover the entire surface of brick pillar, arch or vault. The uncovered lanes remain open.
In some cases (for example, rigid stone masonry walls) the use of reinforced concrete is also recommended in order to develop rigid horizontal slabs to transmit the seismic forces to the vertical bearing system properly. In order to prevent horizontal displacement of the walls, a ring beam of reinforced concrete has to be developed on the slabs' levels (2).

Reinforced concrete is suitable for indirect structural strengthening by additional supporting structures, too (3). The basic idea is to maintain the original structural form, yet observe its weakness or poor technical condition and discharge it from an important part of the vertical load by an additional bearing system. Table 1 includes examples of strengthening with reinforced concrete.

Tab. 1 Strengthening structures using reinforced concrete

Case	Deficiency	Strengthening solution
Vaulted masonry structure Theater of Turda, Romania;	Precarious technical state of the masonry pillars and arches of the basement	Partial covering with reinforced concrete using Pozzolanic cement; Direct strengthening
		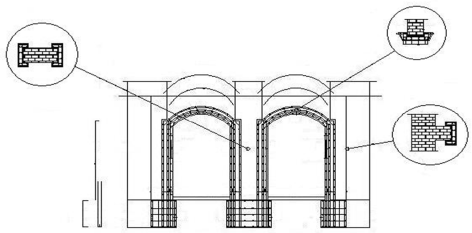
Masonry arches and vaults Basement of the Palace of Justice, Odorheiu-Secuiesc;	Cracks and breaks, detached bricks, large vertical displacements	Reinforced concrete slab on metal beams; Indirect strengthening
		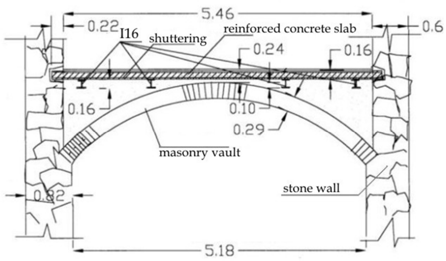

4. CONCLUSIONS

Concerning the practical need as well as international regulations and recommendations, the paper tries to dispel the commonly supported negative perception that the use of reinforced concrete for historical buildings is entirely restricted, which often proves hypocritical.

5. REFERENCES

Bucur-Horváth, I., Popa I., Tănăsoiu, I., (2001) „Study on old masonry structures in brick vaults", Proceedings of the 2nd International Congress on Studies on Ancient Structures, Istanbul, July 2001, Vol.1, pp. 311-322.

Bucur-Horváth, I., Popa, I., Bulbuk, M., Virág, J., (2008), „Historical Constructions – Authenticity and Adaptation to the Modern Demands", Proceedings of the 6th International Conference on Structural Analysis of Historic Constructions SACH, July 2008, Bath, United Kingdom, Volume 1, pp. 169-174.

DESIGN OF PRE-STRESSED CONCRETE BRIDGE GIRDERS – A PRACTICAL APPROACH

Kálmán Koris, István Bódi
Department of Structural Engineering
Budapest University of Technology and Economics
1111 Budapest, Műegyetem rakpart 1-3.

SUMMARY

To facilitate the practical application of European Standards (EN) in Hungary the Department of Structural Engineering at the Budapest University of Technology and Economics was collaborating with the industrial partner SW-Umwelttechnik Ltd. In frames of this collaboration 18 different prefabricated, pre-stressed concrete bridge girders were developed by the exclusive use of EN. Besides the analysis of standalone girders, complete bridge superstructures consisting of the developed beams were also calculated to prove their applicability according to EN. This study introduces the motivation of the work carried out, the aspects and some details of the design process as well as some conclusions on the comparison of the EN and the Hungarian Highway Engineering Regulations in view of the results.

1. INTRODUCTION

After the finalisation of European Standards (EN) in 2006 they were used parallel to the Hungarian Highway Engineering Regulations (*UT 2-3.414:2004*) in Hungary. The UT was primarily based on the Hungarian Standard (MSZ) but it also included some aspects of the EN in terms of approach to the European design regulations. The deadline for the parallel usability of these standards expired on 31st March 2010 and after a nine-month grace period only the EN can be used for the design of engineering structures. To facilitate the practical application of EN the Department of Structural Engineering at the Budapest University of Technology and Economics was collaborating with the industrial partner SW-Umwelttechnik Ltd., one of the largest prefabricating companies in Hungary to control existing prefabricated concrete structural members (originally designed according to MSZ), as well as to develop a range of new prefabricated members by the exclusive use of EN (*Koris et al 2005, Bódi et al 2007*). The aim of this development was also to improve the marketability of the Hungarian prefabricated concrete products in the European market.

As a part of this collaboration new prefabricated, pre-stressed concrete bridge girders were also developed (*Bódi and Koris, 2006*). Altogether 18 different girders with heights of 0.90 m and 1.20 m and lengths between 10.80 m and 32.80 m were designed in detail. Besides the analysis of standalone girders, 8 complete bridge superstructures consisting of the developed beams were calculated to prove their applicability according to EN. Based on the results of detailed analyses the reinforcement and formwork plans of the beams, as well as a short guide for their application were produced.

Designed bridge girders were also examined in terms of diversity of the European Standard and the Hungarian Highway Engineering Regulations. Some of the bridge superstructures mentioned before were also controlled by an independent institution according to the Hungarian Highway Engineering Regulations. Results of these calculations were compared to the results of our previous analyses according to European Standard.

2. DESIGN OF STANDALONE BRIDGE GIRDERS

After considering the typical spans for the application of prefabricated concrete bridge girders in Hungary, two different cross-sections were designed. The beam SHI90 is 90 cm high and can be applied for spans between 10.80–26.80 meters, while the beam SHI120 is 120 cm high and it is suitable for spans between 16.80–32.80 meters. Exact shapes of the cross-sections (Fig. 1) were determined considering the experiences of previous Hungarian road bridge girder types (*Balázs 1995, Koris and Salamak 2007*), as well as the aspects of construction, transportation, erection, economy and durability.

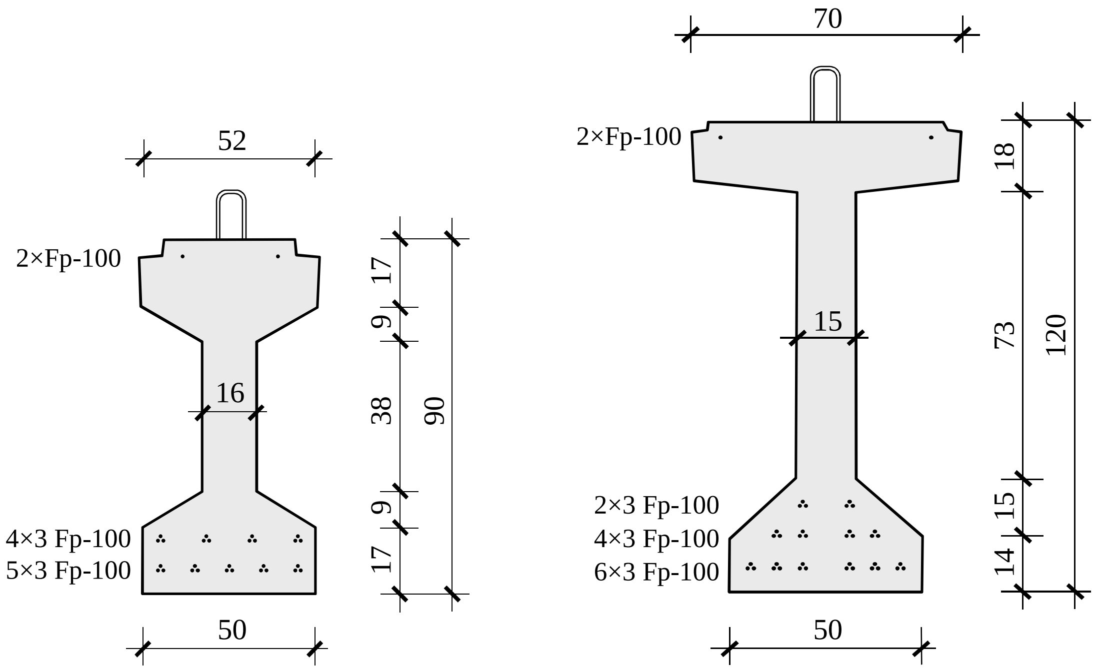

Fig. 1 Cross-sections of beam types SHI90-26.80 and SHI120-32.80

The analysis of the individual beams started with the calculation of the effective pre-stressing force, considering the effect of creep, shrinkage and relaxation according to EN. The distribution of effective pre-stressing force along the length of the beam was determined for each row of the cables. The next step was to control the ultimate limit states including the bending and shear resistances of the girders. The analysed beams are typically used for slab and beam bridges where the prefabricated girder is cooperating with a monolithic reinforced concrete slab. Therefore the ultimate bending moment was also calculated by considering the joint behaviour of the prefabricated beam and the in situ reinforced concrete deck (a 200 mm thick concrete deck was considered in case of SHI90 beams, and a 250 mm thick one in case of SHI120 beams).

The analyses of serviceability limit states (SLS) included the stress limitation, the crack control and the deflection control of the girders. Deflection of the mid-span was calculated in different stages of the construction; namely, after the removal of the formwork, 28 days after concrete casting and in final stage when the beam already supports the weight of the monolithic concrete deck too. Fig. 2 illustrates the maximum deflection of the SHI120 beam 28 days after concrete casting and in final stage as a function of the beam length and the number of the applied tendons.

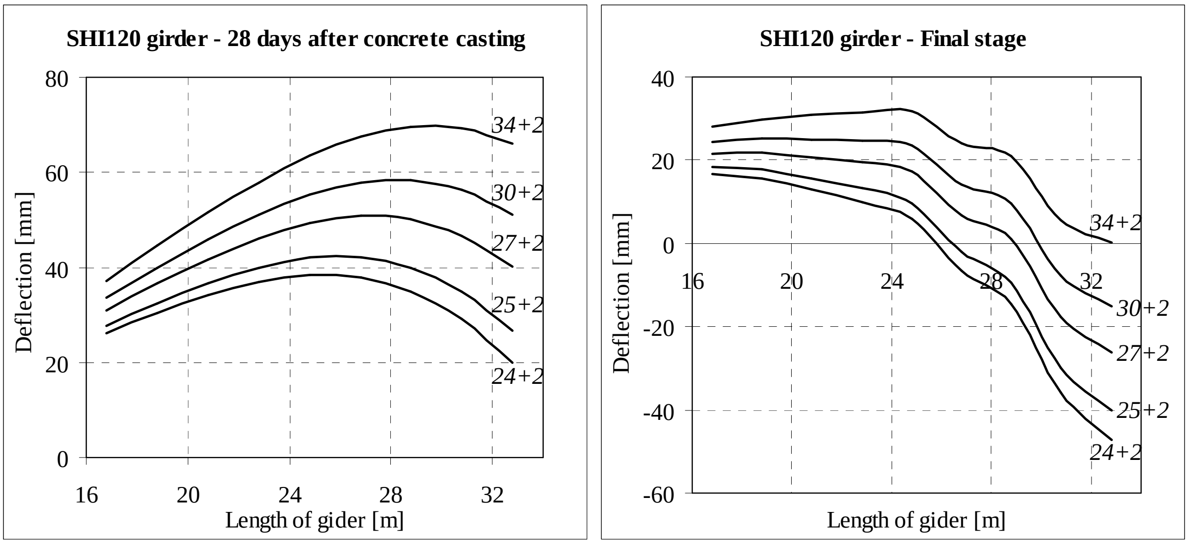

Fig. 2 Deflection of the SHI120 beam 28 days after concrete casting and in final stage.

Besides controlling the ultimate and serviceability limit states, we also analysed the local stress-distribution at the end of the girder. The distribution of transversal tensile stresses at the anchorage of the tendons as well as the necessary reinforcement was determined. Other local effects, like cracking of the corner at the end of the beam, and the local crushing of the concrete at the bearings were controlled, too. Finally, temporary stages were analysed, including the checking of maximum stresses and the possibility of buckling during the lifting of the appropriate girder. After performing the detailed calculation, the formwork and reinforcement plans (containing all the main tendons and steel bars as well as the additional reinforcement) were drawn for each of the 18 pre-stressed beams. A short application guide to the developed beams was also produced.

3. ANALYSES OF BRIDGE SUPERSTRUCTURES

The analysis of standalone bridge girders was followed by the calculation of complete bridge superstructures consisting of the developed beams to prove their applicability according to European Standard. Altogether 8 different bridge superstructures covering the total range of available beam lengths and types were controlled. A possible configuration for a bridge cross-section consisting of SHI120-32.80 beams is displayed in Fig. 3. The internal forces of the sample bridges were calculated by AxisVM civil engineering finite element software, using the appropriate traffic loads for bridges as defined by EN.

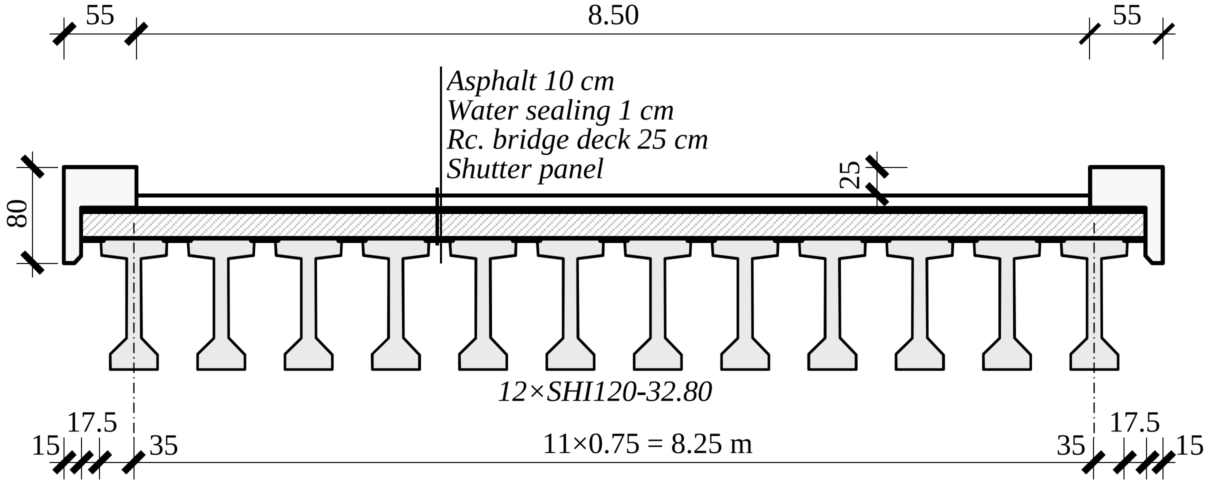

Fig. 3 Cross-section of a bridge superstructure consisting of SHI120-32.80 beams

The resulting forces per prefabricated girder were compared to the previously calculated beam resistance values and all the examined bridge girders proved to be safe against the actions when applied in a bridge superstructure. According to these calculations, the maximum applicable distance between the individual beams was calculated for each beam type separately. The applicable maximum of the unit gross load (excluding the self-weight of the beam) was also determined for both ultimate and serviceability limit states.

4. COMPARISON OF THE RESULTS OBTAINED BY THE EUROPEAN STANDARD AND THE HUNGARIAN HIGHWAY ENGINEERING REGULATIONS

The bridge superstructures mentioned before were also controlled by an independent institution using the Hungarian Highway Engineering Regulations (UT). Considering the differences in live loads (e.g. the tandem load system defined by EN is 25% higher than the concentrated traffic load defined by UT), as well as in safety, combination and dynamic factors, the use of EN delivered about 7% higher design value for bending moment in case of the longest SHI120 beam. However, ultimate limit states were fulfilled in case of both standards. Coming to the comparison of the adequacy in serviceability limit states (SLS), we observed that UT requires slightly more tendons in case of the longest beams to fulfil all the requirements. The main reason for this difference was that in serviceability limit state no tension is allowed by UT in the bottom flange of the girders. The EN is less strict in that manner, requiring only decompression in the same situation. It means that in case of the longest designed beams, the use of European Standard delivers slightly more economical design that the Hungarian Highway Engineering Regulation.

5. CONCLUSIONS

The Department of Structural Engineering at the Budapest University of Technology and Economics was collaborating with the industrial partner SW-Umwelttechnik Ltd. to develop a new range of prefabricated concrete bridge girders using the EN. Standalone prefabricated beams, as well as bridge superstructures consisting of the developed beams were controlled and they proved to be safe against the appropriate traffic actions. Comparing the results obtained by the use of EN and UT standards, we concluded that slightly fewer tendons were required in case of the longest beams by the former standard to be able to fulfil all the requirements of SLS because of the less strict regulations concerning the tensile stresses in the bottom flange.

6. REFERENCES

Balázs, Gy. (1995), „Concrete and reinforced concrete II. – History of concrete and reinforced concrete civil engineering structures“ (in Hungarian), Akadémiai kiadó, Budapest.

Bódi, I., Koris, K. (2006), „Calculation of SHI prestressed bridge girders for administrative qualification process“ (in Hungarian), Budapest University of Technology and Economics, Department of Structural Engineering, Budapest.

Bódi, I., Koris, K., Erdődi, L. (2007), „Parametric analyses of precast reinforced concrete pipes“, Proc. of the 3rd Central European Congress on concrete Engineering – Innovative Materials and Technologies for Concrete Structures, Visegrád, Hungary, pp. 431-436.

Koris, K., Bódi, I., Erdődi, L. (2005), „Parametric analyses of pre-cast concrete structural members“, Proc. of the fib Symposium Keep Concrete Attractive, Hungary, Vol.1, pp. 717-722.

Koris, K., Salamak, M. (2007), „Prefabricated bridge girders in Hungary“ (in Polish), Drogownictwo 62:(11) pp. 367-371.

UT 2-3.414:2004 (2004), „Design standards for road bridges IV. Design of concrete, reinforced concrete and pre-stressed concrete road bridges“ (in Hungarian).

THE EFFECT OF FRICTION ON THE COMPRESSIVE STRENGTH OF CONCRETE SPECIMENS

Miklós Márton[1], Tamás Simon Dr.[1], Adorján Borosnyói Dr.[1]
[1] *Department of Construction Materials and Engineering Geology*
Budapest University of Technology and Economics

SUMMARY

It is known that the friction between the loading plate and the test specimen influences both the shape of the failure and the measurable compressive strength during the testing of compressive strength of concrete. Present paper studies the influences of friction on the measurable compressive strength of concrete specimens. Standard cubes of 150 mm size and C40/50 strength class were tested. During the tests different materials were used between the cube specimens and the loading plates to influence the restraining of the loaded surfaces. It was shown that a movement parameter can characterize the friction between the surfaces.

1. INTRODUCTION

The coefficient of friction is depending on the roughness of the surfaces, the adhesion, the quality of lubrication, the endurance of the contact without movement, the loading rate, the stiffness of the contact points and the rate of slip (Dulácska et al, 2002). If the friction is too high then the material fails in shear.

A loaded specimen deforms in three dimensions. Shortening is realized in the loading direction and elongation takes place perpendicular to the loading direction. The transverse elongation is restrained by the active friction force developing at the contact surfaces. During standard compressive tests the active friction force is always as high as can successfully restrain the transverse elongation of the loaded surfaces. In an unrestrained loaded body the transverse elongation is zero at the axis of the normal force and increases considerably at distances farer from the middle axis (Kausay, 1967; Kotsovos, 1983).

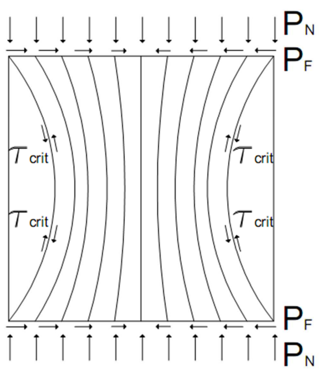

Fig. 1a Shear failure

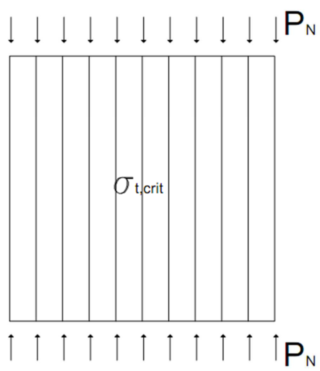

Fig. 1b Failure without restrain

The friction work is proportional to the strain energy, therefore, the active friction force is zero at the axis of the normal force and increases along the contact surface. Only normal force acts along the symmetry axis of the specimen. At other locations the resultant force has also a transverse component that is equal to the active friction force developed at that segment of the loaded surface. Therefore, the direction of the resultant force differs more from the normal force direction at farer locations from the symmetry axis. The trajectories of compressive stresses have the shape of a hyperboloid as a result of the three dimensional stress field. There is no stress from the load within the volume of the specimen located between the extreme compressive stress trajectories and the loaded surface. The highest shear stresses are developed along the extreme compressive stress trajectories that results in the shear failure of the specimen (Fig. 1) (Kausay, 1967; Scheerer, 2009).

2. TEST METHOD

The same batch of C40/50 concrete was used for the preparation of the standard 150 mm cube specimens that were tested both according to EN 12390-3 in compression and for surface friction under controlled conditions detailed in the followings. Friction tests were performed under a constant load of 12 kN. Specimens were loaded vertically by 12 kN normal force and also horizontally with monotonically increasing load by a hydraulic jack. Horizontal load was recorded by a load cell and movement (i.e. slip of the specimen) was recorded by an LVDT. The materials used for the modification of the friction between the specimens and the loading plates were selected with the aim of studying different friction mechanisms. Therefore, solid (rubber sheet and wallboard sheet), granulated (cement, talcum powder, 0/1 mm quartz sand and 1/2 mm quartz sand) and liquid (hydraulic oil) materials were applied. For the solid and granulated materials the layer thickness between the specimens and the loading plates was 2 mm in each case *(Palotás, 1979)*. For comparison, both the compressive strength tests and the friction tests were performed on the concrete specimens without any surface material.

3. RESULTS

Results of the tests are indicated in *Fig 2*. The ranges of the compressive strength of the concrete specimens corresponding to the different surface layers applied are indicated as a function of the movement parameter. The dimensionless movement parameter (δ) in our studies was the ratio of the horizontal load applied by the hydraulic jack at the very moment of the initiation of the slip of the specimen (F_{slip}) under the constant vertical load of F_v = 12 kN ($\delta = F_{slip}/F_v$).

It can be realized that the surface layer dependent compressive strength of the concrete specimens (f_c*) is proportional to the movement parameter (δ) as $f_c^* \propto 2500 \cdot \delta$.

It should be also highlighted that the movement parameter (δ) is not the coefficient of friction but a generalization of it. The movement parameter (δ) covers four different friction type mechanisms:

A. *Real surface friction by sliding of rough surfaces on each other.* This behaviour is indicated in Fig. 2 by 1) as concrete-steel friction and 2) as wallboard plate-concrete friction. During the tests the slips always occurred along the wallboard concrete-plate interfaces and never along the steel-wallboard plate interfaces.
B. *Disturbed surface friction by sliding of rough surfaces on each other with lubrication.* This behaviour is indicated in Fig. 2 by 3) as concrete-steel friction by the application of hydraulic oil. It can be realized that the oil film results a higher value for the movement parameter (δ) due to the increased adhesion at the contact surface, however, the influence on the transverse restraining action of the loading plate is negligible.

C. *Apparent surface friction by the internal friction of granulated materials.* This behaviour is indicated in Fig. 2 by 4) for the talcum powder layer, 5) for the cement layer, 6) for the 0/1 mm quartz sand and 7) for the 1/2 mm quartz sand.
D. *Apparent surface friction by shear action of high deformation capacity solid materials.* This behaviour is indicated in Fig. 2 by 8) for the rubber layer.

Our results confirmed the supposition of other researchers that the surface friction that can restrain the free deformations of a loaded cubic specimen is really proportional to the measurable normal force. It practically also means that the influence can be more pronounced for lower strength concretes and less pronounced for higher strength concretes.

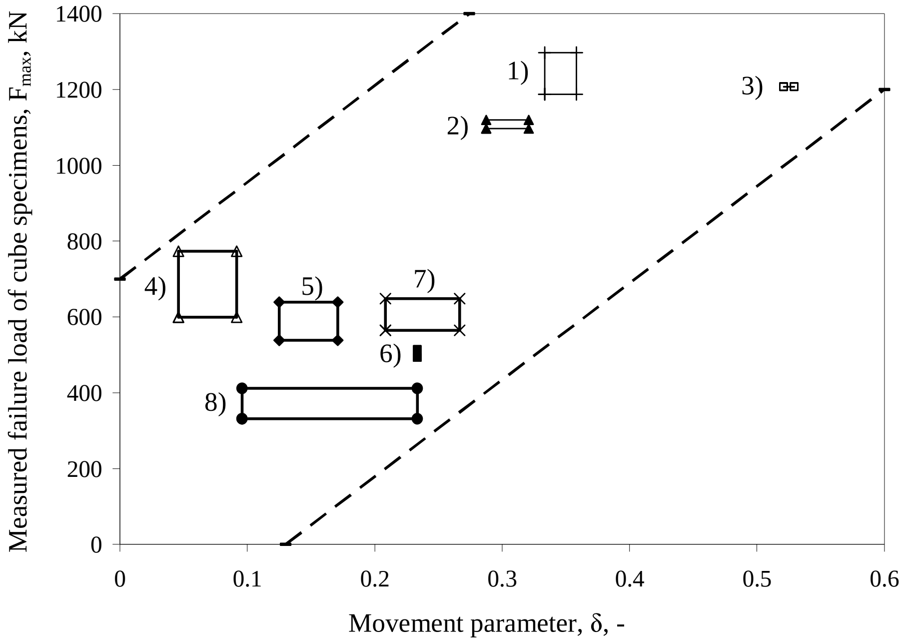

Fig. 2 Measured failure load of cube specimens as a function of the movement parameter

Key: 1) specimens tested according to EN 12390-3 without any surface layer
2) wallboard, wooden plate applied as surface layer
3) hydraulic oil applied as surface layer
4) talcum powder oil applied as surface layer
5) cement applied as surface layer
6) 0/1 mm quartz sand applied as surface layer
7) 1/2 mm quartz sand applied as surface layer
8) rubber plate applied as surface layer

4. DISCUSSION

Typical failure modes of the tested specimens are indicated in Fig. 3. The photographs can also confirm the importance of the surface friction on the behaviour of concrete cube specimens in compression. Failure mode can be changed from the completely restrained shear failure (see also Fig. 1.a) to the unrestrained, rupture type failure (see also Fig. 1.b) by the application of different surface layers. The movement parameter (δ) introduced in present studies can clearly indicate the severity of the restraining action activated or blocked by different materials between the specimens and the loading plates.

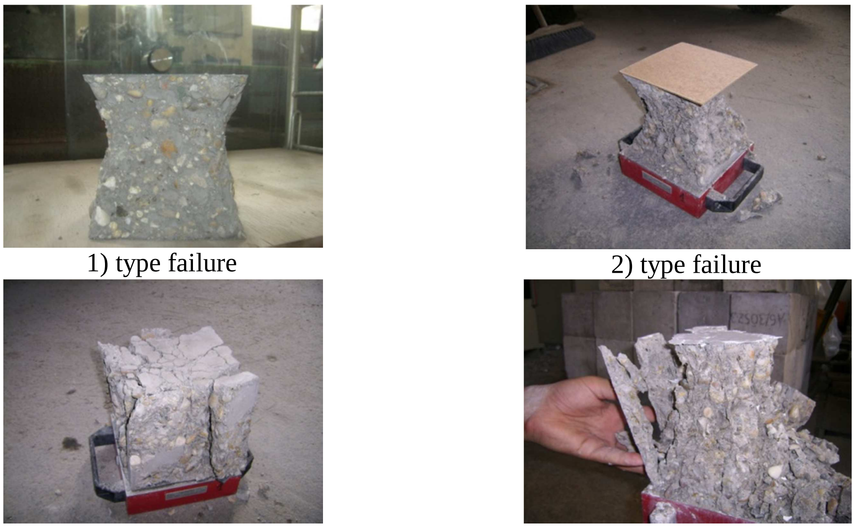

1) type failure 2) type failure

4) type failure 8) type failure

Fig. 3 Typical failure modes

5. CONCLUSIONS

Present paper summarized the influences of friction on the measurable compressive strength of concrete specimens. Standard cubes of 150 mm size and C40/50 strength class were tested. During the tests different materials were used between the cube specimens and the loading plates to influence the restraining of the loaded surfaces. Solid (rubber sheet and wallboard sheet), granulated (cement, talcum powder, 0/1 mm quartz sand and 1/2 mm quartz sand) and liquid (hydraulic oil) materials were applied.
It was shown that a movement parameter can characterize the friction between the surfaces. The dimensionless movement parameter ($\delta = F_{slip}/F_v$) can be defined by laboratory friction tests as the ratio of the horizontal load at the very moment of the initiation of the slip of the specimen (F_{slip}) and the vertical load (F_v).
The movement parameter can be considered as a generalization of the coefficient of friction.
It can be realized that the surface layer dependent compressive strength of the concrete specimens (f_c*) is proportional to the movement parameter (δ) as $f_c^* \propto 2500 \cdot \delta$.

6. ACKNOWLEDGEMENT

Authors express their gratitude to Mr. Mihály *Deák* for his help during the laboratory tests.

7. REFERENCES

Dulácska, E., Csák, B., Orosz, L. (2002) „The friction of concrete”, *Vasbetonépítés* 2002/3 pp. 83-93. (in Hungarian)
Kausay, T., (1967) „The importance of the particle shape in concrete strength”, *Építőanyag*, XIX/3 (1967) pp. 110-115. (in Hungarian)
Kotsovos, D., M. (1983) „Effect of testing techniques on the post-ultimate behaviour of concrete in compression” Material and Structures Volume 16. (1983) pp. 1, 3-16.
Palotás, L., (1979) „Engineering materials, Vol. 2, Timber-Stone-Metals-Binders”, Akadémiai Kiadó, Budapest, 586 p. (in Hungarian)
Scheerer, S., (2009) „High performance lightweight concrete under multiaxial compression” Technische Universitat Dresden,Schriftenreihe Heft 21, pp. 17-52. (in German)

INFLUENCE OF SHEAR RESISTANCE ON DUCTILITY OF BENDED FIBRE REINFORCED ELEMENTS

Jan Vodička[1], Jiří Krátký[1], Hana Hanzlová[2], Jitka Vašková[2]
[1] *Profesional Association for Science, Research and Consultacy, Komornická 15, 160 00 Prague 6.*
[2] *CTU in Prague, Faculty of Civil Engineering, Thákurova 7, 166 29 Prague 6, Departement of Concrete and Masonry Structures*

SUMMARY

The paper deals with types of failure of fibre reinforced beams with standard reinforcement of two ductility classes. It is shown in the graphs of relation between the force and deflection. The types of failure are discussed. There are the basic recommendations how to protect brittle failure of flexural concrete beams.

1. INTRODUCTION

To check possibilities of replacement of shear reinforcement at the reinforced concrete structures by the steel fibres were draft destruction tests simulated the failure due to flexural - shear strength by bending of reinforced concrete beams with the size 100/150/1800mm, with the effective span l = 1500mm, according the Fig.1. All the beams are reinforced by two longitudinal rebars (2 Ø 10) - strength class of reinforcing steel B500, in two variants of ductility class A and C (i.e. B500 A and B500 C e.g. EPSTAL).

To cause rather shear failure than the failure caused by bending moment for test loads were moved the symmetrical forces $F/2$ to the mid point of beam closer to supports – on the distance c = 600mm between the forces, i.e. on the critical shear slenderness of the beam $\lambda_v = a / h = 450 / 150 = 3{,}0$ (see Figure 1). (For testing flexural failure of beams the distance between the forces c = 200mm, was used, i.e. $\lambda_v = 650 / 150 = 4{,}33$.)

For the verification of the influence of steel fibres on the shear and bending load capacity there were compared SFRC beams reinforced not only by rebars (2Ø10) but also by steel fibres of three types (notation SFRC) with concrete beams without fibres reinforced only by longitudinal rebars (2Ø10) (notation RC). The volume ratio $\rho_{v,f}$ for all types of steel fibres is equal $\rho_{v,f}$ = 0,5% (i.e. $m_f \approx 40\text{kg/m}^3$).

For the three used types of steel fibres was demonstrated the influence of type of fibres on the characteristic strengths of concrete in compression and tension by macro-cracking.

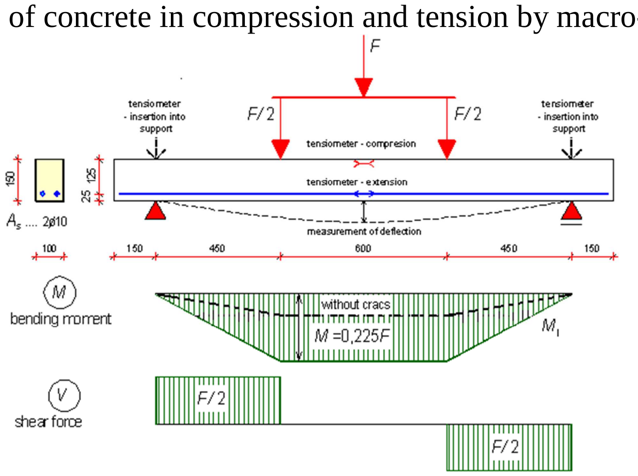

Fig. 1 Adjustment of test flexural – shear strength by bending

2. LOAD BEARING CAPACITY OF TESTED BEAMS

The load bearing capacity of tested beams was affected by nature of failures. The shear failures as shear cracking, anchoring failure or crushing of concrete due to interaction of shear and compression stresses are mostly brittle failures (see Fig. 2.1 and 2.2), contrary to flexural cracking failures that are ductile when the rebars of high ductility are used (B500 C – see Fig. 3.2). Rebars with low ductility (B500 A) have many times caused the tensile failure of rebars (see Fig. 3.1).

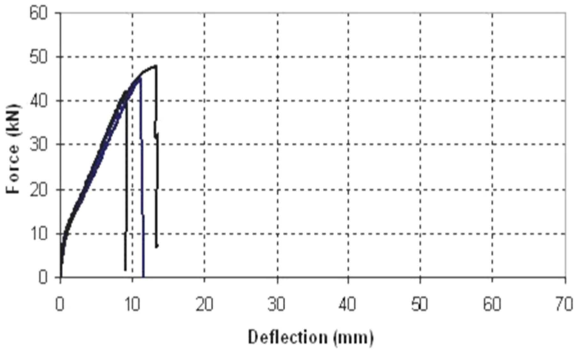

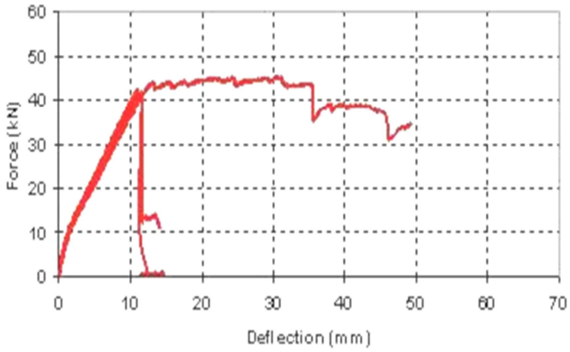

Fig. 2.1 RC beam (2Ø10 of ductility class B500 A) without fibres (Left)
Fig. 2.2 RC beam (2Ø10 of ductility class B500 C) without fibres (Right)

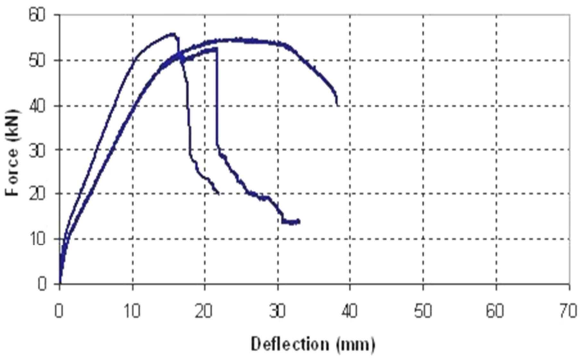

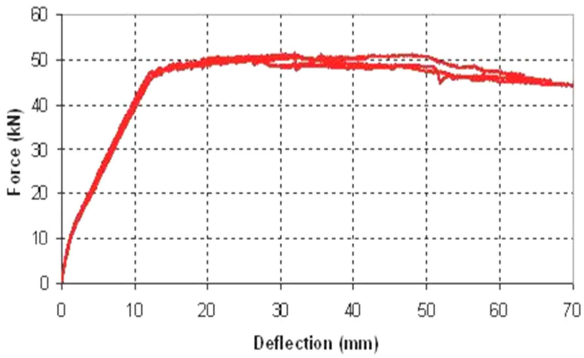

Fig. 3.1 SFRC beam with Dramix 35 (2Ø10 of ductility class B500 A) (Left)
Fig. 3.2 SFRC beam with Dramix 35 (2Ø10 of ductility class B500 C) (Right)

We have two types of failure – shear and flexural failure (see Fig. 4 and Fig. 5). The load bearing capacity of SFRC beams ($\rho_{v,f}$ = 0,5%) is about 10-20% bigger than of RC beams (without fibres).

The ductility of SFRC beams denoted by the influence of the deflection at beams load bearing capacity is greater than that of RC beams about 100% (for B500 A) to 165% - 300% (for B500 C).

Shear cracking

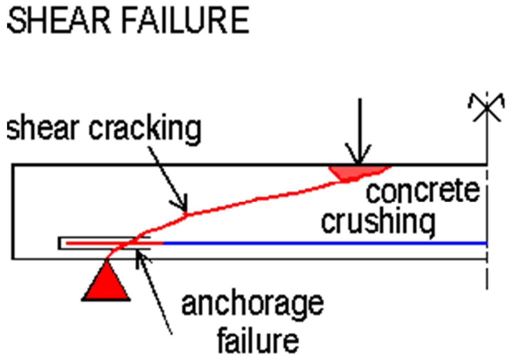

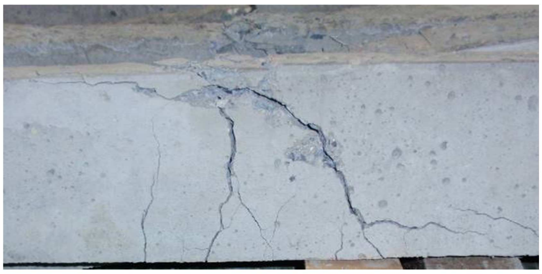

Anchorage failure

Crushing of concrete

Fig. 4 Types of failure – shear failure

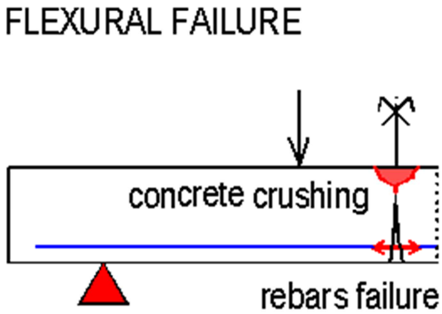

Flexural cracking failure

Rebars tension failure

Fig. 5 Types of failure – flexural failure

3. CONCLUSIONS

With regard to the brittle shear failure it is necessary to prevent its existence. That can be attained by using:

- higher volume ratio of fibres $\rho_{v,f} > 0,5\%$,
- combination of fibres and shear reinforcing steel stirrups of high ductility.

The experimental research verified:

- RC beams reinforced with steel rebars B500A attained deflection δ_m = 9,0 mm (100%) by brittle shear failure, with steel rebars B500C δ_m = 11,5 mm (128%) at the same load bearing capacity F_{um} = 42,0 kN,
- SFRC beams reinforced with steel rebars B500A attained deflection δ_m = 16,0 mm (178%) by brittle shear failure, with steel rebars B500C δ_m = 27,5 mm (305%) by ductile failure at the same load bearing capacity F_{um} = 52,0 kN.

To prevent the primary brittle failure in transverse shear of flexural beams consideration should be given to interaction of fibre-reinforced concrete with stirrups made of steel with high ductility class and ensure the high deflection of beams at flexural failure.

4. ACKNOWLEDGEMENTS

This work was supported by Czech Science Foundation, grant project 103/09/2039 and partial results of grant project 103/07/1275 were utilized.

5. REFERENCES

Krátký, Vodička, Vašková, Determination of Tensile Part of Fibre Concrete Stress-Strain Diagram from Bending Test Measurements, In: Proceedings of 5th Intern. Conference Fibre Concrete - Technology, Design, Application. Praha: ČVUT v Praze, Fakulta stavební, 2009, p. 167-174. ISBN 978-80-01-04381-3

Vašková, J. - Krátký, J. – Vodička, J. - Hanzlová, H. Evaluation of FC for Determination of Design Parameters In: Innovative Concrete Technology in Practice. Vienna: Austrian Society for Concrete and Construction Technology, 2009, p.319-322

Krátký, J. - Vašková, J. - Hanzlová, H. – Vodička, J. General Principles of the Design of Fibre Concrete Structural Elements. In: Proceedings of 6th CCC Congress in Mariánské Lázně 2010 - Concrete Structures for Challenging Times. Praha: ČBS - Česká betonářská společnost ČSSI, 2010, p. 435-438. ISBN 978-80-87158-26-5.

Krátký, J. - Vodička, J. - Vašková, J. - Hanzlová, H.: Assumptions for Design of Fibre Concrete Structural Elements In: Proceedings of Conference Fibre Reinforced Materials. Singapore: CI-PREMIERE PTE LTD, 2010, p. 191-198. ISBN 978-981-08-5198-9.

THE TENSILE BEHAVIOUR OF A NEW CONSTITUTIVE MODEL FOR MASONRY JOINT

Anita Fódi[1], *István Bódi*[1]
[1] *Department of Structural Engineering*
Budapest University of Technology and Economics
1111 Budapest, Műegyetem rakpart 1-3.

SUMMARY

The aim of the paper is to introduce a constitutive model being able to follow the pre-peak softening of the masonry joints. Experimental investigations were performed by a numerical model using this model. By dividing the masonry joint into small pieces, and by ordering different stiffness and tensile strength drawn from Gaussian distribution to each piece the desired behaviour is obtained. The paper presents the effects of the different parameters of the constitutive model.

1. INTRODUCTION

Based on former experimental investigations (*Fódi, Bódi, 2010, 2011*) the occurrence of the failure was stated at the mortar-unit surface of plain and reinforced masonry walls subjected to shear. These failure modes are: (1) tensile stress arises between the unit and mortar, which is characteristic in case of low values of compressive strength. (2) Slip in the bed and head joints in case of low compression and high unit tensile strength. (3) The tensile failure and the diagonal crack of the unit, in case of high compressive stress and low tensile strength. (4) The compressive failure of the joint and the unit. In this paper the tensile behaviour of the unit-mortar joint is investigated numerically.

2. SET OF THE PROBLEM

A numerical model was built to simulate the tensile behaviour of the masonry joint (*Fódi, Bódi, 2011*). It was demonstrated that the joint stiffness at the beginning of the loading matches the experimental results; however, the pre-peak behaviour is not perfect. The failure is too sudden compared to the experiments, which is attributed to the material heterogeneity, not every part of the material fails in the same minute. The joint is assumed to contain microcracks, which makes the behaviour softer in the experiments than in the model and causes an internal mechanism of progressive damage of joints under shear. In the model the plasticity conditions govern the failure. They describe for each point of the solid what kind of stress state results in the plasticity of the point. Flow rules specify how the point of the material behaves after plasticity and they are activated when plasticity conditions are fulfilled. Stiffness degradation does not take place before failure in the model. In this paper the material defects and stiffness degradation of the joint are intended to be built in the model.

3. THE EXPERIMENTS SIMULATED

The tensile behaviour of unit-mortar joint was investigated by *Van der Pluijm, 1997* on 4 different types of bricks. Fig. 1 shows the tensile behaviour of the joint for the brick and mortar most similar to the Hungarian ones. It can be seen that the tensile strength is between 0.14-0.81 N/mm^2 (coefficient of variations: 40 %). The test setup is shown in Fig. 1. One diagram was selected to approximate by numerical calculations.

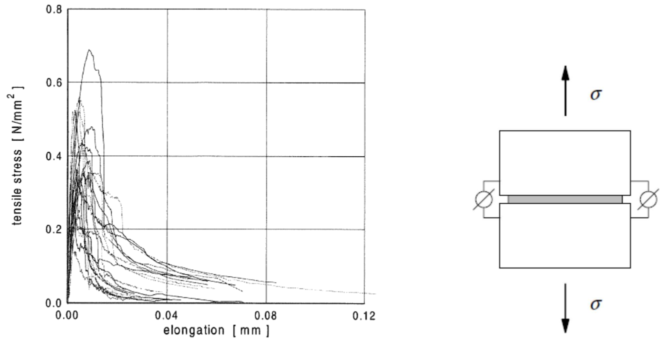

Fig. 1 The experimental investigation of *Van der Pluijm, 1997*

4. THE MODEL INTRODUCED

According to the three types of masonry modelling defined by *Lourenço, 1996* the simplified micromodel was chosen. For the accurate description of the joint area contact with Coulomb slip failure the following parameters are required: cohesion, tensile strength, dilatation and friction angle, normal and shear stiffness. The post-peak behaviour is performed by the dilatancy angle that is activated after the onset of the failure. The dilatancy is the change in volume that occurs through the shear distortion of a material. In *Fódi, Bódi, 2011* it was proved that the joint normal stiffness and the tensile strength have the most dominant effect on the joint tensile behaviour. For simulating the pre-peak softening behaviour, the method developed is to assign different normal stiffness and tensile strength in certain places of the joint already before the loading. Proving this statement a program was implemented in FISH language ordering random stiffness to certain places of the joint according to a given distribution. First, the joint is split into small pieces. Then certain amounts of random stiffness values are drawn from normal or uniform distribution. One stiffness value is joined to every piece of the joint. In the following the different effects of the model parameters are presented.

5. THE EFFECTS OF PARAMETERS INFLUENCING THE MODEL BEHAVIOUR

The following effects can have an influence on the model behaviour: the velocity of the loading, the size of the mesh within the block (because the joint has the same mesh, that the bricks have), the type of the distribution, the amount of the pieces that the joint is split into, the amount of material types that are generated, the properties that have nonzero standard deviation. In this paper all these effects are investigated.

5.1. The effects of the type of the distribution, the loading velocity and the mesh sizes

Fig. 2, diagram 1 shows the contact behaviour in case of zero standard deviation and the tensile strength of 0.35 N/mm^2. Diagram 2 shows if the joint is divided into 12x50 pieces and every piece has the same characteristics and the tensile strength of 0.65 N/mm^2. If one of 40 different normal stiffness values, according to uniform distribution, is assigned to each of the 600 joint pieces almost the same diagram, 3, is obtained. If the stiffness values are generated according to Gaussian distribution with the same standard deviation the desired softening can be obtained. Diagram 5 shows the behaviour with the same parameters as 1, however, with denser mesh. The denser mesh affects only the post-peak behaviour of the joint and the running time is three times longer than in case of a looser mesh. Looser mesh means the loosest mesh density giving the same result as the denser. Therefore, every run was performed with the looser mesh. The loading velocity was chosen for the value that does not alter the behaviour compared to the lowest velocity and provides reasonably quick convergence.

5.2. The effect of the coefficient of variation (COV) of the joint normal stiffness

Different normal stiffness values were assigned to the joint pieces according to normal distribution. Fig. 3 shows the joint behavior for the same parameters as diagram 4. In case of diagram 4, 6 and 7 the COV of the normal stiffness is 56%, 66% and 73%, respectively. It could not be stated clearly that the best applicable value to approximate the experimental diagram is between 66-73 %. For example, diagram 8 presents 56% COV of the normal stiffness and 40 % of the tensile strength.

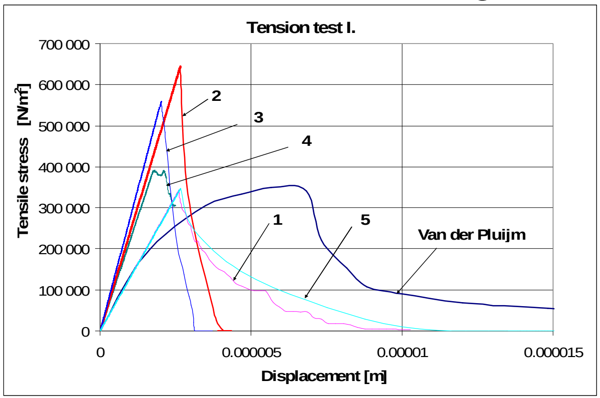

Fig. 2 Stress-displacement diagrams

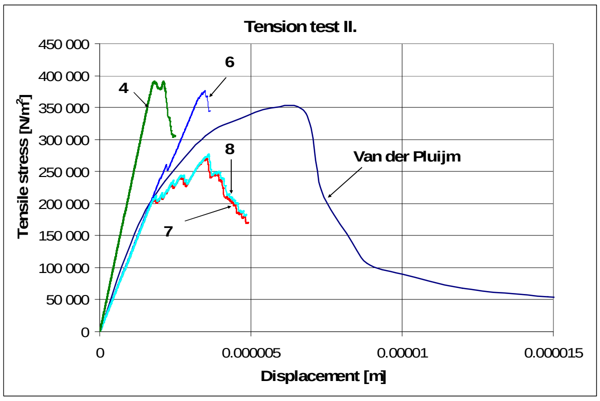

Fig. 3 Effect of the COV of the normal stiffness

5.3. The effect of the coefficient of variation of the joint tensile strength

It is necessary to investigate the effect if only the joint tensile strength has nonzero standard deviation. Diagram 11 shows the result with 0 COV, and tensile strength of 0.35 N/mm^2. 12, 13, 14 and 16 present the 1.42 %, 14.2 %, 33% and 65.7% COV of the tensile strength. Diagram 15 shows the behaviour in case of 33 % COV in the normal stiffness. Diagram 15 is almost the same as the experimental results; it has to be “magnified”, by increasing the tensile strength of the joint to 0.74 N/mm^2 and COV of 65.7 % (diagram 17).

5.4. The effects of the standard deviation of the normal stiffness and the tensile strength

These effects were investigated by splitting the joint into 12x50 pieces. In case of diagram 19 and 20 the normal stiffness and the tensile strength also have the COV of 33 % and 50 % and the tensile strength is 0.9 instead of 0.65 N/mm^2. Diagram 21, 22 and 24 present 50 %COV of the stiffness and 55, 62.5, 30.7 % of the tensile strength. Diagram 22 and 23 have the same, 62.5 % COV of tensile strength, the stiffness values are different (COV 50 and 62.5 %).

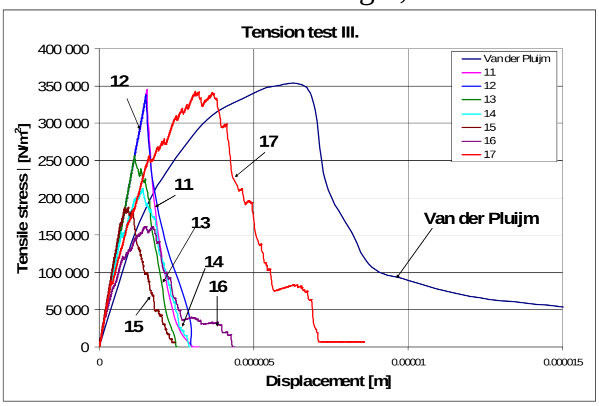

Fig. 4 Effect of the COV of the tensile strength

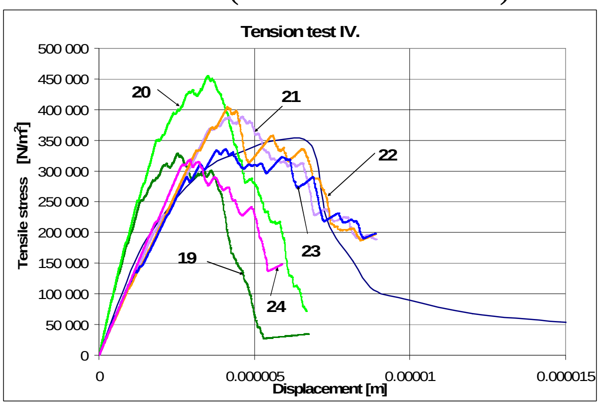

Fig. 5 Effects of the COV of the normal stiffness and tensile strength

5.5. The effect of the number of the joint pieces

Fig. 6 shows how the joint behaves by splitting the joint in the case of a: into 12x50 pieces, b: 6x24, c: 2x1, d: 1 and e: 3x8. Every parameter was the same in all cases, the number of the joint pieces is modified. Both the normal stiffness and the tensile strength have nonzero standard deviation (COV 33% and 50%).

5.6. The effect of the amount of the material types

Fig. 7 shows the effect of the number of material types that can be assigned to the joint pieces. Every other parameter is the same as in Chapter 5.5. In case of a, f, g and h 40, 30, 10 and 5 material types are defined. In the case i 2 types of materials are distributed between 600 joint pieces. Varying the number of the joint pieces and of materials every diagram of Fig. 1 can be obtained. If one single diagram needs to be demonstrated the most pieces and materials have to be defined. If all the diagrams in the envelope of Fig. 1 should be obtained 24 joint pieces are enough in case of 40 material types or for 600 joints 5 types of materials are adequate.

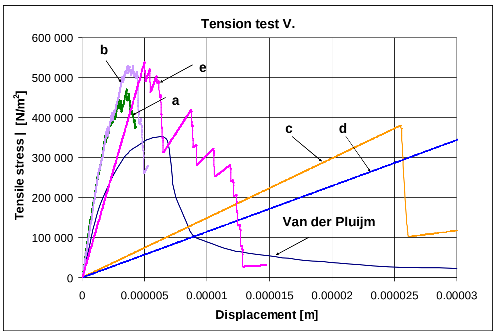

Fig. 6 The effect of the joint pieces

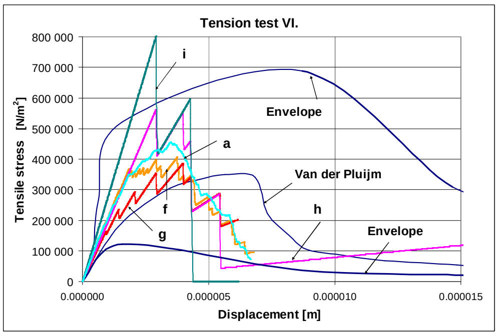

Fig. 7 The effect of the material types

6. CONCLUSIONS AND FURTHER APPLICATIONS

In the paper a constitutive model was introduced that simulates the pre-peak softening of the masonry joint. By separation of the joint into pieces, and by ordering different normal stiffness and tensile strength to every piece drawn from Gaussian distribution the experimental behaviour was obtained. Parameters were suggested for approximation of one single diagram and for the envelope of the experimental series. The here introduced joint constitutive model is intended to implement in the model of masonry structures.

7. ACKNOWLEDGEMENTS

The Authors would like to express their grateful thanks to the Itasca Consultants SAS for providing the program 3DEC in the framework of the Itasca Education Partnership Program.

7. REFERENCES

Fódi, A., Bódi, I., (2010) „Comparison of shear behaviour of masonry walls with and without reinforcement“, POLLACK PERIODICA, Vol. 5. No. 3: pp. 71-82.

Fódi, A., Bódi, I., (2011) ”The behaviour of a simplified micromodel for masonry”, HCTAM, 2011, 11th Hungarian Conference on Theoretical and Applied Mechanics, August 29-31, Miskolc, Hungary (under publication)

Lourenço, P. J. B. B., (1996), „Computational strategies for masonry structures”, Doctoral dissertation, Delft University Press

Pluijm, R. v. D., (1997), „Non-linear behaviour of masonry under tension”, HERON, Vol. 42, No. 1: pp. 25-54.

NUMERICAL MODELLING OF CONCRETE STRUCTURES WITH GFRP MEMBERS

Peter Koteš[1], Katarína Serdelová[1]
[1] *Department of Structures and Bridges*
Civil Engineering Faculty, University of Žilina,
010 26 Žilina, Slovakia, Univerzitná 8215/1

SUMMARY

The paper is focused on numerical modelling of bonding between GFRP formwork and concrete. The stay-in-place GFRP formwork with concrete slab creates composite system *(Naď et al 2009)*. This system is able to use on floors in building structures *(Koteš et al 2009)*. The load-carrying capacity of the composite system is highly influenced by quality of bonding between GFRP formwork and concrete. The results from numerical modelling will be compared with results from experiment.

1. INTRODUCTION

The ATENA software was used for the numerical analyses of push test specimens *(Červenka et al 2009)*. The FEM model corresponding to real specimens from experimental measurements shown in Fig.1 was created. Due to not exactly symmetrical shape of the specimens, the symmetry was not used. It means that the full specimen was modelled, not only half or quarter of specimen. The material characteristics used for modelling are shown in Tab. 1.

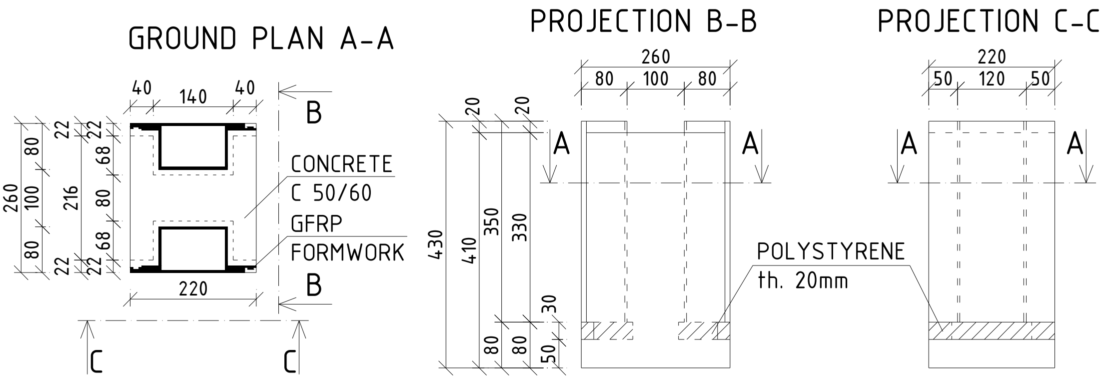

Fig. 1 Arrangement of the sensors

Tab. 1 The review of the used material characteristics

Material	Material element
Concrete	3D Nolinear Cementitious 2, f_{cu} = 50.0 MPa (C40/50)
Reinforcement	Reinforcement, linear, E = 210 GPa; f_y = 500 MPa
Steel plate	3D Elastic Isotropic, E = 210 GPa; f_y = 210 MPa
GFRP profile	3D Bi-linear, steel Von Mises, E = 25000 MPa; strength f_{tk} = 200 MPa; poisson coefficient ν = 0.25

The important part of the work was modelling the contact between internal concrete part and GFRP profile. The material model "3D Interface" was used in Atena. This model is used for contact modelling between two various elements.
The interface material model "3D Interface" is based on Mohr-Coulomb criterion with tension cut off. The constitutive relation for a general three-dimensional case is given in terms of tractions on interface planes and relative sliding and opening displacements and it is given by formulae

$$\begin{Bmatrix} \tau_1 \\ \tau_2 \\ \sigma \end{Bmatrix} = \begin{bmatrix} K_{tt} & 0 & 0 \\ 0 & K_{tt} & 0 \\ 0 & 0 & K_{nn} \end{bmatrix} \begin{Bmatrix} v_1 \\ v_2 \\ u \end{Bmatrix} \tag{1}$$

where: τ is shear stress in direction x and y,
σ is normal stress,
v is relatively displacement on surface,
u is relatively opening of contact,
K_{tt} is initial elastic shear stiffness,
K_{nn} is initial elastic normal stiffness.

The initial failure surface correspond to Mohr-Coulomb condition with tension cut off

$$|\tau| \le c + \sigma \cdot \phi, \quad \text{for } \sigma \le f_t, \tag{2}$$

$$\tau = 0, \quad \text{for } \sigma > f_t,$$

where: c is cohesion,
ø is coefficient of friction,
f_t is tension strength on surface.

After stresses violate this condition, the surface collapses to a residual surface which corresponds to dry friction (Fig. 2).

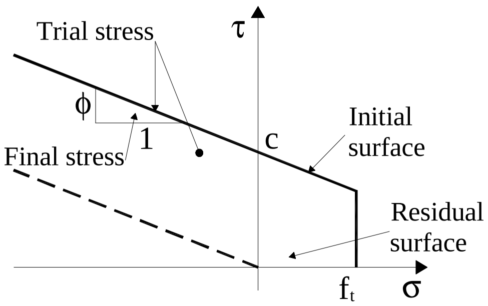

Fig. 2 Failure surface for interface elements

The cohesion c is equal to surface stresses σ_{surf} achieved from the experiment. There was modelled only one representative specimen P2 in the numerical analysis, so, the value of cohesion $c = 9.797 \cdot 10^{-2}$ MN/m^2 was considered. The values of initial elastic normal and shear stiffness are estimated from formulas

$$K_{nn} = \frac{E}{t}, \quad K_{tt} = \frac{G}{t}, \tag{3)(4}$$

where: E is minimal elastic modulus,
G is minimal shear modulus,
t is width of interface zone.

The K_{nn} and K_{tt} get extremely high values (approaching to infinity) because the width of interface zone t between concrete and GFRP girder is approaching to zero value. According to

(Červenka et al 2009), it is not recommended to use so high values because leading to numerical instabilities during calculation. From this reason, the values $K_{nn} = K_{tt} = 6.5 \cdot 10^7$ MN/m^3 were considered.

The value of friction coefficient ø between concrete and GFRP is not generally known, so, it was forecasted to approximate value 0.1. Within the ambit of sensitive analysis, the following values of the friction coefficient were used ø = 0.025; 0.050; 0.075; 0.100; 0.125; 0.150. The 3D model of Push test specimen created in software Atena is shown in Fig. 3.

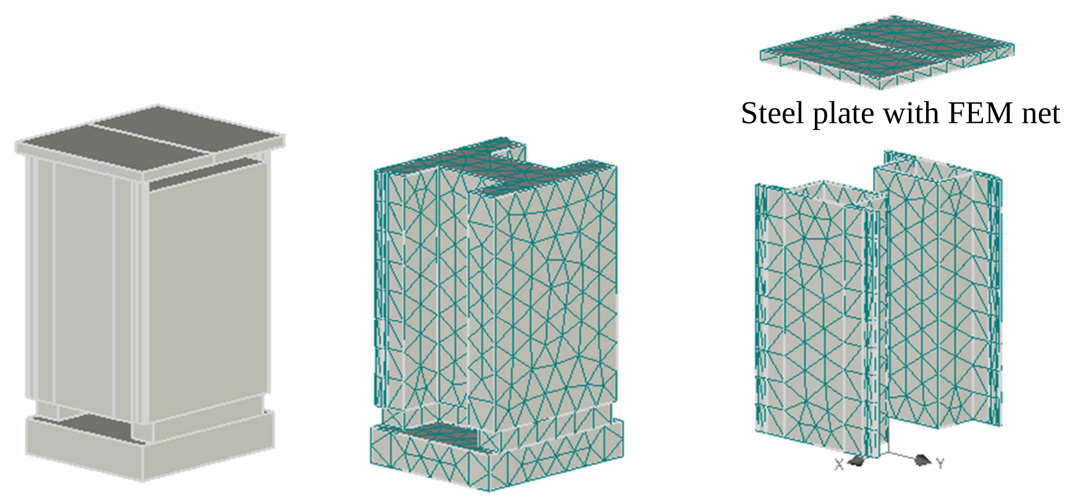

Fig. 3 3D FEM model of Push test specimen

2. RESULTS OF NUMERICAL ANALYSIS

The numerical specimen was loaded step by step by deformation of steel plate 0.1 mm in down direction. At the same time, a force F corresponding to given deformation (as loading) was calculated as response to given deformation by software Atena.

The force increasing F depending to loading by deformation 0.1 mm step by step is shown in Fig. 4. The shown forces F are depended to friction coefficient and they are shown values just in one observed location (monitor). Similar values were achieved in all observed monitors.

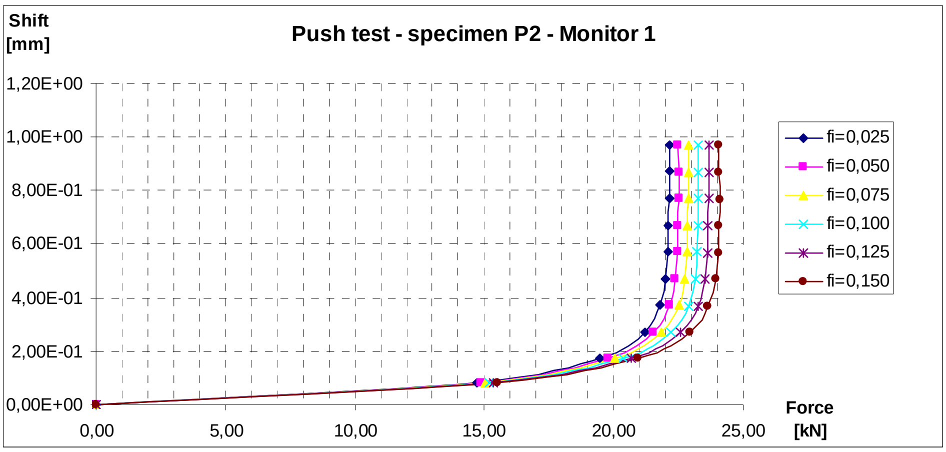

Fig. 4 Increasing of forces F to loading – numerical model

The contact failure occurs at the time when the force is not increasing (Fig. 4). From the results follow that max load force at bond failure F_{max} is very influenced by value of friction coefficient ø. The maximum calculated forces F_{max} and the surface stresses σ_{surf} at the bond failure are shown in Tab. 2 and Fig 5.

Tab. 2 Max load force and surface stress at bond failure

Friction coefficient ø [-]	**0.025**	**0.050**	**0.075**	**0.100**	**0.125**	**0.150**
$\mathbf{F_{max}}$ [kN]	22.13	22.51	22.89	23.27	23.67	24.08
$\boldsymbol{\sigma_{surf}}$ [kN/m^2]	91.86	93.44	95.02	96.60	98.26	99.96

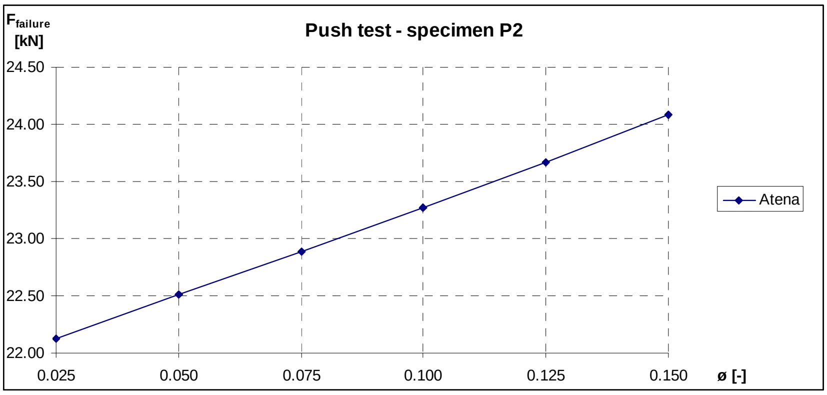

Fig. 5 Max forces F_{max} corresponding to failure – numerical model

The values F_{max} are close to be linear dependence to friction coefficient ø. The optimal value of friction coefficient ø = 0.12 corresponding to experimental results was backward calculated.

3. CONCLUSIONS

The same material characteristics as in experiment were used in the numerical model. The value of friction coefficient ø occurs as questionable parameter in the numerical modelling due to not know common value. From this reason, the sensitivity analysis was executed. This analysis shows the indispensable influence of friction coefficient value on bonding between GFRP and concrete. The optimal value of friction coefficient ø = 0.12 was backward calculated. The experiences and verified parameters of contact from numerical modelling of push test will be used on numerical modelling of entire composite girder. The increasing of bonding between GFRP and concrete can be achieved using appropriate surface treatment, as for example, using rougher surface (lugs) or sand-blast of GFRP surface.

4. ACKNOWLEDGEMENTS

This work was supported by Research Project no. 1/0461/10 supported by Slovak Grant Agency.

5. REFERENCES

Červenka, V. – Červenka, J. – Jendele L. (2009) „ATENA Program Documentation, Part 1, Theory“, www.cervenka.cz.

Koteš P., Vičan J., Nad', Ľ. (2009) “Stay-in-place GFRP formwork, Part 1 – Girders”, XVIII. Russian-Slovak-Polish seminar „Theoretical foundation of civil engineering“, Moscow - Archangelsk, Russia, p. 259-264

Nad' Ľ., Špernoga B., Bajzecer A. (2007) “Structural stay-in-place GFRP formwork-concrete deck: new type of composite structure”, 8-th International Conference FRPRCS-8, Patras, Greece

AUTOMATED PRESTRESSING APPLICATION IN MATHCAD

Sándor Gábor – Álmos
Technical University of Cluj-Napoca
400114 Cluj-Napoca, Romania, Memorandumului str. 28

SUMMARY

The Following paper presents an application sheet, created in MathCAD for designing and verifying Prestressed Concrete Beams, according to EC2. The Application includes several parts, such as: own static module, own cross section calculation module (area and inertia, neutral axis), included materials (both Steel and Concrete), SLS an SLU verifications (diagrams for the entire length of the beam), Design of Shear Resistance, etc.
The paper also presents the modality of creating such an intelligent worksheet and relates of the advantages and disadvantages of using MathCAD for such a delicate matter.

1. INTRODUCTION

The idea of automation the algorithm for the calculation of prestressed concrete members is preoccupying the engineers for a long time, and it is a really delicate matter. Although several software are dedicated to the calculation of such elements, these are very expensive. So came the idea of creating an intelligent worksheet, which is based on an easy to use and well spread software, and is popular enough in the circles of students and planning firms.
The choice fell on MathCAD, because it sits at the base of all precise engineering calculations, and in the same time assures a quick and effective workflow, eliminating the chance of human errors. It is based on an effective and performant mathematical module, is easy to use, so it permits the creation, calculation and formatting of the mathematical formulas within the same file. Its main characteristic is that it doesn't need superior programming skills neither at the creation of worksheets, nor at their usage.

2. THE APPLICATION APAM

APAM (Automatised Prestressing Application in MathCAD) is software dedicated for dimensioning and verifying of prestressed concrete girders. At this moment it is still under development, so it enables the calculation of beams with constant height, but it permits the usage of fully, partially or limited prestressing method. The program is divided into multiple parts (modules) so it is easy to use and user friendly.

2.1. Material Library

The software contains multiple concrete classes defined in EN 1992-1, from C30/37 to C90/105. It enables also the usage of custom materials, for the situation in which the user wants to perform his calculations based on a specific concrete recipe. In a similar way, there are included several types of steel grades (both flexural steel and tendons). These can also be changed to custom ones for the case we would like to work with a specific steel grade or tendon type. The material library grants the user a quick change of materials, if needed, and offers the possibility of a quick preview for the different proprieties of the materials.

2.2. The cross section and its proprieties

In APAM the introduction of the cross section is realized trough different tables. For the concrete section, it is enough to introduce the semi-coordinates of the cross section, the other part being automatically generated based on the introduced coordinates. However, for the reinforcements and the tendons, an exact positioning is required, for each bar.
As a verification of the correctness of the introduced values, the software creates a plot of the cross section, as shown in Fig. 1. This way the possible errors are easy to spot. Using a visual method, the user verifies if the concrete section was correctly introduced, and if the steel bars and tendons are in the correct position.

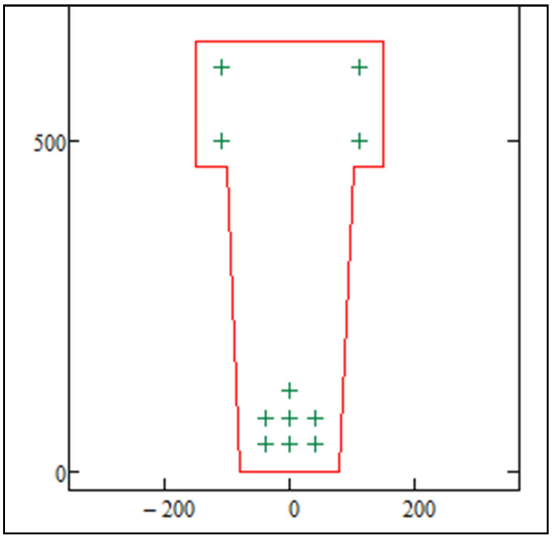

Fig. 1 Cross-section example *(Screen-shot APAM)*

After assuring ourselves of the correctness of the introduced data, the characteristics of the ideal cross section are calculated (I, W, A etc.) for initial and final states and the heights of the neutral axes, for both situations, reported to the lower side of the beam.

2.3. Loads, Load cases, Static calculation

In APAM we can use work with four different load cases: permanent loads, live, snow and wind loads. Within each load case we are able to define a number of maximum six concentrated loads of any position and a distributed load along the beams length. The load combinations are generated automatically according to EN 1990, for ULS (Ultimate Limit State) and SLS (Serviceability Limit State) states. The coefficients ψ used in case of the SLS combinations can be modified according to the NAD. The static calculations run in the background and don't need any type of intervention from the user. Moment diagrams are created for the dominant and significant combinations (Fig. 2).

2.4. Prestressing force. Losses

The initial prestressing tension is given by the user, taking notice of its maximum values calculated by the program. It is recommended, for keeping calculations as simple as possible, to introduce a round value for the initial prestressing tension. The prestress force is calculated automatically.
The calculations of the short term losses can be configured. We can establish which types of losses we want to include in our calculation or which we don't. (Fig. 3)

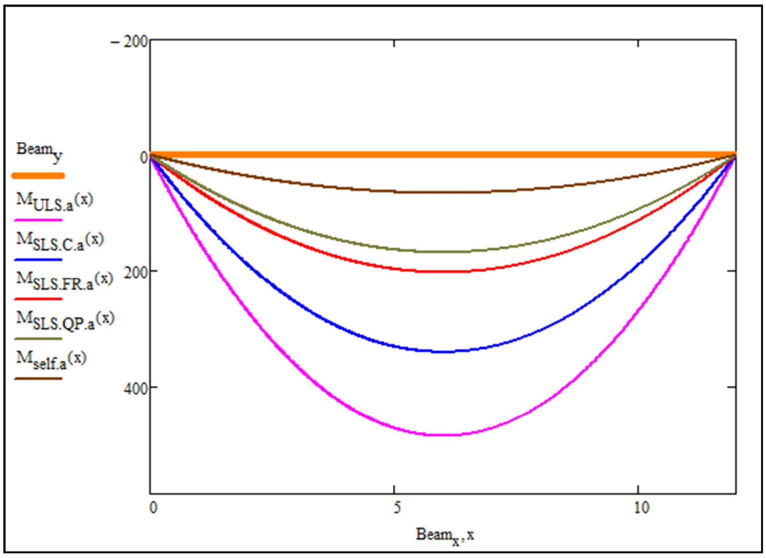

Fig. 2 Moment diagrams for different load combinations *(Screen-shot APAM)*

To find the exact value of the effective prestressing force, losses due to creep, shrinkage and short term relaxation are calculated according to Eurocode 2.
The software determines the values of the losses under the form of percentages too. In this manner we can understand better and trace the changes which intervene.

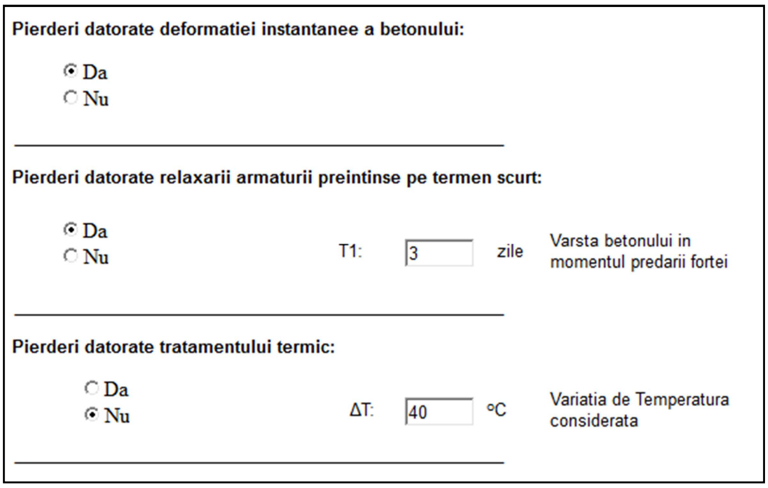

Fig. 3 Configuration of short term losses *(Screen-shot APAM)*

2.5. Initial State, SLS and USL verifications

The initial verifications, which are made when the prestressing force is applied, the SLS verifications for the qvasi-permanent and frequent load combinations are resolved with tension diagrams (Fig. 4). In case of the ULS verifications the dimensions of the compressed zone are calculated and the capable moment is determined. The deformations suffered by the steel reinforcements and tendons located in the tension zone are verified too.

2.6. Shear resistance

The module dedicated to shear design offers multiple possibilities for the user. The diameter of the shear reinforcement can be chosen, as well as the number of sheared bars, and the angle of the compressed concrete rods can be modified according to the user's preferences. The effectiveness of the given reinforcement can be evaluated by the use of specific diagram.

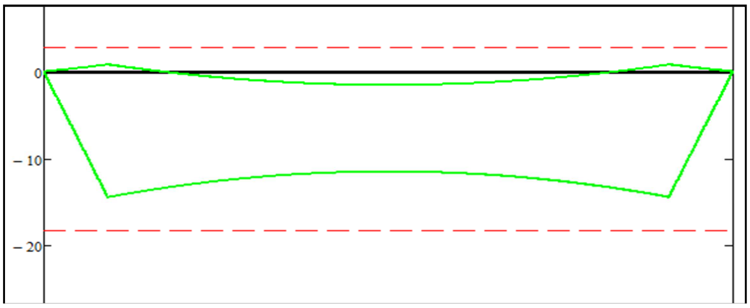

Fig. 4 Tension Diagram for the upper and lower side *(Screen-shot APAM)*

3. TESTING. COMPAREING RESULTS

APAM has been tested since the beginning of the programming process. This has had a positive influence on the program, not only by eliminating the bugs and errors, but also by helping to develop performant and precise algorithms. The results obtained in the testing process were more than satisfying. These were compared with the results offered by Abacus FETT for the same cross-sections. For the properties of the ideal concrete section the differences were less than 0.1%. In case of the prestress-losses and different coefficients differences less than ±3% were registered. Results in the calculation of upper and lower side tensions show that the maximum differences are less than ±5%. In this case the values differ more, because of the way Abacus calculates the tensions. In Abacus, verifications are made for all combinations in different limit states, not only for the maximum combination as in APAM.

4. CONCLUSIONS

APAM is a very promising software, which is still in development. Testing indicates satisfying results, less than 3% deviation from other dedicated software. The use of the software can be easily mastered by anyone, in just a few minutes.

The algorithms and functions which build up the software are programmed in a portable manner, so they can be used by creation of future applications of great success.

Despite its precision and its calculation speed MathCAD isn't the best developing environment for such complex software. Its programming functions are too limited; it contains only a short list of commands, so the coding process is difficult and slow. MathCAD doesn't offer in all cases the possibility of the most elegant programming solution.

5. REFERENCES

***, SR EN 1992-1-1 (2004), "Reguli generale și reguli pentru clădiri"

Kiss Z., Oneț T. (2008) "Proiectarea structurilor de beton armat după SR EN 1992-1", Ed. Abel, Cluj-Napoca 2008

Hurst M. K. (2003) "Prestressed Concrete Design", E & FN Spon, London, 2003

Thomsing M. (2002) "Spann Beton. Grundlagen Berechnungsferfahren Beispiele", 3 Auflage, B.G. Teubner, Stuttgart Leitzig-Wiesbaden, 2002

Petrina M., Cătărig A., Bâlc R., Petrina T., Ciplea C. (2007) "Statica Construcțiilor în formulare matriceală", U. T. Press, Cluj-Napoca, 2007

Bia C., Ille V., Soare M. V. (1983) "Rezistența Materialelor și Teoria Elasticității", Ed. Didactică și Pedagogică, București, 1983

PROPERTIES OF GREEN CONCRETES WITH RECYCLED AGGREGATES FROM CONSTRUCTION AND DEMOLITION WASTES

Lina M. González Oviedo[1], Ana Paola Ozuna[1]
[1]Universidad de los Andes
Cra. 1 N 18A – 12 Bogotá, Colombia

SUMMARY

Construction is an activity that generates a significant impact due to its high demand for natural resources and its high levels of waste production. By recycling these residues in concrete mixtures without affecting the essential properties of concrete, the impact produced by this industry may be reduced. Compressive tests in concrete mixtures, using recycled aggregates, were performed to different concrete designs. While preparing different concrete mixtures that contained 20% and 30% of recycled aggregates that came from mature concretes, it was observed that its resistance was not significantly affected. Moreover, when performing the same test to concrete mixtures containing 20%, 30% and 40% of recycled aggregates from construction and demolition waste, results showed that the resistance was significantly reduced. Even though further tests are required, the results of this investigation suggest that recycled concretes can be used as both, structural and no structural concretes.

1. INTRODUCTION

Throughout time the construction industry has generated a high impact in the environment due to its high demand for natural resources and its high levels of waste production. Waste residues tend to be inert residues mainly constituted by concrete, pavements, gravel, sand and soil. Worldwide, construction waste are recycled and reused in different ways such as recycled aggregates for road construction or new concrete mixtures.

Today, in Colombia the lack of understanding and knowledge by the construction sector has disabled the market to produce new products that come from recycled materials. Recycling and reusing construction wastes generates a more efficient and green construction, therefore it is important to find a way to use them in concrete mixtures without affecting its essential properties.

The purpose of the investigation and whose results are presented herewith was to determine, by performing a compressive test to different concrete mixtures containing different amounts of construction and demolition waste, if concrete resistance is altered, and to what extent.

2. EXPERIMENTAL RESULTS

One of the most important characteristics of concrete is its resistance to compression and tension, as well as its elastic module and its water absorption.

For purpose of this investigation, different experiments were performed in order to determine if recycled aggregates in a concrete mixture are appropriate for use, without modifying the properties of a mixture. Following the ASSHTO, ASTM and NTC standards different concrete mixtures were prepared. These mixtures varied in quantity and type of recycled aggregate. Three mixtures were prepared with a resistance of 31MPa and containing recycled aggregates that only came from old concrete structures; one with no content of recycled aggregates, one with 20% of recycled aggregates and one with 30% of recycled aggregates. Four other mixtures were prepared with a resistance of 28 MPa and recycled aggregates that came from construction and demolition wastes; one mixture with no content of recycled aggregate, one with 20%, one with 30% and one with 40% of recycled aggregates. For each design three cylinders were made and were tested in different dates as seen in tables 1, 2 and 3.

Tab. 1 Concrete Mixtures at 7 days

7 Days	Old Concretes			C&D Waste			
Concrete	**0%**	**20%**	**30%**	**0%**	**20%**	**30%**	**40%**
Weight (kg)	12.86	12.88	12.42	12.44	12.56	11.82	13.24
Height (cm)	30	30	30	30	30	30	30
Diameter (cm)	15	15	15	15	15	15	15
Area (cm2)	176.625	176.625	176.625	176.625	176.625	176.625	176.625
T. resistance (Mpa)	157.5	157.5	157.5	140	140	140	140
Actual Resistance	156.5	150.0	154.9	130.8	127.8	82.13	118.90
Error	0.01	0.05	0.02	0.066	0.09	0.41	0.15
Error between cylinders		0.04	0.01		0.02	0.35	0.08

Tab. 2. Concrete Mixtures at 14 days

14 days	Old Concretes			C&D Waste			
Concrete	**0%**	**20%**	**30%**	**0%**	**20%**	**30%**	**40%**
Weight (kg)	12.78	12.9	12.76	12.74	12.52	12.5	12.94
Height (cm)	30	30	30	30	30	30	30
Diameter (cm)	15	15	15	15	15	15	15
Area (cm2)	176.625	176.625	176.625	176.625	176.625	176.625	176.625
T. resistance (Mpa)	220.5	220.5	220.5	196	196	196	196
Actual Resistance	213.2	212.3	211.3	182.4	170.7	128.23	161.60
Error	0.033	0.037	0.042	0.07	0.13	0.35	0.18
Error between cylinders		0.004	0.01		0.06	0.28	0.11

Tab. 3 Concrete Mixtures at 28 days

28 days	Old Concretes			C&D Waste			
Concrete	**0%**	**20%**	**30%**	**0%**	**20%**	**30%**	**40%**
Weight (kg)	13.84	13.46	13.78	12.46	13.16	12.4	12.46
Height (cm)	30	30	30	30	30	30	30
Diameter (cm)	15	15	15	15	15	15	15
Area (cm2)	176.625	176.625	176.625	176.625	176.625	176.625	176.625
T. resistance (Mpa)	315	315	315	280	280	280	280
Actual Resistance	306.6	303.8	306.3	260.0	224.0	225.5	217.7
Error	0.027	0.036	0.028	0.071	0.20	0.19	0.22
Error between cylinders		0.009	0.001		0.13	0.12	0.15

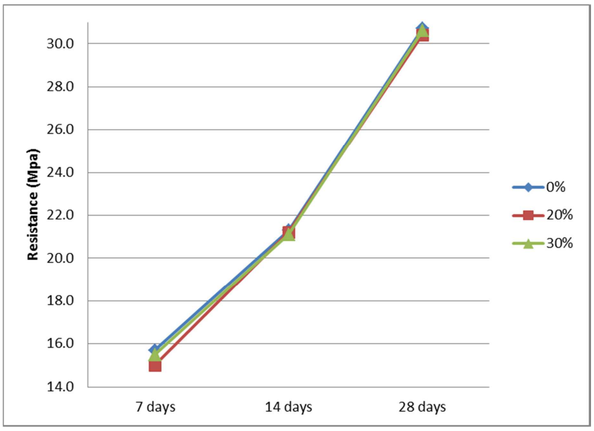

Fig. 1 RA Old Concretes Comparison

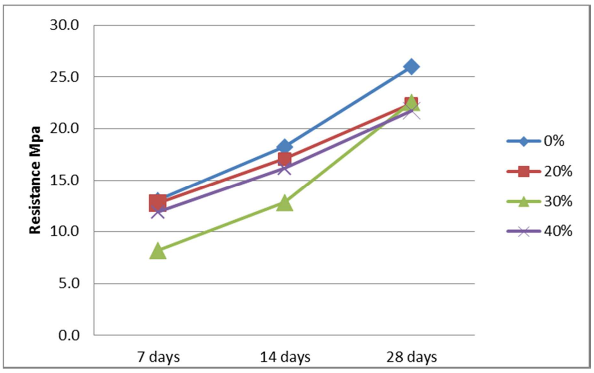

Fig. 2 RA C&D Wastes Comparison

After performing the compression tests, it was observed that the resistances obtained for both cylinders with and without recycled aggregates that came from old concretes was practically the same. There was a loss of 4% in the cylinders that had 30% of recycled aggregates and less than 2% in those with 20% of recycled aggregates as shown in Fig. 1. This depicts that these types of green concretes can be used for both structural and nonstructural concretes, due to the fact that they comply with international standards.

The cylinders that contained recycled aggregates that came from construction and demolition waste had a different behavior. The resistance to compression was significantly altered. Fig. 2 shows how up to 22% of the resistance was lost in the mixture containing 40% of recycled aggregates. To use these types of concretes, only up to 30% of recycled aggregate must be used in order to have a proper resistance. Nonetheless, it is suggested that these types of concretes not be used for structural purposes, but can be used in other projects, for example rigid pavements. It must be taken into consideration the fact that some concretes containing recycled aggregates from construction and demolition waste may not comply with international standards, therefore it is important to perform further test to ensure the quality of these concretes.

Furthermore, it is important to highlight the fact that more water was needed for these mixtures. Mixtures containing recycled aggregates need more water because its percentage of water absorption is higher. This can be explained due to the fact that waste throughout time loses its water content, while aggregates in its natural condition, embedded in different types of soils, can maintain their humidity and water content.

Even though the resistance to a compression test is one of the most important factors to determine in a concrete mixture, further tests most be applied, such as flexion and stability tests. It is important to mention that the type of waste being used, its properties and characteristics may vary, making it possible for them to have a lower resistance than natural aggregates.

3. CONCLUSIONS

Green concretes is an alternative and competitive market that can be created through the acknowledgment that construction and demolition wastes are viable for reusing and recycling as aggregates for any king of concrete, including structural concretes. It's been observed, that up to 30% of recycled aggregates may be used without affecting the principal properties of the mixture. By using these types of concretes a more viable material is introduced to the market, allowing constructions to lowers their costs. In the end, not only are green concretes beneficial as a financial factor, but it is also helping societies reduce their environmental impact in the world.

4. AKNOWLEDGMENTS

I would personally like to thanks the Department of Environmental and Civil Engineering of La Universidad de los Andes for making this possible.

5. REFERENCES

ACPA. (n.d.). Recycling Concrete Pavements.

Agency, E. P. (2010). *Danish Ministry of the Environment*. Retrieved Abril 15, 2011, from http://www.mst.dk/English/Soil+and+Waste/

Aitcin, P. C. (2000). *Cements of Yesterday and Today, Concretes of Tomorrow*.

Akash Raoa, K. N. (2006, Mayo 24). Use of aggregates from recycled construction and demolition waste in concrete. India.

Alcaldia Mayor de Bogota, U. (2009). *Diagnostico del Manejo Integral de los Escombros en Bogota.* Bogota.

American Concrete Pavement Association. (2009). Recycling Concrete Pavementes.

Commission, E. (2010). *Service Contract on Management of Construction and Demolition Waste.*

(n.d.). *Consturction and Demolition Waste Manegments Practices and Their Economic Impacts.*

Sami W. Tabsh, A. S. (2008, Junio 22). Influence of recycled concrete aggregates on strength properties of concrete. Sharjah, United Arab Emirates.

Topcu, I. B. (2003). *Properties of Concretes produced with waste concrete aggregates.*

UAESP. (2011). *UAESP*. Retrieved Abril 20, 2011, from http://www.uesp.gov.co/uaesp_jo/index.php?option=com_content&view=article&id=425&Itemid=174

WBCSD, W. B. (2007). *Recycling Concrete.* Washington DC: WBCSD North America Office.

LOAD BEARING CAPACITY VERIFICATION USING THE GLOBAL SAFETY FACTOR FORMAT

Kálmán Szalai, Tamás Kovács
Department of Structural Engineering, Budapest University of Technology and Economics
1111 Budapest, Műegyetem rkp. 3.

SUMMARY

One half century of Hungarian and almost two decades of European Union experience in the application of the partial safety factor method in structural design led to the conclusion that, in particular cases for recently designed structures and especially for laboratory and on-site investigations of existing structures, the use of the global safety factor format is more advantageous for reliability verification than the recently applied partial safety factor format.

1. INTRODUCTION

This paper compares two safety formats. The first is the *partial safety factor format* as proposed by the Eurocode (EC). In complex load cases, particularly when an action simultaneously affects the action as well as the resistance-side of the relevant design requirement (e.g. the self-weight of earth for cantilever-type (retaining) walls), the application of the partial safety factor format becomes very complicated and difficult. For the supervision of existing structures the values of partial factors recommended for newly-built structures may be lowered because the statistical properties of many geometrical, strength and, sometimes, loading properties can be on-site measured and, consequently, the related uncertainties are eliminated. If expressing the required reliability level by only *one global safety factor* the design procedure becomes more transparent. A limited application of this was proposed as "global resistance format" by the recently published *fib* Model Code 2010 (*fib*, 2010).

2. RELIABILITY BACKGROUND

Reliability analyses of load carrying structures carried out on the basis of minimum whole life cost found the optimum risk against ultimate failure as $p_{RE} \approx 10^{-4}$, to which a reliability index of β=3.719 belongs (*Kármán 1965; Mistéth, 2001*). The sensitivity factors α_E and α_R associated with $R_d(t) = E_d(t)$ may generally be approximated as α_E= -0.6 and α_R=0.8 (thus $\alpha_E^2+\alpha_R^2$=0.36+0.64=1.0) (*Fig. 1*). The EC (*EN, 2002*) sets a minimum value of β=3.8 for RC2 structures and 50 years of reference period, and recommends to take α_E= -0.7 and α_R=0.8. These latter values, which do not fulfil the $\alpha_E^2+\alpha_R^2$=1.0 condition, can be considered as safe-side approximations of the above ones. Assuming normal distribution for both the action-side (E) and the resistance-side (R) and applying α_E= -0.6 and α_R=0.8, the partial risks are resulted in $p_E \approx 1\%$ ($-\alpha_E\beta=0.6\times3.8=2.28 \rightarrow p_E=1.13\%$) and $p_R \approx 1‰$ ($\alpha_R\beta=0.8\times3.8=3.04 \rightarrow p_R=1.18‰$) for β=3.8. The design value of action yields in $E_d = E_m\left(1-\beta\alpha_E^{(-)}\nu_E\right)$ and, by the use of a logarithmic transformation on the resistance-side for numerical reasons, the design value of resistance results in $R_d = R_m \exp\left(\beta\alpha_R^{(+)}\nu_R\right)$. The global safety factor can be deduced as follows:

$$\gamma_{RE} = \exp\left(\beta\alpha_R^{(+)}\nu_R\right)\left(1-\beta\alpha_E^{(-)}\nu_E\right). \tag{1}$$

where ν_R and ν_E are the respective coefficients of variation (COV).

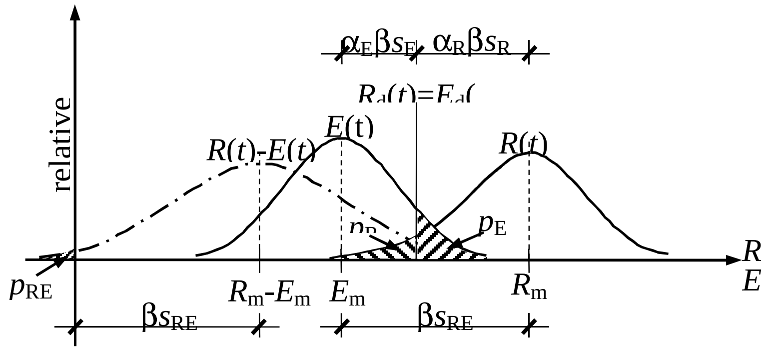

Fig. 1 Interpretation of the reliability index β

When using γ_{RE}, the basic ultimate limit state (ULS) requirement $R_d \geq E_d$ according to the partial safety factor format changes to

$$R_m \geq \gamma_{RE}\, E_m\,. \tag{2}$$

Taking the above partial risks p_R=1.18‰ and p_E=1.13% and assuming that the dominant resistance parameter (e.g. a material strength) as well as the individual (i.e. permanent and variable) actions follow the normal distribution, the respective partial factors derive as

$$\gamma_R = \frac{1-1.645\nu_{Rf}}{1-3.04\nu_R} \quad \text{and} \quad \gamma_E = 1 + 1.645\,\nu_E\,. \qquad \text{(3a and 3b)}$$

The respective COV values are interpreted as

$$\nu_R = \sqrt{\nu_{Rf}^2 + \nu_{Rm}^2 + \nu_{RG}^2} \quad \text{and} \quad \nu_E = \sqrt{\nu_{Ef}^2 + \nu_{Em}^2 + \nu_{EG}^2} \qquad \text{(4a and 4b)}$$

where the index *f* refers to strength (ν_{Rf}) and to the intensity of the considered action (ν_{Ef}) only, moreover indices *m* and *G* refer to the uncertainty of the applied calculation model (ν_{Rm} and ν_{Em}) and geometry (ν_{RG} and ν_{EG}), respectively.

Tab. 1 Partial factors of the EC2 and the respective coefficients of variation

Design variable	**Partial factor**	**Coefficient of variation (COV) based on**	
		partial factors	**on-site measurements**
Actions			
unfavourable permanent action	γ_g=1.15 (=0,85×1,35)	ν_g=0.091	ν_{gf}, ν_{qf}, ν_{Lf1}
favourable permanent action	γ_g=1.35	ν_g=0.213	
traffic loads	γ_q=1.35	ν_q=0.213	
variable actions (other than traffic loads)	γ_q=1.50	ν_q=0.304	
Resistances			
concrete compressive strength	γ_c=1.5	ν_c=0.166	ν_{cf}, ν_{sf},ν_{Lf2}
reinforcing and prestressing steel strength	γ_s=1.15	ν_s=0.066	

According to (*Soukov and Jungwirt, 1997*), the partial factor for concrete, which is set to γ_c=1.5 in the EC, is based on ν_{cf}=0.15, ν_{cm}=0.05 and ν_{cG}=0.05 COV values that yields in ν_c=0.166 from *Eq.(4a)*. In literature, the COV of steel strength is usually taken as ν_{sf}=0.05 while the other two COVs values may be assumed as ν_{sm}=ν_{sG}=0.03, which results in ν_s=0.066 from *Eq.(4b)*. The COV values "based on partial factors" (3rd column) in *Tab.1* correspond to *Eq.(4a)* and *Eq.(4b)* and were deduced from the given partial factors (2nd column) by *Eq.(3a)* and *Eq.(3b)*, respectively.

3. APPLICATION OF THE GLOBAL SAFETY FACTOR FORMAT

The practical application of the global safety factor format will be demonstrated on the following fictitious simply-supported beam with constant cross-section as shown in *Fig. 2*.

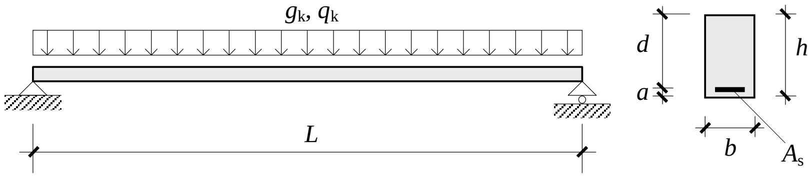

Fig. 2 Notations used in the numerical example

Geometry: L=13.4 m; b=250 mm; h=700 mm; a=30 mm; effective depth: $d = h\text{-}a$ = 700-30 = 670 mm (a included the unfavourable deviation of reinforcement). *Actions*: g_k = 6 kN/m; q_k = 5 kN/m (characteristic values as defined in the EC). *Materials*: concrete: C30/37, f_{ck}=30 N/mm^2, f_{cm}=38 N/mm^2; steel: S500B, f_{yk}=500 N/mm^2.

3.2.1 Verification of bending capacity during design

This section applies to *newly-built structures* by introducing the global safety factor format as a design tool alternative to the widely recommended partial safety factor format. At the time of design the designer has no choice but to apply COV values deduced from the respective partial safety factors given by the relevant standard (see *Tab. 1*). For the sake of simplicity, the nominal values of all geometrical data were taken as design values. In using *Eq.(2)*, the mean value of M_{Rm} and M_{Em} can be calculated as follows:

$$M_{\mathrm{Rm}}\left(f_{\mathrm{ym}}, f_{\mathrm{cm}}\right) = A_{\mathrm{s}} f_{\mathrm{ym}}\left(d - \frac{A_{\mathrm{s}} f_{\mathrm{ym}}}{2bf_{\mathrm{cm}}}\right) \quad \text{and} \quad M_{\mathrm{Em}}(g_{\mathrm{k}}, q_{\mathrm{k}}) = \frac{(g_{\mathrm{k}} + q_{\mathrm{k}})L^2}{8} \tag{5}$$

The mean compressive strength of concrete f_{cm} was taken from the relevant EC2 formula (f_{cm}=f_{ck}+8 N/mm^2). The mean strength of steel f_{ym} was calculated from f_{yk} using constant ν_{sf} according to *Sec. 2*. The resulting standard deviations of both sides were calculated as follows:

$$s_{\mathrm{R}} = \sqrt{\left[\left(\frac{\mathrm{d}}{\mathrm{d}f_{\mathrm{ym}}} M_{\mathrm{Rm}}\left(f_{\mathrm{ym}}, f_{\mathrm{cm}}\right)\right)\nu_{\mathrm{s}} f_{\mathrm{ym}}\right]^2 + \left[\left(\frac{\mathrm{d}}{\mathrm{d}f_{\mathrm{cm}}} M_{\mathrm{Rm}}\left(f_{\mathrm{ym}}, f_{\mathrm{cm}}\right)\right)\nu_{\mathrm{c}} f_{\mathrm{cm}}\right]^2} \tag{6a}$$

$$s_{\mathrm{E}} = \sqrt{\left[\left(\frac{\mathrm{d}}{\mathrm{d}g_{\mathrm{k}}} M_{\mathrm{Em}}\left(g_{\mathrm{k}}, q_{\mathrm{k}}\right)\right)\nu_{\mathrm{g}} g_{\mathrm{k}}\right]^2 + \left[\left(\frac{\mathrm{d}}{\mathrm{d}q_{\mathrm{k}}} M_{\mathrm{Em}}\left(g_{\mathrm{k}}, q_{\mathrm{k}}\right)\right)\nu_{\mathrm{q}} q_{\mathrm{k}}\right]^2} \tag{6b}$$

then the resulting COV values derived as ν_R=s_R/M_{Rm} and ν_E=s_E/M_{Em}. Using β=3.8 according the EC, the global safety factor can be calculated in iterative way from *Eq.(1)*. The applied sensitivity factors α_R and α_E have to fulfil the α_R^2+α_E^2=1.0 condition in each iteration step. The procedure starts with α_R=0.7 and α_E= -0,7 (α_R^2+α_E^2=0.98≈1.0), which corresponds to equal partial risks (p_R=p_E) at both sides of *Eq.(1)*, then they are refined in each step until γ_{RE} remains unchanged compared to the previous step. The value of γ_{RE} converges very quickly. The bending capacity is adequate if γ_{RE} of the last step fulfils *Eq.(2)*. The procedure ended in the 3rd iteration step when γ_{RE3}=1.672 (=γ_{RE2}) was obtained, which fulfilled *Eq.(2)* as follows: $\gamma_{RE3}M_{Em}(g_k, q_k)$=413 kNm < $M_{Rm}(f_{ym}, f_{cm})$=434 kNm. Note that the values of sensitivity factors in the last iteration step (α_{E3}= -0.844 and α_{R3}=0.536) significantly differed from their initial values (α_{E1}= -0.7 and α_{R1}=0.7) as well as from that recommended by the EC (α_E= -0.7 and α_{R3}=0.8). This supports the fact that the introduced global safety factor format is able to take the current variability of action- and resistance-sides into account and to divide the design risk p_{RE} between them accordingly instead of using recommended, constant partial risks p_E and p_R.

3.2.2 Verification of bending capacity for existing structures

This section applies the global safety factor method to existing structures on the basis of the assumption that the necessary statistical properties (i.e. COV values) of the relevant design variables (i.e. load intensities, geometrical properties and strength data) are available from extensive on-site measurements. In this scholastic example, the *mean values* were assumed to be equal to the respective characteristic values for loading data ($g_m=g_k$; $q_m=q_k$), to the respective nominal values for geometrical data ($L_m=L$; $h_m=h$, $b_m=b$; $a_m=a$, $A_{sm}=A_s$) and to values slightly higher than the respective standardized mean values (see *Sec. 3.2.1*) (f_{cm}; f_{ym}). The respective *COV values* were assumed as follows:

- Loading data:
  - permanent load: $\nu_{gf}=0.07$ (< $\nu_g=0.091$ ($\gamma_g=1.15$) in *Tab 1*);
  - live load: $\nu_{qf}=0.24$ (< $\nu_q=0.304$ ($\gamma_q=1.5$) in *Tab 1*);
- Geometrical data:
  - span: $\nu_{Lf}=0.01$;
  - cross-sectional height: $\nu_{hf}=0.02$ (> ν_{Lf});
  - cross-sectional width: $\nu_{bf}=0.02$ (= ν_{hf});
  - reinforcement position: $\nu_{af}=0.3$ (accounting for unfavourable deviation);
  - area of reinforcement: $\nu_{Asf}=0.01$;
- Resistance data
  - concrete strength: $\nu_c=0.17$ (> $\nu_{cf}=0.15$);
  - steel strength: $\nu_s=0.06$ (> $\nu_{sf}=0.05$).

As shown, in contrast to *Sec. 3.2.1*, here all geometrical data are considered fully as random variables with known mean values and COV values. *Eq.(5)* and *Eq.(6a and ab)* were extended accordingly. The procedure ended again in the 3rd iteration step when $\gamma_{RE3}=1.569$ (=γ_{RE2}) was obtained, which fulfilled *Eq.(2)* as follows: $\gamma_{RE3}M_{Em}(g_m, q_m, L_m)=1.569\times247=387$ kNm < $M_{Rm}(f_{ym}, f_{cm}, h_m, b_m, a_m, A_{sm})=439$ kNm.

4. CONCLUSIONS

The application of the global safety factor format for the verification of bending capacity of a simple beam on the basis of standardized safety elements and also of on-site-measured data was introduced. The biggest advantage of this format is that, in each design situation, the total risk can be divided between the action-side and the resistance-side of the design requirement by taking the current variability of both sides into account. This cannot be done when constant partial risks are applied as recommended by the partial safety factor method in the EC.

REFERENCES

EN 1990:2002 Eurocode *Basis of structural design*, CEN, Bruxelles

EN 1992-1-1:2004 Eurocode 2: *Design of concrete structures. Part 1-1: General rules and rules for buildings*, CEN, Bruxelles

fib (2010) *fib Model Code 2010*, fib Bulletin 55-56, *fib*, Lausanne

Kármán, T. (1965) *On the optimum level of safety of structures* (in Hungarian), ÉTI, Budapest

Mistéth, E. (2001) *Design theory* (in Hungarian), Akadémiai Kiadó, Budapest

Soukov, D., Jungwirt, F. (1997) Conformity and safety of concrete according to prEN 206 and Eurocodes, *Leipzig Annual Civil Engineering Report*, No. 2, Leipzig

STATICAL AND DYNAMICAL TESTS OF ADHESIVE PRESTRESSED REINFORCED ELEMENTS CONTAINING FLY ASH

Jure Radić[1, 2], Ružica Rosković[2], Igor Džajić[2], Darija Živni[2]
[1] *University of Zagreb*
Faculty of Civil Engineering
10000 Zagreb, Kačićeva 26, Croatia
[2] *Institut IGH, d.d.*
10000 Zagreb, Janka Rakuše 1, Croatia

SUMMARY

Great costs of building materials are often cited as a disadvantage of prestressed structures. In the previous practice in Croatia, it was used cement of type CEM I 52, 5 R / N as a binder.

After 2006, when standard EN 450-1 was accepted, there are possibilities for flying ash use in concrete, but up to now it had not a practice. National regulations prohibit use of calcium fly ash, because of potential danger for reinforcement corrosion.

In this paper, it was previously made adhesive prestressed reinforced concrete elements with cement replacement with 25% of siliceous and calcium flying ash. All mechanical and durability properties of concrete were investigated, as a load carrying capacity of prestressed beams.

1. INTRODUCTION

In recent years, the durability of reinforced concrete structures is a major concern, because builders must take into consideration the life cycle of concrete at the initial election of the concrete mix. Durability of concrete is highly dependent on the type and quality of cement, the quality and relation components of concrete composition, performance and conditions that the concrete is exposed.

The main factor in predicting the durability of is microstructure of the protective cover of concrete to the reinforcement and connection of pores in the cement paste and transition zone *(Cook et al 1987, Scrivener et al 1987).*

The development of solid-phase relationship is the basis for the development of mechanical properties and the formation of pore structure is the basis for the transport properties. Therefore, concerns for the environment is becoming a necessity for the future, but have made adequate utilization of waste materials at the same time great potential in terms of rationalization.

The use of flying ashes in cement production is nothing new and has long been applying because of cheaper production and increased quantities of cement.

Today is the increasing use of these materials as the mineral supplements by adding directly to the concrete. This world is increasingly used because they have demonstrated good properties of silicon fly ash in a better (denser) structure of concrete, as a result puzzolan reactions.

This paper examines and describes the use of silicon and calcium fly ash in the manufacture of pre-tensioned reinforced concrete elements, with the aim no decrease mechanical and durability properties of products and reduce production costs.

2. PRESTRESSED CONCRETE

Concrete is a material high compressive and low tensile strength. Tensile stresses caused by shrinkage, temperature and external load very quickly reaches tensile strength of concrete and leads to cracking in reinforced concrete structures. After the appearing cracks all tensile stresses are accepted by reinforcement. Crack width limit depending on the duration of load and aggressive environment in order to avoid compromising the durability of the structure.

The aim of prestressing is to eliminate or reduce the tensile normal stresses in all cross-sections and to the action of induced forces. These are the prestressing force. The resulting stresses must be less than the permissible value in all stages of construction and use of the building.

Requirements for the prestressed concrete structures are as follows:

- High compressive strength;
- A small amount of shrinkage;
- Durability.

It is known that the action of a large number of load cycles and fluctuating loads on the structural element is actually fatigue. Due to fatigue, the material is destroyed at much lower stresses than the static tensile strength, sometimes less, and the stresses on the elastic limit. It is essentially a destruction of fatigue.

The purpose of dynamic testing beams of the same geometric characteristics (cross section and span) and the same ways of reinforcing and prestressing was to show possible different effects on the bearing capacity due to the use of three different types of concrete. Therefore it was decided that models beams for testing represent a girders for bridges that are in its service life exposed to fatigue. To investigate the impact of fatigue on the beams bearing capacity, it was supposed that these beams be built in motorway objects with more than two traffic lanes and it would be the first traffic category *(HRN EN 1991-2, 2005)*.

3. EXPERIMENTAL RESEARCH

The purpose of testing was to show the influence of fly ash in the pre-tension load bearing capacity of reinforced concrete elements made of concrete with fly ash before and after a fatigue exposure.

The test specimens were pre-tensioned reinforced concrete beams by two strands diameter 12,5 mm, and reinforced with B500B reinforcement. All beams were reinforced and prestressed in the same way. All reinforced concrete beams were made of the same size, length 3130 mm, and the same cross-sectional properties.

The concrete used to make the beam is different in composition, as described in the following paragraphs and all concretes were designed with compressive strength class C40/50. For the purposes of testing three types of concrete were prepared, whose compositions are shown in (Tab. 1).

Tab. 1 Composition of concrete for testing

	RC	**C1**	**C2**
Cement (CEM I 52.5 N) - kg/m^3	430,0	322,5	322,5
Calcium fly ash (W) - kg/m^3	0	107,5	0
Silicon fly ash (V) - kg/m^3	0	0	107,5
Water - kg/m^3	141,9	146,2	167,7
v/c	0,33	0,34	0,39
Super plasticizer -%	1,1	1,0	1,13
Air -%	1,2	2,2	1,1
Aggregate - kg/m^3	1909,6	1873,6	1809,5
Total - kg/m^3	2486,2	2454,1	2412,1
The consistency of concrete, by shrugging - mm	220	210	210

As shown in (Tab. 1), the aim was to replace 25% of cement CEM I 52.5 N with fly ash to obtain the same consistency of fresh concrete.

Before the static and dynamic testing girders, structural analysis of bearing capacity beams was made. In the calculation of beams, the material nonlinearity has been recognized, and girders were analyzed in the cracked condition in order to take into account the reduction of stiffness of beams and increasing tension in the strands. These results later were used for comparison with those obtained by testing.

Fatigue of beams is performed by cyclical loading of dynamic pulsator. Pulsation is made according to the scheme of four point bending test, as well as static testing. The load pulses ranging from 90 KN to 130 KN, in the cracked zone of prestressed reinforced concrete beams. Pulsation frequencies are carried out between 4 Hz and 6 Hz through 2 million cycles of load changes. The interval of stresses in the strands of smooth prestressing wires had to be less than 190 MPa according to Table 3 of standard nHRN prEN 10138:2005.

During the test, visually was monitored the appearance and spread of cracks.

Fig. 1 The collapse of test specimen

As a result of fatigue there was a reduction in stiffness due to cracking beams tension zone of concrete sections. Reduction of beam stiffness after fatigue proved by testing the stiffness of beams, measuring the Eigen values before and after fatigue exposure beams made of an equal composition of the concrete.

Measurement results are shown in (Tab. 2), the breaking force and deflection on samples of prestressed reinforced concrete beams. Beams were tested before fatigue (static test) and after fatigue through 2 million cycles (dynamic testing).

During the examination of samples before, during and after the collapse, it was determined that there was no appearance of slip strands for prestressing.

Tab. 2: Results of beam load bearing capacity in bending

Property	Concrete	RC	C1	C2
Breaking Force, kN	before fatigue	342	336	334
	after the fatigue	270,7	276,9	286,2
The largest deflection achieved in the mid, mm	before fatigue	108,6	123,3	109,2
	after the fatigue	104,5	117,1	122,0

4. CONCLUSIONS

By fatigue testing, beams have shown that the fracture occurred due to failure of prestressed strands. Not observed significant differences in the behaviour of concrete of different composition either before or after the beams exposure to fatigue. The breaking forces were less as a result of fatigue.

This fatigue testing of prestressed reinforced concrete beams showed that fly ashes can be used in pre-tensioned concrete structures.

Using a specific and acceptable raw materials for pre-proven application, significantly contributes to savings in production, as a major problem in the technology of prestressing reinforced concrete elements. In addition, of course, contributes to environmentally sustainable construction.

5. ACKNOWLEDGEMENTS

The authors are grateful to the Viadukt D.D. Company for assistance in the preparation of prestressed reinforced concrete beams for testing purposes.

6. REFERENCES

Cook, D.J.; Cao, H.T., (1987) “An investigation of the pore structure in fly ash/OPC blends”, Proceedings of the First International Rilem Congress: Pore Structures and Materials Properties, Vol. I, Chapman and Hall, London 1987, pp. 69-76.

Scrivener, K.L.; Pratt, P.L., (1987) The characterization and quantification of cement and concrete microstructures, Proceedings of the First International Rilem Congress: Pore Structures and Materials Properties, Vol. I, Chapman and Hall, London 1987, pp. 61-68

HRN EN 1991-2: 2008 Eurocode 1: Action on structures – Part 2: Traffic loads on bridges, Croatian and European Standard

nHRN prEN 10138-3: 2005 Prestressing steels – Part 3: Strand, Croatian and European Standard

CORELATION BEETWEEN FROST RESISTANCE OF CONCRETE MEASURED BY CIF TEST AND BY MICROSCOPIC ANALYSIS

Ana Hranilović Trubić[1], Ružica Rosković[1], Jure Radić[1]
[1] *Institute IGH d.d.*
1000 Zagreb, Janka Rakuše 1

SUMMARY

Concrete structures should be designed and performed in the way that, under expected environmental conditions, their safety and usability hold over the structure's lifetime with minimal repair and maintenance costs. Long-life concrete must be resistant to destruction when exposed to agressive environment like it is, among other things, the freezing effect without deicing salt.

In this paper proportioning of frost resistant concrete is presented depending on the w/c ratio and amount of cement and admixtures. 15 concrete mixtures have been prepared and all the concrete's physical and mechanical properties have been tested. Methods of testing frost resistance through the air void distribution with linear microscopical analysis are used. The microscopic method in hardened concrete has significantly reduced time necessary for the execution of preliminary testing by the alternating freezing and thawing cycles.
The analysis of the internal damage will be presented by using the CIF-test. The CIF-test basing on this shows the strong correlation between freeze-thaw cycles, frost suction and internal damage of concrete.

1. INTRODUCTION

In this paper, the test results of the concrete freeze-thaw resistance are presented. Concrete resistance is determined by measuring air void characteristics. The test has been conducted using two methods: microscopic analysis and CIF methods (**C**apillary suction, **I**nternal damage and Freeze thaw Test). A criterion for the obtained frost resistance has been the pore spacing factor <0.2mm. The test limit of the CIF-test – the number of freeze thaw cycles until which a relative dynamic modulus of elasticity (RDM) of 80% is reached. 15 different concrete mix compositions are made and the influence of w/c ratio and quantity of air entraining admixture (AEA) on the air void characteristics is analysed. These compositions are presented in Table 1.

2. EXPERIMENTAL WORK

All the mixtures are prepared with same components. A mixing procedure has been performed according to the standard HRN EN 480-1:2005 – admixtures for concrete, mortar and mortar grouting – testing methods – 1. part: Reference concrete and reference mortar for testing (HRN EN 480-1: 1997.). Concrete was placed into the moulds in two layers and each layer was then vibrated on the vibrating table.
The measured air voids parameters are: the total air content, pore spacing factor (L`) and specific surface (α). The total content of air voids is measured using all three methods while the pore spacing factor and specific surface are measured by means of the Air Void Analyser and RapidAir 457 instrument.

Tab.1. Used mix compositions

Mark of mix	w/c	Cement (kg)	Air entrained agent (%)
M1	0,40	300	0,0
M2	0,40	300	1,0
M3	0,40	320	0,5
M4	0,40	340	0,0
M5	0,40	340	1,0
M6	0,45	300	0,5
M7	0,45	320	0,0
M8	0,45	320	0,5
M9	0,45	320	1,0
M10	0,45	340	0,5
M11	0,50	300	0,0
M12	0,50	300	1,0
M13	0,50	320	0,5
M14	0,50	340	0,0
M15	0,50	340	1,0

This method for determination of concrete durability to freezing according to HRN EN 480-11:2005 can be performed with the 7 days old concrete sample. The sample preparation according to HRN EN 480-11:2005 requires about 15 min for cutting from the concrete cube, 120 min for good surface polishing, 60 min for surface contrasting and drying on 60°C and, at the end, 15min for the sample analysis of the final air void characterization in hardened concrete by means of the RapidAir 457 instrument. Total required time for concrete durability testing to freezing according to this method, from the time of the concrete placing into the mould to the time of air void characterization, is about 10 days.Concrete is resistant if it is proved that the spacing factor of entrained air micropores is lesser than 0,20 and the specific surface greater than 25 mm^{-1}.

CIF test usually lasts 56 freeze thaw cycles, i.e. the duration is 28 days of freeze thaw cycles plus 7 days of capillary suction. In order to reduce errors caused by laboratory operators, the loosely adhering scaled material is removed from the test surface by an ultrasonic bath. The scaled material is filtered and dried at 105°C. every four or six freeze-thaw cycles, the amount of scaled material and the ultrasonic transit time of the specimens are measured. Due to the measurement of transit time at a defined height of 35 mm from the test surface the CIF test is nearly independent of the geometry of the specimens, e.g. cubes, drilled cores or precast elements can be used. By using demineralised water as coupling medium, the determination of transit time can be measured easily with high precision.Internal damage is detected by measuring the change of ultrasonic pulse velocity in a height of 35 mm from the test surface.

3. ANALYSIS

Figures 1 to 3 show the results of relative dinamic modulus of elasticity decrease compared with the results of microscopis analysis results (amount of pores, space factor and specific surface) for specimens for which a demineralised water was used as a test liquid. Figure 1 showsresults of RDM decrease and results of pore amount. Figure 2 shows results of RDM decrease and results of space factor. Limit for resistance of concrete to freezing and thawing

action is 0,2 mm, and limit for dynamic modulus of elasticity for test specimens tested to freezing and thawing is decrease od dynamic modulus of elasticity higher than 20%.
Required specific surface for specimens resistive to freezing and thawing action is 25 mm^{-1}.

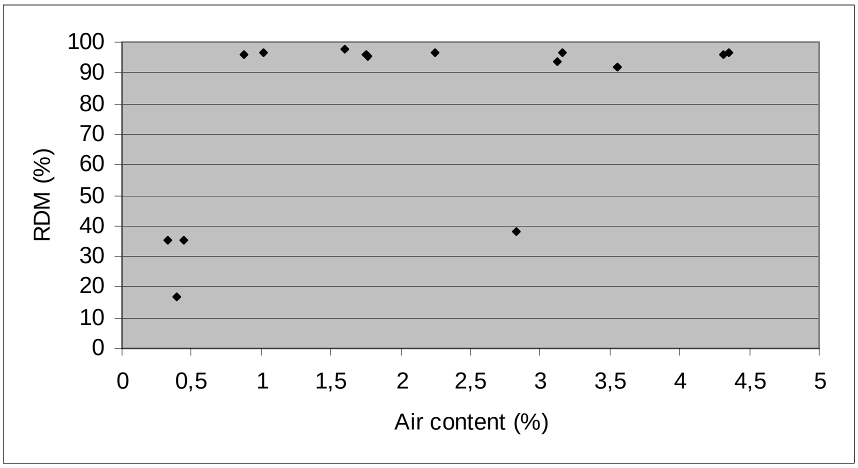

Fig. 1 Comparison of results of RDM decrease and amount of pores (tests in water)

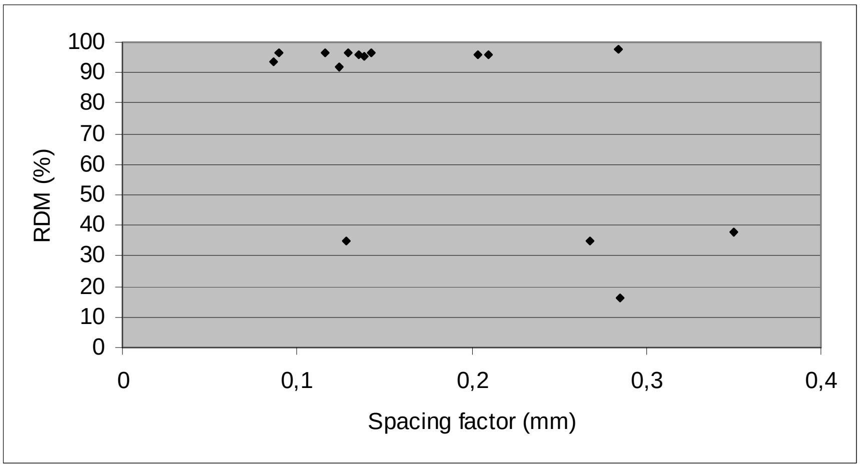

Fig. 2.Comparison of results of RDM decrease and space factor (tests in water)

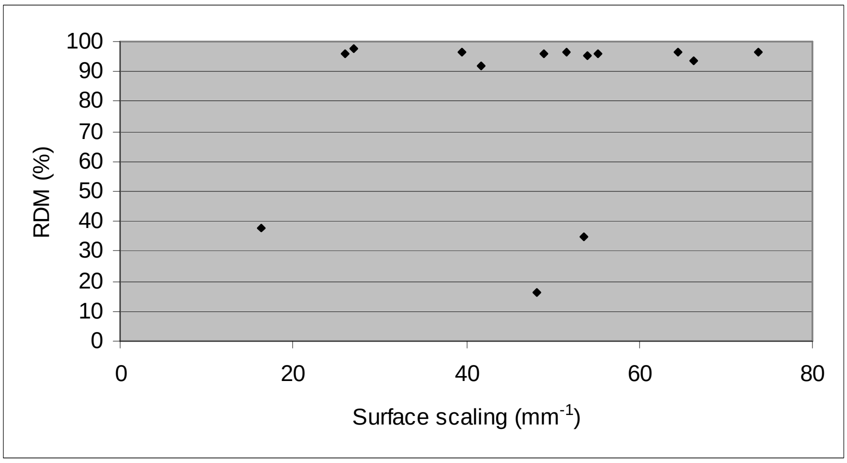

Fig.3 Comparison of results of RDM decrease and specific surface (tests in water)

4. CONCLUSIONS

In this paper, the test results of the concrete freeze-thaw resistance are presented. Concrete resistance is determined by measuring air void characteristics. The test has been conducted using two methods: microscopic analysis and CIF methods.

Compared two test methods (microscopis analysis and CIF method), it is visible that test results have good coincedence. The method of defining the concrete durability to freezing according to HRN EN 480-11:2005 standard is multiply faster than the direct method of testing by cycles of freezing and thawing (CIF method).

5. REFERENCES

Croatian Standard, HRN EN 480-11 Admixtures for concrete, mortar and grout – Test methods – Part 11: Determination of air void characteristics in hardened concrete

Fagerlund, G.: Internal frost attack-state of the art, Proceedings of the International RILEMWorkshop „Frost Resistance of Concrete“, Edited by M.J. Setzer and R. Auberg, E&FN SPON, London (1997) 323-338

Palecki, S., Setzer, M.J.: Investigations of high-performance concrete under frost attack – internal damage and water uptake, „Frost resistance of concrete“ – Proceedings of international rilem workshop, Pro24, Essen, 2002

Recommendations of RILEM TC 176-IDC: test methods of frost resistance of concrete. CIF-test-capillary suction, internal damage and freeze thaw test, reference method and alternative methods A and B, Materials and Structures, vol. 34, 2001, p. 515

Setzer. M.J.: Proceedings of the International RILEM Workshop on Resistance of Concrete to Freezing and Thawing with or without Deicing Chemicals, Proceedings, vol. 34, 1997, p. 157

LCC ANALYSIS IN MAINTENANCE STRATEGY

S. Skaric Palic[1], I. Stipanovic Oslakovic[2], D. Bjegovic[3], J.Radic[4]
[1,2,3,4] *Institute IGH, Zagreb, Croatia*
[3,4] *Faculty of Civil Engineering, University of Zagreb*
[2] *Faculty of Engineering Technology, University of Twente*

SUMMARY

This paper focuses on different repair methods which are evaluated regarding risks and costs and in correlation to the structural service level for concrete structures. An overview of different repair and maintenance measures correlated to the degradation level is presented. In this way direct costs of a certain repair intervention can be directly linked to degradation level. For achieving entire cognition of influence of a certain repair method, direct cost + social cost + environmental impact etc. should be distinguished. Available real data collected from actual repair works performed on existing structures are presented.

1. INTRODUCTION

Analysis of different maintenance strategies (costs, environment, availability…) is the quintessence of every effective and sustainable asset management system. It is a process which should involve all stages from condition assessment of a structure, followed by repair, rehabilitation and maintenance planning, to implementation of monitoring technique. In case of structures with really long life cycles such as concrete bridges this process becomes quite complex because of many maintenance and repair procedures that will occur through its lifespan. Actions that have to be taken through the whole service life of a structure, from construction through all maintenance, repair and rehabilitation processes and finally removal, present enormous impact on economical, technical, social and environmental aspects. This is a well known fact but the problem arises when these influences need to be presented in a measurable way, especially in the same time.

One of the biggest problems in Croatian bridge management practice is that process of a repair planning is most often approached from a short term financial aspect taking into consideration only the direct costs of a certain maintenance solution. All other influences, for example, durability, impact on the environment, social costs such as traffic delays, noise produced during repair process, which are not as transparent as direct costs, are more or less neglected. (*fib Bulletin* 44 (2008), ISO 15686-7, REHABCON Manual (2004), Radić J. et al. Concrete structures: Reoair (2008))]

2. DIRECT COST OF REPAIR ALTERNATIVES

First step in every maintenance planning is assessing condition of a structure. Preliminary categorization of defects during visual inspection in Croatia is usually performed according the Tab. 1, based on the DIN 1076, directives RI-EBW-Pruf 88. Decision about the repair is made based upon categorization of defects first for individual structural elements and then for the entire structure.

Tab. 1 Categorization of defects

Damage category	Type of damage
0	No damage
I	Smaller defects resulted from the construction process
II	Smaller defects resulted from the exploitation
III	Defects that in long term decrease durability of the structure. Repair is needed.
IV	Defects that can, in the foreseeable future, decrease the reliability of the structure, Repair is needed now.
V	Defects that present a serious danger for safety of the structure. Intervention is needed emergently, and if necessary limitation or shutdown of traffic.

In Tab. 2 a connection has been established between degradation category (with some characteristic performance indicators) and direct cost of repair method. For example cost for category IV and V is the same but risks are different because category V means that stability of element or the whole structure is endangered. (Škarić Palić S., Stipanović Oslaković I. (2010)).

Tab. 2 Possible repair methods for some characteristic defects

<table>
<tr><th>Deg. cat.</th><th>Characteristic performance indicators</th><th>Possible repair methods (principle ; method) (HRN EN 1504-9:2001)</th><th>Direct cost €/unit</th></tr>
<tr><td>0</td><td>-</td><td>-</td><td>-</td></tr>
<tr><td rowspan="2">I</td><td>Surface imperfections</td><td rowspan="2">Surface coating (1 [PI], 2 [MC], 5 [PR], 6 [RC]; 1.2, 2.2, 5.1, 6.1)</td><td rowspan="2">25 €/m²</td></tr>
<tr><td>Small cracks (e.g.from shrinkage)</td></tr>
<tr><td rowspan="2">II</td><td>Surface cracks</td><td rowspan="2">Surface coating (1 [PI], 2 [MC], 5 [PR], 6 [RC]; 1.2, 2.2, 5.1, 6.1)</td><td rowspan="2">25 €/m²</td></tr>
<tr><td>Detachment of very thin surface layer</td></tr>
<tr><td rowspan="3">III</td><td>Net cracks in protective layer of concrete</td><td rowspan="3">Reprofilation of concrete depth depending on depth of penetration, cost given for 2 cm (3 [CR]; 3.1, 3.3) – applying mortar by hand or spraying</td><td rowspan="3">90-130€/m²</td></tr>
<tr><td>Contamination of protective layer of concrete (chloride penetration, dealkalisation)</td></tr>
<tr><td>Scaling due to freeze/thaw cycles</td></tr>
<tr><td rowspan="3">IV</td><td>Scaling of protective layer of concrete</td><td rowspan="3">Reprofilation of concrete 8 cm in depth (behind reinforcement), replacement of part of reinforcement (3 [CR]; 3.1, 3.2, 3.3) - applying mortar/concrete by hand or spraying or recasting</td><td rowspan="3">180-230€/m²</td></tr>
<tr><td>Visible products of corrosion of reinforcement</td></tr>
<tr><td>Reduction of reinforcement cross section</td></tr>
<tr><td rowspan="3">V</td><td>Spalling of surface layer of conrete</td><td rowspan="2">Reprofilation of concrete 8 cm or more in depth (behind reinforcement), replacement of part of reinforcement (3 [CR]; 3.1, 3.2, 3.3) - applying mortar/concrete by hand or spraying or recasting</td><td rowspan="2">180-230€/m²</td></tr>
<tr><td>Advanced corrosion of reinforcement (visible)</td></tr>
<tr><td>Significant reduction of reinforcement cross section</td><td>Replacement of element (3 [CR]; 3.4)</td><td>-</td></tr>
</table>

Methods and principles used in Tab. 2 are some of repair methods from standard HRN EN 1504-9:2001, which overall includes 11 principles and 37 methods. Direct costs included in the analysis present current costs on Croatian market and where collected directly from manufacturers and contractors.

When there is more than one repair method which presents a posible solution for recorded degradation, analysis has to be made. But when altenative is between repair options with different costs then almost always option with lower direct cost is chosen and there is no further analysis. (Årskog V., Fossdal S., E. Gjørv O. (2004), Škarić Palić S., Stipanović Oslaković I., Mavar K, Balagija A. (2008), Škarić Palić S., Stipanović Oslaković I. (2010)).
In Tab. 3 an example is presented with two repair options: concrete recasting or applying mortar.

Tab. 3 Direct cost of two repair options regarding degradation type - porous concrete (segregation, mechanical damage, nests in concrete) – 4 cm (Škarić Palić S., Stipanović Oslaković I., Mavar K, Balagija A. (2008))

<table>
<tr><th>Repair option</th><th>1 (3 [CR]; 3.1, 3.3)</th><th>2 (3 [CR]; 3.2)</th></tr>
<tr><td>Definition</td><td>Reprofilation, applying mortar by hand or spraying mortar.</td><td>Recasting concrete.</td></tr>
<tr><td rowspan="5">Steps</td><td>– Removal of concrete by waterjetting – 4 cm</td><td>– Removal of concrete by waterjetting – 8 cm (concrete to be installed properly needs larger thickness)</td></tr>
<tr><td>60€/m^2</td><td>120€/m^2</td></tr>
<tr><td colspan="2">– Repair of reinforcement, adding new bars (up to app 25%)
– Protection of reinforcement (coating)</td></tr>
<tr><td>– Reprofilation of concrete with mortars class R3 or R4 (depending on the structural element, cost for R4) – 4 cm</td><td>– Reprofilation of concrete with concrete, class depending on structural element and environmental condition (cost for C35/45) – 8 cm</td></tr>
<tr><td>50 €/m^2</td><td>35 €/m^2</td></tr>
</table>

3. INDIRECT COSTS

Sometimes indirect costs are easily recognized, for example in Tab 3 for repair option 2 there is twice more waterjetting compared to repair option 1, so impact on the environment is much larger. But that is only a part of the process because reprofilation also entailes further direct costs. In Tab. 4 direct costs are further dismemberd upon: manual labour, mechanization, material itself and other direct costs. In this way a method becomes more transparent and other influences are easier to recognize. Indirect costs (impact on the environment - IE, social cost -SC) can be recognized and should further be analysed from differences in the following (Habert G. (2009), Škarić Palić S., Stipanović Oslaković I. (2010)):

- Material (production, compound, transport) – IE
- Installment (duration, energy consumption) – SC (traffic jams), IE (CO_2 emission)

Tab. 4 Analysis of direst costs

Repair option	**1 (3 [CR]; 3.1, 3.3)**	**2 (3 [CR]; 3.2)**
Definition	Reprofilation, applying mortar by hand or spraying mortar.	Recasting concrete.
Manual labour	8,1 €/m^2	15,4 €/m^2
Mechanization (e.g. agregat, pumps, compressor...)	7,6 €/m^2	2,2 €/m^2
Material (e.g. concrete, mortar, fuel, formwork...)	34,3 €/m^2	17,4 €/m^2

4. CONCLUSION

Purpose of this paper was to present through cost analysis of repair alternatives that process of decision making between different maintenance strategies is not so simple as it is often approached. Without detailed and transparent analysis in all stages of a repair process it is imposible to make a responsible and sustainable desicion.

5. REFERENCES

Årskog V., Fossdal S., E. Gjørv O., "Life-cycle assessment of repair and maintenance systems for concrete structures", International workshop on sustainable development and concrete technology, Beijing, May 20–21, 2004, p 193-200

fib Bulletin 44, (February 2008), Concrete structure management: Guide to ownership and good practice Guide to good practice

Habert G., "Composite UHPFRC Concrete construction for CO2 savings" , ARCHES, Ljubljana, 27-28 August 2009

HRN EN 1504-9: 2001 Products and systems for the protection and repair of concrete structures - Definitions, requirements, quality control and evaluation of conformity – Part 9 General principles for the ise of products and systems.

ISO 15686-7 Buildings and constructed assets – Service life planning – Part 7: Performance evaluation for feedback of service life data from practice

Radić J. et al. Concrete structures: Repair, Hrvatska sveučilišna naklada, Zagreb, 2008. (in Croatian)

REHABCON Manual, (June 2004.), EC DG ENTR-C-2, IPS-2000-0063, EU-Project REHABCON Strategy for maintenance and rehabilitation in concrete structures

Škarić Palić S., Stipanović Oslaković I., Mavar K, Balagija A., „Condition assessment and LCCA of 11 overpasses on Zagreb bypass", Networks for sustainable environment and high quality of life, International Conference and EurekaBuild Event, Dubrovnik, Croatia, 2008, p 141-148

Škarić Palić S., Stipanović Oslaković I., „LCCA and analytical model for selection of optimal repair method in repair design process", ENBRI LCA WORKSHOP – Ljubljana, 21st–22nd May 2010

ROLE OF FLY ASH IN ENHANCEMENT OF RESISTIVITY OF CONCRETE TO PENETRATION OF FLUIDS

Ph.D. Ružica Rosković, B.Sc.Chem.Eng.[1], Prof. Jure Radić, B.Sc.C.E.[1],
Tomislav Jelavić, B.Sc.C.E.[1]
[1] *Institute IGH d.d.*
1000 Zagreb, Janka Rakuše 1

SUMMARY

In this paper it was studied and described possibility of siliceous and calcium fly ash for production of previously prestressed reinforced concrete elements, with the objective to decrease production costs and to improve physically - mechanical and durability properties of concrete as a civil engineering material.
Fly ash as a mineral additive has a great role in a cement replacement and in improvement of permeability properties. Influence of fly ash to cementitious composite material is exceptionally good and desirable, especially for cements with application in aggressive media. For this purpose laboratory investigations of properties of concrete, with certain contents of fly ash was conducted, which was compared with properties of concrete with CEM I 52,5 N cement type, to obtain optimal composition for prestressed reinforced concrete elements.

1. INTRODUCTION

Durability of structures is determined by its ability to resist the physical and environmental influences without losing the functional properties and structural integrity of the original design. Because of deterioration of materials due to corrosion and other effects, structures do not posses required safety and serviceability in operations. With the requirements of 100-year design life for major structures and enormous rehabilitation and repair costs associated with inability to satisfy these requirements, durability of civil engineering structures is today one of the key problems of structures worldwide. Premature loss in durability of structures is mainly caused by wrong selection of materials, poor quality of construction, poor design and non regular or absence of maintenance.
Durability of concrete has been subject of expert studies in the country and abroad. Dominant object of current research of numerous scientists is to track down causes of damage to concrete structures, as well as to find ways or possibilities of diminishing effects of specific deterioration causes and increasing concrete resistance to those effects.
Even today, due to future requirements and obligation of contributing to sustainable development, increasingly demanding requirements for more durable concrete and concrete structures are set, with ultimate goal of reducing consumption of natural resources in the course of production, construction, maintenance and use.

2. ROLE OF FLY ASH

Durability of concrete structures primarily depends on:

- permeability of the concrete;
- occurrence of micro-cracks in the concrete due to accumulation and evaporation of water and cement hydration heat as well as related stress;
- carbonation;
- inadequate protective layer;

- possibility of corrosion of steel reinforcement.

Previous studies have shown that use of mineral admixtures such as fly ash, silica fume, blast-furnace slag, etc. may reduce greatly permeability of concrete and consequently the probability of steel corrosion. When different reactive mineral admixtures are added into concrete at the same time, they develop their own characteristics with the development of time, so that the physical, mechanical and durability properties of concrete will not be reduced when large amount of mineral admixtures are added into concrete. For example, fly ash mostly enhance durability properties with the time and decrease early strength.

In this project mainly the addition of fly ash was researched, while its properties are the most suitable for the application in concrete elements. An advantage gained by adding the fly ash is lower absorption of heat generated as anhydrite phases are formed relative to Portland cement. Excessive heat of the hydration causes certain stresses and gives rise to occurrence of cracks in the concrete. Those cracks represent open to unhindered ingress of fluids, which leads to reduced durability of the structure.

3. EXPERIMENTAL WORK

In this paper it was studied and described possibility of siliceous and calcium fly ash intended use for production of previously prestressed reinforced concrete elements, with the objective of production costs decreasing without disturbing of mechanical and durability properties of concrete as a Civil engineering material.

For laboratory tests of concrete mixtures, objective was to achieve early strengths which would satisfy condition for release of prestressed cables.

For concrete C 40/50 condition was 30N/mm^2 after age of 3 days. Tab. 1 shows obtained measuring results of fresh and hardened concrete properties.

Tab. 1 Fresh and hardened concrete test results

COMPOSITION CODE	PJ1 (CEM I)	PJ2 (CEM I+25% Calcium fly ash)	PJ3 (CEM I+25% Siliceous fly ash)
Consistency by Slump test [mm]	220	210	210
Fresh concrete density [kg/m^3]	2482	2478	2496
Hardened concrete density [kg/m^3]	2468	2471	2458
Compressive strength after 1 day	42,5	39,3	41,7
Compressive strength after 2 days	52,8	51,8	51,2
Compressive strength after 7 days	69,5	62,9	71,6

3.1 Methods and test results of fluid penetration properties

Water permeability of concrete (determination of the penetration depth of water under pressure) was examined according to the standard HRN EN 12390-8 . (Tab.2)

Tab. 2 **Water permeability test results**

Concrete Property	PJ1	PJ2	PJ3
Water penetration depth, mm	19,3	18,7	18,0

Test of **Gas permeability coefficient** was conducted in accordance to the standard HRN EN 993-4 with nitrogen flow through specimen at constant pressure difference at the opposite specimen sides, with the measurement of volume of gas passing through the material in time.

Tab. 3 Gas permeability results for concrete

Concrete Property	PJ1	PJ2	PJ3
Specific coefficient of gas-permeabilityaverage value μ_{sr} (x10^{-13} cm^2)	2,12	2,06	0,85

Capillary absorption (water absorption) is phenomena of water absorption, which under influence of capillary forces penetrates through contact surface into tested material. In this test, increase of specimen mass in conditions defined in the standard HRN EN ISO 15148.

Tab. 4 Test results of water absorption coefficient (capillary absorption)

Concrete Property	PJ1	PJ2	PJ3
Water absorption coefficient (kg/($m^2h^{1/2}$))	0,627	0,481	0,387

Coefficient of chloride diffusion was tested according to the method NT BUILD 492. This approach to chloride ion diffusion was based on the movement of chloride ions under influence of external electric field. (Tab.5)

Tab. 5 Test results of chloride diffusion coefficient

Concrete Property	PJ1	PJ2	PJ3
Chloride diffusion coefficient D_{Cl} (×10^{-12} m^2/s)	6,37	6,11	2,54

3.2 Analysis of test results

Figure 6 shows all four durability properties of concrete: Capillary absorption, Water permeability, Gas permeability and Chloride diffusion for reference concrete PJ 1 compared with concretes PJ 2 and PJ 3.

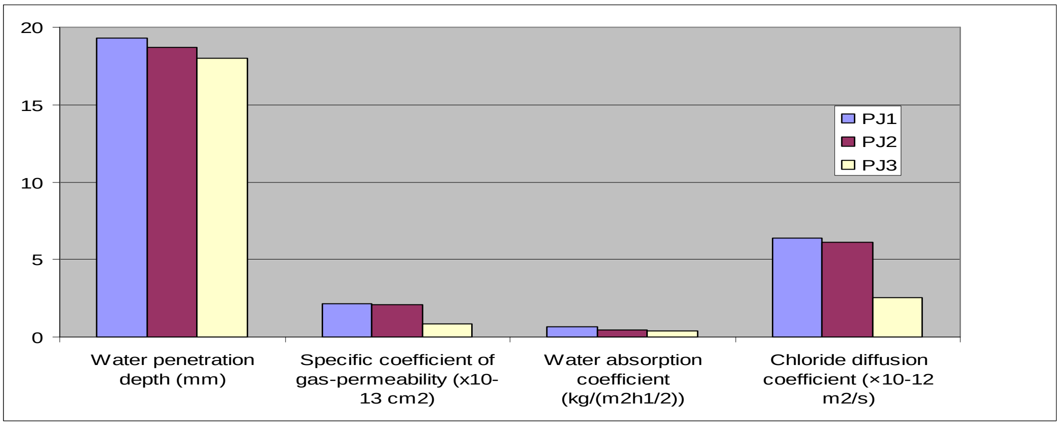

Fig. 1 Presentation of fluids penetration for concretes: PJ 1, PJ 2 i PJ 3.

Water permeability results are equable, with values from 18 to 20 mm, and satisfy conditions for water permeability class VDP 2 according to HRN 1128.

Coefficient of gas permeability results shows that addition of fly ash have minor influence to the coefficient of gas permeability.

Comparison of capillary absorption results for concrete PJ1 with cement CEM 1, PJ2 with cement CEM I + 25% calcium ash and PJ3 with CEM I + 25% siliceous ash shown that ash, due to it`s chemical composition, fills structure of cement matrix, and at that way improve structure of concrete.

One of the most important durability properties, which is also important for concrete assessment in the environments with salts from the sea or with salts which aren`t from the sea is coefficient of chloride diffusion.

Concrete produced from the cements with the calcium fly-ash and concrete with added calcium fly ash, have some lower coefficient of chloride ions diffusion, compared with reference concrete, which is very good. Concrete produced with siliceous fly ash have the best properties, assessed as concrete with very low chloride permeability.

4. CONCLUSIONS

Assuming known influence of fly ash to the improvement of durability properties of concrete, it was compared the properties of reference concrete with cement CEM I, which is in use for fabrication of prestressed girders, with the properties of concrete in wich one part of cement is replaced with certain contents of fly ash.

At this way, in this work, based on laboratory investigations, we try to demonstrate possibility of fly ash use for production of concrete for prestressed reinforced concrete elements. Basic technological criteria of fast increase of compressive strength were satisfied by use of superplastificizer, wherewith usability of these concrete compositions in prestressed girders was proved. Afterwards, advantages of concrete with addition of fly ash were proved with tests of permeability properties.

At this way, by substitution of clinker part with fly ash in constructive elements we can talk about the great potential of fly ash use in economic and technical sense, but also opens the field for further research.

5. REFERENCES

Berndt, M.L. Properties of sustainable concrete containing fly ash, slag and recycled concrete aggregate, Construction and Building Materials,Volume 23, Issue 7, July 2009, pp-2606-2613

Bilodeau, A.; Sivsundaram, V.; Painter, K.E.; Malhotra, V.M. Durability of concrete incorporating high volumes of fly ash from sources in the US, ACI Materials Journal 1994; 91(1): pp-3-12.

Rosković, R.; Bjegović, D. Role of mineral additions in reducing CO_2 emission. Cement and Concrete Research. 35 (2005) , 5; pp-974-978

HRN EN 12390-8:2009 Testing hardened concrete -- Part 8: Depth of penetration of water under pressure

HRN EN 993-4:2008 Methods of test for dense shaped refractory products – Part 4: Determination of permeability to gases

EN ISO 15148:2002 Hygrothermal performance of building materials and products – Determination of water absorption coefficient by partial immersion

NT BUILD 492:1999-11, Concrete, mortar and cement-based repair materials: chloride migration coefficient from non-steady-state migration experiments.

RAISING THE STATE OF THE ART IN STRUCTURAL ENGINEERING THROUGH PREFABRICATION

Dr. Müh. Özgür Bezgin
[1] *Yapı Merkezi Prefabrication Incorporated, Istanbul, Turkiye*
Mimar Sinan Mahallesi, Baraj Yolu Caddesi
No:102, 34935, Sultanbeyli, Istanbul

SUMMARY

Concrete prefabrication provides the design possibilities and the construction method to satisfy the architectural, functional and the structural requirements of a structure within a single step of prefabricated production. Presented here is the design and production history of a prefabricated structural façade that has become the architectural centerpiece of an educational and research establishment.

1. INTRODUCTION

Founded in 1994; The Sabancı University, which is located in the Tuzla district of Istanbul within The Turkish Republic, is a private university dedicated to the advancement of science, technology and arts through research and development. Construction of an academic center that is dedicated to research in the field of nanotechnology was proposed, the conceptual plans of which were brought to our attention by the University's representatives in the early spring of 2009. The proposed research center is known as **SU-NAC;** "**Sabancı University Nanotechnology Research and Application Center"** consists of an 11 meter high two – story building with footprint dimensions of 40 meter length and 60 meter width, which is partially surrounded by an atrium space that is enclosed by a structural façade designed to represent the lattice structure of a nanotube. The 134 meter long structural façade consists of 7,3 meter high and 50 cm thick prefabricated structural elements of high strength C60 grade white concrete that are aligned along a hypothetical oval plan surrounding the rectangular footprint of the two story high building. The structural façade, which is constructed of 53 prefabricated units of three different types, encloses an unobstructed atrium space around the two story building with a footprint area of approximately 1.185 m^2. The atrium space is capped by a heat insulated concrete roof with an area of 1.800 m^2 and weighing 560 kg/m^2 that is supported on steel beams spanning the variable opening space between the two – story building. The structure is located in the highly seismic industrial Marmara Region of the Turkish Republic with maximum absolute ground acceleration values in excess of 0.4g.

2. FUNCTIONAL CHARACTERISTICS

The prefabricated façade formed an important part of the vertical face of the structure measuring approximately 1.000 m^2. Therefore the façade had to satisfy the simultaneous architectural, functional and structural requirements in its design. The structural façade had to be transparent enough to allow the infusion of daylight and at the same time had to be strong and ductile enough to support the lateral and vertical loads due to the heavy roof loads. The two conflicting requirements of the façade had to be resolved within its solid structural part that formed 30% of the total façade area. The remaining 70% of the façade area was covered by the windows. Figure – 1 shows the initial architectural perspective of the structure and figure – 2 shows perspectives of the atrium.

Fig. 1 Architectural perspective of the façade.

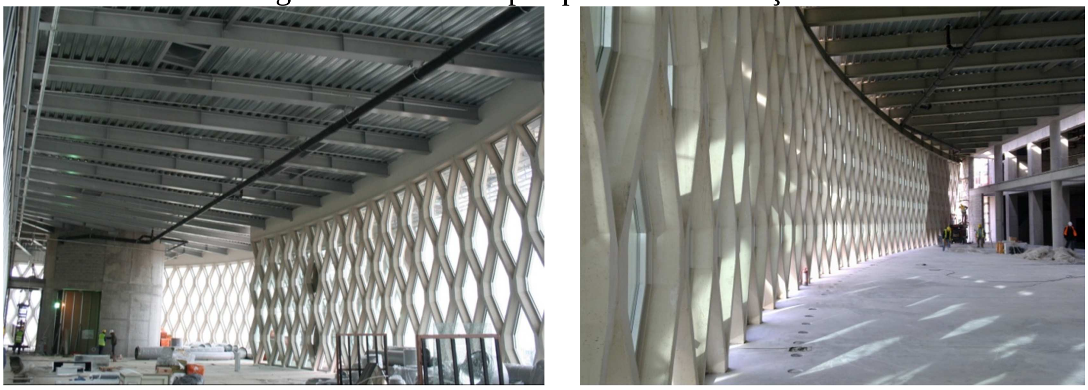

Fig. 2 Interior views of the atrium

3. STRUCTURAL CHARACTERISTICS

The structural façade of SU-NAC shown consist of three types of prefabricated elements that amount to fifty-three elements in total. Following their production and shipment, the prefabricated structural elements are installed within sockets that are prepared within a continuous strip foundation along the total length of the façade. The prefabricated structural façade elements were designed for service level gravity load values of minimum 12.5 Tons and maximum 50 Tons. The reinforcements along the façade were continuous each reinforcement with a total length of 920 cm were bent at 10 locations along its span in order to follow the architecture of the prefabricated structural façade elements.

4. PREFABRICATION AND INSTALLATION

The initial realization and the completion of the project took place in 18 months between March 2009 and August 2010 that included many design and production phases. The structural design of the prefabricated structural elements lasted four months during which many revisions were made and many core design ideas were considered. Production of the continuous reinforcement cage as shown in figure – 3 without any overlaps was an important challenge that had to be overcome for placement into a slender formwork with limited tolerances.

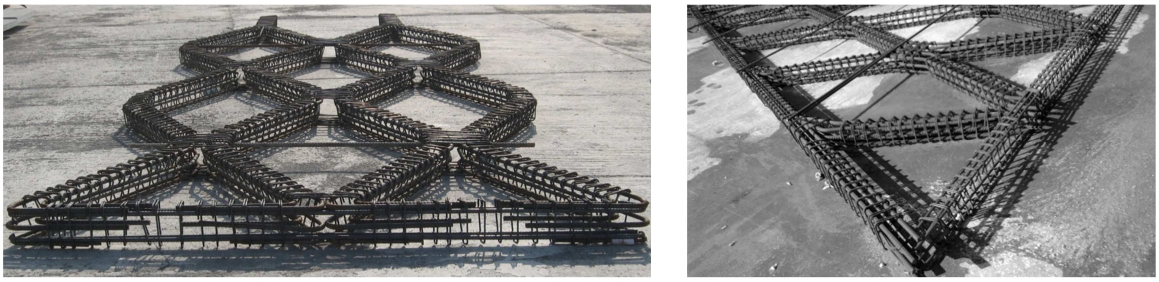

Fig. 3 Reinforcement cages of the prefabricated structural facade elements.

Without the use of any special curing schemes, the products were decast after 12 hours at a strength grade of C30, which was sufficient for the products to be lifted and stored for shipment. Prefabricated structural façade element were later shipped to the site 20 km away from the factory in groups of three units where they were unloaded and placed into pre-prepared socketed strip foundations as shown in figure – 4.

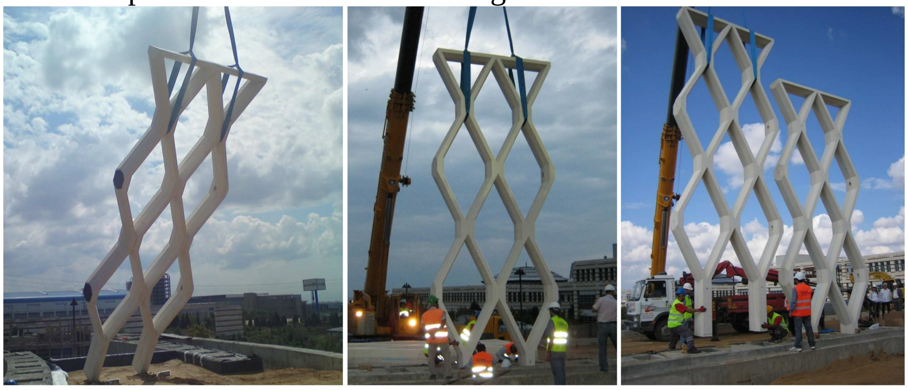

Fig. 4 Installation of prefabricated structural facade elements.

Following their installation, the prefabricated structural façade elements were bolted along their points of contact that allowed for rotation but prevented relative lateral translation between the neighboring elements. Following the completion of the façade which is shown in figure – 5, roof construction took place.

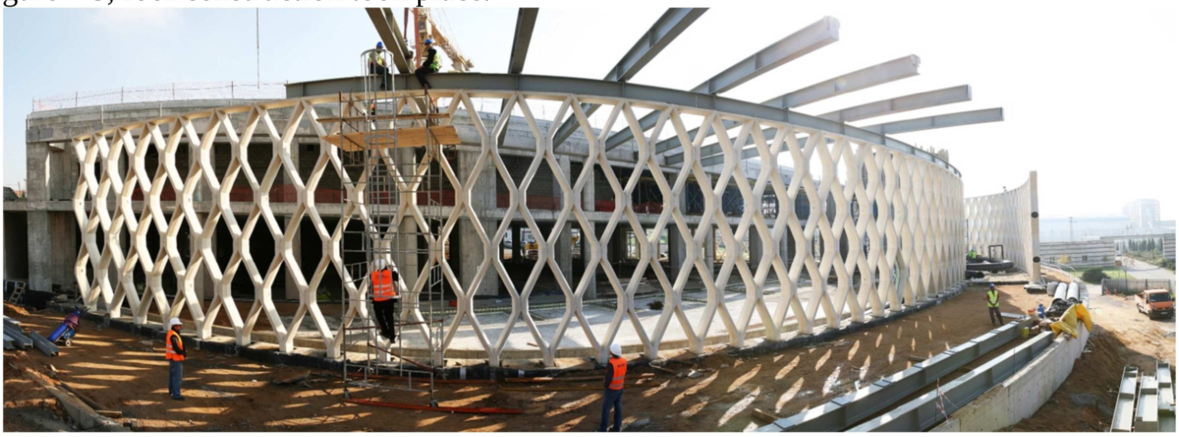

Fig. 5 Completed perspective of the facade ready to receive the roof loadings.

5. CONCLUSION

During the design of the prefabricated elements, the deformations under the imposed loadings were carefully estimated and submitted to the window pane producer for a pane design that allowed for the deformations and expected movements in the construction of the window frames. The prefabricated structural façade design and construction was an important challenge that provided a construction solution that provided the architectural and structural requirements of a façade in a single step of construction. Initial architectural design called for separate vertical support elements for the roof; however the design by YMP incorporated into the façade all the structural requirements that were needed to provide for the large atrium space of SU – NAC.

Fig. 6 Various perspectives of the facade prior to the completion of the Project.

AUTHOR INDEX